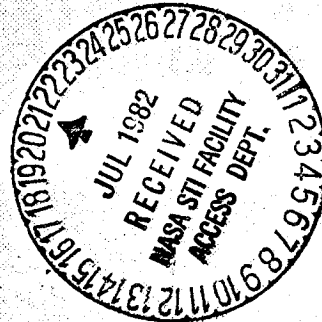


# NASA Technical Memorandum 82473

(NASA-TM-82473) TERRESTRIAL ENVIRONMENT N82-28317  
(CLIMATIC) CRITERIA GUIDELINES FOR USE IN  
AEROSPACE VEHICLE DEVELOPMENT (NASA) 418 p  
HC A18/MF A01 CSCL 22B Unclas  
G3/15 25996

## Terrestrial Environment (Climatic) Criteria Guidelines for Use in Aerospace Vehicle Development, 1982 Revision

JUNE 1982



**NASA**



Terrestrial Environment (Climatic) Criteria Guidelines for Use in  
Aerospace Vehicle Development, 1982 Revision

George C. Marshall Space Flight Center  
Marshall Space Flight Center, Alabama

Jun 82





1. Report No. NASA TM-82473	2. Government Accession No.	3. Recipient's Catalog No. N82-28317	
4. Title and Subtitle Terrestrial Environment (Climatic) Criteria Guidelines for Use in Aerospace Vehicle Development, 1982 Revision		5. Report Date June 1982	
		6. Performing Organization Code	
7. Author(s) Robert E. Turner and C. Kelly Hill, Compilers		8. Performing Organization Report No. ES84	
9. Performing Organization Name and Address  George C. Marshall Space Flight Center Marshall Space Flight Center, Alabama 35812		10. Work Unit No. M-382	
		11. Contract or Grant No.	
12. Sponsoring Agency Name and Address  National Aeronautics and Space Administration Washington, D.C. 20546		13. Type of Report and Period Covered Technical Memorandum	
		14. Sponsoring Agency Code	
15. Supplementary Notes This document was prepared based on the engineering problems which have developed or are anticipated for future programs by design and operational personnel of the NASA field centers. Various staff members of the Atmospheric Sciences Division, Space Sciences Laboratory, MSFC/NASA, contributed to the contents of this document.			
16. Abstract  This document provides guidelines on terrestrial environment data specifically applicable for NASA aerospace vehicles and associated equipment development. The primary geographic areas encompassed are the John F. Kennedy Space Center, Florida; Vandenberg AFB, California; Edwards AFB, California; Michoud Assembly Facility, New Orleans, Louisiana; National Space Technology Laboratory, Bay St. Louis, Mississippi; Lyndon B. Johnson Space Center, Houston, Texas; and the White Sands Missile Range, New Mexico. In addition, a section has been included to provide information on the general distribution of natural environmental extremes in the conterminous United States that may be needed to specify design criteria in the transportation of space vehicle subsystems and components. Although not considered as a specific vehicle design criterion, a section on atmospheric attenuation has been added since certain Earth orbital experiment missions are influenced by the Earth's atmosphere. A summary of climatic extremes for worldwide operational needs is also included. This document presents the latest available information on probable climatic extremes and succeeds information presented in TM X-64589, TM X-64757, and TM X-78118. Information is included on atmospheric chemistry, seismic criteria, and on a mathematical model to predict atmospheric dispersion of aerospace engine exhaust cloud rise and growth. There is also a section on atmospheric cloud phenomena. The information in this report is recommended for use in the development of aerospace vehicle and associated equipment design and operational criteria, unless otherwise stated in contract work specifications.  The environmental data in this report are primarily limited to information below 90 km. Environmental criteria for 90 km and above are being documented in a NASA Technical Memorandum entitled "Space and Planetary Environment Criteria Guidelines for Use in Space Vehicle Development (1982 Revision) (report in process).			
17. Key Words (Suggested by Author(s)) Environment Criteria, Terrestrial Environment, Surface Extremes, Wind, Temperature, Solar Radiation, Humidity, Precipitation, Density, Pressure, Atmospheric Electricity, Cloud Cover Structure, Control Systems		18. Distribution Statement Unclassified - Unlimited  Subject Category 15	
19. Security Classif. (of this report) Unclassified	20. Security Classif. (of this page) Unclassified	21. No. of Pages 418	22. Price A18

REPRODUCED BY  
NATIONAL TECHNICAL  
INFORMATION SERVICE  
U.S. DEPARTMENT OF COMMERCE  
SPRINGFIELD, VA. 22161



NASA Technical Memorandum 82473

**Terrestrial Environment (Climatic)  
Criteria Guidelines for Use in  
Aerospace Vehicle Development,  
1982 Revision**

**Robert E. Turner and C. Kelly Hill, *Compilers***  
*George C. Marshall Space Flight Center*  
*Marshall Space Flight Center, Alabama*



National Aeronautics  
and Space Administration

**Scientific and Technical  
Information Office**

1982

## ACKNOWLEDGMENTS

A large number of aerospace engineers and personnel in varying scientific fields have contributed and assisted in the preparation of this document. The following personnel were responsible for the sections identified as follows:

	SECTION	RESPONSIBLE PERSONS
I.	Summary and Introduction	William W. Vaughan
II.	Winds	George H. Fichtl, O. E. Smith, and Stanley L. Adelfang
III.	Inflight Thermodynamic Properties	Dale L. Johnson
IV.	Precipitation, Fog, and Icing	S. C. Brown, J. C. Sloan, and Dale L. Johnson
V.	Sea State	S. Clark Brown
VI.	Humidity	Charles K. Hill
VII.	Atmospheric Density and Pressure (Surface)	Dale L. Johnson
VIII.	United States Surface Extremes	Charles K. Hill
IX.	Worldwide Surface Extremes	Charles K. Hill
X.	Occurrences of Tornadoes and Hurricanes	Charles K. Hill and Dale L. Johnson
XI.	Atmospheric Electricity	Hugh Christian
XII.	Cloud Phenomena	Jeffrey Anderson, Vernon Keller, and David Bowdle
XIII.	Cloud Cover and Four-D Atmospheric Models	S. Clark Brown and Dale L. Johnson
XIV.	Thermal and Radiation	Harold Euler and Dale L. Johnson
XV.	Atmospheric Chemistry	Richard Cadle
XVI.	Geologic Hazards	Halka Chronic
XVII.	Aerospace Vehicle Effluent Diffusion Modeling for Tropospheric Air Quality and Environmental Assessments	H. E. Cramer and R. K. Dumbauld
XVIII.	Conversion Units	Robert E. Turner

Other members of the Atmospheric Sciences Division, Space Sciences Laboratory, who contributed to the document were Dennis W. Camp, Michael Susko, Robert E. Smith, and Warren Campbell.

Special acknowledgments are given to Dr. William W. Vaughan, Chief, Atmospheric Sciences Division (ES81), for his concerted guidance which led to the completion of the revision of this report.

## FOREWORD

This document provides information relative to the natural environment for altitudes of 90 km to the surface of the Earth. NASA Technical Memorandum TM-78119, entitled "Space and Planetary Environment Criteria Guidelines for Use in Space Vehicle Development, 1982 Revision," provides natural environment information for altitudes above 90 km.

There is no intent to automatically change any references to previous documents in contract scopes of work by the issuance of the 1982 revision of this document.

This document, which succeeds all editions of TM 78118, entitled "Terrestrial Environment (Climatic) Criteria Guidelines for Use in Aerospace Vehicle Development, 1977 Revision" and June 1979 Second Edition, is recommended for use in the development of space vehicles and associated equipment.

The information presented in this document is based on data and models considered to be accurate. However, in those design applications which indicate a critical environment interface the user should consult an environmental specialist to insure application of the most current information and scientific engineering interpretation.

Various programs of NASA's Office for Space Transportation Systems, Office for Aeronautics and Space Technology, Office for Space Science and Applications, and Office for Space Transportation Operations provided resources required for the preparation of this document.

## TABLE OF CONTENTS

	Page
SECTION I. INTRODUCTION .....	1.1
1.1 General .....	1.1
1.2 Main Geographical Areas Covered in Document .....	1.3
SECTION II. WINDS .....	2.1
2.1 Introduction .....	2.1
2.2 Definitions .....	2.3
2.2.1 Ground Winds .....	2.3
2.2.2 Inflight Winds .....	2.4
2.2.3 General .....	2.5
2.3 Ground Winds (1 to 150 m) .....	2.6
2.3.1 Introduction .....	2.6
2.3.2 Considerations in Ground Wind Design Criteria. ....	2.7
2.3.3 Introduction to Exposure Period Analysis. ....	2.7
2.3.4 Development of Extreme Value Concept .....	2.8
2.3.5 Design Wind Profiles for Aerospace Vehicles. ....	2.9
2.3.6 Spectral Ground Wind Turbulence Model .....	2.24
2.3.7 Ground Wind Gust Factors .....	2.31
2.3.8 Ground Wind Shear. ....	2.34
2.3.9 Ground Wind Direction Characteristics .....	2.34
2.3.10 Design Winds for Facilities and Ground Support Equipment. ....	2.35
2.3.11 Ground Winds for Runway Orientation Optimization. ....	2.45
2.4 Inflight Winds .....	2.51
2.4.1 Introduction .....	2.51
2.4.2 Wind Aloft Climatology .....	2.52
2.4.3 Wind Component Statistics .....	2.53
2.4.4 Wind Speed Profiles for Biasing Tilt Program .....	2.62
2.4.5 Design Wind Speed Profile Envelopes .....	2.64
2.4.6 Wind Speed Change Envelopes .....	2.64
2.4.7 Wind Direction Change Envelopes. ....	2.70
2.4.8 Gusts – Vertically Flying Vehicles .....	2.77
2.4.9 Synthetic Wind Speed Profiles. ....	2.82
2.4.10 Characteristic Wind Profiles to a Height of 18 Kilometers. ....	2.86
2.4.11 Vector Wind and Vector Wind Shear Models. ....	2.87
2.4.12 Wind Profile Data Availability. ....	2.90
2.4.13 Atmospheric Turbulence Criteria for Horizontally Flying Vehicles. ....	2.91
2.4.14 Turbulence Model for Flight Simulation .....	2.100
2.4.15 Discrete Gust Model – Horizontally Flying Vehicles. ....	2.109
2.4.16 Flight Regimes For Use of Horizontal and Vertical Turbulence Models (Spectra and Discrete Gusts) .....	2.111

## TABLE OF CONTENTS (Continued)

	Page
2.5 Mission Analysis, Prelaunch Monitoring, and Flight Evaluation. ....	2.111
2.5.1 Mission Planning. ....	2.112
2.5.2 Prelaunch Wind Monitoring. ....	2.115
2.5.3 Post-Flight Evaluation. ....	2.116
REFERENCES. ....	2.120
 SECTION III. INFLIGHT THERMODYNAMIC PROPERTIES. ....	 3.1
3.1 Introduction. ....	3.1
3.2 Atmospheric Temperature. ....	3.1
3.2.1 Air Temperature at Altitude. ....	3.1
3.2.2 Extreme Cold Temperature. ....	3.2
3.3 Atmospheric Pressure. ....	3.2
3.3.1 Definition. ....	3.2
3.3.2 Pressure at Altitude. ....	3.3
3.4 Atmospheric Density. ....	3.3
3.4.1 Definition. ....	3.3
3.4.2 Atmospheric Density at Altitude. ....	3.9
3.5 Simultaneous Values of Temperature, Pressure, and Density at Discrete Altitude Levels. ....	3.9
3.5.1 Introduction. ....	3.9
3.5.2 Method of Determining Simultaneous Value. ....	3.9
3.6 Extreme Atmospheric Profiles for Kennedy Space Center, Florida, Vandenberg AFB, California, and Edwards AFB, California. ....	3.13
3.7 Reference Atmospheres. ....	3.22
3.8 Reentry – Global Reference Atmosphere Model. ....	3.24
3.8.1 Reentry Atmospheric Model. ....	3.24
REFERENCES. ....	3.25
 SECTION IV. PRECIPITATION, FOG, AND ICING. ....	 4.1
4.1 Introduction. ....	4.1
4.2 Definitions. ....	4.1
4.3 Rainfall. ....	4.1
4.3.1 Record Rainfall. ....	4.2
4.3.2 Raindrop Size. ....	4.7
4.3.3 Statistics of Rainfall Occurrences. ....	4.7
4.3.4 Distribution of Rainfall Rates with Altitude. ....	4.8
4.3.5 Types of Ice Formation. ....	4.8
4.3.6 Hydrometeor Characteristics with Altitude. ....	4.13
4.4 Snow. ....	4.14
4.4.1 Snow Loads at Surface. ....	4.14
4.4.2 Snow Particle Size. ....	4.16
4.5 Hail. ....	4.16
4.5.1 Hail at Surface. ....	4.20
4.5.2 Distribution of Hail with Altitude. ....	4.23



## TABLE OF CONTENTS (Continued)

	Page
4.6 Laboratory Test Simulation .....	4.23
4.6.1 Rate of Fall of Raindroplets .....	4.23
4.6.2 Raindrop Size and Distribution .....	4.24
4.6.3 Wind Speed .....	4.24
4.6.4 Temperatures .....	4.24
4.6.5 Recommended Items to Include in Laboratory Rainfall Tests .....	4.25
4.7 Rain Erosion .....	4.27
4.7.1 Introduction .....	4.27
4.7.2 Rain Erosion Criteria .....	4.27
4.8 Fogs .....	4.27
4.9 Precipitation or Fog (VAFB and KSC) .....	4.29
REFERENCES .....	4.31
 SECTION V. SEA STATE .....	 5.1
5.1 Introduction .....	5.1
5.2 Wave Slopes .....	5.3
5.3 Surface Currents .....	5.3
5.4 Sea-State Duration .....	5.5
5.5 Ocean Temperatures .....	5.6
5.6 Atmospheric Conditions .....	5.6
REFERENCES .....	5.9
 SECTION VI. HUMIDITY .....	 6.1
6.1 Definitions .....	6.1
6.2 Vapor Concentration .....	6.2
6.2.1 High Vapor Concentration at Surface .....	6.4
6.2.2 Low Vapor Concentration at Surface .....	6.6
6.2.3 Compartment Vapor Concentration at Surface .....	6.7
6.3 Vapor Concentration at Altitude .....	6.7
6.3.1 High Vapor Concentration at Altitude .....	6.7
6.3.2 Low Vapor Concentration at Altitude .....	6.7
REFERENCES .....	6.11
 SECTION VII. ATMOSPHERIC PRESSURE AND DENSITY (SURFACE) .....	 7.1
7.1 Atmospheric Pressure .....	7.1
7.1.1 Definition .....	7.1
7.1.2 Surface Pressure .....	7.1
7.1.3 Pressure Change .....	7.1
7.1.4 Pressure Decrease with Altitude .....	7.1
7.2 Atmospheric Density .....	7.1
7.2.1 Definition .....	7.1
7.2.2 Surface Density .....	7.4
7.3 Surface Density Variability and Altitude Variations .....	7.5
REFERENCES .....	7.5

## TABLE OF CONTENTS (Continued)

	Page
SECTION VIII. UNITED STATES SURFACE EXTREMES .....	8.1
8.1 Introduction .....	8.1
8.2 Environments Included .....	8.1
8.3 Source of Data .....	8.1
8.4 Extreme Design Environments .....	8.2
8.4.1 Air Temperature .....	8.2
8.4.2 Snowfall — Snow Load .....	8.2
8.4.3 Hail .....	8.9
8.4.4 Atmospheric Pressure .....	8.9
REFERENCES .....	8.16
SECTION IX. WORLDWIDE SURFACE EXTREMES .....	9.1
9.1 Introduction .....	9.1
9.2 Sources of Data .....	9.1
9.3 Worldwide Extremes Over Continents .....	9.2
9.3.1 Temperature .....	9.2
9.3.2 Dew Point .....	9.5
9.3.3 Precipitation .....	9.6
9.3.4 Pressure .....	9.7
9.3.5 Ground Wind .....	9.7
REFERENCES .....	9.10
SECTION X. OCCURRENCES OF TORNADOES AND HURRICANES .....	10.1
10.1 Introduction .....	10.1
10.2 Tornadoes .....	10.1
10.3 Hurricanes and Tropical Storms .....	10.4
10.3.1 Distribution of Hurricane and Tropical Storm Frequencies .....	10.4
REFERENCES .....	10.7
SECTION XI. ATMOSPHERIC ELECTRICITY .....	11.1
11.1 Introduction .....	11.1
11.2 Thunderstorm Electricity .....	11.2
11.2.1 Potential Gradient .....	11.2
11.2.2 Fair-Weather Potential Gradients .....	11.3
11.2.3 Potential Gradients During Thunderstorms .....	11.3
11.2.4 Corona Discharge .....	11.3
11.3 Characteristics of Lightning Discharges .....	11.3
11.3.1 Lightning Currents .....	11.4
11.3.2 Lightning Characteristics for Design on the Launch Pad or During Ground Transportation .....	11.4
11.3.3 Lightning Characteristics for Design During Flight (Triggered Lightning) .....	11.7

## TABLE OF CONTENTS (Continued)

	Page
11.3.4 Current Flow Distribution from a Lightning Discharge .....	11.10
11.3.5 Radio Interference .....	11.10
11.4 Frequency of Occurrence of Thunderstorms .....	11.10
11.4.1 Thunderstorm Days per Year (Isoceraunic Level) .....	11.10
11.4.2 Thunderstorm Occurrence per Day .....	11.11
11.4.3 Thunderstorm Hits .....	11.11
11.5 Frequency of Lightning Strokes to Earth .....	11.13
11.6 Static Electricity .....	11.14
11.7 Electrical Breakdown of the Atmosphere .....	11.14
REFERENCES .....	11.16
 SECTION XII. CLOUD PHENOMENA .....	 12.1
12.1 Introduction .....	12.1
12.2 Cloud Processes .....	12.1
12.3 Basic Cloud Types .....	12.4
BIBLIOGRAPHY .....	12.7
 SECTION XIII. CLOUD COVER AND FOUR-D ATMOSPHERIC MODELS .....	 13.1
13.1 Introduction .....	13.1
13.2 Interaction Model of Microwave Energy and Atmospheric Variables .....	13.1
13.2.1 Scattering and Extinction Properties of Water Clouds Over the Range 10 cm to 10 $\mu$ m .....	13.3
13.2.2 Zenith Opacity due to Atmospheric Water Vapor as a Function of Latitude .....	13.3
13.3 Global Cloud Model .....	13.3
13.3.1 Introduction .....	13.3
13.3.2 Background .....	13.4
13.3.3 The Simulation Procedure .....	13.6
13.3.4 Limitations of the Present Model .....	13.7
13.3.5 The Revised Cloud Model .....	13.8
13.3.6 The Revised Simulation Procedure .....	13.8
13.3.7 Cloud Data for the Revised Model .....	13.9
13.4 Four-Dimensional Atmospheric Models .....	13.9
REFERENCES .....	13.11
 SECTION XIV. THERMAL AND RADIATION .....	 14.1
14.1 Introduction .....	14.1
14.2 Definitions .....	14.1
14.3 Spectral Distribution of Radiation .....	14.2
14.3.1 Introduction .....	14.2
14.3.2 Solar Radiation .....	14.3
14.3.3 Intensity Distribution .....	14.3

## TABLE OF CONTENTS (Continued)

	Page
14.3.4 Atmospheric Transmittance of Solar Radiation . . . . .	14.7
14.3.5 Sky (Diffuse) Radiation . . . . .	14.8
14.4 Average Emittance of Colored Objects . . . . .	14.10
14.5 Computation of Surface Temperature for Several Simultaneous Radiation Sources . . . . .	14.10
14.6 Total Solar Radiation . . . . .	14.10
14.6.1 Introduction . . . . .	14.10
14.6.2 Use of Solar Radiation in Design . . . . .	14.10
14.6.3 Total Solar Radiation Extremes . . . . .	14.17
14.7 Temperature . . . . .	14.20
14.7.1 Air Temperature Near the Surface . . . . .	14.20
14.7.2 Extreme Air Temperature Change . . . . .	14.23
14.7.3 Surface (Skin) Temperature . . . . .	14.23
14.7.4 Compartment Temperature . . . . .	14.23
14.8 Data on Air Temperature Distribution with Altitude . . . . .	14.24
REFERENCES . . . . .	14.25
SECTION XV. ATMOSPHERIC CHEMISTRY (Gaseous and Particulate) . . . . .	
15.1 Introduction . . . . .	15.1
15.2 Gaseous Composition . . . . .	15.1
15.2.1 Ozone ( $O_3$ ) . . . . .	15.1
15.2.2 Nitrous Oxide ( $N_2O$ ) . . . . .	15.3
15.2.3 Nitric Oxide (NO) and Nitrogen Dioxide ( $NO_2$ ) . . . . .	15.3
15.2.4 Nitric Acid Vapor ( $HNO_3$ ) . . . . .	15.3
15.2.5 Hydrogen Sulfide ( $H_2S$ ) . . . . .	15.3
15.2.6 Carbonyl Sulfide (COS) and Carbon Disulfide ( $CS_2$ ) . . . . .	15.3
15.2.7 Ammonia ( $NH_3$ ) . . . . .	15.3
15.2.8 Hydrogen ( $H_2$ ) . . . . .	15.4
15.2.9 Methane ( $CH_4$ ) . . . . .	15.4
15.2.10 Sulfur Dioxide ( $SO_2$ ) . . . . .	15.4
15.2.11 Carbon Monoxide (CO) . . . . .	15.4
15.2.12 Carbon Dioxide ( $CO_2$ ) . . . . .	15.4
15.2.13 Water ( $H_2O$ ) . . . . .	15.5
15.3 Physical and Chemical Properties of Atmospheric Gases . . . . .	15.5
15.3.1 Nitrogen ( $N_2$ ) . . . . .	15.5
15.3.2 Oxygen ( $O_2$ ) . . . . .	15.6
15.3.3 Argon (A), Neon (Ne), Krypton (Kr), Xenon (Xe), and Helium (He) . . . . .	15.6
15.3.4 Nitrous Oxide ( $N_2O$ ) . . . . .	15.6
15.3.5 Nitric Oxide (NO) . . . . .	15.6
15.3.6 Nitrogen Dioxide ( $NO_2$ ) . . . . .	15.6
15.3.7 Nitric Acid Vapor ( $HNO_3$ ) . . . . .	15.6
15.3.8 Ammonia ( $NH_3$ ) . . . . .	15.7
15.3.9 Ozone ( $O_3$ ) . . . . .	15.7
15.3.10 Hydrogen ( $H_2$ ) . . . . .	15.7
15.3.11 Hydrogen Sulfide ( $H_2S$ ) . . . . .	15.7

## TABLE OF CONTENTS (Continued)

	Page
15.3.12 Carbon Disulfide (CS <sub>2</sub> ) and Carbonyl Sulfide (COS) . . . . .	15.7
15.3.13 Sulfur Dioxide (SO <sub>2</sub> ) . . . . .	15.7
15.3.14 Carbon Monoxide (CO) . . . . .	15.8
15.3.15 Carbon Dioxide (CO <sub>2</sub> ) . . . . .	15.8
15.3.16 Methane (CH <sub>4</sub> ) . . . . .	15.8
15.4 The Corrosive Effects of Gases . . . . .	15.8
15.4.1 Rusting . . . . .	15.9
15.4.2 Oxidation of Rubber and Synthetic Plastics . . . . .	15.9
15.4.3 "Weathering" of Paints . . . . .	15.9
15.4.4 Corrosion by Sulfur Dioxide and Hydrogen Sulfide . . . . .	15.9
15.4.5 Nitric Acid Vapor and Hydrogen Chloride . . . . .	15.10
15.5 Particles . . . . .	15.10
15.5.1 Sources of Particles . . . . .	15.10
15.5.2 Physical Properties . . . . .	15.11
15.5.3 Particle Size Distributions . . . . .	15.12
15.5.4 Variation With Altitude . . . . .	15.13
15.5.5 Corrosion and Abrasion by Particles . . . . .	15.13
15.6 Snow, Hail, and Rain . . . . .	15.14
REFERENCES . . . . .	15.15
 SECTION XVI. GEOLOGIC HAZARDS . . . . .	 16.1
16.1 Introduction . . . . .	16.1
16.2 Specific Hazards . . . . .	16.1
16.2.1 Earthquakes . . . . .	16.1
16.2.2 Tsunamis and Seiches . . . . .	16.1
16.2.3 Slope Processes . . . . .	16.2
16.2.4 Floods . . . . .	16.3
16.2.5 Volcanic Hazards . . . . .	16.5
16.2.6 Expanding Ground . . . . .	16.6
16.2.7 Ground Subsidence . . . . .	16.7
16.2.8 Other Hazards . . . . .	16.8
16.2.9 Conclusions . . . . .	16.8
16.3 Geology and Geologic Hazards at Edwards Air Force Base, California . . . . .	16.8
16.3.1 Geology . . . . .	16.8
16.3.2 Geologic Hazards . . . . .	16.10
16.4 Geology and Geologic Hazards of Vandenberg Air Force Base, California . . . . .	16.12
16.4.1 Introduction . . . . .	16.12
16.4.2 Geology . . . . .	16.13
16.4.3 Geologic Hazards . . . . .	16.13
16.4.4 Conclusions . . . . .	16.17
16.5 Geology and Geologic Hazards at Cape Canaveral and Kennedy Space Center, Florida . . . . .	16.18
16.5.1 Introduction . . . . .	16.18
16.5.2 Geologic Hazards of Cape Canaveral and Kennedy Space Center . . . . .	16.18

## TABLE OF CONTENTS (Concluded)

	Page
16.6 Seismic Environment . . . . .	16.20
16.6.1 GSE Categories and Requirements . . . . .	16.20
16.6.2 Types of Design Analyses . . . . .	16.20
16.6.3 Dynamic Analysis . . . . .	16.21
16.6.4 Static Analysis. . . . .	16.21
REFERENCES . . . . .	16.26
SECTION XVII. AEROSPACE VEHICLE EFFLUENT DIFFUSION MODELING FOR TROPOSPHERIC AIR QUALITY AND ENVIRONMENTAL ASSESSMENTS . . . . .	
	17.1
17.1 Introduction . . . . .	17.1
17.2 The NASA/MSFC REED Code . . . . .	17.2
17.2.1 Overview of the REED Code . . . . .	17.2
17.2.2 Launch Types and Vehicle Parameters . . . . .	17.2
17.2.3 Meteorological Layers . . . . .	17.2
17.2.4 REED Code Cloud and Plume Rise Models . . . . .	17.2
17.2.5 Source Dimensions, Material Distribution, and Spatial Position of the Stabilized Ground-Cloud. . . . .	17.2
17.2.6 Turbulence Profile Algorithm . . . . .	17.2
17.2.7 REED Code Dispersion Models . . . . .	17.2
17.3 Toxicity Criteria . . . . .	17.3
REFERENCES . . . . .	17.3
SECTION XVIII. CONVERSION UNITS. . . . .	
	18.1
18.1 Physical Constants and Conversion Factors. . . . .	18.1
REFERENCES . . . . .	18.17

## TECHNICAL MEMORANDUM TM

**TERRESTRIAL ENVIRONMENT (CLIMATIC) CRITERIA GUIDELINES  
FOR USE IN AEROSPACE VEHICLE DEVELOPMENT  
1982 REVISION****SUMMARY**

Atmospheric phenomena play a significant role in the design and flight of aerospace vehicles and in the integrity of the associated aerospace systems and structures. Environmental design criteria guidelines in this report are based on statistics of atmospheric and climatic phenomena relative to various aerospace industrial, operational, and vehicle launch locations. This revision contains new and updated material in most sections.

Specifically, aerospace vehicle design guidelines are established for the following environmental phenomena and presented by sections: Winds; Inflight Thermodynamic Properties; Precipitation, Fog, and Icing; Sea State; Humidity; Atmospheric Density and Pressure (Surface); United States Surface Extremes; Worldwide Surface Extremes; Tornadoes and Hurricanes; Atmospheric Electricity; Cloud Phenomena; Four-D Atmospheric and Cloud Cover Models; Thermal Radiation; Atmospheric Chemistry; and Geologic Hazards. The last section in this document includes conversion constants.

Atmospheric data are presented and analyzed for application to aerospace vehicle design studies. The atmospheric parameters are scaled to show the probability of reaching or exceeding certain limits to assist in establishing design and operating criteria. Additional information on the different parameters may be found in the numerous references cited in the text following each section.

**SECTION I. INTRODUCTION****1.1 General**

For climatic extremes, there is no known physical upper or lower bound except for certain conditions; for example, wind speed does have a strict physical lower bound of zero. Therefore, for any observed extreme condition, there is a finite probability of its being exceeded. Consequently, climatic extremes for design must be accepted with the knowledge that there is some risk of the values being exceeded. Also, the accuracy of measurement of many environmental parameters is not as precise as desired. In some cases, theoretical estimates of extreme values are believed to be more representative than those indicated by empirical distributions from short periods of record. Therefore, theoretical values are given considerable weight in selecting extreme values for some parameters, i.e., the peak surface winds. Criteria guidelines are presented for various percentiles based on available data samples. Caution should be exercised in the interpretation of these percentiles in vehicle studies to ensure consistency with physical reality and the specific design and operational problems of concern.

Aerospace vehicles are not normally designed for launch and flight in severe weather conditions such as hurricanes, thunderstorms, and squalls. Atmospheric parameters associated with severe weather which may be hazardous to space vehicles are strong ground and inflight winds, strong wind shears, turbulence, icing conditions, and electrical activity. The guidelines given usually provide information relative to severe weather characteristics, which may be included in design studies if required.

Environmental data in this report are primarily limited to information below 90 km. Specific space vehicle natural environmental design criteria are normally specified in the appropriate organizational space vehicle design ground rules and design criteria data documentation. The information in this document is recommended for use in the development of space vehicles and associated equipment design criteria unless otherwise stated in contract work specifications.

The data in all sections are based on conditions which have actually occurred, or are statistically probable in nature, over a longer reference period than the available data based on established models.

Assessment of the natural environment in the early stages of an aerospace vehicle development program will be advantageous in developing a vehicle with a minimum operational sensitivity to the environment. For those areas of the environment that need to be monitored prior to and during tests and operations, this early planning will permit development of the required measuring and communication systems for accurate and timely monitoring of the environment.

A knowledge of the Earth's atmospheric environmental parameters is necessary for the establishment of design requirements for space vehicles and associated equipment. Such data are required to define the design condition for fabrication, storage, transportation, test, preflight, and inflight design conditions and should be considered for both the whole system and the components which make up the system. One of the purposes of this document is to provide guideline data on natural environmental conditions for the various major geographic locations which are applicable to the design of space vehicle and associated equipment.

Good engineering judgment must be exercised in the application of the Earth's atmospheric data to space vehicle design analysis. Consideration must be given to the overall vehicle mission and performance requirements. Knowledge still is lacking on the relationships between some of the atmospheric variates which are required as inputs to the design of space vehicles. Also, interrelationships between space vehicle parameters and atmospheric variables cannot always be clearly defined. Therefore, a close working relationship and team philosophy should exist between the design/operational engineer and the respective organization's aerospace meteorologists. Although, ideally, a space vehicle design should accommodate all expected operational atmospheric conditions, it is neither economically nor technically feasible to design space vehicles to withstand all atmospheric extremes. For this reason, consideration should be given to protection of space vehicles from some extremes by use of support equipment and by using specialized forecast personnel to advise on the expected occurrence of critical environmental conditions. The services of specialized forecast personnel may be very economical in comparison with more expensive designing which would be necessary to cope with all environmental possibilities.

In general this document does not specify how the designer should use the data in regard to a specific space vehicle design. Such specifications may be established only through analysis and study of a particular design problem. Although of operational significance, descriptions of some atmospheric conditions have been omitted since they are not of direct concern for structural and control system design. Induced environments (vehicle caused) may be more critical than natural environments for certain vehicle operational situations, and in some cases the combination of natural and induced environments will be more severe than either environment alone. Induced environments are considered in other space vehicle criteria documents, which should be consulted for such data.

The environment criteria data presented in this document were formulated based on discussions with and requests from engineers involved in space vehicle development and operations; therefore, they represent responses to actual engineering problems and are not just a general compilation of environmental data. This report is used extensively by the Marshall Space Flight Center (MSFC), other NASA centers, various other government agencies, and their associated contractors in design and operational studies. Considerably more information is available on topics covered in this report than is presented here. Users of this document



who have questions or require further information on the data provided may direct their requests to the Atmospheric Sciences Division (ES81), Space Sciences Laboratory, Marshall Space Flight Center, Alabama 35812.

## 1.2 Main Geographical Areas Covered in Document

- a. John F. Kennedy Space Center, Florida.
- b. Vandenberg AFB, California.
- c. Edwards Air Force Base, California.
- d. Lyndon B. Johnson Space Center, Houston, Texas.
- e. White Sands Missile Range, New Mexico.
- f. Michoud Assembly Facility, New Orleans, Louisiana.
- g. National Space Technology Laboratory (NSTL), Bay St. Louis, Mississippi.

This document does not include the subject of environmental test procedures. Reference should be made to Department of Defense MIL-STD-810C Environmental Test Methods (1975)\* available from the National Technical Information Service, Springfield, Virginia, 22161. This document covers procedures for: Low Pressure (Altitude), High and Low Temperature, Temperature Shock, Temperature Altitude and Temperature-Humidity Altitude, Solar Radiation, Rain, Humidity, Fungus, Salt Fog, Dust (Fine Sand), and Space Simulations (Unmanned Test). An excellent comparison of the various international environmental testing standards may be found in the Journal of Environmental Sciences, Vol XXIV, Number 2, March/April 1981.

\*Revision being considered by DOD.



## SECTION II. WINDS

### 2.1 Introduction

An aerospace vehicle's response to atmospheric disturbances, and especially wind, must be carefully evaluated to insure an acceptable design relative to operational requirements. The choice of criteria depends upon the specific launch location(s), vehicle configuration, and mission. Vehicle design, operation, and flight procedures must be separated into particular phases for proper assessment of environmental influences and impacts upon the life history of each vehicle and all associated systems. These phases include such things as (1) initial purpose and concept of the vehicle, (2) preliminary engineering design for flight, (3) structural design, (4) vehicle guidance and flight control design, (5) optimizations of design limits regarding the various environmental factors, and (6) final assessment of environmental capability for launch and flight operations. The proper selection, analyses, and interpretation of wind information are essential requirements of atmospheric scientists responsible for establishing the environmental wind criteria to support all aerospace programs and missions.

Winds are characterized by three-dimensional motions of the air, composed of very large to very small scale spatial and temporal variations. The variability of wind is caused and governed by the rotation of the Earth, geographic characteristics, and the available solar energy reaching the Earth's atmosphere and surface. This energy drives the large-scale global circulation in which massive wave patterns form and significant imbalances are established among major atmospheric pressure regimes. Due to the Earth-Sun orbital behavior, seasonal wind variations occur and may be seen in synoptic weather changes that affect all locations. Other dominating factors that cause the winds to vary so drastically are land-sea influences, geographic locations, terrain type, elevation, available water, vegetation, and a vast assortment of other natural and manmade constituents.

Because the wind environment affects the design of aerospace vehicles and their operations, it is necessary to use good technical judgment and to apply sound engineering principles in preparing wind criteria that are descriptive and concise. Although wind criteria contained in this report were especially prepared for application in aerospace vehicle programs, it is important to note that much of this information is directly applicable in other programs, such as aeronautical engineering, architecture, atmospheric diffusion, wind and solar energy conversion research, atmospheric sound propagation, and many others.

The synthetic ground and inflight wind criteria concept has its major value and contribution to the design during the initial and intermediate phases of the development cycles of aerospace vehicles. Although a certain overall vehicle performance capability in terms of probability may be stated as a guideline, it is not realistic to expect a design to be developed that will precisely meet this specified performance capability because of the many unknowns in the vehicle characteristics and design criteria. Many advancements have been achieved regarding aerospace vehicle design, operations, and flight, but it is still not possible to make exact statements on the overall design risks or operational capabilities of a vehicle. Therefore, it makes good engineering sense to establish a set of idealized or synthetic ground and inflight wind models which characterize such features as wind magnitude versus height, gust factors, turbulence spectra, and wind shear phenomena, and vector properties of winds. These models may then be referenced and used in a consistent manner to establish preliminary and intermediate design criteria necessary to ensure completion of the expected missions through application of proper wind criteria in the vehicle development. Furthermore, representative wind models aid in isolating those features of the winds (ground and inflight) that are design critical to vehicle ground and inflight operations.

It is an accepted practice to use the synthetic wind criteria approach described herein for NASA space vehicle developments during the preliminary and intermediate design phases. These criteria should be

carefully formulated to ensure that the appropriate study models are used in the vehicle design studies and to be consistent in applying wind criteria from one vehicle to another in structural/control system simulation models. The synthetic wind profile features may readily be employed to isolate critical design problems without resorting to lengthy and elaborate computer routines which are unjustified with respect to other design input parameters which also require special attention. In some cases, for example, the designer may use close approximations of steady-state wind limits for design and operational assessments. Other features of the wind forcing function may be accomplished by using combinations of steady-state winds, wind shears, and gusts. For steady-state wind limits, a multitude of mission and vehicle performance analyses can rapidly be accomplished relative to launch windows, etc., using representative historical records of the steady-state inflight wind data and available ground wind data sets. Such records, described in this section, are available for all major launch sites. These statistical records and the synthetic profile concept are also adequate for bias of pitch and yaw programs, range safety studies, preliminary and final abort analyses, water entry of space vehicle components (Space Shuttle solid rocket motor water entry, for example) and related space vehicle operational problems.

When adequately documented and referenced, the synthetic wind criteria concept provides a powerful tool for ensuring consistent design inputs for all users, and it essentially avoids the problem of any oversight errors which may be costly to correct in later vehicle development phases. Furthermore, they enable design engineers at various locations to simultaneously conduct studies and compare their results on a standard basis.

During the later stages of a vehicle development program, when adequate vehicle response data are available, it is highly desirable, if not mandatory, to simulate the vehicle ascent flight and response to actual wind velocity profiles. However, these wind profiles should contain an adequate frequency content (gusts, turbulence, embedded jets, extreme shears, etc.) to encompass the significant frequencies of response of the vehicle to winds (control mode frequencies, first bending mode frequency, liquid propellant slosh modes, etc.). Anything short of this suggested approach would correspond to the use of only another preliminary design approximation of the natural environment. The current acceptable practice is to use a selection of detailed inflight wind profiles (resolution to about one cycle per 100 m) obtained by the FPS-16 Radar/Jimsphere technique for the launch sites of concern. These data and their availability are discussed in pertinent subsections in this document. The number of flight performance simulations and detailed wind profiles selected will depend upon the particular vehicle and the design problems involved and how well the vehicle performance characteristics were identified during the preliminary and intermediate design phase. The vehicle simulation to detailed inflight wind profiles should constitute a verification of the design. It should provide the necessary information to ensure a design optimization with added routines to isolate any critical areas requiring further analysis to refine vehicle control and structural responses to wind. The profiles used should constitute a selection of representative data from the available detailed wind profile record. The selection must portray adequate statistical confidence of wind velocity variability required for vehicle design and development and especially to meet mission objectives. Such goals can only be reached through collaboration among vehicle design groups and the cognizant organization concerned with preparing and interpreting environmental wind criteria.

Special attention is placed on techniques for developing synthetic vector wind profiles for aerospace vehicle applications — this information is presented within this section and illustrates how several statistical wind models can be derived. More specifically, synthetic vector wind and vector wind shear criteria models can now be generated for use in vehicle design and flight studies using analytical techniques where statistical probabilities and distributions of vector winds are more ideally presented and understood.

For the preflight simulation and flight evaluation of a space vehicle related to the wind environment it is recommended that established ground wind reference height anemometers and detailed inflight wind profiles measured by the FPS-16 Radar/Jimsphere system be used to obtain reliable data. A rapid reduction

scheme to ensure a prompt input into prelaunch flight simulation programs is required. During the pre-launch phase, accurate and near real-time wind data are mandatory, especially if critical, or near critical, launch wind conditions exist. Furthermore, adequate flight simulations cannot be made without timely and accurate launch wind profile data.

The information given in this section constitutes wind models and criteria guidelines applicable to various design problems. The selected risk levels employed are characterized by ground and inflight winds required for the design and depend upon the design philosophy used by management for the development efforts. To maximize vehicle performance flexibility, it is considered best to utilize those wind data associated with the minimum acceptable risk levels. In addition, the critical mission-related parameters such as exposure time of a vehicle being affected by natural environment quantities, launch windows, reentry periods, launch turnaround periods, etc., should carefully be considered. Initial design work using unbiased (wind) trajectories on the basis of nondirectional ground or inflight winds may be used unless the vehicle and its mission are well known and the exact launch azimuth and time(s) are established and adhered to throughout the program. In designs that use wind-biased trajectories and directional (vector) wind criteria, rather severe wind constraints can result if the vehicle is used for other missions, different flight azimuths, or in another vehicle configuration. Therefore, caution must be exercised in using wind criteria models to ensure consistency with the physical interpretation of each specific vehicle design problem. Several references are cited throughout this section which discuss special and specific problems related to the development and specification of wind environments for aerospace vehicle programs.

## 2.2 Definitions

The following terms are used in this section with the meanings specified here.

### 2.2.1 Ground Winds

Ground Winds are winds which affect space vehicles during ground operations and immediately on launch and, for purposes of this document, can be considered to be winds below a height of approximately 150 m above the natural grade (ground winds are sometime referred to as surface winds).

Average wind speed – See steady-state wind speed.

Free-standing winds are the ground winds that are applied to the vehicle when it is standing on the launch pad (with or without fuel) after any service structure, support, or shelter has been removed.

Gust is a sudden increase in the ground wind speed. It is frequently expressed as a deviation from a mean wind speed. A sudden decrease in the wind speed is sometimes also referred to as a gust (negative).

Gust factor is the ratio of peak ground wind speed to the average or mean ground wind speed over a finite time period.

Launch design winds are the peak ground winds for which the vehicle can be launched, normally involving a stated design wind at a reference height plus the associated peak wind profile (~99.9 percent) shape.

On-pad winds are the ground winds at a given reference height plus associated peak wind profile (~99.9 percent) that are applied when the vehicle is on the launch pad with protective measures in place, i.e., service structures, support, or shelter.

Peak wind speed is the maximum (essentially, instantaneous) wind speed measured during a specified reference period, such as hour, day, or month at a given reference height.

Steady-state or average wind speed is the mean, over a period of approximately 10 min, of the ground wind speed measured at a fixed reference height. It is usually assumed constant as, for example, in spectral calculations. Thus, the steady-state or average wind should be the mean which filters out, over a sufficient duration, the effects that would very definitely contribute to the random responses of aerospace vehicles and structures. The average wind speed is sometimes referred to as the quasi-steady-state wind.

Reference height (ground winds) is the height above the ground surface (natural grade) to which wind speeds are referred for the establishment of climatological conditions, for construction of design wind profiles, and for statements of an operational wind constraint. Normally during the design and development phase, a reference height near the base of the vehicle (usually given as the 10- or 18.3-m level) is used. After completion of vehicle development, the operational constraints may be stated with respect to a reference height near the top of the vehicle.

Causes of high ground winds are summarized as follows:

- a. Tornadoes: Upper limit unknown; estimated approximately 103 m/sec (200 knots).
- b. Hurricanes: By definition, a storm of tropical origin with winds greater than 33 m/sec (64 knots), upper limit unknown; speeds have been measured exceeding 90 m/sec (175 knots).
- c. Tropical Storms: By definition, a storm with winds less than 33 m/sec (64 knots) and greater than 17 m/sec (33 knots).
- d. Thunderstorms: Upper limit not defined; typical values approximately 23 m/sec (45 knots); severe thunderstorm by definition greater than 26 m/sec (50 knots) (Ref. 2.1).
- e. Frontal Passages: Without thunderstorms, winds usually less than 18 m/sec (35 knots); with squalls, same as for thunderstorms.
- f. Pressure Gradients: Long-duration gusty winds; winds usually less than 31 m/sec (60 knots).

### 2.2.2 Inflight Winds

Inflight winds are those winds above a height of approximately 150 m.

Design verification data tapes are a selection of detailed wind profile data compiled from FPS-16 Radar/Jimsphere data records for use in vehicle final design verification analysis. They consist of a representative monthly selection of wind profiles from which the integrated response of a vehicle to the combined effect of speed, direction, shear, and turbulence (gusts) may be derived. They have application to computation of final reference values of launch delay risk for a given vehicle mission.

Design wind speed profile envelopes are envelopes of scalar or vector component or resultant wind speeds representing the extreme steady-state inflight wind value for any selected altitude that have a specified probability of not being exceeded during a given reference period.

Detail wind profile is a wind profile measured by the FPS-16 Radar/Jimsphere or equivalent technique and having a resolution to at least one cycle per 100 m. Application is intended for final design verification purposes and launch delay risk calculations.

Steady-state inflight wind, in this document, refers to the mean wind speed as measured with the rawinsonde system and averaged over approximately 1000 m in the vertical direction. The assigned height of this wind measurement will be the middle of the 1000-m layer.

Reference height (inflight winds) is that referred to in constructing a synthetic wind profile.

Scale-of-distance is the vertical distance (thickness of layer) between two wind measurements used in computing wind shears.

Serial complete data represent the completion of a sample of rawinsonde data (selected period) by filling in (inserting) missing data by interpolation, by extrapolation, or by use of data from nearby stations. This operation is performed by meteorological personnel familiar with the data.

Shear build-up envelope is the curve determined by combining the reference height wind speed from the wind speed profile envelope with the shears (wind speed change) below the selected altitude (reference height). The shear build-up envelope curve usually starts at zero altitude difference (scale-of-distance) and wind speed and ends at the design wind speed value at the referenced altitude for inflight wind response studies.

Synthetic wind speed profile is a design wind profile representing the combination of a reference height design wind with associated envelope shears (wind speed change) and gusts for engineering design and mission analysis purposes.

Wind speed change envelopes (wind shear) represent the values of the change in wind speed over various increments of altitude (100 to 5000 m), computed for a given probability level and associated reference height or related wind speed value at the reference height. These values are combined, and an envelope of the wind speed change is found useful in constructing synthetic wind profiles. Usually the 99 percentile probability level is used for design purposes.

Wind shear is equal to the difference between wind speeds measured at two specific positions divided by the distance between the two positions.

### 2.2.3 General

Calm winds are those winds with a speed less than 0.5 m/sec (1 knot).

Component wind speed is the equivalent wind speed that any selected wind vector would have if resolved to a specific direction; that is, a wind from the northeast (45-degree azimuth) of 60 m/sec would have a component from the east (90-degree azimuth) of 42.4 m/sec. This northeast wind would be equivalent to a 42.4 m/sec head wind on the vehicle, if the vehicle is launched on an east (90-degree) azimuth.

Percentile: The percentile is that value of a variable at or below which lies the given percent of a set of data. The relationship between the mean, standard deviation ( $\sigma$ ), and percentile (P) of a normal or Gaussian distribution function is as follows for selected values:

Mean  $\pm$  n $\sigma$ P = Percentile = Probability  $\times$  100

Minimum	0.000
Mean - 3 $\sigma$	0.135
Mean - 2 $\sigma$	2.275
Mean - 1 $\sigma$	15.866
Mean $\pm$ 0 $\sigma$	50.000
Mean + 1 $\sigma$	84.134
Mean + 2 $\sigma$	97.725
Mean + 3 $\sigma$	99.865
Maximum	100.000

Scalar wind is the magnitude of the wind vector.

Vector wind includes magnitude and direction of the wind.

Wind direction is the direction from which the wind is blowing, measured clockwise from true North.

Windiest monthly reference period is the month that has the highest tropospheric wind speeds at a given probability level.

### 2.3 Ground Winds (1 to 150 m)

#### 2.3.1 Introduction

Ground winds for aerospace vehicle applications are defined in this document to be those winds in the lowest 150 m of the atmosphere. A vehicle positioned vertically on-pad may penetrate this entire region. The winds in this layer of the atmosphere are characterized by very complicated three-dimensional flow patterns with rapid variations in magnitude and direction in space and time. An engineering requirement exists for models which define the structure of wind in this layer because of the complicated and possible critical manner in which a vehicle might respond to certain aspects of the flow in this layer, both when the vehicle is stationary on the launch pad and during the first few seconds after launch. The forces generated by von Karman vortex shedding are an example of the effect of wind on space vehicles. These forces can result in base bending moments while the vehicle is on the launch pad and pitch and yaw plane angular accelerations and vehicle drift during lift-off. Other equally important examples can be cited. The basic treatment of the ground wind problem relative to vertically oriented vehicles on-pad and during lift-off has been to estimate the risk of encountering crucial aspects of wind along the vertical. It should be noted that, in addition to the engineering requirements for on-pad and launch winds for vertically ascending vehicles, a requirement for ground wind models also exists for horizontally flying vehicles for take-off and landing. In a space vehicle context, this is especially true for the return flight of the Space Shuttle Orbiter vehicle. This aspect of the natural wind environment is discussed in Sections 2.4.13 through 2.4.15.

With the evolution of larger and more sophisticated space vehicles, the requirements for more adequate ground wind information have increased. For example, to fulfill the need to provide improved ground wind data, the 150-Meter Ground Winds Tower Facility was constructed on Merritt Island, Kennedy



Space Center, Florida, in close proximity to Launch Complex 39. Wind and temperature profile data from this facility have been used in many studies that have contributed to a significant portion of the information in this chapter on wind shaping, gusts, and turbulence spectra. Similar towers are in operation at the various national ranges.

Because ground wind data are applied by space vehicle engineers in numerous ways, dependent upon the specific problem, various viewpoints and kinds of analytical techniques were used to obtain the environmental models presented here. Program planning, for instance, requires considerable climatological insight to determine the frequency and persistence distributions for wind speeds and wind directions. However, for design purposes the space vehicle must withstand certain unique predetermined structural loads that are generated from exposure to known peak ground wind conditions. Ground wind profiles and the ground wind turbulence spectra contribute to the development of the design ground wind models. Surface roughness, thermal environment, and various transient local and large-scale meteorological systems influence the ground wind environment for each launch site.

### 2.3.2 Considerations in Ground Wind Design Criteria

To establish the ground wind design criteria for aerospace vehicles, several important factors must be considered.

- a. Where is the vehicle to operate?
- b. What is the launch location?
- c. What are the proposed vehicle missions?
- d. How many hours, days, or months will the vehicle be exposed to ground winds?
- e. What are the consequences of operational constraints that may be imposed upon the vehicle because of wind constraints?
- f. What are the consequences if the vehicle is destroyed or damaged by ground winds?
- g. What are the cost and engineering practicalities for designing a functional vehicle to meet the desired mission requirements?
- h. What is the risk that the vehicle will be destroyed or damaged by excessive wind loading?

In view of this list of questions or any similar list that a design group may enumerate, it becomes obvious that the establishment of ground wind environment design criteria for a space vehicle requires an interdisciplinary approach involving the several engineering and scientific disciplines. Furthermore, the process is an iterative one. To begin the iterative process, specific information on ground winds is required.

### 2.3.3 Introduction to Exposure Period Analysis

Valid, quantitative answers to such questions as the following are of primary concern in the design, mission planning, and operations of space vehicles:

- a. What is the probability that the peak ground wind at some specified reference height will exceed (or not exceed) a given magnitude in some specified time period?
- b. Given a design wind profile in terms of peak wind speed versus height from 10 to 150 m, what is the probability that the design wind profile will be exceeded in some specified time period?

Given a statistical sample of peak wind measurements for a specific location, the first question can be answered in as much detail as a statistical analyst finds necessary and sufficient. This first question has been thoroughly analyzed for Kennedy Space Center and partially for Vandenberg AFB, and to a lesser degree for other locations of interest.

The analysis becomes considerably more complex in answering the second question. A wind profile is required, and, to develop the model, measurements of the wind profiles by properly instrumented ground wind towers are required as well as a program for scheduling the measurements and data reduction. Every instantaneous wind profile is unique; similarity is a matter of degree. Given the peak wind speed at one height, there is a whole family of possible profiles extending from the specified wind at that height. Thus for each specified wind speed at a given height, there is a statistical distribution of wind profiles. Recommended profile shapes for Kennedy Space Center and other locations are given in this report. The analysis needed to answer the second question is not complete, but we can assume that, given a period of time, the design wind profile shape will occur for a specified wind speed at a given height. In the event that a thunderstorm passes over the vehicle, it is logical to assume that the design wind profile shape (~99.9 shape) will occur and that the chance of the design wind profile being exceeded is the same as the probability that the peak wind during the passage of the thunderstorm will strike the vehicle or point of interest.

#### 2.3.4 Development of Extreme Value Concept

It has been estimated from wind tunnel tests that only a few seconds are required for the wind to produce near steady-state drag loads on a vehicle such as the Space Shuttle in an exposed condition on the launch pad. For this and other reasons (Section 2.3.5), we have adopted the peak wind speed as our fundamental measurement of wind. Equally important, when the engineering applications of winds can be made in terms of peak wind speeds, it is possible to obtain an appropriate statistical sample that conforms to the fundamental principles of extreme value theory. One hour is a convenient and physically meaningful minimum time interval from which to select the peak wind. The reader is referred to Section 2.3.5.5.1 for details concerning averaging times in the context of structural response. An hourly peak wind speed sample has been established for Kennedy Space Center from wind information on continuous recording charts. Representative peak wind samples for Vandenberg AFB have been derived from hourly steady-state wind measurements using statistical and physical principles.

##### 2.3.4.1 Envelope of Distributions

In the development of the statistics for peak winds, it was recognized that the probability of hourly, daily, and monthly peak winds exceeding (or not exceeding) specified values varied with time of day and from month to month. In other words, the distributions of like variables were different for the various reference periods. Even so, the Gumbel distribution was an excellent fit to the samples of all hourly, daily, monthly, bimonthly (in two combinations), and trimonthly (in three combinations) periods taken over the complete period of record, justifying the use of these distributions. However, in establishing vehicle wind design criteria for the peak winds versus exposure time, it is desired to present a simple set of wind statistics in such a manner that every reference period and exposure time would not have to be examined to determine the probability that the largest peak wind during the exposure time would exceed some specified magnitude.

To accomplish this objective, envelopes of the distributions of the largest peak winds for various time increments from which the extremes were taken for the various reference periods were constructed. For example, to obtain the envelope distribution of hourly peak winds for the month of March, the largest peak wind was selected at each percentage point from the 24 peak wind distributions (one for each hour). The annual envelope distribution is the envelope of the 12 hourly envelopes (one for each month).

Selected envelopes of distributions are given in Section 2.3.5. It is recommended that these envelopes of distributions be used for vehicle wind design considerations. This recommendation is made under the assumption that it is not known what time of day or season of year critical vehicle operations are to be conducted; furthermore, it is not desirable to design a vehicle to operate only during selected hours or months. Should all other design alternatives fail to lead to a functionally engineered vehicle with an acceptable risk of not being compromised by wind loads, then distributions for peak winds by time of day for monthly reference periods may be considered for limited missions. For vehicle operations, detailed statistics of peak winds for specific missions are meaningful for management decisions, in planning missions, and in establishing mission rules and alternatives to the operational procedures. To present the wind statistics for these purposes is beyond the scope of this document. Each space mission has many facets that make it difficult to generalize and to present the statistics in brief form. Specific data for these applications are available upon request.

### 2.3.5 Design Wind Profiles for Aerospace Vehicles

Specific information about the wind profile is required to calculate ground wind loads on space vehicles. The Earth's surface is a rigid boundary that exerts a frictional force on the lower layers of the atmosphere, causing the wind to vanish at the ground. In addition, the characteristic length and velocity scales of the mean (steady-state) flow in the first 150 m (boundary layer) of the atmosphere combine to yield extremely high Reynolds numbers with values that range between approximately  $10^6$  and  $10^8$ , so that for most conditions (wind speeds  $> 1$  m/sec) the flow is fully turbulent. The lower boundary condition, the thermal and dynamic stability properties of the boundary layer, the distributions of the large-scale pressure, the Coriolis forces, and the structure of the turbulence combine to yield an infinity of wind profiles.

Data on basic wind speed profiles given in this section are to be used for vehicle design. With respect to design practices, the application of peak winds and the associated turbulence spectra and discrete gusts should be considered. The maximum response obtained for the selected risk levels for each physically realistic combination of conditions should be employed in the design. Care should be exercised so that wind inputs are not taken into account more than once. For example, the discrete gust and spectrum of turbulence are representations of the same thing, namely atmospheric turbulence. Thus, one should not calculate the responses of a vehicle due to the discrete gust and spectrum and then combine the results by addition, root-sum-square, or any other procedure since these inputs represent the same thing. Rather, the responses should be calculated with each input and then enveloped.

#### 2.3.5.1 Philosophy

An example of a peak wind speed is given in Figure 2.3.1. Peak wind statistics have three advantages over mean wind statistics. First, peak wind statistics do not depend upon an averaging operation as do mean wind statistics. Second, to construct a mean wind sample, a chart reader or weather observer must perform an "eyeball" average of the wind data, causing the averaging process to vary from day to day according to the mood of the observer, and from observer to observer. Hourly peak wind speed readings avoid this subjective averaging process. Third, to monitor winds during the countdown phase of a space vehicle launch, it is easier to monitor the peak wind speed than the mean wind speed.

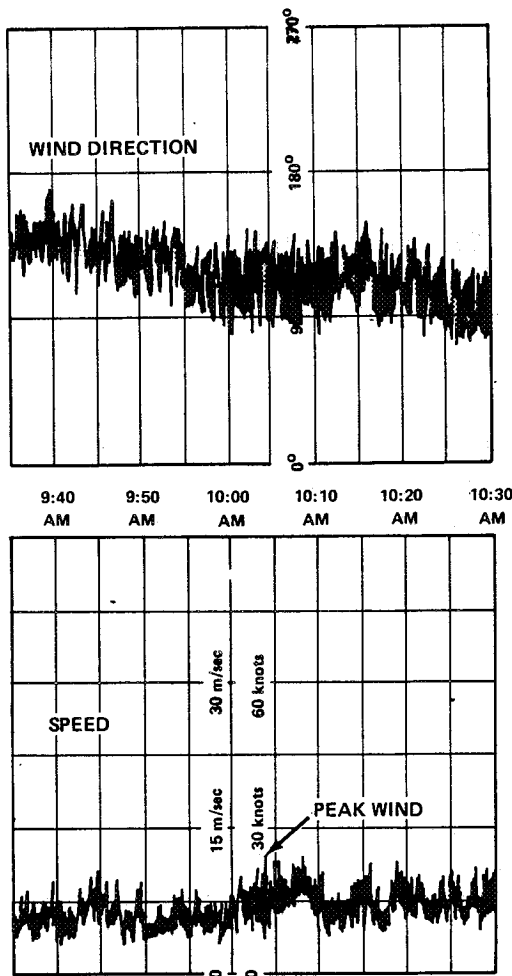


Figure 2.3.1 Example of peak wind speed records.

O. E. Smith, et al. (Ref. 2.2) have performed extensive statistical analyses with peak wind speed samples measured at the 10-m level. In the course of the work he and his collaborators introduced the concept of exposure period probabilities into the design and operation of space vehicles. By determining the distribution functions of peak wind speeds for various periods of exposure (hour, day, month, year, etc.), it is possible to determine the probability of occurrence of a certain peak wind speed magnitude occurring during a prescribed period of exposure of a space vehicle to the natural environment. Thus, if an operation requires, for example, 1 hour to complete, and if the critical wind loads on the space vehicle can be defined in terms of the peak wind speed, then it is the probability of occurrence of the peak wind speed during a 1-hour period that gives a measure of the risk of the occurrence of structural failure. Similarly, if an operation requires 1 day to complete, then it is the probability of occurrence of the peak wind speed during a 1-day period that gives a measure of the risk of structural failure.

All probability statements concerning the capabilities of the space vehicles that are launched at NASA's Kennedy Space Center are prescribed in terms of Smith's peak wind speed exposure statistics. These peak wind statistics are usually transformed to the 18.3-m (60-ft) reference level for design purposes (or higher levels for operational applications). However, to perform loading and response calculations resulting from steady-state and random turbulence drag loads

and von Karman vortex shedding loads, the engineer requires information about the vertical variation of the mean wind and the structure of turbulence in the atmospheric boundary layer. The philosophy is to extrapolate the peak wind statistics up into the atmosphere via a peak wind profile, and the associated steady-state or mean wind profile is obtained by applying a gust factor that is a function of wind speed and height.

### 2.3.5.2 Peak Wind Profile Shapes

To develop a peak wind profile model, approximately 6000 hourly peak wind speed profiles measured at NASA's ground wind tower facility at Kennedy Space Center have been analyzed. The sample, composed of profiles of hourly peak wind speeds measured at the 18-, 30-, 60-, 90-, 120-, and 150-m levels, showed that the variation of the peak wind speed in the vertical, below 150 m, for engineering purposes, could be described with a power law relationship given by

$$u(z) = u_{18.3} \left( \frac{z}{18.3} \right)^k, \quad (2.1)$$

where  $u(z)$  is the peak wind speed at height  $z$  in meters above natural grade and  $u_{18.3}$  is a known peak wind speed at  $z = 18.3$  m. The peak wind is referenced to the 18.3-m level because this level has been selected as the standard reference for the Kennedy Space Center launch area. A reference level should always be stated when discussing ground winds to avoid confusion in interpretation of risk statements and structural load calculations.

A statistical analysis of the peak wind speed profile data revealed that, for engineering purposes,  $k$  is distributed normally for any particular value of the peak wind speed at the 18.3-m level. Thus, for a given percentile level of occurrence,  $k$  is approximately equal to a constant for  $u_{18.3} \leq 2$  m/sec. For  $u_{18.3} > 2$  m/sec,

$$k = c(u_{18.3})^{-3/4}, \quad (2.2)$$

where  $u_{18.3}$  has the units of meter per second. The parameter  $c$ , for engineering purposes, is distributed normally with mean value 0.52 and standard deviation 0.36 and has units of  $m^{3/4} \text{ sec}^{-3/4}$ . The distribution of  $k$  as a function of  $u_{18.3}$  is depicted in Figure 2.3.2. The  $\bar{k} + 3\sigma$  values are used in design studies.

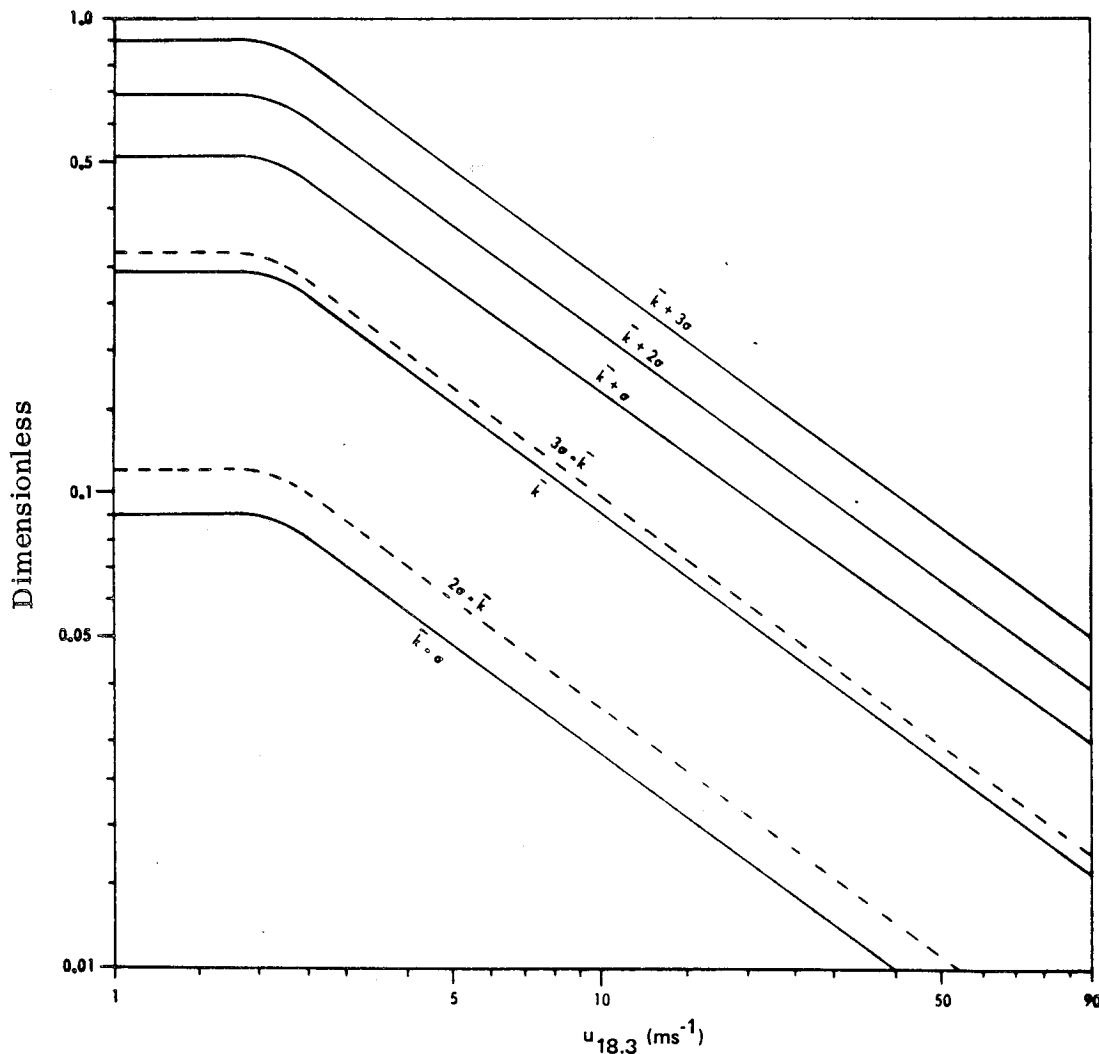


Figure 2.3.2 Distribution of the peak wind profile parameter  $k$  for various wind speeds at the 18.3-m level for the Eastern Test Range.

### 2.3.5.3 Instantaneous Extreme Wind Profiles

The probability that the hourly peak wind speeds at all levels occur simultaneously is small. Accordingly, the practice of using peak wind profiles introduces some conservatism into the design criteria; however, the probability is relatively large that when the hourly peak wind occurs at the 18.3-m level, the wind at the other levels almost take on the hourly peak values.

To gain some insight into this question, approximately 35 hours of digitized magnetic tape data were analyzed. The data were digitized at 0.2-sec intervals in real time and partitioned into 0.5-, 2-, 5-, and 10-min samples. The vertical average peak wind speed  $\bar{u}_P$  and the 18-m mean wind  $\bar{u}_{18}$  were calculated for each sample. In addition, the instantaneous vertical average wind speed time history at 0.2-sec intervals was calculated for each sample, and the peak instantaneous vertical average wind speed  $u_I$  was selected for each sample. The quantity  $\bar{u}_I/\bar{u}_P$  was then interpreted to be a measure of how well the peak wind profile approximates the instantaneous extreme wind profile. Figure 2.3.3 is a plot of  $\bar{u}_I/\bar{u}_P$  as a function of  $\bar{u}_{18}$ . The data points tend to scatter about a mean value of  $\bar{u}_I/\bar{u}_P \approx 0.93$ ; however, some of the data points have values equal to 0.98. These results justify the use of peak wind profiles for engineering purposes.

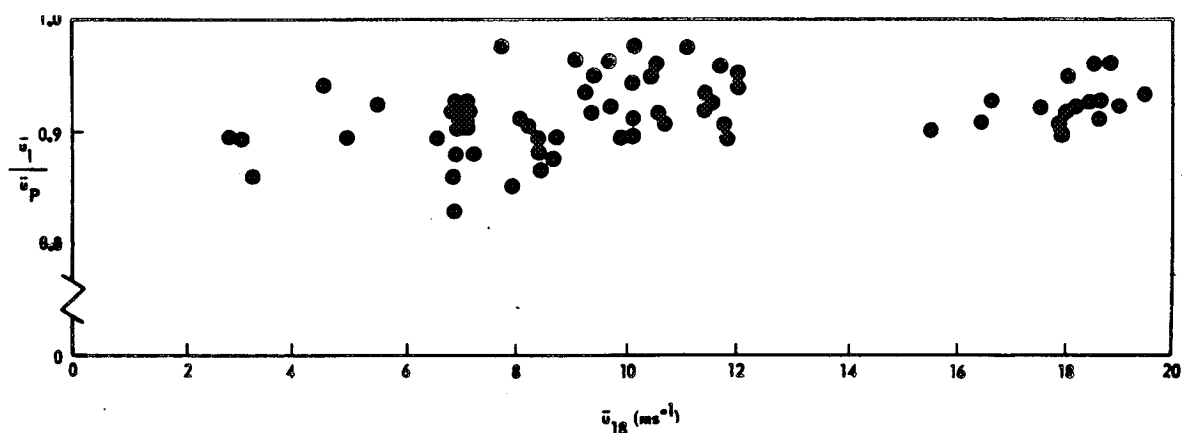


Figure 2.3.3 The ratio  $\bar{u}_I/\bar{u}_P$  as a function of the 18.3-m mean wind speed ( $\bar{u}_{18}$ ) for a 10-min sampling period.

### 2.3.5.4 Peak Wind Profile Shapes for Other Test Ranges and Sites

Detailed analyses of wind profile statistics are not available for other test ranges and sites. The exponent  $k$  in equation (2.1) is a function of wind speed, surface roughness, etc. For moderate surface roughness conditions, the extreme value of  $k$  is usually equal to 0.2 or less during high winds ( $\geq 15$  m/sec). For design and planning purposes for test ranges and sites other than Kennedy Space Center, it is recommended that the values of  $k$  given in Table 2.3.1 be used. These values of  $k$  are the only values used in this report for sites other than Kennedy Space Center and represent estimates for 99.87 percentile, or mean + 3 (0.13 percent risk), values for the peak wind speed profile shape.

TABLE 2.3.1 VALUES OF  $k$  TO USE FOR TEST RANGES  
OTHER THAN KENNEDY SPACE CENTER

$k$ Value	18.3-m Level Peak Wind Speed ( $\text{ms}^{-1}$ )
$k = 0.2$	$7 \leq u_{18.3} < 22$
$k = 0.14$	$22 \leq u_{18.3}$

### 2.3.5.5 Aerospace Vehicle Design Wind Profiles

The data presented in this section provide basic peak wind speed profile (envelope) information for test, free-standing, launch, and lift-off conditions to ensure satisfactory performance of the space vehicle. To establish vehicle response requirements, the peak design surface winds are assumed to act normal to the longitudinal axis of the vehicle on the launch pad and to be from the most critical direction.

#### 2.3.5.5.1 Design Wind Profiles for Kennedy Space Center

Peak wind profiles are characterized by two parameters, the peak wind speed at the 18.3-m level and the shape parameter  $k$ . Once these two quantities are defined, the peak wind speed profile envelope is completely specified. Accordingly, to construct a peak wind profile envelope for the Kennedy Space Center, in the context of launch vehicle loading and response calculations, two pieces of information are required. First, the risk of exceeding the design wind peak speed at the reference level for a given period must be specified. Once this quantity is given, the design peak wind speed at the reference level is automatically specified (Figure 2.3.4). Second, the risk associated with compromising the structural integrity of the vehicle, once the reference level design wind occurs, must be specified. This second quantity and the reference level peak wind speed will determine the value of  $k$  that is to be used in equation (2.1).

It is recommended that the  $\bar{k} + 3\sigma$  value of  $k$  be used for the design of space vehicles. Thus, if a space vehicle designed to withstand a particular value of peak wind speed at the 18.3-m reference level is exposed to that peak wind speed, the vehicle has at least a 99.865-percent chance of withstanding possible peak wind profile conditions.

Operational ground wind constraints for established vehicles should be determined for a reference level (above natural grade) near the top of the vehicle while on the launch pad. The profile may be calculated using equations (2.1) and (2.2) with a value of  $k = \bar{k} - 3\sigma$ . This will produce a peak wind profile envelope associated with an upper reference level ground wind constraint. Tables for these calculations and those associated with the design reference level are available for various wind speeds and  $k$  values applicable to Kennedy Space Center upon request to the Atmospheric Sciences Division, Space Sciences Laboratory, NASA, Marshall Space Flight Center, Alabama 35812.

Table 2.3.2 contains peak wind speed profiles for various envelope values of peak wind speed at the 10-m level for fixed values of risk for the worst monthly-hourly reference periods of the year for a 1-hour exposure. To construct these profiles, the 1-hour exposure period statistics for each hour in each month were constructed. This exercise yielded 288 distribution functions (12 months times 24 hours), which were enveloped to yield the largest or "worst" 10-m level peak wind speed associated with a given level of risk for all monthly-hourly reference periods. Thus, for example, according to Table 2.3.2 there is at most a 10-percent risk that the peak wind speed will exceed 13.9 m/sec (27.0 knots) during any particular hour in any

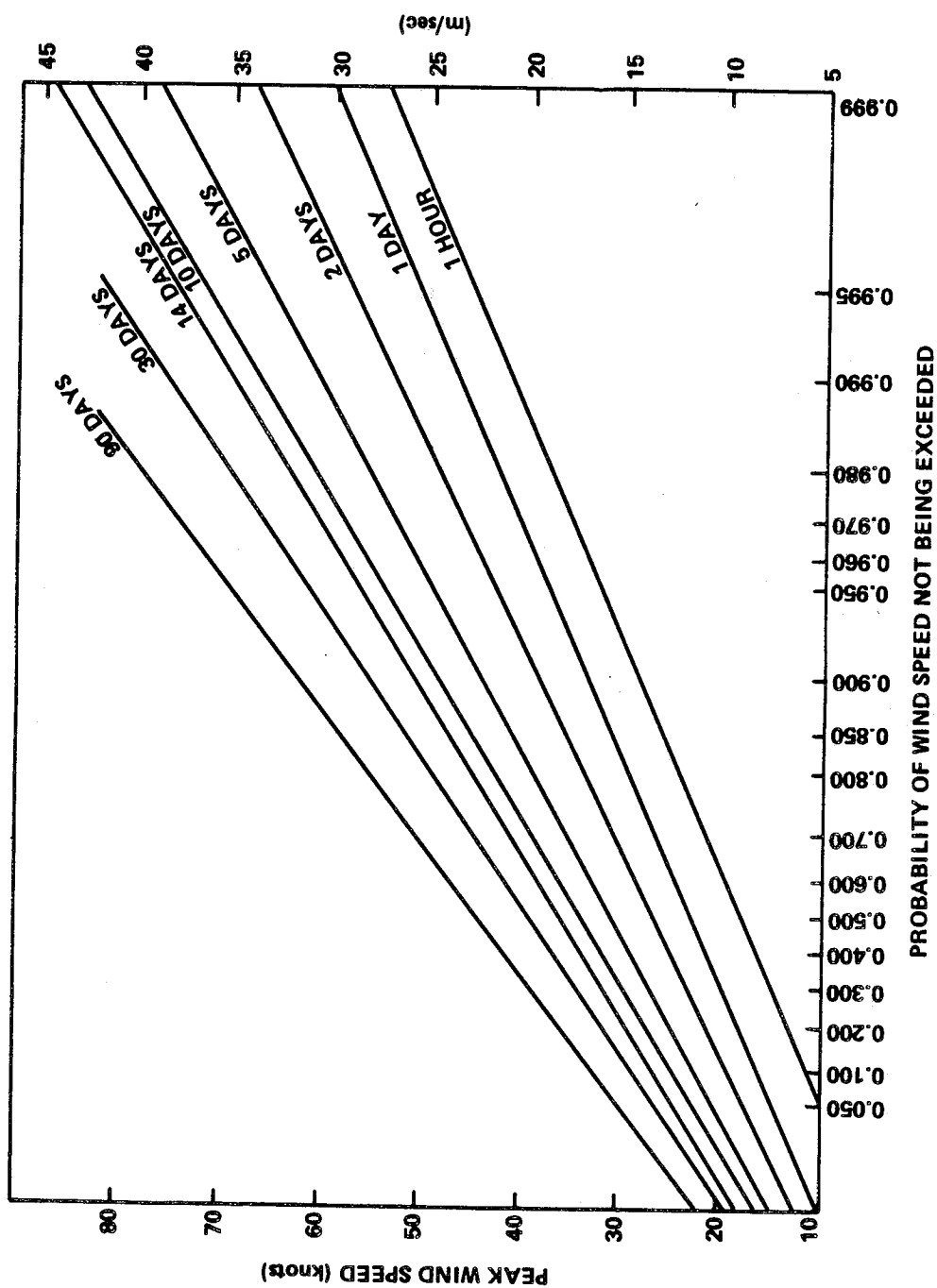


Figure 2.3.4 18.3-m reference level; Kennedy Space Center peak wind speed for windiest reference period versus probability for several exposure periods applicable to vehicle design criteria development.



particular month at the 10-m level; and if a peak wind speed equal to 13.9 m/sec (27.0 knots) should occur at the 10-m level, then there is only a 0.135-percent chance that the peak wind speed will exceed 24.1 m/sec (46.8 knots) at the 152.4-m level or the corresponding values given at the other heights.

Tables 2.3.3 through 2.3.5 contain peak wind profile envelopes for various values of peak wind speed at the 10-m level and fixed values of risk for various exposure periods. The 1-day exposure values of peak wind speed were obtained by constructing the daily peak wind statistics for each month and then enveloping these distributions to yield the worst 1-day exposure, 10-m level peak wind speed for a specified value of risk (daily-monthly reference period). The 30-day exposure envelope peak wind speeds were obtained by constructing the monthly peak wind statistics for each month and then constructing the envelope of the distributions (monthly-annual reference period). The 10-day exposure statistics were obtained by interpolating between the 1- and 30-day exposure period results. The envelopes of the 90-day exposure period statistics are the 90-day exposure statistics associated with the 12 trimonthly periods (January-February-March, February-March-April, March-April-May, and so forth) (90-day-annual reference period). Finally, the 365-day exposure period statistics were calculated with the annual peak wind sample (17 data points) to yield one distribution. Tables 2.3.3 through 2.3.5 contain the largest or "worst" 10-m level peak wind speed associated with a given level of risk for the stated exposure periods.

It is recommended that the data in Tables 2.3.2 through 2.3.5 be used as the basis for space vehicle design for Kennedy Space Center operations. Wind profile statistics for the design of permanent ground support equipment are discussed in subsection 2.3.10.

Mean wind profiles or steady-state wind profiles can be obtained from the peak wind profiles by dividing the peak wind by the appropriate gust factor (subsection 2.3.7). It is recommended that the 10-min gust factors be used for structural design purposes. Application of the 10-min gust factors to the peak wind profile corresponds to averaging the wind speed over a 10-min period. This averaging period appears to result in a stable mean value of the wind speed. Within the range of variation of the data, the 1-hour and 10-min gust factors are approximately equal for sufficiently high wind speed. This occurs because the spectrum of the horizontal wind speed near the ground is characterized by a broad energy gap centered at a frequency approximately equal to 0.000278 Hz (1 cycle/hr) and typically extends over the frequency domain  $0.000139 \text{ Hz (0.5 cycles/hr)} < \omega < 0.0014 \text{ Hz (5 cycles/hr)}$ . The Fourier spectral components associated with frequencies less than 0.000278 Hz (1 cycle/hr) corresponds to the meso- and synoptic-scale motions, while the remaining high-frequency spectral components correspond to mechanically and thermally produced turbulence. Thus, a statistically stable estimate of the mean or steady-state wind speed can be obtained by averaging over a period in the range from 10 min to an hour. Since this period is far longer than any natural period of structural vibration, it assures that effects caused by the mean wind properly represent steady-state, nontransient effects. The steady-state wind profiles, calculated with the 10-min gust factors, that correspond to those in Tables 2.3.2 through 2.3.5 are given in Tables 2.3.6 through 2.3.9.

#### 2.3.5.5.2 Design Ground Wind Profiles for Other Locations

Tables 2.3.10 through 2.3.17 contain recommended design ground wind profiles for several different risks of exceeding the 10-m level peak wind speed and 10-min mean wind speed for a 1-hour exposure period. These tables are based on the same philosophy as Table 2.3.2 and Table 2.3.6 for Kennedy Space Center. The locations for which data are provided include White Sands Missile Range, New Mexico; Edwards AFB, California; Vandenberg AFB, California; and National Space Technology Laboratory, Mississippi.

TABLE 2.3.2 PEAK WIND SPEED PROFILE ENVELOPES FOR VARIOUS VALUES OF RISK OF EXCEEDING THE 10-m LEVEL PEAK WIND SPEED FOR 1-hr EXPOSURE (hourly-monthly reference period) FOR KENNEDY SPACE CENTER<sup>1</sup>

Height		Risk (%)									
		20		10		5		1		0.1	
(m)	(ft)	knots	ms <sup>-1</sup>	knots	ms <sup>-1</sup>	knots	ms <sup>-1</sup>	knots	ms <sup>-1</sup>	knots	ms <sup>-1</sup>
10.0	33	22.9	11.8	27.0	13.9	30.8	15.8	39.5	20.3	51.9	26.7
18.3	60	26.3	13.5	30.5	15.7	34.4	17.7	43.4	22.3	56.0	28.8
30.5	100	29.5	15.2	33.8	17.4	37.9	19.5	47.0	24.2	59.8	30.8
61.0	200	34.5	17.8	38.9	20.0	43.0	22.1	52.3	26.9	65.4	33.6
91.4	300	37.8	19.5	42.2	21.7	46.4	23.9	55.7	28.7	68.9	35.4
121.9	400	40.4	20.8	44.7	23.0	48.9	25.2	58.3	30.0	71.5	36.8
152.4	500	42.5	21.9	46.8	24.1	51.0	26.2	60.3	31.0	73.6	37.8

TABLE 2.3.3 PEAK WIND SPEED PROFILE ENVELOPES FOR A 10-PERCENT RISK VALUE OF EXCEEDING THE 10-m LEVEL PEAK WIND SPEED FOR VARIOUS REFERENCE PERIODS OF EXPOSURE FOR KENNEDY SPACE CENTER<sup>1</sup>

Height		Exposure (days)									
		1		10		30		90		365	
(m)	(ft)	knots	ms <sup>-1</sup>	knots	ms <sup>-1</sup>	knots	ms <sup>-1</sup>	knots	ms <sup>-1</sup>	knots	ms <sup>-1</sup>
10.0	33	32.1	16.5	46.9	24.1	53.9	27.7	61.0	31.4	70.0	36.0
18.3	60	35.8	18.4	51.0	26.2	58.2	29.9	65.3	33.6	74.5	38.3
30.5	100	39.2	20.2	54.7	28.1	62.0	31.9	69.3	35.7	78.5	40.4
61.0	200	44.4	22.8	60.2	31.0	67.6	34.8	75.0	38.6	84.4	43.4
91.4	300	47.8	24.6	63.6	32.7	71.1	36.6	78.5	40.4	88.0	45.3
121.9	400	50.3	25.9	66.2	34.1	73.7	37.9	81.1	41.7	90.6	46.6
152.4	500	52.4	27.0	68.3	35.1	75.8	39.0	83.2	42.8	92.8	47.7

1. Recommended for design criteria development.

TABLE 2.3.4 PEAK WIND SPEED PROFILE ENVELOPES FOR A 5-PERCENT RISK VALUE OF EXCEEDING THE 10-m LEVEL PEAK WIND SPEED FOR VARIOUS REFERENCE PERIODS OF EXPOSURE FOR KENNEDY SPACE CENTER<sup>2</sup>

Height		Exposure (days)									
		1		10		30		90		365	
(m)	(ft)	knots	ms <sup>-1</sup>	knots	ms <sup>-1</sup>	knots	ms <sup>-1</sup>	knots	ms <sup>-1</sup>	knots	ms <sup>-1</sup>
10.0	33	36.1	18.5	52.3	26.9	60.1	30.9	67.9	34.9	77.7	40.0
18.3	60	39.8	20.5	56.5	29.1	64.4	33.1	72.4	37.3	82.4	42.4
30.5	100	43.3	22.3	60.3	31.0	68.3	35.1	76.4	39.3	86.5	44.5
61.0	200	48.6	25.0	65.9	33.9	74.0	38.1	82.2	42.3	92.5	47.6
91.4	300	52.0	26.8	69.4	35.7	77.6	40.0	85.8	44.2	96.1	49.4
121.9	400	54.5	28.0	72.0	37.0	80.2	41.3	88.5	45.5	98.8	50.8
152.4	500	56.6	29.1	74.1	38.1	82.3	42.3	90.6	46.6	101.0	52.0

TABLE 2.3.5 PEAK WIND SPEED PROFILE ENVELOPES FOR A 1-PERCENT RISK VALUE OF EXCEEDING THE 10-m LEVEL PEAK WIND SPEED FOR VARIOUS REFERENCE PERIODS OF EXPOSURE FOR KENNEDY SPACE CENTER<sup>2</sup>

Height		Exposure (days)									
		1		10		30		90		365	
(m)	(ft)	knots	ms <sup>-1</sup>	knots	ms <sup>-1</sup>	knots	ms <sup>-1</sup>	knots	ms <sup>-1</sup>	knots	ms <sup>-1</sup>
10.0	33	45.0	23.1	64.7	33.3	74.0	38.1	83.4	42.9	95.4	49.1
18.3	60	49.0	25.2	69.1	35.6	78.6	40.4	88.2	45.4	100.3	51.6
30.5	100	52.6	27.1	73.1	37.6	82.8	42.6	92.4	47.5	104.7	53.9
61.0	200	58.1	30.0	78.8	40.6	88.6	45.6	98.4	50.6	110.9	57.1
91.4	300	61.5	31.6	82.4	42.4	92.3	47.5	102.1	52.5	114.6	59.0
121.9	400	64.1	33.0	85.1	43.8	95.0	48.9	104.8	53.9	117.4	60.4
152.4	500	66.1	34.0	87.2	44.9	97.1	50.0	107.0	55.0	119.6	61.5

2. Recommended for design criteria development.

TABLE 2.3.6 10-min MEAN WIND SPEED PROFILE ENVELOPES FOR VARIOUS VALUES OF RISK OF EXCEEDING THE 10-m LEVEL MEAN WIND SPEED FOR A 1-hr EXPOSURE (hourly-monthly reference period) FOR KENNEDY SPACE CENTER

Height		Risk (%)									
		20		10		5		1		0.1	
(m)	(ft)	knots	ms <sup>-1</sup>	knots	ms <sup>-1</sup>	knots	ms <sup>-1</sup>	knots	ms <sup>-1</sup>	knots	ms <sup>-1</sup>
10.0	33	14.1	7.2	16.6	8.6	19.1	9.8	24.6	12.7	32.4	16.7
18.3	60	17.1	8.8	19.9	10.3	22.6	11.7	28.7	14.8	37.2	19.1
30.5	100	20.0	10.3	23.1	11.9	26.0	13.4	32.6	16.8	41.6	21.4
61.0	200	24.7	12.7	28.1	14.5	31.3	16.1	38.3	19.7	48.1	24.7
91.4	300	27.8	14.3	31.3	16.1	34.7	17.9	42.0	21.6	52.1	26.8
121.9	400	30.3	15.6	33.9	17.4	37.3	19.2	44.8	23.0	55.1	28.3
152.4	500	32.3	16.6	35.9	18.5	39.4	20.3	47.0	24.2	57.5	29.6

TABLE 2.3.7 10-min MEAN WIND SPEED PROFILE ENVELOPES FOR A 10-PERCENT RISK VALUE OF EXCEEDING THE 10-m LEVEL MEAN WIND SPEED FOR VARIOUS REFERENCE PERIODS OF EXPOSURE FOR KENNEDY SPACE CENTER

Height		Exposure (days)									
		1		10		30		90		365	
(m)	(ft)	knots	ms <sup>-1</sup>	knots	ms <sup>-1</sup>	knots	ms <sup>-1</sup>	knots	ms <sup>-1</sup>	knots	ms <sup>-1</sup>
10.0	33	20.0	10.3	29.3	15.1	33.7	17.3	38.1	19.6	43.8	22.5
18.3	60	23.6	12.1	33.8	17.4	38.7	19.9	43.3	22.3	49.5	25.5
30.5	100	27.1	13.9	38.0	19.5	43.1	22.2	48.2	24.8	54.6	28.1
61.0	200	32.4	16.7	44.2	22.7	49.6	25.5	55.1	28.3	62.1	31.9
91.4	300	35.8	18.4	48.1	24.7	53.8	27.7	59.4	30.6	66.6	34.3
121.9	400	38.5	19.8	51.0	26.2	56.8	29.2	62.6	32.2	69.9	36.0
152.4	500	40.6	20.9	53.3	27.4	59.2	30.5	65.1	33.5	72.6	37.3

TABLE 2.3.8 10-min MEAN WIND SPEED PROFILE ENVELOPES FOR A 5-PERCENT RISK OF EXCEEDING THE 10-m LEVEL MEAN WIND SPEED FOR VARIOUS REFERENCE PERIODS OF EXPOSURE FOR KENNEDY SPACE CENTER

Height		Exposure (days)									
		1		10		30		90		365	
(m)	(ft)	knots	ms <sup>-1</sup>	knots	ms <sup>-1</sup>	knots	ms <sup>-1</sup>	knots	ms <sup>-1</sup>	knots	ms <sup>-1</sup>
10.0	33	22.5	11.6	32.7	16.8	37.6	19.3	42.5	21.9	48.6	25.0
18.3	60	26.3	13.5	37.5	19.3	42.8	22.0	48.1	24.7	54.8	28.2
30.5	100	30.0	15.4	41.9	21.6	47.5	24.4	53.2	27.4	60.2	31.0
61.0	200	35.5	18.3	48.4	24.9	54.5	28.0	60.4	31.1	68.1	35.0
91.4	300	39.2	20.2	52.5	27.0	58.7	30.2	64.9	33.4	72.9	37.5
121.9	400	41.9	21.6	55.5	28.6	61.9	31.8	68.2	35.1	76.3	39.3
152.4	500	44.0	22.6	57.9	29.8	64.4	33.1	70.9	36.4	79.1	40.7

TABLE 2.3.9 10-min MEAN WIND SPEED PROFILE ENVELOPES FOR A 1-PERCENT RISK VALUE OF EXCEEDING THE 10-m LEVEL MEAN WIND SPEED FOR VARIOUS REFERENCE PERIODS OF EXPOSURE FOR KENNEDY SPACE CENTER

Height		Exposure (days)									
		1		10		30		90		365	
(m)	(ft)	knots	ms <sup>-1</sup>	knots	ms <sup>-1</sup>	knots	ms <sup>-1</sup>	knots	ms <sup>-1</sup>	knots	ms <sup>-1</sup>
10.0	33	28.1	14.5	40.9	21.0	46.3	23.8	52.2	26.9	59.7	30.7
18.3	60	32.5	16.7	46.5	23.9	52.2	26.9	58.6	30.1	66.7	34.3
30.5	100	36.6	18.8	51.4	26.4	57.6	29.6	64.3	33.1	72.9	37.5
61.0	200	42.6	21.9	58.6	30.1	65.2	33.5	72.5	37.3	81.6	42.0
91.4	300	47.2	24.3	63.0	32.4	69.9	36.0	77.4	39.8	86.9	44.7
121.9	400	49.4	25.4	66.3	34.1	73.4	37.8	81.0	41.7	90.7	46.7
152.4	500	51.7	26.6	68.9	35.4	76.1	39.1	83.8	43.1	93.7	48.2

TABLE 2.3.10 SURFACE PEAK WIND SPEED PROFILE ENVELOPES FOR VARIOUS VALUES OF RISK OF EXCEEDING THE 10-m LEVEL PEAK WIND SPEED FOR 1-hr EXPOSURE (hourly-monthly reference period) FOR NATIONAL SPACE TECHNOLOGY LABORATORY AREA

Height		Risk (%)									
		20		10		5		1		0.1	
(m)	(ft)	knots	ms <sup>-1</sup>	knots	ms <sup>-1</sup>	knots	ms <sup>-1</sup>	knots	ms <sup>-1</sup>	knots	ms <sup>-1</sup>
10.0	33	19.8	10.2	23.9	12.3	27.6	14.2	37.2	19.1	53.0	27.3
18.3	60	22.4	11.5	27.0	13.9	31.2	16.0	42.0	21.5	57.7	29.7
30.5	100	24.8	12.8	29.9	15.4	34.5	17.8	46.5	23.9	61.9	31.8
61.0	200	28.4	14.6	34.3	17.7	39.6	20.4	53.4	27.4	68.1	35.1
91.4	300	30.8	15.9	37.2	19.2	43.0	22.1	57.9	29.8	72.2	37.2
121.9	400	32.7	16.8	39.4	20.3	45.5	23.4	61.4	31.5	75.2	38.7
152.4	500	34.2	17.6	41.3	21.3	47.7	24.5	64.3	33.0	77.5	39.9

TABLE 2.3.11 SURFACE MEAN WIND SPEED PROFILE ENVELOPES FOR VARIOUS VALUES OF RISK OF EXCEEDING THE 10-m LEVEL 10-min MEAN WIND SPEED FOR 1-hr EXPOSURE (hourly-monthly reference period) FOR NATIONAL SPACE TECHNOLOGY LABORATORY AREA

Height		Risk (%)									
		20		10		5		1		0.1	
(m)	(ft)	knots	ms <sup>-1</sup>	knots	ms <sup>-1</sup>	knots	ms <sup>-1</sup>	knots	ms <sup>-1</sup>	knots	ms <sup>-1</sup>
10.0	33	14.1	7.3	17.1	8.8	19.7	10.1	26.6	13.7	37.9	19.5
18.3	60	16.0	8.2	19.3	9.9	22.3	11.4	30.0	15.4	41.2	21.2
30.5	100	17.7	9.1	21.4	11.0	24.7	12.7	33.2	17.1	44.2	22.8
61.0	200	20.3	10.5	24.5	12.6	28.3	14.6	38.2	19.6	48.6	25.0
91.4	300	22.0	11.3	26.6	13.7	30.7	15.8	41.4	21.3	51.6	26.6
121.9	400	23.3	12.0	28.2	14.5	32.5	16.7	43.8	22.5	53.7	27.7
152.4	500	24.4	12.6	29.5	15.2	34.1	17.5	45.9	23.6	55.4	28.5

TABLE 2.3.12 SURFACE PEAK WIND SPEED PROFILE ENVELOPES FOR VARIOUS VALUES OF RISK OF EXCEEDING THE 10-m LEVEL PEAK WIND SPEED FOR 1-hr EXPOSURE (hourly-monthly reference period) FOR VANDENBERG AFB, CALIFORNIA<sup>3</sup>

Height		Risk (%)									
		20		10		5		1		0.1	
(m)	(ft)	knots	ms <sup>-1</sup>	knots	ms <sup>-1</sup>	knots	ms <sup>-1</sup>	knots	ms <sup>-1</sup>	knots	ms <sup>-1</sup>
10.0	33	20.0	10.3	23.8	12.3	27.5	14.2	35.8	18.4	47.3	24.3
18.3	60	22.5	11.6	26.8	13.8	31.0	16.0	40.3	20.8	51.4	26.5
30.5	100	25.0	12.9	29.7	15.3	34.3	17.7	44.7	23.0	55.2	28.5
61.0	200	28.7	14.8	34.1	17.6	39.4	20.3	51.3	26.4	60.9	31.3
91.4	300	31.1	16.0	37.0	19.0	42.8	22.0	55.7	28.7	64.4	33.2
121.9	400	32.9	16.9	39.2	20.2	45.3	23.3	59.0	30.4	67.1	34.5
152.4	500	34.4	17.7	41.0	21.1	47.4	24.4	61.7	31.7	69.2	35.6

TABLE 2.3.13 SURFACE MEAN WIND SPEED PROFILE ENVELOPES FOR VARIOUS VALUES OF RISK OF EXCEEDING THE 10-m LEVEL 10-min MEAN WIND SPEED FOR 1-hr EXPOSURE (hourly-monthly reference period) FOR VANDENBERG AFB, CALIFORNIA<sup>3</sup>

Height		Risk (%)									
		20		10		5		1		0.1	
(m)	(ft)	knots	ms <sup>-1</sup>	knots	ms <sup>-1</sup>	knots	ms <sup>-1</sup>	knots	ms <sup>-1</sup>	knots	ms <sup>-1</sup>
10.0	33	14.3	7.4	17.0	8.9	19.6	10.1	25.6	13.1	33.8	17.4
18.3	60	16.1	8.3	19.2	9.9	22.1	11.4	28.8	14.8	36.7	18.9
30.5	100	17.8	9.2	21.2	10.9	24.5	12.6	31.9	16.4	39.5	20.3
61.0	200	20.5	10.5	24.4	12.6	28.1	14.5	36.7	18.9	43.5	22.4
91.4	300	22.2	11.4	26.4	13.6	30.5	15.7	39.8	20.5	46.0	23.7
121.9	400	23.5	12.1	28.0	14.4	32.3	16.7	42.1	21.7	47.9	24.7
152.4	500	24.6	12.7	29.3	15.1	33.8	17.4	44.0	22.7	49.4	25.5

3. Formerly Western Test Range.

TABLE 2.3.14 SURFACE PEAK WIND SPEED PROFILE ENVELOPES FOR VARIOUS VALUES OF RISK OF EXCEEDING THE 10-m LEVEL PEAK WIND SPEED FOR 1-hr EXPOSURE (hourly-monthly reference period) FOR WHITE SANDS MISSILE RANGE

Height		Risk (%)									
		20		10		5		1		0.1	
(m)	(ft)	knots	ms <sup>-1</sup>	knots	ms <sup>-1</sup>	knots	ms <sup>-1</sup>	knots	ms <sup>-1</sup>	knots	ms <sup>-1</sup>
10.0	33	15.3	7.9	20.9	10.7	24.7	12.7	34.3	17.7	52.1	26.8
18.3	60	17.3	8.9	23.6	12.1	27.9	14.3	38.7	20.0	56.7	29.2
30.5	100	19.1	9.9	26.1	13.4	30.9	15.9	42.9	22.1	60.9	31.3
61.0	200	22.0	11.3	30.0	15.4	35.5	18.2	49.3	25.4	66.9	34.4
91.4	300	23.8	12.3	32.6	16.7	38.5	19.8	53.4	27.6	71.0	36.5
121.9	400	25.2	13.0	34.5	17.7	40.8	21.0	56.6	29.2	73.9	38.0
152.4	500	26.4	13.7	36.1	18.5	42.7	22.0	59.3	30.6	76.2	39.2

TABLE 2.3.15 SURFACE MEAN WIND SPEED PROFILE ENVELOPES FOR VARIOUS VALUES OF RISK OF EXCEEDING THE 10-m LEVEL 10-min MEAN WIND SPEED FOR 1-hr EXPOSURE (hourly-monthly reference period) FOR WHITE SANDS MISSILE RANGE

Height		Risk (%)									
		20		10		5		1		0.1	
(m)	(ft)	knots	ms <sup>-1</sup>	knots	ms <sup>-1</sup>	knots	ms <sup>-1</sup>	knots	ms <sup>-1</sup>	knots	ms <sup>-1</sup>
10.0	33	10.9	5.6	14.9	7.7	17.6	9.1	24.5	12.6	37.2	19.2
18.3	60	12.3	6.4	16.9	8.6	19.9	10.2	27.7	14.3	40.5	20.8
30.5	100	13.7	7.1	18.7	9.6	22.1	11.3	30.7	15.8	43.4	22.4
61.0	200	15.7	8.1	21.4	11.0	25.3	13.0	35.2	18.2	47.8	24.6
91.4	300	17.0	8.8	23.3	11.9	27.5	14.1	38.2	19.7	50.7	26.1
121.9	400	18.0	9.3	24.6	12.6	29.1	15.0	40.4	20.9	52.8	27.1
152.4	500	18.9	9.8	25.8	13.2	30.5	15.7	42.3	21.9	54.4	28.0



TABLE 2.3.16 SURFACE PEAK WIND SPEED PROFILE ENVELOPES FOR VARIOUS VALUES OF RISK OF EXCEEDING THE 10-m LEVEL PEAK WIND SPEED FOR 1-hr EXPOSURE (hourly-monthly reference period) FOR EDWARDS AIR FORCE BASE

Height		Risk (%)									
		20		10		5		1		0.1	
(m)	(ft)	knots	ms <sup>-1</sup>	knots	ms <sup>-1</sup>	knots	ms <sup>-1</sup>	knots	ms <sup>-1</sup>	knots	ms <sup>-1</sup>
10.0	33	24.4	12.6	28.3	14.6	31.5	16.2	38.4	19.8	47.0	24.2
18.3	60	27.6	14.2	32.0	16.5	35.6	18.3	43.4	22.4	51.1	26.3
30.5	100	30.5	15.8	35.4	18.3	39.4	20.3	48.0	24.8	54.9	28.3
61.0	200	35.0	18.1	40.6	21.0	45.2	23.3	55.1	28.4	60.3	31.1
91.4	300	38.0	19.6	44.1	22.7	49.1	25.2	59.8	30.8	64.0	33.0
121.9	400	40.3	20.8	46.7	24.1	52.0	26.7	63.4	32.7	66.6	34.3
152.4	500	42.2	21.8	48.9	25.2	54.4	28.0	66.4	34.2	68.8	35.4

TABLE 2.3.17 SURFACE MEAN WIND SPEED PROFILE ENVELOPES FOR VARIOUS VALUES OF RISK OF EXCEEDING THE 10-m LEVEL 10-min MEAN WIND SPEED FOR 1-hr EXPOSURE (hourly-monthly reference period) FOR EDWARDS AIR FORCE BASE

Height		Risk (%)									
		20		10		5		1		0.1	
(m)	(ft)	knots	ms <sup>-1</sup>	knots	ms <sup>-1</sup>	knots	ms <sup>-1</sup>	knots	ms <sup>-1</sup>	knots	ms <sup>-1</sup>
10.0	33	17.4	9.0	20.2	10.4	22.5	11.6	27.4	14.1	33.6	17.3
18.3	60	19.7	10.2	22.8	11.8	25.4	13.1	31.0	16.0	36.5	18.8
30.5	100	21.8	11.3	25.3	13.0	28.1	14.5	34.4	17.7	39.2	20.2
61.0	200	25.0	12.9	29.0	15.0	32.3	16.6	39.4	20.3	43.1	22.2
91.4	300	27.1	14.0	31.5	16.2	35.0	18.0	42.7	22.0	45.7	23.5
121.9	400	28.8	14.9	33.4	17.2	37.1	19.1	45.3	23.3	47.6	24.5
152.4	500	30.1	15.6	34.9	18.0	38.9	20.0	47.4	24.4	49.1	25.3

The peak/mean wind profiles were constructed with a 1.4 gust factor and mean  $+3\sigma$  value of  $k$ , as given in subsection 2.3.5.4. Some additional general ground wind data are given in References 2.3 and 2.4 for several other locations. See Section V for a discussion of low-level profiles over water used for Space Shuttle Solid Rocket Booster (SRB) water entry studies.

#### 2.3.5.5.3 Frequency of Calm Winds

Generally, design criteria wind problems are concerned with high wind speeds, but a condition of calm or very low speeds may also be important. For example, with no wind to disperse venting vapors such as LOX, a poor visibility situation could develop around the vehicle. Calm wind conditions can also have significant implications relative to the atmospheric diffusion of vehicle exhaust clouds. In addition, calm wind in conjunction with high solar heating can result in significantly high vehicle compartment temperatures. Table 2.3.18 shows the frequency of calm winds at the 10-m level for Kennedy Space Center as a function of time of day and month. The maximum percentage of calms appears in the summer and during the early morning hours, with the minimum percentage appearing throughout the year during the afternoon. Similar tables for other locations are available upon request.

#### 2.3.6 Spectral Ground Wind Turbulence Model

Under most conditions ground winds are fully developed turbulent flows. This is particularly true when the wind speed is greater than a few meters per second or the atmosphere is unstable, or when both conditions exist. During nighttime conditions when the wind speed is typically low and the stratification is stable, the intensity of turbulence is small if not nil. Spectral methods are a particularly useful way of representing the turbulent portion of the ground wind environment for launch vehicle design purposes, as well as for use in diffusion calculations of toxic fuels and atmospheric pollutants.

##### 2.3.6.1 Introduction

At a fixed point in the atmospheric boundary layer, the instantaneous wind vector fluctuates in time about the horizontal steady-state wind vector. The vector departure of the horizontal component of the instantaneous wind vector from the quasi-steady wind vector is the horizontal vector component of turbulence. This vector departure can be represented by two components, the longitudinal and the lateral components of turbulence which are parallel and perpendicular to the steady-state wind vector in the horizontal plane (Figure 2.3.5). The model contained herein is a spectral representation of the characteristics of the longitudinal and lateral components of turbulence. The model analytically defines the spectra of these components of turbulence for the first 200 m of the boundary layer. In addition, it defines the longitudinal and lateral cospectra, quadrature spectra, and the corresponding coherence functions associated with any pair of levels in the boundary layer. Details concerning the model can be found in References 2.5, 2.6, and 2.7.

##### 2.3.6.2 Turbulence Spectra

The longitudinal and lateral spectra of turbulence at frequency  $\omega$  and height  $z$  can be represented by a dimensionless function of the form

TABLE 2.3.18 FREQUENCY (%) OF CALM WIND AT THE 10-m LEVEL, KENNEDY SPACE CENTER

Hour EST	Month												Annual
	Jan	Feb	Mar	Apr	May	June	July	Aug	Sept	Oct	Nov	Dec	
00	4.8	4.0	3.6	1.3	7.3	9.2	11.7	13.7	6.3	6.9	6.3	6.0	6.8
01	2.8	1.3	2.4	1.7	8.9	8.3	10.9	14.1	7.1	4.8	6.3	6.5	6.3
02	4.8	2.2	3.6	2.9	7.7	10.0	11.7	13.7	10.4	7.3	5.4	4.0	7.0
03	5.2	3.1	2.0	3.8	8.5	12.1	11.3	17.3	12.1	5.2	2.9	3.2	7.3
04	2.8	4.4	2.4	3.8	5.2	13.8	14.5	13.7	10.8	5.2	4.6	2.8	7.0
05	4.4	4.0	3.2	2.9	9.7	16.3	15.3	18.5	13.3	3.6	4.6	4.4	8.4
06	4.4	4.0	4.4	2.9	8.9	16.3	19.8	19.0	13.3	3.2	5.0	5.2	8.9
07	3.6	4.4	4.8	6.3	10.5	16.7	18.1	19.4	15.8	4.4	5.4	5.6	9.6
08	3.6	6.6	6.5	2.9	2.4	5.4	6.0	6.9	4.6	4.0	8.8	4.4	5.2
09	3.6	1.8	2.0	2.1	2.8	3.8	4.8	1.6	4.2	0.8	4.6	5.6	3.1
10	0.4	1.8	1.6	1.7	0.4	3.8	4.0	2.8	2.1	*	1.3	2.4	1.8
11	0.4	1.3	1.2	1.7	0.8	1.3	2.4	0.8	2.9	0.8	1.7	0.8	1.3
12	1.6	0.4	*	*	*	0.8	0.8	0.4	1.3	0.4	2.1	1.2	0.8
13	2.0	0.4	*	*	0.4	1.3	0.4	1.6	0.8	0.4	1.7	0.4	0.8
14	0.8	4.0	0.8	0.4	0.4	0.8	1.2	1.6	1.3	0.8	*	0.4	0.7
15	0.4	1.3	*	*	*	0.8	0.4	1.6	2.5	0.4	0.4	0.4	0.7
16	0.4	0.4	0.4	*	0.8	0.4	0.8	0.4	1.3	0.8	*	0.8	0.5
17	1.6	0.4	*	0.4	0.4	2.1	0.8	3.2	2.1	1.6	1.7	2.0	1.4
18	4.0	1.8	0.8	0.4	1.6	2.5	3.2	4.0	2.9	1.2	5.0	7.7	2.9
19	2.8	3.5	2.0	*	1.6	5.0	2.8	5.2	4.6	1.2	7.1	6.5	3.5
20	4.4	3.5	2.8	1.7	3.2	6.7	5.6	8.5	7.5	1.6	6.3	6.0	4.8
21	5.2	4.0	3.2	1.3	4.8	7.5	10.5	8.9	8.3	4.4	5.0	6.0	5.8
22	3.6	2.2	2.4	1.7	6.0	7.5	7.7	12.9	7.9	4.8	6.3	5.2	5.7
23	5.6	3.5	4.8	0.8	6.5	8.3	10.5	15.3	10.0	5.6	4.6	5.2	6.8
All Hours	3.1	2.5	2.3	1.7	4.1	6.7	7.3	8.6	6.4	2.9	4.0	3.9	4.5

\* values &lt; 0.4 percent

2.26

$$\frac{\omega S(\omega)}{\beta u_*^2} = \frac{c_1 f/f_m}{\left[1 + 1.5(f/f_m)^{c_2}\right]^{(5/3)c_2}}, \quad (2.3)$$

where

$$f = \frac{\omega z}{u(z)} \quad (2.4)$$

$$f_m = c_3 \left(\frac{z}{z_r}\right)^{c_4} \quad (2.5)$$

$$\beta = \left(\frac{z}{z_r}\right)^{c_5} \quad (2.6)$$

$$u_* = c_6 \bar{u}(z_r) \quad (2.7)$$

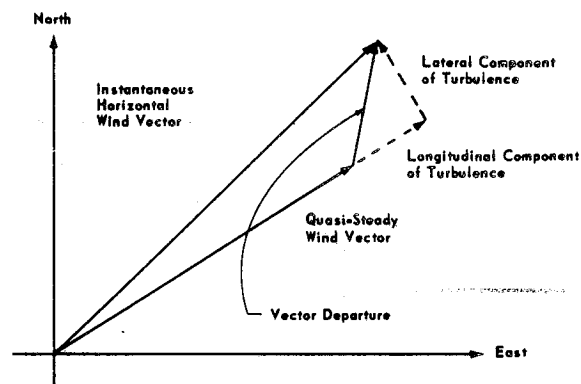


Figure 2.3.5 The relationship between the quasi-steady and the horizontal instantaneous wind vectors and the longitudinal and lateral components of turbulence.

In these equations  $z_r$  is a reference height equal to 18.3 m (60 ft);  $\bar{u}(z)$  is the quasi-steady wind speed at height  $z$ ; and the quantities  $c_i$  ( $i = 1, 2, 3, 4, 5$ ) are dimensionless constants that depend upon the site and the stability. The frequency  $\omega$  is defined with respect to a structure or vehicle at rest relative to the Earth. The reader is referred to Sections 2.4.13 and 2.4.14 for the definition of turbulence spectral inputs for application to the take-off and landing of conventional aeronautical systems and the landing of the Shuttle Orbiter vehicle. The spectrum  $S(\omega)$  is defined so that integration over the domain  $0 \leq \omega \leq \infty$  yields the variance of the turbulence. Engineering values of  $c_i$  are given in Table 2.3.19 for the longitudinal spectrum and in Table 2.3.20 for the lateral spectrum. The constant  $c_6$  can be estimated with the equation

$$c_6 = \frac{0.4}{\ln\left(\frac{z_r}{z_0}\right) - \Psi}, \quad (2.8)$$

where  $z_0$  is the surface roughness length of the site and  $\Psi$  is a parameter that depends upon the stability. If  $z_0$  is not available for a particular site, then an estimate of  $z_0$  can be obtained by taking 10 percent of the typical height of the surface obstructions (grass, shrubs, trees, rocks, etc.) over a fetch from the site with length equal to approximately 1500 m. The parameter  $\Psi$  vanishes for strong wind conditions and is of order unity for light wind unstable daytime conditions at the Kennedy Space Center. Typical values of  $z_0$  for various surfaces are given in Table 2.3.21.

The function given by equation (2.3) is depicted in Figures 2.3.6 and 2.3.7. Upon prescribing the steady-state wind profile  $u(z)$  and the site ( $z_0$ ), the longitudinal and lateral spectra are completely specified functions of height  $z$  and frequency  $\omega$ . A discussion of the units of the various parameters mentioned previously is given in subsection 2.3.6.4.

TABLE 2.3.19 DIMENSIONLESS CONSTANTS FOR THE LONGITUDINAL SPECTRUM OF TURBULENCE FOR KENNEDY SPACE CENTER

Condition	$c_1$	$c_2$	$c_3$	$c_4$	$c_5$
Light Wind Daytime Conditions	2.905	1.235	0.04	0.87	-0.14
Strong Winds	6.198	0.845	0.03	1.00	-0.63

TABLE 2.3.20 DIMENSIONLESS CONSTANTS FOR THE LATERAL SPECTRUM OF TURBULENCE FOR KENNEDY SPACE CENTER

Condition	$c_1$	$c_2$	$c_3$	$c_4$	$c_5$
Light Wind Daytime Conditions	4.599	1.144	0.033	0.72	-0.04
Strong Winds	3.954	0.781	0.1	0.58	-0.35

TABLE 2.3.21 TYPICAL VALUES OF SURFACE ROUGHNESS LENGTH ( $z_0$ ) FOR VARIOUS TYPES OF SURFACES

Type of Surface	$z_0$ (m)	$z_0$ (ft)
Mud flats, ice	$10^{-5}$ - $3 \cdot 10^{-5}$	$3 \cdot 10^{-5}$ - $10^{-4}$
Smooth sea	$2 \cdot 10^{-4}$ - $3 \cdot 10^{-4}$	$7 \cdot 10^{-4}$ - $10^{-3}$
Sand	$10^{-4}$ - $10^{-3}$	$3 \cdot 10^{-4}$ - $3 \cdot 10^{-3}$
Snow surface	$10^{-3}$ - $6 \cdot 10^{-3}$	$3 \cdot 10^{-4}$ - $2 \cdot 10^{-2}$
Mown grass ( $\sim 0.01$ m)	$10^{-3}$ - $10^{-2}$	$3 \cdot 10^{-3}$ - $3 \cdot 10^{-2}$
Low grass, steppe	$10^{-2}$ - $4 \cdot 10^{-2}$	$3 \cdot 10^{-2}$ - $10^{-1}$
Fallow field	$2 \cdot 10^{-2}$ - $3 \cdot 10^{-2}$	$6 \cdot 10^{-2}$ - $10^{-1}$
High grass	$4 \cdot 10^{-2}$ - $10^{-1}$	$10^{-1}$ - $3 \cdot 10^{-1}$
Palmetto	$10^{-1}$ - $3 \cdot 10^{-1}$	$3 \cdot 10^{-1}$ - 1
Suburbia	1 - 2	3 - 6
City	1 - 4	3 - 13

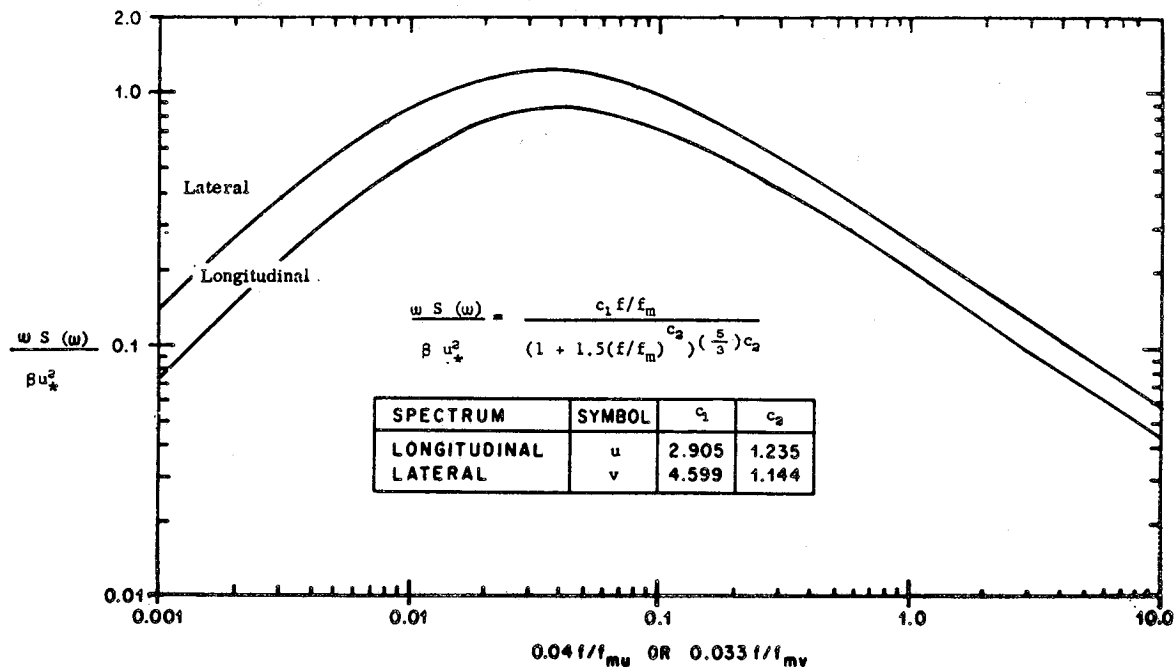


Figure 2.3.6  $\omega S(\omega)/\beta u_*^2$  versus  $0.04f/f_m$  (longitudinal) and  $0.033f/f_m$  (lateral) for light wind daytime conditions.

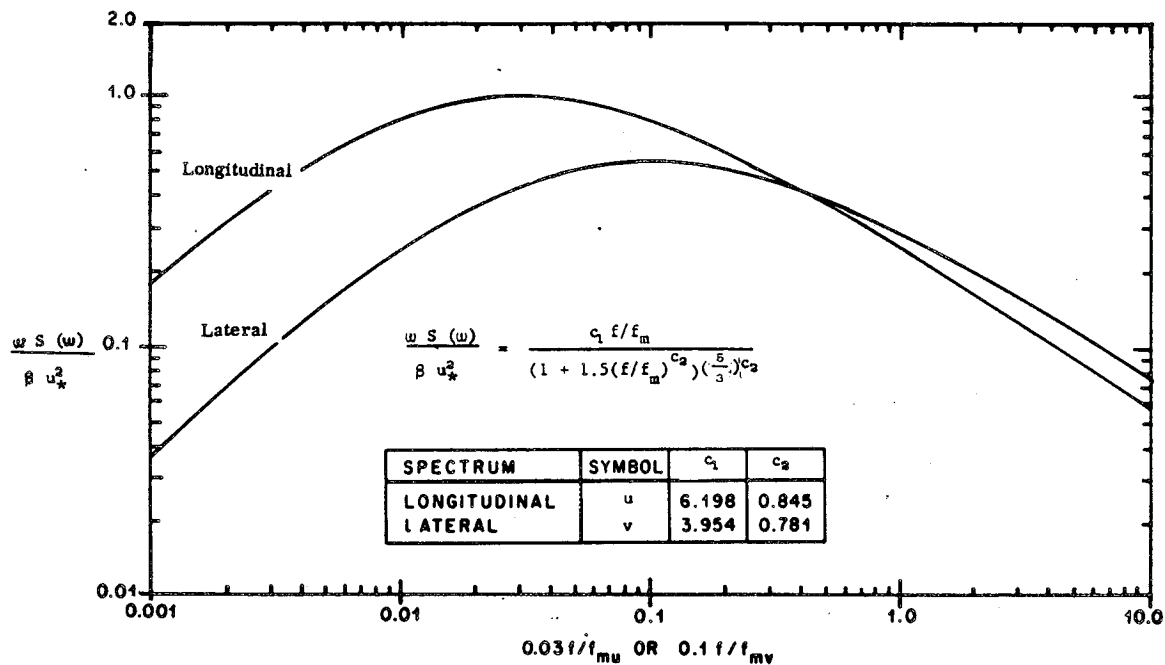


Figure 2.3.7  $\omega S(\omega)/\beta u_*^2$  versus  $0.03f/f_m$  (longitudinal) and  $0.1f/f_m$  (lateral) for strong wind conditions.

### 2.3.6.3 The Cospectrum and Quadrature Spectrum

The cospectrum and the quadrature spectrum associated with either the longitudinal or lateral components of turbulence levels  $z_1$  and  $z_2$  can be represented by the following:

$$C(\omega, z_1, z_2) = \sqrt{S_1 S_2} \exp \left( -0.3465 \frac{\Delta f}{\Delta f_{0.5}} \right) \cos(2\pi\gamma\Delta f) \quad (2.9)$$

$$Q(\omega, z_1, z_2) = \sqrt{S_1 S_2} \exp \left( -0.3465 \frac{\Delta f}{\Delta f_{0.5}} \right) \sin(2\pi\gamma\Delta f) \quad (2.10)$$

where

$$\Delta f = \frac{\omega z_2}{\bar{u}(z_2)} - \frac{\omega z_1}{\bar{u}(z_1)} \quad (2.11)$$

The quantities  $S_1$  and  $S_2$  are the longitudinal or lateral spectra at levels  $z_1$  and  $z_2$ , respectively, and  $\bar{u}(z_1)$  and  $\bar{u}(z_2)$  are the steady-state wind speeds at levels  $z_1$  and  $z_2$ . The quantity  $\Delta f_{0.5}$  is a nondimensional function of stability, and values of this parameter for the Eastern Test Range are given in Table 2.3.22. The nondimensional quantity  $\gamma$  should depend upon height and stability. However, it has only been possible to detect a dependence on height at Kennedy Space Center. Based upon analysis of turbulence data measured at the NASA 150-Meter Ground Winds Tower Facility at the Kennedy Space Center, the values of  $\gamma$  in Table 2.3.23 are suggested for the Eastern Test Range. The quantity  $\Delta f_{0.5}$  can be interpreted by constructing the coherence function, which is defined to be

$$\text{coh}(\omega, z_1, z_2) = \frac{C^2 + Q^2}{S_1 S_2} \quad (2.12)$$

TABLE 2.3.22 VALUES OF  $\Delta f_{0.5}$  FOR KENNEDY SPACE CENTER

Turbulence Component	Light Wind Daytime Conditions	Strong Winds
Longitudinal	0.04	0.036
Lateral	0.06	0.045

TABLE 2.3.23 VALUES OF  $\gamma$  FOR KENNEDY SPACE CENTER

Turbulence Component	$(z_1 + z_2)/2 \leq 100$ m	$(z_1 + z_2)/2 > 100$ m
Longitudinal	0.7	0.3
Lateral	1.4	0.5

Substituting equations (2.9) and (2.10) into equation (2.12) yields

$$\text{coh}(\omega, z_1, z_2) = \exp \left( -0.693 \frac{\Delta f}{\Delta f_{0.5}} \right) \quad (2.13)$$

It is clear from this relationship that  $\Delta f_{0.5}$  is that value of  $\Delta f$  for which the coherence (coh) is equal to 0.5.

#### 2.3.6.4 Units

The spectral model of turbulence presented in subsections 2.3.6.2 and 2.3.6.3 is a dimensionless model. Accordingly, the user is free to select the system of units he desires, except that  $\omega$  must have the units of cycles per unit time. Table 2.3.24 gives the appropriate metric and U. S. customary units for the various quantities in the model.

TABLE 2.3.24 METRIC AND U. S. CUSTOMARY UNITS OF VARIOUS QUANTITIES IN THE TURBULENCE MODEL

Quantity	Metric Units	U. S. Customary Units
$\omega$	Hz	Hz
$S(\omega), Q(\omega), C(\omega)$	$\text{m}^2 \text{s}^{-2}/\text{Hz}$	$\text{ft}^2 \text{s}^{-2}/\text{Hz}$
$f, f_m, \Delta f, \Delta f_{0.5}$	Dimensionless	Dimensionless
$z, z_r, z_0$	m	ft
$u, u_*$	$\text{ms}^{-1}$	$\text{ft s}^{-1}$
$\beta$	Dimensionless	Dimensionless
Coh	Dimensionless	Dimensionless
$\gamma$	Dimensionless	Dimensionless
$\Psi$	Dimensionless	Dimensionless



### 2.3.7 Ground Wind Gust Factors

The gust factor  $G$  is defined to be

$$G = \frac{u}{\bar{u}} \quad (2.14)$$

where

$u$  = maximum wind speed at height  $z$  within an averaging period of length  $\tau$  in time

$\bar{u}$  = mean wind speed associated with the averaging period  $\tau$ , given by

$$\bar{u} = \frac{1}{\tau} \int_0^{\tau} u_i(t) dt \quad (2.15)$$

$u_i(t)$  = instantaneous wind speed at time  $t$

$t$  = time reckoned from the beginning of the averaging period.

If  $\tau = 0$ , then  $\bar{u} = u$  according to equation (2.15), and it follows from equation (2.14) that  $G = 1.0$ . As  $\tau$  increases,  $\bar{u}$  departs from  $u$ , and  $\bar{u} \leq u$  and  $G > 1.0$ . Also, as  $\tau$  increases, the probability of finding a maximum wind of a given magnitude increases. In other words, the maximum wind speed increases as  $\tau$  increases. In the case of  $\bar{u} \rightarrow 0$  and  $u \geq 0$  ( $\bar{u} = 0$  might correspond to windless free convection),  $G \rightarrow \infty$ . As  $\bar{u}$  or  $u$  increases,  $G$  tends to decrease for fixed  $\tau > 0$ ; while for very high wind speeds,  $G$  tends to approach a constant value for given values of  $z$  and  $\tau$ . Finally, as  $z$  increases,  $G$  decreases. Thus, the gust factor is a function of the averaging time  $\tau$  over which the mean wind speed is calculated, the height  $z$ , and the wind speed (mean or maximum).

#### 2.3.7.1 Gust Factor as a Function of Peak Wind Speed ( $u_{18.3}$ ) at Reference Height for Kennedy Space Center

Investigations (Ref. 2.8) of gust factor data have revealed that the vertical variation of the gust factor can be described with the following relationship:

$$G = 1 + \frac{1}{g_0} \left( \frac{18.3}{z} \right)^p, \quad (2.16)$$

where  $z$  is the height in meters above natural grade. The parameter  $p$ , a function of the 18.3-m peak wind speed in meters per second, is given by

$$p = 0.283 - 0.435 e^{-0.2 u_{18.3}} \quad (2.17)$$

2.32

The parameter  $g_0$ , depends on the averaging time and the 18.3-m peak wind speed and is given by

$$g_0 = 0.085 \left( \ln \frac{\tau}{10} \right)^2 - 0.329 \left( \ln \frac{\tau}{10} \right) + 1.98 - 1.887 e^{-0.2 u_{18.3}}, \quad (2.18)$$

where  $\tau$  is given in minutes and,  $u_{18.3}$  in meters per second.

These relationships are valid for  $u_{18.3} \geq 4$  m/sec and  $\tau \leq 10$  min. In the interval  $10 \text{ min} \leq \tau \leq 60$  min,  $G$  is a slowly increasing monotonic function of  $\tau$ , and for all engineering purposes the 10-min gust factor ( $\tau = 10$  min) can be used as estimates of the gust factors associated with averaging times greater than 10 min and less than 60 min ( $10 \text{ min} \leq \tau \leq 60$  min).

The dependence of the gust factor upon the averaging time and the peak wind speed is shown in Figure 2.3.8. Figure 2.3.9 illustrates the dependence of the 10-min gust factors upon the peak wind speed and height.

The calculated mean gust factors for 10 min for values of  $u_{18.3}$  in the interval  $4.63 \text{ m/sec} \leq u_{18.3} \leq \infty$  are presented in Table 2.3.25 in both the U. S. Customary and Metric units for  $u_{18.3}$  and  $z$ . As an example, the gust factor profile for  $\tau = 10$  min and  $u_{18.3} = 9.27$  m/sec (18 knots) is given in Table 2.3.26.

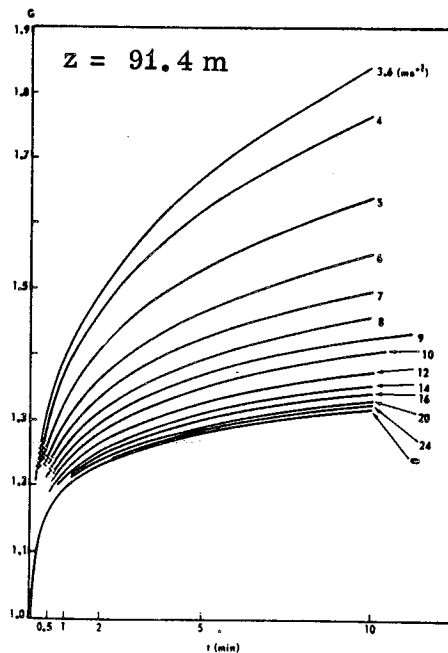


Figure 2.3.8 Gust factor as a function of time for various values of  $u_{18.3}$  in the interval.

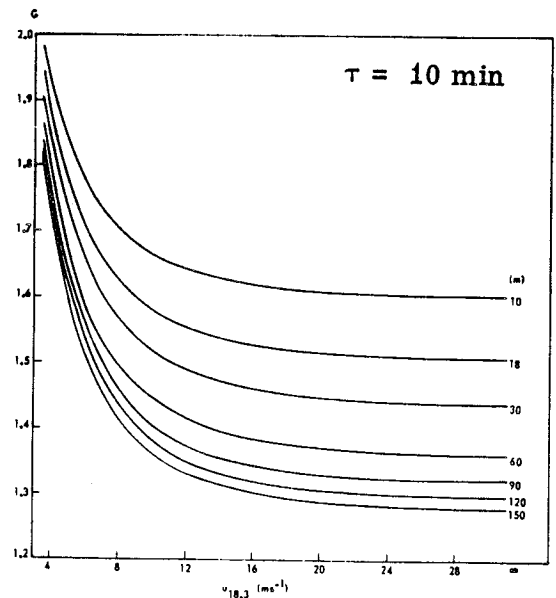


Figure 2.3.9 Gust factor as a function of peak wind ( $u$ ) for various heights.

Since the basic wind statistics are given in terms of hourly peak winds, use the  $\tau = 10$  min gust factors to convert the peak winds to mean winds by dividing by  $G$ . All gust factors in these sections are expected values for any particular set of values for  $u$ ,  $\tau$ , and  $z$ .

TABLE 2.3.25 10-min GUST FACTORS FOR KENNEDY SPACE CENTER

60-ft (18.3-m) peak wind kts (ms <sup>-1</sup> )	Height Above Natural Grade in Feet (meters)						
	33 (10.0)	60 (18.3)	100 (30.5)	200 (61.0)	300 (91.4)	400 (121.9)	500 (152.4)
9.0 (4.63)	1.868	1.812	1.767	1.710	1.679	1.658	1.642
10.0 (5.15)	1.828	1.766	1.718	1.657	1.624	1.602	1.585
11.0 (5.66)	1.795	1.729	1.678	1.614	1.580	1.556	1.539
12.0 (6.18)	1.768	1.699	1.645	1.579	1.544	1.520	1.502
13.0 (6.69)	1.746	1.674	1.618	1.550	1.514	1.489	1.471
14.0 (7.21)	1.727	1.652	1.595	1.525	1.488	1.464	1.446
15.0 (7.72)	1.712	1.634	1.576	1.505	1.467	1.442	1.424
16.0 (8.24)	1.698	1.619	1.559	1.487	1.449	1.424	1.406
17.0 (8.75)	1.686	1.606	1.545	1.472	1.434	1.409	1.390
18.0 (9.27)	1.676	1.594	1.532	1.459	1.421	1.395	1.377
19.0 (9.78)	1.668	1.584	1.522	1.447	1.409	1.384	1.365
20.0 (10.30)	1.660	1.575	1.512	1.437	1.399	1.374	1.355
25.0 (12.87)	1.634	1.545	1.480	1.403	1.365	1.339	1.321
30.0 (15.44)	1.619	1.528	1.462	1.385	1.346	1.321	1.302
$\infty$ ( $\infty$ )	1.599	1.505	1.437	1.359	1.320	1.295	1.277

TABLE 2.3.26 GUST FACTOR PROFILE FOR  $\tau = 10$  min  
AND  $u_{18.3} = 9.27$  m/sec (18 knots)

Height		Gust Factor (G)
(ft)	(m)	
33	10.0	1.676
60	18.3	1.594
100	30.5	1.532
200	61.0	1.459
300	91.4	1.421
400	121.9	1.395
500	152.4	1.377

### 2.3.7.2 Gust Factors for Other Locations

For design purposes, the gust factor value of 1.4 will be used over all altitudes of the ground wind profile at other test ranges. This gust factor should correspond to approximately a 10-min averaging period.

### 2.3.8 Ground Wind Shear

Wind shear near the surface, for design purposes, is a shear that acts upon a space vehicle, free-standing on the pad, or at time of liftoff. For overturning moment calculations the wind shear shall be computed by first subtracting the 10-min mean wind speed at the height corresponding to the base of the vehicle from the peak wind speed at the height corresponding to the top of the vehicle (see Section 2.3.5.5 for mean and peak wind profiles) and then dividing the difference by the distance between the two profiles. The reader should consult References 2.9 through 2.17 for a detailed discussion of the statistical properties of wind shear near the ground for engineering applications.

### 2.3.9 Ground Wind Direction Characteristics

Figure 2.3.1 (Section 2.3.5) shows a time trace of wind direction (section of a wind direction recording chart). This wind direction trace may be visualized as being composed of a mean wind direction plus fluctuations about the mean. An accurate measure of ambient wind direction near the ground is difficult to

obtain sometimes because of the interference of the structure that supports the instrumentation and other obstacles in the vicinity of the measurement location (Ref. 2.18). This is particularly true for launch pads; therefore, care must be exercised in locating wind sensors in order to obtain representative measurements of wind direction.

General information such as that which follows is available and may be used to specify conditions for particular studies. For instance, the variation of wind direction as a function of mean wind speed and height from analysis of NASA's 150-Meter Ground Winds Tower Facility data at Kennedy Space Center is discussed in Reference 2.2. A graph is shown in Reference 2.2 that gives values of the standard deviation of the wind direction  $\sigma_\theta$  as a function of height for a sampling time of approximately 5 min.

### 2.3.10 Design Winds for Facilities and Ground Support Equipment

#### 2.3.10.1 Introduction

In this section, the important relationships between desired lifetime  $N$ , calculated risk  $U$ , design return period  $T_D$ , and design wind  $W_D$  will be described for use in facilities design for several locations.

a. The desired lifetime  $N$  is expressed in years, and preliminary estimates must be made as to how many years the proposed facility is to be used.

b. The calculated risk  $U$  is a probability expressed either as a percentage or as a decimal fraction. Calculated risk, sometimes referred to as design risk, is a probability measure of the risk the designer is willing to accept that the facility will be destroyed by wind loading in less time than the desired lifetime.

c. The design return period  $T_D$  is expressed in years and is a function of desired lifetime and calculated risk.

d. The design wind  $W_D$  is a function of the desired lifetime and calculated risk and is derived from the design return period and a probability distribution function of yearly peak winds.

#### 2.3.10.2 Development of Relationships

From the theory of repeated trial probability we can derive the following expression:

$$N = \frac{\ln(1 - U)}{\ln\left(1 - \frac{1}{T_D}\right)} \quad (2.19)$$

Equation (2.19) gives the important relationships for the three variables, calculated risk  $U$ , design return period  $T_D$ , and desired lifetime  $N$ . If estimates for any two variables are available, the third can be determined from this equation.

Design return period  $T_D$ , calculated with equation (2.19), for various values of desired lifetime  $N$  and design risk are given in Table 2.3.27. The table presents the exact and adopted values for design return

TABLE 2.3.27 EXACT AND ADOPTED VALUES FOR DESIGN RETURN PERIOD ( $T_D$ , years) VERSUS DESIRED LIFETIME ( $N$ , years) FOR VARIOUS DESIGN RISKS ( $U$ )

N (years)	Design Return Period (years)									
	U = 50%		U = 20%		U = 10%		U = 5%		U = 1%	
	Exact	Adopted	Exact	Adopted	Exact	Adopted	Exact	Adopted	Exact	Adopted
1	2	2	15	5	10	10	20	20	100	100
10	15	15	45	50	95	100	196	200	996	1000
20	29	30	90	100	190	200	390	400	1991	2000
25	37	40	113	125	238	250	488	500		
30	44	50	135	150	285	300	585	600		
50	73	100	225	250	475	500	975	1000		
100	145	150	449	500	950	1000	1950	2000		

period versus desired lifetime for various design risks. The adopted values for  $T_D$  are in some cases greatly oversized to facilitate a convenient use of the tabulated probabilities for the distributions of yearly peak winds.

### 2.3.10.3 Design Winds for Facilities at Kennedy Space Center

To obtain the design wind, it is required that the wind speed corresponding to the design return period be determined. Since the design return period is a function of risk, either of two procedures can be used to determine the design wind: One is through a graphical or numerical interpolation procedure; the second is based on an analytical function. A knowledge of the distribution of yearly peak winds is required for both procedures. For the greatest statistical efficiency in arriving at a knowledge of the probability that peak winds will be less than or equal to some specified value of yearly peak winds, the choice of an appropriate probability distribution function is made, and the parameters for the function are estimated from the sample of yearly peak winds. From an investigation leading to the distribution of hourly, daily, monthly, and yearly peaks it was learned that the Gumbel distribution was an excellent fit for the 17 years of yearly peak ground winds at the 10-m level for Kennedy Space Center. The distribution of yearly peak wind (10-m level), as obtained by the Gumbel distribution, is tabulated for various percentiles together with the corresponding return periods in Table 2.3.28. The values for the parameters  $\alpha$  and  $\mu$  for this distribution are also given in this table.

The design wind can now be determined by making a choice for desired lifetime and design risk and by taking the design return period from Table 2.3.27 and looking up the wind speed corresponding to the return period given in Table 2.3.28. For combinations not tabulated in Tables 2.3.27 and 2.3.28, the design return period can be interpolated.

TABLE 2.3.28 GUMBEL DISTRIBUTION FOR YEARLY PEAK WIND SPEED,  
10-m REFERENCE LEVEL, INCLUDING HURRICANE WINDS,  
KENNEDY SPACE CENTER

Return Period (years)	Probability	y	m/sec	knots
2	0.50	0.36651	25.45	49.47
5	0.80	1.49994	31.79	61.79
10	0.90	2.25037	35.98	69.95
15	0.933	2.66859	38.33	74.50
20	0.95	2.97020	40.01	77.77
30	0.967	3.39452	42.38	82.39
45	0.978	3.80561	44.68	86.86
50	0.98	3.90191	45.22	87.90
90	0.9889	4.49523	48.54	94.35
100	0.99	4.60015	49.12	95.49
150	0.9933	5.00229	51.37	99.86
200	0.995	5.29581	53.01	103.05
250	0.996	5.51946	54.26	105.48
300	0.9967	5.71218	55.34	107.58
400	0.9975	5.99021	56.90	110.60
500	0.9980	6.21361	58.14	113.02
600	0.9983	6.37628	58.75	114.20
1 000	0.9990	6.90726	62.02	120.56
10 000	0.9999	9.21029	74.90	145.60
$\alpha^{-1} = 5.5917 \text{ m/sec (10.8695 knots)} \quad \mu = 23.4 \text{ m/sec (45.49 knots)}$ $\Phi = e^{-e^{-y}} \quad , \text{ where } y = \alpha[x - \mu]$				

#### 2.3.10.4 Procedure to Determine Design Winds for Facilities

The design wind,  $W_D$  as a function of desired lifetime,  $N$  and calculated risk,  $U$  for the Gumbel distribution of peak winds at the 10-m reference level, can be derived as

$$W_D = \frac{1}{\alpha} \left\{ -\ln [-\ln(1 - U)] + \ln N \right\} + \mu \quad , \quad (2.20)$$

where  $\alpha$  and  $\mu$  are estimated from the sample of yearly peak winds.

2.38

Taking the values for  $\alpha^{-1} = 5.5917$  m/sec (10.8695 knots) and for  $\mu = 23.4$  m/sec (45.49 knots) from Table 2.3.28 and evaluating equation (2.20) for selected values of N and U, yields the data in Table 2.3.29.

A convenient plot for design wind versus desired lifetime is illustrated in Figure 2.3.10. The slopes of the lines in Figure 2.3.10 are equal.

TABLE 2.3.29 FACILITY DESIGN WIND  $W_{D10}$  WITH RESPECT TO THE  
10-m REFERENCE LEVEL PEAK WIND SPEED FOR VARIOUS  
LIFETIMES (N), KENNEDY SPACE CENTER

U	1 - U	$-\ln [-\ln(1 - U)]$	Design Wind ( $W_{D10}$ ) for Various Lifetimes (N) *							
			N = 1		N = 10		N = 30		N = 100	
			(m/sec)	(knots)	(m/sec)	(knots)	(m/sec)	(knots)	(m/sec)	(knots)
0.63212	0.36788	0	23.40	45.49	36.28	70.52	42.42	82.46	49.15	95.55
0.50	0.50	0.36651	25.45	49.47	38.33	74.50	44.47	86.44	51.20	99.53
0.4296	0.5704	0.57722	26.62	51.76	39.50	76.79	45.65	88.73	52.38	101.82
0.40	0.60	0.67173	27.16	52.79	40.03	77.82	46.18	89.76	52.92	102.85
0.30	0.70	1.03093	29.17	56.70	42.04	81.72	48.19	93.67	54.92	106.75
0.20	0.80	1.49994	31.79	61.79	44.66	86.82	50.81	98.76	57.54	111.85
0.10	0.90	2.25037	35.99	69.95	48.86	94.98	55.00	106.92	61.74	120.01
0.05	0.95	2.97020	40.01	77.77	52.88	102.80	59.03	114.74	65.76	127.83
0.01	0.99	4.60016	49.12	95.49	62.00	120.52	68.14	132.46	74.88	145.55

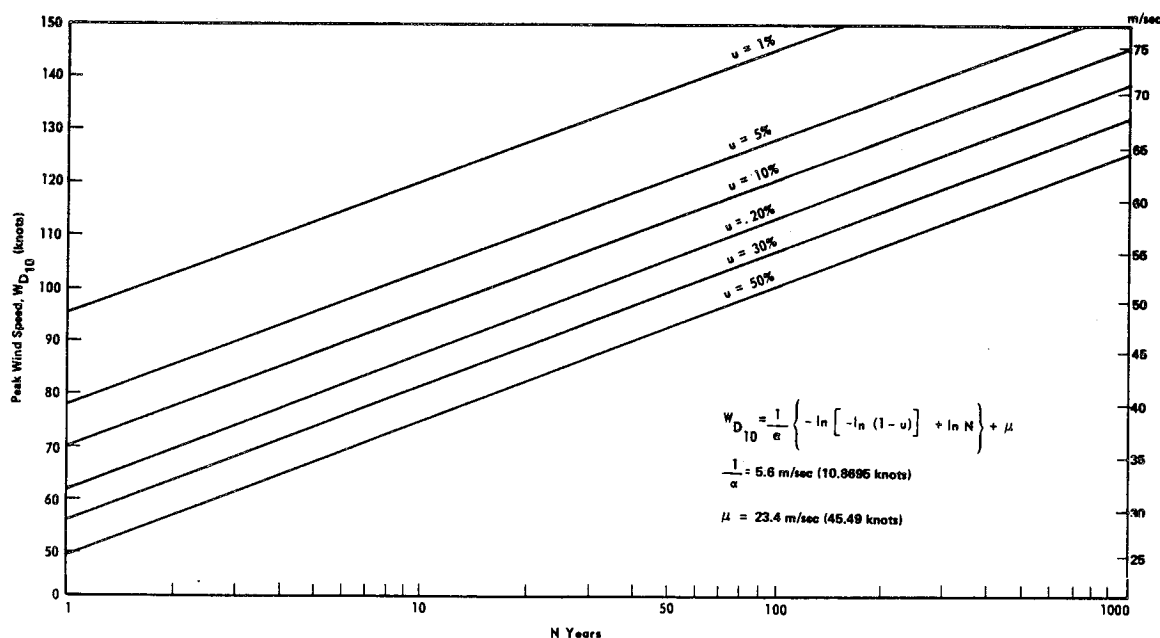


Figure 2.3.10 Facility design wind  $W_{D10}$  with respect to the 10-m reference level peak wind speed for various lifetimes (N), Kennedy Space Center.

\*Values of N are given in years.



### 2.3.10.5 Requirements for Wind Load Calculations

The design wind for a structure cannot be determined solely by wind statistics at a particular height. The design engineer is most interested in designing a structure which satisfies the user's requirements for utility, which will have a small risk of failure within the desired lifetime of the structure, and which can carry a sufficiently large wind load and be constructed at a sufficiently low cost. The total wind loading on a structure is composed of two interrelated components, steady-state drag wind loads, and dynamic wind loads (time-dependent drag loads, vortex shedding forces, etc.). The time required for a structure to respond to the drag wind loads dictates the averaging time for the design wind profile. In general, the structure response time depends upon the shape and size of the structure. The natural frequency of the structure and the size and shape of the structure and its components are important in estimating the dynamic wind load. It is conceivable that a structure could be designed to withstand very high wind speeds without structural failure and still oscillate in moderate wind speeds. If such a structure, for example, is to be used to support a precision tracking radar, then there may be little danger of overloading the structure by high winds; but the structure might be useless for its intended purpose if it were to oscillate in a moderate wind. Also, a building may have panels or small members that could respond to dynamic loading in such a way that long-term vibrations could cause failure, without any structural failure of the main supporting members. Since dynamic wind loading requires an intricate knowledge of the particular facility and its components, no attempt is made here to state generalized design criteria for dynamic wind loading. The emphasis in this section is upon winds for estimating drag wind loads in establishing design wind criteria for structures. Reference is made to Section 2.3.5 for information appropriate to dynamic wind loads.

### 2.3.10.6 Wind Profile Construction

Given the peak wind at the 10-m level, the peak wind profile can be constructed with the peak wind profile law from Section 2.3.5. Steady-state wind profiles can be obtained by using appropriate gust factors which are discussed in Section 2.3.7.

To illustrate the procedures and operations in deriving the wind profile and the application of the gust factor, three examples are worked out for Kennedy Space Center. Peak wind speeds at the 10-m level of 36, 49, and 62 m/sec (70, 95, and 120 knots) have been selected for these examples. These three wind speeds were selected because they correspond to a return period of 10, 100, and 1000 years for a peak wind at the 10-m level at Kennedy Space Center (see Table 2.3.32). Table 2.3.34 contains the risks of exceeding these peak winds for various values of desired lifetime.

Table 2.3.31 gives the peak design wind profiles corresponding to the desired lifetimes and calculated risks presented in Table 2.3.30. These profiles were calculated with equation (2.22).

### 2.3.10.7 Use of Gust Factors Versus Height

In estimating the drag load on a particular structure, it may be determined that wind force of a given magnitude must act on the structure for some period (for example, 1 min) to produce a critical drag load. To obtain the wind profile corresponding to a time averaged wind, the peak wind profile values are divided by the required gust factors. The gust factors for winds greater than 15 m/sec (29 knots) versus height given in Table 2.3.32 are taken from Section 2.3.7. This operation may seem strange to someone who is accustomed to multiplying the given wind by a gust factor in establishing the design wind. This is because most literature on this subject gives the reference wind as averaged over some time increment (for example, 1, 2, or 5 min) or in terms of the "fastest mile" of wind that has a variable averaging time depending upon the

2.40

TABLE 2.3.30 CALCULATED RISK (U) VERSUS DESIRED LIFETIME (N, years)  
FOR ASSIGNED DESIGN WINDS RELATED TO PEAK WINDS AT THE  
10-m REFERENCE LEVEL, KENNEDY SPACE CENTER

N (years)	$W_{D_{10}} = 36 \text{ m/sec}$ (70 knots) $T_D = 10 \text{ years}$ U%	$W_{D_{10}} = 49 \text{ m/sec}$ (95 knots) $T_D = 100 \text{ years}$ U%	$W_{D_{10}} = 62 \text{ m/sec}$ (120 knots) $T_D = 1000 \text{ years}$ U%
1	10	1.0	0.1
10	65	10	1
20	88	18	2
25	93	22	2.5
30	95.8	26	3
50	99.5	39.5	5
100	99.997	63.397	10
$T_D = \text{Design return period}$			

TABLE 2.3.31 DESIGN<sup>4</sup> PEAK WIND PROFILES FOR DESIGN WIND RELATIVE TO THE  
10-m REFERENCE LEVEL, KENNEDY SPACE CENTER

Height		$W_{D_{10}} = 36 \text{ m/sec}$ (70 knots)		$W_{D_{10}} = 49 \text{ m/sec}$ (95 knots)		$W_{D_{10}} = 62 \text{ m/sec}$ (120 knots)	
(ft)	(m)	(knots)	(ms <sup>-1</sup> )	(knots)	(ms <sup>-1</sup> )	(knots)	(ms <sup>-1</sup> )
33	10	70.0	36.0	95.0	48.9	120.0	61.8
60	18.3	74.5	38.4	99.9	51.4	125.2	64.5
100	30.5	78.6	40.4	104.2	53.7	129.8	66.8
200	61.0	84.4	43.4	110.4	56.8	136.2	70.1
300	91.4	88.0	45.3	114.2	58.8	140.2	72.2
400	121.9	90.7	46.7	117.0	60.2	143.0	73.62
500	152.4	92.8	47.8	119.1	61.3	145.3	74.8

4. See Table 2.3.30 for calculated risk values versus desired lifetime for these design winds.

TABLE 2.3.32 GUST FACTORS FOR VARIOUS AVERAGING TIMES ( $\tau$ ) FOR  
PEAK WINDS  $> 15$  m/sec (30 knots) AT THE 10-m REFERENCE LEVEL  
VERSUS HEIGHT, KENNEDY SPACE CENTER

Height		Various Averaging Times ( $\tau$ , min )				
(ft)	(m)	$\tau=0.5$	$\tau=1$	$\tau=2$	$\tau=5$	$\tau=10$
33	10	1.318	1.372	1.435	1.528	1.599
60	18.3	1.268	1.314	1.366	1.445	1.505
100	30.5	1.232	1.271	1.317	1.385	1.437
200	61.0	1.191	1.223	1.261	1.316	1.359
300	91.4	1.170	1.199	1.232	1.282	1.320
400	121.9	1.157	1.183	1.214	1.260	1.295
500	152.4	1.147	1.172	1.201	1.244	1.277

wind speed. The design wind profiles for the three examples (that is, in terms of the peak winds of 36, 49, and 62 m/sec (70, 95, and 120 knots) at the 10-m level) for various averaging times  $\tau$ , given in minutes, are illustrated in Tables 2.3.33, 2.3.34, and 2.3.35. Following the procedures presented by this example, the design engineer can objectively derive several important design parameters that can be used in meeting the objective of designing a facility that will (1) meet the requirements for utility and desired lifetime, (2) withstand a sufficiently large wind loading with a known calculated risk of failure, caused by wind loads, and (3) allow him to proceed with trade-off studies between the design parameters and to estimate the cost of building a structure to best meet these design objectives.

TABLE 2.3.33 DESIGN<sup>5</sup> WIND PROFILES FOR VARIOUS AVERAGING TIMES ( $\tau$ )  
FOR PEAK DESIGN WIND OF 36.0 m/sec (70 knots) RELATIVE TO THE  
10-m REFERENCE LEVEL, KENNEDY SPACE CENTER

Height		Design Wind Profiles for Various Averaging Times ( $\tau$ ) in minutes											
(ft)	(m)	$\tau=0$		$\tau=0.5$		$\tau=1$		$\tau=2$		$\tau=5$		$\tau=10$	
		(m/sec)	(knots)	(m/sec)	(knots)	(m/sec)	(knots)	(m/sec)	(knots)	(m/sec)	(knots)	(m/sec)	(knots)
33	10	36.0	70.0	27.3	53.1	26.2	51.0	25.1	48.8	23.6	45.8	22.5	43.8
60	18.3	38.3	74.5	30.2	58.8	29.2	56.7	28.0	54.5	26.5	51.6	25.5	49.5
100	30.5	40.4	78.6	32.8	63.8	31.8	61.8	30.7	59.7	29.2	56.8	28.1	54.7
200	61.0	43.4	84.4	36.5	70.9	35.5	69.0	34.4	66.9	33.0	64.1	31.9	62.1
300	91.4	45.3	88.0	38.7	75.2	37.8	73.4	36.7	71.4	35.3	68.6	34.3	66.7
400	121.9	46.7	90.7	40.3	78.4	39.5	76.7	38.4	74.7	37.0	72.0	36.0	70.0
500	152.4	47.7	92.8	41.6	80.9	40.7	79.2	39.8	77.3	38.4	74.6	37.4	72.7

5. See Table 2.3.30 for calculated risk values versus desired lifetime for these design winds.

2.42

TABLE 2.3.34 DESIGN<sup>6</sup> WIND PROFILES FOR VARIOUS AVERAGING TIMES ( $\tau$ )  
FOR PEAK DESIGN WIND OF 49.0 m/sec (95 knots) RELATIVE TO THE  
10-m REFERENCE LEVEL, KENNEDY SPACE CENTER

Height		Design Wind Profiles for Various Averaging Times ( $\tau$ ) in minutes											
(ft)	(m)	$\tau=0$		$\tau=0.5$		$\tau=1$		$\tau=2$		$\tau=5$		$\tau=10$	
		(m/sec)	(knots)	(m/sec)	(knots)	(m/sec)	(knots)	(m/sec)	(knots)	(m/sec)	(knots)	(m/sec)	(knots)
33	10	48.9	95.0	37.1	72.1	35.6	69.2	34.1	66.2	32.0	62.2	30.6	59.4
60	18.3	51.4	99.9	40.5	78.8	39.1	76.0	37.6	73.1	35.5	69.1	34.2	66.4
100	30.5	53.6	104.2	43.5	84.6	42.2	82.0	40.7	79.1	38.7	75.2	37.3	72.5
200	61.0	56.8	110.4	47.7	92.7	46.5	90.3	45.0	87.5	43.2	83.9	41.8	81.2
300	91.4	58.7	114.2	50.2	97.6	49.0	95.2	47.7	92.7	45.8	89.1	44.5	86.5
400	121.9	60.2	117.0	52.0	101.1	50.9	98.9	49.6	96.4	47.8	92.9	46.5	90.3
500	152.4	61.3	119.1	53.4	103.8	52.3	101.6	51.0	99.2	49.2	95.7	48.0	93.3

TABLE 2.3.35 DESIGN WIND<sup>6</sup> PROFILES FOR VARIOUS AVERAGING TIMES ( $\tau$ )  
FOR PEAK DESIGN WIND OF 62.0 m/sec (120 knots) RELATIVE TO THE  
10-m REFERENCE LEVEL, KENNEDY SPACE CENTER

Height		Design Wind Profiles for Various Averaging Times ( $\tau$ ) in minutes											
(ft)	(m)	$\tau=0$		$\tau=0.5$		$\tau=1$		$\tau=2$		$\tau=5$		$\tau=10$	
		(m/sec)	(knots)	(m/sec)	(knots)	(m/sec)	(knots)	(m/sec)	(knots)	(m/sec)	(knots)	(m/sec)	(knots)
33	10	61.7	120.0	46.8	91.0	45.0	87.5	43.0	83.6	40.4	78.5	38.6	75.0
60	18.3	64.4	125.2	50.8	98.7	49.0	95.3	47.2	91.7	44.6	86.6	42.8	83.2
100	30.5	66.8	129.8	54.2	105.4	52.5	102.1	50.7	98.6	48.2	93.7	46.5	90.3
200	61.0	70.1	136.2	58.9	114.4	57.3	111.4	55.6	108.0	53.2	103.5	51.5	100.2
300	91.4	72.1	140.2	61.6	119.8	60.1	116.9	58.5	113.8	56.3	109.4	54.6	106.2
400	121.9	73.6	143.0	63.6	123.6	62.2	120.9	60.6	117.8	58.4	113.5	56.8	110.4
500	152.4	74.7	145.3	65.2	126.7	63.8	124.0	62.2	121.0	60.1	116.8	58.5	113.8

#### 2.3.10.8 Recommended Design Risk Versus Desired Lifetime

Unfortunately, there is not a clear-cut precedent from building codes to follow in recommending design risk for a given desired lifetime of a structure. This could be because the consequences of total loss of a structure due to wind forces differ according to the purpose of the structure. Conceivably, a value analysis in terms of original investment cost, replacement cost, safety of property and human life, loss of national prestige, and many other factors could be made to give a measure of the consequences for the loss of a particular structure in arriving at a decision as to what risk management is willing to accept for the loss within the desired lifetime of the structure. If the structure is an isolated shed then obviously its loss is not as great as a structure that would house many people or a structure that is critical to the mission of a large

6. See Table 2.3.30 for calculated risk values versus desired lifetime for these design winds.

organization; nor is it as potentially unsafe as the loss of a nuclear power plant or storage facility for explosives or highly radioactive materials. To give a starting point for design studies aimed at meeting the design objectives, it is recommended that a design risk of 10 percent for the desired lifetime be used in determining the wind loading on structures that have a high replacement cost. Should the loss of the structure be extremely hazardous to life or property, or critical to the mission of a large organization, then a design risk of 5 percent or less for the desired lifetime is recommended. These are subjective recommendations involving arbitrary assumptions about the design objectives. Note that the larger the desired lifetime, the greater the design risk is for a given wind speed (or wind loading). Therefore, realistic appraisals should be made for desired lifetimes.

### 2.3.10.9 Design Winds for Facilities at Vandenberg AFB, White Sands Missile Range, Edwards Air Force Base, National Space Technology Laboratory, Bay St. Louis, Mississippi

#### 2.3.10.9.1 The Wind Statistics

The basic wind statistics for these five locations are taken from Reference 2.19, which presents isotach maps for the United States for the 50, 98, and 99 percentile values for the yearly maximum "fastest mile" of wind at the 30-ft (~ 10-m) reference height above natural grade. By definition, the fastest mile is the fastest wind speed in miles per hour of any mile of wind during a specified period (usually taken as the 24-hour observational day), and the largest of these in a year for the period of record constitutes the statistical sample of yearly fastest mile. From this definition, it is noted that the fastest mile as a measure of wind speed has a variable averaging time; for example, if the wind speed is 60 miles per hour, the averaging time for the fastest mile of wind is 1 min. For a wind speed of 120 miles per hour, the averaging time for the fastest mile of wind is 0.5 min. Thom (Ref. 2.19) reports that the Fréchet probability distribution function fits his samples of fastest mile very well. The Fréchet distribution function is given as

$$F(x) = e^{-\left(\frac{x}{\beta}\right)^{-\gamma}}, \quad (2.21)$$

where the two parameters  $\beta$  and  $\gamma$  are estimated from the sample by the maximum likelihood method. From Thom's maps of the 50, 98, and 99 percentiles of fastest mile of wind for yearly extremals, we have estimated (interpolated) for these percentiles for the five locations and calculated the values for the parameters  $\beta$  and  $\gamma$  for the Fréchet distribution function and computed several additional percentiles, as shown in Table 2.3.36. To have units consistent with the other sections of this document, the percentiles and the parameters  $\beta$  and  $\gamma$  have been converted from miles per hour to knots and m/sec. Thus, Table 2.3.36 gives the Fréchet distribution for the fastest mile of winds at the 30-ft (~ 10-m) level for the five locations with the units in knots and m/sec.

The discussion in Section 2.3.10.2, devoted to desired lifetime, calculated risk, and design winds with respect to the wind statistics at a particular height (10-m level) is applicable here, except that the reference statistics are with respect to the fastest mile converted to knots and m/sec. See also Reference 2.20.

#### 2.3.10.9.2 Conversion of Fastest Mile to Peak Winds

It was mentioned in Section 2.3.10.3 that the Fréchet distribution for the 17-year sample of yearly peak winds for Kennedy Space Center was an acceptable fit to this sample. The Fréchet distributions for the

---

7. Includes New Orleans, Louisiana.

2.44

TABLE 2.3.36 FRÉCHET DISTRIBUTION OF FASTEST MILE WIND AT THE 10-m HEIGHT OF YEARLY EXTREMES FOR THE INDICATED STATIONS

P Probability	T <sub>D</sub> Return Period (years)	Fastest Mile Wind					
		National Space Technology Lab		Vandenberg AFB		Edwards AFB	
		(m/sec)	(knots)	(m/sec)	(knots)	(m/sec)	(knots)
0.50	2	22.1	42.9	18.0	34.9	11.3	22.0
0.80	5	26.6	51.8	21.6	42.0	15.0	29.1
0.90	10	30.1	58.6	24.4	47.4	18.1	35.2
0.95	20	33.9	65.9	27.4	53.3	21.6	42.0
0.98	50	39.6	76.9	31.8	61.9	27.3	53.0
0.99	100	44.4	86.4	35.7	69.4	32.4	63.1
0.9933	150	47.4	92.2	38.0	73.9	35.1	68.3
0.995	200	49.7	96.7	39.9	77.6	38.6	75.0
0.996	250	51.6	100.4	41.4	80.4	40.8	79.3
0.99667	300	53.2	103.5	42.6	82.9	42.7	83.1
0.9975	400	55.8	108.4	44.6	86.7	45.8	89.1
0.998	500	57.9	112.5	46.2	89.9	48.5	94.2
0.99833	600	59.4	115.5	47.5	92.3	50.5	98.1
0.99875	800	62.6	121.6	50.3	97.7	54.0	105.0
0.999	1000	64.9	126.1	51.8	100.6	57.6	111.9
$\gamma$	Unitless	6.08075		6.19591		4.02093	
$1/\gamma$	Unitless	0.16445		0.16140		0.24870	
$\ln \beta$	Unitless	3.70093		3.49620		2.99989	
$\beta$	m/sec	20.829		16.968		10.322	
	(knots)	(40.488)		(32.983)		(20.065)	

fastest mile were obtained from Thom's analysis for Kennedy Space Center. From these two distributions (the Fréchet for the peak winds as well as for the fastest mile), the ratio of the percentiles of the fastest mile to the peak winds were taken. This ratio varied from 1.12 to 1.09, over the range of probabilities from 30 to 99 percent. Thus we adopted 1.10 as a factor to multiply the statistics of the fastest mile of wind to obtain peak (instantaneous) wind statistics. This procedure is based on the evidence of only one station. A gust factor of 1.10 is often applied to the fastest mile statistics in facility design work to account for gust loads.

#### 2.3.10.9.3 The Peak Wind Profile

The peak wind profile law adopted for the five locations for peak winds at the 10-m level greater than 22.6 m/sec (44 knots) is

$$u = u_{10} \left( \frac{z}{10} \right)^{1/7} \quad (2.2)$$

where  $u_{10}$  is the peak wind at the 10-m height and  $u$  is the peak wind at height  $z$  in meters.

#### 2.3.10.9.4 The Mean Wind Profile

To obtain the mean wind profile for various averaging times, the gust factors given in Section 2.3.7, are applied to the peak wind profile as determined by equation (2.22).

#### 2.3.10.9.5 Design Wind Profiles for Station Locations

The design peak wind profiles for the peak winds in Table 2.3.31 are obtained from the adopted peak wind power law given by equation (2.22), and the mean wind profiles for various averaging times are obtained by dividing by the gust factors for the various averaging times. (The gust factors versus height and averaging times are presented in Table 2.3.32.) The resulting selected design wind profiles for design return periods of 10, 100, and 1000 years for the four stations are given in Tables 2.3.40 through 2.3.46, in which values of  $\tau$  are given in minutes. The design risk versus desired lifetime for the design return periods of 10, 100, and 1000 years is presented in Table 2.3.30.

#### 2.3.11 Ground Winds for Runway Orientation Optimization

Runway orientation is influenced by a number of factors; for example, winds, terrain features, population interference, etc. In some cases the frequency of occurrence of crosswind components of some significant speed has received insufficient consideration. Aligning the runway with the prevailing wind will not insure that crosswinds will be minimized. In fact, two common synoptic situations (one producing light easterly winds, and the other causing strong northerly winds) might exist in such a relationship that a runway oriented with the prevailing wind might be the least useful to an aircraft constrained by crosswind components. Two methods, one empirical, the other theoretical, of determining the optimum runway orientation to minimize critical crosswind component speeds are available (Ref. 2.21).

TABLE 2.3.37 PEAK WINDS (fastest mile values times 1.10) FOR THE 10-m REFERENCE LEVEL FOR 10-, 100-, AND 1000-YEAR RETURN PERIODS

T <sub>D</sub> (years)	Peak Winds					
	National Space Technology Lab		Vandenberg AFB		Edwards AFB	
	(m/sec)	(knots)	(m/sec)	(knots)	(m/sec)	(knots)
10	33.2	64.5	26.8	52.1	19.9	38.7
100	48.9	95.0	39.3	76.3	35.7	69.4
1000	71.4	138.7	56.9	110.7	63.4	123.2

TABLE 2.3.38 FACILITIES DESIGN WIND AS A FUNCTION OF AVERAGING  
TIME ( $\tau$ ) FOR A PEAK WIND OF 33.2 m/sec (64.5 knots)  
(10-year return period) FOR NATIONAL SPACE  
TECHNOLOGY LABORATORY

Height		Facilities Design Wind as a Function of Averaging Time ( $\tau$ ) in minutes											
(ft)	(m)	$\tau=0$ (peak)		$\tau=0.5$		$\tau=1$		$\tau=2$		$\tau=5$		$\tau=10$	
		(m/sec)	(knots)	(m/sec)	(knots)	(m/sec)	(knots)	(m/sec)	(knots)	(m/sec)	(knots)	(m/sec)	(knots)
33	10	33.2	64.5	25.2	48.9	24.2	47.0	23.1	44.9	21.7	42.2	20.7	40.3
60	18.3	36.2	70.3	28.5	55.4	27.5	53.5	26.5	51.5	25.1	48.7	24.0	46.7
100	30.5	38.9	75.6	31.6	61.4	30.6	59.5	29.5	57.4	28.1	54.6	27.1	52.6
200	61.0	43.0	83.5	36.1	70.1	35.1	68.3	34.1	66.2	32.6	63.4	31.6	61.4
300	91.4	45.5	88.5	38.9	75.6	38.0	73.8	36.9	71.8	35.5	69.0	34.5	67.0
400	121.9	47.4	92.2	41.0	79.7	40.1	77.9	39.0	75.9	37.7	73.2	36.6	71.2
500	152.4	48.5	94.3	42.3	82.2	41.4	80.5	40.4	78.5	39.0	75.8	38.0	73.8

TABLE 2.3.39 FACILITIES DESIGN WIND AS A FUNCTION OF AVERAGING  
TIME ( $\tau$ ) FOR A PEAK WIND OF 48.9 m/sec (95.0 knots)  
(100-year return period) FOR NATIONAL SPACE  
TECHNOLOGY LABORATORY

Height		Facilities Design Wind as a Function of Averaging Time ( $\tau$ ) in minutes											
(ft)	(m)	$\tau=0$ (peak)		$\tau=0.5$		$\tau=1$		$\tau=2$		$\tau=5$		$\tau=10$	
		(m/sec)	(knots)	(m/sec)	(knots)	(m/sec)	(knots)	(m/sec)	(knots)	(m/sec)	(knots)	(m/sec)	(knots)
33	10	48.9	95.0	37.1	72.1	35.6	69.2	34.1	66.2	32.0	62.2	30.6	59.4
60	18.3	53.3	103.6	42.0	81.7	40.5	78.8	39.0	75.8	36.9	71.7	35.4	68.8
100	30.5	57.3	111.4	46.5	90.4	45.1	87.6	43.5	84.6	41.4	80.4	40.8	79.3
200	61.0	63.3	123.0	53.1	103.3	51.8	100.6	50.2	97.5	48.1	93.5	46.6	90.5
300	91.4	67.0	130.3	57.3	111.4	55.9	108.7	54.4	105.8	52.3	101.6	50.8	98.7
400	121.9	69.9	135.8	60.4	117.4	59.1	114.8	57.6	111.9	55.5	107.8	54.0	104.9
500	152.4	71.4	138.8	62.2	121.0	60.9	118.4	59.5	115.6	57.4	111.6	55.9	108.7



TABLE 2.3.40 FACILITIES DESIGN WIND AS A FUNCTION OF AVERAGING TIME ( $\tau$ ) FOR A PEAK WIND OF 71.4 m/sec (138.7 knots) (1000-year return period) FOR NATIONAL SPACE TECHNOLOGY LABORATORY

Height		Facilities Design Wind as a Function of Averaging Time ( $\tau$ ) in minutes											
(ft)	(m)	$\tau=0$ (peak)		$\tau=0.5$		$\tau=1$		$\tau=2$		$\tau=5$		$\tau=10$	
		(m/sec)	(knots)	(m/sec)	(knots)	(m/sec)	(knots)	(m/sec)	(knots)	(m/sec)	(knots)	(m/sec)	(knots)
33	10	26.8	52.1	20.3	39.5	19.5	38.0	18.7	36.3	17.5	34.1	16.8	32.6
60	18.3	29.2	56.8	23.0	44.8	22.2	43.2	21.4	41.6	20.2	39.3	19.4	37.7
100	30.5	31.4	61.1	25.5	49.6	24.7	48.1	23.9	46.4	22.7	44.1	21.9	42.5
200	61.0	34.7	67.5	29.2	56.7	28.4	55.2	27.5	53.5	26.4	51.3	25.6	49.7
300	91.4	36.8	71.5	31.4	61.1	30.7	59.6	29.8	58.0	28.7	55.8	27.9	54.2
400	121.9	38.3	74.5	33.1	64.4	32.4	63.0	31.6	61.4	30.4	59.1	29.6	57.5
500	152.4	39.1	76.1	34.1	66.3	33.4	64.9	32.6	63.3	31.5	61.2	30.7	59.6

TABLE 2.3.41 FACILITIES DESIGN WIND AS A FUNCTION OF AVERAGING TIME ( $\tau$ ) FOR A PEAK WIND OF 26.8 m/sec (52.1 knots) (10-year return period) FOR VANDENBERG AFB AND WHITE SANDS MISSILE RANGE

Height		Facilities Design Wind as a Function of Averaging Time ( $\tau$ ) in minutes											
(ft)	(m)	$\tau=0$ (peak)		$\tau=0.5$		$\tau=1$		$\tau=2$		$\tau=5$		$\tau=10$	
		(m/sec)	(knots)	(m/sec)	(knots)	(m/sec)	(knots)	(m/sec)	(knots)	(m/sec)	(knots)	(m/sec)	(knots)
33	10	71.4	138.7	54.1	105.2	52.0	101.1	49.7	96.7	46.7	90.8	44.6	86.7
60	18.3	77.8	151.2	61.3	119.2	59.2	115.1	56.9	110.7	53.8	104.6	51.7	100.5
100	30.5	83.7	162.7	68.0	132.1	65.8	128.0	63.5	123.5	60.4	117.5	58.2	113.2
200	61.0	92.4	179.6	77.6	150.8	75.6	146.9	73.3	142.4	70.2	136.5	68.0	132.2
300	91.4	97.9	190.3	83.6	162.6	81.6	158.7	79.5	154.5	76.3	148.4	74.2	144.2
400	121.9	102.0	198.2	88.1	171.3	86.2	167.5	84.0	163.3	80.9	157.3	78.8	153.1
500	152.4	104.3	202.7	90.9	176.7	89.0	173.0	86.8	168.8	83.8	162.9	81.6	158.7

**TABLE 2.3.42 FACILITIES DESIGN WIND AS A FUNCTION OF AVERAGING TIME ( $\tau$ ) FOR A PEAK WIND OF 39.3 m/sec (76.3 knots) (100-year return period) FOR VANDENBERG AFB AND WHITE SANDS MISSILE RANGE**

Height		Facilities Design Wind as a Function of Averaging Time ( $\tau$ ) in minutes											
(ft)	(m)	$\tau=0$ (peak)		$\tau=0.5$		$\tau=1$		$\tau=2$		$\tau=5$		$\tau=10$	
		(m/sec)	(knots)	(m/sec)	(knots)	(m/sec)	(knots)	(m/sec)	(knots)	(m/sec)	(knots)	(m/sec)	(knots)
33	10	39.3	76.3	29.8	57.9	28.6	55.6	27.4	53.2	25.7	49.9	24.5	47.7
60	18.3	42.8	83.2	33.7	65.6	32.6	63.3	31.3	60.9	29.6	57.6	28.4	55.3
100	30.5	46.0	89.5	37.3	72.6	36.2	70.4	35.0	68.0	33.2	64.6	32.0	62.3
200	61.0	50.8	98.8	42.7	83.0	41.6	80.8	40.3	78.4	38.6	75.1	37.4	72.7
300	91.4	53.9	104.7	46.0	89.5	44.9	87.3	43.7	85.0	42.0	81.7	40.8	79.3
400	121.9	56.1	109.1	48.5	94.3	47.4	92.2	46.2	89.9	44.6	86.6	43.3	84.2
500	152.4	57.4	111.5	50.0	97.2	48.9	95.1	47.7	92.8	46.1	89.6	44.9	87.3

**TABLE 2.3.43 FACILITIES DESIGN WIND AS A FUNCTION OF AVERAGING TIME ( $\tau$ ) FOR A PEAK WIND OF 56.9 m/sec (110.7 knots) (1000-year return period) FOR VANDENBERG AFB AND WHITE SANDS MISSILE RANGE**

Height		Facilities Design Wind as a Function of Averaging Time ( $\tau$ ) in minutes											
(ft)	(m)	$\tau=0$ (peak)		$\tau=0.5$		$\tau=1$		$\tau=2$		$\tau=5$		$\tau=10$	
		(m/sec)	(knots)	(m/sec)	(knots)	(m/sec)	(knots)	(m/sec)	(knots)	(m/sec)	(knots)	(m/sec)	(knots)
33	10	56.9	110.7	43.2	84.0	41.5	80.7	39.7	77.1	37.2	72.4	35.6	69.2
60	18.3	62.1	120.7	49.0	95.2	47.3	91.9	45.5	88.4	43.0	83.5	41.3	80.2
100	30.5	66.8	129.8	54.2	105.4	52.5	102.1	50.7	98.6	48.2	93.7	46.5	90.3
200	61.0	73.7	143.3	61.9	120.3	60.3	117.2	58.4	113.6	56.0	108.9	54.2	105.4
300	91.4	78.1	151.9	66.8	129.8	65.2	126.7	63.4	123.3	61.0	118.5	59.2	115.1
400	121.9	81.4	158.2	70.3	136.7	68.8	133.7	67.0	130.3	64.6	125.6	62.9	122.2
500	152.4	83.2	161.8	72.6	141.1	71.0	138.1	69.3	134.7	66.9	130.1	65.2	126.7

**TABLE 2.3.44 FACILITIES DESIGN WIND AS A FUNCTION OF AVERAGING TIME ( $\tau$ ) FOR A PEAK WIND OF 19.9 m/sec (38.7 knots) (10-year return period) FOR EDWARDS AFB**

Height		Facilities Design Wind as a Function of Averaging Time ( $\tau$ ) in minutes											
(ft)	(m)	$\tau=0$ (peak)		$\tau=0.5$		$\tau=1$		$\tau=2$		$\tau=5$		$\tau=10$	
		(knots)	(m/sec)	(knots)	(m/sec)	(knots)	(m/sec)	(knots)	(m/sec)	(knots)	(m/sec)	(knots)	(m/sec)
33	10	38.7	19.9	29.4	15.1	28.2	14.5	27.0	13.9	25.3	13.0	24.2	12.4
60	18.3	42.1	21.7	33.2	17.1	32.0	16.5	30.8	15.8	29.1	15.0	28.0	14.4
100	30.5	45.1	23.2	36.6	18.8	35.5	18.3	34.2	17.6	32.6	16.8	31.4	16.2
200	61.0	50.1	25.8	42.1	21.7	41.0	21.1	39.7	20.4	38.1	19.6	36.9	19.0
300	91.4	53.1	27.3	45.4	23.4	44.3	22.8	43.1	22.2	41.4	21.3	40.2	20.7
400	121.9	55.3	28.4	47.8	24.6	46.7	24.0	45.6	23.5	43.9	22.6	42.7	22.0
500	152.4	57.1	29.4	49.8	25.6	48.7	25.1	47.5	24.4	45.9	23.6	44.7	23.0

TABLE 2.3.45 FACILITIES DESIGN WIND AS A FUNCTION OF AVERAGING  
TIME ( $\tau$ ) FOR A PEAK WIND OF 35.7 m/sec (69.4 knots)  
(100-year return period) FOR EDWARDS AFB

Height		Facilities Design Wind as a Function of Averaging Time ( $\tau$ ) in minutes											
(ft)	(m)	$\tau=0$ (peak)		$\tau=0.5$		$\tau=1$		$\tau=2$		$\tau=5$		$\tau=10$	
		(knots)	(m/sec)	(knots)	(m/sec)	(knots)	(m/sec)	(knots)	(m/sec)	(knots)	(m/sec)	(knots)	(m/sec)
33	10	69.4	35.7	52.7	27.1	50.6	26.0	48.4	24.9	45.4	23.4	43.4	22.3
60	18.3	75.5	38.8	59.5	30.6	57.5	29.6	55.3	28.4	52.2	26.9	50.2	25.8
100	30.5	80.9	41.6	65.7	33.8	63.7	32.8	61.4	31.6	58.4	30.0	56.3	29.0
200	61.0	89.9	46.2	75.5	38.8	73.5	37.8	71.3	36.7	68.3	35.1	66.2	34.1
300	91.4	95.2	49.0	81.4	41.9	79.4	40.8	77.3	39.8	74.3	38.2	72.1	37.1
400	121.9	99.2	51.0	85.7	44.1	83.9	43.2	81.7	42.0	78.7	40.5	76.6	39.4
500	152.4	102.4	52.7	89.3	45.9	87.4	45.0	85.3	43.9	82.3	42.3	80.2	41.3

TABLE 2.3.46 FACILITIES DESIGN WIND AS A FUNCTION OF AVERAGING  
TIME ( $\tau$ ) FOR A PEAK WIND OF 63.3 m/sec (123.0 knots)  
(1000-year return period) FOR EDWARDS AFB

Height		Facilities Design Wind as a Function of Averaging Time ( $\tau$ ) in minutes											
(ft)	(m)	$\tau=0$ (peak)		$\tau=0.5$		$\tau=1$		$\tau=2$		$\tau=5$		$\tau=10$	
		(knots)	(m/sec)	(knots)	(m/sec)	(knots)	(m/sec)	(knots)	(m/sec)	(knots)	(m/sec)	(knots)	(m/sec)
33	10	123.0	63.3	93.3	48.0	89.7	46.1	85.7	44.1	80.5	41.4	76.9	39.6
60	18.3	133.8	68.8	105.5	54.3	101.8	52.4	98.0	50.4	92.6	47.6	88.9	45.7
100	30.5	143.2	73.7	116.2	59.8	112.7	58.0	108.7	55.9	103.4	53.2	99.7	51.3
200	61.0	159.3	82.0	133.8	68.8	130.3	67.0	126.3	65.0	121.0	62.2	117.2	60.3
300	91.4	168.7	86.8	144.2	74.2	140.7	72.4	136.9	70.4	131.6	67.7	127.8	65.7
400	121.9	175.8	90.4	151.9	78.1	148.6	76.4	144.8	74.5	139.5	71.8	135.8	69.9
500	152.4	181.5	93.4	158.2	81.4	154.9	79.7	151.1	77.7	145.9	75.1	142.1	73.1

In the empirical method the runway crosswind components are computed for all azimuth and wind speed categories in the wind rose (Ref. 2.21). From these values the optimum runway orientation can be selected that will minimize the risk of occurrence of any specified crosswind speed.

The theoretical method requires that the wind components are bivariate normally distributed; i.e., a vector wind data sample is resolved into wind components in a rectangular coordinate system and the bivariate normal elliptical distribution is applied to the data sample of component winds. For example, let  $x_1$  and  $x_2$  be normally distributed variables with parameters  $(\xi_1, \sigma_1)$  and  $(\xi_2, \sigma_2)$ .  $\xi_1$  and  $\xi_2$  are the respective means, while  $\sigma_1$  and  $\sigma_2$  are the respective standard deviations. Let  $\rho$  be the correlation coefficient which is a measure of the dependence between  $x_1$  and  $x_2$ . Now, the bivariate normal density function is

$$p(x_1, x_2) = \left[ 2\pi\sigma_1\sigma_2(1-\rho^2)^{1/2} \right]^{-1} \exp \left\{ -\frac{1}{2(1-\rho^2)} \left[ \left( \frac{x_1 - \xi_1}{\sigma_1} \right)^2 - 2\rho \left( \frac{x_1 - \xi_1}{\sigma_1} \right) \left( \frac{x_2 - \xi_2}{\sigma_2} \right) + \left( \frac{x_2 - \xi_2}{\sigma_2} \right)^2 \right] \right\} \quad (2.2)$$

Let  $\alpha$  be any arbitrary angle in the rectangular coordinate system. From the statistics in the  $(x_1, x_2)$  space, the statistics for any rotation of the axes of the bivariate normal distribution through any arbitrary angle  $\alpha$  may be computed (Ref. 2.22). Let  $\Delta\alpha$  denote the desired increments for which runway orientation accuracy is required; e.g., one may wish to minimize the probability of crosswinds with a runway orientation accuracy down to  $\Delta\alpha = 10$  degrees. This means we must rotate the bivariate normal axes through every 10 degrees. It is only necessary to rotate the bivariate normal surface through 180 degrees since the distribution is symmetric in the other two quadrants. Let  $(y_1, y_2)$  denote the bivariate normal space after rotation. This rotation process will result in 18 sets of statistics in the  $(y_1, y_2)$  space. The quantity  $y_1$  is the head wind component, while  $y_2$  is the crosswind component. Since we are concerned with minimizing the probability of cross winds ( $y_2$ ) only, we now examine the marginal distribution  $p(y_2)$  for the 18 orientations ( $\alpha$ ). Since  $p(y_1, y_2)$  is bivariate normal, the 18 marginal distributions  $p(y_2)$  must be univariate normal:

$$p(y_2) = \left[ \sigma_2(2\pi)^{1/2} \right]^{-1} \exp \left\{ -\frac{1}{2} \left[ (y_2 - \xi_2)/\sigma_2 \right]^2 \right\} \quad (2.3)$$

$\xi_2$  and  $\sigma_2$  are replaced by their sample estimates  $\bar{Y}_2$  and  $S_{y_2}$ . Now, let

$$z = \frac{Y_2 - \bar{Y}_2}{S_{y_2}} \quad , \quad (2.4)$$

where  $y_2$  is the critical crosswind of interest. The quantity  $z$  is a standard normal variable, and the probability of its exceedance is easily calculated from the tables of the standard normal integral. Since a right or left crosswind ( $y_2$ ) is a constraint to an aircraft, the critical region (exceedance region) for the normal distribution is two-tailed; i.e., we are interested in twice the probability of exceeding  $|y_2|$ . Let this probability of exceedance or risk equal  $R$ . Now, the orientation for which  $R$  is a minimum is the desired optimum

runway orientation. The procedure described may be used for any station. Only parameters estimated from the data are required as input. Consequently, many runways and locations may be examined rapidly.

Either the empirical or theoretical method may be used to determine an aircraft runway orientation that minimizes the probability of critical crosswinds. Again, it is emphasized that the wind components must be bivariate normally distributed to use the theoretical method. In practical applications, the following steps are suggested:

1. Test the component wind samples for bivariate normality if these samples are available.
2. If the component winds are available and cannot be rejected as bivariate normal using the bivariate normal goodness-of-fit test, use the theoretical method since it is more expedient and easily programmed.
3. If the component wind data samples are not available and there is doubt concerning the assumption of bivariate normality of the wind components, use the empirical method.

## 2.4 Inflight Winds

### 2.4.1 Introduction

Inflight wind speed profiles are used in vehicle design studies primarily to establish structural and control system capabilities and compute performance requirements. The inflight wind speeds selected for vehicle design may not represent the same percentile value as the design surface wind speed. The selected wind speeds (inflight and surface) are determined by the desired vehicle launch capability and can differ in the percentile level since the inflight and surface wind speeds differ in degree of persistence for a given reference time period and can be treated as being statistically independent for engineering purposes.

Wind information for inflight design studies is presented in two basic forms: discrete or synthetic profiles and measured profile samples. There are certain limitations to each of these wind input forms, and their utility in design studies depends upon a number of considerations such as, (1) accuracy of basic measurements, (2) complexity of input to vehicle design, (3) economy and practicality for design use, (4) ability to represent significant features of the wind profile, (5) statistical assumption versus physical representation of the wind profile, (6) ability of input to ensure control system and structural integrity of the vehicle, and (7) flexibility of use in design trade-off studies.

An accurate and adequate number of measured wind profiles are necessary for developing a valid statistical description of the wind profile. Fortunately, current records of data from some locations (Kennedy Space Center in particular) fulfill these requirements, although a continuing program of data acquisition is vital to further enhance the confidence of the statistical information generated. Various methods and sensors for obtaining inflight profiles include the rawinsonde, the FPS-16 Radar/Jimsphere, and the rocketsonde. The statistical analyses performed on the inflight wind profiles provide detailed descriptions of the upper winds and an understanding of the profile characteristics, such as temporal and height variations, as well as indications of the frequency and the persistence of transient meteorological systems.

The synthetic type of wind profile is the oldest method used to present inflight design wind data. The synthetic wind profile data are presented in this document because this method of presentation provides a reasonable approach for most design studies when properly used, especially during the early design periods.

Also, the concept of synthetic wind profiles is generally understood and employed in most aerospace organizations for design computations. It should be understood that the synthetic wind profile includes the wind speed, wind speed change, maximum wind layer thickness, and gusts that are required to establish vehicle design values.

Currently, launch vehicles for use at various launch sites and in comprehensive space research missions and payload configurations are designed by use of synthetic vector wind and wind shear models with regard to specific wind directions. However, if a vehicle is not restricted to a given launch site, and flight azimuth and a specific configuration and mission, wind components (head, tail, left cross or right cross) are often used. Component wind profiles are sometimes used and for a given percentile, the magnitudes of component winds are equal to or less than those of the scalar winds. Component or directional dependent winds should not be employed in initial design studies unless specifically authorized by the cognizant design organization. Vector wind and vector wind shear models may be more applicable<sup>8</sup> and were used for the Space Shuttle vehicle.

Selection of a set of detailed wind profiles for final design verification and launch delay risk calculations requires the matching of vehicle simulation resolution and technique to frequency or information content of the profile. A detailed wind profile data set is available for Kennedy Space Center and Vandenberg AFB. Programs are currently underway to develop data sets for other test ranges. Detailed wind profile data sets for design verification use are for Kennedy Space Center, Florida, and Vandenberg AFB, California (see Section 2.4.12.1). Selected samples of detailed wind profiles are available for other locations.

The synthetic wind profile provides a conditionalized wind shear/gust state with respect to the given design wind speed. Therefore, in concept, the synthetic wind profile should produce a vehicle design which has a launch delay risk not greater than a specified value which is generally the value associated with the design wind speed. This statement, although generally correct, depends on the control system response characteristics, the vehicle structural integrity, etc. A joint condition of wind shear, gust, and speeds is given in design verification selection of detailed wind profiles. Therefore, the resulting launch delay risk for a given vehicle design is the specified value of risk computed from the vehicle responses associated with the various profiles. For the synthetic profile a vehicle inflight wind speed capability and maximum launch delay risk may be stated which is conditional upon the wind/gust design values. However, for the selection of detailed wind profiles only a vehicle launch risk value may be given, since the wind characteristics are treated as a joint condition. These two differences in philosophy should be understood to avoid misinterpretation of vehicle response calculation comparisons. In both cases allowance for dispersions in vehicle characteristics should be made prior to flight simulation through the wind profiles and establishment of vehicle design response or operational launch delay risk values. The objective is to insure that a space vehicle will accommodate the desired percentage of wind profiles or conditions in its non-nominal flight mode.

#### 2.4.2 Wind Aloft Climatology

The development of design wind speed profiles and associated shears and gusts requires use of the measured wind speed and wind direction data collected at the area of interest for some reasonably long period of time, i.e., 10 years or longer. The subject of wind climatology for an area, if treated in detail, would make up a voluminous document. The intent here is to give a brief treatment of selected topics that are frequently considered in space vehicle development and operations problems and provide references to more extensive information.

---

8. Considerable effort has been expended to formulate a vector wind and vector wind shear model for use in the Space Shuttle design and operational analysis studies. Reference should be made to Section 2.4.1 for more details on this subject.

Considerable data summaries (monthly and seasonal) exist on wind aloft statistics for the world. However, it is necessary to interpret these data in terms of the engineering design problem and design philosophy. For example, wind requirements for performance calculations relative to aircraft fuel consumption requirements must be derived for the specific routes and design reference period. Such data are available on request.

### 2.4.3 Wind Component Statistics

Wind component statistics are used in mission planning to provide information on the probability of exceeding a given wind speed in the pitch or yaw planes and to bias the tilt program at a selected launch time. The vector wind and vector wind shear model discussed in Section 2.4.11 is directly applicable to the description of these input data.

The wind component statistics are computed for various launch azimuths (15-degree intervals were selected at MSFC) for each month for the pitch plane (range) and yaw plane (cross range) at Kennedy Space Center and Vandenberg AFB, California. References 2.23 through 2.25 contain information on the statistical distributions of wind speeds and vector wind components for the various vehicle flight centers and test ranges.

#### 2.4.3.1 Upper Wind Correlations

Coefficients of correlations of wind components between altitude levels with means and standard deviations at altitude levels may be used in a statistical model to derive representative wind profiles. A method of preparing synthetic wind profiles by use of correlation coefficients between wind components is described in Reference 2.26. In addition, these correlation data are applicable to certain statistical studies of vehicle responses (Ref. 2.27).

Data on correlations of wind between altitude levels for various geographical locations are presented in References 2.28, 2.29, and 2.30. The reports give values of the interlevel and intralevel coefficients of linear correlations between wind components. Because of the occurrence of the regular increase of winds with altitude below and the decrease of winds above the 10- to 14-km level, the correlation coefficients decrease with greater altitude separation of the levels being correlated. Likewise, the highest correlation coefficients between components occur in the 10- to 14-km level.

Correlations between wind components separated by a horizontal distance are now becoming available. The reader is referred to the work of Buell (Refs. 2.31 and 2.32) for a detailed discussion of the subject.

#### 2.4.3.2 Thickness of Strong Wind Layers

Wind speeds in the middle latitudes generally increase with altitude to a maximum between 10- and 14-km. Above 14 km, the wind speeds decrease with altitude, then increase at higher altitude, depending upon season and location. Frequently, these winds exceed 50 m/sec in the jet stream, a core of maximum winds over the midlatitudes in the 10- to 14-km altitudes. The vertical extent of the core of maximum winds, or the sharpness of the extent of peak winds on the wind profile is important in some vehicle design studies. For information concerning the thickness of strong wind layers the reader is referred to Reference 2.33.

Table 2.4.1 shows design values of vertical thickness (based on maximum thickness) of the wind layers for wind speeds for Kennedy Space Center. Similar data for Vandenberg AFB are given in Table 2.4.2. At both ranges, the thickness of the layer decreases with increase of wind speed; that is, the sharpness of the wind profile in the vicinity of the jet core becomes more pronounced as wind speed increases.

TABLE 2.4.1 DESIGN THICKNESS FOR STRONG WIND LAYERS  
AT KENNEDY SPACE CENTER

Quasi-Steady-State Wind Speed ( $\pm 5 \text{ ms}^{-1}$ )	Maximum Thickness (km)	Altitude Range (km)
50	4	8.5 to 16.5
75	2	10.5 to 15.5
92	1	10.0 to 14.0

TABLE 2.4.2 DESIGN THICKNESS FOR STRONG WIND LAYERS AT  
VANDENBERG AFB, CALIFORNIA

Quasi-Steady-State Wind Speed ( $\pm 5 \text{ ms}^{-1}$ )	Maximum Thickness (km)	Altitude Range (km)
50	4	8.0 to 16
75	2	9.5 to 14

#### 2.4.3.3 Exceedance Probabilities

The probability of inflight winds exceeding or not exceeding some critical wind speed for a specified time duration may be of considerable importance in mission planning, and in many cases more information than just the occurrence of critical winds is desired. If a dual launch, with the second vehicle being launched 1 to 3 days after the first, is planned and if the launch opportunity extends over a 10-day period, what is the probability that winds below (or above) critical levels will last for the entire 10 days? What is the probability of 2 or 3 consecutive days of favorable winds in the 10-day period? Suppose the winds are favorable on the scheduled launch day, but the mission is delayed for other reasons. Now, what is the probability that the winds will remain favorable for 3 or 4 more days? Answers to these questions could also be used for certain design considerations involving specific vehicles prepared for a given mission and launch window. A body of statistics is available from the Atmospheric Sciences Division, which can be used to answer these and possibly other related questions. An example of the kind of wind persistence statistics that are available is given in Figure 2.4.1. This figure gives the probability of the maximum wind speed in the 10- to 15-km region being less than, equal to, or greater than 50 and 75  $\text{ms}^{-1}$ , as the case may be for various multiples of 12 hours for the month of January. Thus, for example, there is approximately an 18 percent chance that the wind speed will be greater than or equal to 50 m/sec for ten consecutive 12-hour periods in January.



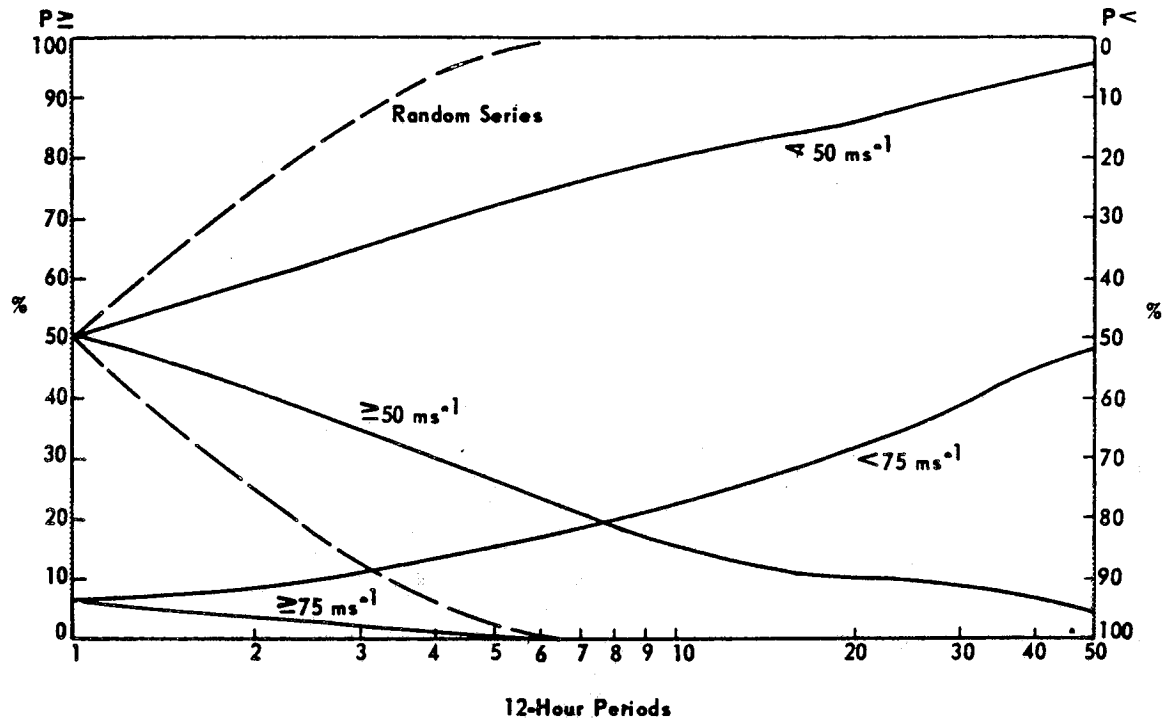


Figure 2.4.1 Probability of the maximum wind speed in the 10- to 15-km layer being less than, equal to, or greater than specified values for k-consecutive 12-hr periods during January at Kennedy Space Center.

#### 2.4.3.4 Design Scalar Wind Speeds (10-15 km Altitude Layer)

The distributions of design scalar wind speed in the 10- to 15-km altitude layer over the United States are shown in Figure 2.4.2 for the 95 percentile and Figure 2.4.3 for the 99 percentile values. The line of local maximum in the isopleths (maximum wind speeds) is shown by heavy lines with arrows. These winds occur at approximately the level of maximum dynamic pressure for most space vehicles.

#### 2.4.3.5 Temporal Wind Changes

Atmospheric wind fields change with time. Significant wind direction and speed changes can occur over time scales as short as a few minutes or less. There is no upper bound limit on the time scale over which the wind field can change. To develop real time wind biasing programs for space vehicle control purposes, which involve the use of wind profiles observed a number of hours prior to launch, it is necessary that consideration be given to the changes in wind speed and direction that can occur during the time elapsed from entering the biasing profile into the vehicle control system logic to the time of launch. Thus, for example, if the observed wind profile 8 hours prior to launch is to be used as a wind biasing profile, then consideration should be given to the dispersions in wind direction and speed that could occur over this period of time. Wind speed and direction change data are also useful for mission operation purposes. Results of studies conducted by the Atmospheric Sciences Division to define these dispersions in a statistical context are presented herein. Specialized data tapes containing pairs of FPS-16 Jimsphere measured detail wind profiles over time periods of 3 hours to 12 hours are available upon request to the Atmospheric Sciences Division.

To account for the differences between the dynamics of the flow in the atmospheric boundary layer and the free atmosphere, the atmosphere is usually partitioned at the 2-km level in studies of the temporal

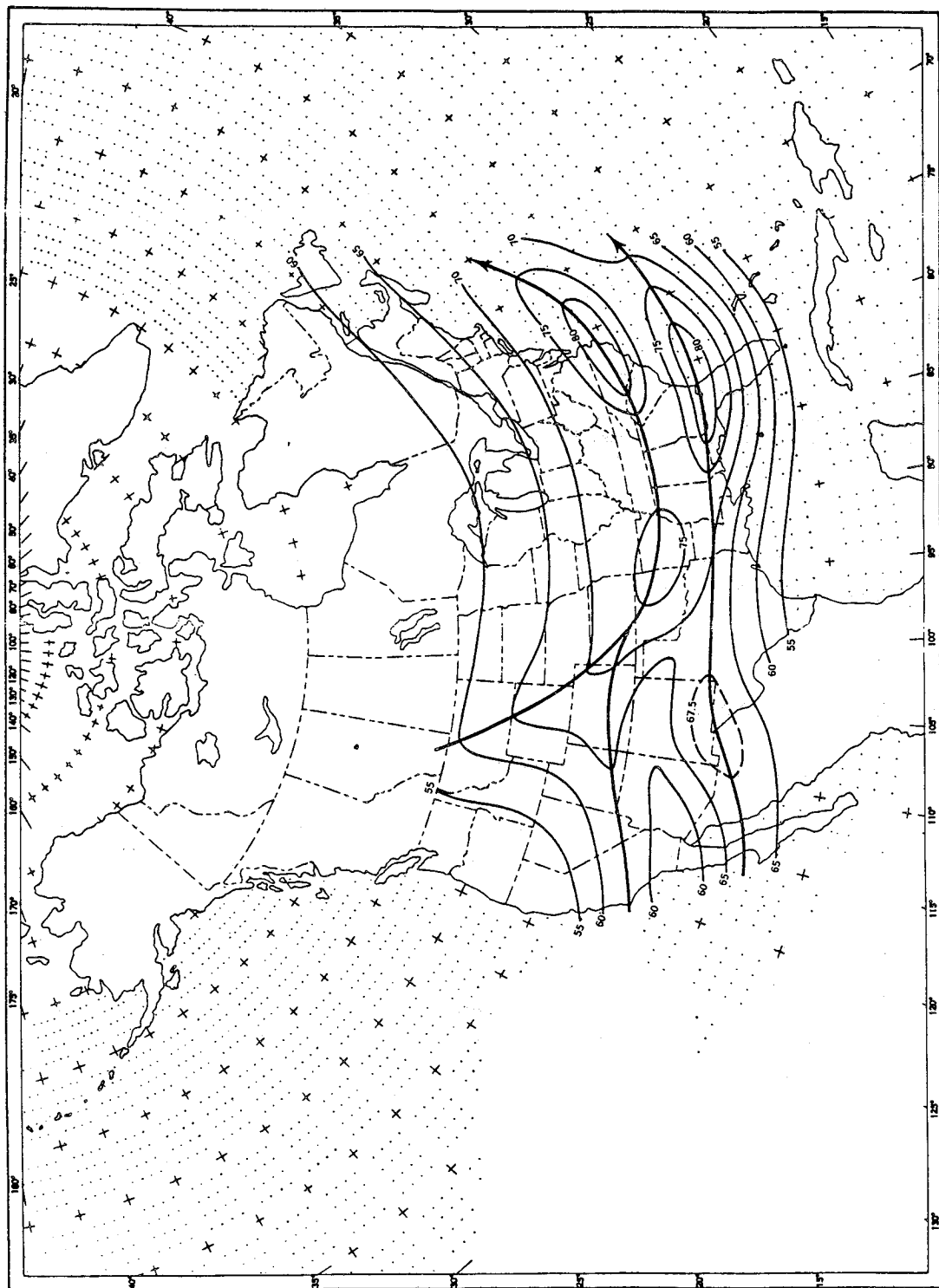


Figure 2.4.2 Design scalar wind speeds (m/sec) 95 percentile envelope analysis prepared from windiest month and maximum winds in the 10- to 15-km layer.

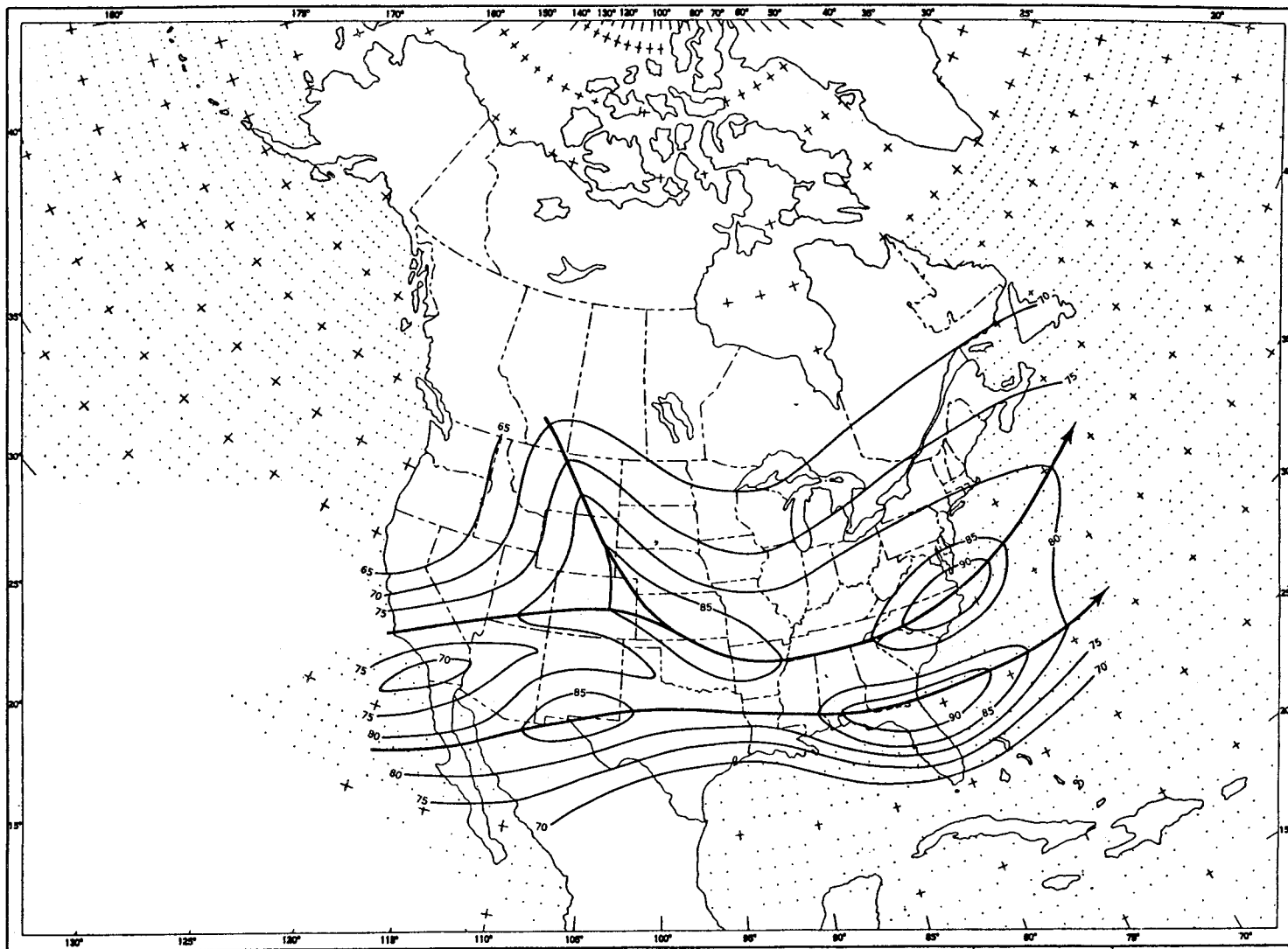


Figure 2.4.3 Design scalar wind speeds (m/sec) 99 percentile envelope analysis prepared from windiest month and maximum winds in the 10- to 15-km layer.

ORIGINAL PHOTO  
OF POOR QUALITY

changes in the wind field. Below the 2-km level the flow is significantly influenced by the surface of the Earth and is predominantly a turbulent one. In the free atmosphere above the 2-km level the flow is for all practical purposes free of the effects of the surface of the Earth.

Figures 2.4.4 and 2.4.5 contain idealized 99 percent wind direction and speed changes as a function of elapsed time and observed or reference wind speed for altitudes between 150 m and 2 km for Kennedy Space Center. The wind speed may increase or decrease from the reference profile value; thus, envelopes of each category are presented in Figure 2.4.5. Figures 2.4.6 and 2.4.7 are the idealized 99 percent wind direction and speed changes as a function of elapsed time and observed or reference wind speed for altitudes between 2 to 16 km.

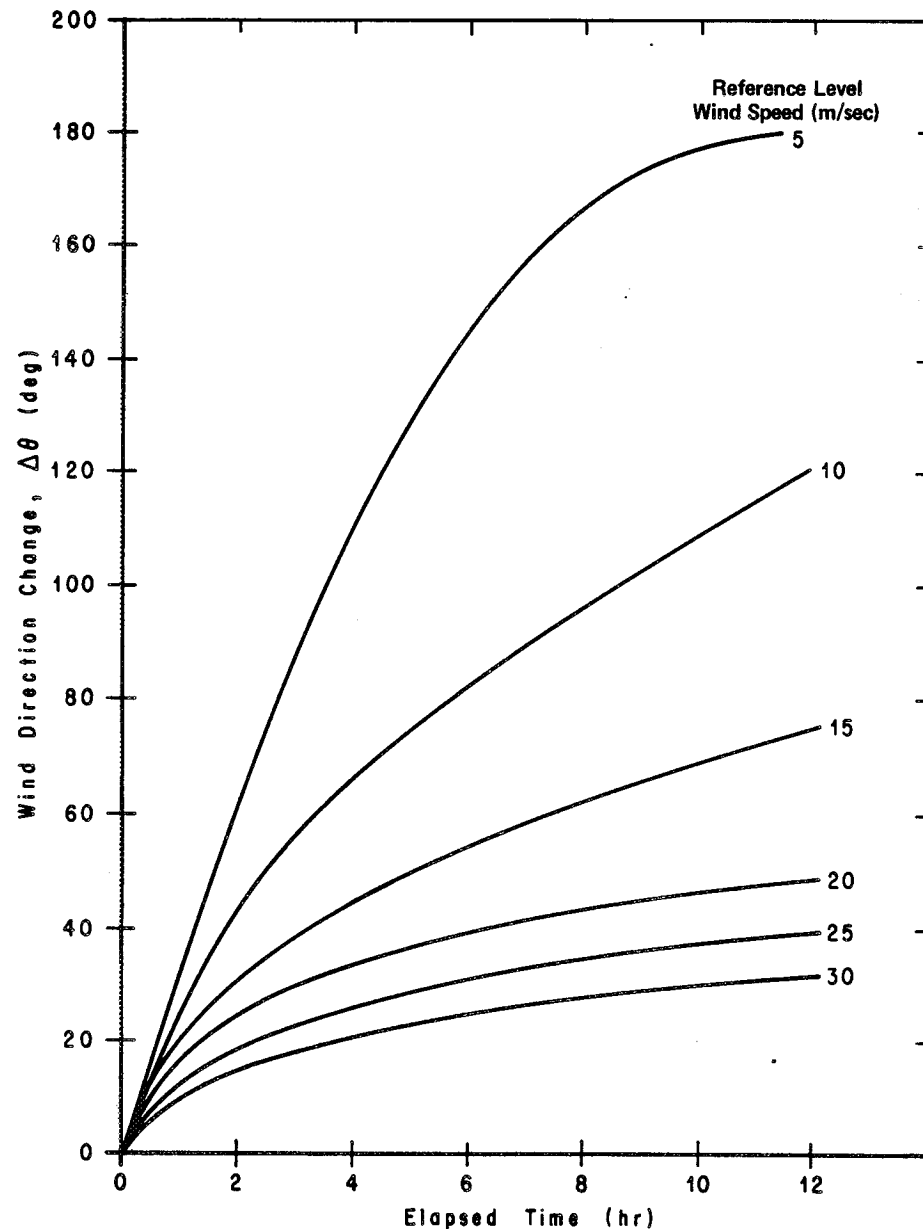


Figure 2.4.4 Idealized 99 percent wind direction change as a function of time and wind speed in the 150-m to 2-km altitude region of the Kennedy Space Center.

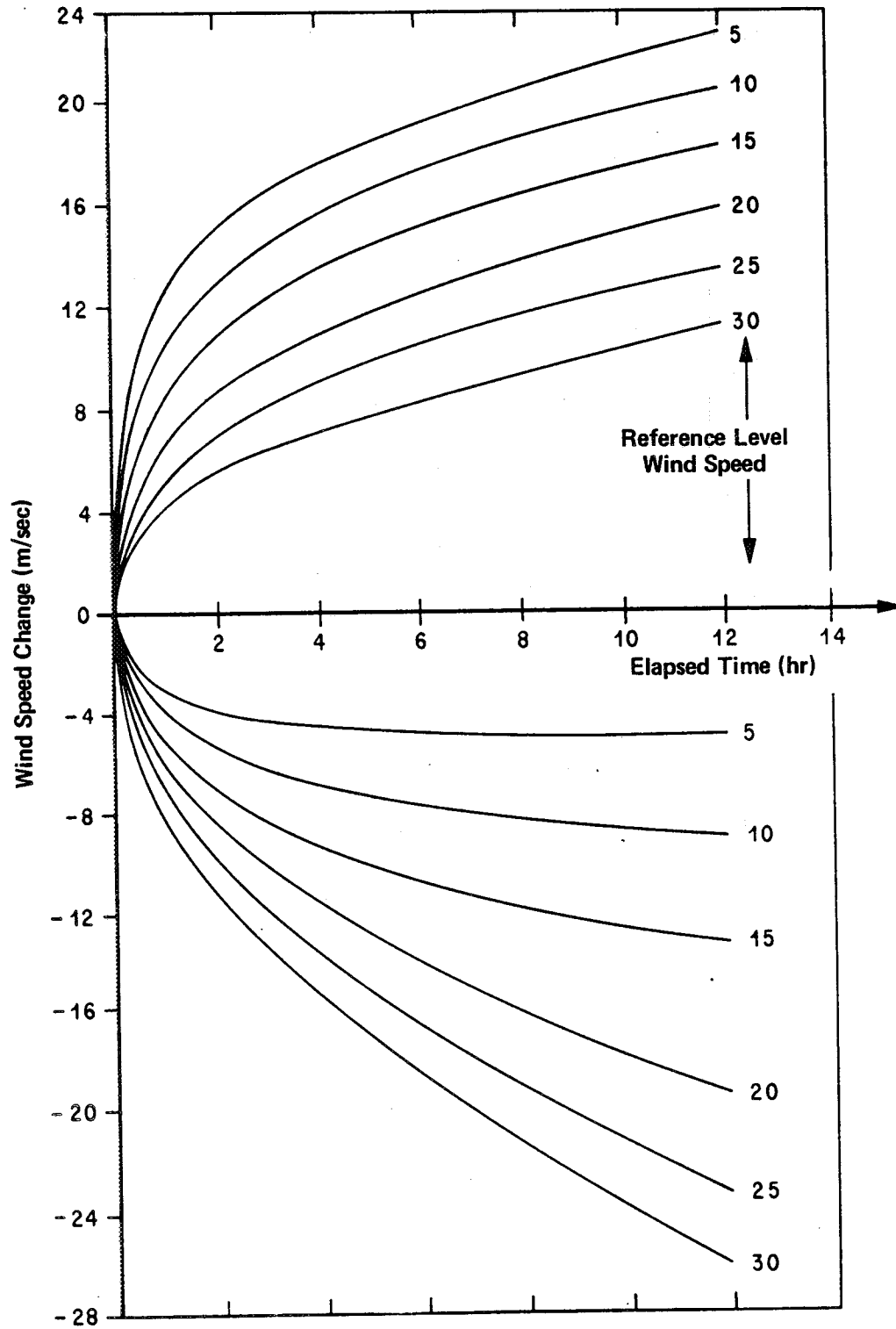


Figure 2.4.5 Idealized 99 percent wind speed change as a function of time and wind speed in the 150-m to 2-km altitude region of the Kennedy Space Center.

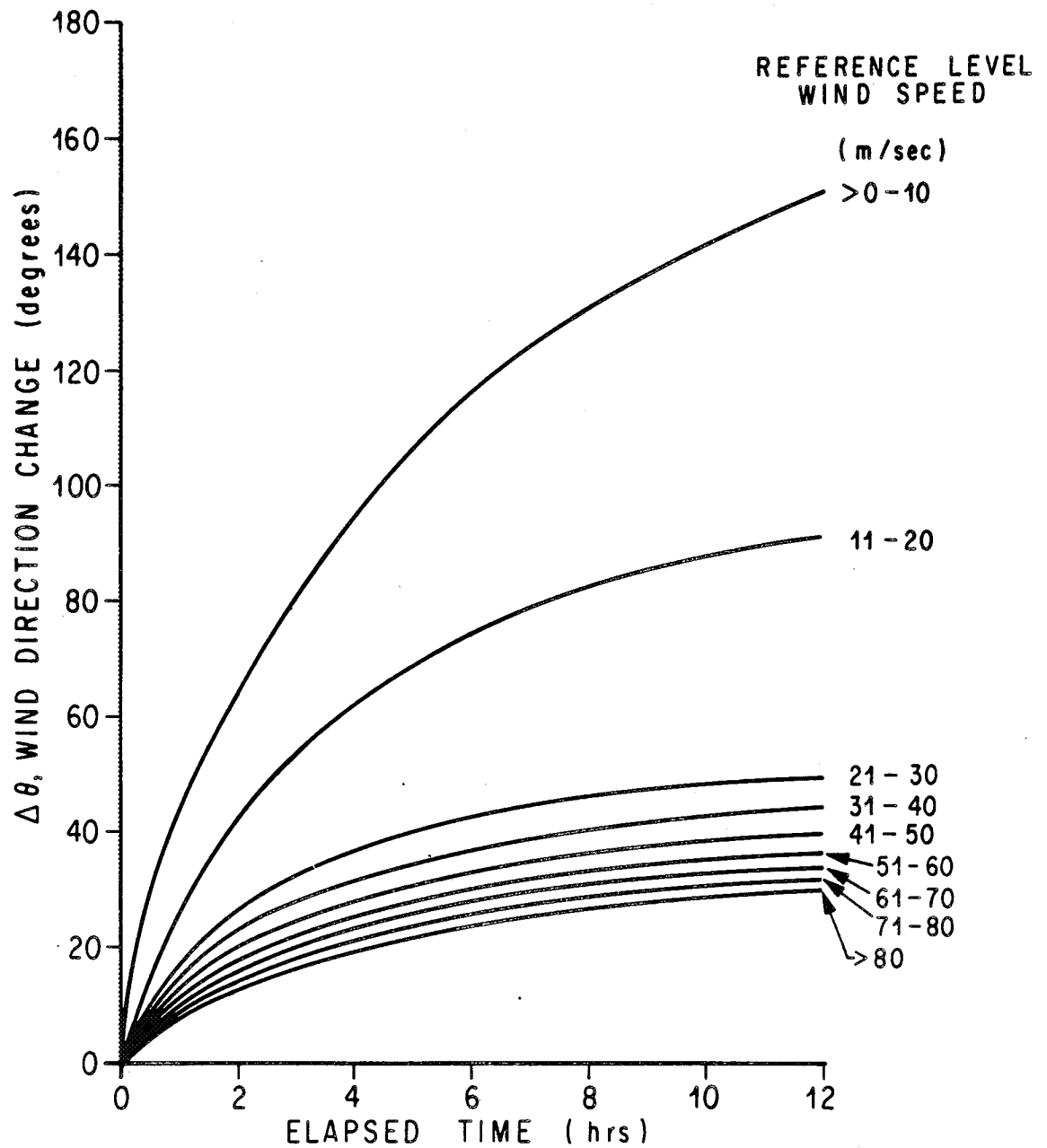
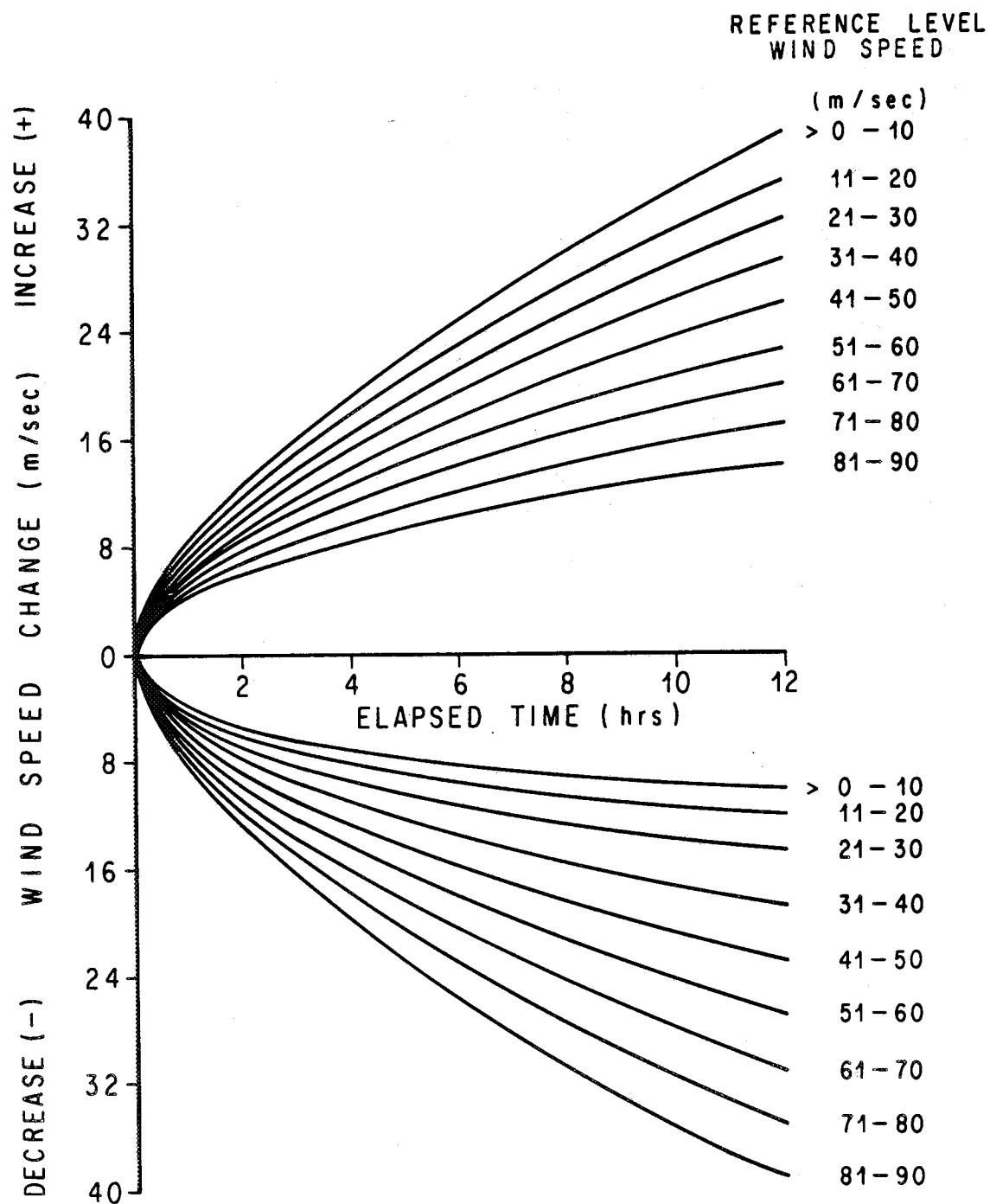
ORIGINAL PAGE IS  
OF POOR QUALITY

Figure 2.4.6 Idealized 99 percent wind direction change as a function of time and wind speed in the 2- to 16-km region of the Kennedy Space Center.



**Figure 2.4.7** Idealized 99 percent wind speed change as a function of time and wind speed in the 2- to 16-km region of the Kennedy Space Center.

A few cautionary statements regarding the preceding data are in order. They are applicable only to the Kennedy Space Center launch area because differences are known to exist in the data with the geographical sites. Conclusions should not be drawn relative to frequency content and phase relationships of the wind profile since the data given herein provide only envelope conditions for ranges of speed and direction changes. Direction correlations have not been developed between the changes of wind direction and wind speed.

Additional information concerning wind speed and direction changes can be found in reports by Camp and Susko (Ref. 2.34) and Camp and Fox for Santa Monica (Ref. 2.35).

Temporal vector wind change at Kennedy Space Center (KSC), Florida, and Vandenberg Air Force Base (VAFB), California, has been studied by Adelfang (Refs. 2.36 and 2.37). The joint distribution of the four variables represented by the  $u$  and  $v$  components of the wind vector at an initial time and after a specified elapsed time is hypothesized to be quadrivariate normal. The fourteen statistics of this distribution are presented according to monthly reference period for altitudes from 0 to 27 km. These statistics are used to calculate percentiles of the theoretical distribution of wind component change with respect to time (univariate normal distribution), the joint distribution of wind component change (bivariate normal), the modulus of vector wind change (Rayleigh), and the vector wind at a future time given the vector wind at an initial time (conditional bivariate normal); the large body of statistics contained in these references are not repeated herein. For the purpose of illustrating the application of these statistics, the 95 percentile vector wind change ellipses for time intervals of 12, 24, 36, 48, 60, and 72 hr at 6, 12, and 18 km during April at KSC and during January at VAFB have been calculated. Each ellipse illustrated in Figure 2.4.8 was calculated from the bivariate normal statistics of vector wind change given in the referenced reports; each ellipse encompasses 95 percent of the wind change expected for the indicated time interval. The methodology for calculation of wind or wind change ellipses for any percentile is described by Smith (Ref. 2.38). The wind change ellipses illustrated in Figure 2.4.8 clearly indicate: the strong variation of wind change with altitude at both locations, the larger wind changes at VAFB, and the relatively small increase in wind change for time intervals greater than 36 hr.

#### 2.4.4 Wind Speed Profiles for Biasing Tilt Program

In attempting to maintain a desired flight path for a space vehicle through a strong wind region, the vehicle control system could introduce excessive bending moments and orbit anomalies. To reduce this problem, it is sometimes desirable to wind bias the pitch program; that is, to tilt the vehicle sufficiently to produce the desired flight path and minimize maximum dynamic pressure level loads with the expected wind profile. Since most inflight strong winds over Kennedy Space Center are winter westerlies, it is sometimes expedient to use the monthly or seasonal pitch plane median wind speed profile for bias analyses.

Head and tail wind components and right and left crosswind components from 0- to 70-km altitudes were computed for every 15 degrees of flight azimuth for the Kennedy Space Center launch area and were published by NASA (Refs. 2.24 and 2.25). Similar calculations for other ranges are available upon request.

It is not usually necessary to bias the vehicle in the yaw plane because of the flight azimuths normally used at Kennedy Space Center and Vandenberg Air Force Base. For applications where both pitch and yaw biasing are used, monthly vector mean winds may be more efficient for wind biasing. Such statistics will be made available upon request or see Reference 2.38 and Section 2.4.11.



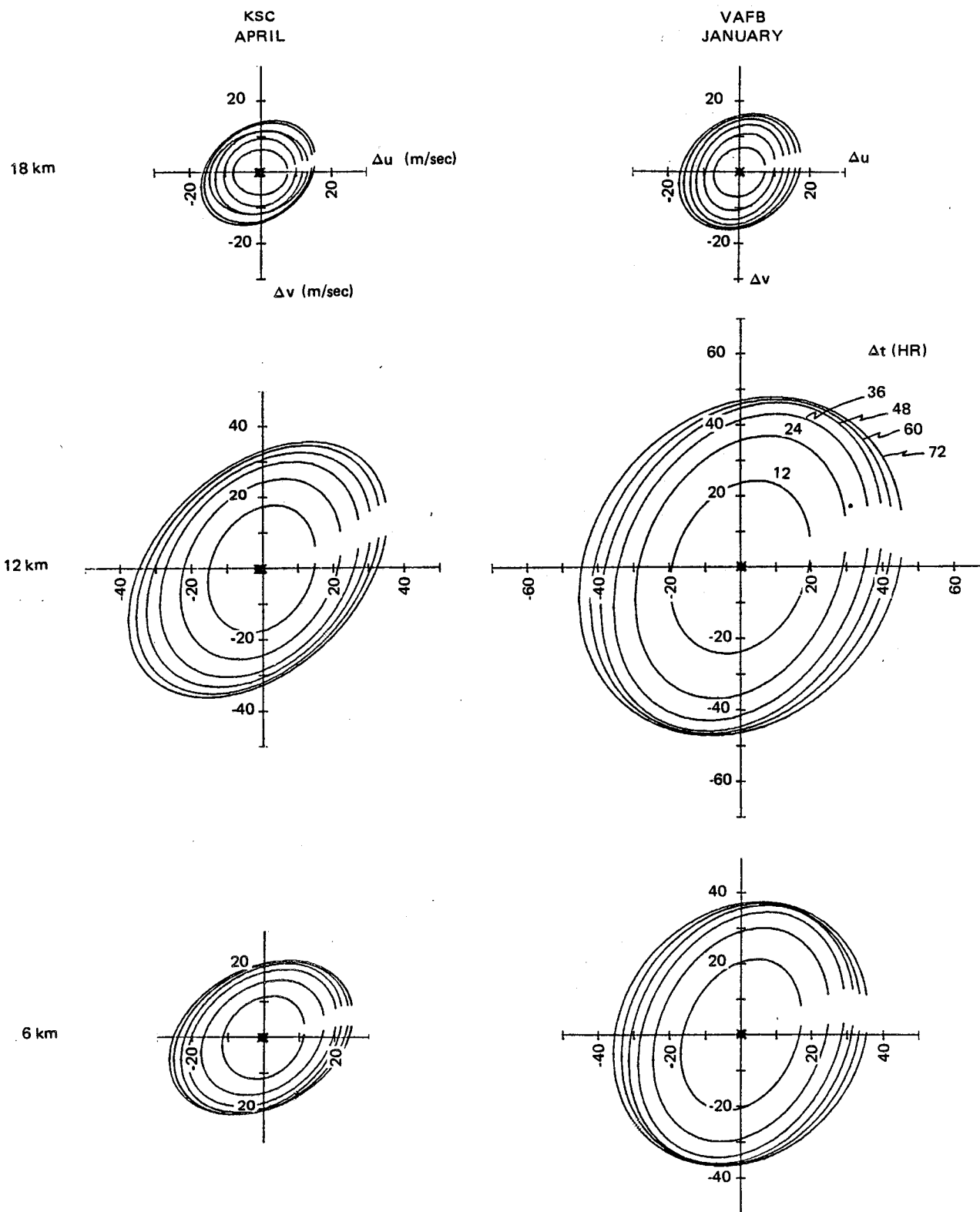


Figure 2.4.8 April KSC and January VAFB 95 percentile wind change ( $\Delta u$  and  $\Delta v$ ) ellipses at 6, 12, and 18 km for time intervals of 12, 24, 36, 48, 60, and 72 hr.

#### 2.4.5 Design Wind Speed Profile Envelopes

The wind data given in Section 2.4.5.1 are not expected to be exceeded by the given percentage of time (time as related to the observational interval of the data sample) based upon the windiest monthly reference period. To obtain the profiles, monthly frequency distributions are combined for each percentile level to give the envelope over all months. The profiles represent horizontal wind flow referenced to the Earth's surface. Vertical wind flow is negligible except for that associated with gusts or turbulence. The scalar wind speed envelopes are normally applied without regard to flight directions to establish the initial design requirements. Directional wind criteria for use with the synthetic wind profile techniques should be applied with care and specific knowledge of the vehicle mission and flight path, since severe wind constrain could result for other flight paths and missions.

##### 2.4.5.1 Scalar Wind Speed Envelopes<sup>9</sup>

Scalar wind speed profile envelopes are presented in Tables 2.4.3 through 2.4.6 and Figures 2.4.9 through 2.4.12. These are idealized steady-state scalar wind speed profile envelopes for four active or potential operational space vehicle launch or landing sites; i.e., Kennedy Space Center, Florida; Vandenberg AFB California; White Sands Missile Range, New Mexico; and Edwards Air Force Base, California. Table 2.4.7 and Figure 2.4.13 envelope the 95 and 99 percentile steady-state scalar wind speed profile envelopes from the same four locations. They are applicable for design criteria when initial design or operational capability has not been restricted to a specific launch site or may involve several geographical locations. However, if the specific geographical location for application has been determined as being near one of the four referenced sites then the relevant data should be applied.

This section provides design nondirectional wind data for various percentiles; therefore, the specific percentile wind speed envelope applicable to design should be specified in the appropriate space vehicle specification documentation. For engineering convenience the design wind speed profile envelopes are given as linear segments between altitude levels; therefore, the tabular values are connected, when graphed, by straight lines between the points.

#### 2.4.6 Wind Speed Change Envelopes

This section provides representative information on wind speed change (shear) for scales of distance  $\Delta H \leq 5000$  m. Wind speed change is defined as the total magnitude (speed) change between the wind vector at the top and bottom of a specified layer, regardless of wind direction. Wind shear is the wind speed change divided by the altitude interval. When applied to space vehicle synthetic wind profile criteria, it is frequently referred to as a wind buildup or back-off rate depending upon whether it occurs below (buildup) or above (back-off) the reference height of concern. Thus, a buildup wind value is the change in wind speed which a vehicle may experience while ascending vertically through a specified layer to the known altitude. Back-off magnitudes describe the speed change which may be experienced above the chosen level. Both buildup and back-off wind speed change data are presented in this section as a function of reference level wind vector

- 
9. This section and several others that follow present data and instructions relative to the development and use of scalar synthetic wind profiles in aerospace vehicle design analyses and related studies. In many cases these will prove adequate for preliminary design investigations. However, a vector synthetic wind profile design input may prove more adequate when a more realistic synthetic wind profile input is desirable. The reader should consult Section 2.4.11 for more details on vector wind and vector wind shear models. In either case, the most realistic test of an aerospace vehicle performance is flight simulation through detailed wind profile data sets (see Section 2.4.12.1).

TABLE 2.4.3 SCALAR WIND SPEED  $V$  (m/sec) STEADY-STATE ENVELOPES AS FUNCTIONS OF ALTITUDE  $H$  (km) FOR VARIOUS PROBABILITIES  $P$  (%) FOR KENNEDY SPACE CENTER

Altitude	Percentile				
	(km)	50	75	90	95
1	8	13	16	19	24
6	23	31	39	44	52
11	43	55	66	73	88
12	45	57	68	75	92
13	43	56	67	74	86
20	7	12	17	20	25
23	7	12	17	20	25
40	43	57	70	78	88
50	75	83	91	95	104
58	85	96	106	112	123
60	85	96	106	112	123
75	15	22	28	30	37
80	15	22	28	30	37

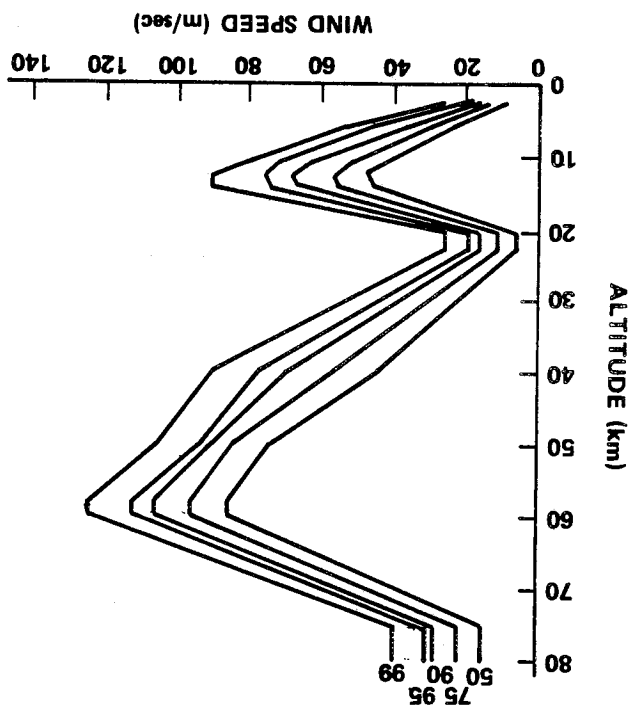


Figure 2.4.9 Scalar wind speed profile envelopes, steady-state, for Kennedy Space Center.

TABLE 2.4.4 SCALAR WIND SPEED  $V$ (m/sec) STEADY-STATE ENVELOPES AS FUNCTIONS OF ALTITUDE  $H$  (km) FOR VARIOUS PROBABILITIES  $P$  (%) FOR VANDENBERG AFB, CALIFORNIA

Altitude (km)	Percentile				
	50	75	90	95	99
1	7	10	13	15	19
6	20	29	36	41	50
10	31	43	53	60	73
11	32	44	55	62	79
12	32	44	55	62	79
20	6	10	14	17	26
23	6	10	14	17	26
40	55	67	82	90	105
50	79	96	111	120	132
58	83	107	128	140	164
60	83	107	128	140	164
75	50	65	87	98	118
80	50	65	87	98	118

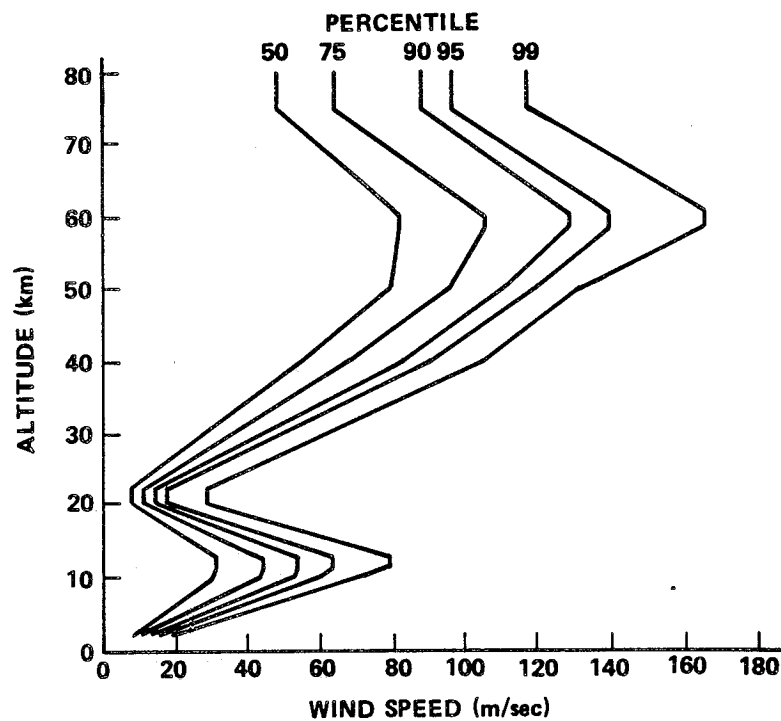


Figure 2.4.10 Scalar wind speed profile envelopes; steady-state for Vandenberg AFB, California.

TABLE 2.4.5 SCALAR WIND SPEED  $V$  (m/sec) STEADY-STATE ENVELOPES AS FUNCTIONS OF ALTITUDE  $H$  (km) FOR VARIOUS PROBABILITIES  $P$  (%) FOR WHITE SANDS MISSILE RANGE

P = 50		P = 75		P = 90		P = 95		P = 99	
H	V	H	V	H	V	H	V	H	V
1	4	1	7	1	11	1	13	1	22
2	5	2	8	2	12	2	15	2	22
						7	50	7	68
		9	45	8	49	9	67	9	88
11	42	10	53	11	71	11	76		
13	42	12	55	13	63	12	78	14	88
				15	45	15	52	15	69
20	10	20	14	20	20	20	24	20	41
23	10	23	14	23	20	23	24	23	41
50	85	50	104	50	120	50	130	50	150
60	85	60	104	60	120	60	130	60	150
75	60	75	77	75	93	75	102	75	120
80	60	80	77	80	93	80	102	80	120

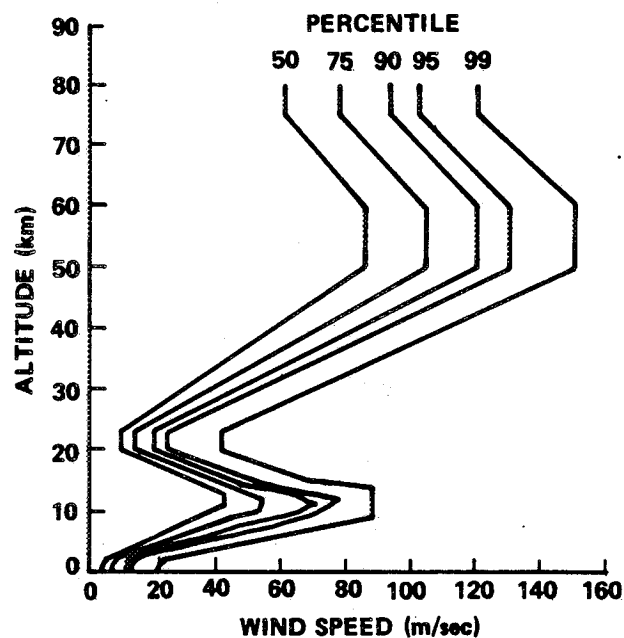


Figure 2.4.11 Scalar wind speed profile envelopes, steady state, for White Sands Missile Range.

TABLE 2.4.6 SCALAR WIND SPEED  $V$  (m/sec) STEADY-STATE ENVELOPES AS FUNCTIONS OF ALTITUDE  $H$  (km) FOR VARIOUS PROBABILITIES  $P$  (%) FOR EDWARDS AIR FORCE BASE

P = 50		P = 75		P = 90		P = 95		P = 99	
H	V	H	V	H	V	H	V	H	V
1	8	1	11	1	16	1	17	1	25
2	8	2	12	2	16	2	18	2	28
				5	30	5	36	5	56
10	29			10	51	10	61	10	77
12	32	11	44	11	56			12	77
15	25	13	39	12	56	12	61	14	65
18	13	17	21	17	28	16	38	16	43
20	9	20	13	20	19	20	23	20	30
23	9	23	13	23	19	23	23	23	30
50	85	50	104	50	120	50	130	50	150
60	85	60	104	60	120	60	130	60	150
75	60	75	77	75	93	75	102	75	120
80	60	80	77	80	93	80	102	80	120

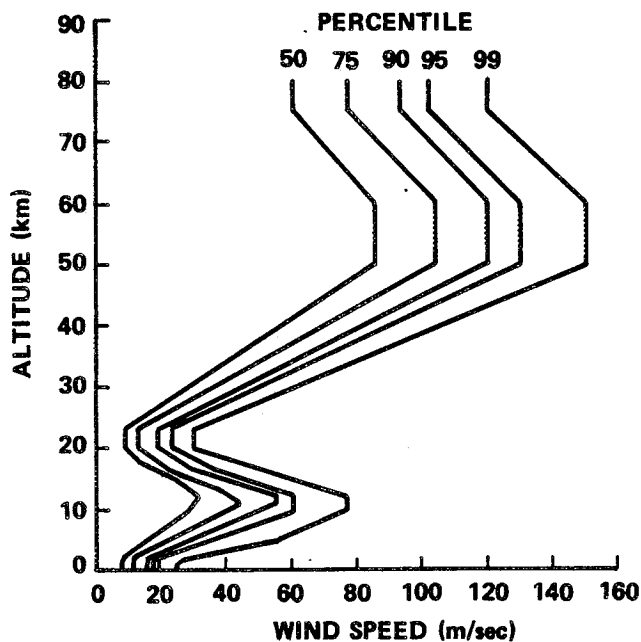


Figure 2.4.12 Scalar wind speed profile envelopes, steady state, for Edwards Air Force Base.

TABLE 2.4.7 SCALAR WIND SPEED  $V$  (m/sec) STEADY-STATE ENVELOPES AS FUNCTIONS OF ALTITUDE  $H$  (km) FOR TWO PROBABILITIES  $P$  (%) ENCOMPASSING ALL FOUR LOCATIONS

P = 95				P = 99			
H	V	H	V	H	V	H	V
1	22	17	44	1	28	15	70
3	31	20	29	3	38	20	41
		23	29	5	56	23	41
6	54	50	150	6	60	50	170
		60	150	7	68	60	170
10	75	75	120	9	88	75	135
11	76	80	120	11	88	80	135
12	78			12	92		
13	74			13	88		
				14	88		

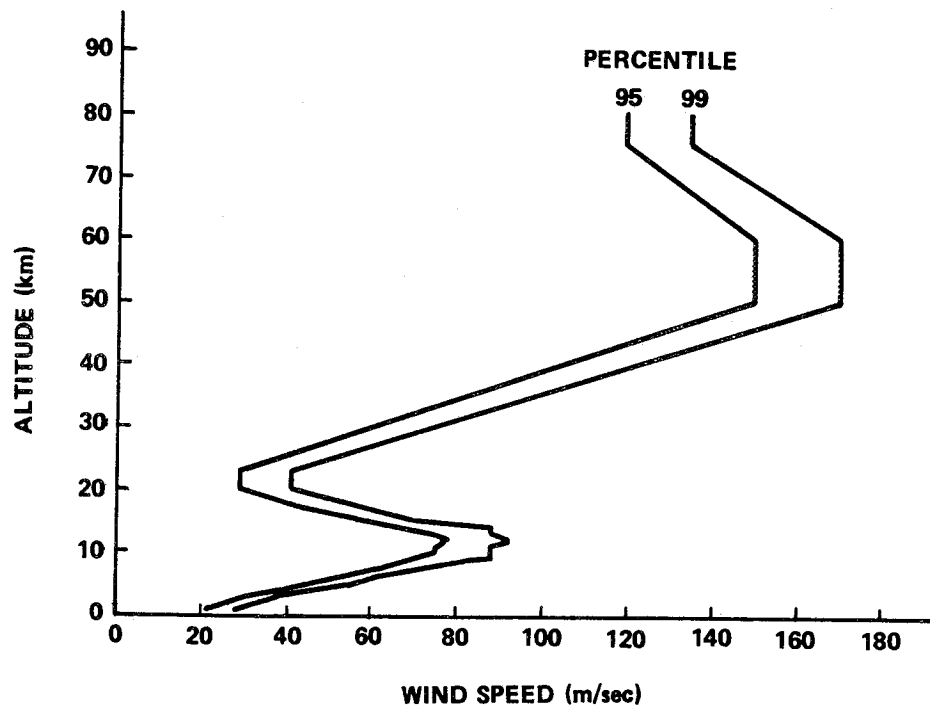


Figure 2.4.13 Scalar wind speed profile envelopes, steady state for all four locations.

magnitude and geographic location. Wind buildup or back-off may be determined for a vehicle with other than a vertical flight path by multiplying the wind speed change by the cosine of the angle between the vertical axis and the vehicle trajectory. Wind shears for scales of distance  $\Delta H \geq 1000$  m thickness are computed from rawinsonde and rocketsonde observations, while the small-scale shears associated with scales of distance  $\Delta H < 1000$  m are computed from a relationship developed by Fichtl (Ref. 2.39) based on experimental results from FPS-16 radar/Jimsphere balloon wind sensor measurements of the detail wind profile structure. This relationship states that the back-off or buildup wind shear  $\Delta u$  for  $\Delta H < 1000$  m for a given risk of exceedance is related to the  $\Delta H = 1000$  m shear,  $(\Delta u)_{1000}$ , at the same risk of exceedance, through the expression

$$\Delta u = (\Delta u)_{1000} \left( \frac{\Delta H}{1000} \right)^{0.7}, \quad (2.26)$$

where  $\Delta H$  has units of meters.

An envelope of the 99 percentile wind speed buildup is used currently in constructing synthetic wind profiles. For most design studies, the use of this 99 percentile scalar buildup wind shear data is warranted. The envelopes for back-off shears have application to certain design studies and should be considered where appropriate. These envelopes are not meant to imply perfect correlation between shears for the various scales of distance; however, certain correlations do exist, depending upon the scale of distance and the wind speed magnitude considered. This method of describing the wind shear for vehicle design has proven to be especially acceptable in preliminary design studies since the dynamic response of the structure or control system of a vehicle is essentially influenced by specific wavelengths as represented by a given wind shear. Construction of synthetic profiles for vehicle design applications is described in Section 2.4.9.

Wind speed change (shear) statistics for various locations differ primarily because of prevailing meteorological conditions, orographic features, and data sample size. Significant differences, especially from an engineering standpoint, are known to exist in the shear profiles for different locations. Therefore, consistent vehicle design shear data representing five active or potentially operational space vehicle launch or landing sites are presented in Tables 2.4.8 through 2.4.15; i.e., for Kennedy Space Center, Vandenberg AFB, White Sands Missile Range, and Edwards Air Force Base. Tables 2.4.16 and 2.4.17 envelope the 99 percentile shears from these four locations. They are applicable for design criteria when initial design or operational capability has not been restricted to a specific launch site or may involve several geographical locations. However, if the specific geographic location for application has been determined as being near one of the four referenced sites, then the relevant data should be applied. Equation (2.26) was used to construct Tables 2.4.8 through 2.4.17 for scales of distance.

#### 2.4.7 Wind Direction Change Envelopes

This section provides representative information on wind direction change  $\Delta \theta$  for scales of distance  $\Delta H \leq 4$  km. Wind direction change is defined as the total change in direction of wind vectors at the top and bottom of a specified layer. Wind direction changes can occur above or below a reference point in the atmosphere. As in the case of the wind speed changes in Section 2.4.6, we will call changes below the reference level buildup wind changes and those above the reference level back-off wind direction changes. These changes can be significantly different. For example, if the reference point is at the 4-km level, the buildup changes between the 1- and 4-km levels will be distinctly different from the back-off changes between the



TABLE 2.4.8 BUILDUP DESIGN ENVELOPES OF 99 PERCENTILE WIND SPEED CHANGE,  
1- TO 80-km ALTITUDE REGION, KENNEDY SPACE CENTER

Wind Speed at Reference Altitude (m/sec)	Scales of Distance (m)									
	5000	4000	3000	2000	1000	800	600	400	200	100
> 90	65.6	59.5	52.3	43.5	34.0	29.0	23.8	17.9	11.2	6.8
= 80	60.4	55.5	49.7	42.0	32.7	27.7	22.7	17.0	10.6	6.5
= 70	56.0	51.7	47.0	40.4	31.2	26.6	21.8	16.4	10.1	6.2
= 60	51.3	48.5	44.5	38.6	30.0	25.6	21.1	15.8	9.8	6.0
= 50	46.5	45.0	41.2	36.5	28.5	24.4	20.0	15.0	9.2	5.7
= 40	38.5	37.7	36.8	34.9	26.5	22.6	18.5	13.8	8.6	5.3
= 30	28.0	27.5	26.5	24.5	20.8	17.8	14.5	10.8	6.7	4.1
= 20	17.6	17.3	16.6	15.8	14.6	12.5	10.2	7.2	4.7	2.9

TABLE 2.4.9 BACK-OFF DESIGN ENVELOPES OF 99 PERCENTILE WIND SPEED CHANGE,  
1- TO 80-km ALTITUDE REGION, KENNEDY SPACE CENTER

Wind Speed at Reference Altitude (m/sec)	Scales of Distance (m)									
	5000	4000	3000	2000	1000	800	600	400	200	100
> 90	77.5	74.4	68.0	59.3	42.6	36.4	29.7	22.4	13.8	8.5
= 80	71.0	68.0	63.8	56.0	40.5	34.7	28.5	21.4	13.2	8.1
= 70	63.5	61.0	57.9	52.0	38.8	33.1	27.0	20.3	12.5	7.7
= 60	56.0	54.7	52.3	47.4	36.0	31.0	25.3	18.9	11.7	7.2
= 50	47.5	47.0	46.2	43.8	33.0	28.3	23.2	17.5	10.7	6.6
= 40	39.0	38.0	37.0	35.3	29.5	25.3	20.6	15.5	9.6	5.9
= 30	30.0	30.0	29.4	26.9	22.6	19.4	15.8	11.9	7.3	4.5
= 20	18.0	17.5	16.7	15.7	14.2	12.2	9.9	7.5	4.6	2.8

TABLE 2.4.10 BUILDUP DESIGN ENVELOPES OF 99 PERCENTILE WIND SPEED CHANGE,  
1- TO 80-km ALTITUDE REGION, VANDENBERG AFB

Wind Speed at Reference Altitude (m/sec)	Scales of Distance (m)									
	5000	4000	3000	2000	1000	800	600	400	200	100
> 90	62.1	59.9	57.8	51.5	35.2	30.1	24.6	18.4	11.5	7.0
= 80	58.7	57.7	55.6	48.8	33.5	29.0	23.6	17.8	11.0	6.7
= 70	55.0	54.5	53.4	48.1	33.0	28.8	23.0	16.8	10.5	6.5
= 60	50.4	49.9	49.0	44.0	32.7	27.9	22.8	16.2	9.7	5.3
= 50	45.4	44.8	43.7	40.0	29.9	25.4	21.8	15.6	9.2	5.0
= 40	38.9	38.7	37.2	34.9	25.1	22.4	19.1	14.9	8.8	4.7
= 30	30.0	29.4	28.3	25.4	19.9	17.8	14.8	11.5	7.1	4.2
= 20	20.0	19.8	19.5	18.4	15.0	13.1	10.9	8.0	4.7	2.6

TABLE 2.4.11 BACK-OFF DESIGN ENVELOPES OF 99 PERCENTILE WIND SPEED CHANGE,  
1- TO 80-km ALTITUDE REGION, VANDENBERG AFB

Wind Speed at Reference Altitude (m/sec)	Scales of Distance (m)									
	5000	4000	3000	2000	1000	800	600	400	200	10
> 90	66.9	62.5	57.7	49.9	37.5	32.1	26.1	19.7	12.0	7.
= 80	64.1	60.8	56.6	48.3	36.9	31.5	25.6	19.1	11.6	6.
= 70	62.0	59.2	54.8	47.1	36.0	31.0	25.0	18.6	11.2	6.
= 60	57.1	54.5	51.3	45.4	32.6	28.5	23.0	17.1	10.2	5.
= 50	49.6	47.8	45.7	42.1	30.1	25.9	20.8	15.5	9.2	5.
= 40	39.4	38.8	37.9	35.5	25.9	23.5	19.6	14.0	8.2	4.
= 30	29.9	29.3	28.3	26.3	20.5	18.6	15.8	12.2	8.0	4.
= 20	19.8	19.5	19.0	17.7	13.4	12.2	10.7	9.0	6.3	4.

TABLE 2.4.12 BUILDUP DESIGN ENVELOPES OF 99 PERCENTILE WIND SPEED CHANGE,  
1- TO 80-km ALTITUDE REGION, WHITE SANDS MISSILE RANGE

Wind Speed at Reference Altitude (m/sec)	Scales of Distances (m)									
	5000	4000	3000	2000	1000	800	600	400	200	10
> 90	70.7	67.0	61.2	52.4	42.0	36.0	29.4	22.1	13.6	8.
= 80	66.0	63.0	57.7	50.0	40.2	34.5	28.1	21.2	13.0	8.
= 70	60.2	57.0	53.0	46.5	38.0	32.6	26.6	20.0	12.3	7.
= 60	52.4	50.0	46.5	42.3	35.5	30.5	24.9	18.7	11.5	7.
= 50	44.8	43.0	40.2	36.5	32.0	28.3	23.1	17.4	10.7	6.
= 40	36.4	35.3	33.8	31.0	27.5	23.6	19.3	14.5	8.9	5.
= 30	27.4	26.5	25.6	24.3	20.6	17.7	14.4	10.8	6.7	4.
= 20	18.4	17.7	17.3	16.5	15.0	12.9	10.5	7.9	4.9	3.

TABLE 2.4.13 BACK-OFF DESIGN ENVELOPES OF 99 PERCENTILE WIND SPEED CHANGE,  
1- TO 80-km ALTITUDE REGION, WHITE SANDS MISSILE RANGE

Wind Speed at Reference Altitude (m/sec)	Scales of Distance (m)									
	5000	4000	3000	2000	1000	800	600	400	200	10
> 90	66.2	62.0	57.0	50.0	37.0	31.7	25.9	19.5	12.0	7.
= 80	62.0	58.5	54.0	48.0	35.8	30.7	25.1	18.9	11.6	7.
= 70	57.5	54.5	50.7	44.3	34.2	29.3	23.9	18.0	11.1	6.
= 60	52.6	49.2	45.5	40.5	32.8	28.1	23.0	17.3	10.6	6.
= 50	45.0	42.8	40.1	37.0	31.0	26.6	21.7	16.3	10.0	6.
= 40	36.5	35.5	34.8	33.5	29.3	25.1	20.5	15.4	9.5	5.
= 30	27.4	27.0	26.4	24.8	22.0	19.3	15.8	11.8	7.3	4.
= 20	17.7	17.3	16.7	15.8	14.1	12.1	9.9	7.4	4.6	2.

TABLE 2.4.14 BUILDUP DESIGN ENVELOPES OF 99 PERCENTILE WIND SPEED CHANGE,  
1- TO 80-km ALTITUDE REGION, EDWARDS AIR FORCE BASE

Wind Speed at Reference Altitude (m/sec)	Scales of Distance (m)									
	5000	4000	3000	2000	1000	800	600	400	200	100
> 90	69.0	65.0	59.5	52.0	39.5	33.9	27.7	20.8	12.8	7.9
= 80	64.9	61.8	56.9	50.0	38.2	32.8	26.7	20.1	12.4	7.6
= 70	59.0	57.0	53.0	46.8	37.0	31.7	25.9	19.5	12.0	7.4
= 60	51.8	50.4	47.8	43.6	35.5	30.5	24.9	18.7	11.5	7.1
= 50	44.8	43.6	41.3	38.2	31.8	27.5	22.4	16.9	10.4	6.4
= 40	36.5	35.5	34.3	32.0	26.5	23.0	18.8	14.1	8.7	5.3
= 30	28.0	27.3	26.3	24.5	20.8	17.8	14.6	11.0	6.7	4.2
= 20	18.0	17.7	17.4	16.7	15.2	13.0	10.6	8.0	4.9	3.0

TABLE 2.4.15 BACK-OFF DESIGN ENVELOPES OF 99 PERCENTILE WIND SPEED CHANGE,  
1- TO 80-km ALTITUDE REGION, EDWARDS AIR FORCE BASE

Wind Speed at Reference Altitude (m/sec)	Scales of Distance (m)									
	5000	4000	3000	2000	1000	800	600	400	200	100
> 90	75.2	72.0	67.3	59.0	42.8	36.7	30.2	22.5	13.9	8.5
= 80	68.0	66.3	62.5	55.5	40.8	35.0	28.6	21.5	13.2	8.1
= 70	60.4	59.0	56.8	51.4	38.7	33.2	27.0	20.4	12.5	7.7
= 60	53.0	51.8	49.3	45.0	36.0	30.9	25.2	19.0	11.7	7.2
= 50	44.5	43.3	41.5	38.4	32.0	27.5	22.4	16.9	10.4	6.4
= 40	35.7	35.3	34.5	33.0	27.0	23.2	18.9	14.2	8.8	5.4
= 30	27.1	27.0	26.9	26.3	21.4	18.4	15.0	11.3	6.9	4.3
= 20	18.0	17.0	16.6	15.7	14.2	12.2	9.9	7.5	4.6	2.8

TABLE 2.4.16 BUILDUP DESIGN ENVELOPES OF 99 PERCENTILE WIND SPEED CHANGE,  
1- TO 80-km ALTITUDE REGION, FOR ALL FOUR LOCATIONS

Wind Speed at Reference Altitude (m/sec)	Scales of Distance (m)									
	5000	4000	3000	2000	1000	800	600	400	200	100
> 90	71.0	67.0	61.2	52.4	42.0	36.0	29.4	22.1	13.6	8.4
= 80	66.5	63.0	57.7	50.0	40.2	34.5	28.1	21.2	13.0	8.0
= 70	61.2	58.5	53.8	48.1	38.0	32.6	26.6	20.0	12.3	7.6
= 60	54.4	52.5	50.0	44.2	35.5	30.5	24.9	18.7	11.5	7.1
= 50	46.5	45.0	43.7	40.0	33.0	28.3	23.2	17.4	10.7	6.6
= 40	38.9	38.7	37.2	34.9	27.6	23.7	19.3	14.9	8.9	5.5
= 30	30.0	29.4	28.3	25.4	20.8	17.8	14.8	11.5	7.1	4.2
= 20	20.0	19.8	19.5	18.4	15.2	13.1	10.9	8.0	4.9	3.0

TABLE 2.4.17 BACK-OFF DESIGN ENVELOPES OF 99 PERCENTILE WIND SPEED CHANGE, 1- TO 80-km ALTITUDE REGION, FOR ALL FOUR LOCATIONS

Wind Speed at Reference Altitude (m/sec)	Scales of Distance (m)									
	5000	4000	3000	2000	1000	800	600	400	200	100
> 90	77.5	74.4	68.0	59.3	42.8	36.7	30.2	22.5	13.9	8.5
= 80	71.0	68.0	63.8	56.0	40.8	35.0	28.6	21.5	13.2	8.1
= 70	63.5	61.0	57.9	52.0	38.8	33.2	27.0	20.4	12.5	7.7
= 60	57.1	54.7	52.3	47.4	36.0	31.0	25.3	19.0	11.7	7.2
= 50	49.6	47.8	46.2	43.8	33.0	28.3	23.2	17.5	10.7	6.6
= 40	39.4	38.8	37.9	35.5	29.5	25.3	20.6	15.5	9.6	5.9
= 30	30.0	30.0	29.4	26.9	22.6	19.4	15.8	12.2	7.3	4.6
= 20	19.8	19.5	19.0	17.7	14.2	12.2	10.7	9.0	6.3	4.3

5- and 7-km levels. This results from the fact that variations of wind direction tend to be larger in the atmospheric boundary layer (0-2 km) than in the free atmosphere above the atmospheric boundary layer. In this light the following model is recommended as an integrated wind direction change criterion for design studies. The model consists of the 8-16 km 99 percent direction changes in Figure 2.4.14 and a set of functions  $R(\Delta H, H_T, \bar{u}_T)$  to transfer these changes to any reference level  $H_T$  above the 1-km level, where  $\bar{u}_T$  is the reference level wind speed. The quantity  $R$  is defined such that multiplication of the 8-16 km wind direction changes by  $R(\Delta H, H_T, \bar{u}_T)$  will yield the changes in wind direction over a layer of thickness  $\Delta H$  with top or bottom of the reference level located at height  $H_T$  above sea level and reference level wind speed equal to  $\bar{u}_T$ . The functions  $R(\Delta H, H_T, \bar{u}_T)$  for back-off and buildup wind direction changes are defined as

Back-off:

$$R = R^*, \quad 1 \leq H_T < 1.5 \text{ km}$$

$$R = 2(1-R^*)(H_T - 1.5) + R^*, \quad 1.5 \leq H_T < 2 \text{ km}$$

$$R = 1 \quad 2 \text{ km} \leq H_T$$

Buildup:

$$R = R^*, \quad 0 < H_T \leq 2 \text{ km}$$

$$R = \left[ \frac{R^* - 1}{2} \right] \left[ 1 - \cos \pi (\Delta H - H_T + 3) \right] + 1, \quad 1 < \Delta H \leq H_T - 2$$

$$\left. \begin{array}{l} \\ \\ R = R^*, \quad H_T - 2 < \Delta H \leq H_T \end{array} \right\} \quad , \quad 2 < H_T \leq 3 \text{ km}$$

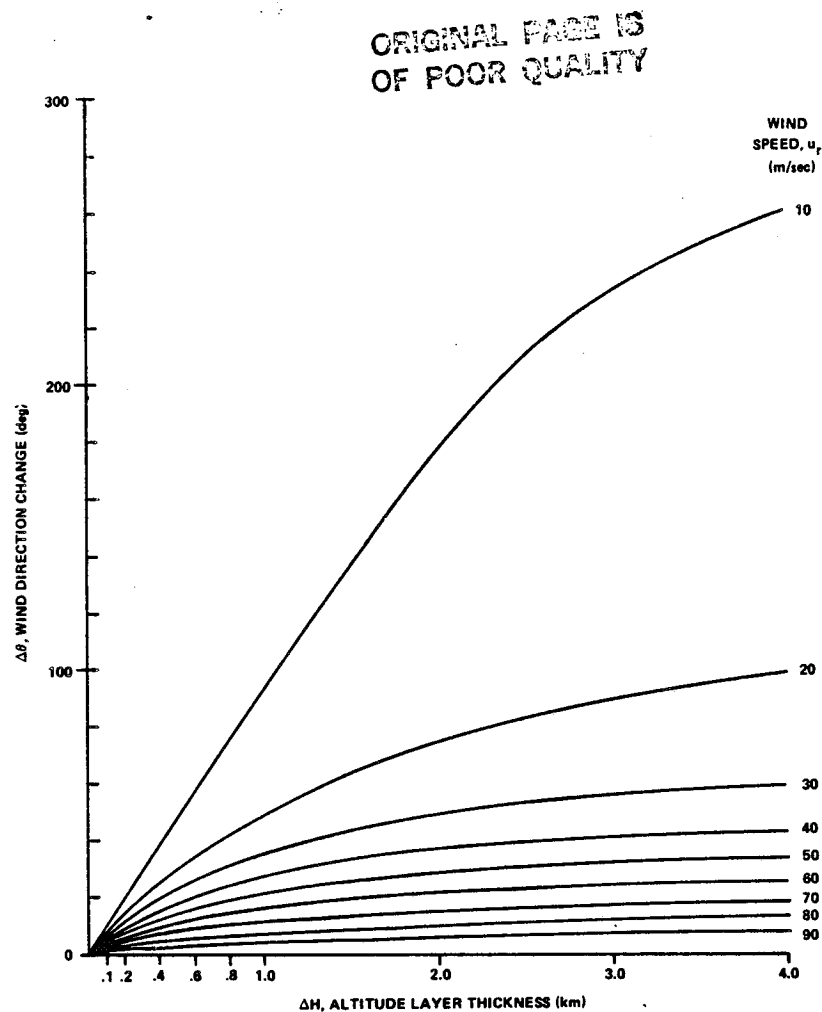


Figure 2.4.14 Idealized 99 percent wind direction change as a function of wind speed for varying layers in the 8-16 km altitude region of Kennedy Space Center.

$$R = 1, 0 < \Delta H \leq H_T - 3 \text{ km}$$

$$R = \left[ \frac{R^* - 1}{2} \right] \left[ 1 - \cos \pi (\Delta H - H_T + 3) \right] + 1, H_T - 3 < \Delta H \leq H_T - 2 \quad \left. \vphantom{\left[ \frac{R^* - 1}{2} \right]} \right\}, 3 < H_T \leq 6 \text{ km}$$

$$R = R^*, H_T - 2 < \Delta H \leq 4 \text{ km}$$

$$R = 1,$$

$$6 \text{ km} \leq H_T,$$

where  $\Delta H$ , and  $H_T$  have units of kilometers and  $R$  is a nondimensional quantity. The quantity  $R^*$  is a function of  $\Delta H$  and  $\bar{u}_T$  and is given in Figure 2.4.15.

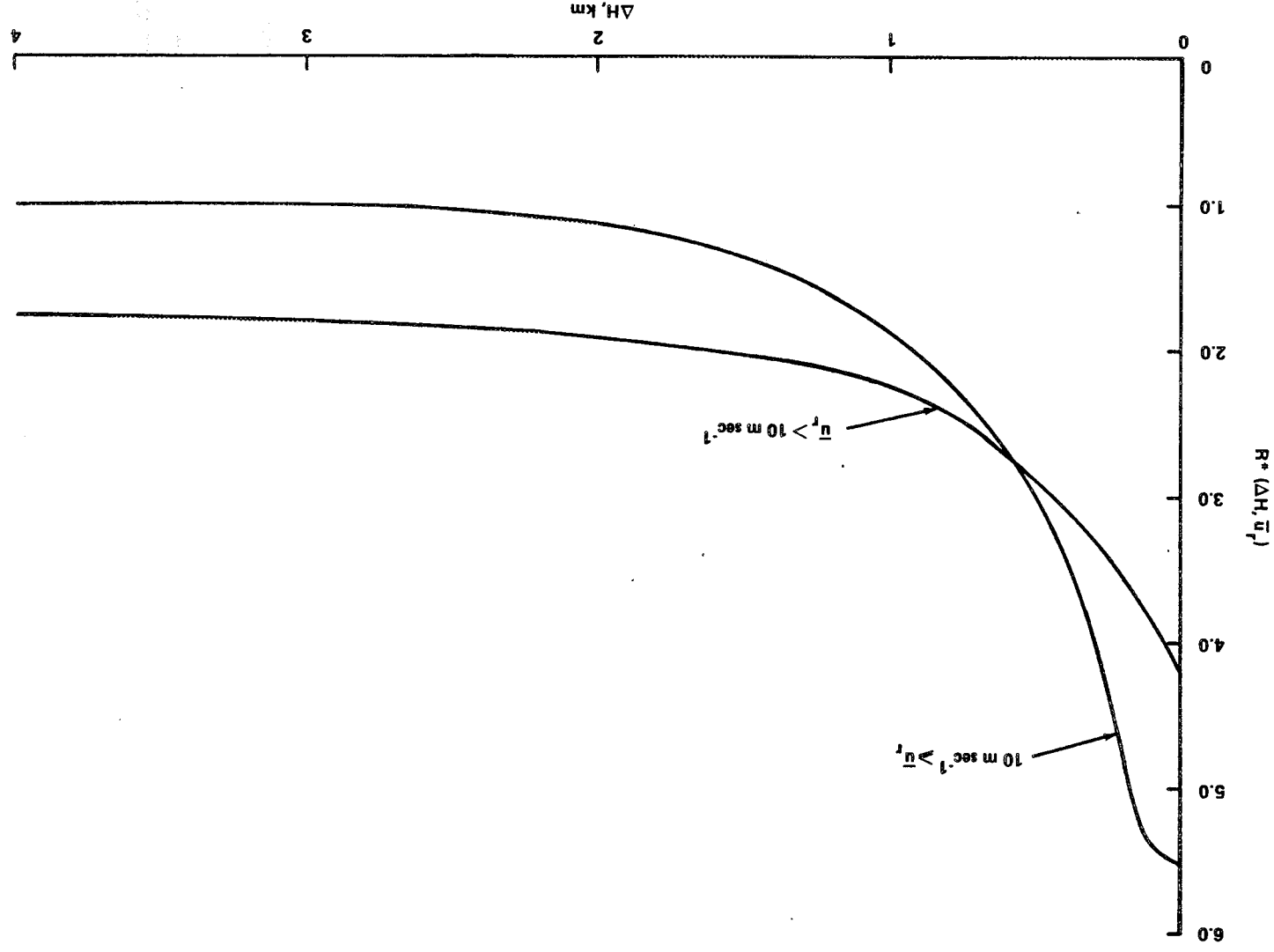


Figure 2.4.15 The function  $R^*$  versus  $\Delta H$  for various categories of wind speed  $u_r$

To apply these wind direction change data, one first constructs a synthetic wind profile (see Section 2.4.9), wind profile envelopes and wind shear envelopes, with or without gust (see Section 2.4.8), as the case may be. A point (reference point) at height  $H_r$  above sea level of potential concern on this synthetic wind profile is selected for analysis. One then turns the wind direction above or below this point according to the schedule of wind direction changes given by the preceding model. Thus, for example, if the 12-km reference point wind speed and direction are  $20 \text{ m sec}^{-1}$  and  $90^\circ$  (east wind i.e., a wind blowing from the east), then according to the wind direction change model discussed previously the wind directions at 0.2, 0.6, 1.0, 2.0, 3.0, and 4.0 km below or above the 12-km reference point, as the case may be, are  $107^\circ$ ,  $123^\circ$ ,  $140^\circ$ ,  $165^\circ$ ,  $180^\circ$ , and  $190^\circ$  for clockwise turning of the wind vector starting with the reference point wind vector at 12 km and looking toward the Earth. Counterclockwise turning is also permissible. The direction of rotation of the wind vector should be selected to produce the most adverse wind situation from a vehicle response point of view.

In view of the unavailability of wind direction change statistics above the 16-km level, at this time, it is recommended that the preceding procedure be used for  $H_r > 16 \text{ km}$ .<sup>10</sup>

## 2.4.8 Gusts – Vertically Flying Vehicles

The steady-state inflight wind speed envelopes presented in Section 2.4.5 do not contain the gust (high frequency content) portion of the wind profile. The steady-state wind profile measurements have been defined as those obtained by the rawinsonde system. These measurements represent wind speeds averaged over approximately 1000 m in the vertical and, therefore, eliminate features with smaller scales. These smaller scale features are contained in the detailed profiles measured by the FPS-16 Radar/Jimsphere system.

A number of attempts have been made to represent the high frequency content of vertical wind profiles in a suitable form for use in vehicle design studies. Most of the attempts resulted in gust information that could be used for specific applications, but, to date, no universal gust representation has been formulated. Information on discrete and continuous gust representations is given below relative to vertically ascending space vehicles.

### 2.4.8.1 Discrete Gusts

Discrete gusts are specified in an attempt to represent, in a physically reasonable manner, characteristics of small-scale motions associated with vertical wind velocity profiles. Gust structure usually is quite complex and it not always understood. For vehicle design studies, discrete gusts are usually idealized because of their complexity and to enhance their utilization.

Well-defined, sharp-edged, and repeated sinusoidal gusts are important types in terms of their influence upon space vehicles. Quasi-square-wave gusts with amplitudes of approximately 9 m/sec have been measured. These gusts are frequently referred to as embedded jets or singularities in the vertical wind profile. By definition, a gust is a wind speed in excess of the defined steady-state value; therefore, these gusts are employed on top of the steady-state wind profile values.

If a design wind speed profile envelope without a wind shear envelope is to be used in a design study, it is recommended that the associated discrete gust vary in length from 60 to 300 m. The leading and trailing

---

10. See Section 2.4.14.2 for wind direction change statistics valid below the 1-km level for take-off and landing design studies.

2.78

edge<sup>11</sup> should conform to a 1-cosine buildup of 30 m and a corresponding decay also over 30 m, as shown Figure 2.4.16. The plateau region of the gust can vary in thickness from zero to 240 m. An analytical expression for the value of this gust of height H above natural grade is given by

$$\left. \begin{aligned} u_g &= \frac{A}{2} \left\{ 1 - \cos \left[ \frac{\pi}{30} (H - H_b) \right] \right\}, & H_b \leq H \leq H_b + 30 \text{ m} \\ u_g &= A, & H_b + 30 \text{ m} \leq H \leq H_b + \lambda - 30 \text{ m} \\ u_g &= \frac{A}{2} \left\{ 1 - \cos \left[ \frac{\pi}{30} (H - H_b - \lambda) \right] \right\}, & H_b + \lambda - 30 \text{ m} \leq H \leq H_b + \lambda \end{aligned} \right\} \quad (2.7)$$

where  $H_b$  is the height of the base of the gust above natural grade,  $\lambda$  is the gust thickness ( $60 \leq \lambda \leq 300 \text{ m}$ ),  $A$  is the gust amplitude, and MKS units are understood.

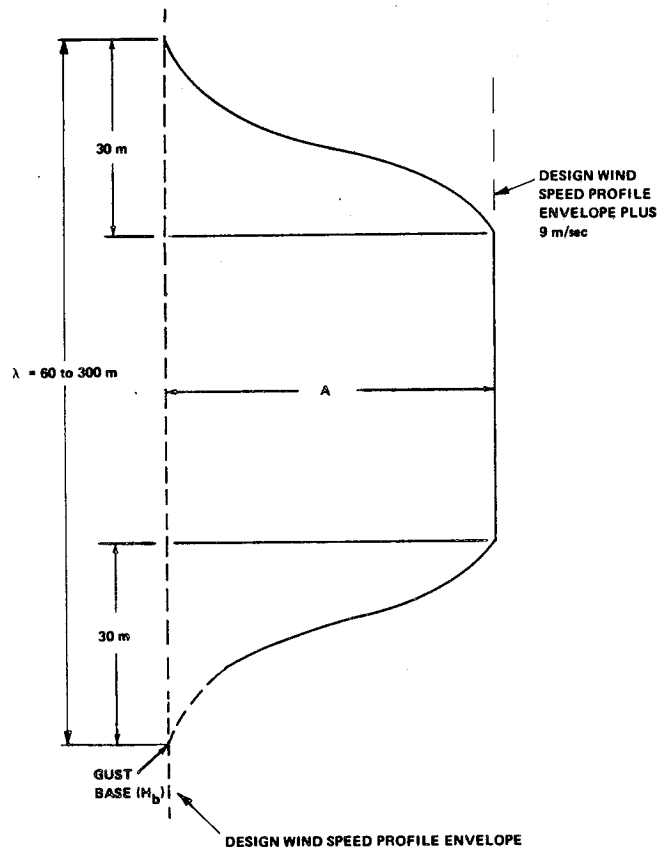


Figure 2.4.16 Relationship between discrete gust and/or embedded jet characteristics (quasi-square-wave shape) and the design wind speed profile envelope.

11. Leading and trailing edges are used here in the sense that as height H increases, one first encounters the gust leading edge and then the trailing edge.



The gust amplitude is a function of  $H_b$  and for design purposes the 1 percent risk gust amplitude is given by

$$\left. \begin{aligned} A &= 6 \text{ m/sec}, H_b < 300 \text{ m} \\ A &= \frac{3}{700} (H_b - 300) + 6, 300 \text{ m} \leq H_b \leq 1000 \text{ m} \\ A &= 9 \text{ m/sec}^{-1}, 1000 \text{ m} < H_b \end{aligned} \right\} \quad (2.28)$$

If a wind speed profile envelope with a buildup wind shear envelope (Section 2.4.6) is to be used in a design study, it is recommended that the previously mentioned discrete gust be modified by replacing the leading edge 1-cosine shape with the following formula

$$u_g = 10A \left\{ \left( \frac{H - H_b}{30} \right)^{0.9} - 0.9 \left( \frac{H - H_b}{30} \right) \right\}, H_b \leq H \leq H_b + 30 \text{ m} \quad (2.29)$$

The height of the gust base  $H_b$  corresponds to the point where the design wind speed profile envelope intersects the design buildup shear envelope. If a discrete gust is to be used with a back-off wind shear envelope, then the 1-cosine trailing edge shall be given by

$$u_g = 10A \left\{ \left( \frac{H_b + \lambda - H}{30} \right)^{0.9} - 0.9 \left( \frac{H_b + \lambda - H}{30} \right) \right\}, H_b + \lambda - 30 \text{ m} \leq H \leq H_b + \lambda \quad (2.30)$$

and the leading edge shall conform to a 1-cosine shape. In this case the height,  $H_b + \lambda$ , of the end of the gust corresponds to the point where the design wind speed profile envelope intersects the design back-off shear envelope. This modification of the 1-cosine shape at the leading and trailing edges, as the case may be, results in a continuous merger of the shear envelope and the discrete gust. See Section 2.4.9 for further details. When applying the discrete gust with wind shears the discrete gust and shears should be reduced to 0.85 of the original value to account for the nonperfect correlation between wind shears and gusts (see Section 2.4.9.2 for details).

Another form of discrete gust that has been observed is approximately sinusoidal in nature, where gusts occur in succession. Figure 2.4.17 illustrates the estimated number of consecutive sinusoidal type gusts that may occur and their respective amplitudes for design purposes. It is extremely important when applying these gusts in vehicle studies to realize that these are pure sinusoidal representations that have never been observed in nature. The degree of purity of these sinusoidal features on the vertical wind profiles has not been established. These gusts should be superimposed symmetrically upon the steady-state profile. The data presented here on sinusoidal gusts are at best preliminary and should be treated as such in design studies.

2.80

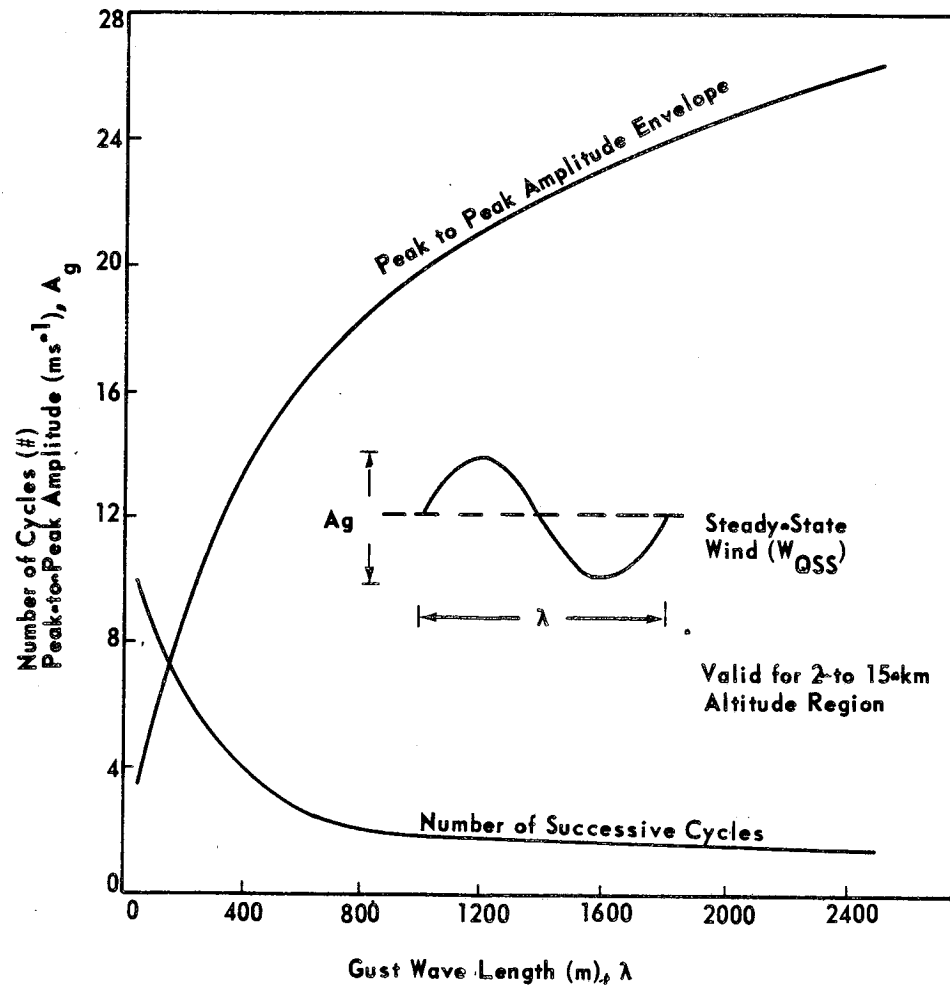


Figure 2.4.17 Best estimate of expected ( $\geq 99$  percentile) gust amplitude and number of cycles as a function of gust wavelength.

#### 2.4.8.2 Spectra

In general, the small-scale motions associated with vertical detailed wind profiles are characterized by a superposition of discrete gusts and many random frequency components. Spectral methods have been employed to specify the characteristics of this superposition of small-scale motions.

A digital filter was developed to separate small-scale motions from the steady-state wind profile. The steady-state wind profile defined by the separation process approximates those obtained by the rawinsonde system.<sup>12</sup> Thus, a spectrum of small-scale motions is representative of the motions included in the FPS-16 radar/Jimsphere measurements, which are not included in the rawinsonde measurements. Therefore, a spectrum of those motions should be considered in addition to the steady-state wind profiles to obtain an equivalent representation of the detailed wind profile. Spectra of the small-scale motions for various probability levels have been determined and are presented in Figure 2.4.18. The spectra were computed from approximately 1200 detailed wind profile measurements by computing the spectra associated with each

12. This definition was selected to enable use of the much larger rawinsonde data sample in association with a continuous-type gust representation.

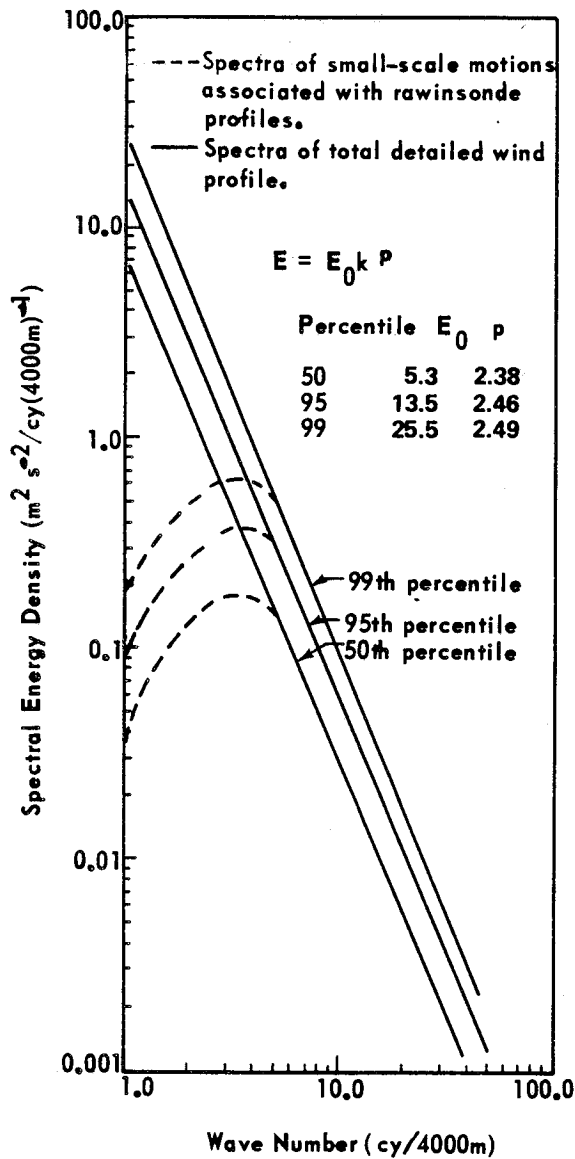


Figure 2.4.18 Spectra of detailed wind profiles.

profile and then determining the probabilities of occurrence of spectral density as a function of wave numbers (cycles/4000 m). Thus the spectra represent envelopes of spectral density for the given probability levels. Spectra associated with each profile were computed over the altitude range between approximately 4 and 16 km. It has been shown that energy (variance) of the small-scale motions is not vertically homogeneous; that is, it is not constant with altitude. The energy content over limited altitude intervals and for limited frequency bands may be much larger than that represented by the spectra in Figure 2.4.18. This should be kept in mind when interpreting the significance of vehicle responses when employing the spectra of small-scale motions. Additional details on this subject are available upon request. Envelopes of spectra for detailed profiles without filtering (solid lines) are also shown in Figure 2.4.18. These spectra are well represented for wave numbers  $\geq 5$  cycles per 4000 m by the equation

$$E(k) = E_0 k^{-p}, \quad (2.31A)$$

where  $E$  is the spectral density at any wave number  $k$  (cycles/4000 m) between 1 and 20,  $E_0 = E(1)$ , and  $p$  is a constant for any particular percentile level of occurrence of the power spectrum.

Spectra of the total wind speed profiles may be useful in control systems and other slow response parametric studies for which the spectra of small-scale motions may not be adequate.

The power spectrum recommended for use in elastic body studies is given by the following expression:

$$E(\kappa) = \frac{683.4 (4000 \kappa)^{1.62}}{1 + 0.0067 (4000 \kappa)^{4.05}} \quad (2.31B)$$

where the spectrum  $E(\kappa)$  is defined so that integration over the domain  $0 \leq \kappa \leq \infty$  yields the variance of the turbulence. In this equation  $E(\kappa)$  is now the power spectral density [ $m^2 \text{ sec}^{-2} / (\text{cycles per meter})$ ] at wave number  $\kappa$  (cycles per meter). This function represents the 99 percentile scalar wind spectra for small-scale motions given by the dashed curve and its solid line extension into the high wave number region in Figure 2.4.18. The associated design turbulence loads are obtained by multiplying the load standard deviations by a factor of three. (Spectra for meridional and zonal components are available upon request.)

Vehicle responses obtained from application of these turbulence spectra should be added to rigid vehicle responses resulting from use of the synthetic wind speed and wind shear profile (with the 0.85 factor on shears) but without a discrete gust.

#### 2.4.9 Synthetic Wind Speed Profiles

Methods of constructing synthetic wind speed profiles are described herein. One method uses design wind speed profile envelopes (Section 2.4.5) and discrete gusts or spectra (Section 2.4.8) without consideration of any lack of correlation between the shears and gusts. Another method takes into account the relationships between the wind shear and gust characteristics.

##### 2.4.9.1 Synthetic Wind Speed Profiles for Vertical Flight Path Considering Only Speeds and Shears

In the method that follows, correlation between the design wind speed profile envelope and wind shear envelope is considered. The method is illustrated with the 95 percentile design nondirectional (scalar) wind speed profile and the 99 percentile scalar wind speed buildup envelope for Kennedy Space Center (KSC) (Fig. 2.4.19) and is stated as follows:

- a. Start with a speed on the design wind speed profile envelope at a selected (reference) altitude.
- b. Subtract the amount of the shear (wind speed change) for each required altitude layer from the value of the wind speed profile envelope at the selected altitude. Figure 2.4.19 presents an example of a 99 percentile shear buildup envelope starting from a reference altitude of 11 km on the KSC 95 percentile wind speed profile envelope (Fig. 2.4.8). The 10 km wind speed of 41.3 m/sec is determined by subtracting 31.7 m/sec — a linearly interpolated shear value for 73 m/sec from the 100 m column of Table 2.4.9 — from 73 m/sec.
- c. Plot values obtained for each altitude layer at the corresponding altitudes. (The value of 41.3 m/sec, obtained in the example in b, would be plotted at 10 km.) Continue plotting values until a 5000-m layer is reached (5000 m below the selected altitude).
- d. Draw a smooth curve through the plotted points starting at the selected altitude on the wind speed profile envelope. The lowest point is extended from the origin with a straight line tangent to the plotted shear buildup curve. This curve then becomes the shear buildup envelope.

##### 2.4.9.2 Synthetic Wind Speed Profiles for Vertical Flight Path Considering Relationships Between Speeds, Shears, and Gusts

In the construction of a synthetic wind speed profile, the lack of perfect correlation between the wind shear and gust can be taken into account by multiplying the shears (wind speed changes) (Section 2.4.6) and the recommended design discrete gusts (Section 2.4.8) by a factor of 0.85 before constructing the synthetic wind profile. This is equivalent, as an engineering approximation, to taking the combined 99 percentile values for the gusts and shears in a perfectly correlated manner. This approach was used successfully in the Apollo/Saturn vehicle development program.

Thus, to construct the synthetic wind speed profiles (considering relationships between shears, speeds, and gusts, using the design wind speed envelopes given in Section 2.4.5), the procedure that follows

- 2

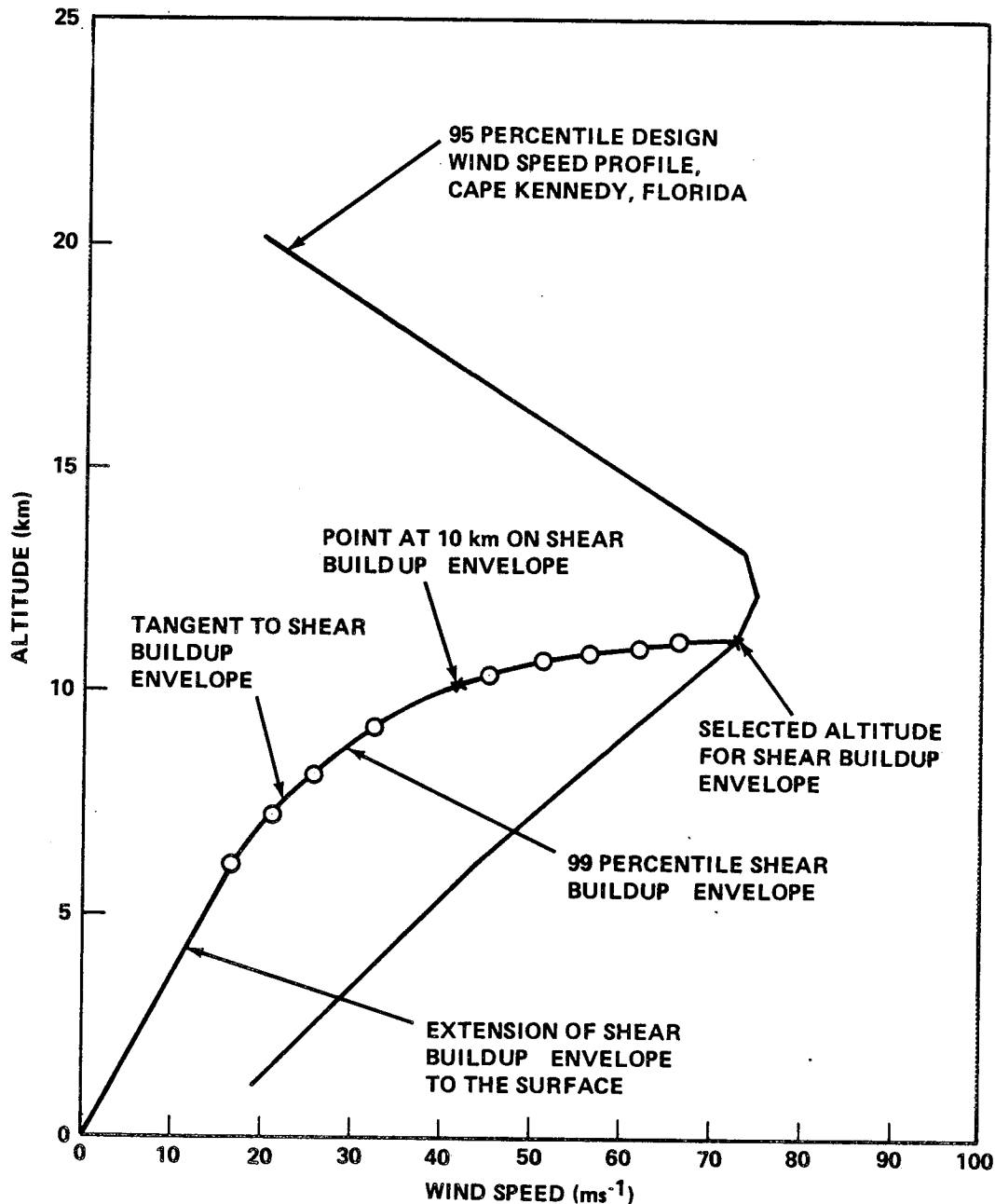


Figure 2.4.19 Example of synthetic wind profile construction, without addition of gust.

is used. Figures 2.4.20 and 2.4.21 show an example using the 95 percentile design wind speed profile envelope, the 99 percentile wind speed buildup envelope, and the modified 1-cosine discrete gust shape.

- a. Construct the shear buildup envelope in the way described in Section 2.4.9.1, except multiply the values of wind speed change used for each scale-of-distance by 0.85. (In the example for the selected altitude of 11 km, the point at 10 km will be found by using the wind speed change of  $31.2 \times 0.85$ , or 26.5 m/sec.) This value subtracted from 73 m/sec then gives a value of 46.5 m/sec for the point plotted at 10 km instead of the value of 41.8 m/sec used when shear and gust relationships were not considered.

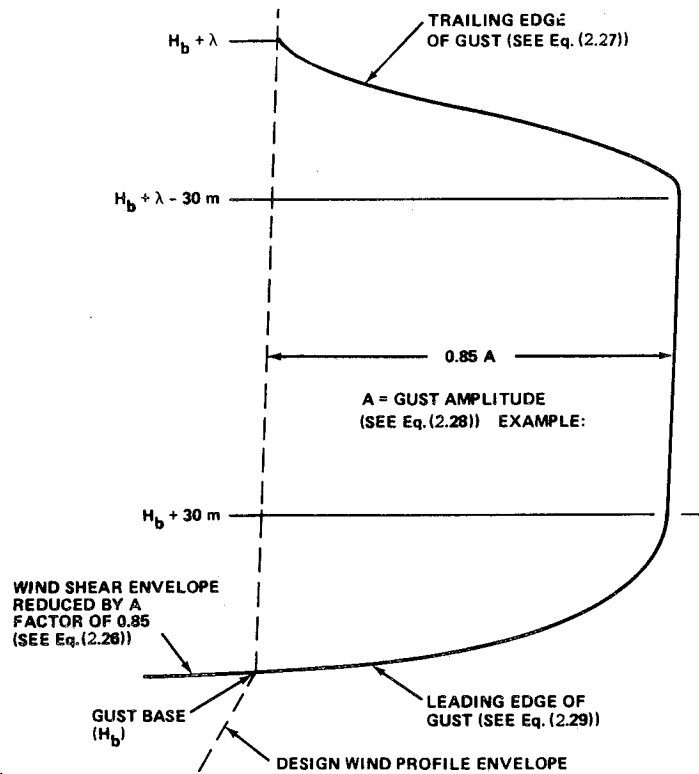


Figure 2.4.20 Relationship between revised gust shape, design wind profile envelope, and speed buildup (shear) envelope.

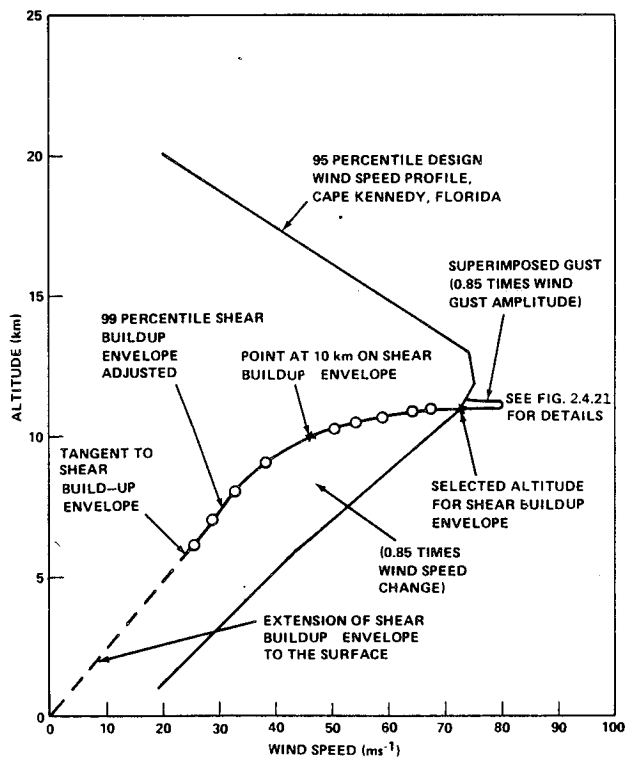


Figure 2.4.21 Example of synthetic wind profile construction, with relationship of wind shears and gusts assumed.

b. The discrete gust is superimposed on the buildup wind shear envelope/wind speed profile envelope by adding the gust given by equation (2.27) with leading edge in the region  $H_b \leq H \leq H_b + 30$  m replaced with equation (2.29). The base of the discrete gust is located at the intersection of the buildup wind shear envelope and the wind speed profile envelope (see Fig. 2.4.21). The gust amplitude,  $A$ , shall be decreased by a factor of 0.85 to account for the nonperfect correlation between shears and gusts. Figure 2.4.21 gives an example of a synthetic profile with shears and gust in combination.

c. When the gust ends at the design wind envelope, the synthetic wind profile may follow the design wind speed envelope or shear back-off profile. If the synthetic wind profile follows the design wind speed envelope, then the trailing edge of the discrete gust will be a 1-cosine shape as given by equation (2.27). If the synthetic wind profile follows the shear back-off profile, then the trailing edge of the discrete gust will be that given by equation (2.30). This modified gust shape will guarantee a continuous transition from the gust to the back-off shear envelope. Vehicle response through both the wind profile envelope with gusts and the synthetic wind profile with shears and gusts in combination should be examined.

d. If a power spectrum representation (see Section 2.4.8.2) is used, then disregard all previous references to discrete gusts. Use the 0.85 factor on shears and apply the spectrum as given in Section 2.4.8.2.

#### 2.4.9.3 Synthetic Wind Profile Merged to the Ground Wind Profile

Up to this point we have considered only those wind shear envelopes which are linearly extrapolated to a zero wind condition at the ground. This procedure does not allow for the possibility of the vehicle (Space Shuttle) to enter a wind shear envelope/gust above the  $H = 1000$  m in a perturbed state resulting from excitations of the control system by the ground wind profile and the associated ground wind shears and gusts. To allow for these possibilities, it is recommended that the wind shear envelopes which begin above the 3000-m level be combined with the wind profile envelope and discrete gust as stated in Section 2.4.9.2; however, a linear extrapolation shall be used to merge the wind defined by the shear envelope at the 3000-m level with the 1000-m wind on the wind profile envelope.

The steady-state ground wind profile up to the 150-m level is defined by the peak wind profile (see Section 2.3.5.2) reduced to a steady-state wind profile by division with a 10-min average gust factor profile (see Section 2.3.7.1). To merge this steady-state wind profile into the 1000-m level steady-state wind speed envelope, the steady-state wind speed in the layer between 150 to 300 m shall take on a constant value equal to the steady-state wind at the 150-m level defined by the peak wind profile and gust factor profile between the surface of the Earth and the 150-m level. The flow between the 300-m level and the 1000-m level shall be obtained by linear interpolation. If the discontinuities in slope of the wind profile at the 150-, 300- and 1000-m levels resulting from this merging procedure introduce significant false vehicle responses, it is recommended that this interpolation procedure be replaced with a procedure involving a smooth continuous function which closely approximates the piece-wise linear segment interpolation function between the 150- and 1000-m levels with continuous values of wind speed and slope at the 150- and 1000-m levels.

#### 2.4.9.4 Synthetic Wind Speed Profiles for Nonvertical Flight Path

To apply the synthetic wind profile for other than vertical flight, multiply the wind shear buildup and back-off values by the cosine of the angle between the vertical axis (Earth-fixed coordinate system) and the vehicle's flight path. The gust (or turbulence spectra) is applied directly to the vehicle without respect to the flight path angle. The synthetic wind profile is otherwise developed according to procedures given in Section 2.4.9.2.

## 2.4.10 Characteristic Wind Profiles to a Height of 18 Kilometers

## 2.4.10.1 Features of Wind Profiles

A significant problem in space vehicle design is to provide assurance of an adequate design for flight through wind profiles of various configurations. During the major design phase of a space vehicle, the descriptions of various characteristics of the wind profile are employed in determining the applicable vehicle response requirement. Since much of the vehicle is in a preliminary status of design and the desired detail data on structural dynamic modes and other characteristics are not known at this time, the use of statistical and synthetic representations of the wind profile is desirable. However, after the vehicle design has been finalized and tests have been conducted to establish certain dynamic capabilities and parameters, it is desirable to evaluate the total system by simulated dynamic flight through wind profiles containing adequate frequency resolution (Ref. 2.40). The profiles shown in Figures 2.4.22 through 2.4.27 are profiles of scalar wind measured by the FPS-16 radar/Jimsphere wind measuring system, and they illustrate the following: (1) jet stream winds, (2) sinusoidal variation in wind with height, (3) high winds over a broad altitude band, (4) light wind speeds, and (5) discrete gusts.

These profiles show only a few of the possible wind profiles that can occur. Jet stream winds (Fig. 2.4.22) are quite common to the various test ranges during the winter months and can reach magnitudes in excess of 100 m/sec. These winds occur over a limited altitude range, making the wind shears very large. Figure 2.4.23 depicts winds having sinusoidal behavior in the 10- to 14-km region. These types of winds can create excessive loads upon a vertically rising vehicle, particularly if the reduced forcing frequencies couple with the vehicle control frequencies and result in additive loads. Periodic variations in the vertical wind profile are not uncommon. Some variations are of more concern than others, depending upon wavelength and,

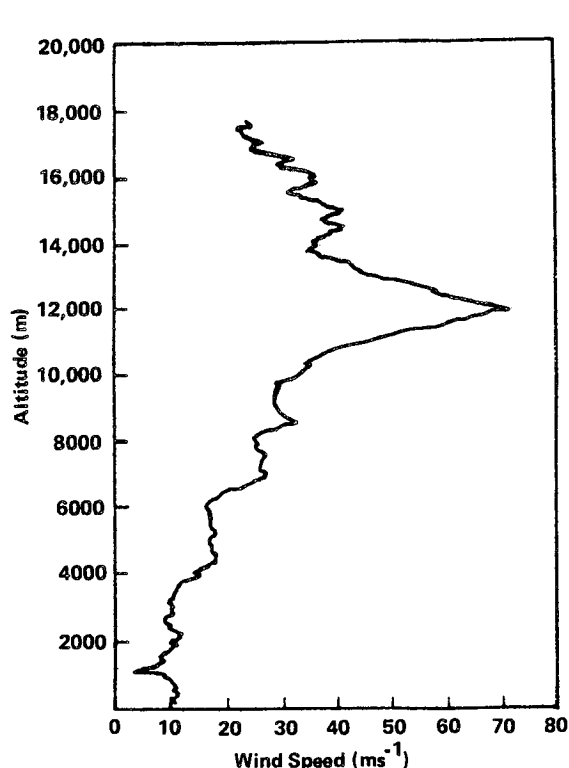


Figure 2.4.22 Example of jet stream winds.

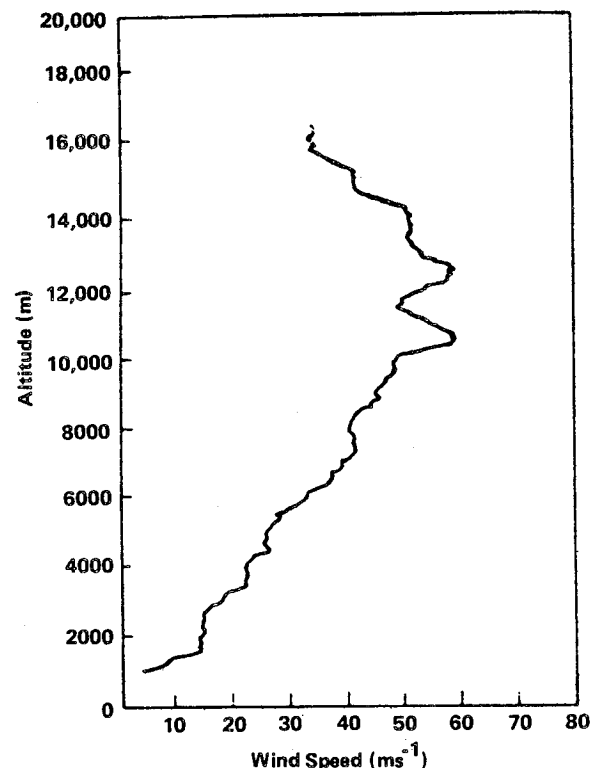


Figure 2.4.23 Example of sine wave flow in the 10- to 14-km altitude region.



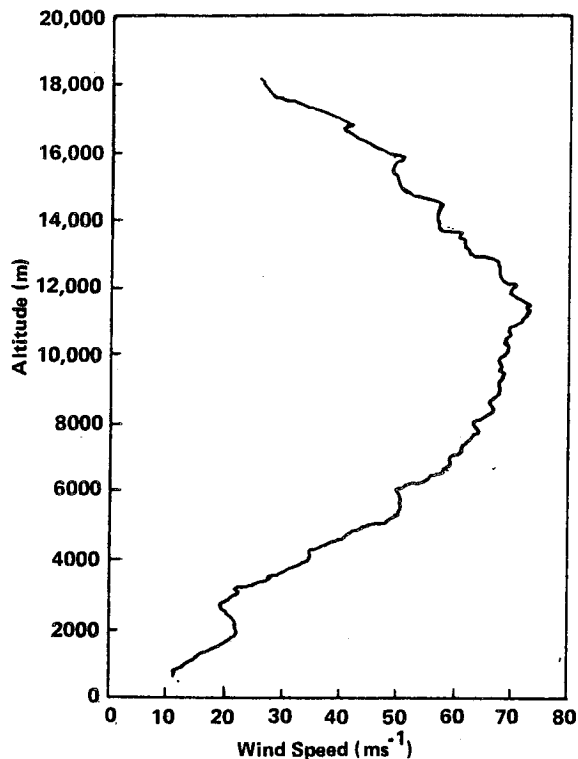


Figure 2.4.24 Example of high wind speeds over a deep altitude layer.

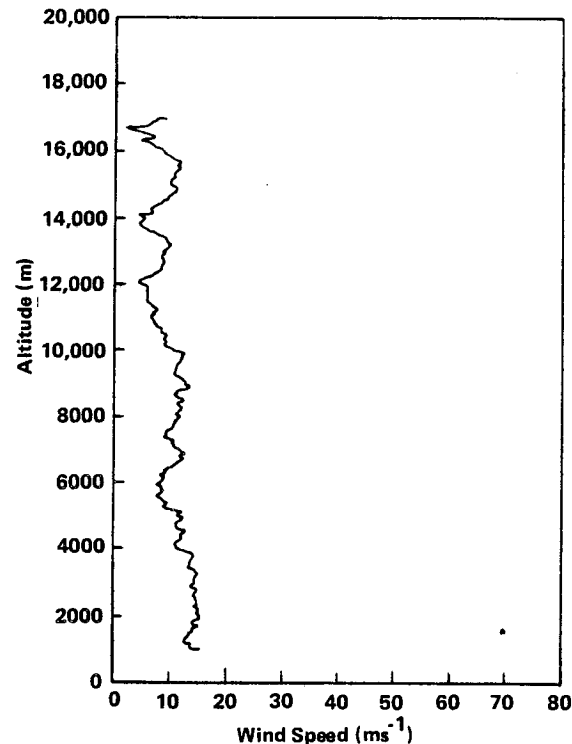


Figure 2.4.25 Example of low wind speeds.

course, amplitude. Figure 2.4.24 is an interesting example of high wind speeds that occurred over 6 km in depth. Such flow is not uncommon for the winter months. Figure 2.4.25 shows scalar winds of very low values. These winds were generally associated with easterly flow over the entire altitude interval (surface to 16 km) at Kennedy Space Center, Florida. The last examples (Figures 2.4.26 and 2.4.27) illustrate two samples of discrete gusts.

## 2.4.11 Vector Wind and Vector Wind Shear Models

### 2.4.11.1 Vector Wind Profile Models

This subsection presents the concepts for a vector wind profile model, an outline of procedures to compute synthetic vector wind profiles (SVWP) followed by examples, and some suggestions for alternate approaches. Applications of the theoretical relationships between the variables and the parameters of the multivariate probability distribution function presented in Section XV are made. The vector wind profile models presented in this section have potential applications for aerospace vehicle ascent and reentry analysis for the altitude range from 1 to 27 km for Kennedy Space Center, Florida, and Vandenberg AFB, California (Ref. 2.38).

### 2.4.11.2 Vector Wind Profile Model Concepts

Purpose of a Model. What is a model? One definition is that a model is a representation of one or more attributes of a thing or concept. Hence, our objective in modeling the atmospheric winds is to simplify the complexity of the real wind profiles by a few attributes or characteristics to make the real wind profiles

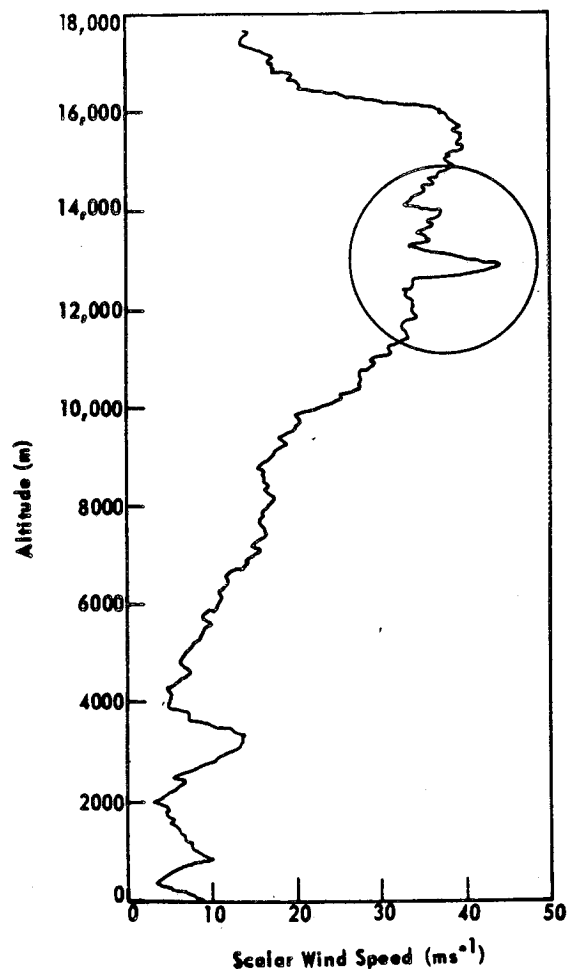


Figure 2.4.26 Example of a discrete gust observed at 1300Z on January 21, 1968, at Kennedy Space Center.

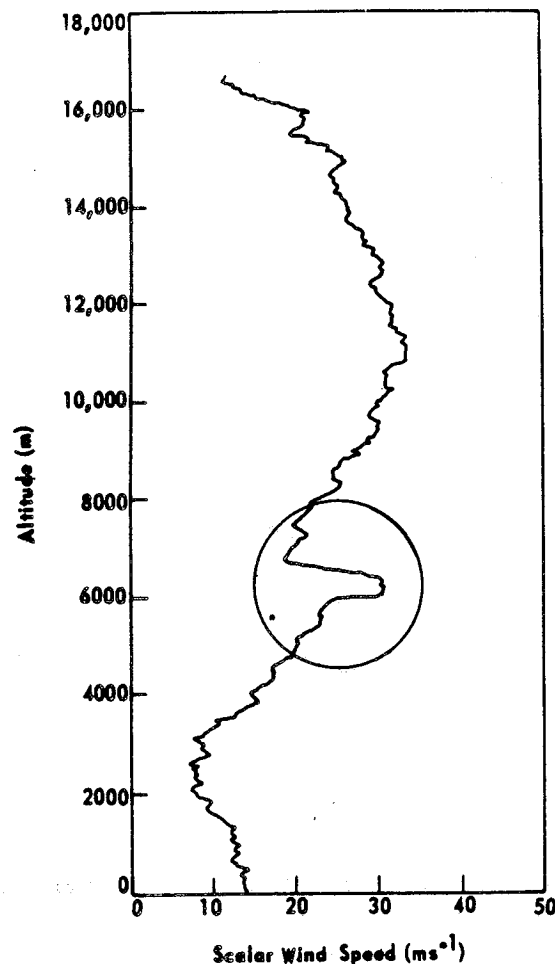


Figure 2.4.27 Example of a discrete gust observed by a Jimsphere released at 2103Z on November 8, 1967, at Kennedy Space Center.

more understandable and less complicated for certain engineering applications. The modeling tools are those of mathematical probability theory and statistical analysis of wind data samples. Hopefully, through these methods, a wind model can be derived that will be a cost saving device for use in aerospace vehicle programs and still be sufficiently representative of the real wind profiles to answer engineering questions that arise in the aerospace vehicle analysis. However, the most realistic test of aerospace vehicle performance is an evaluation by flight simulations through detailed wind profiles. A sample of 150 detailed wind profiles (Jimsphere wind profiles) for each month for Kennedy Space Center has been made available. A sample of 150 detailed wind profiles for each month which have all the power spectra characteristics that measured Jimsphere profiles have for Vandenberg AFB has been made available for flight simulations for aerospace vehicle flights from Vandenberg AFB. These two detailed wind profile data samples have the same moment statistical parameters at 1-km intervals (within statistical confidences) as the 14 parameters presented in the referenced report (Ref. 2.38). This was the basis for the selection of the 150 detailed wind profiles for each month.

**Synthetic Vector Wind Model.** In this discussion it is assumed that the reader is familiar with the synthetic scalar wind profile model presented in this report. By definition, the synthetic scalar wind profile model is the locus of wind speeds versus altitude obtained from conditional wind shears given a specified wind speed at a reference altitude. The profile is constructed by subtracting the conditional wind shears from the specified wind speed. The scalar wind shears are a function of wind speed only. The SVWP<sup>13</sup> extends this concept to the vector wind representation. For the SVWP the vector wind shears are a function of: (a) the reference altitude; (b) the given wind vector at the reference altitude, which makes the conditional vector wind shears wind-azimuth dependent; (c) the conditional wind shears; and (d) the monthly reference period.

For a given wind vector, the SVWP has three dimensions, whereas the synthetic scalar wind profile has two dimensions. A wind vector is selected at the reference altitude  $H_0$ , and the conditional vector wind shears are computed for altitudes  $H$  below and above  $H_0$ . The conditional vector shears are then subtracted from the given wind vector at  $H_0$ . For two-point separation in altitude ( $H_0 - H$ ), the cone formed by this procedure contains a specified percentage of the wind vectors at altitude  $H$  for the given wind vector at  $H_0$ . The base is an ellipse in which a specified percentage (usually taken as 99 percent) of the wind vectors will lie given the wind vector at  $H_0$ . The interest in modeling the wind profile is to make some logical or orderly choice to arrive at the conditional wind vectors versus altitude. It is illustrated in Reference 2.38 that there are an infinite number of paths along the surface of the conditional cone from reference altitude  $H_0$  down to the level  $H$ . Hence, a choice of an orderly path along the surface of the conditional cone of wind vectors should be dictated by the desired scientific or engineering application. A step-by-step procedure is given to compute the SVWP that is in-plane with the given wind vector. This in-plane profile has two branches: one is the smallest conditional vector wind and has the largest shears, and the other is the outer branch, which has the largest in-plane conditional wind vector but not necessarily the largest conditional shear. Also presented is the SVWP derived from the tangent intercepts to the conditional vector winds. These out-of-plane synthetic vector wind profiles have two branches: a right-turning wind direction and a left-turning wind direction with respect to altitude. The two-part, in-plane SVWP and the two-part, out-of-plane SVWP give a total of four synthetic vector wind profiles.

Actual examples of the conditional vector winds are shown in Reference 2.38. The examples were derived from the December wind parameters for Vandenberg AFB. The reference altitude  $H_0$  is 10 km; the given wind vector at  $H_0$  is from 330 degrees at 57.8 m/sec or, in terms of the components,  $u^* = 28$  m/sec and  $v^* = -50$  m/sec. Instead of conditional ellipses, 99 percent conditional circles have been computed for each altitude at 1-km intervals from 0 to 27 km altitude. As presented, the dashed line connecting the center of the conditional circles versus altitude is the conditional mean vector. The smooth curve connecting the intercepts of the conditional circles is the in-plane SVWP that has the largest conditional shears.

#### 2.4.11.3 Computation of the Synthetic Vector Wind Profile

Discussion in Reference 2.38 is sufficiently detailed for a computer program development to code the procedures to compute the SVWP. Digressions are made in the procedures to clarify some points. The primary objectives, however, are to illustrate some applications of the probability theory of vector winds and to show the use of the tabulated wind statistical parameters to compute synthetic vector wind profiles.

#### 2.4.12 Wind Profile Data Availability

##### 2.4.12.1 Kennedy Space Center, Florida, and Vandenberg AFB, California, Jimsphere Wind Design Assessment and Verification Data Tape

The Jimsphere wind design assessment and verification data tapes serve as a very special data set for wind aloft vehicle response and other analytical studies. When properly integrated into a flight-simulation program (Space Shuttle, for example), vehicle operational risks can be more accurately assessed relative to the true representation of wind velocity profile characteristics. The wind velocity profiles contain wind vectors for each 25 m in altitude from near surface to an altitude of approximately 18 km. The high frequency resolution is one cycle per 100 m with an rms error of approximately 0.5 m/sec for velocities averaged over a 50-m height interval. Launch probability statements may be specified from flight simulations and related analyses. Through in-depth mathematical and statistical interpretations of these data, specific criteria can be generated on details of vector winds, gusts, shears, and the wind flow field interrelationships.

Two special Jimsphere wind profile data sets of 150 profiles per month are available for Kennedy Space Center, Florida, and Vandenberg AFB, California. In addition, a set of Jimsphere wind profiles for 3.5-hr, 7-hr, and 10.5-hr pairs grouped according to summer, winter, and transition seasonal months has been prepared for KSC. A similar set of 3.5-hr wind profile pairs is planned for Vandenberg AFB when adequate data become available. These data sets were selected based on an extensive statistical and physical analysis of the vector wind profile characteristics and their representativeness. They have been specified for use in the Space Shuttle program for system design assessment, performance analysis, and prelaunch wind-loads calculations.

These data sets are available on magnetic computer tapes upon request to the Atmospheric Sciences Division, Space Sciences Laboratory, NASA/George C. Marshall Space Flight Center, Marshall Space Flight Center, Alabama 35812. There are also a large number of Jimsphere wind velocity profile data available for Kennedy Space Center, Point Mugu, White Sands Missile Range, Green River, Wallops Island, and Vandenberg AFB, California.

##### 2.4.12.2 Availability of Serial Completed Rawinsonde Wind Velocity Profiles

Serially complete, edited, and corrected rawinsonde wind profile data at 1-km intervals to approximately 30 km are available for 19 years (two observations per day) for Kennedy Space Center, for 9 years (four observations per day) for Santa Monica, and for 14 years (two observations per day) for Vandenberg Air Force Base. A representative serial complete rawinsonde wind profile data set is available for the Wallops Flight Center (12 years, two observations per day). Qualified requestors in aerospace, scientific, and engineering organizations may obtain these data, which are also on magnetic tapes, upon request to the Chief, Atmospheric Sciences Division, Space Sciences Laboratory, NASA/George C. Marshall Space Flight Center, Marshall Space Flight Center, Alabama 35812. They are also available as card deck 600 from the National Climatic Center, NOAA, Asheville, North Carolina 28801.

##### 2.4.12.3 Availability of Rocketsonde Wind Velocity Profiles

Rocketsonde wind profile data at 1-km intervals from approximately 20 to 75 km have been collected for over 10 years from various launch sites around the world. These data can be obtained from the World Data Center A, Asheville, North Carolina 28801.

#### 2.4.12.4 Utility of Data

All wind profile data records should be checked carefully by the user before employing them in any vehicle response calculations. Wherever practical, the user should become familiar with the representativeness of the data and frequency content of the profile used, as well as the measuring system and reduction schemes employed in handling the data. For those organizations that have aerospace meteorology oriented groups or individuals on their staffs, consultations should be held with them. Otherwise, various government groups concerned with aerospace vehicle design and operation can be of assistance. Such action by the user can prevent expensive misuse and error in interpretation of the data relative to the intended application.

#### 2.4.13 Atmospheric Turbulence Criteria for Horizontally Flying Vehicles

This section presents the continuous turbulence random model for the design of aerospace vehicles capable of flying horizontally, or nearly so, through the atmosphere. In general both the continuous random model (Sections 2.4.13 and 2.4.14) and the discrete model (Section 2.4.15) are used to calculate vehicle responses, with the procedure producing the larger response being used for design.

To a reasonable degree of approximation, inflight atmospheric turbulence experienced by horizontally flying vehicles can be assumed to be homogeneous, stationary, Gaussian, and isotropic. Under some conditions, these assumptions might appear to be drastic, but for engineering purposes they seem to be appropriate, except for low-level flight in approximately the first 300 m of the atmosphere. It has been found that the spectrum of turbulence first suggested by von Karman appears to be a good analytical representation of atmospheric turbulence. The longitudinal spectrum is given by

$$\Phi_u(\Omega, L) = \sigma^2 \frac{2L}{\pi} \frac{1}{[1 + (1.339 L\Omega)^2]^{5/6}}, \quad (2.32)$$

where  $\sigma^2$  is the variance of the turbulence,  $L$  is the scale of turbulence, and  $\Omega$  is the wave number in units of radians per unit length. The spectrum is defined so that

$$\sigma^2 = \int_0^{\infty} \Phi_u(\Omega, L) d\Omega. \quad (2.33)$$

The theory of isotropic turbulence predicts that the spectra  $\Phi_w$  of the lateral and vertical components of turbulence are related to the longitudinal spectrum through the differential equation

$$\Phi_w = \frac{1}{2} \left( \Phi_u - \Omega \frac{d\Phi_u}{d\Omega} \right). \quad (2.34)$$

2.92

Substitution of equation (2.32) into equation (2.34) yields

$$\Phi_w = \sigma^2 \frac{L}{\pi} \frac{1 + \frac{8}{3} (1.339 L\Omega)^2}{[1 + (1.339 L\Omega)^2]^{11/6}} \quad (2.35)$$

The nondimensional spectra  $2\pi\Phi_u/\sigma^2L$  are depicted in Figure 2.4.28 as a function of  $\Omega L$ . As  $L\Omega \rightarrow \infty$ ,  $\Phi_u$  and  $\Phi_w$  asymptotically behave like

$$\Phi_u \sim \sigma^2 \frac{2L}{\pi} \frac{(L\Omega)^{-5/3}}{(1.339)^{5/3}} \quad (L\Omega \rightarrow \infty) \quad (2.36)$$

$$\Phi_w \sim \sigma^2 \frac{8L}{3\pi} \frac{(L\Omega)^{-5/3}}{(1.339)^{5/3}} \quad (L\Omega \rightarrow \infty) \quad (2.37)$$

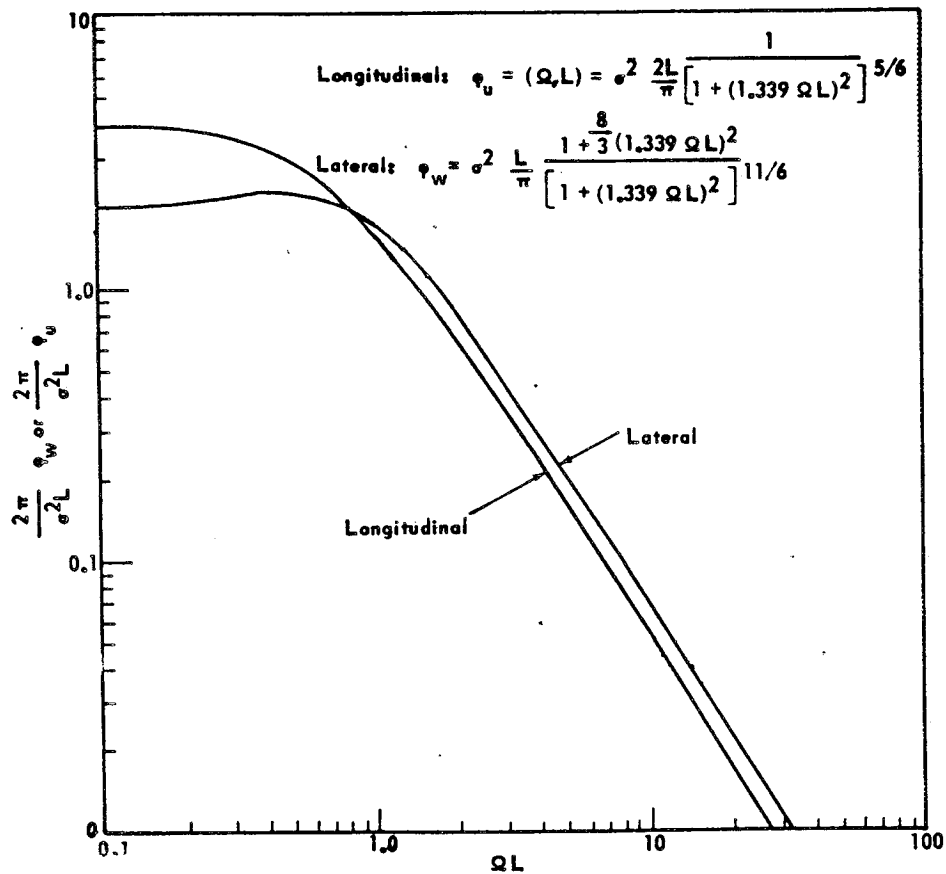


Figure 2.4.28 The dimensionless longitudinal and lateral  $2\pi\Phi_u/\sigma^2L$  and  $2\pi\Phi_w/\sigma^2L$  spectra as functions of the dimensionless frequency  $L\Omega$ .

consistent with the concept of the Kolmogorov inertial subrange. In addition,  $\Phi_w/\Phi_u \rightarrow 4/3$  as  $\Omega L \rightarrow \infty$ .

Design values of the scale of turbulence  $L$  are given in Table 2.4.18. Experience indicates that the scale of turbulence increases as height increases in the first 762 m (2500 ft)<sup>14</sup> of the atmosphere, and typical values of  $L$  range from 10 m (~30 ft) near the surface to 610 m (2000 ft) at approximately a 762-m (2500-ft) altitude. Above the 762-m (2500-ft) level, typical values of  $L$  are in the order of 762 to 1829 m (2500 to 6000 ft). The scales of turbulence in Table 2.4.18 above the 300-m level are probably low, and they would be expected to give a somewhat conservative or high number of load or stress exceedances per unit length of flight. The scale of turbulence indicated for the first 304.8 m of the atmosphere in Table 2.4.18 is a typical value. The use of this average scale of turbulence may be approximate for load studies; however, it is inappropriate for control system and flight simulation purposes, in which event the vertical variation of the scale of turbulence in the first 300 m of the atmosphere should be taken into account.

The power spectrum analysis approach is applicable only to stationary Gaussian continuous turbulence, but atmospheric turbulence is neither statistically stationary nor Gaussian over long distances. The statistical quantities used to describe turbulence vary with altitude, wind direction, terrain roughness, atmospheric stability, and a host of other variables. Nevertheless, it is valid to a sufficient degree of engineering approximation to recommend that atmospheric turbulence be considered locally Gaussian and stationary and that the total flight history of a horizontally flying vehicle be considered to be composed of an ensemble of exposures to turbulence of various intensities, all using the same power spectrum shape. Furthermore, it is recommended that the following statistical distribution of rms gust intensities be used:

$$p(\sigma) = \frac{P_1}{b_1} \sqrt{\frac{2}{\pi}} \exp\left(-\frac{\sigma^2}{2b_1^2}\right) + \frac{P_2}{b_2} \sqrt{\frac{2}{\pi}} \exp\left(-\frac{\sigma^2}{2b_2^2}\right), \quad (2.38)$$

where  $b_1$  and  $b_2$  are the standard deviations of  $\sigma$  in nonstorm and storm turbulence. The quantities  $P_1$  and  $P_2$  denote the fractions of flight time or distance flown in nonstorm and storm turbulence. It should be noted that if  $P_0$  is the fraction of flight time or distance in smooth air, then

$$P_0 + P_1 + P_2 = 1. \quad (2.39)$$

The recommended design values of  $P_1$ ,  $P_2$ ,  $b_1$ , and  $b_2$  are given in Table 2.4.18. Note that over rough terrain  $b_2$  can be extremely large in the first 304 m (1000 ft) above the terrain and the  $b$ 's for the vertical, the lateral, and the longitudinal standard deviations of the turbulence are not equal. Thus in the first 304 m (1000 ft) of the atmosphere above rough terrain, turbulence is significantly anisotropic and this anisotropy must be taken into account in engineering calculations.

An exceedance model of gust loads and stresses can be developed with the preceding information. Let  $y$  denote any load quantity that is a dependent variable in a linear system of response equations (for example, bending moment at a particular wing station). This system is forced by the longitudinal, lateral, and vertical components of turbulence and, upon producing the Fourier transform of the system, it is possible to obtain the spectrum of  $y$ . This spectrum will be proportional to the input turbulence spectra, the function of proportionality being the system transfer function. Upon integrating the spectrum of  $y$  over the domain  $0 < \Omega < \infty$ , we obtain the relationship

14. U. S. customary units are used in the section in parentheses to maintain continuity with source of data – Air Force Flight Dynamics Laboratory and other documentation.

TABLE 2.4.18 PARAMETERS FOR THE TURBULENCE MODEL FOR HORIZONTALLY FLYING VEHICLES

Altitude		Mission Segment *	Turbulence Component **	P <sub>1</sub> (unitless)	b <sub>1</sub>		P <sub>2</sub> (unitless)	b <sub>2</sub>		L	
(m)	(ft)				(m/sec)	(ft/sec)		(m/sec)	(ft/sec)	(m)	(ft)
0 - 304.8	0 - 1 000	Low Level Contour (rough terrain)	V	1.00	0.82	2.7	10 <sup>-5</sup>	3.25	10.65	152.4	500
0 - 304.8	0 - 1 000	Low Level Contour (rough terrain)	L, L	1.00	0.94	3.1	10 <sup>-5</sup>	4.29	14.06	152.4	500
0 - 304.8	0 - 1 000	C, C, D	V, L, L	1.00	0.77	2.51	0.005	1.54	5.04	152.4	500
304.8 - 672	1 000 - 2 500	C, C, D	V, L, L	0.42	0.92	3.02	0.0033	1.81	5.94	533.4	1750
672 - 1 524	2 500 - 5 000	C, C, D	V, L, L	0.30	1.04	3.42	0.0020	2.49	8.17	762	2500
1 524 - 3 048	5 000 - 10 000	C, C, D	V, L, L	0.15	1.09	3.59	0.00095	2.81	9.22	762	2500
3 048 - 6 096	10 000 - 20 000	C, C, D	V, L, L	0.062	1.00	3.27	0.00028	3.21	10.52	762	2500
6 096 - 9 144	20 000 - 30 000	C, C, D	V, L, L	0.025	0.96	3.15	0.00011	3.62	11.88	762	2500
9 144 - 12 192	30 000 - 40 000	C, C, D	V, L, L	0.011	0.89	2.93	0.000095	3.00	9.84	762	2500
12 192 - 15 240	40 000 - 50 000	C, C, D	V, L, L	0.0046	1.00	3.28	0.000115	2.69	8.81	762	2500
15 240 - 18 288	50 000 - 60 000	C, C, D	V, L, L	0.0020	1.16	3.82	0.000078	2.15	7.04	762	2500
18 288 - 21 336	60 000 - 70 000	C, C, D	V, L, L	0.00088	0.89	2.93	0.000057	1.32	4.33	762	2500
21 336 - 24 384	70 000 - 80 000	C, C, D	V, L, L	0.00038	0.85	2.80	0.000044	0.55	1.80	762	2500
above 24 384	above 80 000	C, C, D	V, L, L	0.00025	0.76	2.50	0	0	0	762	2500

\* Climb, cruise, and descent (C, C, D).

\*\* Vertical, lateral, and longitudinal (V, L, L).



$$\sigma_y = A\sigma, \quad (2.40)$$

where  $A$  is a positive constant that depends upon the system parameters and the scale of turbulence, and  $\sigma_y$  is the standard deviation of  $y$ .

If the output  $y$  is considered to be Gaussian for a particular value of  $\sigma$ , then the expected number of fluctuations of  $y$  that exceed  $y^*$  with positive slope per unit distance with reference to a zero mean is

$$N(y^*) = N_0 \exp \left( -\frac{y^{*2}}{2\sigma_y^2} \right), \quad (2.41)$$

where  $N_0$  is the expected number of zero crossings of  $y$  unit distance with  $h$  positive slope and is given by

$$N_0 = \frac{1}{2\pi\sigma_y} \left[ \int_0^\infty \Omega^2 \Phi_y(\Omega) d\Omega \right]^{1/2}. \quad (2.42)$$

In this equation,  $\Phi_y$  is the spectrum of  $y$  and

$$\sigma_y = \left[ \int_0^\infty \Phi_y(\Omega) d\Omega \right]^{1/2}. \quad (2.43)$$

The standard deviation of  $\sigma_y$  is related to standard deviation of turbulence through equation (2.40), and  $\sigma$  is distributed according to equation (2.38). Accordingly, the number of fluctuations of  $y$  that exceed  $y^*$  for standard deviations of turbulence in the interval  $\sigma$  to  $\sigma + d\sigma$  is  $N(y^*) p(\sigma) d\sigma$ , so that integration over the domain  $0 < \sigma < \infty$  yields

$$\frac{M(y^*)}{N_0} = P_1 \exp \left( -\frac{|y^*|}{b_1 A} \right) + P_2 \exp \left( -\frac{|y^*|}{b_2 A} \right), \quad (2.44)$$

where  $M(y^*)$  is the overall expected number of fluctuations of  $y$  that exceed  $y^*$  with positive slope. To apply this equation, the engineer needs only to calculate  $A$  and  $N_0$  and specify the risk of failure he wishes to accept. The appropriate values of  $P_1$ ,  $P_2$ ,  $b_1$ , and  $b_2$  are given in Table 2.4.18. Figures 2.4.29 and 2.4.30 give plots of  $M(y^*)/N_0$  as a function of  $|y^*|/A$  for the various altitudes for the design data given in Table 2.4.18. Table 2.4.19 provides a summary of the units of the various quantities in this model.

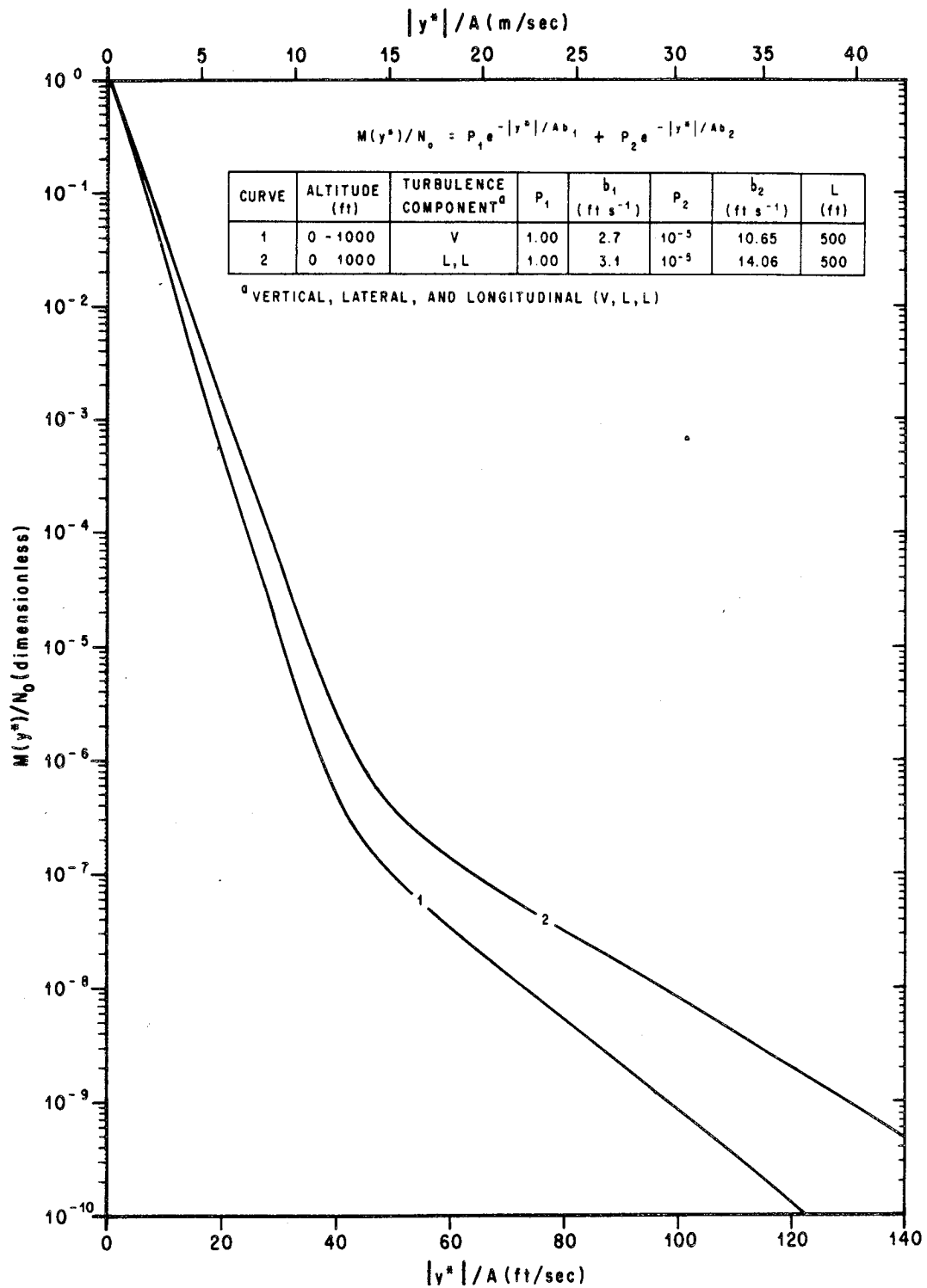


Figure 2.4.29 Exceedance curves for the vertical, lateral, and longitudinal components of turbulence for the 0- to 1000-ft altitude range.

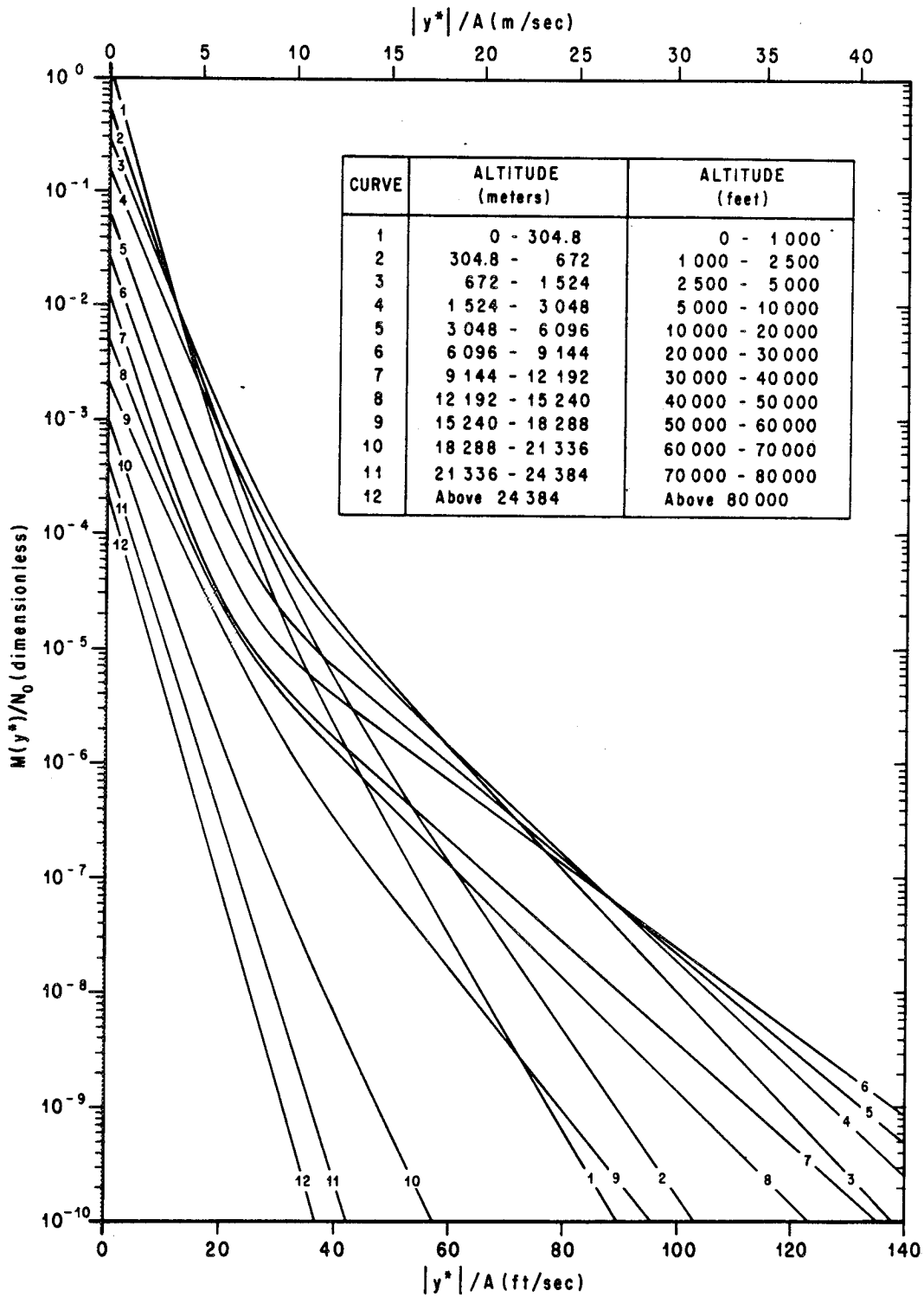


Figure 2.4.30 Exceedance curves for the vertical, lateral, and longitudinal components of turbulence for various altitude ranges.

TABLE 2.4.19 METRIC AND U.S. CUSTOMARY UNITS OF VARIOUS QUANTITIES IN THE TURBULENCE MODEL FOR HORIZONTALLY FLYING VEHICLES

Quantity	Metric Units	U. S. Customary Units
$\Omega$	rad/m	rad/ft
$\Phi_u, \Phi_w$	$m^2/sec^2/rad/m$	$ft^2/sec^2/rad/ft$
$\sigma^2$	$m^2/sec^2$	$ft^2/sec^2$
L	m	ft
$b_1, b_2$	m/sec	ft/sec
$P_1, P_2$	dimensionless	dimensionless
$\sigma_y/A$	m/sec	ft/sec
$ y^* /A$	m/sec	ft/sec
$N_0, N, M$	rad/sec	rad/sec

#### 2.4.13.1 Application of Power Spectral Model

To apply equation (2.44), the engineer can either calculate A and  $N_0$  and then calculate the load quantity  $y^*$  for a specified value of  $M(y^*)$ , or calculate A and calculate the load quantity  $y^*$  for a specified value of  $M(y^*)/N_0$ . These design criteria were consistent with the limit load capabilities of present day commercial aircraft. The criterion in which  $M(y^*)$  is specified is suitable for a mission analysis approach to the design problem. The criterion in which  $M(y^*)/N_0$  is specified is suitable for a design envelope approach to aircraft design.

In the design envelope approach, it is assumed that the airplane operates 100 percent of the time at its critical design envelope point. The philosophy is that if the vehicle can operate 100 percent of the time at any point on the envelope, it can surely operate adequately in any combination of operating points on the envelope. A new vehicle is designed on a limit load basis for a specified value of  $M/N_0$ . Accordingly,  $M/N_0 = 6 \times 10^{-9}$  is suitable for the design of commercial aircraft. To apply this criterion, all critical altitudes, weights, and weight distributions are specified configurations with equation (2.44) for  $M/N_0 = 6 \times 10^{-9}$ .

In the mission analysis approach, a new aircraft is designed on a limit load basis for  $M = 2 \times 10^{-5}$  load exceedances per hour. To apply this criterion, the engineer must construct an ensemble of flight profiles which define the expected range of payloads and the variation with time of speed, altitude, gross weight, and center of gravity position. These profiles are divided into mission segments, or blocks, for analysis; and average or effective values of the pertinent parameters are defined for each segment. For each mission segment, values of A and  $N_0$  are determined by dynamic analysis. A sufficient number of load and stress quantities are included in the dynamic analysis to assure that stress distributions throughout the structure are realistically or conservatively defined. Now the contribution of  $M(y^*)$  from the  $i$ th flight segment is

$t_i M_i (y^*/T)$ , where  $t_i$  is the amount of time spent in the  $i$ th flight regime (mission segment),  $T$  is the total time flown by the vehicle over all mission segments, and  $M_i(y^*)$  is the exceedance rate associated with the  $i$ th segment. The total exceedance rate for all mission segments,  $k$  say, is

$$M(y^*) = \sum_{i=1}^k \frac{t_i}{T} N_{0i} \left( P_1 e^{-|y^*|/b_1 A} + P_2 e^{-|y^*|/b_2 A} \right) \quad (2.45)$$

where subscript  $i$  denotes the  $i$ th mission segment. The limit gust load quantity  $|y^*|$  can be calculated with this formula upon setting  $M(y^*) = 2 \times 10^{-5}$  exceedances per hour.

The previously mentioned limit load design criteria were derived for commercial aircraft which are normally designed for 50,000-hr lifetimes. Therefore, to apply these criteria to horizontally flying aerospace vehicles which will have relatively short lifetimes would be too conservative. However, it is possible to modify these criteria so that they will reflect a shorter vehicle lifetime. The probability  $F_p$  that a load will be exceeded in a given number of flight hours  $T$  is

$$F_p = 1 - e^{-TM} \quad (2.46)$$

If it is assumed that the limit load criterion  $M = 2 \times 10^{-5}$  exceedances per hour is associated with an aircraft with a lifetime  $T$  equal to 50,000 hours, this means that  $F_p = 0.63$ ; i.e., there is a 63 percent chance that an aircraft design for a 50,000-hr operating lifetime will exceed its limit load capability at least once during its operating lifetime. This high failure probability, based on limit loads, is not excessive in view of the fact that an aircraft will receive many inspections on a routine basis during its operating lifetime. In addition, after safety factors are applied to the design limit loads, the ultimate load exceedance rate will be on the order of  $10^{-8}$  exceedances per hour. Substitution of this load exceedance rate into equation (2.46) for  $T = 50,000$  hr yields a failure probability, on an ultimate load basis, of  $F_p = 0.0005$ . This means that there will be only a 0.05 percent chance that an aircraft will exceed its ultimate load capability during its operating lifetime of 50,000 hr. Thus, a failure probability of  $F_p = 0.63$  on a limit load basis is reasonable for design. Let us now assume that  $F_p = 0.63$  is the limit load design failure probability so that equation (2.46) can be used to calculate design values of  $M$  associated with a specified vehicle lifetime. Thus, for example, if we expect a vehicle to fly only 100 hr, then according to equation (2.46), we have  $M = 10^{-2}$  exceedances per hour. Similarly, if we expect a vehicle to be exposed to the atmosphere for 1000 hr of flight, then  $M = 10^{-3}$  exceedances per hour.

The corresponding design envelope criterion can be obtained by dividing the preceding calculated values of  $M$  by an appropriate value of  $N_0$ . In the case of the 50,000 hr criterion, we have  $M/N_0 = 6 \times 10^{-9}$  and  $M = 2 \times 10^{-5}$  exceedances per hour, so that an estimate of  $N_0$  for purposes of obtaining a design criterion is  $N_0 = 0.333 \times 10^4 \text{ hr}^{-1}$ . Thus upon solving equation (2.46) for  $M$  and dividing by  $N_0 = 0.333 \times 10^4 \text{ hr}^{-1}$ , the design envelope criterion takes the form

$$\frac{M}{N_0} = \frac{3 \times 10^{-4}}{T} \quad (2.47)$$

where we have used  $F_p = 0.63$ . Thus, for a 100-hr aircraft, the design envelope criterion is  $M/N_0 = 3 \times 10^{-6}$  and for a 1000-hr aircraft  $M/N_0 = 3 \times 10^{-7}$ .

It is recommended that the power spectral approach be used in place of the standard discrete gust methods. Reasonably discrete gusts undoubtedly occur in the atmosphere; however, there is accumulating evidence that the preponderance of gusts are better described in terms of continuous turbulence models. It has long been accepted that clear air turbulence at moderate intensity levels is generally continuous in nature. Thunderstorm gust velocity profiles are now available in considerably quantity, and they almost invariably display the characteristics of continuous turbulence. Also, low-level turbulence is best described with power spectral methods. A power spectral method of load analysis is not necessarily more difficult to apply than a discrete gust method. The present static load "plunge-only discrete gust methods" can, in fact, be converted to a power spectral basis by making a few simple modifications in the definitions of the gust alleviation factor and the design discrete gust. To be sure, this simple rigid-airplane analysis does not exploit the full potentiality of the power spectral approach, but it does account more realistically for the actual mix of gust gradient distances in the atmosphere and the variation of gust intensity with gradient distance.

#### 2.4.14 Turbulence Model for Flight Simulation<sup>15</sup>

For simulation of turbulence in either an analog or digital fashion, the turbulence realizations are to be generated by passing a white noise process through a passive filter. The model of turbulence as given in Section 2.4.13 is not particularly suited for the simulation of turbulence with white noise because the von Karman spectra given by equations (2.32) and (2.35) are irrational. Thus, for engineering purposes, the Dryden spectra may be used for simulation of continuous random turbulence. They are given by

$$\text{Longitudinal: } \Phi_u(\Omega) = \sigma^2 \frac{2L}{\pi} \frac{1}{1 + (L\Omega)^2} \quad (2.48)$$

$$\text{Lateral and Vertical: } \Phi_w(\Omega) = \sigma^2 \frac{L}{\pi} \frac{1 + 3(L\Omega)^2}{[1 + (L\Omega)^2]^2} \quad (2.49)$$

Since these spectra are rational, a passive filter may be generated. It should be noted that the Dryden spectra are somewhat similar to the von Karman spectra. As  $\Omega L \rightarrow 0$ , the Dryden spectra asymptotically approach the von Karman spectra. As  $\Omega L \rightarrow \infty$ , the Dryden spectra behave like  $(\Omega L)^{-2}$ , while the von Karman spectra behave like  $(\Omega L)^{-5/3}$ . Thus, the Dryden spectra depart from the von Karman spectra by a factor proportional to  $(\Omega L)^{-1/3}$  as  $\Omega L \rightarrow \infty$ , so that at sufficiently large values of  $\Omega L$  the Dryden spectra will fall below the von Karman spectra. However, this deficiency in spectral energy of the Dryden spectra with respect to the von Karman spectra is not serious from an engineering point of view. If the capability to use the von Karman spectra is already available, the user should use it in flight simulation rather than the Dryden spectra.

The spectra as given by equations (2.48) and (2.49) can be transformed from the wave number ( $\Omega$ ) domain to the frequency domain ( $\omega$ , rad/sec) with a Jacobian transformation by noting that  $\Omega = \omega/V$ , so that

15. Details on simulations should be requested from Atmospheric Sciences Division, Space Sciences Laboratory, MSFC.

$$\Phi_u(\omega) = \frac{L}{V} \frac{2\sigma^2}{\pi} \frac{1}{1 + (L\omega/V)^2} \quad (2.50)$$

$$\Phi_w(\omega) = \frac{L}{V} \frac{\sigma^2}{\pi} \frac{1 + 3(L\omega/V)^2}{[1 + (L\omega/V)^2]^2} \quad (2.51)$$

The quantity  $V$  is the magnitude of the mean wind vector relative to the aerospace vehicle,  $\vec{u} - \vec{C}$ . The quantities  $\vec{u}$  and  $\vec{C}$  denote the velocity vectors of the mean flow of the atmosphere and the aerospace vehicle relative to the Earth. In the region above the 300-m level the longitudinal component of turbulence is defined to be the component of turbulence parallel to the mean wind vector relative to the aerospace vehicle ( $\vec{u} - \vec{C}$ ). The lateral and vertical components of turbulence are perpendicular to the relative mean wind vector and act in the lateral and vertical directions relative to the vehicle flight path.

#### 2.4.14.1 Transfer Functions

Atmospheric turbulence can be simulated by passing white noise through filters with the following frequency response functions:

$$\text{Longitudinal: } F_u(j\omega) = \frac{(2k)^{1/2}}{a + j\omega} \quad (2.52)$$

$$\text{Lateral and Vertical: } F_w(j\omega) = \frac{(3k)^{1/2} (3^{-1/2} a + j\omega)}{(a + j\omega)^2}, \quad (2.53)$$

where

$$a = \frac{V}{L} \quad (2.54)$$

$$k = \frac{a\sigma^2}{\pi} \quad (2.55)$$

To generate the three components of turbulence, three distinct uncorrelated Gaussian white noise sources should be used.

To define the rate of change of gust velocities about the pitch, yaw, and roll axes for simulation purposes, a procedure consistent with the preceding formulation can be found in Section 3.7.5, "Application of Turbulence Models and Analyses," of Reference 2.41. This should be checked for applicability.

## 2.4.14.2 Boundary Layer Turbulence Simulation

The turbulence in the atmospheric boundary layer, defined here for engineering purposes to be approximately the first 300 m of the atmosphere, is inherently anisotropic. To simulate this turbulence as realistically as possible, the differences between the various scales and intensities of turbulence should be taken into account. There are various problems associated with developing an engineering model of turbulence for simulation purposes. The most outstanding one concerns how one should combine the landing or take-off steady-state wind and turbulence conditions near the ground (18.3-m level, for example) with the steady-state wind and turbulence conditions at approximately the 300-m level. The wind conditions near the ground are controlled by local conditions and are usually derived from considerations of the risks associated with exceeding the design take-off or landing wind condition during any particular mission. The turbulence environments at and above the 300-m level are controlled by relatively large scale conditions rather than local landing or take-off wind conditions, and these turbulence environments are usually derived from considerations of the risks associated with exceeding the design turbulence environment during the total life or total exposure time of the vehicle to the natural environment. The use of the risk associated with exceeding the design wind environment near the ground during a given mission rather than the use of the risk of exceeding the design turbulence environment during the total life of the vehicle is justified on the basis that, if the landing conditions are not acceptable, the pilot has the option to land at an alternate airfield and thus avoid the adverse landing wind conditions at the primary landing site. Similarly, in the take-off problem, the pilot can wait until the adverse low-level wind and turbulence conditions have subsided before taking off. The use of the risk associated with exceeding the design turbulence environment during the total life of the vehicle above the atmospheric boundary layer to develop design turbulence environments for vehicle design studies is justified because the pilot does not have the option of avoiding adverse flight turbulence conditions directly ahead of the vehicle. In addition, the art of forecasting inflight turbulence has not progressed to the point where a flight plan can be established which avoids inflight turbulence with a reasonable small risk so that design environments can be established on a per flight basis rather than on a total lifetime basis.

How does one then establish a set of values for  $L$  and  $\sigma$  for each component of turbulence which merges together these two distinctly different philosophies? It is recommended that design values for each component of turbulence be established at the 18.3-m and at the 304.8-m levels based on the previously stated philosophies. Once these values of  $\sigma$  and  $L$  are established, the corresponding values between the 18.3- and 304.8-m levels can be obtained with the following interpolation formulae

$$\sigma(H) = \sigma_{18.3} \left( \frac{H}{18.3} \right)^p \quad (2.56)$$

$$L(H) = L_{18.3} \left( \frac{H}{18.3} \right)^q \quad (2.57)$$

where  $\sigma(H)$  and  $L(H)$  are the values of  $\sigma$  and  $L$  at height  $H$  above natural grade,  $\sigma_{18.3}$  and  $L_{18.3}$  are the values of  $\sigma$  and  $L$  at the 18.3-m level, and  $p$  and  $q$  are constants selected such that the appropriate values of  $\sigma$  and  $L$  occur at the 304.8-m level. Representative values of  $L_{18.3}$  for the Dryden spectrum are given by



$$L_{u18.3} = 31.5 \text{ m} ; L_{v18.3} = 18.4 \text{ m} ; L_{w18.3} = 10.0 \text{ m} , \quad (2.58)$$

where subscripts u, v, and w denote the longitudinal, lateral, and vertical components of turbulence. The corresponding design values of  $\sigma_{18.3}$  are given by

$$\sigma_{u18.3} = 2.5 u_{*o} \quad (2.59)$$

$$\sigma_{v18.3} = 1.91 u_{*o} \quad (2.60)$$

$$\sigma_{w18.3} = 1.41 u_{*o} \quad (2.61)$$

where  $u_{*o}$  is the surface friction velocity which is given by

$$u_{*o} = 0.4 \frac{\bar{u}_{18.3}}{\ln \left( \frac{18.3}{z_o} \right)} \quad (2.62)$$

The quantity  $\bar{u}_{18.3}$  is the mean wind or steady-state wind at the 18.3-m level,  $z_o$  is the surface roughness length (see Section 2.3.6.2), and SI units are understood. The quantity  $u_{18.3}$  is related to the 18.3-m level peak wind speed  $u_{18.3}$  (see Section 2.3.4) through the equation

$$\bar{u}_{18.3} = \frac{u_{18.3}}{G_{18.3}} , \quad (2.63)$$

where  $G_{18.3}$  is the 18.3-m level gust factor (see Section 2.3.7.1) associated with a 1-hr average wind. This gust factor is a function of the 18.3-m level peak wind speed so that, upon specifying  $u_{18.3}$  and the surface roughness length, the quantity  $u_{*o}$  is defined by equation (2.62) and the standard deviations of turbulence are in turn defined by equations (2.59) through (2.61).

The values of  $L$  and  $\sigma$  must satisfy the Dryden isotropy conditions demanded by the equation of mass continuity for incompressible flow. These isotropy conditions are given by

$$\frac{\sigma_u^2}{L_u} = \frac{\sigma_v^2}{L_v} = \frac{\sigma_w^2}{L_w} \quad (2.64)$$

and must be satisfied at all altitudes. The length scales given by equation (2.58) and the standard deviations of turbulence given by equations (2.59) through (2.61) were selected so that they satisfy the isotropy condition given by equation (2.64); i.e.,

$$\frac{\sigma_{u18.3}^2}{L_{u18.3}} = \frac{\sigma_{v18.3}^2}{L_{v18.3}} = \frac{\sigma_{w18.3}^2}{L_{w18.3}} \quad (2.65)$$

At the 304.8-m level, equation (2.64) is automatically satisfied because  $\sigma_u = \sigma_v = \sigma_w$  and  $L_u = L_v = L_w$  at the 304.8-m level.

To calculate the value of  $\sigma_{304.8}$  appropriate for performing a simulation, the following procedure is used to calculate the design instantaneous gust from which the design value of  $\sigma_{304.8}$  shall be obtained. The procedure consists of specifying the vehicle lifetime  $T$ ; calculating the limit load design value of  $M/N_0$  with equation (2.47); and then calculating the limit load instantaneous gust velocity,  $w^*$ , say, with equation (2.44) for  $A = 1$  with the values of  $P_1$ ,  $P_2$ ,  $b_1$ , and  $b_2$  associated with the 0-304.8 m height interval for climb, cruise, descent in Table 2.4.18. The instantaneous gust velocity  $w^*$  should be associated with the 99.98 percent value of gust velocity for a given realization of turbulence. In addition, the turbulence shall be assumed to be Gaussian, so that the value of  $\sigma_{304.8}$  for performing a simulation shall be obtained by dividing  $w^*$  by 3.5. This value of  $\sigma_{304.8}$  and the values of  $\sigma$  at the 18.3-m level [see equations (2.59) through (2.61)] shall be used to determine the values of  $p$  for each component of turbulence with equation (2.56); i.e.,

$$p = 0.356 \ln \left( \frac{\sigma_{304.8}}{\sigma_{18.3}} \right) \quad (2.66)$$

The integral scale of turbulence at the 304.8-m level appropriate for simulation of turbulence with the Dryden turbulence model is  $L_{304.8} = 190$  m. This scale of turbulence and the 18.3-m level scales of turbulence given by equation (2.58) yield the following values of  $q$  appropriate for the simulation of turbulence with the Dryden turbulence model in the atmospheric boundary layer:

$$q_u = 0.64 \quad ; \quad q_v = 0.83 \quad ; \quad q_w = 1.05 \quad (2.67)$$

The vertical distributions of  $\sigma$  and  $L$  given by equations (2.56) and (2.57) satisfy the isotropy condition given by equation (2.64).

Below the 18.3-m level  $\sigma$  and  $L$  shall take on constant values equal to corresponding 18.3-m level values.

The steady-state wind profile to be used with this model shall be obtained by the procedure given in Section 2.4.9.3 for merging ground winds and inflight wind profile envelopes.

To determine the steady-state wind direction  $\Theta(z)$  at any level  $H$  between the surface and the 1000-m level, use the following formula

$$\Theta(H) = \Theta_{1000} + \left[ 2 \left( \frac{H - 1000}{1000} \right) + \left( \frac{H - 1000}{1000} \right)^2 \right] \Delta ,$$

where  $\Theta_{1000}$  is the selected 1000-m level wind direction and  $H$  is altitude above the surface of the Earth in meters. The quantity  $\Delta$  is the angle between the wind vectors at the 10- and 1000-m levels. This quantity for engineering purposes is distributed according to a Gaussian distribution with mean value and standard deviation given by

$$\bar{\Delta} = 31^\circ , \quad \bar{u}_{1000} \leq 4 \text{ m sec}^{-1} ,$$

$$\bar{\Delta} = 31 - 2.183 \ln(\bar{u}_{1000}/4) , \quad \bar{u}_{1000} > 4 \text{ m sec}^{-1}$$

$$\sigma_{\Delta} = 64^\circ , \quad \bar{u}_{1000} \leq 4 \text{ m sec}^{-1} ,$$

$$\sigma_{\Delta} = 63e^{-0.0531(\bar{u}_{1000} - 4)} , \quad \bar{u}_{1000} > 4 \text{ m sec}^{-1} ,$$

where  $\bar{u}_{1000}$  is the 1000-m level steady-state wind speed. To avoid unrealistic wind direction changes,  $\Delta$ , between the surface and the 1000-m level, only those values of  $\Delta$  that occur in the interval  $-180^\circ \leq 0 \leq 180^\circ$  should be used. It is recommended that  $\pm 1$  percent risk wind direction changes be used for vehicle design studies.

To apply this model, the longitudinal component of turbulence shall be assigned to be that component of turbulence parallel to the horizontal component of the relative wind vector. The lateral component of turbulence is perpendicular to the longitudinal component and lies in the horizontal plane. The vertical component of turbulence is orthogonal to the horizontal plane.

The following procedure shall be used to calculate profiles of  $\sigma$  and  $L$  in the first 304.8 m of the atmosphere for simulation of turbulence with the Dryden turbulence model:

- a. Specify the peak wind speed at the 18.3-m level consistent with the accepted risk of exceeding the design 18.3-m level peak wind speed.
- b. Calculate the steady-state wind speed at the 18.3-m level with equation (2.63).
- c. Calculate the surface friction velocity with equation (2.62).
- d. Calculate the 18.3-m levels standard deviations of turbulence with equations (2.59) through (2.61).

e. Calculate the 304.8-m level standard deviation of turbulence consistent with the accepted risks of encountering the design instantaneous gust during the total exposure of the vehicle to the natural environments (remember  $\sigma_u = \sigma_v = \sigma_w$  at the 304.8-m level).

f. Calculate  $p_u$ ,  $p_v$ , and  $p_w$  with equation (2.66).

g. Calculate the distribution of  $\sigma$  and  $L$  with equations (2.56) and (2.57) for the altitudes at and between the 18.3- and 304.8-m levels.

h. Below the 18.3-m level  $\sigma$  and  $L$  shall take on constant values equal to the 18.3-m levels values of  $\sigma$  and  $L$ .

The reader should consult Reference 2.42 for a detailed discussion concerning the philosophy and problem associated with the simulation of turbulence for engineering purposes.

#### 2.4.14.3 Turbulence Simulation in the Free Atmosphere (above 304.8 m)

To simulate turbulence in the free atmosphere (above 304.8 m) it is recommended that equations (2.44) and (2.47) and the supporting data in Table 2.4.18 be used to specify the appropriate values of  $\sigma$ . The turbulence at these altitudes can be considered to be isotropic for engineering purposes so that the integral scales and intensities of turbulence are independent of direction. Past studies have shown that when the Dryden turbulence model is being used, the scales of turbulence  $L = 533.4$  m in the 304.8 to 672 m altitude band and  $L = 762$  m above the 672-m level in Table 2.4.18 should be replaced with the values  $L = 300$  m and  $L = 533$  m, respectively (Ref. 2.41). This reduction in scales tends to bring the Dryden spectra in line with the von Karman spectra over the band of wave numbers of the turbulence which are of primary importance in the design of aerospace vehicles. Accordingly, it is recommended that these reduced scales be used in the simulation of turbulence above the 304.8-m level when the Dryden model is being used.

To calculate the values of  $\sigma$  above the 304.8-m level appropriate for performing a simulation of turbulence, it is recommended that the procedure used to calculate the 304.8-m level value of  $\sigma$  be used. The appropriate values of  $P_1$ ,  $P_2$ ,  $b_1$ , and  $b_2$  for the various altitude bands above the 304.8-m level are given in Table 2.4.18.

#### 2.4.14.4 Design Floor on Gust Environments

If the design lifetime,  $T$ , is sufficiently small, it is possible that the turbulence models described herein for horizontally and nearly horizontally flying vehicles will result in a vehicle design gust environment which is characterized by discrete gusts with amplitudes less than  $9 \text{ m sec}^{-1}$  for  $dm/L > 10$  in Figure 2.4.31 above the 1-km level. This is especially true for altitudes above the 18-km level. In view of the widespread acceptance of the  $9 \text{ m sec}^{-1}$  gust as a minimum gust amplitude for design studies in the aerospace community and in view of the increased uncertainty in gust data as altitude increases, it is recommended that a floor be established on gust environments for altitudes above the 1-km level so that the least permissible value of  $\sigma$  shall be  $3.4 \text{ m sec}^{-1}$  above the 1-km level.

#### 2.4.14.5 Multimission Turbulence Simulation

The effects of atmospheric turbulence in both horizontal and near-horizontal flight, during reentry, or atmospheric flight of aerospace vehicles, are important for determining design, control, and "pilot-in-the-loop" effects. A nonrecursive model (based on the realistic von Karman spectra) is described. Aerospace

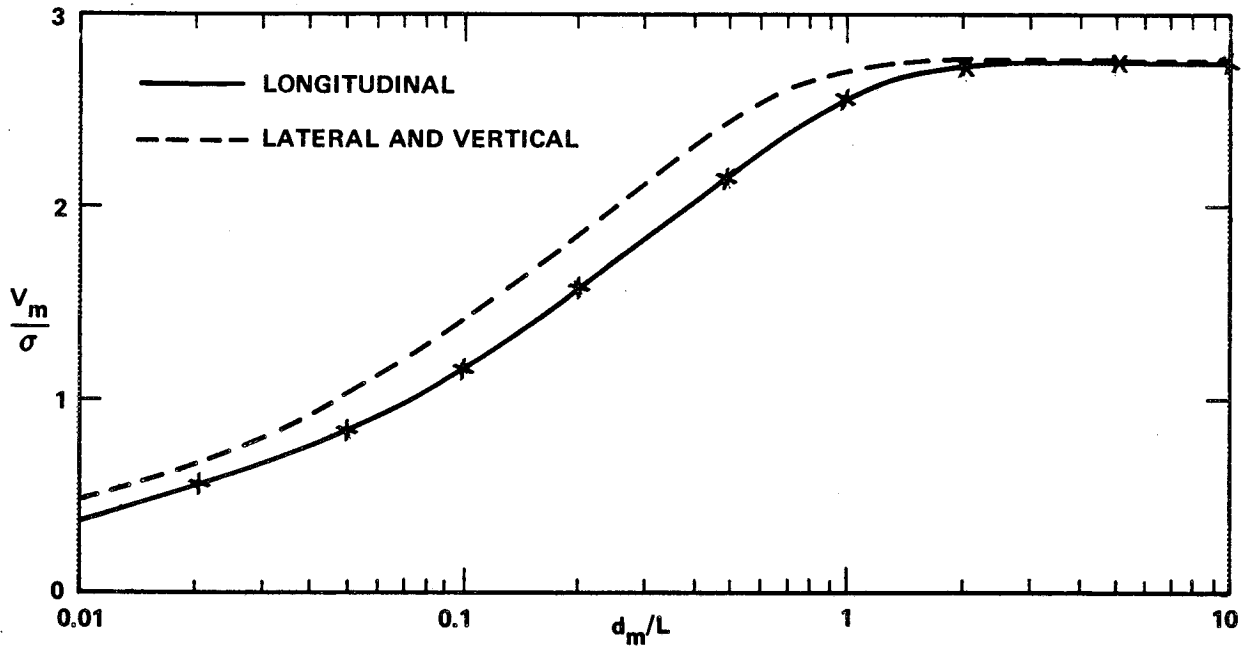


Figure 2.4.31 Nondimensional discrete gust magnitude  $V_m/\sigma$  as a function of nondimensional gust half-width.

vehicles will respond not only to turbulent gusts, but also to spatial gradients of instantaneous gusts (roll, pitch, and yaw). The model described (Reference 2.43) simulates vertical and horizontal instantaneous gusts, and three of the nine instantaneous gust gradients, as shown in Table 2.4.20.

TABLE 2.4.20 SIMULATED QUANTITIES

Variable	Spectrum	Comments
$U_1$	$\Phi_{11}$	Longitudinal gust
$U_2$	$\Phi_{22}$	Transverse gust
$U_3$	$\Phi_{33}$	Vertical gust
$\partial U_2 / \partial X_1$	$\Phi_{22/33}$	Yaw*
$\partial U_3 / \partial X_1$	$\Phi_{33/11}$	Pitch
$\partial U_3 / \partial X_2$	$\Phi_{33/22}$	Roll

\*  $X_1, X_2, X_3$  are aircraft fixed coordinates with  $X_1$  along the flight path,  $X_2$  the lateral direction, and  $X_3$  vertically upward.

Simulation of turbulence is achieved by passing a white noise process through a filter whose transfer function yields a von Karman power spectrum. The von Karman spectral functions are:

$$\Phi_{ii} = \frac{55\sigma^2}{36a\pi^2} \frac{[(aLk)^2 - (aLk_i)^2]}{[1 + (aLk)^2]^{17/6}} \quad (2.68)$$

$$\Phi_{ii/jj} = \frac{55\sigma^2}{36\pi^2 a^3 L^2} \frac{(aLk_i)^2 [(aLk)^2 - (aLk_i)^2]}{[1 + (aLk)^2]^{17/6}} \quad (2.69)$$

where

$a$  = von Karman constant (1.339)

$\sigma^2$  = variance of turbulence

$k$  = magnitude of wave number vector

$k_i$  =  $i$ th component of wave number

$L$  = length scale of turbulence

$\Phi_{ii}$  = three-dimensional gust spectrum

$\Phi_{ii/jj}$  = three-dimensional gust gradient spectrum.

Simulating turbulence with a von Karman spectrum is not a simple process, and generating von Karman turbulence fast enough for real-time simulations is difficult. One procedure for real-time simulations involves generating a large number of data tape sets for each new mission profile. An alternative approach was suggested by Fichtl (Reference 2.44). In this approach the turbulent spectra are represented in non-dimensional form using the length scale of turbulence, the standard deviation of turbulence, and vehicle true air speed. One set of nondimensional turbulence is generated based on the von Karman spectrum. These tapes can be Fourier analyzed to assure the spectra conform to von Karman's model. To run any mission profile, an efficient real-time routine reads the tapes and transforms them to dimensional format giving the desired output. Copies of gust and gust gradient simulation tapes are available for Space Shuttle applications upon request to the Chief of the Atmospheric Sciences Division, NASA Marshall Space Flight Center.

The conversion to dimensional values is accomplished as follows:

$$u_i^* = \sigma_i U_i \quad , \quad (2.70)$$

where

$u_i^*$  = dimensional gust

$\sigma_i$  = standard deviation of  $i$ th gust component

$$\frac{\partial u_i^*}{\partial x_j^*} = \frac{\sigma_i}{L_j} \frac{\partial u_i}{\partial x_j} \quad (2.71)$$

where

$\partial u_i^* / \partial x_j^* =$  dimensional gust gradient

$L_j =$  jth length scale of turbulence

$$\Delta t^* = a L_1 T / V \quad (2.72)$$

where

$\Delta t^* =$  dimensional time step

$T =$  dimensionless time step.

Note that  $\Delta t^*$  is not a constant because  $L_1$  and  $V$  vary with altitude. To obtain dimensional time,  $t_N^*$ , a summation process is involved,

$$t_N^* = \sum_{n=0}^N \Delta t_n^* = a T \sum_{n=0}^N L_{in} / V_n \quad (2.73)$$

For digital simulations, turbulence generated with uneven time steps is undesirable. A simple interpolation routine is used to obtain values of turbulence at equal time steps. Specific values of  $\sigma_i$  must be determined for specific applications. Sections 2.4.14.2 through 2.4.14.4 prescribe the technique for specifying the standard deviation. Values of the turbulent length scales and standard deviations are given in Table 2.4.24.

#### 2.4.15 Discrete Gust Model – Horizontally Flying Vehicles

Often it is useful for the engineer to use discrete gusts in load and flight control system calculations of horizontally flying vehicles. The discrete gust is defined as follows:

$$V_d = 0, \quad x < 0$$

$$V_d = \frac{V_m}{2} \left( 1 - \cos \frac{\pi x}{d_m} \right), \quad 0 \leq x \leq 2d_m$$

$$V_d = 0, \quad x > 2d_m,$$

TABLE 2.4.21 VARIATION OF STANDARD DEVIATION AND LENGTH SCALE WITH ALTITUDE\*

Altitude (m)	Standard Deviation of Turbulence			Integral Scales of Turbulence		
	$\sigma_1$ (m/sec)	$\sigma_2$ (m/sec)	$\sigma_3$ (m/sec)	$L_1$ (m)	$L_2$ (m)	$L_3$ (m)
10	2.31	1.67	1.15	21	11	5
20	2.58	1.98	1.46	33	19	11
30	2.75	2.20	1.71	43	28	17
40	2.88	2.36	1.89	52	35	23
50	2.98	2.49	2.05	61	42	29
60	3.07	2.61	2.19	68	49	35
70	3.15	2.71	2.32	75	56	41
80	3.22	2.81	2.43	82	63	47
90	3.28	2.89	2.54	89	69	53
100	3.33	2.97	2.64	95	75	59
200	3.72	3.53	3.38	149	134	123
304.8	3.95/4.37	3.95/4.37	3.95/4.39	196/300	190/300	192/300
400	4.39	4.39	4.39	300	300	300
500	4.39	4.39	4.39	300	300	300
600	4.39	4.39	4.39	300	300	300
700	4.39	4.39	4.39	300	300	300
762	4.39/5.70	4.39/5.70	4.39/5.70	300/533	300/533	300/533
800	5.70	5.70	5.70	533	533	533
900	5.70	5.70	5.70	533	533	533
1524	5.70/5.79	5.70/5.79	5.70/5.79	533	533	533
2000	5.79	5.79	5.79	533	533	533
3048	5.79/5.52	5.79/5.52	5.79/5.52	533	533	533
4000	5.52	5.52	5.52	533	533	533
5000	5.52	5.52	5.52	533	533	533
6096	5.52/5.27	5.52/5.27	5.52/5.27	533	533	533
7000	5.27	5.27	5.27	533	533	533
8000	5.27	5.27	5.27	533	533	533
9144	5.27/4.22	5.27/4.22	5.27/4.22	533	533	533
10000	4.22	4.22	4.22	533	533	533
20000	6.01	6.01	4.22	6691	6691	955

\*Double entries for a tabulated altitude indicate a step change in standard deviation or integral scale at that altitude.



where  $x$  is distance and  $V_m$  is maximum velocity of the gust which occurs at position  $x = d_m$  in the gust. To apply the model, the engineer specifies several values of the gust half-width,  $d_m$ , so as to cover the range of frequencies of the system to be analyzed. To calculate the gust parameter  $V_m$  one enters Figure 2.4.30 with  $d_m/L$  and reads out  $V_m/\sigma$ . Figure 2.4.30 is based on the Dryden spectrum of turbulence. Accordingly, the procedures outlined in Sections 2.4.14.2 and 2.4.14.3 can be used for the specification of the  $\sigma$ 's and  $L$ 's to determine the gust magnitude  $V_m$  from Figure 2.4.30. In the boundary layer, three values of  $V_m$  will occur at each altitude, one for each component of turbulence. In the free atmosphere the lateral and vertical values of  $V_m$  are equal at each altitude. In general both the continuous random gust model (Sections 2.4.13 and 2.4.14) and the discrete gust models are often used to calculate vehicle responses, with the procedure producing the larger response being used for design.

#### 2.4.16 Flight Regimes For Use of Horizontal and Vertical Turbulence Models (Spectra and Discrete Gusts)

Sections 2.4.8, 2.4.13, and 2.4.15 contain turbulence (spectra and discrete gusts) models for response calculations of vertically ascending and horizontally flying aerospace vehicles.

The turbulence model for the horizontally flying vehicles was derived from turbulence data gathered with airplanes. The turbulence model for the vertically ascending or descending vehicles was derived from wind profile measurements made with vertically ascending Jimsphere balloons and smoke trails. In many instances aerospace vehicles neither fly in a pure horizontal flight mode nor ascend or descend in a strictly vertical flight path. At this time there does not appear to be a consistent way of combining the turbulence models for horizontal and vertical flight so as to be applicable to the design of aerospace vehicles with other than near horizontal or vertical flight paths without being unduly complicated or overly conservative. In addition, the unavailability of a sufficient large data sample of turbulence measurements in three dimensions precludes the development of such a combined model.

Accordingly, in lieu of the availability of a combined turbulence model and for the sake of engineering simplicity, the turbulence model in Section 2.4.8 should be applied to ascending and descending aerospace vehicles when the angle between the flight path and the local vertical is less than or equal to 30 degrees. Similarly, the turbulence model in Sections 2.4.13 and 2.4.15 should be applied to aerospace vehicles when the angle between the flight path and the local horizontal is less than or equal to 30 degrees. In the remaining flight path region between 30 degrees from the local vertical and 30 degrees from the local horizontal, both turbulence models should be independently applied and the most adverse responses used in the design.

### 2.5 Mission Analysis, Prelaunch Monitoring, and Flight Evaluation

Wind information is useful in the following three general cases of mission analysis:

- a. Mission Planning. Since this activity will normally take place well in advance of the mission, the statistical attributes of the wind are used.
- b. Prelaunch Operations. Although wind statistics are useful at the beginning of this period, the emphasis is placed upon forecasting and wind monitoring.
- c. Postflight Evaluation. The effect of the observed winds on the flight is analyzed.

## 2.5.1 Mission Planning

From wind climatology, the optimum time (month and time of day) and place to conduct the operation can be identified. Missions with severe wind constraints may have such a low probability of success that the risk is unacceptable. Feasibility studies based upon wind statistics can identify these problem areas and answer questions such as: "Is the mission feasible as planned?" and "If the probable risk of mission delay or failure is unacceptably high, can it be reduced by rescheduling to a lighter wind period?"

The following examples are given to illustrate the use of some of the many wind statistics available to the mission planner.

If it is necessary to remove the wind loads damper from a large launch vehicle for a number of hours and this operation must be scheduled some days in advance, the well-known diurnal ground wind variation should be considered for this problem. If, for example, 10.3 m/sec (20 knots) were the critical wind speed, there is a 1-percent risk at 0600 EST, but a 13-percent risk at 1500 EST in July. Obviously, the midday period in the summer should be avoided for this operation. Since these probability values apply to 1-hr exposure periods, it is important to recognize that the wind risk depends not only upon wind speed but also upon exposure time. From Figure 2.5.1, the risk in percentage associated with a 15.4 m/sec (30-knot) wind at 10 m in February at Kennedy Space Center can be obtained for various exposure times. The upper curve shows the risk increasing from 1 percent for 1-hr exposure starting at 0400 EST to 9.3 percent for 12-hr exposure starting at 0400 EST. In this case the exposure period extends through the high risk part of the day. The lower curve illustrates the minimum risk associated with each exposure period. The lowest risk, of course, can be realized if the starting times are changed to avoid the windy portion of the day. Although there is no space here for the tabulation, wind risk probabilities by month and starting hour for exposure periods from 1 hr to 365 days are available upon request.

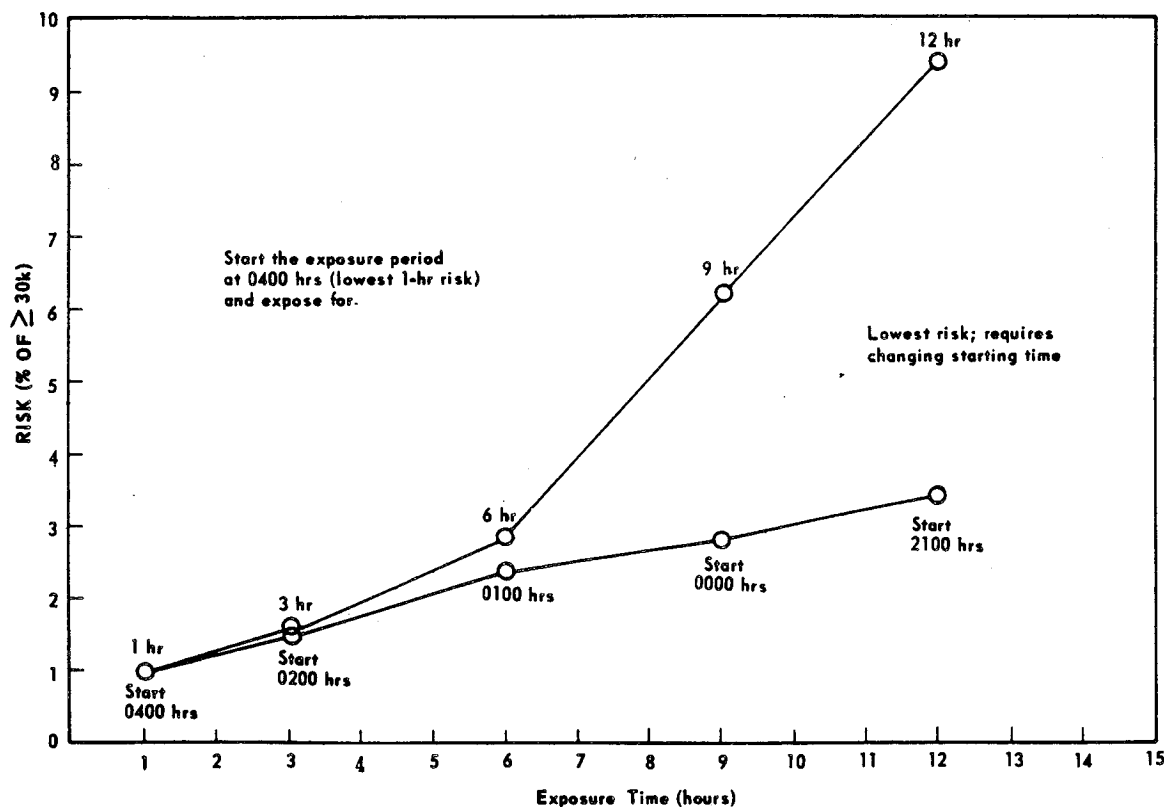


Figure 2.5.1 Example of wind risk for various exposure times.

When winds aloft are considered for mission planning purposes, again the first step might be to acquire general climatological information on the area of concern. From Figure 2.5.2 it is readily apparent that for Kennedy Space Center most strong winds occur during winter in the 10- to 15-km altitude region (this applies also to nearly all midlatitude locations). It is also true that these strong winds are usually westerly.

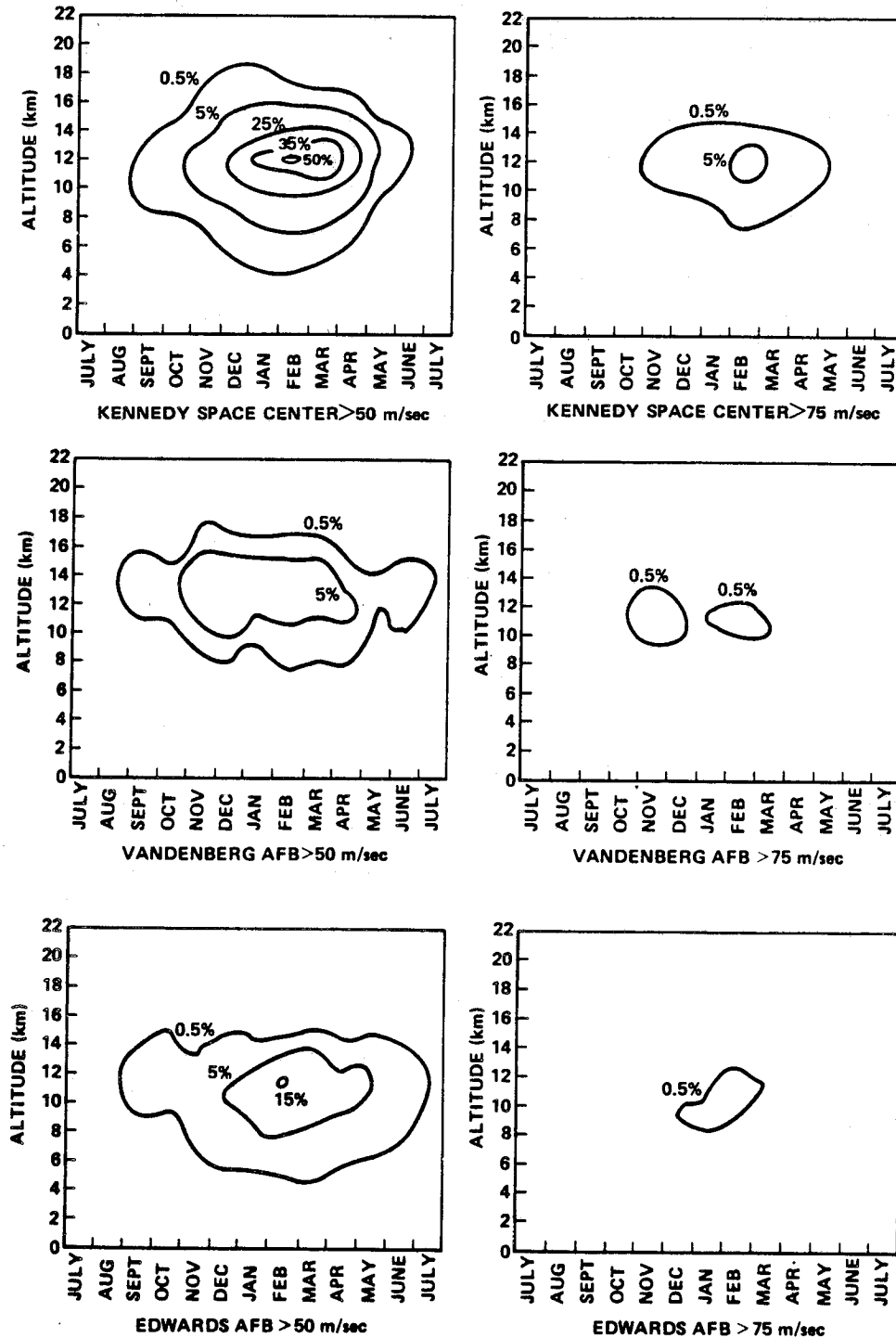


Figure 2.5.2 Frequency of scalar wind speed exceeding given wind speed as a function of altitude for stations indicated.

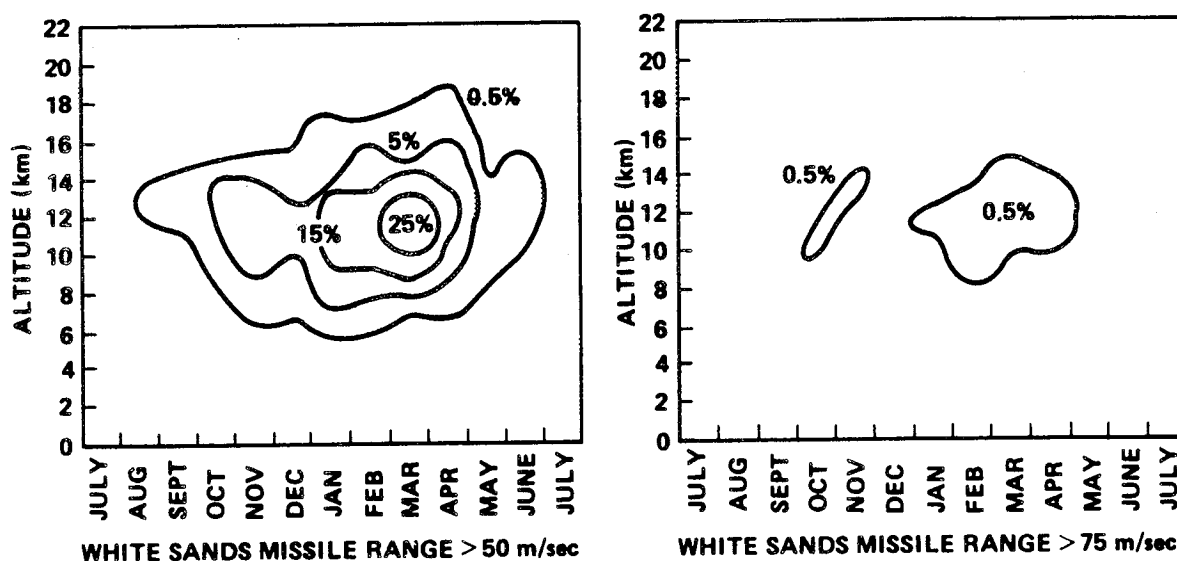


Figure 2.5.2 Frequency of scalar wind speed exceeding given wind speed as a function of altitude for stations indicated (Concluded).

Next, the mission analyst might ask if a particular mission is feasible. If, for example, the flight is to take place in January and 10- to 15-km altitude winds  $\geq 50$  m/sec are critical, the probability of favorable winds on any day in January is 0.496. With such a low probability of success, this mission may not be feasible. But, to continue the example, if it is necessary that continuously favorable winds exist for 3 days (perhaps for a dual launch), the probability of success will decrease to 0.256. Obviously an alternate mission schedule must be planned or else the scheduled space vehicle must be provided additional capability through redesign.

Perhaps the vehicle can remain on the pad in a state of near readiness awaiting launch for several days. In this case it would be desirable to know that the probability of occurrence of at least one favorable wind speed, for example, in a 4-day period is 0.813. If greater flexibility of operation is desired, one might require four favorable opportunities in 4 days. This probability is 0.550. Now, if consecutive favorable opportunities are required, for example, four consecutive successes in eight periods, the probability of success will be somewhat lower (0.431).

The mission planner might also gain some useful information from the persistence of the wind aloft. The probability of winds  $< 50$  m/sec on any day in January is 0.496. But if a wind speed  $< 50$  m/sec does occur, then the probability that the next observed wind 12 hr later would be  $< 50$  m/sec is 0.82, a rather dramatic change. Furthermore, if the wind continues below 50 m/sec for five observations, the probability that it will remain there for one more 12-hr period is 0.92.

As the time of the operation approaches T-4 to T-1 days, the conditional probability statements assume a more significant role. At this point, as the winds will usually be monitored, the appropriate conditional probability value can be identified and used to greater advantage.

The preceding examples are intended to illustrate the type of analysis that can be accomplished to provide objective data for program decisions. This may best be accomplished by a close working relationship between the analyst and those concerned with the decision.

## 2.5.2 Prelaunch Wind Monitoring

Inflight winds constitute the major atmospheric forcing function in space vehicle and missile design and operations. A frequency content of the wind profile near the bending mode frequencies or wind shear with the characteristics of a step input may exceed the vehicle's structural capabilities (especially on forward stations for the small-scale variations of the wind profiles). Wind profiles with high speeds and shears exert high structural loads at all stations on a large space vehicle, and when the influences of bending dynamics are high, even a profile with low speeds and high shears can create large loads (Ref. 2.45).

Because of the possibility of launch into unknown winds, operational missile systems must accept some inflight loss risk in exchange for a rapid-launch capability. But research and development missiles, and space vehicles in particular, cost so much that the overall success of a flight outweighs the consideration of launch delays caused by excessive inflight wind loads. If the exact wind profile could be known in advance, it would be a relatively simple task to decide upon the launch date and time. However, there is little hope of accurately forecasting the detailed wind profile very much into the future.

Over the years, these situations have increasingly put emphasis on prelaunch monitoring of inflight winds. Now, finally, prelaunch and profile determination techniques essentially preclude the risk of launching a space vehicle or research and development missile into an inflight wind condition that would cause it to fail.

The development and operational deployment of the FPS-16 radar/Jimsphere system (Ref. 2.46) significantly minimize vehicle failure risks when properly integrated into a flight simulation program. The Jimsphere sensor, when tracked with the FPS-16 or other radar with equal tracking capability, provides a very accurate "all weather" detailed wind profile measurement. FPS-16 radars are available at all national test ranges.

In general, the system provides a wind profile measurement from the surface to an altitude of 17 km in slightly less than 1 hr, a vertical spatial frequency resolution of 1 cycle per 100 m, and an rms error of about 0.5 m/sec or less for wind velocities averaged over 50-m intervals. The resolution of these data permits calculating the structural loads associated with the first bending mode and generally the second mode of missiles and space vehicles during the critical, high dynamic pressure phase of flight. This provides better than an order-of-magnitude accuracy improvement over the conventional rawinsonde wind profile measuring system.

By employing the appropriate data transmission resources, a detailed wind profile from the FPS-16 radar can be ready for input to the vehicle's flight simulation program within a few minutes after tracking of the Jimsphere. The flight simulation program provides flexibility relative to vehicle dynamics and other parameters in order to make maximum use of the detailed wind profiles.

If very critical wind conditions exist and the mission requirement dictates a maximum effort to launch with provision for last-minute termination of the operation, then a contingency plan that will provide essentially real-time wind profile and flight simulation data may be employed. This is done while the Jimsphere balloon is still in flight.

An example of the FPS-16 radar/Jimsphere system data appears in Figure 2.5.3 — the November 8 and 9, 1967, sequence observed during prelaunch activities for the first Apollo/Saturn-V test flight, AS-501. Reference 2.47 contains additional sequential Jimsphere wind profile sets for Kennedy Space Center and Point Mugu, California, respectively. The persistence over a period of 1 hr of some small-scale features in the wind profile structure, as well as the rather distinct changes that developed in the profiles over a period of a few hours, is evident.

Note: Times between Jimsphere measurements  
not constant.  
Jimsphere balloon rise time to  
16 km  $\approx$  50 min.

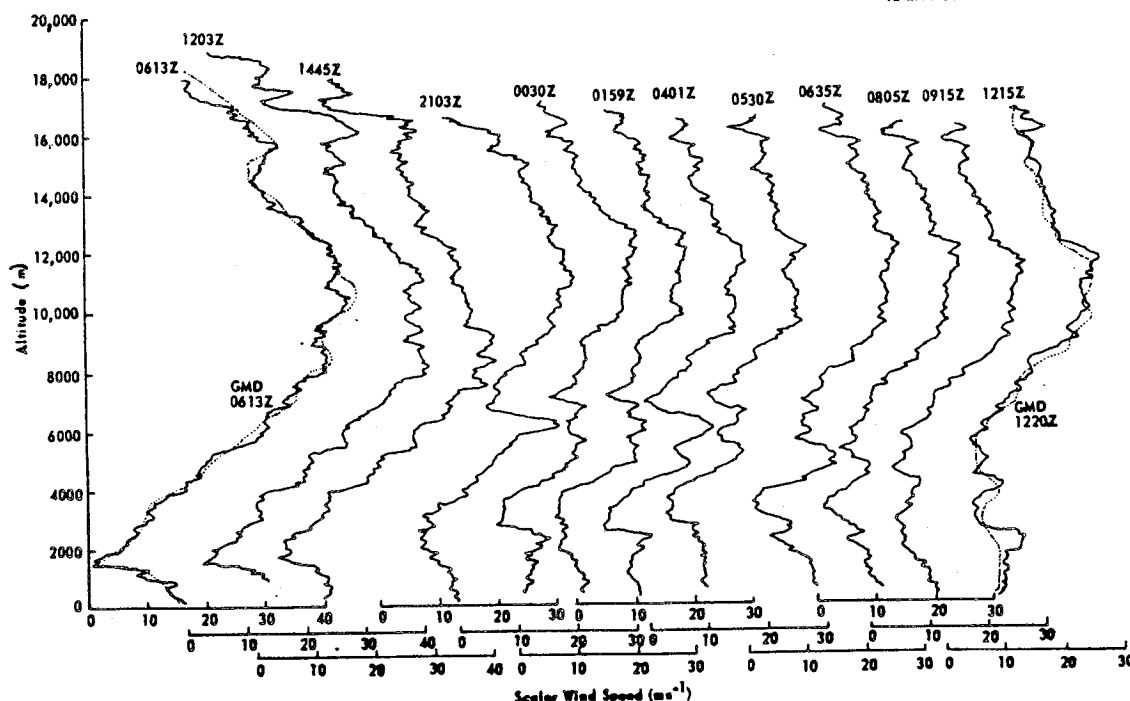


Figure 2.5.3 Example of the FPS-16 radar/Jimsphere system data, November 8-9, 1967.

The FPS-16 radar/Jimsphere system (Fig. 2.5.4) was routinely used in the prelaunch monitoring of NASA's Apollo/Saturn and the Space Shuttle flights. The wind profile data were transmitted to the Johnson Space Center and Marshall Space Flight Center, and the flight simulation results were sent to the launch complex at Kennedy Space Center.

An FPS-16 radar/Jimsphere operational measurement program capability exists at all the national test ranges to obtain detailed wind profile data for use in space vehicle and missile response studies, airplane turbulence analysis, atmospheric turbulence investigations, and mesometeorological studies. Sequential measurements similar to the Saturn-V data shown here — of eight to ten Jimsphere wind profiles approximately 1 hr apart — were made on at least 1 day per month for each location. Single profile measurements were also made daily at Kennedy Space Center.

### 2.5.3 Post-Flight Evaluation

#### 2.5.3.1 Introduction

Because of the variable effects of the atmosphere upon a large space vehicle at launch and during flight, various meteorological parameters were measured at the time of each space vehicle launch, including wind and thermodynamic data at the Earth's surface and up to an altitude of at least 90 km. To make the data available, meteorological tapes were prepared, presentations were made at flight evaluation meetings, memoranda of data tabulations were prepared and distributed, and a summary was written. Reference 2.48 for Space Shuttle STS-1 is an example of one of the reports with an atmospheric section.

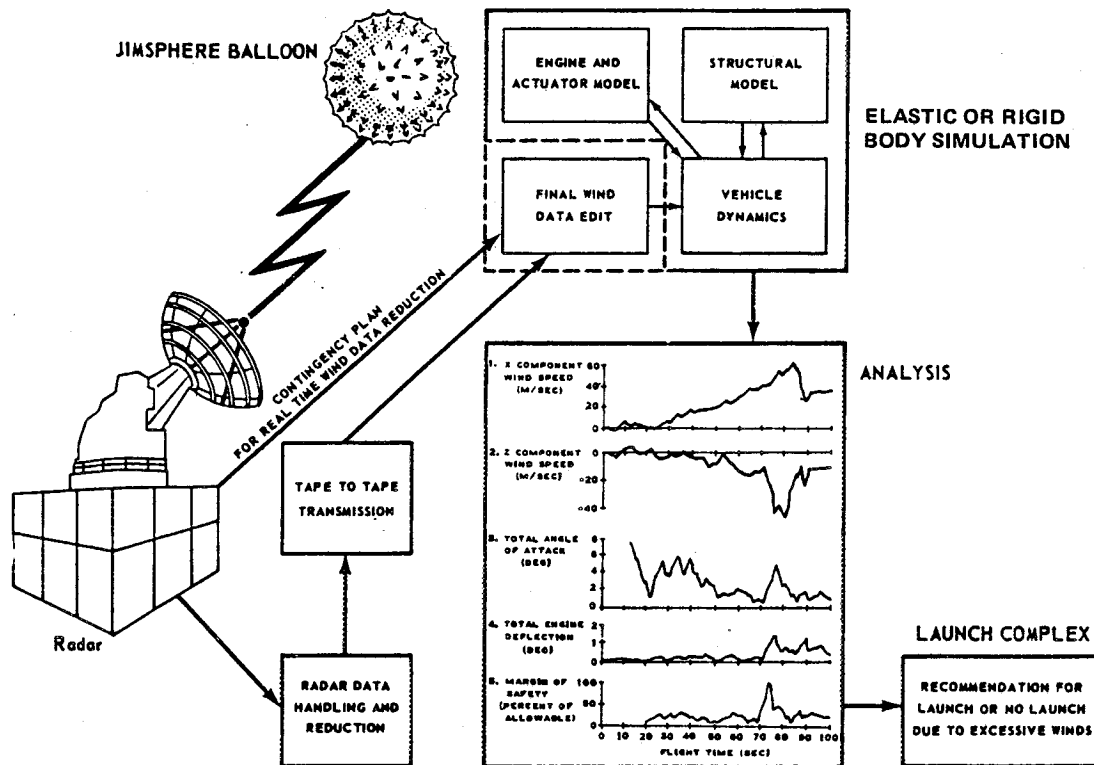


Figure 2.5.4 Operation of the FPS-16 radar/Jimsphere system.

### 2.5.3.2 Meteorological Tapes

Shortly after the launch of each space vehicle, under the cognizance of the Marshall Space Flight Center, a meteorological ascent data tape was prepared by combining the FPS-16 radar/Jimsphere wind profile data and the rawinsonde and rocketsonde wind profile and thermodynamic data (temperature, pressure, and humidity) observed as near the vehicle launch time as feasible. This was done under the supervision of the Marshall Space Flight Center's Atmospheric Sciences Division. The meteorological tape was normally available within 3 days after launch time and provided data to approximately 90 km. In the meteorological data tape, thermodynamic and wind data above the measured data are given by the Global Reference Atmosphere (2.49) values. To prevent unnatural jumps in the data when the two types are merged, the data were carefully examined to pick the best altitude for the merging, and a ramping procedure was employed. The meteorological data tapes were made available to all government and contractor groups for their use in the space vehicle launch and flight evaluation. This provides a consistent set of data for all evaluation studies and ensures the best available information of the state of the atmosphere during launch. For Space Shuttle launches, an SRB descent meteorological data tape was constructed using rawinsonde data taken from a ship stationed near the SRB impact site. Twenty parameters of data were included in the meteorological data tape at 100 ft increments of altitude<sup>16</sup> in Table 2.5.1.

16. Altitude increments of 100 ft were chosen to provide for maximum engineering value and for use of the available atmospheric data and do not necessarily represent the attainable frequency of response of the measurements.

2.118

Pad winds and thermodynamic data were measured and recorded at different heights above the launch pad starting several hours before launch time. Reference 2.50 summarizes atmospheric data observations for 155 flights of NASA/MSFC-related launches. Records and summary reports are maintained on the atmospheric parameters for MSFC-sponsored vehicle test flights conducted at Kennedy Space Center, Florida. Requests for summaries of these atmospheric data, or related questions on specific topics, should be directed to the Atmospheric Sciences Division, Space Sciences Laboratory, NASA-Marshall Space Flight Center, Alabama 35812.



TABLE 2.5.1 FORMAT OF METEOROLOGICAL TAPE

Word	Symbol	Description	Units
1	LAT	Latitude	degrees, + N
2	LON	Longitude	degrees, + E to 360
3	FLAG	0 = measured data, 1 = modeled data 2 = combined measured and modeled data	
4	—	Spare	
5	ALT	Geometric altitude	ft
6	WS	Horizontal wind speed	ft/s
7	WD	Direction horizontal wind is coming from relative to true north, North being 0 deg., increasing positively clockwise	deg
8	TE	Ambient temperature	deg C
9	PR	Ambient pressure	millibars
10	D	Ambient density	gram/m <sup>3</sup>
11	DW	Dew point	deg C
12	TEU	Ambient temperature systematic* uncertainty	deg C
13	PRU	Ambient pressure systematic uncertainty	millibars
14	DU	Ambient density systematic uncertainty	gram/m <sup>3</sup>
15	HWSUS	Horizontal wind speed systematic uncertainty	ft/s
16	HWSUN	Horizontal wind speed noise or** fluctuation uncertainty	ft/s
17	VWSUN	Vertical wind speed noise or fluctuation uncertainty	ft/s
18	HWDUS	Horizontal wind direction systematic uncertainty	deg
19	HWDUN	Horizontal wind direction noise or fluctuation uncertainty	deg
20		Spare	

## REFERENCES

- 2.1 Carter, E. A. and Schuknecht, L. A., "Peak Wind Statistics Associated with Thunderstorms at Cape Kennedy, Florida." NASA CR-61304, NASA-George C. Marshall Space Flight Center, Marshall Space Flight Center, Alabama, August 1969.
- 2.2 Smith, O. E.; Falls, L. W.; and Brown, S. C., "Research Achievements Review," Vol. II, Report No. 10, "Terrestrial and Space Environment Research at MSFC," NASA TM X-53706, NASA-George C. Marshall Space Flight Center, Marshall Space Flight Center, Alabama, 1967.
- 2.3 Lee, Russel F.; Goodge, Grant W.; and Crutcher, H. L., "Surface Climatological Information for Twelve Selected Stations for Reentry Vehicles," NASA CR-61319, Marshall Space Flight Center, Alabama, 1970.
- 2.4 Goodge, G. W., Bilton, T. H.; and Quinlin, F. T., "Surface Climatological Information for Twenty Selected Stations for Reentry Vehicles," NASA CR-61342, Marshall Space Flight Center, Alabama, 1971.
- 2.5 Fichtl, G. H. and McVehil, G. E., "Longitudinal and Lateral Spectra of Turbulence in the Atmospheric Boundary Layer at the Kennedy Space Center," Journal of Applied Meteorology, vol. 9, No. 1, Feb. 1970, pp. 51-63.
- 2.6 Blackadar, Alfred K., et al., "Investigation of the Turbulent Wind Field Below 150M Altitude at the Eastern Test Range," NASA CR-1410, NASA-George C. Marshall Space Flight Center, Marshall Space Flight Center, Alabama, Aug. 1969.
- 2.7 McVehil, G. E. and Camnitz, H. G., "Ground Wind Characteristics at Kennedy Space Center," NASA CR-1418, NASA-George C. Marshall Space Flight Center, Marshall Space Flight Center, Alabama, Sept. 1969.
- 2.8 Fichtl, G. H., Kaufman, J. W., and Vaughan, W. W., "Characteristics of Atmospheric Turbulence as Related to Wind Loads on Tall Structures." Journal of Spacecraft and Rockets, vol. 6, No. 12, Dec. 1969, pp. 1396-1403.
- 2.9 Fichtl, G. H., "Problems in the Simulation of Atmospheric Boundary Layer Flows." AGARD-CP-140 (1973) 2-1. (Paper presented AGARD Flight Mechanics Panel Symposium on "Flight in Turbulence," England, May 1973.)
- 2.10 Fichtl, G. H., "Wind Shear Near the Ground and Aircraft Operations." Journal of Spacecraft and Rockets, Vol. 9, No. 11, November 1972, pp. 765-770.
- 2.11 Fichtl, G. H., "Probability Distribution of Vertical Longitudinal Shear Fluctuations." Journal of Applied Meteorology, Vol. 11, No. 6, September 1972, pp. 918-925.
- 2.12 Fichtl, G. H., "Standard Deviation of Vertical Two-Point Longitudinal Velocity Differences in the Boundary Layer." Boundary-Layer Meteorology, Vol. 2, 1971, pp. 137-151.
- 2.13 Luers, J. K. and Reese, J. B., "Effects of Shear and Aircraft Landing," NASA CR-2287, NASA-George C. Marshall Space Flight Center, Alabama, July 1973.

- 2.14 Luers, J. K., "A Model of Wind Shear and Turbulence in the Surface Boundary Layer," NASA CR-2288, NASA-George C. Marshall Space Flight Center, Alabama, July 1973.
- 2.15 Sowa, Danies, "Low-Level Wind Shear," D. C. Flight Approach, No. 20, Douglas Aircraft Co., Long Beach, CA, 1974.
- 2.16 Barr, Neal M.; Gangaas, D.; and Schaeffer, D. R., "Wind Models for Flight Simulator Certification of Landing and Approach Guidance and Control Systems," Report No. FAA-RD-74-206, U. S. Department of Transportation, Federal Aviation Administration, Washington, D. C. 20590, December, 1974.
- 2.17 Lewell, W. S. and Williamson, Guy G., "Wind Shear and Turbulence Around Airports," NASA CR-2752, NASA-George C. Marshall Space Flight Center, Alabama, October 1976.
- 2.18 Camp, D. W. and Kaufman, J. W., "Comparison of Tower Influence on Wind Velocity for NASA's 150-meter Meteorological Tower and a Wind Tunnel Model of the Tower." Journal of Geophysical Research, vol. 75, No. 6, February 20, 1970.
- 2.19 Thom, H. C. S., "New Distributions of Extreme Winds in the United States," Journal of the Structural Division Proceedings of the American Society of Civil Engineers, ST-7, July 1968, pp. 1787-1801.
- 2.20 Thom, H. C. S., "Distribution of Extreme Winds over Oceans." J. Waterways, Harbors and Coastal Engr. Div., Proc. Am. Soc. Civ. Engr., February 1973, pp. 1-17.
- 2.21 Falls, L. W. and Brown, S. C., "Optimum Runway Orientation Relative to Crosswinds." NASA TN D-6930, September 1972.
- 2.22 Falls, L. W. and Crutcher, H. L., "Determination of Statistics for any Rotation of Axes of a Bivariate Normal Elliptical Distribution." NASA TM X-64595, May 1971.
- 2.23 IRIG Document No. 104-63, Range Reference Atmosphere Documents published by Secretariat, Range Commander's Council, White Sands Missile Range, New Mexico.

a. The following reference atmospheres have been published:

- (1) Atlantic Missile Range Reference Atmosphere for Cape Kennedy, Florida (Part I), 1963.
- (2) White Sands Missile Range Reference Atmosphere (Part I), 1964.
- (3) Fort Churchill Missile Range Reference Atmosphere for Fort Churchill, Canada (Part I), 1964.
- (4) Pacific Missile Range Reference Atmosphere for Eniwetok, Marshall Islands (Part I), 1964.
- (5) Fort Greely Missile Range Reference Atmosphere (Part I), 1964.
- (6) Eglin Gulf Test Range Reference Atmosphere for Eglin AFB, Florida (Part I), 1965.
- (7) Pacific Missile Range Reference Atmosphere for Point Arguello, California (Part I), 1965.

- (8) Wallops Island Test Range Reference Atmosphere (Part I), 1965.
  - (9) Eastern Test Range Reference Atmosphere for Ascension Island, South Atlantic (Part I), 1966.
  - (10) Lihue, Kauai, Hawaii Reference Atmosphere (Part I), 1970.
  - (11) Johnson Island Test Site Reference Atmosphere (Part I), 1970.
  - (12) Edwards Air Force Base Reference Atmosphere (Part I), 1972.
  - (13) Kwajalein Missile Range, Kwajalein, Marshall Islands, Reference Atmosphere (Part I), 1974.
  - (14) Cape Kennedy, Florida Reference Atmosphere (Part II), 1971.
  - (15) White Sands Missile Range Reference Atmosphere (Part II), 1971.
  - (16) Wallops Island Test Range Reference Atmosphere (Part II), 1971.
  - (17) Fort Greely Missile Range Reference Atmosphere (Part II), 1971.
  - (18) Pacific Missile Test Center Reference Atmosphere (Part II), November 1975.
- 2.24 Falls, L. W., "Normal Probabilities for Cape Kennedy Wind Components – Monthly Reference Periods for all Flight Azimuths – Altitudes 0 to 70 Kilometers," NASA TM X-64771, NASA-George C. Marshall Space Flight Center, Marshall Space Flight Center, Alabama, April 16, 1973.
  - 2.25 Falls, L. W., "Normal Probabilities for Vandenberg AFB Wind Components – Monthly Reference Periods for all Flight Azimuths, 0- to 70-km Altitudes," NASA TM X-64897, NASA-George C. Marshall Space Flight Center, Marshall Space Flight Center, Alabama, January 1975.
  - 2.26 Henry, Robert M., "A Statistical Model for Synthetic Wind Profiles for Aerospace Vehicle Design and Launching Criteria." NASA TN D-1813, 1963.
  - 2.27 Bieber, Raymond E., "Missile Structural Loads by Non-Stationary Statistical Methods." Technical Report No. LMSD 49703, Lockheed Missile and Space Division, Huntsville, Alabama 35807, April 1959. (Also available as DDC AD220595 or NTIS PB157733.)
  - 2.28 Vaughan, William W., "Interlevel and Intralevel Correlations of Wind Components for Six Geographical Locations." NASA TN D-561, Dec. 1960.
  - 2.29 Daniels, Glenn, E.; and Smith, Orvel E., "Scalar and Component Wind Correlations Between Altitude Levels for Cape Kennedy, Florida, and Santa Monica, California," NASA TN D-3815, Apr. 1968.
  - 2.30 Cochrane, James A.; Henry, Robert M.; and Weaver, William L., "Revised Upper Air Wind Data for Wallops Island Based on Serially Completed Data for the Years 1956 to 1964." NASA TN D-4570, NASA-Langley Research Center, Langley Station, Hampton, Virginia, May 1968.
  - 2.31 Buell, C. E., "Correlation Functions for Wind and Geopotential on Isobaric Surfaces." Journal of Applied Meteorology, vol. II, No. 1, Feb. 1972, pp. 51-59.

- 2.32 Buell, C. E., "Variability of Wind with Distance and Time on an Isobaric Surface." *Journal of Applied Meteorology*, vol. II, No. 7, Oct. 1972, pp. 1085-1091.
- 2.33 Truppi, Lawrence E., "Probabilities of Zero Wind Shear Phenomena Based on Rawinsonde Data Records," NASA TM X-53452, NASA-George C. Marshall Space Flight Center, Marshall Space Flight Center, Alabama, Apr. 27, 1966.
- 2.34 Camp, Dennis W. and Susko, Michael, "Percentage Levels of Wind Speed Differences Computed by Using Rawinsonde Wind Profile Data from Cape Kennedy, Florida," NASA TM X-53461, NASA-George C. Marshall Space Flight Center, Marshall Space Flight Center, Alabama, May 12, 1966.
- 2.35 Camp, Dennis W. and Fox, Patricia A., "Percentage Levels of Wind Speed Differences Computed by Using Rawinsonde Wind Profile Data from Santa Monica, California." NASA TM X-53428, NASA-George C. Marshall Space Flight Center, Marshall Space Flight Center, Alabama, Oct. 21, 1966.
- 2.36 Adelfang, Stanley I., "Analysis of Vector Wind Change with Respect to Time for Cape Kennedy, Florida." NASA CR-15077, NASA-George C. Marshall Space Flight Center, Marshall Space Flight Center, Alabama, August 1978.
- 2.37 Adelfang, Stanley I., "Analysis of Vector Wind Change with Respect to Time for Vandenberg Air Force Base, California." NASA CR-150776, NASA-George C. Marshall Space Flight Center, Marshall Space Flight Center, Alabama, August 1978.
- 2.38 Smith, O. E.; "Vector Wind and Vector Wind Shear Models 0 to 27 km Altitude for Cape Kennedy, Florida, and Vandenberg AFB, California," NASA TM X-73319, NASA-George C. Marshall Space Flight Center, Marshall Space Flight Center, Alabama, July 1976.
- 2.39 Fichtl, G. H., "Small-Scale Wind Shear Definition for Aerospace Vehicle Design." *Journal of Spacecraft and Rockets*, vol. 9, No. 2, Feb. 1972, pp. 79-83.
- 2.40 Fichtl, G. H.; Camp, D. W.; and Vaughan, W. W., "Detailed Wind and Temperature Profiles." *Clear Air Turbulence and Its Detection*, Edited by Yih-Hc Pao and Arnold Goldberg, Plenum Press, New York, 1969, pp. 308-333.
- 2.41 Chalik, C. R., et al., "Background Information and User Guide for MIL-F-8758B ASG, 'Military Specification - Flying Qualities for Piloted Airplanes,' " AFFDL-TR-69-72, Air Force Flight Dynamics Laboratory, Air Force Systems Command, Wright-Patterson Air Force Base, Ohio August 1969.
- 2.42 Dutton, J. A., "Broadening Horizons in Prediction of the Effects of Atmospheric Turbulence on Aeronautical Systems." AIAA Selected Reprints Series/Vol. XIII, *The Earth's Atmosphere*, W. W. Vaughan and L. L. DeVries, Editors, Published by the American Institute of Aeronautics and Astronautics, New York.
- 2.43 Tatom, Frank B. and Smith, S. Ray, "Advanced Shuttle Simulation Turbulence Tapes (SSTT) Users Guide." Engineering Analysis, Incorporated, Contract NAS8-33818, September 29, 1981.
- 2.44 Fichtl, George H., "A Technique for Simulating Turbulence for Aerospace Vehicle Flight Simulation Studies." NASA TM 78141, November 1977.

- 2.45 Ryan, Robert S.; Scoggins, James R.; and King, Alberta W., "Use of Wind Shears in the Design of Aerospace Vehicles." *Journal of Spacecraft and Rockets*, vol. 4, No. 11, Nov. 1967, pp. 1526-1532.
- 2.46 Vaughan, William W., "New Wind Monitoring System Protects R and D Launches." *Journal of Astronautics and Aeronautics*, Dec. 1968, pp. 41-43.
- 2.47 Johnson, D. L. and W. W. Vaughan, "Sequential High-Resolution Wind Profile Measurements," NASA TP-1354, December 1978.
- 2.48 Johnson, D. L., G. Jasper, and S. C. Brown, "Atmospheric Environment For Space Shuttle (STS-1) Launch," NASA TM-82436, July 1981.
- 2.49 Justus, C. G., G. R. Fletcher, F. E. Gramling, and W. B. Pace, "The NASA/MSFC Global Reference Atmospheric Model – MOD 3 (with Spherical Harmonic Wind Model)," NASA CR-3256, March 1980.
- 2.50 Johnson, D. L., "Summary of Atmospheric Data Observations for 155 Flights of MSFC/ABMA Related Aerospace Vehicles," NASA TM X-64796, NASA-George C. Marshall Space Flight Center, Marshall Space Flight Center, Alabama, December 5, 1973.

## SECTION III. INFLIGHT THERMODYNAMIC PROPERTIES

### 3.1 Introduction

This section presents the inflight thermodynamic parameters (temperature, pressure, and density) of the atmosphere. Mean and extreme values of the thermodynamic parameters given here can be used in application of many aerospace problems, such as (1) research planning and engineering design of remote Earth sensing systems; (2) vehicle design and development; and (3) vehicle trajectory analysis, dealing with vehicle thrust, dynamic pressure, aerodynamic drag, aerodynamic heating, vibration, structural and guidance limitations, and reentry analysis. Atmospheric density plays a very important role in most of the preceding problems. The first part of this section gives median and extreme values of these thermodynamic variables with respect to altitude. An approach is presented for temperature, pressure, and density as independent variables, with a method to obtain simultaneous values of these variables at discrete altitude levels. A subsection on reentry is presented, giving atmospheric models to be used for reentry heating, trajectory, etc., analyses.

Standard Sea Level Values used are (Ref. 3.1):

	Metric Units	U. S. Customary Units
Temperature	15.0°C or 288.15°K	59°F or 518.67°R
Pressure	1.013250 × 10 <sup>5</sup> Newton m <sup>-2</sup> (Newton m <sup>-2</sup> is equivalent to a Pascal (Pa) in SI units)	2116.22 lb ft <sup>-2</sup> or 14.696 lb in <sup>-2</sup>
Density	1.2250 kg m <sup>-3</sup>	0.076474 lb ft <sup>-3</sup>

### 3.2 Atmospheric Temperature

#### 3.2.1 Air Temperature at Altitude

Median and extreme air temperatures for the following list of test ranges were compiled from frequency distributions of radiosonde measured temperature data from 0 through 30 km altitude. Mean and extreme temperatures for the different test ranges above 30 km altitude were obtained from rocketsonde observations.

- Kennedy Space Center (KSC) air temperature values with altitude are given in Table 3.1 (Ref. 3.2).
- Vandenberg Air Force Base (VAFB) air temperature values with altitude are given in Table 3.2 (Ref. 3.3).
- White Sands Missile Range (WSMR) air temperature values with altitude are given in Table 3.3 (Ref. 3.4).
- Edwards Air Force Base (EAFB) air temperature values with altitude are given in Table 3.4 (Ref. 3.4).

A comprehensive listing of the extremes of surface temperature for different locations of interest can be obtained from Table 14.2 of this document.

TABLE 3.1 KENNEDY SPACE CENTER, FLORIDA, AIR TEMPERATURES  
AT VARIOUS ALTITUDES

Geometric Altitude (km)	Minimum		Median		Maximum	
	(° C)	(° F)	(° C)	(° F)	(° C)	(° F)
SFC (0.005 MSL)	-3.9	25	23.5	74	37.2	99
1	-8.9	16	17.4	63	27.8	82
2	-10.0	14	12.2	54	21.1	70
3	-11.1	12	7.1	45	16.1	61
4	-13.9	7	1.8	35	11.1	52
5	-20.0	-4	-4.1	25	5.0	41
6	-26.1	-15	-10.5	13	-1.1	30
7	-33.9	-29	-17.4	1	-7.2	19
8	-41.1	-42	-24.8	-13	-13.9	7
9	-50.0	-58	-32.4	-26	-21.1	-6
10	-56.1	-69	-40.0	-40	-30.0	-22
16.2	-80.0	-112	-70.3	-95	-57.8	-72
20	-76.1	-105	-62.8	-81	-47.8	-54
30	-58.9	-74	-42.4	-44	-30.0	-22
35	-47.4	-53	-30.6	-23	-14.6	6
40	-36.7	-34	-17.8	0	1.9	35
45	-23.0	-9	-6.3	21	12.8	55
50	-18.2	-1	-2.5	27	22.0	72
55	-34.4	-30	-12.4	10	18.9	66
60	-28.5	-19	-26.1	-15	17.0	63
*						

\*For higher altitudes, see Ref. 3.2, item 13 of Ref. 3.4, and paragraph 3.6 of this report.

### 3.2.2 Extreme Cold Temperature

Extreme cold temperatures during aircraft flight, when compartments are not heated, are given in Table 3.5. Hot compartment temperatures are given in Section XIV, paragraph 14.7.4.

## 3.3 Atmospheric Pressure

### 3.3.1 Definition

Atmospheric pressure (also called barometric pressure) is the force exerted, as a consequence of gravitational attraction, by the mass of the column of air of unit cross section lying directly above the area in question. It is expressed as force per unit area (Newtons per square meter or Newtons per square centimeter).



TABLE 3.2 VANDENBERG AIR FORCE BASE, CALIFORNIA, AIR  
TEMPERATURES AT VARIOUS ALTITUDES

Geometric Altitude (km)	Minimum		Median		Maximum	
	(° C)	(° F)	(° C)	(° F)	(° C)	(° F)
SFC (0.1 MSL)	-3.3	26	13.0	55	37.8	100
1	-3.6	26	13.3	56	33.4	92
2	-7.0	19	10.1	50	28.0	82
3	-15.2	5	5.1	41	17.6	64
4	-22.6	-9	-1.0	30	12.1	54
5	-29.7	-22	-7.5	18	3.3	38
6	-35.6	-32	-14.4	6	-2.7	27
7	-43.3	-46	-21.8	-7	-9.9	14
8	-47.4	-53	-29.5	-21	-15.9	3
9	-51.3	-60	-37.3	-35	-26.8	-16
10	-57.0	-71	-44.6	-48	-31.2	-24
16.3	-76.0	-105	-64.0	-83	-51.0	-60
20	-74.9	-103	-59.8	-76	-49.0	-56
30	-63.7	-83	-42.7	-45	-29.4	-21
40	-42.2	-44	-19.3	-3	17.8	64
45	-30.5	-23	-5.8	21	27.6	82
50	-18.2	-1	-2.0	28	28.0	82
55	-21.8	-7	-6.8	20	31.6	89
60	-25.1	-13	-20.5	-5	35.7	96
*						

\*For higher altitudes, see Refs. 3.3 and 3.6, and item 18 of Ref. 3.4.

### 3.3.2 Pressure at Altitude

Atmospheric pressure extremes for all four locations (KSC, VAFB, WSMR, and EAFB) are given in Table 3.6. These values were taken from pressure frequency distributions of radiosonde observations from the four test ranges. Pressure means and extremes were computed above 25 km altitude using rocketsonde observations.

Mean and extreme values of station pressure for many locations of interest are given in Table 7.1 of Section VII, whereas median values aloft are given in Tables 3.7, 3.8, 3.9, and in Ref. 3.4.

## 3.4 Atmospheric Density

### 3.4.1 Definition

Density ( $\rho$ ) is the ratio of the mass of a substance to its volume. (It is also defined as the reciprocal of specific volume.) Density is usually expressed in grams per cubic centimeter or kilograms per cubic meter.

TABLE 3.3 WHITE SANDS MISSILE RANGE, NEW MEXICO, AIR TEMPERATURES  
AT VARIOUS ALTITUDES

Geometric Altitude (km)	Minimum		Median		Maximum	
	(°C)	(°F)	(°C)	(°F)	(°C)	(°F)
SFC (1.3 MSL)	-23.9	-11	18.1	65	41.7	107
2	-11.7	11	13.1	56	31.1	88
3	-18.9	-2	6.2	43	22.2	72
4	-23.9	-11	-0.2	32	12.8	55
5	-31.1	-24	-6.7	20	6.1	43
6	-36.1	-33	-13.6	7	0.0	32
7	-42.2	-44	-20.5	-5	-7.2	19
8	-48.9	-56	-29.8	-22	-13.9	7
9	-55.0	-67	-36.7	-34	-21.1	-6
10	-60.0	-76	-43.3	-46	-27.2	-17
16.5	-80.0	-112	-67.1	-89	-47.8	-54
20	-77.8	-108	-60.0	-76	-52.2	-62
30	-58.9	-74	-43.2	-46	-26.1	-15
35	-52.2	-62	-32.2	-26	-7.8	18
40	-41.8	-43	-18.7	-2	5.0	41
45	-30.5	-23	-4.7	24	19.6	67
50	-29.1	-20	-1.6	29	25.9	79
55	-28.7	-20	-4.6	24	30.2	86
60	-35.8	-32	-20.4	-5	28.0	82
65	-36.5	-34	-38.1	-37	31.3	88
*						

\*For higher altitudes, see item 14 of Ref. 3.4.

TABLE 3.4 EDWARDS AFB, CALIFORNIA, TEMPERATURES AT VARIOUS ALTITUDES

Geometric Altitude (km)	Minimum		Median		Maximum	
	(°C)	(°F)	(°C)	(°F)	(°C)	(°F)
SFC (0.7 MSL)	-15.6	4	17.3	63	45.0	113
1	-6.0	21	16.2	61	35.3	96
2	-12.9	9	11.4	53	26.2	79
3	-16.9	2	5.3	42	19.0	66
4	-23.4	-10	-1.3	30	10.7	51
5	-29.7	-21	-8.2	17	5.2	41
6	-35.2	-31	-15.3	4	-2.9	27
7	-42.0	-44	-22.8	-9	-12.1	10
8	-48.9	-56	-30.5	-23	-17.4	1
9	-55.0	-67	-38.3	-37	-24.2	-12
10	-58.8	-74	-45.7	-50	-30.8	-23
17.8	-78.0	-108	-63.3	-82	-53.0	-63
20	-73.5	-100	-60.2	-76	-49.6	-57
25	-73.2	-100	-52.3	-62	-40.4	-41
30	-66.1	-87	-45.1	-49	-29.1	-20
40	-42.2	-44	-19.3	-3	17.8	64
45	-30.5	-23	-5.8	21	27.6	82
50	-18.2	-1	-2.0	28	28.0	82
55	-21.8	-7	-6.8	20	31.6	89
60	-25.1	-13	-20.5	-5	35.7	96
*						

\*For higher altitudes, see Ref. 3.7, and item 18 of Ref. 3.4.

TABLE 3.5 LOW TEMPERATURE EXTREMES FOR ALL LOCATIONS  
(KSC, VAFB, WSMR, AND EAFB)

Maximum Flight Altitude (Geometric) of Aircraft Used for Transport		Compartment Cold Temperature Extreme	
(m)	(ft)	(°C)	(°F)
3 048	10 000	-25.0	-13
4 572	15 000	-35.0	-31
6 096	20 000	-45.0	-49
7 620	25 000	-50.0	-58
9 144	30 000	-57.0	-71
10 668	35 000	-65.0	-85
12 192	40 000	-70.0	-94
13 716	45 000	-75.0	-103

TABLE 3.6 ATMOSPHERIC PRESSURE-HEIGHT EXTREMES  
FOR ALL LOCATIONS (KSC, VAFB, WSMR, AND EAFB)

Geometric Altitude (above mean sea level) (km) (ft)		Pressure			
		Maximum		Minimum	
		(mb)	(lb in. <sup>-2</sup> )	(mb)	(lb in. <sup>-2</sup> )
0	0	(Use values in Table 7.1 for surface pressure for each station)			
3	9 800	730	10.6	680	9.86
6	19 700	510	7.40	457	6.63
10	32 800	295	4.28	251	3.64
15	49 200	135	1.96	116	1.68
20	65 600	60	$8.7 \times 10^{-1}$	51	$7.4 \times 10^{-1}$
25	82 000	30	$4.4 \times 10^{-1}$	22	$3.2 \times 10^{-1}$
30	98 400	14.5	$2.1 \times 10^{-1}$	10.4	$1.5 \times 10^{-1}$
35	114 800	7.4	$1.1 \times 10^{-1}$	4.9	$7.1 \times 10^{-2}$
40	131 200	3.8	$5.5 \times 10^{-2}$	2.4	$3.5 \times 10^{-2}$
45	147 600	2.0	$2.9 \times 10^{-2}$	1.2	$1.7 \times 10^{-2}$
50	164 000	1.2	$1.7 \times 10^{-2}$	$6.1 \times 10^{-1}$	$8.8 \times 10^{-3}$
55	180 400	$6.0 \times 10^{-1}$	$8.7 \times 10^{-3}$	$3.1 \times 10^{-1}$	$4.5 \times 10^{-3}$
60	196 800	$3.2 \times 10^{-1}$	$4.6 \times 10^{-3}$	$1.6 \times 10^{-1}$	$2.3 \times 10^{-3}$
65	213 300	$1.7 \times 10^{-1}$	$2.5 \times 10^{-3}$	$8.3 \times 10^{-2}$	$1.2 \times 10^{-3}$
70	229 700	$8.5 \times 10^{-2}$	$1.2 \times 10^{-3}$	$4.1 \times 10^{-2}$	$5.9 \times 10^{-4}$
75	246 100	$3.1 \times 10^{-2}$	$4.5 \times 10^{-4}$	$2.1 \times 10^{-2}$	$3.0 \times 10^{-4}$
80	262 500	$1.4 \times 10^{-2}$	$2.0 \times 10^{-4}$	$8.9 \times 10^{-3}$	$1.3 \times 10^{-4}$
85	278 900	$5.9 \times 10^{-3}$	$8.6 \times 10^{-5}$	$3.7 \times 10^{-3}$	$5.4 \times 10^{-5}$
90	295 300	$2.6 \times 10^{-3}$	$3.8 \times 10^{-5}$	$1.4 \times 10^{-3}$	$2.0 \times 10^{-5}$

TABLE 3.7 KENNEDY SPACE CENTER (PATRICK) REFERENCE  
ATMOSPHERE (PRA-63) (Ref. 3.2)

GEOMETRIC ALTITUDE	PRESSURE	KINETIC TEMPERATURE	VIRTUAL TEMPERATURE	DENSITY	KINEMATIC VISCOSITY	COEFFICIENT OF VISCOSITY	SPEED OF SOUND
meters	newtons cm <sup>-2</sup>	degrees K	degrees K	kg m <sup>-3</sup>	m <sup>2</sup> sec <sup>-1</sup>	newton-sec m <sup>-2</sup>	m sec <sup>-1</sup>
0.	1.01325e+01	2.96777e+02	2.99372e+02	1.19354e+00	1.484e-05	1.23024e-05	3.46857e+02
1000.	3.06034e+00	2.30533e+02	2.32443e+02	1.07934e+00	1.66873e-05	1.80114e-05	3.42819e+02
2000.	8.05211e-01	2.85322e+02	2.86508e+02	9.79027e-01	1.81379e-05	1.77575e-05	3.39336e+02
3000.	7.13350e-01	2.90251e+02	2.90971e+02	8.85256e-01	1.97797e-05	1.75121e-05	3.36028e+02
4000.	6.31517e-01	2.74919e+02	2.75319e+02	7.99166e-01	2.15830e-05	1.72482e-05	3.32625e+02
5000.	5.57143e-01	2.59022e+02	2.59274e+02	7.20342e-01	2.35266e-05	1.69592e-05	3.28959e+02
6000.	4.90087e-01	2.62679e+02	2.62744e+02	6.49834e-01	2.56031e-05	1.66377e-05	3.24948e+02
7000.	4.29577e-01	2.55717e+02	2.55730e+02	5.84515e-01	2.78202e-05	1.62848e-05	3.20579e+02
8000.	3.75320e-01	2.48232e+02	2.48374e+02	5.26518e-01	3.02084e-05	1.59053e-05	3.15910e+02
9000.	3.26436e-01	2.40733e+02	2.40734e+02	4.72433e-01	3.28242e-05	1.55092e-05	3.11038e+02
10000.	2.82775e-01	2.33148e+02	2.33146e+02	4.22546e-01	3.57541e-05	1.51080e-05	3.06097e+02
11000.	2.43731e-01	2.25675e+02	2.25675e+02	3.76384e-01	3.90766e-05	1.47078e-05	3.01153e+02
12000.	2.09028e-01	2.18226e+02	2.18226e+02	3.33021e-01	4.30461e-05	1.43352e-05	2.96545e+02
13000.	1.78610e-01	2.12931e+02	2.12931e+02	2.92322e-01	4.73227e-05	1.40088e-05	2.92500e+02
14000.	1.51990e-01	2.08157e+02	2.08157e+02	2.54326e-01	5.19445e-05	1.37454e-05	2.88928e+02
15000.	1.29235e-01	2.04826e+02	2.04826e+02	2.19203e-01	5.68536e-05	1.35353e-05	2.86052e+02
16000.	1.09118e-01	2.03402e+02	2.03402e+02	1.87176e-01	6.18997e-05	1.34579e-05	2.85652e+02
17000.	9.22535e-02	2.02853e+02	2.02853e+02	1.59456e-01	6.80663e-05	1.34475e-05	2.85523e+02
18000.	7.80573e-02	2.05371e+02	2.05371e+02	1.32392e-01	7.42617e-05	1.35853e-05	2.87238e+02
19000.	6.62508e-02	2.07786e+02	2.07786e+02	1.09623e-01	8.05876e-05	1.37247e-05	2.88970e+02
20000.	5.63156e-02	2.10354e+02	2.10354e+02	9.31937e-02	8.74400e-05	1.38679e-05	2.90751e+02
21000.	4.79430e-02	2.12914e+02	2.12914e+02	7.84476e-02	9.48837e-05	1.40038e-05	2.92511e+02
22000.	4.08991e-02	2.15374e+02	2.15374e+02	6.61932e-02	1.02707e-04	1.41459e-05	2.94199e+02
23000.	3.49430e-02	2.17698e+02	2.17698e+02	5.59311e-02	1.11927e-04	1.42731e-05	2.95775e+02
24000.	2.99187e-02	2.19812e+02	2.19812e+02	4.74788e-02	1.22608e-04	1.43893e-05	2.97215e+02
25000.	2.55504e-02	2.21723e+02	2.21723e+02	4.03577e-02	1.34939e-04	1.44938e-05	2.98508e+02
26000.	2.20381e-02	2.23444e+02	2.23444e+02	3.43824e-02	1.48259e-04	1.45871e-05	2.99612e+02
27000.	1.89574e-02	2.24935e+02	2.24935e+02	2.93515e-02	1.62763e-04	1.46736e-05	3.00694e+02
28000.	1.63273e-02	2.26478e+02	2.26478e+02	2.51190e-02	1.78112e-04	1.47489e-05	3.01661e+02
29000.	1.40715e-02	2.28004e+02	2.28004e+02	2.14438e-02	1.94616e-04	1.48652e-05	3.02309e+02
30000.	1.21462e-02	2.30792e+02	2.30792e+02	1.83340e-02	2.12207e-04	1.49827e-05	3.02858e+02
31000.	1.05001e-02	2.33023e+02	2.33023e+02	1.56973e-02	2.31254e-04	1.51020e-05	3.03098e+02
32000.	9.09058e-03	2.35312e+02	2.35312e+02	1.34577e-02	2.51254e-04	1.52235e-05	3.03518e+02
33000.	7.89143e-03	2.37661e+02	2.37661e+02	1.15527e-02	2.72847e-04	1.53475e-05	3.03906e+02
34000.	6.84252e-03	2.40065e+02	2.40065e+02	9.92010e-03	2.95808e-04	1.54741e-05	3.04061e+02
35000.	5.94830e-03	2.42525e+02	2.42525e+02	8.54646e-03	3.20460e-04	1.56031e-05	3.04137e+02
36000.	5.16071e-03	2.45029e+02	2.45029e+02	7.36541e-03	3.46817e-04	1.57340e-05	3.04052e+02
37000.	4.51747e-03	2.47581e+02	2.47581e+02	6.35834e-03	3.75165e-04	1.58664e-05	3.03777e+02
38000.	3.94473e-03	2.50161e+02	2.50161e+02	5.49341e-03	4.05247e-04	1.59995e-05	3.03377e+02
39000.	3.44364e-03	2.52743e+02	2.52743e+02	4.75481e-03	4.37285e-04	1.61323e-05	3.02819e+02
40000.	3.02091e-03	2.55302e+02	2.55302e+02	4.12202e-03	4.71971e-04	1.62637e-05	3.02031e+02
41000.	2.64912e-03	2.57833e+02	2.57833e+02	3.57935e-03	5.08491e-04	1.63924e-05	3.01092e+02
42000.	2.32242e-03	2.60294e+02	2.60294e+02	3.11347e-03	5.47351e-04	1.65167e-05	3.00024e+02
43000.	2.04541e-03	2.62627e+02	2.62627e+02	2.71305e-03	5.88493e-04	1.66351e-05	2.98842e+02
44000.	1.80451e-03	2.64871e+02	2.64871e+02	2.36845e-03	6.32505e-04	1.67457e-05	2.97465e+02
45000.	1.59541e-03	2.66925e+02	2.66925e+02	2.07148e-03	6.78818e-04	1.68450e-05	2.95949e+02
46000.	1.39947e-03	2.68825e+02	2.68825e+02	1.81515e-03	7.26848e-04	1.69342e-05	2.94414e+02
47000.	1.21534e-03	2.70623e+02	2.70623e+02	1.59358e-03	7.76284e-04	1.70075e-05	2.92848e+02
48000.	1.05105e-03	2.72186e+02	2.72186e+02	1.40157e-03	8.27462e-04	1.70634e-05	2.91255e+02
49000.	9.36503e-04	2.73757e+02	2.73757e+02	1.23476e-03	8.80901e-04	1.71077e-05	2.89638e+02
50000.	8.53212e-04	2.75179e+02	2.75179e+02	1.09655e-03	9.35933e-04	1.71348e-05	2.87952e+02
51000.	7.82342e-04	2.76405e+02	2.76405e+02	9.78035e-04	9.94714e-04	1.71535e-05	2.86120e+02
52000.	6.63219e-04	2.77474e+02	2.77474e+02	8.65262e-04	1.06702e-03	1.71636e-05	2.84158e+02
53000.	5.35347e-04	2.78315e+02	2.78315e+02	7.59578e-04	1.14201e-03	1.71670e-05	2.82039e+02
54000.	4.51531e-04	2.78957e+02	2.78957e+02	6.62532e-04	1.22497e-03	1.71666e-05	2.79845e+02
55000.	4.03525e-04	2.79470e+02	2.79470e+02	5.80867e-04	1.30917e-03	1.71641e-05	2.77523e+02
56000.	3.58526e-04	2.79893e+02	2.79893e+02	5.07568e-04	1.39340e-03	1.71604e-05	2.75116e+02
57000.	3.17335e-04	2.79917e+02	2.79917e+02	4.46631e-04	1.47513e-03	1.71553e-05	2.72693e+02
58000.	2.79511e-04	2.79854e+02	2.79854e+02	3.92184e-04	1.55367e-03	1.71486e-05	2.70279e+02
59000.	2.43213e-04	2.79702e+02	2.79702e+02	3.42786e-04	1.62734e-03	1.71403e-05	2.67841e+02
60000.	2.09442e-04	2.79471e+02	2.79471e+02	3.00891e-04	1.69321e-03	1.71308e-05	2.65359e+02
61000.	1.78184e-04	2.79161e+02	2.79161e+02	2.61800e-04	1.74947e-03	1.71197e-05	2.62818e+02
62000.	1.54962e-04	2.78781e+02	2.78781e+02	2.27452e-04	1.80000e-03	1.71070e-05	2.60237e+02
63000.	1.34541e-04	2.78321e+02	2.78321e+02	1.99448e-04	1.84608e-03	1.70928e-05	2.57597e+02
64000.	1.16601e-04	2.77781e+02	2.77781e+02	1.75133e-04	1.88843e-03	1.70770e-05	2.54941e+02
65000.	1.00363e-04	2.77161e+02	2.77161e+02	1.53523e-04	1.92587e-03	1.70598e-05	2.52287e+02
66000.	8.70954e-05	2.76471e+02	2.76471e+02	1.34347e-04	1.95847e-03	1.70471e-05	2.49658e+02
67000.	7.50591e-05	2.75711e+02	2.75711e+02	1.17343e-04	1.98608e-03	1.70348e-05	2.47052e+02
68000.	6.45530e-05	2.74881e+02	2.74881e+02	1.02240e-04	2.00897e-03	1.70217e-05	2.44443e+02
69000.	5.54142e-05	2.73991e+02	2.73991e+02	8.89979e-05	2.02887e-03	1.70077e-05	2.41819e+02
70000.	4.74675e-05	2.73051e+02	2.73051e+02	7.77141e-05	2.04514e-03	1.70025e-05	2.39261e+02
71000.	4.05760e-05	2.72071e+02	2.72071e+02	6.84933e-05	2.05795e-03	1.70013e-05	2.36737e+02
72000.	3.46109e-05	2.71051e+02	2.71051e+02	6.09306e-05	2.06795e-03	1.70013e-05	2.34237e+02
73000.	2.94567e-05	2.70001e+02	2.70001e+02	5.49354e-05	2.07296e-03	1.70013e-05	2.31737e+02
74000.	2.50135e-05	2.68921e+02	2.68921e+02	4.93547e-05	2.07796e-03	1.70013e-05	2.29237e+02
75000.	2.12002e-05	2.67781e+02	2.67781e+02	4.40689e-05	2.08296e-03	1.70013e-05	2.26737e+02
76000.	1.79241e-05	2.66601e+02	2.66601e+02	3.92339e-05	2.08796e-03	1.70013e-05	2.24237e+02
77000.	1.51198e-05	2.65381e+02	2.65381e+02	3.48491e-05	2.09296e-03	1.70013e-05	2.21737e+02
78000.	1.27248e-05	2.64121e+02	2.64121e+02	3.08581e-05	2.09796e-03	1.70013e-05	2.19237e+02
79000.	1.06343e-05	2.62821e+02	2.62821e+02	2.71918e-05	2.10296e-03	1.70013e-05	2.16737e+02
80000.	8.94924e-06	2.61481e+02	2.61481e+02	2.38011e-05	2.10796e-03	1.70013e-05	2.14237e+02
81000.	7.47284e-06	2.60101e+02	2.60101e+02	2.07361e-05	2.11296e-03	1.70013e-05	2.11737e+02
82000.	6.23539e-06	2.58681e+02	2.58681e+02	1.79339e-05	2.11796e-03	1.70013e-05	2.09237e+02
83000.	5.18721e-06	2.57221e+02	2.57221e+02	1.54256e-05	2.12296e-03	1.70013e-05	2.06737e+02
84000.	4.31634e-06	2.55721e+02	2.55721e+02	1.30500e-05	2.12796e-03	1.70013e-05	2.04237e+02
85000.	3.59147e-06	2.54181e+02	2.54181e+02	1.08500e-05	2.13296e-03	1.70013e-05	2.01737e+02
86000.	2.98350e-06	2.52601e+02	2.52601e+02	9.05000e-06	2.13796e-03	1.70013e-05	1.99237e+02
87000.	2.48504e-06	2.50981e+02	2.50981e+02	7.57305e-06	2.14296e-03	1.70013e-05	1.96737e+02
88000.	2.06715e-06	2.49321e+02	2.49321e+02	6.39107e-06	2.14796e-03	1.70013e-05	1.94237e+02
89000.	1.72243e-06	2.47621e+02	2.47621e+02	5.42158e-06	2.15296e-03	1.70013e-05	1.91737e+02
90000.	1.44435e-06	2.45881e+02	2.45881e+02	4.62158e-06	2.15796e-03	1.70013e-05	1.89237e+02



TABLE 3.8 VANDENBERG AFB REFERENCE ATMOSPHERE (VRA-71) (Ref. 3.3)

GEOMETRIC ALTITUDE	PRESSURE	KINETIC TEMPERATURE	VIRTUAL TEMPERATURE	DENSITY	KINEMATIC VISCOSITY	COEFFICIENT OF VISCOSITY	SPEED OF SOUND
meters	newtons cm <sup>-2</sup>	degrees K	degrees K	kg m <sup>-3</sup>	m <sup>2</sup> sec <sup>-1</sup>	newton-sec m <sup>-2</sup>	m sec <sup>-1</sup>
0.	1.0189504+01	2.858177+02	2.8715277+02	1.2251775+01	1.4384405-05	1.7794150-05	3.3970470+02
1000.	9.0477741+00	2.8542566+02	2.8699751+02	1.0981225+00	1.6216058-05	1.7812529-05	3.3961291+02
2000.	8.0243502+00	2.8329711+02	2.8359425+02	9.8575554-01	1.7913862-05	1.7958691-05	3.3759326+02
3000.	7.1046558+00	2.7821440+02	2.7842334+02	8.3892961-01	1.9535771-05	1.7417372-05	3.3450165+02
4000.	6.2761809+00	2.717236+02	2.7234561+02	7.0776189-01	2.1316859-05	1.7112362-05	3.3082996+02
5000.	5.5286658+00	2.6563135+02	2.6576157+02	6.0468038-01	2.3153579-05	1.6787203-05	3.2682695+02
6000.	4.8538800+00	2.5871193+02	2.5878914+02	5.2842553-01	2.5155218-05	1.6437062-05	3.2249129+02
7000.	4.2453096+00	2.5137873+02	2.5142259+02	4.6392735-01	2.7304746-05	1.6052801-05	3.1786335+02
8000.	3.6977586+00	2.4369403+02	2.4371449+02	4.0859970-01	2.9632266-05	1.5663607-05	3.1285134+02
9000.	3.2071387+00	2.3535146+02	2.3539045+02	3.6357411-01	3.2207045-05	1.5250423-05	3.0789330+02
10000.	2.7706815+00	2.2650072+02	2.2650072+02	3.2242641-01	3.5177528-05	1.4859917-05	3.0322244+02
11000.	2.3796741+00	2.2133779+02	2.2133779+02	2.8335754-01	3.8432351-05	1.4505341-05	2.9856203+02
12000.	2.0378622+00	2.1778613+02	2.1778613+02	2.4593437-01	4.2060947-05	1.4207811-05	2.9358435+02
13000.	1.7407523+00	2.1502240+02	2.1502240+02	2.1201038-01	4.6009260-05	1.4120552-05	2.8939544+02
14000.	1.4832321+00	2.1289403+02	2.1289403+02	1.8248443-01	5.0666966-05	1.4000983-05	2.8520124+02
15000.	1.2630643+00	2.1101376+02	2.1101376+02	1.5710137-01	5.5574156-05	1.3904901-05	2.8120395+02
16000.	1.0740324+00	2.0946158+02	2.0946158+02	1.342758-01	6.0735000-05	1.3792737-05	2.7733774+02
17000.	9.1290847-01	2.0833955+02	2.0833955+02	1.13225517-01	6.6252571-05	1.3733457-05	2.7370126+02
18000.	7.7604645-01	2.1039268+02	2.1039268+02	9.7851134-01	7.2075284-05	1.3707081-05	2.6977721+02
19000.	6.6155133-01	2.1166832+02	2.1166832+02	8.4082416-01	7.8106581-05	1.3741033-05	2.6557730+02
20000.	5.6393707-01	2.1778162+02	2.1778162+02	7.2619110-01	8.4675866-05	1.4035972-05	2.6284225+02
21000.	4.8036311-01	2.1536418+02	2.1536418+02	6.3770999-01	9.149514-05	1.4145373-05	2.5942363+02
22000.	4.046343-01	2.1777692+02	2.1777692+02	5.651049-01	9.8651338-05	1.4251967-05	2.5657832+02
23000.	3.5099534-01	2.1318086+02	2.1318086+02	5.025416-01	1.0709956-05	1.4352530-05	2.5367034+02
24000.	3.0077469-01	2.2069008+02	2.2069008+02	4.4749698-01	1.1639381-05	1.4446741-05	2.5080132+02
25000.	2.5325416-01	2.2135423+02	2.2135423+02	3.916643-01	1.2700363-05	1.4550570-05	2.4786653+02
26000.	2.1205890-01	2.2311148+02	2.2311148+02	3.4657364-01	1.3907229-05	1.4668995-05	2.4494739+02
27000.	1.7609374-01	2.2436256+02	2.2436256+02	3.0641456-01	1.5279501-05	1.4803803-05	2.4202757+02
28000.	1.4640577-01	2.2603759+02	2.2603759+02	2.7089117-01	1.6824778-05	1.4970351-05	2.3914787+02
29000.	1.2414239-01	2.2714065+02	2.2714065+02	2.4150601-01	1.8713054-05	1.4848574-05	2.3627934+02
30000.	1.0206691-01	2.2844426+02	2.2844426+02	2.1645321-01	2.0860608-05	1.4963557-05	2.3343116+02
31000.	8.0546330-02	2.3259450+02	2.3259450+02	1.9797153-01	2.3449446-05	1.5079353-05	2.3057215+02
32000.	6.3123502-02	2.3466267+02	2.3466267+02	1.81214637-01	2.6187373-05	1.5180873-05	2.2790968+02
33000.	5.0013563-02	2.3673119+02	2.3673119+02	1.6783119-01	2.9151691-05	1.5293437-05	2.2508444+02
34000.	3.6532667-02	2.3884258+02	2.3884258+02	1.5611610-01	3.2406839-05	1.5400839-05	2.2213994+02
35000.	2.9521743-02	2.4103703+02	2.4103703+02	1.4504768-01	3.6024678-05	1.5520252-05	2.1913525+02
36000.	2.4776554-02	2.4335058+02	2.4335058+02	1.3411708-01	4.0011140-05	1.5646202-05	2.1627460+02
37000.	2.0906180-02	2.4579478+02	2.4579478+02	1.2319433-01	4.4573365-05	1.5773532-05	2.1342939+02
38000.	1.8347555-02	2.4877562+02	2.4877562+02	1.1277770-01	4.9826678-05	1.5907357-05	2.1059371+02
39000.	1.5377026-02	2.5109366+02	2.5109366+02	1.0369810-01	5.5639358-05	1.6047047-05	2.0775533+02
40000.	1.3008215-02	2.5389379+02	2.5389379+02	9.5224862-02	6.1912084-05	1.6191175-05	2.0482404+02
41000.	1.0836420-02	2.5675467+02	2.5675467+02	8.5772217-02	6.8667959-05	1.6337515-05	2.0182123+02
42000.	9.1339577-02	2.5961737+02	2.5961737+02	7.8049844-02	7.5808585-05	1.6482991-05	1.9870700+02
43000.	7.6336093-02	2.6237946+02	2.6237946+02	7.0993312-02	8.3570753-05	1.6633690-05	1.9547332+02
44000.	6.2895222-02	2.6506471+02	2.6506471+02	6.4725865-02	9.1219677-05	1.6754759-05	1.9234216+02
45000.	5.1566305-02	2.6773143+02	2.6773143+02	5.8593363-02	9.9707714-05	1.6877477-05	1.8915044+02
46000.	4.1904100-02	2.6918390+02	2.6918390+02	5.2937750-02	1.0767778-05	1.6987989-05	1.8584799+02
47000.	3.4227031-02	2.7047061+02	2.7047061+02	4.7806507-02	1.1672633-05	1.7027854-05	1.8239348+02
48000.	2.836504-02	2.7097270+02	2.7097270+02	4.3034174-02	1.2728103-05	1.7052811-05	1.7899523+02
49000.	2.3752739-02	2.7047461+02	2.7047461+02	3.8704948-02	1.3906948-05	1.7023115-05	1.7509384+02
50000.	2.0455115-02	2.7111662+02	2.7111662+02	3.4862549-02	1.5170714-05	1.7051507-05	1.7010733+02
51000.	1.7450636-02	2.7127369+02	2.7127369+02	3.16007037-02	1.7777625-05	1.7067771-05	1.6517357+02
52000.	1.4605708-02	2.7077585+02	2.7077585+02	2.84997924-02	2.0052652-05	1.7043536-05	1.5988156+02
53000.	1.2344143-02	2.6376022+02	2.6376022+02	2.5741944-02	2.2553560-05	1.6993517-05	1.5295623+02
54000.	1.0478015-02	2.6826166+02	2.6826166+02	2.3026166-02	2.5306703-05	1.6917808-05	1.4638402+02
55000.	8.4382453-03	2.6535233+02	2.6535233+02	2.0575237-02	2.7931122-05	1.6822337-05	1.4017637+02
56000.	6.9667007-03	2.6409184+02	2.6409184+02	1.8403158-02	3.1092461-05	1.6700875-05	1.3577843+02
57000.	5.615756-03	2.6153532+02	2.6153532+02	1.6330711-02	3.4902517-05	1.6590072-05	1.2919329+02
58000.	4.3682362-03	2.5873022+02	2.5873022+02	1.4594443-02	3.9520649-05	1.6439394-05	1.2245963+02
59000.	3.2710367-03	2.5574928+02	2.5574928+02	1.2625577-02	4.4105342-05	1.6287139-05	1.1505106+02
60000.	2.3754115-03	2.5261192+02	2.5261192+02	1.0755510-02	4.9227845-05	1.6127656-05	1.0619222+02
61000.	1.7039015-03	2.4937169+02	2.4937169+02	9.4497169-03	5.4954765-05	1.5958839-05	9.656913+01
62000.	1.2156504-03	2.4606511+02	2.4606511+02	8.1406511-03	6.1417089-05	1.5787579-05	8.6446738+01
63000.	8.5834757-04	2.4272032+02	2.4272032+02	7.0726500-03	6.702127-05	1.5613533-05	7.6123265+01
64000.	6.375800-03	2.3978440+02	2.3978440+02	6.0661984-03	7.2952721-05	1.5433349-05	6.610517+01
65000.	4.698055-03	2.3605390+02	2.3605390+02	5.2600390-03	7.9403301-05	1.5271141-05	5.6900647+01
66000.	3.4031056-03	2.3278436+02	2.3278436+02	4.555474-03	8.7032473-05	1.5080910-05	4.8585949+01
67000.	2.3350478-04	2.2956021+02	2.2956021+02	3.9503376-03	9.5927724-05	1.4917555-05	4.0773397+01
68000.	1.7707160-04	2.2640073+02	2.2640073+02	3.395965-03	1.0333327-05	1.4746916-05	3.3163655+01
69000.	1.2693220-04	2.2330920+02	2.2330920+02	2.9336920-03	1.13941253-05	1.4573723-05	2.6995703+01
70000.	8.7624817-04	2.2028350+02	2.2028350+02	2.5130767-03	1.2581055-05	1.4411118-05	2.0753372+01
71000.	6.4859703-04	2.1731552+02	2.1731552+02	2.1435024-03	1.3976204-05	1.4252683-05	1.5552241+01
72000.	4.2355436-04	2.1439684+02	2.1439684+02	1.8824123-03	1.5814328-05	1.4091690-05	1.0957970+01
73000.	3.0137195-04	2.1144119+02	2.1144119+02	1.6449427-03	1.774430-05	1.3933980-05	7.3153326+00
74000.	2.084853-04	2.0850000+02	2.0850000+02	1.418217-03	2.0726567-05	1.3767049-05	5.2952223+00
75000.	1.4223794-04	2.0563354+02	2.0563354+02	1.2053379-03	2.3614461-05	1.3603951-05	3.8746957+00
76000.	1.0250770-04	2.0260577+02	2.0260577+02	1.055777-03	2.6511169-05	1.3437306-05	2.8534546+00
77000.	7.882458-04	1.9944355+02	1.9944355+02	9.2438548-04	2.9304423-05	1.3254226-05	2.0311344+00
78000.	5.855186-04	1.9610583+02	1.9610583+02	8.0616629-04	3.2236629-05	1.3063349-05	1.4073096+00
79000.	4.335155-04	1.9251422+02	1.9251422+02	7.0551422-04	3.5307030-05	1.2955776-05	9.7314833+00
80000.	3.1243729-04	1.8860110+02	1.8860110+02	6.0681378-04	3.8481378-05	1.2823957-05	7.2530724+00
81000.	2.216307-05	1.8421839+02	1.8421839+02	5.243393+02	4.1710079-05	1.2777743-05	5.7214134+00
82000.	1.6773015-05	1.8065000+02	1.8065000+02	4.5171522-04	4.5171522-05	1.2631173-05	4.6944122+00
83000.	1.2436167-05	1.7605000+02	1.7605000+02	3.9059000+02	4.9059000+02	1.2461713-05	3.6944122+00
84000.	8.429003-05	1.8065000+02	1.8065000+02	3.4096153-05	5.4096153-05	1.2363173-05	2.6944122+00
85000.	6.5275370-05	1.8065000+02	1.8065000+02	3.0365000+02	6.0365000+02	1.2163173-05	1.6944122+00
86000.	4.764308-05	1.8065000+02	1.8065000+02	2.6622298-05	6.6622298-05	1.2163173-05	1.6944122+00
87000.	3.1334790-05	1.8065000+02	1.8065000+02	2.0124761+00	7.0124761+00	1.2163173-05	1.6944122+00
88000.	2.069278-05	1.8065000+02	1.8065000+02	1.4194790+00	7.4194790+00	1.2163173-05	1.6944122+00
89000.	1.2690308-05	1.8065000+02	1.8065000+02	9.1827847-05	9.1827847-05	1.2163173-05	1.6944122+00

TABLE 3.9 EDWARDS AFB REFERENCE ATMOSPHERE (ERA-75) (Ref. 3.7)

GEOMETRIC ALTITUDE	PRESSURE	KINETIC TEMPERATURE	VIRTUAL TEMPERATURE	DENSITY	KINEMATIC VISCOSITY	COEFFICIENT OF VISCOSITY	SPEED OF SOUND
meters	newtons cm <sup>-2</sup>	degrees K	degrees K	kg m <sup>-3</sup>	m <sup>2</sup> sec <sup>-1</sup>	newton-sec m <sup>-2</sup>	m sec <sup>-1</sup>
704.	9.3197999+03	2.8927295+02	2.9024438+02	1.1210501+00	1.6009931+05	1.7997936+05	3.4154145+02
1000.	9.5174369+02	2.8935619+02	2.9030666+02	1.0829572+00	1.6567809+05	1.7951944+05	3.4143229+02
2000.	8.9027162+00	2.8935157+02	2.9049736+02	9.7979598+01	1.8075135+05	1.7709940+05	3.3824919+02
3000.	7.9123340+00	2.87821671+02	2.78841472+02	8.8743099+01	1.9618973+05	1.7410485+05	3.3449716+02
4000.	6.3242364+00	2.7212336+02	2.7233608+02	8.0227467+01	2.1318857+05	1.7112362+05	3.3082996+02
5000.	5.5286650+00	2.6567136+02	2.6574157+02	7.2468080+01	2.3163579+05	1.6784203+05	3.2680685+02
6000.	4.8634600+00	2.5821188+02	2.5828004+02	6.5325510+01	2.5155218+05	1.6437062+05	3.2295129+02
7000.	4.2953086+00	2.5113978+02	2.5112249+02	5.8827869+01	2.7304746+05	1.6062801+05	3.1706835+02
8000.	3.8677686+00	2.4344803+02	2.4330488+02	5.2855270+01	2.9632266+05	1.5663607+05	3.1295134+02
9000.	3.2071977+00	2.3586146+02	2.3587045+02	4.7357911+01	3.2207045+05	1.5252423+05	3.0789330+02
10000.	2.3706481+00	2.2850072+02	2.2850241+02	4.2352241+01	3.5177528+05	1.4859917+05	3.0302224+02
11000.	2.3797471+00	2.2193979+02	2.2193979+02	3.7353759+01	3.8832351+05	1.4505341+05	2.9860008+02
12000.	2.3758423+00	2.1728113+02	2.1728113+02	3.2691835+01	4.3608231+05	1.4227811+05	2.9583572+02
13000.	1.7407523+00	2.1502790+02	2.1502790+02	2.8201088+01	5.0092260+05	1.4124562+05	2.9395944+02
14000.	1.4439331+00	2.1288933+02	2.1288933+02	2.4288845+01	5.7488266+05	1.4008981+05	2.9250124+02
15000.	1.2430643+00	2.1101874+02	2.1101874+02	2.0855009+01	6.6674156+05	1.3904901+05	2.9120963+02
16000.	1.0780324+00	2.0884258+02	2.0884258+02	1.7884258+01	7.7358000+05	1.3818273+05	2.9013272+02
17000.	9.1270847+01	2.0883855+02	2.0883855+02	1.5225517+01	9.0528671+05	1.3782081+05	2.8927721+02
18000.	7.7408455+01	2.1038286+02	2.1038286+02	1.2851183+01	1.0728433+05	1.3741008+05	2.9165773+02
19000.	6.6155133+01	2.1166882+02	2.1166882+02	1.0882416+01	1.2810581+05	1.4034372+05	2.9288225+02
20000.	5.4338303+01	2.1339162+02	2.1339162+02	9.2013190+00	1.5253386+05	1.4314573+05	2.9491924+02
21000.	4.8086911+01	2.1536180+02	2.1536180+02	7.7770908+00	1.8188511+05	1.4537647+05	2.9753823+02
22000.	4.1864433+01	2.1733892+02	2.1733892+02	6.5825416+00	2.1659138+05	1.4730515+05	2.9993397+02
23000.	3.5099534+01	2.1914084+02	2.1914084+02	5.5825416+00	2.5709056+05	1.4843741+05	2.9674094+02
24000.	3.0077669+01	2.2084008+02	2.2084008+02	4.7427480+00	3.0323812+05	1.4933741+05	2.9789132+02
25000.	2.5025116+01	2.2194423+02	2.2194423+02	4.0532336+00	3.5790343+05	1.4506670+05	2.9866653+02
26000.	2.3205870+01	2.2311188+02	2.2311188+02	3.4457270+00	4.2031222+05	1.4588975+05	2.9947338+02
27000.	1.9099714+01	2.2493256+02	2.2493256+02	2.9491950+00	4.9379501+05	1.4634803+05	3.0027575+02
28000.	1.6408522+01	2.2680388+02	2.2680388+02	2.6289412+00	5.8282788+05	1.4730351+05	3.0143187+02
29000.	1.4120899+01	2.2814086+02	2.2814086+02	2.3594011+00	6.8719054+05	1.4840674+05	3.0279339+02
30000.	1.2006481+01	2.3063634+02	2.3063634+02	2.0801965+00	8.0808600+05	1.4961557+05	3.0431145+02
31000.	1.0564830+01	2.3258950+02	2.3258950+02	1.8325895+00	9.5494946+05	1.5078363+05	3.0572815+02
32000.	8.1233802+00	2.3466262+02	2.3466262+02	1.6354035+00	1.1214437+05	1.5188873+05	3.0707090+02
33000.	7.0019567+00	2.3673119+02	2.3673119+02	1.4283197+00	1.3156191+05	1.5296338+05	3.0849199+02
34000.	6.2512442+00	2.3885656+02	2.3885656+02	1.2685326+00	1.5431405+05	1.5409839+05	3.0981395+02
35000.	5.9521349+00	2.4103708+02	2.4103708+02	1.1007467+00	1.8094790+05	1.5525252+05	3.1123525+02
36000.	5.1726480+00	2.4335058+02	2.4335058+02	9.6412688+00	2.1111590+05	1.5648202+05	3.1272402+02
37000.	4.5076480+00	2.4579778+02	2.4579778+02	8.3916438+00	2.4478365+05	1.5773532+05	3.1429057+02
38000.	4.1333455+00	2.4837543+02	2.4837543+02	7.4827700+00	2.8824474+05	1.5970737+05	3.1593331+02
39000.	3.7770724+00	2.5108264+02	2.5108264+02	6.7468101+00	3.3643850+05	1.6040747+05	3.1765333+02
40000.	3.4084150+00	2.5388728+02	2.5388728+02	6.1277733+00	3.9224462+05	1.6191175+05	3.1942405+02
41000.	3.1344920+00	2.5675467+02	2.5675467+02	5.5772217+00	4.5670959+05	1.6333515+05	3.2122122+02
42000.	2.9138673+00	2.5964737+02	2.5964737+02	5.1085583+00	5.3085583+05	1.6482871+05	3.2300002+02
43000.	2.7033609+00	2.6239786+02	2.6239786+02	4.6150753+00	6.1507053+05	1.6623480+05	3.2482402+02
44000.	2.5085323+00	2.6500371+02	2.6500371+02	4.2124674+00	7.1212674+05	1.6754752+05	3.2677401+02
45000.	2.3266305+00	2.6731429+02	2.6731429+02	3.8596663+00	8.2107314+05	1.6870477+05	3.2776014+02
46000.	2.1588400+00	2.6918890+02	2.6918890+02	3.5283263+00	9.4222228+05	1.6972861+05	3.2890792+02
47000.	1.9972708+00	2.7070611+02	2.7070611+02	3.2332573+00	1.0772693+05	1.7072861+05	3.2994948+02
48000.	1.8483504+00	2.7208726+02	2.7208726+02	2.9681883+00	1.2234800+05	1.7162861+05	3.2994948+02
49000.	1.7047671+00	2.7344442+02	2.7344442+02	2.7344442+00	1.3804648+05	1.7248157+05	3.3010733+02
50000.	1.5660115+00	2.7472736+02	2.7472736+02	2.5070377+00	1.5577725+05	1.7067771+05	3.3017857+02
51000.	1.4346768+00	2.7598585+02	2.7598585+02	2.2858330+00	1.7494352+05	1.7043536+05	3.2988156+02
52000.	1.3184118+00	2.7720222+02	2.7720222+02	2.0731944+00	1.9538800+05	1.6992517+05	3.2925423+02
53000.	1.2178915+00	2.6826166+02	2.6826166+02	1.8685186+00	2.2506703+05	1.6917808+05	3.2834042+02
54000.	1.1302458+00	2.6635233+02	2.6635233+02	1.6856366+00	2.6831122+05	1.6822337+05	3.2714987+02
55000.	1.0527081+00	2.6449915+02	2.6449915+02	1.5272234+00	3.1692661+05	1.6708879+05	3.2577843+02
56000.	0.9847670+00	2.6265392+02	2.6265392+02	1.3853031+00	3.6902517+05	1.6580092+05	3.2419829+02
57000.	0.9259756+00	2.6081322+02	2.6081322+02	1.2557482+00	4.2952049+05	1.6436394+05	3.2259533+02
58000.	0.8720862+00	2.5897828+02	2.5897828+02	1.1365433+00	4.9810534+05	1.6286194+05	3.2095104+02
59000.	0.8220862+00	2.5713822+02	2.5713822+02	1.0275851+00	5.7422585+05	1.6125654+05	3.1861922+02
60000.	0.7754195+00	2.5526112+02	2.5526112+02	9.2758514+00	6.5946345+05	1.5958838+05	3.1654918+02
61000.	0.7307840+00	2.5337169+02	2.5337169+02	8.2903481+00	7.5417989+05	1.5787579+05	3.1469338+02
62000.	0.6875608+00	2.5148511+02	2.5148511+02	7.4272680+00	8.6702127+05	1.5613589+05	3.1232245+02
63000.	0.6453767+00	2.4959263+02	2.4959263+02	6.6695325+00	9.8953251+05	1.5438349+05	3.1016513+02
64000.	0.6048000+00	2.4769790+02	2.4769790+02	5.9793780+00	1.1263301+05	1.5263141+05	3.0800647+02
65000.	0.5658055+00	2.4579828+02	2.4579828+02	5.3508924+00	1.2702873+05	1.5089010+05	3.0585991+02
66000.	0.5283104+00	2.4389872+02	2.4389872+02	4.7758146+00	1.4277724+05	1.4916755+05	3.0373397+02
67000.	0.4920478+00	2.4199920+02	2.4199920+02	4.2468150+00	1.5943127+05	1.4746918+05	3.0163455+02
68000.	0.4569720+00	2.4009968+02	2.4009968+02	3.7594757+00	1.7702517+05	1.4579723+05	2.9957003+02
69000.	0.4229774+00	2.3819916+02	2.3819916+02	3.3130747+00	1.9548185+05	1.4415118+05	2.9753372+02
70000.	0.3899703+00	2.3629864+02	2.3629864+02	2.9074366+00	2.1479209+05	1.4252683+05	2.9552241+02
71000.	0.3579703+00	2.3439812+02	2.3439812+02	2.5324233+00	2.3507428+05	1.4091690+05	2.9352707+02
72000.	0.3269703+00	2.3249760+02	2.3249760+02	2.1969427+00	2.5704430+05	1.3930980+05	2.9153326+02
73000.	0.2969703+00	2.3059708+02	2.3059708+02	1.8969427+00	2.8272663+05	1.3769949+05	2.8952232+02
74000.	0.2679703+00	2.2869656+02	2.2869656+02	1.6219427+00	3.0941461+05	1.3600358+05	2.8747967+02
75000.	0.2389703+00	2.2679604+02	2.2679604+02	1.3669427+00	3.3711176+05	1.3430306+05	2.8535846+02
76000.	0.2109703+00	2.2489552+02	2.2489552+02	1.1219427+00	3.6580848+05	1.3254226+05	2.8311344+02
77000.	0.1829703+00	2.2299500+02	2.2299500+02	9.0000000+00	3.9450520+05	1.3078149+05	2.8073096+02
78000.	0.1549703+00	2.2109448+02	2.2109448+02	7.7777778+00	4.2320192+05	1.2902052+05	2.7814833+02
79000.	0.1269703+00	2.1919396+02	2.1919396+02	6.5555556+00	4.5189864+05	1.2725955+05	2.7530724+02
80000.	0.0989703+00	2.1729344+02	2.1729344+02	5.3333333+00	4.8059536+05	1.2550858+05	2.7214104+02
81000.	0.0709703+00	2.1539292+02	2.1539292+02	4.1111111+00	5.0929208+05	1.2375761+05	2.6949122+02
82000.	0.0429703+00	2.1349240+02	2.1349240+02	2.8888889+00	5.3798880+05	1.2200664+05	2.6694122+02
83000.	0.0149703+00	2.1159188+02	2.1159188+02	1.6666667+00	5.6668552+05	1.2025569+05	2.6439122+02
84000.	0.0000000+00	2.0969136+02	2.0969136+02	0.4444444+00	5.9538224+05	1.1850474+05	2.6184122+02
85000.	0.0000000+00	2.0779084+02	2.0779084+02	0.2222222+00	6.2407896+05	1.1675379+05	2.5929122+02
86000.	0.0000000+00	2.0589032+02	2.0589032+02	0.0000000+00	6.5277568+05	1.1500284+05	2.5674122+02
87000.	0.0000000+00	2.0398980+02	2.0398980+02	0.0000000+00	6.8147240+05	1.1325189+05	2.5419122+02
88000.	0.0000000+00	2.0208928+02	2.0208928+02	0.0000000+00	7.1016912+05	1.1150094+05	2.5164122+02
89000.	0.0000000+00	2.0018876+02	2.0018876+02	0.0000000+00	7.3886584+05	1.0975000+05	

### 3.4.2 Atmospheric Density at Altitude

The density of the atmosphere decreases rapidly with height, decreasing to one-half of the surface at approximately 7 km altitude. Density is also variable at a fixed altitude, with the greatest relative variability occurring at approximately 70 km altitude in the high northern latitudes ( $60^{\circ}\text{N}$ ). Other altitudes of maximum density variability occur around 16 km and 0 km. Altitudes of minimum variability (isopycnic levels) occur around 8, 24, and 90 km altitude.

Density varies with latitude in each hemisphere, with the mean annual density near the surface increasing toward the poles. In the region around 8 km in the northern hemisphere, for example, the density variation with latitude and season is small (isopycnic level). Above 8 km to approximately 28 km, the mean annual density decreases toward the north. Mean monthly densities between 30 and 90 km increase toward the north in July and toward the equator in January.

Considerable data are now available on the mean density and its variability below 30 km at the various test ranges from the data collected for preparation of the IRIG Range Reference Atmospheres (Ref. 3.4). Additional information on the seasonal variability of density below 30 km is presented in Ref. 3.8. Above 30 km, the data are less plentiful and the accuracy of the temperature measurements (used to compute some densities) decreases with altitude.

Extreme minimum and maximum values of density for the Eastern Test Range and Vandenberg AFB are given in Table 3.10. These extreme density values approach the  $\pm 3\sigma$  (corresponding to the normal distribution) density values. The relative density deviations for Kennedy Space Center and Vandenberg AFB, as given in Table 3.10, are respectively defined as percentage departures from the Patrick Reference Atmosphere (Ref. 3.2) and the Vandenberg Reference Atmosphere (Ref. 3.3).

Median values of surface density for different locations of interest are given in Table 7.2 of Section VII, with nominal values with altitude being given in Tables 3.7 through 3.9 and in Reference 3.4.

## 3.5 Simultaneous Values of Temperature, Pressure, and Density at Discrete Altitude Levels

### 3.5.1 Introduction

This subsection presents simultaneous values for temperature, pressure, and density as guidelines for aerospace vehicle design considerations. The necessary assumptions and the lack of sufficient statistical data samples restrict the precision by which these data can presently be presented; therefore, the analysis is limited to Kennedy Space Center.

### 3.5.2 Method of Determining Simultaneous Value

An aerospace vehicle design problem that often arises in considering natural environmental data is stated by way of the following question: "How should the extremes (maxima and minima) of temperature, pressure, and density be combined (a) at discrete altitude levels? (b) versus altitude?" As an example, suppose one desires to know what temperature and pressure should be used simultaneously with a maximum density at a discrete altitude. From statistical principles set forth by Dr. C. E. Buell in Reference 3.9, the solution results by allowing mean density plus three standard deviations to represent maximum density and using the coefficients of variation, correlations, and mean values as expressed in equation (3.1).

TABLE 3.10 DENSITY HEIGHT MAXIMUM ( $\approx +3$  SIGMA), AND MINIMUM ( $\approx -3$  SIGMA)  
FOR KENNEDY SPACE CENTER, FLORIDA AND  
VANDENBERG AFB, CALIFORNIA

Altitude <sup>a</sup>		Kennedy Space Center Density				Vandenberg AFB Density			
		Maximum		Minimum		Maximum		Minimum	
		(kg m <sup>-3</sup> )	% Deviation from PRA-63	(kg m <sup>-3</sup> )	% Deviation from PRA-63	(kg m <sup>-3</sup> )	% Deviation from VRA-71	(kg m <sup>-3</sup> )	% Deviation from VRA-71
(km)	(ft)								
0	0	1.326	12.0	1.141	-3.6	1.302	5.3	1.140	-7.8
2	6 600	1.047	6.1	9.497×10 <sup>-1</sup>	-3.0	1.046	6.1	9.518×10 <sup>-1</sup>	-3.5
4	13 100	8.287×10 <sup>-1</sup>	3.7	7.824×10 <sup>-1</sup>	-2.1	8.484×10 <sup>-1</sup>	5.7	7.766×10 <sup>-1</sup>	-3.3
6	19 700	6.706×10 <sup>-1</sup>	3.2	6.355×10 <sup>-1</sup>	-2.2	6.906×10 <sup>-1</sup>	5.7	6.299×10 <sup>-1</sup>	-3.6
8	26 200	5.428×10 <sup>-1</sup>	3.1	5.055×10 <sup>-1</sup>	-4.0	5.601×10 <sup>-1</sup>	6.0	4.971×10 <sup>-1</sup>	-6.0
10	32 800	4.352×10 <sup>-1</sup>	3.0	3.938×10 <sup>-1</sup>	-6.8	4.624×10 <sup>-1</sup>	9.5	3.835×10 <sup>-1</sup>	-9.2
15	49 200	2.345×10 <sup>-1</sup>	7.0	1.979×10 <sup>-1</sup>	-9.7	2.337×10 <sup>-1</sup>	12.0	1.851×10 <sup>-1</sup>	-11.3
20	65 600	1.002×10 <sup>-1</sup>	7.5	8.751×10 <sup>-2</sup>	-6.1	1.001×10 <sup>-1</sup>	8.8	8.420×10 <sup>-2</sup>	-8.5
25	82 000	4.274×10 <sup>-2</sup>	5.9	3.790×10 <sup>-2</sup>	-6.1	4.460×10 <sup>-2</sup>	10.0	3.634×10 <sup>-2</sup>	-10.4
30	98 400	1.976×10 <sup>-2</sup>	7.8	1.700×10 <sup>-2</sup>	-7.3	2.085×10 <sup>-2</sup>	13.0	1.634×10 <sup>-2</sup>	-11.5
35	114 800	9.427×10 <sup>-3</sup>	10.3	7.640×10 <sup>-3</sup>	-10.6	9.786×10 <sup>-3</sup>	13.8	7.505×10 <sup>-3</sup>	-12.8
40	131 200	4.637×10 <sup>-3</sup>	12.5	3.512×10 <sup>-3</sup>	-14.8	4.747×10 <sup>-3</sup>	15.0	3.424×10 <sup>-3</sup>	-17.0
50	164 000	1.275×10 <sup>-3</sup>	16.3	8.630×10 <sup>-4</sup>	-21.3	1.325×10 <sup>-3</sup>	22.0	8.473×10 <sup>-4</sup>	-22.0
60	196 800	3.946×10 <sup>-4</sup>	19.4	2.465×10 <sup>-4</sup>	-25.4	4.422×10 <sup>-4</sup>	35.0	2.359×10 <sup>-4</sup>	-28.0
70	229 700	1.100×10 <sup>-4</sup>	23.6	6.666×10 <sup>-5</sup>	-25.1	1.203×10 <sup>-4</sup>	32.0	6.197×10 <sup>-5</sup>	-32.0
80	262 500	2.342×10 <sup>-5</sup>	19.0	1.596×10 <sup>-5</sup>	-18.9	2.617×10 <sup>-5</sup>	26.0	1.433×10 <sup>-5</sup>	-31.0
90	295 300	3.684×10 <sup>-6</sup>	10.9	2.930×10 <sup>-6</sup>	-11.8	4.177×10 <sup>-6</sup>	20.0	2.785×10 <sup>-6</sup>	-20.0

a. Geometric altitude above mean sea level.

ORIGINAL PAGE IS  
OF POOR QUALITY



$$\text{maximum } \rho = (\bar{\rho} + 3\sigma_{\rho}) = \bar{\rho} \left( 1 + 3 \frac{\sigma_{\rho}}{\bar{\rho}} \right) = \bar{\rho} \left\{ 1 + 3 \left[ \underbrace{\left( \frac{\sigma_P}{\bar{P}} \right) r(P\rho)}_{(A)} - \underbrace{\left( \frac{\sigma_T}{\bar{T}} \right) r(\rho T)}_{(B)} \right] \right\} \quad (3.1)$$

The associated values for pressure and temperature are the last two terms of equation (3.1), (A) and (B), multiplied by  $\bar{P}$  and  $\bar{T}$ , respectively, and then this result is added to  $\bar{P}$  and  $\bar{T}$ , respectively. Appropriate values of  $r$  and CV are obtained from Table 3.11.

TABLE 3.11 COEFFICIENTS OF VARIATION AND DISCRETE ALTITUDE LEVEL CORRELATION COEFFICIENTS BETWEEN PRESSURE – DENSITY  $r(P\rho)$ ; PRESSURE – TEMPERATURE  $r(PT)$ ; AND DENSITY – TEMPERATURE  $r(\rho T)$ , KENNEDY SPACE CENTER, ANNUAL

Altitude (km)	Coefficients of Variation (CV)			Correlation Coefficients (r)		
	$\sigma(\rho)/\bar{\rho}$ (percent)	$\sigma(P)/\bar{P}$ (percent)	$\sigma(T)/\bar{T}$ (percent)	$r(P\rho)$ (unitless)	$r(PT)$ (unitless)	$r(\rho T)$ (unitless)
0	1.8000	.6000	1.5000	.6250	-0.3500	-0.9500
1	1.7000	.5500	1.6000	.3382	-0.0156	-0.9462
2	1.5000	.8000	1.5900	.1508	.3609	-0.8675
3	1.1800	.9800	1.5700	-0.0485	.6606	-0.7818
4	.9700	.8500	1.4000	-0.1799	.7318	-0.8021
5	.8000	.8700	1.3400	-0.2864	.8203	-0.7830
6	.7400	.8400	1.2600	-0.2690	.8246	-0.7666
7	.8800	.9800	1.4200	-0.1633	.7913	-0.7324
8	.9000	1.1300	1.4700	-0.0364	.7910	-0.6402
9	1.1800	1.4700	1.6200	.2678	.7124	-0.4854
10	1.6300	1.7500	1.7200	.4840	.5588	-0.4553
11	1.8800	1.8000	1.7800	.5328	.4485	-0.5174
12	2.1500	1.8700	1.8500	.5841	.3320	-0.5717
13	2.3800	1.9000	1.8500	.6470	.1946	-0.6220
14	2.6200	1.9200	1.7700	.7373	-0.0066	-0.6804
15	2.7800	1.8800	1.6700	.8107	-0.2238	-0.7520
16	2.8800	1.8400	1.7100	.8262	-0.3154	-0.7953
17	2.8800	1.8000	1.7000	.8338	-0.3537	-0.8113
18	2.7500	1.7500	1.7000	.8036	-0.2706	-0.7904
19	2.5000	1.7800	1.6700	.7449	-0.0492	-0.7031
20	2.2700	1.8500	1.6500	.6969	.1625	-0.5944
21	2.0800	1.9500	1.6200	.6786	.3325	-0.4672
22	1.9800	2.1200	1.5700	.7087	.4565	-0.3041
23	1.9200	2.3200	1.4800	.7721	.5659	-0.0870
24	1.9500	2.4000	1.4300	.8032	.5831	-0.0157
25	2.000	2.4300	1.4200	.8116	.5682	-0.0196
26	2.0800	2.5000	1.5000	.8006	.5565	-0.0523
27	2.1500	2.6000	1.5800	.7948	.5640	-0.0528
28	2.2300	2.6700	1.7500	.7591	.5584	-0.1161
29	2.3700	2.6300	1.8700	.7249	.4877	-0.2479
30	2.5200	2.6300	1.9200	.7228	.4211	-0.3224
31	2.7000	2.7000	2.000	.7257	.3704	-0.3704
32	2.8800	2.7500	2.0800	.7279	.3142	-0.4222
33	3.0700	2.7300	2.1700	.7260	.2310	-0.5014
34	3.2700	2.6800	2.2300	.7361	.1223	-0.5817
35	3.4800	2.6000	2.3200	.7454	.0027	-0.6647
36	3.7000	2.5000	2.4300	.7587	-0.1263	-0.7421
37	3.9200	2.3700	2.5500	.7793	-0.2686	-0.8129
38	4.1200	2.4600	2.6300	.7947	-0.3096	-0.8232
39	4.3300	2.6400	2.6900	.8084	-0.3199	-0.8163
40	4.5500	2.7900	2.7680	.8220	-0.3442	-0.8176
41	4.7500	2.8600	3.0200	.7958	-0.3046	-0.8192
42	4.9300	2.9200	3.2600	.7712	-0.2706	-0.8215
43	5.1300	3.000	3.3400	.7850	-0.3075	-0.8309
44	5.3200	3.1800	3.3500	.8037	-0.3270	-0.8252
45	5.5000	3.2400	3.6000	.7797	-0.2912	-0.8261
46	5.6700	3.3200	3.8300	.7571	-0.2539	-0.8242
47	5.8300	3.4100	3.9800	.7489	-0.2402	-0.8232
48	5.9800	3.4800	4.1900	.7284	-0.2090	-0.8223
49	6.1300	3.5900	4.1400	.7572	-0.2540	-0.8241
50	6.2700	3.6900	4.1900	.7644	-0.2633	-0.8232
51	6.4200	3.8200	4.0800	.7984	-0.3201	-0.8260
52	6.5500	3.9100	4.1800	.7950	-0.3103	-0.8234
53	6.7000	4.0100	4.2700	.7953	-0.3089	-0.8222
54	6.8000	4.0700	4.3100	.7990	-0.3164	-0.8232
55	6.9200	4.1400	4.3700	.8016	-0.3220	-0.8241
56	7.0300	4.2100	4.4200	.8043	-0.3267	-0.8244
57	7.1500	4.2800	4.4700	.8081	-0.3351	-0.8258
58	7.2700	4.3600	4.5100	.8127	-0.3434	-0.8263
59	7.3700	4.4200	4.5400	.8172	-0.3530	-0.8277
60	7.4700	4.4800	4.5900	.8188	-0.3565	-0.8283

TABLE 3.11 COEFFICIENTS OF VARIATION AND DISCRETE ALTITUDE LEVEL  
CORRELATION COEFFICIENTS BETWEEN PRESSURE – DENSITY  $r(P\rho)$ ;  
PRESSURE – TEMPERATURE  $r(PT)$ ; AND DENSITY – TEMPERATURE  
 $r(\rho T)$ , KENNEDY SPACE CENTER, ANNUAL (Concluded)

Altitude (km)	Coefficients of Variation (CV)			Correlation Coefficients (r)		
	$\sigma(\rho)/\bar{\rho}$ (percent)	$\sigma(P)/\bar{P}$ (percent)	$\sigma(T)/\bar{T}$ (percent)	$R(P\rho)$ (unitless)	$r(PT)$ (unitless)	$r(\rho T)$ (unitless)
61	7.5700	4.5400	4.6300	.8217	-0.3629	-0.8293
62	7.6500	4.7000	4.8600	.7926	-0.2805	-0.8076
63	7.7500	4.9000	5.0000	.7778	-0.2256	-0.7878
64	7.8300	5.1500	5.1500	.7602	-0.1558	-0.7602
65	7.9000	5.3800	5.3800	.7342	-0.0781	-0.7342
66	7.9800	5.5700	5.4400	.7324	-0.0505	-0.7170
67	8.0300	5.6600	5.4700	.7326	-0.0408	-0.7099
68	8.0700	5.7700	5.4000	.7437	-0.0429	-0.6998
69	8.1000	5.8200	5.5100	.7331	-0.0215	-0.6957
70	8.1200	5.8700	5.4900	.7369	-0.0208	-0.6911
71	8.1200	5.8900	5.4700	.7392	-0.0205	-0.6885
72	8.0700	5.7900	5.3800	.7459	-0.0426	-0.6973
73	8.1200	5.6500	5.2900	.7615	-0.1008	-0.7216
74	8.0700	5.5000	5.1700	.7733	-0.1432	-0.7383
75	7.9000	5.2900	5.4100	.7313	-0.0901	-0.7452
76	7.6800	4.9900	5.6500	.6779	-0.0383	-0.7606
77	7.3800	5.0100	6.1600	.5628	.1390	-0.7403
78	7.0500	5.0400	6.5200	.4587	.2771	-0.7267
79	6.6800	5.1100	6.8400	.3508	.4045	-0.7145
80	6.3200	5.2700	6.7800	.3265	.4730	-0.6784
81	5.9500	5.3600	6.7200	.2975	.5342	-0.6482
82	5.5800	5.5200	6.6600	.2800	.5942	-0.6057
83	5.2500	5.1300	6.6100	.1891	.6259	-0.6475
84	4.9200	4.7800	6.5600	.0855	.6645	-0.6877
85	4.6300	4.4700	6.5100	-0.0232	.7032	-0.7272
86	4.4000	4.1900	6.4500	-0.1271	.7363	-0.7647
87	4.2000	3.9600	6.4000	-0.2296	.7694	-0.7983
88	4.0200	4.0500	6.3400	-0.2344	.7874	-0.7838
89	3.8800	4.1400	6.2800	-0.2255	.7986	-0.7665
90	3.7800	4.0400	5.9600	-0.1608	.7798	-0.7432

In general, the three extreme  $\rho$ ,  $P$ , and  $T$  equations of interest are

$$\text{extreme } \rho = (\bar{\rho} \pm M\sigma_{\rho}) = \bar{\rho} \left[ 1 \pm M \left( \frac{\sigma_{\rho}}{\bar{\rho}} \right) \right] = \bar{\rho} \left\{ 1 \pm M \left[ \left( \frac{\sigma_P}{\bar{P}} \right) r(P\rho) - \left( \frac{\sigma_T}{\bar{T}} \right) r(\rho T) \right] \right\} \quad (3.2)$$

$$\text{extreme } P = (\bar{P} \pm M\sigma_P) = \bar{P} \left[ 1 \pm M \left( \frac{\sigma_P}{\bar{P}} \right) \right] = \bar{P} \left\{ 1 \pm M \left[ \left( \frac{\sigma_{\rho}}{\bar{\rho}} \right) r(P\rho) + \left( \frac{\sigma_T}{\bar{T}} \right) r(PT) \right] \right\} \quad (3.3)$$

$$\text{extreme } T = (\bar{T} \pm M\sigma_T) = \bar{T} \left[ 1 \pm M \left( \frac{\sigma_T}{\bar{T}} \right) \right] = \bar{T} \left\{ 1 \pm M \left[ \left( \frac{\sigma_P}{\bar{P}} \right) r(PT) - \left( \frac{\sigma_{\rho}}{\bar{\rho}} \right) r(\rho T) \right] \right\} \quad (3.4)$$

where  $M$  denotes the multiplication factor to give the desired deviation. The values of  $M$  for the normal distribution and the associated percentile levels are as follows:

	M		Percentile
mean	-3	standard deviations	0.135
mean	-2	standard deviations	2.275
mean	-1	standard deviations	15.866
mean	$\pm 0$	standard deviations = median	50.000
mean	+1	standard deviations	84.134
mean	+2	standard deviations	97.725
mean	+3	standard deviations	99.865

The two associated atmospheric parameters that deal with a third extreme parameter are listed, in more detail, in the following chart.

	For Extreme Density	For Extreme Temperature	For Extreme Pressure
$P_{\text{assoc.}} =$	$\bar{P} \left[ 1 \pm \left\{ M \left( \frac{\sigma_P}{\bar{P}} \right) r(P\rho) \right\} \right]$	$\bar{P} \left[ 1 \pm \left\{ M \left( \frac{\sigma_P}{\bar{P}} \right) r(PT) \right\} \right]$	
$T_{\text{assoc.}} =$	$\bar{T} \left[ 1 \pm \left\{ M \left( \frac{\sigma_T}{\bar{T}} \right) r(\rho T) \right\} \right]$		$\bar{T} \left[ 1 \pm \left\{ M \left( \frac{\sigma_T}{\bar{T}} \right) r(PT) \right\} \right]$
$\rho_{\text{assoc.}} =$		$\bar{\rho} \left[ 1 \pm \left\{ M \left( \frac{\sigma_\rho}{\bar{\rho}} \right) r(\rho T) \right\} \right]$	$\bar{\rho} \left[ 1 \pm \left\{ M \left( \frac{\sigma_\rho}{\bar{\rho}} \right) r(P\rho) \right\} \right]$

Use + sign when extreme parameter is maximum.

Use - sign when extreme parameter is minimum.

It must be emphasized that this procedure is to be used at discrete altitudes only. Whenever extreme profiles of pressure, temperature, and density are required for engineering application, the use of these correlated variables at discrete altitudes is not satisfactory. Subsection 3.6 deals directly with this problem, since a profile of extreme pressure, temperature, or density from 0 to 90 km altitude is unrealistic in the real atmosphere.

### 3.6 Extreme Atmospheric Profiles for Kennedy Space Center, Florida, Vandenberg AFB, California, and Edwards AFB, California

Given in this section are the two extreme density profiles that correspond to the summer (hot) and winter (cold) extreme atmospheres for Kennedy Space Center, Florida (Tables 3.12A and 3.12B); Vandenberg Air Force Base, California (Tables 3.13A and 3.13B); and Edwards AFB, California (Tables 3.14A and 3.14B) (see Ref. 3.6 and 3.7 for detailed information pertaining to the Vandenberg and Edwards extreme atmospheres, respectively). Associated values of extreme temperature and pressure versus altitude are also tabulated. These extreme atmospheric profiles should be used in ascent design analyses at all altitudes. For re-entry studies they apply only from 30 km to the surface for vehicles to be used at Kennedy Space Center, Florida; Vandenberg AFB, California; or Edwards AFB, California. For those aerospace vehicles with ferrying capability, design calculations should use these extreme profiles in conjunction with the hot or cold day design ambient air temperatures over runways from paragraph 8.4.1 of Section VIII. The extreme atmosphere producing the maximum vehicle design requirement should be utilized to determine the design.

The envelopes of deviations of density in Table 3.10 imply that a typical individual extreme density profile may be represented by a similarly shaped profile, that is, deviations of density either all negative or all positive from sea level to 90 km altitude. However, examination of many individual density profiles

3.14

TABLE 3.12A KENNEDY SPACE CENTER SUMMER (HOT)  
ATMOSPHERE (KHA-71)

Geometric Altitude	Geopotential Altitude	Virtual Temperature	Kinetic Temperature	Pressure	Density	Rel. Dev. (T°) with res- pect to PRA-63	Rel. Dev. (P) with res- pect to PRA-63	Rel. Dev. (D) with res- pect to PRA-63
Z(m)	H(m)	T° (*K)	T (*K)	P(N/cm²)	D(kg/m³)	RD(T°)%	RD(P)%	RD(D)%
0.	0.	3.0990000+02	3.0740000+02	1.0100000+01	1.1353705+00	3.52	-6.9	-4.07
1000.	339.5	3.0313637+02	3.0105000+02	9.0346817+00	1.0382755+00	1.56	-2.21	-3.31
2000.	1996.0	2.9637273+02	2.9470000+02	8.0614293+00	9.4757068-01	1.47	1.7	-3.21
3000.	2339.5	2.8960905+02	2.8835000+02	7.1741153+00	8.6296655-01	1.07	4.4	-2.52
4000.	2992.0	2.8244546+02	2.8200000+02	6.3668963+00	7.8418111-01	2.74	6.2	-1.87
5000.	4119.2	2.7608127+02	2.7565001+02	5.6342022+00	7.1093916-01	2.53	1.13	-1.37
6000.	5586.1	2.6931818+02	2.6931818+02	4.9707268+00	6.4297218-01	2.00	1.43	-1.06
7000.	7392.7	2.6255455+02	2.6255455+02	4.3714321+00	5.8001870-01	2.67	1.74	-0.31
8000.	9795.0	2.5579091+02	2.5579091+02	3.8315199+00	5.2142367-01	2.00	2.07	-0.97
9000.	13075.0	2.4902728+02	2.4902728+02	3.3468479+00	4.6813915-01	1.44	2.49	-0.37
10000.	19770.0	2.4226364+02	2.4226364+02	2.9113117+00	4.1872392-01	1.51	2.98	-0.91
11000.	10955.0	2.3550000+02	2.3550000+02	2.5238402+00	3.7334363-01	4.35	3.55	-0.31
12000.	11361.0	2.2820000+02	2.2820000+02	2.1780131+00	3.3249312-01	4.29	4.10	-0.10
13000.	12055.7	2.2090000+02	2.2090000+02	1.8705877+00	2.9499874-01	1.76	4.73	0.32
14000.	12950.1	2.1360000+02	2.1360000+02	1.5983606+00	2.6088215-01	2.61	5.16	2.05
15000.	14044.2	2.0630000+02	2.0630000+02	1.3583010+00	2.2936894-01	1.72	5.35	4.66
16000.	15937.9	1.9900000+02	1.9900000+02	1.1475476+00	2.0088866-01	-1.09	5.17	7.33
17000.	16931.4	1.9162277+02	1.9162277+02	9.6617676-01	1.6995547-01	-2.19	4.73	7.27
18000.	17924.8	2.0000000+02	2.0000000+02	8.1369526-01	1.4173245-01	-2.59	4.19	7.05
19000.	19917.4	2.0416667+02	2.0416667+02	6.8712577-01	1.1728379-01	-1.74	3.70	5.66
20000.	19909.9	2.0833333+02	2.0833333+02	5.8222915-01	9.7358475-02	-0.96	3.79	4.47
21000.	20902.1	2.1250000+02	2.1250000+02	5.0883667-01	8.1133631-02	-0.19	3.23	3.48
22000.	21894.0	2.1566667+02	2.1566667+02	4.2201626-01	6.8172810-02	0.14	3.17	2.97
23000.	22886.5	2.1883333+02	2.1883333+02	3.6056887-01	5.7401234-02	0.77	3.16	2.51
24000.	23879.0	2.2200000+02	2.2200000+02	3.0875046-01	4.8447590-02	1.00	3.21	2.06
25000.	24871.9	2.2516667+02	2.2516667+02	2.6498604-01	4.0994491-02	1.55	3.30	1.60
26000.	25864.8	2.2833333+02	2.2833333+02	2.2793980-01	3.4775516-02	2.13	3.44	1.15
27000.	26857.9	2.3150000+02	2.3150000+02	1.9649475-01	2.9570541-02	2.93	3.64	0.73
28000.	27850.9	2.3466667+02	2.3466667+02	1.6972565-01	2.5199219-02	3.07	3.07	0.29
29000.	28843.0	2.3783333+02	2.3783333+02	1.4687393-01	2.1516243-02	4.04	4.35	0.30
30000.	29835.0	2.4100000+02	2.4100000+02	1.2732124-01	1.9405121-02	4.42	4.02	0.39
31000.	30827.1	2.4416667+02	2.4416667+02	1.1056625-01	1.5773346-02	4.73	5.32	0.52
32000.	31819.2	2.4733333+02	2.4733333+02	9.6198730-02	1.3586524-02	5.11	5.36	0.72
33000.	32811.3	2.5050000+02	2.5050000+02	8.3870697-02	1.0065735-02	5.67	7.06	1.32
34000.	33803.4	2.5366667+02	2.5366667+02	7.3279037-02	7.3279037-02	5.90	7.70	1.70
35000.	34795.5	2.5683333+02	2.5683333+02	6.4129087-02	6.4129087-02	6.11	8.27	2.14
36000.	35787.6	2.6000000+02	2.6000000+02	5.6184777-02	5.6184777-02	6.13	9.06	2.71
37000.	36779.7	2.6288611+02	2.6288611+02	4.9269104-02	4.9269104-02	6.24	9.75	3.31
38000.	37771.8	2.6576923+02	2.6576923+02	4.3294535-02	4.3294535-02	6.36	11.17	4.49
39000.	38763.9	2.6865385+02	2.6865385+02	3.8097067-02	3.8097067-02	6.41	11.92	5.06
40000.	39756.0	2.7153846+02	2.7153846+02	3.3570537-02	3.3570537-02	6.54	12.61	5.60
41000.	40748.1	2.7442308+02	2.7442308+02	2.9622116-02	2.9622116-02	6.69	13.30	6.10
42000.	41740.2	2.7730769+02	2.7730769+02	2.6172104-02	2.6172104-02	6.80	13.90	6.56
43000.	42732.3	2.8019231+02	2.8019231+02	2.3153610-02	2.3153610-02	6.89	14.63	7.06
44000.	43724.4	2.8307692+02	2.8307692+02	2.0507717-02	2.0507717-02	7.17	15.43	7.59
45000.	44716.5	2.8596154+02	2.8596154+02	1.8386378-02	1.8386378-02	7.54	16.21	8.13
46000.	45708.6	2.8884615+02	2.8884615+02	1.6148109-02	1.6148109-02	7.93	17.01	8.70
47000.	46700.7	2.9173077+02	2.9173077+02	1.4355888-02	1.4355888-02	8.32	17.81	9.27
48000.	47692.8	2.9461538+02	2.9461538+02	1.2777675-02	1.2777675-02	8.71	18.61	9.84
49000.	48684.9	2.9750000+02	2.9750000+02	1.1384040-02	1.1384040-02	9.10	19.41	10.41
50000.	49677.0	2.9750000+02	2.9750000+02	1.0186231-02	1.0186231-02	9.49	19.15	9.32
51000.	50669.1	2.9325000+02	2.9325000+02	9.0407466-03	1.0739715-03	9.88	20.16	10.26
52000.	51661.2	2.8900000+02	2.8900000+02	8.0399930-03	9.6910378-04	10.27	21.09	11.10
53000.	52653.3	2.8475000+02	2.8475000+02	7.1372587-03	8.7313598-04	10.66	21.72	11.90
54000.	53645.4	2.8050000+02	2.8050000+02	6.3243675-03	7.8543025-04	11.05	22.47	12.70
55000.	54637.5	2.7625000+02	2.7625000+02	5.5935943-03	7.0539075-04	11.44	23.22	13.50
56000.	55629.6	2.7200000+02	2.7200000+02	4.9378836-03	6.3245458-04	11.83	23.97	14.30
57000.	56621.7	2.6775000+02	2.6775000+02	4.3505454-03	5.6608540-04	12.22	24.72	15.10
58000.	57613.8	2.6350000+02	2.6350000+02	3.8253748-03	5.0578808-04	12.61	25.47	15.90
59000.	58605.9	2.5925000+02	2.5925000+02	3.3566785-03	4.5108956-04	13.00	26.22	16.70
60000.	59598.0	2.5500000+02	2.5500000+02	2.9390943-03	4.0150946-04	13.39	26.97	17.50
61000.	60590.1	2.5075000+02	2.5075000+02	2.5678229-03	3.5675335-04	13.78	27.72	18.30
62000.	61582.2	2.4650000+02	2.4650000+02	2.2383559-03	3.1631772-04	14.17	28.47	19.10
63000.	62574.3	2.4225000+02	2.4225000+02	1.9464898-03	2.7987802-04	14.56	29.22	19.90
64000.	63566.4	2.3800000+02	2.3800000+02	1.6884898-03	2.4709821-04	14.95	30.00	20.70
65000.	64558.5	2.3375000+02	2.3375000+02	1.4609194-03	2.1766889-04	15.34	30.75	21.50
66000.	65550.6	2.2950000+02	2.2950000+02	1.2605929-03	1.9129334-04	15.73	31.50	22.30
67000.	66542.7	2.2525000+02	2.2525000+02	1.0846486-03	1.6770816-04	16.12	32.25	23.10
68000.	67534.8	2.2100000+02	2.2100000+02	9.3052387-04	1.4666247-04	16.51	33.00	23.90
69000.	68526.9	2.1675000+02	2.1675000+02	7.9586029-04	1.2791753-04	16.90	33.75	24.70
70000.	69519.0	2.1250000+02	2.1250000+02	6.7856073-04	1.1126780-04	17.29	34.50	25.50
71000.	70511.1	2.0825000+02	2.0825000+02	5.7664156-04	9.6510648-05	17.68	35.25	26.30
72000.	71503.2	2.0400000+02	2.0400000+02	4.8844814-04	8.3469629-05	18.07	36.00	27.10
73000.	72495.3	1.9975000+02	1.9975000+02	4.1236877-04	7.1975231-05	18.46	36.75	27.90
74000.	73487.4	1.9550000+02	1.9550000+02	3.4700393-04	6.1864117-05	18.85	37.50	28.70
75000.	74479.5	1.9125000+02	1.9125000+02	2.9097080-04	5.3004503-05	19.24	38.25	29.50
76000.	75471.6	1.8700000+02	1.8700000+02	2.4319172-04	4.6252975-05	19.63	39.00	30.30
77000.	76463.7	1.8275000+02	1.8275000+02	2.0245552-04	4.0253811-05	20.02	39.75	31.10
78000.	77455.8	1.7850000+02	1.7850000+02	1.6777892-04	3.5263811-05	20.41	40.50	31.90
79000.	78447.9	1.7425000+02	1.7425000+02	1.3800621-04	3.0334485-05	20.80	41.25	32.70
80000.	79440.0	1.7000000+02	1.7000000+02	1.1290073-04	2.6315139-05	21.19	42.00	33.50
81000.	80432.1	1.6575000+02	1.6575000+02	9.2306137-05	2.2893204-05	21.58	42.75	34.30
82000.	81424.2	1.6150000+02	1.6150000+02	7.5511932-05	1.9504837-05	21.97	43.50	35.10
83000.	82416.3	1.5725000+02	1.5725000+02	6.1855116-05	1.674332-05	22.36	44.25	35.90
84000.	83408.4	1.5300000+02	1.5300000+02	5.0659180-05	1.4038513-05	22.75	45.00	36.70
85000.	84400.5	1.4875000+02	1.4875000+02	4.1408538-05	1.1850260-05	23.14	45.75	37.50
86000.	85392.6	1.4450000+02	1.4450000+02	3.3922195-05	9.9713593-06	23.53	46.50	38.30
87000.	86384.7	1.4025000+02	1.4025000+02	2.7647018-05	8.4710650-06	23.92	47.25	39.10
88000.	87376.8	1.3600000+02	1.3600000+02	2.2735596-05	7.1096806-06	24.31	48.00	39.90
89000.	88368.9	1.3175000+02	1.3175000+02	1.8634796-05	6.0394928-06	24.70	48.75	40.70
90000.	89361.0	1.2750000+02	1.2750000+02	1.5134811-05	5.1070709-06	25.09	49.50	41.50

TABLE 3.12B KENNEDY SPACE CENTER WINTER (COLD)  
ATMOSPHERE (KCA-71)

Geometric Altitude	Geopotential Altitude	Virtual Temperature	Kinetic Temperature	Pressure	Density	Rel. Dev. (T*) with res- pect to PRA-63	Rel. Dev. (P) with res- pect to PRA-63	Rel. Dev. (D) with res- pect to PRA-63
Z(m)	H(m)	T* (*K)	T (*K)	P (N/cm <sup>2</sup> )	D (kg/m <sup>3</sup> )	RD(T)%	RD(P)%	RD(D)%
0.	0.	2.7500000+02	2.7450000+02	1.0270000+01	1.3009944+00	-3.14	-3.14	2.32
1000.	223.5	2.7000000+02	2.6960000+02	9.059171+00	1.1689934+00	-7.67	-7.67	7.30
2000.	1336.5	2.6500000+02	2.6470000+02	7.9735277+00	1.0481959+00	-7.91	-7.91	7.00
3000.	739.5	2.6000000+02	2.5980000+02	7.0004350+00	9.3797119+01	-7.46	-7.46	5.95
4000.	2392.5	2.5500000+02	2.5470000+02	6.1305847+00	8.2752835+01	-7.39	-7.39	4.90
5000.	4989.5	2.5000000+02	2.5000000+02	5.3594730+00	7.4616589+01	-7.16	-7.16	3.51
6000.	7995.1	2.4523591+02	2.4523591+02	4.6646548+00	6.6278397+01	-5.65	-4.92	1.96
7000.	10822.7	2.4044706+02	2.4044706+02	4.0522883+00	5.8710627+01	-6.07	-5.69	1.36
8000.	13373.0	2.3595761+02	2.3595761+02	3.5107186+00	5.182328+01	-4.37	-5.46	-1.17
9000.	15675.0	2.3160561+02	2.3160561+02	3.0333381+00	4.5620410+01	-3.77	-7.19	-2.40
10000.	17700.0	2.2767153+02	2.2767153+02	2.6141402+00	4.0002266+01	-2.42	-7.55	-5.27
11000.	19565.7	2.2401892+02	2.2401892+02	2.2471262+00	3.4951847+01	-1.74	-7.61	-7.15
12000.	21271.0	2.2058508+02	2.2058508+02	1.925518+00	3.0436223+01	-1.77	-7.15	-7.53
13000.	22855.7	2.1733175+02	2.1733175+02	1.6489457+00	2.6415523+01	-2.15	-7.70	-6.62
14000.	24350.1	2.1428577+02	2.1428577+02	1.4071002+00	2.2809338+01	-3.35	-7.41	-10.05
15000.	24744.2	2.1157970+02	2.1157970+02	1.1935198+00	1.9732939+01	-3.76	-7.03	-9.94
16000.	25037.7	2.0949258+02	2.0949258+02	1.0219132+00	1.6953508+01	-7.13	-6.61	-9.47
17000.	25231.4	2.0749304+02	2.0749304+02	8.6531102+01	1.4460154+01	-2.79	-6.20	-9.75
18000.	25324.5	2.0583237+02	2.0583237+02	7.3453635+01	1.2283195+01	-1.44	-5.95	-7.19
19000.	25317.4	2.0446620+02	2.0446620+02	6.2346069+01	1.0437007+01	1.34	-5.01	-6.13
20000.	25202.1	2.0332348+02	2.0332348+02	5.2929262+01	8.8729208+02	-6.64	-6.01	-5.33
21000.	25000.0	2.0239611+02	2.0239611+02	4.4953001+01	7.4658779+02	-1.41	-6.23	-6.27
22000.	24728.6	2.1030961+02	2.1030961+02	3.8218424+01	6.3147604+02	-1.12	-6.54	-4.57
23000.	24385.6	2.1219170+02	2.1219170+02	3.2513529+01	5.3736919+02	-2.52	-6.30	-4.65
24000.	23976.9	2.1362211+02	2.1362211+02	2.7700539+01	4.5168950+02	-2.89	-7.42	-4.85
25000.	23517.4	2.1517109+02	2.1517109+02	2.3622344+01	3.8223467+02	-2.94	-7.96	-5.26
26000.	23015.5	2.1673259+02	2.1673259+02	2.0166165+01	3.2796351+02	-2.37	-8.50	-5.76
27000.	22474.2	2.1842757+02	2.1842757+02	1.7237638+01	2.7482916+02	-2.88	-9.05	-6.38
28000.	21937.7	2.2007615+02	2.2007615+02	1.4746703+01	2.3465394+02	-2.34	-9.47	-7.07
29000.	21402.8	2.2170900+02	2.2170900+02	1.2632431+01	1.9857147+02	-2.04	-10.22	-7.40
30000.	20871.0	2.2331153+02	2.2331153+02	1.0832073+01	1.6910702+02	-1.16	-10.79	-7.87
31000.	20347.1	2.2488554+02	2.2488554+02	9.2998346+02	1.4416779+02	-3.55	-11.79	-8.13
32000.	20000.0	2.2644043+02	2.2644043+02	7.9957733+02	1.2301918+02	-2.79	-12.07	-8.57
33000.	19744.4	2.2799975+02	2.2799975+02	6.8840331+02	1.0507172+02	-4.07	-12.71	-9.21
34000.	19477.6	2.2960097+02	2.2960097+02	5.9314604+02	8.9853973+02	-4.32	-13.40	-9.49
35000.	19166.4	2.3125000+02	2.3125000+02	5.1093379+02	7.6963609+02	-4.65	-14.12	-9.94
36000.	18814.0	2.3382940+02	2.3382940+02	4.4116489+02	6.571515+02	-4.57	-14.75	-11.37
37000.	18435.2	2.3642857+02	2.3642857+02	3.8143088+02	5.6209221+02	-4.51	-15.56	-11.57
38000.	18022.1	2.3901786+02	2.3901786+02	3.3035589+02	4.8152172+02	-4.45	-16.24	-12.34
39000.	17570.8	2.4160714+02	2.4160714+02	2.8661022+02	4.1323890+02	-4.41	-16.91	-13.08
40000.	17095.1	2.4415643+02	2.4415643+02	2.4901237+02	3.5523605+02	-4.35	-17.57	-13.32
41000.	16581.1	2.4678571+02	2.4678571+02	2.1667652+02	3.0585937+02	-4.28	-18.21	-14.55
42000.	16036.9	2.4937500+02	2.4937500+02	1.8820863+02	2.6376449+02	-4.19	-18.74	-15.29
43000.	15452.2	2.5196428+02	2.5196428+02	1.6474552+02	2.2778053+02	-4.05	-19.46	-16.05
44000.	14837.7	2.5455357+02	2.5455357+02	1.4394226+02	1.9698486+02	-3.89	-20.05	-16.83
45000.	14182.0	2.5714286+02	2.5714286+02	1.2533651+02	1.7059479+02	-3.63	-20.62	-17.62
46000.	13490.5	2.5973214+02	2.5973214+02	1.1074660+02	1.4797821+02	-3.30	-21.15	-18.46
47000.	12765.7	2.6232143+02	2.6232143+02	9.6825027+02	1.2858047+02	-2.87	-21.63	-19.36
48000.	12000.0	2.6491071+02	2.6491071+02	8.5055041+02	1.1187174+02	-2.31	-22.05	-20.20
49000.	11195.0	2.6750000+02	2.6750000+02	7.4903328+02	9.7817115+02	-1.61	-22.47	-21.10
50000.	10341.1	2.6750000+02	2.6750000+02	6.5834379+02	8.5726990+02	-1.15	-22.71	-21.91
51000.	9424.2	2.6750000+02	2.6750000+02	5.7941055+02	7.5457335+02	-0.79	-22.99	-22.52
52000.	8470.6	2.6750000+02	2.6750000+02	5.0931116+02	6.6395879+02	-0.07	-23.19	-23.25
53000.	7489.1	2.6607143+02	2.6607143+02	4.4871795+02	5.8748772+02	-0.29	-23.35	-23.57
54000.	6471.1	2.6464286+02	2.6464286+02	3.9456653+02	5.1935687+02	-0.53	-23.47	-23.82
55000.	5445.2	2.6321423+02	2.6321423+02	3.4663939+02	4.5875263+02	-0.84	-23.59	-24.00
56000.	4394.3	2.6178572+02	2.6178572+02	3.0420338+02	4.0691104+02	-1.37	-23.65	-24.68
57000.	33415.7	2.6035714+02	2.6035714+02	2.6690495+02	3.5713458+02	-1.85	-23.67	-25.00
58000.	22737.1	2.5892957+02	2.5892957+02	2.3394566+02	3.1478500+02	-2.40	-23.65	-25.44
59000.	12276.0	2.5750000+02	2.5750000+02	2.0493507+02	2.7727747+02	-2.92	-23.67	-25.79
60000.	5355.7	2.5607143+02	2.5607143+02	1.7946230+02	2.4408292+02	-3.63	-23.44	-26.12
61000.	60326.6	2.5464286+02	2.5464286+02	1.5695310+02	2.1473479+02	-4.31	-23.24	-26.41
62000.	61125.1	2.5321423+02	2.5321423+02	1.3722539+02	1.8792230+02	-5.02	-22.99	-26.66
63000.	62295.4	2.5178572+02	2.5178572+02	1.1901118+02	1.6587944+02	-5.76	-22.71	-26.86
64000.	63747.3	2.5035714+02	2.5035714+02	1.0467529+02	1.4562313+02	-6.53	-22.24	-27.01
65000.	64253.0	2.4892857+02	2.4892857+02	9.1317415+01	1.2776279+02	-7.22	-21.77	-27.07
66000.	64231.7	2.4750000+02	2.4750000+02	7.9591589+01	1.1192064+02	-7.91	-21.14	-27.11
67000.	64209.3	2.4607143+02	2.4607143+02	6.9297552+01	9.8073482+01	-8.95	-20.41	-27.07
68000.	64173.0	2.4464286+02	2.4464286+02	6.0273170+01	8.5805893+01	-9.79	-19.76	-26.91
69000.	64144.5	2.4321423+02	2.4321423+02	5.2362318+01	7.4997425+01	-10.62	-19.00	-26.69
70000.	64114.6	2.4178572+02	2.4178572+02	4.5454579+01	6.5495014+01	-11.47	-18.37	-26.37
71000.	64084.3	2.4035714+02	2.4035714+02	3.9408634+01	5.7145119+01	-12.31	-17.65	-26.07
72000.	64054.3	2.3892857+02	2.3892857+02	3.4146309+01	4.9815655+01	-13.16	-16.87	-25.46
73000.	64024.1	2.3750000+02	2.3750000+02	2.9575343+01	4.3401718+01	-14.01	-16.23	-24.86
74000.	64000.0	2.3607143+02	2.3607143+02	2.5612631+01	3.7884127+01	-14.87	-15.57	-24.15
75000.	64022.6	2.3464286+02	2.3464286+02	2.2135302+01	3.2925129+01	-15.74	-14.87	-23.37
76000.	64097.3	2.3321423+02	2.3321423+02	1.9212246+01	2.8688431+01	-16.59	-14.14	-22.59
77000.	64172.9	2.3178572+02	2.3178572+02	1.6645303+01	2.4969101+01	-17.48	-13.40	-21.85
78000.	64247.5	2.3035714+02	2.3035714+02	1.4385223+01	2.1701813+01	-18.39	-12.67	-21.19
79000.	64322.1	2.2892857+02	2.2892857+02	1.2365341+01	1.8788338+01	-19.30	-11.95	-20.51
80000.	64396.0	2.2750000+02	2.2750000+02	1.0559136+01	1.6231238+01	-20.27	-11.20	-19.82
81000.	64469.7	2.2607143+02	2.2607143+02	9.1113408+00	1.4154732+01	-21.31	-10.47	-19.13
82000.	64543.2	2.2464286+02	2.2464286+02	7.8145255+00	1.2319863+01	-22.37	-9.74	-18.44
83000.	64616.4	2.2321423+02	2.2321423+02	6.6990716+00	1.0700285+01	-23.42	-9.01	-17.75
84000.	64689.7	2.2178572+02	2.2178572+02	5.7196012+00	9.2762901+00	-24.47	-8.28	-17.06
85000.	64762.9	2.2035714+02	2.2035714+02	4.8654079+00	8.0223083+00	-25.52	-7.55	-16.37
86000.	64836.0	2.1892857+02	2.1892857+02	4.1329370+00	6.9224450+00	-26.57	-6.82	-15.68
87000.	64909.1	2.1750000+02	2.1750000+02	3.5031226+00	5.9589480+00	-27.62	-6.09	-14.99
88000.	64982.2	2.1607143+02	2.1607143+02	2.9604435+00	5.1109661+00	-28.67	-5.36	-14.30
89000.	65055.3	2.1464286+02	2.1464286+02	2.4953273+00	4.3857098+00	-29.72	-4.63	-13.61
90000.	65128.4	2.1321423+02	2.1321423+02	2.0947456+00	3.7453175+00	-30.77	-3.90	-12.92



TABLE 3.13A VANDENBERG SUMMER (HOT) ATMOSPHERE (VHA-73) (Ref. 3.6)

GEO- METRIC ALTITUDE	GEO- POTENTIAL ALTITUDE	VIRTUAL TEMPERATURE	KINETIC TEMPERATURE	PRESSURE	DENSITY	REL. DEV. (T°) WITH RESPECT TO VRA-71	REL. DEV. (P) WITH RESPECT TO VRA-71	REL. DEV. (D) WITH RESPECT TO VRA-71
Z(m)	H(m)	T° (°K)	T (°K)	P (N/cm <sup>2</sup> )	D(kg/m <sup>3</sup> )	RD(T°)%	RD(P)%	RD(D)%
0.	0.	3.1270000+02	3.1040000+02	1.0100000+01	1.1252041+00	8.90	-1.88	-6.98
1000.	999.5	3.0564445+02	3.0360000+02	9.0433741+00	1.0307463+00	6.50	-0.05	-6.15
2000.	1998.8	2.9858889+02	2.9680000+02	8.0764169+00	9.4226634-01	5.29	.65	-4.41
3000.	2997.7	2.9153334+02	2.9000000+02	7.1933711+00	8.5957158-01	4.71	1.25	-3.30
4000.	3996.3	2.8447778+02	2.8320000+02	6.3887244+00	7.8235557-01	4.45	1.79	-2.54
5000.	4994.6	2.7742223+02	2.7640001+02	5.6572052+00	7.1039269-01	4.39	2.32	-1.97
6000.	5992.5	2.7036667+02	2.6960000+02	4.9937766+00	6.4344846-01	4.47	2.88	-1.53
7000.	6990.2	2.6331112+02	2.6280000+02	4.3936325+00	5.8128933-01	4.73	3.49	-1.19
8000.	7987.5	2.5625556+02	2.5600000+02	3.8521923+00	5.2368783-01	5.15	4.18	-.93
9000.	8984.5	2.4920000+02	2.4920000+02	3.3650957+00	4.7042153-01	5.64	4.92	-.67
10000.	9981.3	2.4053334+02	2.4053334+02	2.9268444+00	4.2389880-01	5.27	5.64	.35
11000.	10977.7	2.3186667+02	2.3186667+02	2.5326658+00	3.8051989-01	4.77	6.43	1.87
12000.	11973.7	2.2320000+02	2.2320000+02	2.1795295+00	3.4017810-01	2.48	6.95	4.37
13000.	12969.5	2.1453334+02	2.1453334+02	1.8645094+00	3.0276635-01	-.23	7.11	7.36
14000.	13965.0	2.0586667+02	2.0586667+02	1.5847846+00	2.6817733-01	-3.30	6.80	10.43
15000.	14960.1	1.9720000+02	1.9720000+02	1.3376402+00	2.3630346-01	-6.55	5.90	13.31
16000.	15954.9	1.9570000+02	1.9570000+02	1.1241226+00	2.0610632-01	-6.57	4.66	12.02
17000.	16949.5	1.9720000+02	1.9720000+02	9.4465147-01	1.6687632-01	-5.57	3.48	9.61
18000.	17943.7	2.0073846+02	2.0073846+02	7.9573023-01	1.3810093-01	-4.59	2.53	7.44
19000.	18937.6	2.0427692+02	2.0427692+02	6.7212328-01	1.1462151-01	-3.49	1.60	5.33
20000.	19931.2	2.0781538+02	2.0781538+02	5.6937122-01	9.5439698-02	-2.61	.97	3.73
21000.	20924.4	2.1135385+02	2.1135385+02	4.8373771-01	7.9729042-02	-1.86	.61	2.53
22000.	21917.4	2.1489231+02	2.1489231+02	4.1213909-01	6.6814438-02	-1.13	.41	1.52
23000.	22910.0	2.1843077+02	2.1843077+02	3.5205753-01	5.6153625-02	-.32	.29	-.56
24000.	23902.4	2.2196923+02	2.2196923+02	3.0146263-01	4.7317459-02	.58	.21	-.41
25000.	24894.4	2.2550769+02	2.2550769+02	2.5873474-01	3.9969986-02	1.60	.19	-1.39
26000.	25886.1	2.2904615+02	2.2904615+02	2.2257759-01	3.3848221-02	2.66	.25	-2.30
27000.	26877.5	2.3258462+02	2.3258462+02	1.9194649-01	2.8744659-02	3.66	.52	-2.98
28000.	27868.6	2.3612308+02	2.3612308+02	1.6595856-01	2.4485870-02	4.44	1.15	-3.18
29000.	28859.4	2.3966154+02	2.3966154+02	1.4382187-01	2.0913849-02	5.05	1.64	-3.24
30000.	29849.9	2.4320000+02	2.4320000+02	1.2477411-01	1.7872536-02	5.54	2.23	-3.14
31000.	30840.0	2.4631765+02	2.4631765+02	1.0854021-01	1.5351728-02	5.90	2.90	-2.84
32000.	31829.9	2.4943529+02	2.4943529+02	9.4560565-02	1.3207052-02	6.30	3.64	-2.50
33000.	32819.4	2.5255294+02	2.5255294+02	8.2517347-02	1.1382030-02	6.68	4.43	-2.11
34000.	33808.7	2.5567059+02	2.5567059+02	7.2130870-02	9.8276710-03	7.05	5.26	-1.66
35000.	34797.6	2.5878823+02	2.5878823+02	6.3160133-02	8.5018768-03	7.36	6.13	-1.17
36000.	35786.2	2.6190588+02	2.6190588+02	5.5398216-02	7.3685989-03	7.62	7.01	-.57
37000.	36774.5	2.6502353+02	2.6502353+02	4.8666973-02	6.3975410-03	7.82	7.91	.08
38000.	37762.5	2.6814117+02	2.6814117+02	4.2817249-02	5.5634384-03	7.96	8.81	.79
39000.	38750.2	2.7125882+02	2.7125882+02	3.7723102-02	4.8452492-03	8.04	9.71	1.55
40000.	39737.5	2.7437647+02	2.7437647+02	3.3279228-02	4.2256546-03	8.07	10.62	2.36
41000.	40724.6	2.7749411+02	2.7749411+02	2.9397174-02	3.6904526-03	8.08	11.52	3.18
42000.	41711.4	2.8061176+02	2.8061176+02	2.6056630-02	3.2279282-03	8.09	12.42	4.01
43000.	42697.8	2.8372941+02	2.8372941+02	2.3039207-02	2.8282852-03	8.13	13.33	4.81
44000.	43683.9	2.8684706+02	2.8684706+02	2.0444488-02	2.4829949-03	8.14	14.25	5.55
45000.	44669.6	2.8996470+02	2.8996470+02	1.8168831-02	2.1834793-03	8.17	15.20	6.20
46000.	45655.3	2.9308235+02	2.9308235+02	1.6164093-02	1.9223480-03	8.88	16.18	6.71
47000.	46640.5	2.9620000+02	2.9620000+02	1.4385190-02	1.6918819-03	9.51	17.22	7.64
48000.	47625.4	2.9620000+02	2.9620000+02	1.2818198-02	1.5075772-03	9.31	18.27	8.19
49000.	48610.0	2.9620000+02	2.9620000+02	1.1421840-02	1.3433490-03	9.51	19.27	8.92
50000.	49594.3	2.9620000+02	2.9620000+02	1.0177627-02	1.1970084-03	9.24	20.37	10.20
51000.	50578.3	2.9620000+02	2.9620000+02	9.0689635-03	1.066158-03	9.19	21.31	11.10
52000.	51561.9	2.9620000+02	2.9620000+02	8.0805098-03	9.504369-04	9.39	22.32	11.82
53000.	52545.3	2.9620000+02	2.9620000+02	7.1950161-03	8.5820842-04	8.27	23.32	13.91
54000.	53528.4	2.8791429+02	2.8791429+02	6.3955581-03	7.7381164-04	7.33	24.23	15.75
55000.	54511.1	2.8377143+02	2.8377143+02	5.6750142-03	6.9666314-04	6.54	25.04	17.37
56000.	55493.6	2.7962857+02	2.7962857+02	5.0267339-03	6.2623221-04	5.88	25.77	18.78
57000.	56475.7	2.7548571+02	2.7548571+02	4.4443536-03	5.6202674-04	5.33	26.41	20.01
58000.	57457.5	2.7134286+02	2.7134286+02	3.9221644-03	5.0357592-04	4.87	26.97	21.67
59000.	58439.1	2.6720000+02	2.6720000+02	3.4547555-03	4.5044625-04	4.48	27.45	21.99
60000.	59420.3	2.6305714+02	2.6305714+02	3.0370307-03	4.0222382-04	4.13	27.86	22.79
61000.	60401.2	2.5891429+02	2.5891429+02	2.6644552-03	3.5852188-04	3.83	28.21	23.48
62000.	61381.8	2.5477143+02	2.5477143+02	2.3327088-03	3.1897581-04	3.54	28.48	24.09
63000.	62362.1	2.5062857+02	2.5062857+02	2.0378721-03	2.8325033-04	3.26	28.69	24.63
64000.	63342.1	2.4648571+02	2.4648571+02	1.7762542-03	2.5102877-04	2.97	28.83	25.12
65000.	64321.4	2.4234286+02	2.4234286+02	1.5446758-03	2.2201657-04	2.66	28.91	25.57
66000.	65301.2	2.3820000+02	2.3820000+02	1.3400006-03	1.9594312-04	2.33	28.93	26.00
67000.	66280.3	2.3405714+02	2.3405714+02	1.1594701-03	1.7254829-04	1.96	28.87	26.40
68000.	67259.3	2.2991429+02	2.2991429+02	1.0006714-03	1.5160394-04	1.55	28.75	26.78
69000.	68237.5	2.2577143+02	2.2577143+02	8.6121321-04	1.3288224-04	1.10	28.55	27.15
70000.	69215.7	2.2162857+02	2.2162857+02	7.3911667-04	1.1619067-04	.61	28.28	27.50
71000.	70193.5	2.1748571+02	2.1748571+02	6.3246489-04	1.0133731-04	-.08	27.92	27.82
72000.	71171.1	2.1334286+02	2.1334286+02	5.3967237-04	8.8149071-05	-.49	27.47	28.09
73000.	72148.3	2.0920000+02	2.0920000+02	4.5900583-04	7.6471567-05	-1.08	26.92	28.30
74000.	73125.3	2.0505714+02	2.0505714+02	3.8919926-04	6.6153764-05	-1.69	26.26	28.43
75000.	74101.9	2.0091429+02	2.0091429+02	3.295102-04	5.7053579-05	-2.29	25.48	28.42
76000.	75078.3	1.9677143+02	1.9677143+02	2.7727127-04	4.9075842-05	-2.88	24.56	28.26
77000.	76054.3	1.9262857+02	1.9262857+02	2.3281574-04	4.2071342-05	-3.42	23.51	27.88
78000.	77030.0	1.8848571+02	1.8848571+02	1.9671169-04	3.5943508-05	-3.89	22.29	27.24
79000.	78005.4	1.8434286+02	1.8434286+02	1.6204834-04	3.0591488-05	-4.24	20.91	26.26
80000.	78980.4	1.8020000+02	1.8020000+02	1.3420582-04	2.5044710-05	-4.45	19.33	24.90
81000.	79955.4	1.8020000+02	1.8020000+02	1.1112200-04	2.0145099-05	-2.22	17.82	20.49
82000.	80929.9	1.8020000+02	1.8020000+02	9.1691288-05	1.7744064-05	-.25	16.73	17.62
83000.	81904.1	1.8020000+02	1.8020000+02	7.5950622-05	1.4689445-05	-.25	16.10	16.39
84000.	82878.0	1.8020000+02	1.8020000+02	6.2980652-05	1.2176514-05	-.25	15.48	15.77
85000.	83851.6	1.8020000+02	1.8020000+02	5.2146911-05	1.0068893-05	-.25	14.85	15.13
86000.	84824.9	1.8020000+02	1.8020000+02	4.3191910-05	8.3389282-06	-.25	14.22	14.50
87000.	85798.0	1.8020000+02	1.8020000+02	3.5724639-05	6.8847435-06	-.25	13.58	13.86
88000.	86770.7	1.8020000+02	1.8020000+02	2.9678345-05	5.7106018-06	-.25	12.94	13.22
89000.	87743.1	1.8020000+02	1.8020000+02	2.4518966-05	4.7130584-06	-.25	12.30	12.58
90000.	88715.1	1.8020000+02	1.8020000+02	2.0151138-05	3.9081573-06	-.25	11.65	11.93

TABLE 3.13B VANDENBERG WINTER (COLD) ATMOSPHERE (VCA-73) (Ref. 3.6)

GEO- METRIC ALTITUDE	GEO- POTENTIAL ALTITUDE	VIRTUAL TEMPERATURE	KINETIC TEMPERATURE	PRESSURE	DENSITY	REL. DEV. (T) WITH RESPECT TO VRA-71	REL. DEV. (P) WITH RESPECT TO VRA-71	REL. DEV. (D) WITH RESPECT TO VRA-71
Z(m)	H(m)	T° (°K)	T (°K)	P (N/cm <sup>2</sup> )	D(kg/m <sup>3</sup> )	RD(T) %	RD(P) %	RD(D) %
0.	999.0	2.7270000+02	2.7210000+02	1.0180000+01	1.3004703+00	-5.03	-1.10	5.20
1000.	999.8	2.6666000+02	2.6648000+02	8.9693283+00	1.1704464+00	-6.98	-1.87	6.57
2000.	1998.8	2.6122000+02	2.6086000+02	7.8809177+00	1.0510132+00	-7.89	-1.79	6.62
3000.	2997.7	2.5548000+02	2.5524000+02	6.9047076+00	9.4151269+01	-8.24	-2.81	5.92
4000.	3996.3	2.4972000+02	2.4962000+02	6.0312658+00	8.4131451+01	-8.30	-3.90	4.80
5000.	4994.6	2.4400000+02	2.4400000+02	5.2517759+00	7.4681523+01	-8.19	-5.01	3.47
6000.	5992.5	2.3830000+02	2.3830000+02	4.5580398+00	6.6633385+01	-7.92	-6.09	1.98
7000.	6990.2	2.3260000+02	2.3260000+02	3.9423968+00	5.9055721+01	-7.49	-7.14	1.37
8000.	7987.5	2.2690000+02	2.2690000+02	3.3976520+00	5.2165361+01	-6.90	-8.12	-1.31
9000.	8984.5	2.2120000+02	2.2120000+02	2.9171181+00	4.5451659+01	-6.23	-9.04	-2.99
10000.	9981.3	2.2086667+02	2.2086667+02	2.4993697+00	3.9421944+01	-3.34	-9.79	-6.69
11000.	10977.7	2.2053333+02	2.2053333+02	2.1409279+00	3.3419378+01	-7.63	-10.63	-9.46
12000.	11973.7	2.2020000+02	2.2020000+02	1.8334731+00	2.9006479+01	1.11	-10.03	-11.61
13000.	12969.5	2.1986667+02	2.1986667+02	1.5698082+00	2.4872811+01	2.25	-9.82	-11.80
14000.	13965.7	2.1953333+02	2.1953333+02	1.3437376+00	2.1323162+01	3.12	-9.45	-12.19
15000.	14960.1	2.1920000+02	2.1920000+02	1.1499446+00	1.8275709+01	3.88	-8.96	-12.37
16000.	15954.0	2.1886667+02	2.1886667+02	9.8387086+01	1.5660159+01	4.49	-8.39	-12.33
17000.	16949.5	2.1853333+02	2.1853333+02	8.4159365+01	1.3415970+01	4.64	-7.81	-11.89
18000.	17943.7	2.1820000+02	2.1820000+02	7.1969167+01	1.1490234+01	3.71	-7.26	-10.59
19000.	18937.6	2.1870000+02	2.1870000+02	6.1554150+01	9.8050058+02	3.32	-6.96	-9.91
20000.	19931.2	2.1920000+02	2.1920000+02	5.2659444+01	8.3690010+02	2.72	-6.63	-9.05
21000.	20924.4	2.1970000+02	2.1970000+02	4.5065654+01	7.1458278+02	2.01	-6.28	-8.11
22000.	21917.4	2.2020000+02	2.2020000+02	3.8582201+01	6.1038803+02	1.32	-6.00	-7.25
23000.	22910.0	2.2070000+02	2.2070000+02	3.3044670+01	5.2159878+02	.71	-5.85	-6.57
24000.	23902.4	2.2120000+02	2.2120000+02	2.8312334+01	4.4589290+02	.24	-5.87	-6.13
25000.	24894.4	2.2170000+02	2.2170000+02	2.4265535+01	3.8130028+02	-1.12	-6.05	-5.94
26000.	25886.1	2.2220000+02	2.2220000+02	2.0803276+01	3.2615742+02	-.41	-6.32	-5.90
27000.	26877.5	2.2270000+02	2.2270000+02	1.7840172+01	2.7907043+02	-.74	-6.59	-5.85
28000.	27868.6	2.2320000+02	2.2320000+02	1.5304207+01	2.3886475+02	-1.28	-6.70	-5.53
29000.	28859.4	2.2370000+02	2.2370000+02	1.3134525+01	2.0454262+02	-1.95	-7.12	-5.20
30000.	29849.9	2.2420000+02	2.2420000+02	1.1278137+01	1.7524437+02	-2.71	-7.61	-5.64
31000.	30840.0	2.2470000+02	2.2470000+02	9.6878738+02	1.5020203+02	-3.39	-8.17	-4.95
32000.	31829.9	2.2520000+02	2.2520000+02	8.3202466+02	1.2770590+02	-4.03	-8.80	-4.97
33000.	32819.4	2.2570000+02	2.2570000+02	7.1553249+02	1.0661954+02	-3.94	-9.46	-5.74
34000.	33808.7	2.2620000+02	2.2620000+02	6.1612920+02	9.3486013+02	-3.87	-10.10	-6.48
35000.	34797.6	2.2670000+02	2.2670000+02	5.3127079+02	7.9472872+02	-3.83	-10.74	-7.18
36000.	35786.2	2.2720000+02	2.2720000+02	4.5877666+02	6.8298111+03	-3.84	-11.37	-7.83
37000.	36774.5	2.2770000+02	2.2770000+02	3.9674339+02	5.8514099+03	-3.90	-12.02	-8.45
38000.	37762.5	2.2820000+02	2.2820000+02	3.4357967+02	5.0206642+03	-4.02	-12.68	-9.02
39000.	38750.2	2.2870000+02	2.2870000+02	2.9792671+02	4.3138564+03	-4.17	-13.35	-9.57
40000.	39737.5	2.2920000+02	2.2920000+02	2.5866051+02	3.7113266+03	-4.37	-14.03	-10.10
41000.	40724.6	2.2970000+02	2.2970000+02	2.2482605+02	3.1668689+03	-4.58	-14.73	-10.64
42000.	41711.4	2.3020000+02	2.3020000+02	1.9566269+02	2.7571029+03	-4.78	-15.43	-11.19
43000.	42697.5	2.3070000+02	2.3070000+02	1.7048912+02	2.3811340+03	-4.95	-16.15	-11.78
44000.	43683.9	2.3120000+02	2.3120000+02	1.4876175+02	2.0595932+03	-5.06	-16.86	-12.43
45000.	44669.8	2.3170000+02	2.3170000+02	1.2999268+02	1.7443018+03	-5.06	-17.56	-13.17
46000.	45655.3	2.3220000+02	2.3220000+02	1.1371536+02	1.5476761+03	-4.90	-18.25	-14.03
47000.	46640.5	2.3270000+02	2.3270000+02	9.9526405+03	1.3428264+03	-4.54	-18.90	-15.65
48000.	47625.4	2.3320000+02	2.3320000+02	8.7191319+03	1.1764016+03	-4.71	-19.55	-16.57
49000.	48610.0	2.3370000+02	2.3370000+02	7.6385498+03	1.0306020+03	-4.54	-20.23	-16.44
50000.	49594.3	2.3420000+02	2.3420000+02	6.6919231+03	9.0289450+04	-4.78	-20.85	-16.88
51000.	50578.3	2.3470000+02	2.3470000+02	5.8625937+03	7.9998797+04	-4.82	-21.58	-17.61
52000.	51561.9	2.3520000+02	2.3520000+02	5.1332330+03	6.9265652+04	-4.65	-22.26	-18.47
53000.	52545.3	2.3570000+02	2.3570000+02	4.4989681+03	6.1026216+04	-4.80	-22.90	-19.02
54000.	53528.4	2.3620000+02	2.3620000+02	3.9384305+03	5.3709328+04	-4.78	-23.54	-19.70
55000.	54511.1	2.3670000+02	2.3670000+02	3.4440768+03	4.7223997+04	-4.62	-24.15	-20.48
56000.	55493.6	2.3720000+02	2.3720000+02	3.0088639+03	4.1485059+04	-4.33	-24.74	-21.33
57000.	56475.7	2.3770000+02	2.3770000+02	2.6263249+03	3.6413980+04	-3.93	-25.30	-22.24
58000.	57457.5	2.3820000+02	2.3820000+02	2.2906935+03	3.1939316+04	-3.42	-25.82	-23.19
59000.	58439.1	2.3870000+02	2.3870000+02	1.9965887+03	2.7995395+04	-2.84	-26.29	-24.14
60000.	59420.3	2.3920000+02	2.3920000+02	1.7391419+03	2.4523735+04	-2.18	-26.72	-25.06
61000.	60401.2	2.3970000+02	2.3970000+02	1.5140176+03	2.1469926+04	-1.47	-27.09	-26.00
62000.	61381.8	2.4020000+02	2.4020000+02	1.3173056+03	1.8785143+04	-.71	-27.40	-26.88
63000.	62362.1	2.4070000+02	2.4070000+02	1.1454892+03	1.6426374+04	.09	-27.64	-27.71
64000.	63342.1	2.4120000+02	2.4120000+02	9.9539518+04	1.4354014+04	.91	-27.82	-28.47
65000.	64321.8	2.4170000+02	2.4170000+02	8.6441278+04	1.2535653+04	1.74	-27.93	-29.18
66000.	65301.2	2.3878065+02	2.3878065+02	7.5002193+04	1.0937738+04	2.58	-27.55	-29.76
67000.	66280.3	2.3739355+02	2.3739355+02	6.5010309+04	9.5433113+05	3.41	-27.90	-30.27
68000.	67259.0	2.3600645+02	2.3600645+02	5.6287288+04	8.3935469+05	4.24	-27.75	-30.69
69000.	68237.5	2.3461936+02	2.3461936+02	4.8666954+04	7.2222710+05	5.06	-27.52	-31.01
70000.	69215.7	2.3323226+02	2.3323226+02	4.2019844+04	6.2745095+05	5.88	-27.19	-31.23
71000.	70193.5	2.3184517+02	2.3184517+02	3.6225796+04	5.4427624+05	6.69	-26.76	-31.35
72000.	71171.1	2.3045807+02	2.3045807+02	3.1198025+04	4.7175884+05	7.49	-26.23	-31.37
73000.	72148.3	2.2970797+02	2.2970797+02	2.6816368+04	4.0837268+05	8.31	-25.58	-31.29
74000.	73125.3	2.2768387+02	2.2768387+02	2.3046970+04	3.5318852+05	9.16	-24.82	-31.13
75000.	74101.9	2.2629678+02	2.2629678+02	1.9808292+04	3.0550003+05	10.05	-23.95	-30.89
76000.	75078.3	2.2490968+02	2.2490968+02	1.7026424+04	2.6429176+05	11.01	-22.94	-30.59
77000.	76054.3	2.2352258+02	2.2352258+02	1.4659405+04	2.2873878+05	12.07	-21.81	-30.23
78000.	77030.0	2.2213549+02	2.2213549+02	1.2646675+04	1.9424028+05	13.27	-20.54	-29.85
79000.	78005.4	2.2074839+02	2.2074839+02	1.0934830+04	1.7206192+05	14.67	-19.13	-29.48
80000.	78980.4	2.1936129+02	2.1936129+02	9.4366073+05	1.4400207+05	16.31	-17.58	-29.13
81000.	79955.4	2.1797420+02	2.1797420+02	8.1052780+05	1.2470789+05	18.28	-15.86	-28.87
82000.	80929.9	2.1658710+02	2.1658710+02	6.8445205+05	1.0972977+05	19.89	-13.90	-28.19
83000.	81904.1	2.1520000+02	2.1520000+02	5.7823956+05	9.3090994+05	19.13	-11.63	-25.82
84000.	82878.0	2.1520000+02	2.1520000+02	4.9337446+05	7.9488436+05	19.13	-9.36	-23.91
85000.	83851.6	2.1520000+02	2.1520000+02	4.2093396+05	6.8143606+05	19.13	-7.03	-21.95
86000.	84824.6	2.1520000+02	2.1520000+02	3.5912990+05	5.8139562+05	19.13	-4.64	-19.95
87000.	85798.0	2.1520000+02	2.1520000+02	3.0642449+05	4.9605370+05	19.13	-2.21	-17.91
88000.	86770.7	2.1520000+02	2.1520000+02	2.6143789+05	4.2325258+05	19.13	.29	-15.81
89000.	87743.1	2.1520000+02	2.1520000+02	2.2305846+05	3.6412070+05	19.13	2.84	-13.67
90000.	88715.1	2.1520000+02	2.1520000+02	1.9032955+05	3.0813813+05	19.13	5.45	-11.48

TABLE 3.14A EDWARDS SUMMER (HOT) ATMOSPHERE (EHA-75) (Ref. 3.7)

GEO- METRIC ALTITUDE	GEO- POTENTIAL ALTITUDE	VIRTUAL TEMPERATURE	KINETIC TEMPERATURE	PRESSURE	DENSITY	REL. DEV. (T°) WITH RESPECT TO ERA-74	REL. DEV. (P) WITH RESPECT TO ERA-74	REL. DEV. (D) WITH RESPECT TO ERA-74
Z(m)	H(m)	T° (°K)	T (°K)	P (N/cm²)	D(kg/m³)	RD(T%)	RD(P%)	RD(D%)
706.	705.2	3.1805000+02	3.1805000+02	8.2900000+00	1.0175555+00	9.23	-2.16	-10.44
1000.	998.9	3.1209859+02	3.1209859+02	8.9927101+00	1.0037755+00	7.61	-1.95	-8.89
2000.	1997.5	3.0146334+02	3.0146334+02	8.0421432+00	9.2934106+01	5.82	-1.23	-6.66
3000.	2995.7	2.9323000+02	2.9323000+02	7.1692100+00	8.5172755+01	5.22	-.61	-5.54
4000.	3993.7	2.8448333+02	2.8448333+02	6.3701680+00	7.7865946+01	4.79	-.02	-4.59
5000.	4991.3	2.7676334+02	2.7676334+02	5.6405716+00	7.0999023+01	4.42	.53	-3.72
6000.	5988.6	2.6915544+02	2.6915544+02	4.9766757+00	6.4413065+01	4.36	1.08	-3.14
7000.	6985.6	2.6190455+02	2.6190455+02	4.3758856+00	5.8191729+01	4.59	1.67	-2.80
8000.	7982.3	2.5492273+02	2.5492273+02	3.8339298+00	5.2393019+01	5.03	2.32	-2.58
9000.	8978.6	2.4810455+02	2.4810455+02	3.3465977+00	4.6995209+01	5.64	3.05	-2.44
10000.	9974.7	2.4123065+02	2.4123065+02	2.9107930+00	4.2035543+01	6.07	3.91	-2.04
11000.	10970.5	2.3413387+02	2.3413387+02	2.5210631+00	3.7510884+01	5.86	4.81	-.99
12000.	11965.9	2.2703710+02	2.2703710+02	2.1738746+00	3.3356114+01	4.69	5.64	-.92
13000.	12961.0	2.1994032+02	2.1994032+02	1.8650988+00	2.9551155+01	2.67	6.24	3.47
14000.	13956.2	2.1284355+02	2.1284355+02	1.5932018+00	2.5551155+01	2.36	6.50	6.14
15000.	14950.3	2.0574678+02	2.0574678+02	1.3532391+00	2.2076429+01	-2.03	6.35	8.56
16000.	15944.5	1.9863000+02	1.9863000+02	1.1425509+00	2.0081875+01	-4.83	5.74	11.11
17000.	16938.4	2.0315000+02	2.0315000+02	9.6412691+01	1.6533133+01	-2.87	5.05	8.16
18000.	17931.9	2.0769000+02	2.0769000+02	8.1639213+01	1.3693001+01	-1.17	4.70	5.94
19000.	18925.2	2.1215000+02	2.1215000+02	6.9370273+01	1.1392114+01	.28	4.63	4.33
20000.	19918.1	2.1422692+02	2.1422692+02	5.9109888+01	9.6119186+02	.42	4.69	4.25
21000.	20910.7	2.1630384+02	2.1630384+02	5.0030077+01	8.1219940+02	.46	4.76	4.29
22000.	21903.0	2.1838077+02	2.1838077+02	4.3092430+01	6.8781142+02	.49	4.84	4.33
23000.	22895.0	2.2045769+02	2.2045769+02	3.6879513+01	5.8276230+02	.59	4.92	4.31
24000.	23886.7	2.2253461+02	2.2253461+02	3.1610081+01	4.9486573+02	.84	5.04	4.16
25000.	24878.1	2.2461154+02	2.2461154+02	2.7132461+01	4.2083160+02	1.19	5.05	3.82
26000.	25869.1	2.2668846+02	2.2668846+02	2.3320557+01	3.5839356+02	1.60	5.01	3.40
27000.	26859.9	2.2876538+02	2.2876538+02	2.0070293+01	3.0563484+02	1.96	5.08	3.11
28000.	27850.3	2.3084231+02	2.3084231+02	1.7295921+01	2.6100494+02	2.10	5.44	3.22
29000.	28840.5	2.3291923+02	2.3291923+02	1.4926132+01	2.2323105+02	2.09	5.55	3.39
30000.	29830.3	2.3499615+02	2.3499615+02	1.2900001+01	1.9123856+02	1.98	5.68	3.63
31000.	30819.8	2.3707308+02	2.3707308+02	1.1164329+01	1.6407257+02	1.93	5.83	3.83
32000.	31809.0	2.3915000+02	2.3915000+02	9.6093582+02	1.4084936+02	1.91	5.99	4.00
33000.	32797.9	2.4295333+02	2.4295333+02	8.3927593+02	1.2034792+02	2.63	6.20	3.48
34000.	33786.5	2.4675666+02	2.4675666+02	7.2992877+02	1.0305168+02	3.31	6.51	3.09
35000.	34774.8	2.5056000+02	2.5056000+02	6.3610809+02	8.8447494+03	3.95	6.89	2.82
36000.	35762.7	2.5436333+02	2.5436333+02	5.5063488+02	7.6092947+03	4.53	7.34	2.69
37000.	36750.4	2.5816666+02	2.5816666+02	4.8030504+02	6.5619659+03	5.03	7.84	2.67
38000.	37737.7	2.6197000+02	2.6197000+02	4.2048144+02	5.6715698+03	5.47	8.39	2.77
39000.	38724.7	2.6577333+02	2.6577333+02	3.7471504+02	4.9119873+03	5.85	8.99	2.97
40000.	39711.5	2.6957666+02	2.6957666+02	3.2981136+02	4.2625066+03	6.18	9.62	3.24
41000.	40697.9	2.7338000+02	2.7338000+02	2.9076445+02	3.7055760+03	6.48	10.29	3.58
42000.	41684.0	2.7718333+02	2.7718333+02	2.5881953+02	3.2275963+03	6.77	11.00	3.96
43000.	42669.6	2.8098666+02	2.8098666+02	2.2720108+02	2.8166123+03	7.08	11.75	4.35
44000.	43655.3	2.8479000+02	2.8479000+02	2.0137253+02	2.4629745+03	7.47	12.54	4.72
45000.	44640.5	2.8859333+02	2.8859333+02	1.7879410+02	2.1563862+03	7.96	13.39	5.03
46000.	45625.3	2.9239666+02	2.9239666+02	1.5899658+02	1.8949432+03	8.62	14.31	5.24
47000.	46609.9	2.9620000+02	2.9620000+02	1.4151964+02	1.6644580+03	9.51	15.32	5.30
48000.	47594.2	2.9620000+02	2.9620000+02	1.2610335+02	1.4831359+03	9.31	16.35	6.44
49000.	48578.1	2.9620000+02	2.9620000+02	1.1236006+02	1.3215718+03	9.51	17.34	7.15
50000.	49561.8	2.9620000+02	2.9620000+02	1.0014529+02	1.1776111+03	9.24	18.42	8.41
51000.	50545.1	2.9620000+02	2.9620000+02	8.9218640+03	1.0493260+03	9.19	19.34	9.30
52000.	51528.1	2.9620000+02	2.9620000+02	7.9498910+03	9.3500988+04	9.39	20.33	10.01
53000.	52510.9	2.9205714+02	2.9205714+02	7.0783657+03	8.4429538+04	8.27	21.32	12.06
54000.	53493.3	2.8791429+02	2.8791429+02	6.2918555+03	7.6126856+04	7.33	22.22	13.87
55000.	54475.4	2.8377143+02	2.8377143+02	5.5830145+03	6.8536967+04	6.54	23.02	15.46
56000.	55457.2	2.7962857+02	2.7962857+02	4.9452281+03	6.1607957+04	5.88	23.73	16.85
57000.	56436.7	2.7548571+02	2.7548571+02	4.3723237+03	5.5291355+04	5.33	24.36	18.06
58000.	57419.9	2.7134286+02	2.7134286+02	3.8580056+03	4.9541217+04	4.87	24.91	19.11
59000.	58400.7	2.6720000+02	2.6720000+02	3.3987260+03	4.4314373+04	4.48	25.39	20.61
60000.	59381.3	2.6305714+02	2.6305714+02	2.9871829+03	3.9570264+04	4.13	25.79	20.80
61000.	60361.6	2.5891429+02	2.5891429+02	2.6214478+03	3.5270774+04	3.83	26.13	21.48
62000.	61341.6	2.5477143+02	2.5477143+02	2.2944933+03	3.1380439+04	3.54	26.40	22.06
63000.	62321.2	2.5062857+02	2.5062857+02	2.0048475+03	2.7866054+04	3.26	26.60	22.61
64000.	63300.6	2.4648571+02	2.4648571+02	1.7474222+03	2.4696028+04	2.97	26.75	23.09
65000.	64279.6	2.4234286+02	2.4234286+02	1.5195846+03	2.1841669+04	2.66	26.82	23.54
66000.	65258.4	2.3820000+02	2.3820000+02	1.3182655+03	1.9276726+04	2.33	26.84	23.95
67000.	66236.8	2.3405714+02	2.3405714+02	1.1400494+03	1.6975212+04	1.96	26.79	24.35
68000.	67214.9	2.2991429+02	2.2991429+02	9.8444938+04	1.4914501+04	1.55	26.66	24.73
69000.	68192.6	2.2577143+02	2.2577143+02	8.4729949+04	1.3072944+04	1.10	26.47	25.09
70000.	69170.3	2.2162857+02	2.2162857+02	7.2718143+04	1.1430716+04	.61	26.20	25.43
71000.	70147.5	2.1748571+02	2.1748571+02	6.2217712+04	9.9694729+05	.08	25.85	25.75
72000.	71124.4	2.1334286+02	2.1334286+02	5.3091286+04	8.6722613+05	-.49	25.40	26.02
73000.	72101.0	2.0920000+02	2.0920000+02	4.5130035+04	7.5270228+05	-1.08	24.86	26.22
74000.	73077.3	2.0505714+02	2.0505714+02	3.8289347+04	6.5082788+05	-1.69	24.21	26.36
75000.	74053.3	2.0091429+02	2.0091429+02	3.2409137+04	5.6139469+05	-2.29	23.44	26.34
76000.	75029.0	1.9677143+02	1.9677143+02	2.7274609+04	4.8282385+05	-2.88	22.54	26.18
77000.	76004.4	1.9262857+02	1.9262857+02	2.2905303+04	4.1399419+05	-3.42	21.50	25.81
78000.	76979.5	1.8848571+02	1.8848571+02	1.9156933+04	3.5381767+05	-3.89	20.31	25.17
79000.	77954.3	1.8434286+02	1.8434286+02	1.5933712+04	2.9909630+05	-4.24	18.95	24.22
80000.	78928.8	1.8020000+02	1.8020000+02	1.3200096+04	2.5506019+05	-4.45	17.40	22.87
81000.	79903.0	1.8020000+02	1.8020000+02	1.0919571+04	2.1103859+05	-2.22	15.91	18.54
82000.	80876.8	1.8020000+02	1.8020000+02	9.0289115+05	1.7678943+05	-.25	14.83	15.12
83000.	81850.4	1.8020000+02	1.8020000+02	7.4744225+05	1.4859610+05	-.25	14.22	14.51
84000.	82823.7	1.8020000+02	1.8020000+02	6.1964757+05	1.1974335+05	-.25	13.60	13.89
85000.	83796.7	1.8020000+02	1.8020000+02	5.1270668+05	9.9201202+06	-.25	12.99	13.27
86000.	84769.3	1.8020000+02	1.8020000+02	4.2341139+05	8.2015991+06	-.25	12.36	12.64
87000.	85741.7	1.8020000+02	1.8020000+02	3.5085678+05	6.7825317+06	-.25	11.74	12.02
88000.	86713.8	1.8020000+02	1.8020000+02	2.9077530+05	5.6247711+06	-.25	11.11	11.39
89000.	87685.5	1.8020000+02	1.8020000+02	2.4003982+05	4.6634674+06	-.25	10.48	10.76
90000.	88657.0	1.8020000+02	1.8020000+02	1.9807416+05	3.8452148+06	-.25	9.84	10.11



TABLE 3.14B EDWARDS WINTER (COLD) ATMOSPHERE (ECA-75) (Ref. 3.7)

GEO- METRIC ALTITUDE	GEO- POTENTIAL ALTITUDE	VIRTUAL TEMPERATURE	KINETIC TEMPERATURE	PRESSURE	DENSITY	REL. DEV. (T*) WITH RESPECT TO ERA-74	REL. DEV. (P) WITH RESPECT TO ERA-74	REL. DEV. (D) WITH RESPECT TO ERA-74
Z(m)	H(m)	T* (°K)	T (°K)	P (N/cm <sup>2</sup> )	D(kg/m <sup>3</sup> )	RD(T) %	RD(P) %	RD(D) %
706.	705.2	2.7365000+02	2.7315000+02	9.3400000+00	1.1353954+00	-6.01	-1.11	5.22
1000.	998.9	2.7169868+02	2.7123291+02	9.0436318+00	1.1595598+00	-6.32	-1.40	5.25
2000.	1997.5	2.6556651+02	2.6471218+02	7.9626412+00	1.0465218+00	-6.96	-2.21	5.11
3000.	2995.7	2.5842434+02	2.5819145+02	6.9882666+00	9.4204977-01	-7.27	-3.11	4.48
4000.	3993.7	2.5178717+02	2.5156707+02	6.1123285+00	8.4668942-01	-7.43	-4.07	3.62
5000.	4991.3	2.4515000+02	2.4515000+02	5.3270900+00	7.5700013-01	-7.51	-5.05	2.66
6000.	5988.6	2.3965000+02	2.3965000+02	4.6267853+00	6.7257345-01	-7.08	-6.02	1.14
7000.	6985.6	2.3415000+02	2.3415000+02	4.0054143+00	5.9592430-01	-6.51	-6.94	-4.46
8000.	7982.3	2.2865000+02	2.2865000+02	3.4555265+00	5.2649399-01	-5.80	-7.78	-2.11
9000.	8978.6	2.2315000+02	2.2315000+02	2.9706049+00	4.6375200-01	-4.99	-8.53	-3.73
10000.	9974.7	2.2248333+02	2.2248333+02	2.5483341+00	3.9902337-01	-2.17	-9.03	-7.01
11000.	10970.5	2.2181667+02	2.2181667+02	2.1850370+00	3.4317250-01	.29	-9.16	-9.42
12000.	11965.9	2.2115000+02	2.2115000+02	1.8727532+00	2.9500646-01	1.97	-8.99	-10.75
13000.	12961.0	2.2048333+02	2.2048333+02	1.6043217+00	2.5378568-01	2.93	-8.64	-11.24
14000.	13955.8	2.1981667+02	2.1981667+02	1.3737173+00	2.1770802-01	3.62	-8.18	-11.39
15000.	14950.3	2.1915000+02	2.1915000+02	1.1756991+00	1.8689287-01	4.35	-7.60	-11.45
16000.	15944.5	2.1848333+02	2.1848333+02	1.0057510+00	1.6636523-01	4.67	-6.95	-11.10
17000.	16938.4	2.1781667+02	2.1781667+02	8.5996912-01	1.3750401-01	4.45	-6.30	-10.02
18000.	17931.9	2.1715000+02	2.1715000+02	7.3495366-01	1.1790656-01	3.35	-5.74	-8.80
19000.	18925.2	2.1731667+02	2.1731667+02	6.2800190-01	1.0067124-01	2.73	-5.29	-7.80
20000.	19918.1	2.1748333+02	2.1748333+02	5.3667863-01	8.5965850-02	1.94	-4.94	-6.75
21000.	20910.7	2.1765000+02	2.1765000+02	4.5869091-01	7.3417381-02	1.08	-4.71	-5.73
22000.	21903.0	2.1781667+02	2.1781667+02	3.9208290-01	6.2708206-02	.23	-4.62	-4.83
23000.	22895.0	2.1798333+02	2.1798333+02	3.3518764-01	5.3567505-02	-.54	-4.64	-4.13
24000.	23886.7	2.1815000+02	2.1815000+02	2.8658279-01	4.5764786-02	-1.15	-4.77	-3.66
25000.	24878.1	2.1903125+02	2.1903125+02	2.4511787-01	3.8985798-02	-1.32	-5.09	-3.82
26000.	25869.1	2.1991250+02	2.1991250+02	2.0978271-01	3.3232181-02	-1.43	-5.53	-4.11
27000.	26859.9	2.2079375+02	2.2079375+02	1.7965517-01	2.8345894-02	-1.59	-5.94	-4.37
28000.	27850.3	2.2167500+02	2.2167500+02	1.5394886-01	2.4193466-02	-1.95	-6.16	-4.33
29000.	28840.5	2.2255625+02	2.2255625+02	1.3200119-01	2.0662117-02	-2.45	-6.67	-4.32
30000.	29830.3	2.2343750+02	2.2343750+02	1.1325157-01	1.7657204-02	-3.04	-7.22	-4.32
31000.	30819.8	2.2431875+02	2.2431875+02	9.7223701-02	1.5098938-02	-3.55	-7.82	-4.42
32000.	31809.0	2.2520000+02	2.2520000+02	8.3514365-02	1.2948991-02	-4.03	-8.46	-4.62
33000.	32797.9	2.2608125+02	2.2608125+02	7.1818008-02	1.1002544-02	-3.94	-9.12	-5.39
34000.	33786.5	2.2696250+02	2.2696250+02	6.1841039-02	9.3830738-03	-3.87	-9.77	-6.13
35000.	34774.8	2.2784375+02	2.2784375+02	5.3324127-02	8.0138092-03	-3.83	-10.41	-6.84
36000.	35762.7	2.2872500+02	2.2872500+02	4.6047458-02	6.8513303-03	-3.84	-11.05	-7.49
37000.	36750.4	2.2960625+02	2.2960625+02	3.9820938-02	5.8730812-03	-3.90	-11.69	-8.11
38000.	37737.7	2.3048750+02	2.3048750+02	3.4485111-02	5.0324949-03	-4.02	-12.35	-8.69
39000.	38724.7	2.3136875+02	2.3136875+02	2.9902954-02	4.3298111-03	-4.17	-13.03	-9.24
40000.	39711.5	2.3225000+02	2.3225000+02	2.5902125-02	3.7250938-03	-4.37	-13.71	-9.77
41000.	40697.9	2.3313125+02	2.3313125+02	2.2561185-02	3.2086792-03	-4.58	-14.41	-10.30
42000.	41684.0	2.3401250+02	2.3401250+02	1.9638176-02	2.7647408-03	-4.78	-15.12	-10.86
43000.	42669.8	2.3489375+02	2.3489375+02	1.7112656-02	2.3899994-03	-4.95	-15.84	-11.45
44000.	43655.3	2.3577500+02	2.3577500+02	1.4932050-02	2.0672607-03	-5.06	-16.55	-12.11
45000.	44640.5	2.3665625+02	2.3665625+02	1.3047066-02	1.7909775-03	-5.06	-17.26	-12.85
46000.	45625.3	2.3753750+02	2.3753750+02	1.1413879-02	1.5535202-03	-4.90	-17.94	-13.72
47000.	46609.9	2.3841875+02	2.3841875+02	9.9894762-03	1.3477931-03	-4.54	-18.60	-14.73
48000.	47594.2	2.3929999+02	2.3929999+02	8.7515234-03	1.1607566-03	-4.71	-19.26	-15.26
49000.	48578.1	2.4018125+02	2.4018125+02	7.6668501-03	1.0344262-03	-4.54	-19.94	-16.13
50000.	49561.6	2.4106250+02	2.4106250+02	6.7167425-03	9.0621996-04	-4.78	-20.56	-16.57
51000.	50545.1	2.4194375+02	2.4194375+02	5.8843326-03	7.9390049-04	-4.82	-21.29	-17.31
52000.	51528.1	2.4282500+02	2.4282500+02	5.1550770-03	6.9551697-04	-4.65	-21.97	-18.17
53000.	52510.9	2.4370625+02	2.4370625+02	4.5156181-03	6.1251270-04	-4.80	-22.62	-18.72
54000.	53493.3	2.4458750+02	2.4458750+02	3.9530086-03	5.3908073-04	-4.78	-23.25	-19.40
55000.	54475.4	2.4546875+02	2.4546875+02	3.4568083-03	4.7398329-04	-4.62	-23.87	-20.18
56000.	55457.2	2.4635000+02	2.4635000+02	3.0199671-03	4.1638064-04	-4.33	-24.46	-21.04
57000.	56438.7	2.4723125+02	2.4723125+02	2.6360655-03	3.6548161-04	-3.93	-25.02	-21.90
58000.	57419.9	2.4811250+02	2.4811250+02	2.2991598-03	3.2056808-04	-3.42	-25.54	-22.90
59000.	58400.7	2.4899375+02	2.4899375+02	2.0039630-03	2.8998631-04	-2.84	-26.02	-23.86
60000.	59381.3	2.4987500+02	2.4987500+02	1.7455506-03	2.4613547-04	-2.18	-26.44	-24.80
61000.	60361.6	2.5075625+02	2.5075625+02	1.5196228-03	2.1548581-04	-1.47	-26.82	-25.73
62000.	61341.6	2.5163750+02	2.5163750+02	1.3221478-03	1.8654141-04	-.71	-27.13	-26.61
63000.	62321.2	2.5251875+02	2.5251875+02	1.1497116-03	1.6486597-04	.09	-27.38	-27.44
64000.	63300.6	2.5340000+02	2.5340000+02	9.9906682-04	1.4407182-04	.91	-27.55	-28.21
65000.	64279.6	2.5428125+02	2.5428125+02	8.6760521-04	1.2580705-04	1.74	-27.66	-28.89
66000.	65258.4	2.5516250+02	2.5516250+02	7.5278520-04	1.0977697-04	2.58	-27.68	-29.50
67000.	66236.8	2.5604375+02	2.5604375+02	6.5249681-04	9.5687866-05	3.41	-27.63	-30.02
68000.	67214.9	2.5692500+02	2.5692500+02	5.6492328-04	8.3339691-05	4.24	-27.48	-30.44
69000.	68192.8	2.5780625+02	2.5780625+02	4.8845291-04	7.2479725-05	5.06	-27.25	-30.76
70000.	69170.3	2.5868750+02	2.5868750+02	4.2174339-04	6.2973022-05	5.88	-26.92	-30.98
71000.	70147.5	2.5956875+02	2.5956875+02	3.6359310-04	5.4621220-05	6.69	-26.49	-31.10
72000.	71124.4	2.6045000+02	2.6045000+02	3.1306743-04	4.7340393-05	7.49	-25.95	-31.11
73000.	72101.0	2.6133125+02	2.6133125+02	2.6913643-04	4.0983200-05	8.31	-25.31	-31.04
74000.	73077.3	2.6221250+02	2.6221250+02	2.3127556-04	3.5848551-05	9.16	-24.55	-30.88
75000.	74053.3	2.6309375+02	2.6309375+02	1.9875049-04	3.0649185-05	10.05	-23.67	-30.64
76000.	75029.0	2.6397500+02	2.6397500+02	1.7086029-04	2.6510239-05	11.01	-22.66	-30.33
77000.	76004.4	2.6485625+02	2.6485625+02	1.4707565-04	2.2944450-05	12.07	-21.52	-29.94
78000.	76979.5	2.6573750+02	2.6573750+02	1.2694359-04	1.9889831-05	13.27	-20.25	-29.60
79000.	77954.3	2.6661875+02	2.6661875+02	1.0971069-04	1.7259922-05	14.67	-18.83	-29.22
80000.	78928.8	2.6750000+02	2.6750000+02	9.4690323-05	1.4405748-05	16.31	-17.27	-28.87
81000.	79903.0	2.6838125+02	2.6838125+02	8.1262589-05	1.2022260-05	18.28	-15.55	-28.60
82000.	80876.2	2.6926250+02	2.6926250+02	6.8721771-05	1.002541-05	19.89	-13.58	-27.92
83000.	81850.4	2.7014375+02	2.7014375+02	5.8037340-05	9.3953013-06	19.13	-11.31	-25.55
84000.	82823.7	2.7102500+02	2.7102500+02	4.9518347-05	8.0164671-06	19.13	-9.02	-23.63
85000.	83796.7	2.7190625+02	2.7190625+02	4.2247176-05	6.8399666-06	19.13	-6.68	-21.67
86000.	84769.3	2.7278750+02	2.7278750+02	3.6045611-05	5.8352351-06	19.13	-4.29	-19.68
87000.	85741.7	2.7366875+02	2.7366875+02	3.0755102-05	4.9785376-06	19.13	-1.84	-17.60
88000.	86713.8	2.7455000+02	2.7455000+02	2.6241243-05	4.2478442-06	19.13	.66	-15.50
89000.	87685.5	2.7543125+02	2.7543125+02	2.2386909-05	3.6240816-06	19.13	3.22	-13.35
90000.	88657.0	2.7631250+02	2.7631250+02	1.9102097-05	3.0427062-06	19.13	5.84	-11.15



shows that when large positive deviations of density occur at the surface, correspondingly large negative deviations will occur near 15 km altitude and above. Such a situation occurs during the winter season (cold atmosphere). The reverse is also true — density profiles with large negative deviations at lower levels will have correspondingly large positive deviations at higher levels. This situation occurs in the summer season (hot atmosphere) (Figs. 3.1, 3.2 and 3.3).

The two extreme Kennedy Space Center density profiles of Figure 3.1 are shown as percent deviations from the Patrick Reference Atmosphere, 1963 density profile (Ref. 3.2). The two profiles obey the hydrostatic equation and the ideal gas law. The extreme density profiles shown here to 30 km altitude were observed in the atmosphere. The results shown above 30 km are somewhat speculative because of the limited data from this region of the atmosphere. Isopycnic levels (levels of minimum density variation) are noted at approximately 8 and 86 km. Another level of minimum density variability is seen at 24 km, and levels of maximum variability occur at 0, 15, and 68 km altitude. The associated extreme virtual temperature profiles for Kennedy Space Center are given in Figure 3.4.

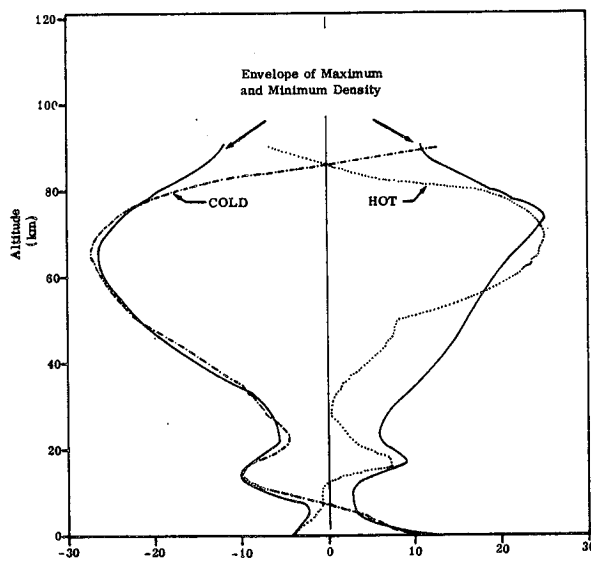


Figure 3.1 Relative deviations (%) of extreme Kennedy Space Center density profiles with respect to PRA-63.

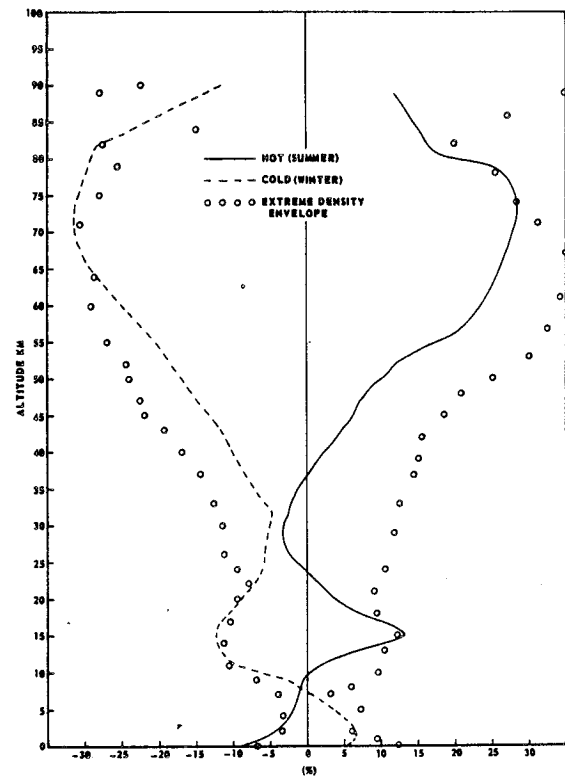


Figure 3.2 Relative deviations (%) of extreme Vandenberg density profiles with respect to VRA-71.

The two Vandenberg extreme density profiles are shown in Figure 3.2 as percent deviations from the Vandenberg Reference Atmosphere, 1971. Levels of minimum density variation are located at  $\sim 8$ , 30 and 90 km altitude. Levels of maximum variability occur at 0, 15 and 73 km. The Hot and Cold Vandenberg virtual temperature profiles are shown in Figure 3.5.

The two Edwards AFB extreme density profiles are shown in Figure 3.3 as percent deviations from the Edwards Reference Atmosphere, 1975. The Hot and Cold Edwards virtual temperature profiles are shown in Figure 3.6. These extreme density and temperature profiles again have structures similar to the

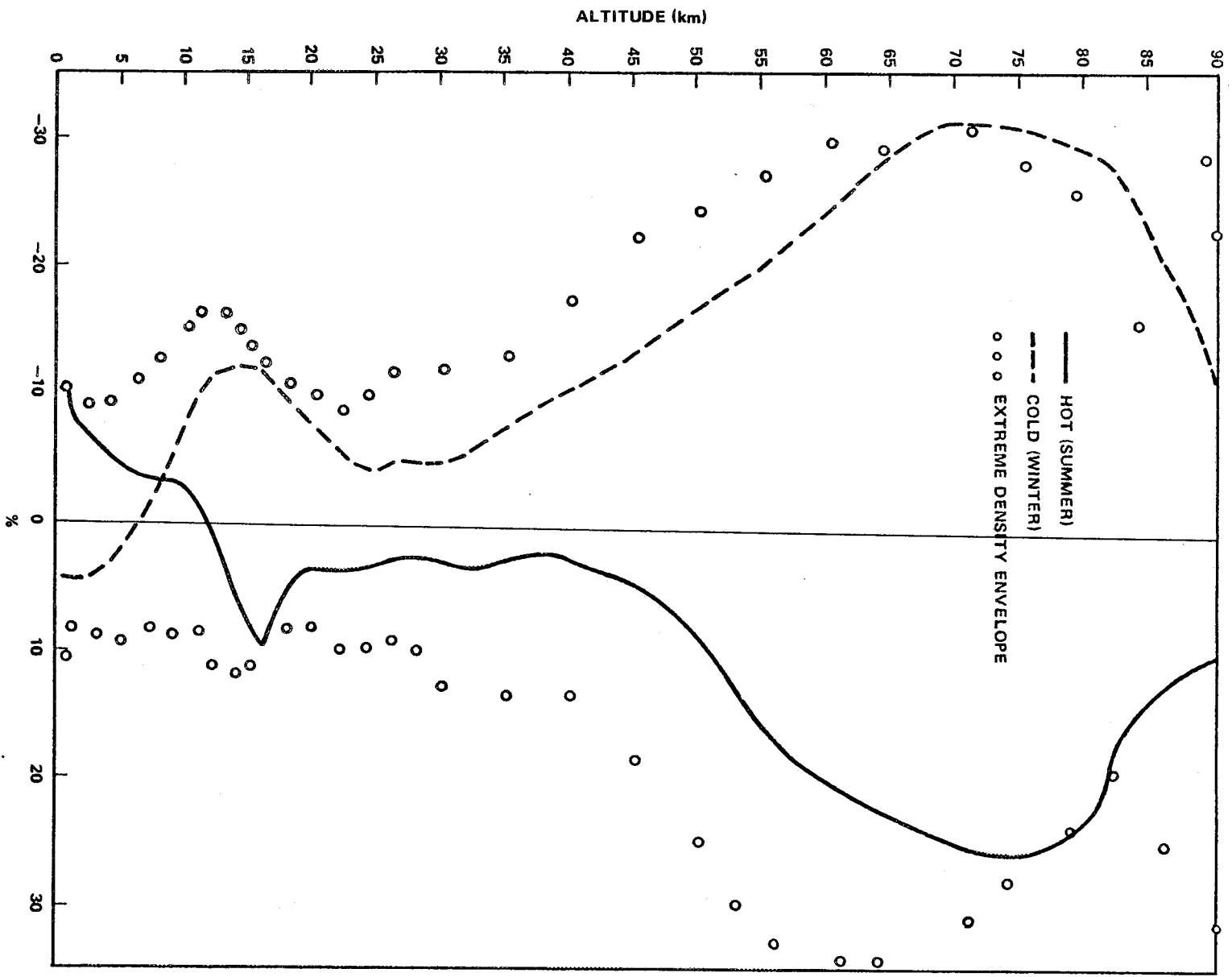


Figure 3.3 Relative deviations (%) of extreme Edwards density profiles with respect to ERA-75.

Kennedy and Vandenberg models. Temperatures below approximately 10 km altitude are virtual temperatures. Virtual temperature includes moisture to avoid computation of specific gas constant for moist air.

$$T_v = T(1 + 0.61 w) \quad , \quad (3.5)$$

where

$T_v$  = virtual temperature ( $^{\circ}\text{K}$ )

$T$  = kinetic temperature ( $^{\circ}\text{K}$ )

$w$  = mixing ratio, grams of water vapor/  
kilograms of dry air (g/kg).

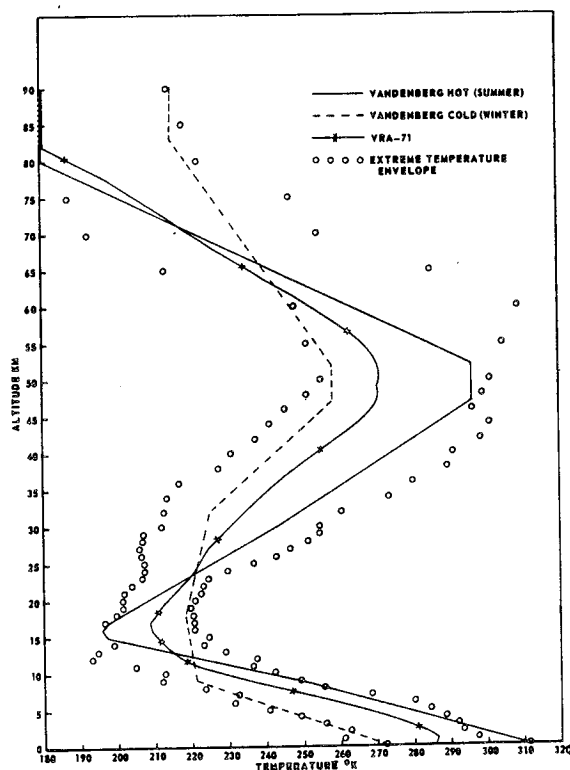


Figure 3.5 Virtual temperature profiles of the Vandenberg hot, cold, and VRA-71.

is given as Table 3.7 from Reference 3.2. The computer subroutine used to prepare these values is available from the Atmospheric Sciences Division, Space Sciences Laboratory, MSFC, NASA, as Computer Subroutine PRA-63. Criteria for orbital studies are in Reference 3.5.

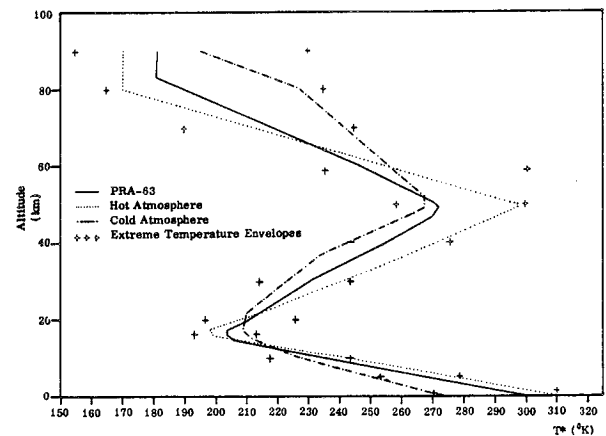


Figure 3.4 Virtual temperature profiles of the Kennedy Space Center hot, cold, and PRA-63.

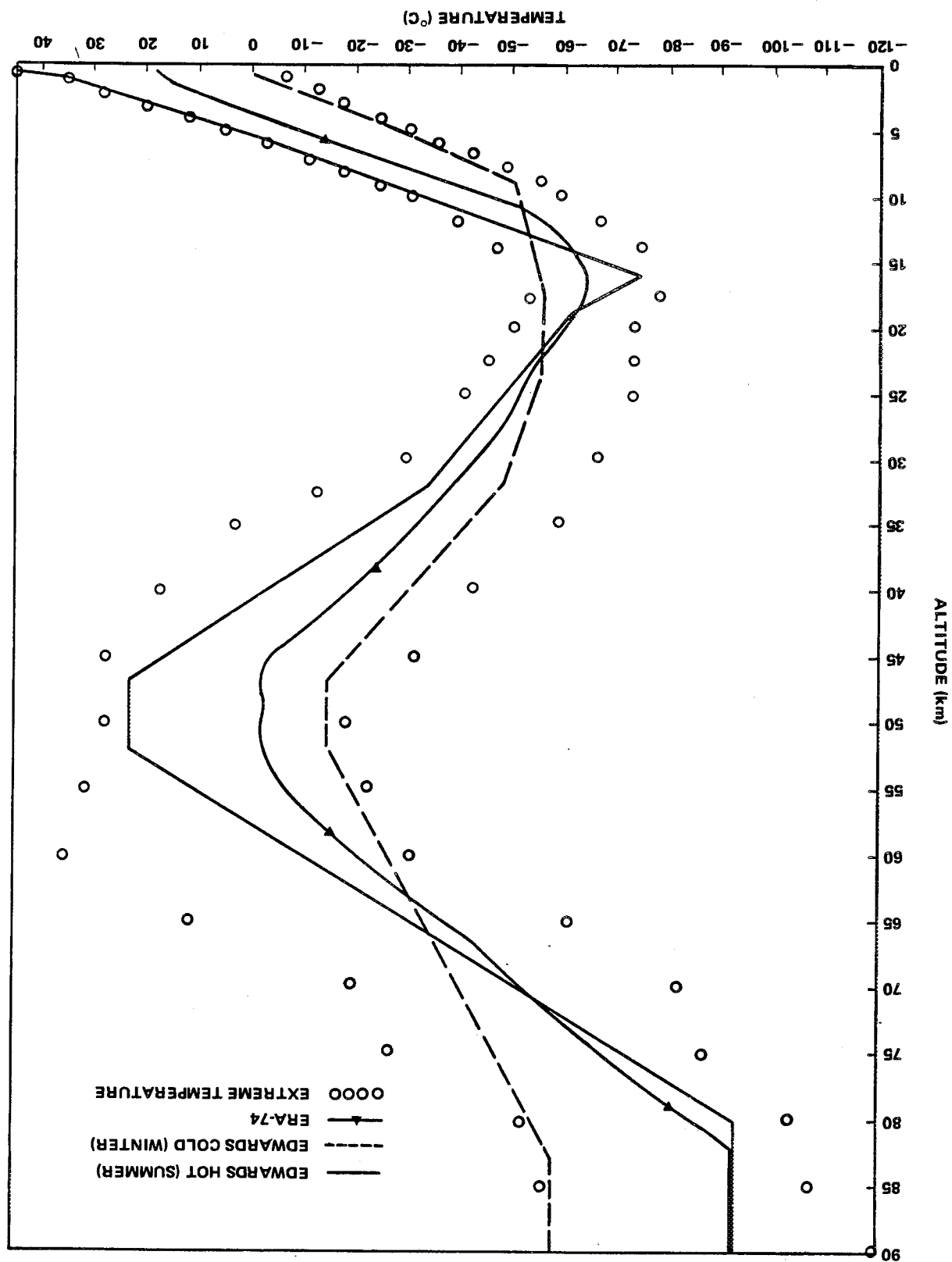
Tables 3.12 A and B, 3.13 A and B, and 3.14 A and B give the numerical data used to prepare Figures 3.1 through 3.6. These three sets of extreme atmospheres are available as computerized subroutines upon request from the NASA-MSFC Space Sciences Laboratory, Atmospheric Sciences Division.

### 3.7 Reference Atmospheres

In design and preflight analysis of space vehicles, special nominal atmospheres are used to represent the mean or median thermodynamic conditions with respect to altitude. For general worldwide design, the U. S. Standard Atmosphere, 1976 (US 76) (Ref. 3.1), is used, but more specific atmospheres are needed at each launch area. A group of Range Reference Atmospheres (Ref. 3.4) have been prepared to represent the thermodynamic medians in the first 30 km at various launch areas. Reference 3.10 (supplemental atmospheres) together with Reference 3.11, which describes the Global Reference Atmosphere Model (GRAM), are also used.

The Patrick Reference Atmosphere (PRA-63) is a more extensive reference atmosphere presenting data to 700 km for the Kennedy Space Center. Because of the utility of this atmosphere, a simplified version

Figure 3.6 Virtual temperature profiles of the Edwards hot, cold, and ERA-75.



ORIGINAL PAGE IS  
OF POOR QUALITY

Reference atmospheres are also available for Vandenberg AFB (Ref. 3.3 and Table 3.8) and Edwards AFB (Ref. 3.7 and Table 3.9). These provide an annual atmospheric model to 700 km and have been designated as Computer Subroutines VRA-71 and ERA-75, respectively.

In Tables 3.7, 3.8 and 3.9 the values are given in standard computer printout, where the two-digit numbers that are at the end of the tabular value (number preceded by E) indicate the power of 10 by which the respective principal value must be multiplied. For example, a tabular value indicated as 2.9937265E 02 is 299.37265 or .15464054E-04 is 0.000015464054.

### 3.8 Reentry – Global Reference Atmosphere Model

#### 3.8.1 Reentry Atmospheric Model

The atmospheric model to be used for all reentry analyses except lower altitudes specified in subsection 3.6 is the NASA-MSFC Global Reference Atmosphere Model (GRAM) (Ref. 3.11). This model generates realistic profiles of atmospheric variables – wind, pressure, temperature, and density – along any vehicle trajectory from orbital altitudes to sea level on a worldwide basis.

The model has been computerized and is available to give these variables and their structure as a function of the three spatial coordinates – latitude, longitude, and altitude – and of the time domain (seasonal). The GRAM model is a composite of other atmospheric models together with new techniques to join models and simulate perturbations. This computer program is available upon request to the Atmospheric Sciences Division, Space Sciences Laboratory, Marshall Space Flight Center, Alabama 35812.

## REFERENCES

- 3.1 "U. S. Standard Atmosphere, 1976," United States Government Printing Office, Washington, D.C., October 1976.
- 3.2 Smith, Orvel E.; and Weidner, Don K., "A Reference Atmosphere for Patrick AFB, Florida, Annual (1963 Revision)," NASA TM X-53139, September 23, 1964.
- 3.3 Carter, E. A.; and Brown, S. C., "A Reference Atmosphere for Vandenberg AFB, California, Annual (1971 Version)." NASA TM X-64590, NASA-Marshall Space Flight Center, Alabama, May 10, 1971.
- 3.4 IRIG Document No. 104-63, Range Reference Atmosphere Documents published by Secretariat, Range Commander's Council, White Sands Missile Range, New Mexico. The following reference atmospheres have been published under this title:
  - (1) Atlantic Missile Range Reference Atmosphere for Cape Kennedy, Florida (Part I), Sept. 1963.
  - (2) White Sands Missile Range Reference Atmosphere (Part I), Aug. 1964.
  - (3) Fort Churchill Missile Range Reference Atmosphere for Fort Churchill, Canada (Part I), Dec. 1964.
  - (4) Pacific Missile Range Reference Atmosphere for Eniwetok, Marshall Islands (Part I), Dec. 1964.
  - (5) Fort Greely Missile Range Reference Atmosphere (Part I), Nov. 1964.
  - (6) Pacific Missile Range Reference Atmosphere for Point Arguello, California (Part I), Aug. 1965.
  - (7) Eglin Gulf Test Range Reference Atmosphere, Eglin AFB, Florida (Part I), Aug. 1965.
  - (8) Wallops Island Test Range Reference Atmosphere (Part I), Sept. 1965.
  - (9) Eastern Test Range Reference Atmosphere for Ascension Island, South Atlantic (Part I), July 1966.
  - (10) Lihu, Kauai, Hawaii Reference Atmosphere (Part I), January 1970.
  - (11) Johnston Island Test Site Reference Atmosphere (Part I), January 1970.
  - (12) Edwards Air Force Base Reference Atmosphere (Part I), Sept. 1972.
  - (13) Cape Kennedy, Florida Reference Atmosphere (Part II), July 1971.
  - (14) White Sands Missile Range Reference Atmosphere (Part II), July 1971.
  - (15) Wallops Island Test Range Atmosphere (Part II), July 1971.

## REFERENCES (Continued)

- (16) Fort Greely Missile Range Reference Atmosphere (Part II), July 1971.
  - (17) Kwajalein Missile Range, Kwajalein, Marshall Islands Reference Atmosphere (Part I), October 1974.
  - (18) Pacific Missile Test Center Reference Atmosphere for Point Arguello, California (Part II), November 1975.
- 
- 3.5 "Space and Planetary Environment Criteria Guidelines for Use in Space Vehicle Development, 1977 Revision." NASA TM-78119, November 1977.
  - 3.6 Johnson, D. L.; "Hot and Cold Atmospheres for Vandenberg AFB, California (1973 Version)," NASA TM X-64756, NASA-Marshall Space Flight Center, Alabama, June 26, 1973.
  - 3.7 Johnson, D. L.; "Hot, Cold, and Annual Reference Atmospheres for Edwards Air Force Base, California (1975 Version)." NASA TM X-64970, November 1975.
  - 3.8 Smith, J. W., "Density Variations and Isopycnic Layer." Journal of Applied Meteorology, vol. 3, No. 3, June 1964, pp. 290-298.
  - 3.9 Buell, C. E., "Some Relations Among Atmospheric Statistics." Journal of Meteorology, vol. 11, June 1954, pp. 238-244.
  - 3.10 "U. S. Standard Atmosphere Supplements 1966." United States Government Printing Office, Washington, D. C. 20402, 1966.
  - 3.11 Justus, C. G., et al., "The NASA/MSFC Global Reference Atmospheric Model – MOD 3 (With Spherical Harmonic Wind Model)." NASA CR-3256, NASA/Marshall Space Flight Center, Huntsville, Ala., March 1980.



## SECTION IV. PRECIPITATION, FOG, AND ICING

### 4.1 Introduction

Precipitation, fog, and icing are atmospheric phenomena of interest to the design, fabrication, and flight of aerospace vehicles. In some arid areas of the world, however, precipitation does not occur for several years. Likewise, in areas of moderate to heavy rainfall, there are periods of time without rain. Because precipitation does occur in discrete events, statistical representation may be misleading; therefore, caution must be taken to ensure that data relative to the desired location are used. Definitions used in this section are given in the following paragraphs.

### 4.2 Definitions

Precipitation is usually defined as all forms of hydrometeors, liquid, or solid, which are free in the atmosphere and reach the ground. In this report the definition is extended to those hydrometeors which do not reach the ground but impinge on a flying surface, such as space vehicles. Accumulation is reported in depth over a horizontal surface, i.e., millimeters or inches for the liquid phase, and in depth or depth-of-water equivalent for the frozen phase.

Snow is defined as all forms of frozen precipitation except large hail. It encompasses snow pellets, snow grains, ice crystals, ice pellets, and small hail.

Hail is precipitation in the form of balls or irregular lumps of ice and is always produced by convective clouds. Through established convention, to be classified as hail the diameter of the ice must be 5 mm or more and the specific gravity must be between 0.60 and 0.92.

Freezing rain is rain that falls in liquid form but freezes upon impact to form a coating of glaze upon the ground or exposed objects.

Small hail is precipitation in the form of semitransparent round or conical grains of frozen water under 5 mm in diameter. Each grain consists of a nucleus of soft hail (ball of snow) surrounded by a very thin ice layer. The grains are not crisp and do not usually rebound when striking a hard surface.

Drizzle: Drizzle consists of droplets which are so small that they make no precipitable impact on surfaces. If individual droplets make a distinct splash on striking the ground or a water surface, they should be recorded as rain (Ref. 4.1).

Mist: Mist is composed of a suspension of very small water droplets in the air. Mist reduces the horizontal visibility at the Earth's surface, as does fog, rain, snow, and other hydrospheric and lithospheric substances.

The previously described precipitation forms are sufficiently different that each must be considered separately in design problems.

### 4.3 Rainfall

There are four major rainfall-producing atmospheric conditions: (1) the monsoon, which produces the heaviest precipitation over long periods (most world records of rainfall rates for periods greater than

12 hours are a result of monsoons), (2) thunderstorms, which generate high rates of precipitation for short periods, (3) cold and warm frontal systems, frequently accompanied by bands of steady light rain. Frontal-produced rain can persist for several days, depending upon the movement of synoptic scale weather systems (thunderstorms may occur with frontal systems to give heavier rain), and (4) hurricanes, which produce heavy rain associated with winds. These four rainfall types are defined in the following paragraphs.

**Monsoon:** The monsoon is a seasonal wind which blows for long periods of time, usually several months from one direction. When these winds blow from the water to land with increasing elevation from the water, the orographic lifting of the moisture-laden air releases precipitation in heavy amounts. In Cherrapunji, India, 9144 mm (360 in.) of rain has fallen in a 1-month period from monsoon rains. The amount of rain from monsoons at low elevations is considerably less than at higher elevations.

**Thunderstorm:** In general, the thunderstorm (local storm) is produced either by lifting of unstable moist air, heating of the land mass, lifting by frontal systems, or a combination of these conditions. Cumulonimbus clouds, which are produced by these storms, are always accompanied by lightning and thunder. The thunderstorm is a consequence of atmospheric instability and is defined loosely as an overturning of air layers in order to achieve a stable condition. Strong wind gusts, heavy rain, severe electrical discharges, and sometimes hail occur with the thunderstorm, with the most frequent and severe occurrences in the late afternoons and evenings.

**Rain shower:** Precipitation from a convective cloud. Showers are characterized by the suddenness with which they start and stop, by the rapid changes of intensity, and usually by rapid changes in the appearance of the sky.

**Cold and warm front precipitation:** When two masses of air meet — one more dense than the other — the lighter air mass (warm) will slide up over the more dense air mass (cold). If sufficient moisture is in the air mass being lifted, then the moisture will be condensed out and fall as precipitation, either rain or snow, depending on the temperature of air masses.

**Hurricanes:** A hurricane is a severe “tropical storm” which forms over the various oceans and seas, nearly always in tropical latitudes. At maturity the tropical cyclone (storm) is one of the most intense and feared storms in the world: Winds exceeding 90 m/s (175 knots) have been measured, and rainfall can be torrential. The wind speed must exceed 33 m/s (64 knots) for the storm to be classified as a hurricane.

Orographic effects should not be overlooked in a discussion of rainfall. Islands located in persistent moist air flow receive extreme rainfall as a result of the moist air being lifted to the condensation level (frequently only 2000 to 5000 ft altitude), with resulting persistent rain. This phenomenon accounts for wide variations in precipitation amounts between locations in close proximity in mountainous areas.

#### 4.3.1 Record Rainfall

In design analysis, the maximum amounts of rainfall for various periods need to be considered. These extreme values vary considerably in different areas of the world, but in areas of similar climatic conditions the extreme values are similar.

##### 4.3.1.1 World Record Rainfall

To best study the maximum amounts of rainfall that have occurred worldwide for different periods, log-log graph paper is used. Figure 4.1 shows these worldwide values and the envelope of these values as a straight line with the equation

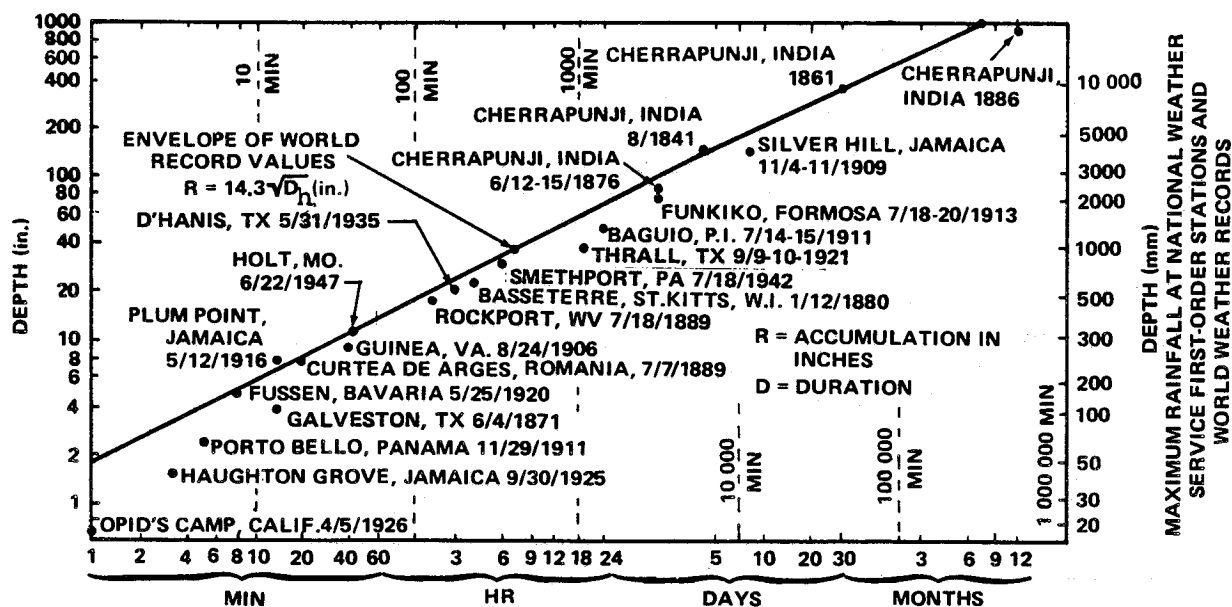


Figure 4.1 World record rainfalls and an envelope of world record values. (After R. D. Fletcher and D. Sartos, Air Weather Service Tech. Report No.105-81, 1951.)

$$R = 363.0 \sqrt{D_h} \text{ (mm)} \quad \text{or} \quad R = 14.3 \sqrt{D_h} \text{ (in.)} \quad (4.1)$$

where  $R$  is the depth of rainfall in millimeters for period  $D$ , and  $D_h$  is the duration of rainfall in hours.

#### 4.3.1.2 Design Rainfall Rates

For design and testing, the rate of rainfall per unit time is more useful than the total depth of rainfall. The normal rates used are shown in millimeters per hour or inches per hour. Figure 4.2 shows the envelope of world record values plotted as the rate per hour (inches and millimeters) versus duration. The Kennedy Space Center and Vandenberg AFB design rainfall rate curves are also shown in Figure 4.2 with the 5-year and 100-year return periods for a few select stations. The 5-year and 100-year return period data were taken from Rainfall Intensity-Duration-Frequency curves published by the U. S. Department of Commerce, Weather Bureau (Ref. 4.2). These data were analyzed by the Extreme Value Method of Gumble (Ref. 4.3).

The term "return period" is a measure of the average time interval between occurrences of a specific event. For example, the 99th percentile rainfall rate for Tampa, Florida, is approximately 10 in./hr for a duration of 6 min (from Fig. 4.2 and Table 4.1). On the average this rainfall rate can be expected to return in 100 years at Tampa. Return periods can be expressed as probabilities, as shown in Table 4.1.

Values of design rainfall for various locations and worldwide extremes of rainfall are given in Tables 4.2, 4.3, 4.4, and 4.5 with values of the corresponding drop size. The worldwide extremes would not normally be used for design of space vehicles but may be needed for facility design, tracking stations, etc. The values of rainfall rates are represented with the following equation:

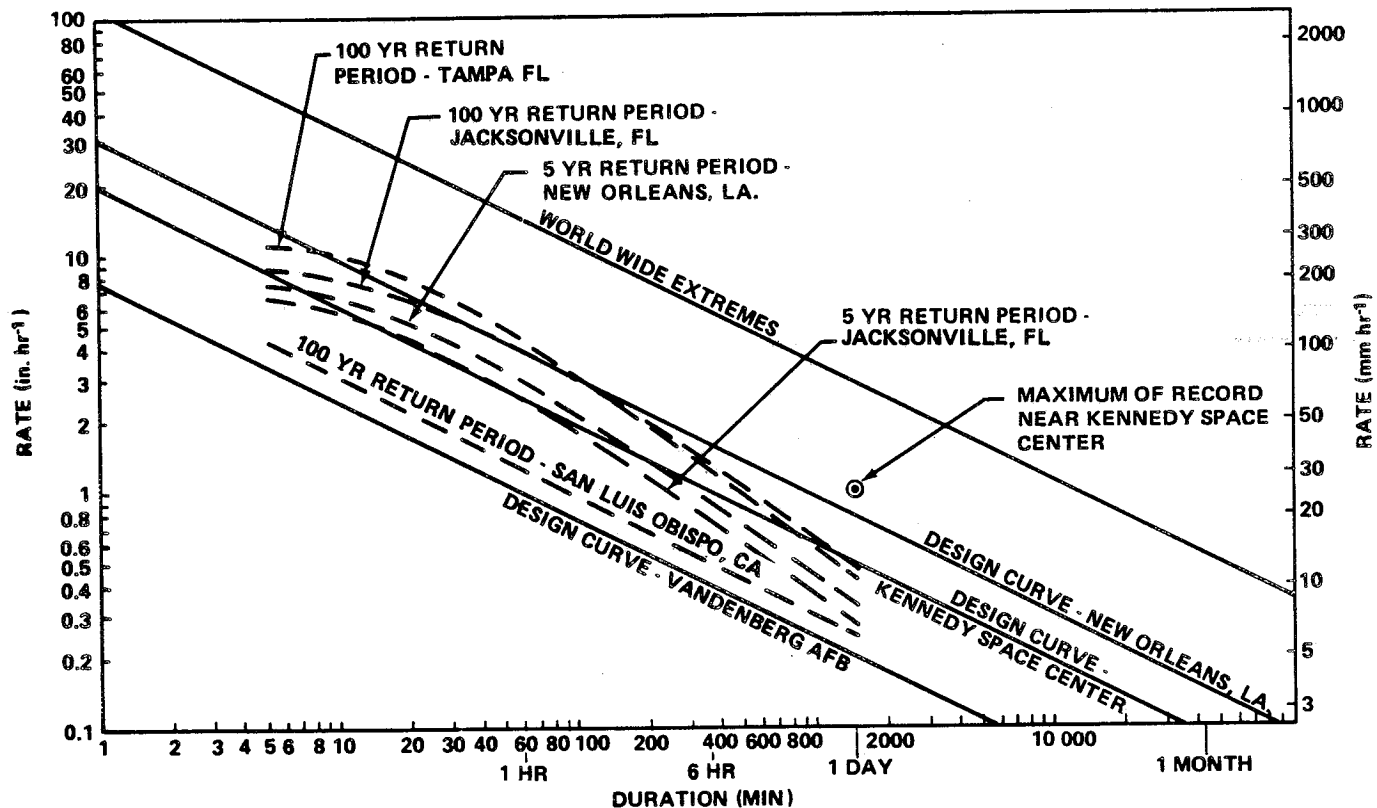


Figure 4.2 Design rainfall rates.

TABLE 4.1 RELATIONSHIP OF RETURN PERIODS  
TO PROBABILITIES

Return Period	Percentile	Return Period	Percentile
(yr)	(%)	(yr)	(%)
2	50	50	98
5	80	100	99
10	90	1000	99.9

$$r = \frac{C\sqrt{D_m}}{D_m} = \frac{C}{\sqrt{D_m}}$$

(4.2)

where

r = rate per hour

 $D_m$  = time in minutes

C = constant for location as given in Table 4.6.

TABLE 4.2 DESIGN RAINFALL, KENNEDY SPACE CENTER, FLORIDA:  
AND HUNTSVILLE, ALABAMA; BASED ON YEARLY LARGEST  
RATE FOR STATED DURATIONS

Time Period	Rainfall Rate		Rainfall Total Accumulation		Raindrop Size		Average Rate of Fall
					Average	Largest	
	mm hr <sup>-1</sup>	in. hr <sup>-1</sup>	mm	in.	mm	mm	m sec <sup>-1</sup>
1 min	492	19.4	8	0.3	2.0	6.0	6.5
5 min	220	8.7	18	0.7	2.0	5.8	6.5
15 min	127	5.0	32	1.25	2.0	5.7	6.5
1 hr	64	2.5	64	2.5	2.0	5.0	6.5
6 hr	26	1.0	156	6.1	1.8	5.0	6.5
12 hr	18	0.7	220	8.7	1.6	4.5	6.5
24 hr	13	0.5	311	12.2	1.5	4.5	6.5

TABLE 4.3 DESIGN RAINFALL, NEW ORLEANS, LOUISIANA; BASED ON  
YEARLY LARGEST RATE FOR STATED DURATIONS

Time Period	Rainfall Rate		Rainfall Total Accumulation		Raindrop Size		Average Rate of Fall
					Average	Largest	
	mm hr <sup>-1</sup>	in. hr <sup>-1</sup>	mm	in.	mm	mm	m sec <sup>-1</sup>
1 min	787	31.0	13	0.5	2.1	6.0	6.5
5 min	352	13.9	29	1.2	2.0	6.0	6.5
15 min	203	8.0	51	2.0	2.0	5.7	6.5
1 hr	102	4.0	102	4.0	2.0	5.5	6.5
6 hr	41	1.6	249	9.8	1.9	5.0	6.5
12 hr	29	1.2	352	13.9	1.8	5.0	6.5
24 hr	21	0.8	498	19.6	1.6	5.0	6.5

TABLE 4.4 DESIGN RAINFALL, VANDENBERG AFB, CALIFORNIA;  
EDWARDS AFB, CALIFORNIA; AND WHITE SANDS MISSILE RANGE, NEW MEXICO;  
BASED ON YEARLY LARGEST RATE FOR STATED DURATIONS

Time Period	Rainfall Rate		Rainfall Total Accumulation		Raindrop Size		Average Rate of Fall
					Average	Largest	
	mm hr <sup>-1</sup>	in. hr <sup>-1</sup>	mm	in.	mm	mm	m sec <sup>-1</sup>
1 min	197	7.7	3	0.1	2.0	5.6	6.5
5 min	88	3.5	7	0.3	2.0	5.3	6.5
15 min	51	2.0	13	0.5	2.0	5.0	6.5
1 hr	25	1.0	25	1.0	1.8	5.0	6.5
6 hr	10	0.4	62	2.4	1.5	4.6	6.0
12 hr	7	0.3	88	3.5	1.3	4.3	5.8
24 hr	5	0.2	124	4.9	1.3	4.0	5.5

TABLE 4.5 DESIGN RAINFALL, WORLDWIDE EXTREMES, BASED ON  
YEARLY LARGEST RATE FOR STATED DURATIONS

Time Period	Rainfall Rate		Rainfall Total Accumulation		Raindrop Size		Average Rate of Fall
					Average	Largest	
	mm hr <sup>-1</sup>	in. hr <sup>-1</sup>	mm	in.	mm	mm	m sec <sup>-1</sup>
1 min	2813	110.8	47	1.8	2.5	6.0	6.5
5 min	1258	49.5	105	4.1	2.2	6.0	6.5
15 min	726	28.6	182	7.1	2.1	6.0	6.5
1 hr	363	14.3	363	14.3	2.0	6.0	6.5
6 hr	148	5.8	890	35.3	2.0	5.8	6.5
12 hr	105	4.1	1258	49.5	2.0	5.5	6.5
24 hr	74	2.9	1779	70.1	2.0	5.2	6.5

TABLE 4.6 CONSTANTS TO USE WITH EQUATION (4.2)  
FOR RAINFALL RATES

	Kennedy Space Center, Huntsville	New Orleans	Vandenberg AFB, Edwards AFB, White Sands Missile Range	Worldwide Extremes
in. hr <sup>-1</sup> mm hr <sup>-1</sup>	19.365 491.87	30.984 786.99	7.746 196.75	110.767 2813.48
Values given in Table No.	2	3	4	5

#### 4.3.2 Raindrop Size

A knowledge of raindrop sizes is required to (1) simulate rainfall tests in the laboratory, (2) know the rate of fall of the raindrops and impact energy, and (3) use in erosion tests of materials.

At the surface, the size of the raindrops varies with the rate of rainfall per unit time; the heavier the rainfall, the larger the drops. Any one rainstorm will contain a variety of sizes of raindrops ranging from less than 0.5 mm (the lower limit of size measurement) to greater than 4.0 mm. The more intense the storm (the higher the rate of rainfall), the larger some of the drops will be. Reference 4.4 shows data on probability of occurrence of various raindrop sizes with relation to types of rain-producing storms: (1) thunderstorms, (2) rain showers, and (3) continuous rain. Thunderstorms have the greatest occurrence of the larger drops (over 2 mm). Rain showers have the next greatest occurrence, while the continuous rain produces the lowest occurrence of the larger drops. Rain drop sizes below 2 mm in diameter occur with near equal probability from all types of storms. In comparing drop sizes with various rainfall rates, the larger drops occurred with the highest probability from the highest rainfall rates. Raindrops over 6 mm in diameter are not expected to occur frequently because the rate of fall breaks these large drops into smaller ones.

#### 4.3.3 Statistics of Rainfall Occurrences

One set of statistical data on precipitation will not be satisfactory for all needs in design; therefore, several sets of statistical data are presented in this section as follows.

##### 4.3.3.1 Design Rainfall Rates

The design rainfall rates in Figure 4.2 and Tables 4.2, 4.3, 4.4, and 4.5 are based on precipitation occurrences; i.e., if precipitation is occurring, what is the probability of exceeding a rate? These data are based on occurrences over a year and would be used in design of items continuously exposed, such as launch facilities.

#### 4.3.3.2 Probability that Precipitation Will Not Exceed a Specific Amount in Any One Day

Values for each month with the probability that precipitation will not exceed a specified amount in any one day are given for several selected sites of aerospace vehicle design interest — Kennedy Space Center, FL; Edwards Air Force Base, and Vandenberg Air Force Base, CA, and New Orleans, LA — in Tables 4.7 through 4.10, respectively. The values in the tables should not be interpreted to mean that the amount of precipitation occurs uniformly over the 24-hour period, since it is more likely that most or all of the amounts occurred in a short period of the day.

#### 4.3.3.3 Rainfall Rates Versus Duration for 50th, 95th, and 99th Percentile, Given a Day with Rain for the Highest Rain Month, Kennedy Space Center, Florida

Rainfall rates for various durations for the 50th, 95th, and 99th percentile, given a day with rain in the highest rain month, are given in Table 4.11 for the Kennedy Space Center, Florida. The precipitation amounts should not be interpreted to mean that the rain fell uniformly for a brief period for the referenced time periods with no rain the remainder of the time period. As an example, the 99th percentile total of 49 mm (1.93 in.) (i.e., left column, 99th percentile, 1-hr duration as shown on Table 4.11) could have occurred as follows: 25 mm (0.98 in.) could have fallen during a 5-min period within a particular hour, with an additional 24 mm (0.95 in.) of rainfall for another 5-min period, making a total of 49 mm (1.93 in.) for a total of about 10 min. Subsequently, no rain would have fallen for 50 min of the hypothetical 1-hr period. The 99th percentile rainfall data are referenced in that such extremes are important to consider in vehicle and facility design studies. Table 4.2 has rainfall rates listed as well as total accumulation, raindrop size, etc., for various periods for Kennedy Space Center and Huntsville, which are also valuable data to use as vehicle criteria.

#### 4.3.4 Distribution of Rainfall Rates with Altitude

Rainfall rates normally decrease with altitude when rain is striking the ground. The rainfall rates at various altitudes in percent of the surface rates are given in Table 4.12 for all areas (Ref. 4.5).

Precipitation above the ground is generally colder than at the ground and frequently occurs as super-cooled drops which may cause icing on objects moving through the drops. Such icing can be expected to occur when the air temperature is about  $-2.2^{\circ}\text{C}$  ( $28^{\circ}\text{F}$ ). The major factors that influence the rate of ice formation are (1) the amount of liquid water, (2) the droplet size, (3) air speed, and (4) the size and shape of the airfoil (Ref. 4.6).

#### 4.3.5 Types of Ice Formation

The type of ice which will form on the outside exposed surfaces of cryogenic tanks is related to the temperature of the tank surface, the precipitation rate, drop size, and wind velocity (or tank velocity). In general, the larger the drop size and the higher the temperature, precipitation rate, and wind speed, the denser the ice will form until a condition is reached where surface temperatures are too high for ice formation. If the precipitation is at too high a temperature at relatively high precipitation rates and wind speed, it may warm the tank sufficiently to melt ice which formed previously.

Table 4.13 summarizes ice types for various tank wall temperatures with moderate precipitation (over  $10 \text{ mm hr}^{-1}$ ).



TABLE 4.7 PROBABILITY THAT PRECIPITATION WILL NOT EXCEED A SPECIFIC AMOUNT IN ANY ONE DAY, KENNEDY SPACE CENTER, FLORIDA

Amount		Jan	Feb	March	Apr	May	June
(in.)	(mm)	%	%	%	%	%	%
0.00	0.00	68.1	60.8	62.2	70.6	64.2	54.7
Trace	Trace	77.1	71.4	71.3	80.0	76.2	65.7
0.01	0.25	79.0	74.3	72.5	82.7	79.4	68.4
0.05	1.27	84.8	79.4	77.5	86.6	84.7	74.1
0.10	2.54	87.1	82.3	81.6	89.3	89.4	75.8
0.25	6.35	90.0	85.8	87.8	93.5	92.9	82.8
0.50	12.70	93.9	91.6	91.6	95.9	96.4	90.8
1.00	25.40	97.1	96.1	96.3	98.0	99.3	97.1
2.50	63.50	99.4	100.0	99.5	99.5	100.0	99.8
5.00	127.00	100.0	100.0	99.8	99.8	100.0	100.0
Amount		July	Aug	Sept	Oct	Nov	Dec
(in.)	(mm)	%	%	%	%	%	%
0.00	0.00	56.8	52.6	40.0	47.4	62.1	64.2
Trace	Trace	65.8	63.9	53.9	61.6	74.2	78.1
0.01	0.25	68.4	66.2	57.5	63.9	77.2	81.0
0.05	1.27	73.2	69.4	62.7	72.0	83.9	86.8
0.10	2.54	75.8	74.9	67.9	76.8	86.9	89.4
0.25	6.35	83.5	80.7	75.8	85.5	90.8	93.3
0.50	12.70	88.3	88.4	83.7	91.3	92.6	96.5
1.00	25.40	93.8	93.6	92.2	95.5	96.2	99.1
2.50	63.50	99.6	99.7	97.4	99.4	99.2	100.0
5.00	127.00	99.6	100.0	99.8	99.7	99.5	100.0

The 100% values in the table indicate no chance of exceeding certain amounts of precipitation during most of the months, however, it should be realized that the length of available data records is not long and that there is always a chance of any meteorological extreme of record being exceeded.

TABLE 4.8 PROBABILITY THAT PRECIPITATION WILL NOT EXCEED A SPECIFIC AMOUNT IN ANY ONE DAY, EDWARDS AFB, CALIFORNIA

Amount		Jan	Feb	March	Apr	May	June
(in.)	(mm)	%	%	%	%	%	%
0.00	0.00	81.7	81.8	82.6	86.7	95.1	98.8
Trace	Trace	88.0	88.9	89.6	93.8	98.6	99.5
0.01	0.25	88.9	89.5	91.3	94.8	99.0	99.5
0.05	1.27	91.7	92.1	93.8	96.4	99.1	99.5
0.10	2.54	93.5	93.5	95.5	97.6	99.4	99.5
0.25	6.35	96.9	95.6	98.0	99.0	100.0	99.9
0.50	12.70	98.8	98.3	99.1	99.6	100.0	100.0
1.00	25.40	99.8	99.6	99.8	100.0	100.0	100.0
2.50	63.50	100.0	100.0	99.9	100.0	100.0	100.0
5.00	127.00	100.0	100.0	100.0	100.0	100.0	100.0
Amount		July	Aug	Sept	Oct	Nov	Dec
(in.)	(mm)	%	%	%	%	%	%
0.00	0.00	94.7	95.2	94.6	93.0	89.8	85.2
Trace	Trace	99.0	98.1	97.8	95.8	94.2	90.8
0.01	0.25	99.3	98.1	98.2	96.1	94.4	91.4
0.05	1.27	99.7	98.9	98.9	97.2	96.4	93.7
0.10	2.54	99.7	99.3	98.9	98.2	97.0	94.9
0.25	6.35	100.0	99.6	99.2	99.2	98.4	96.7
0.50	12.70	100.0	99.9	99.8	99.6	99.3	99.0
1.00	25.40	100.0	100.0	99.9	99.7	100.0	99.9
2.50	63.50	100.0	100.0	100.0	100.0	100.0	100.0
5.00	127.00	100.0	100.0	100.0	100.0	100.0	100.0

The 100% values in the table indicate no chance of exceeding certain amounts of precipitation during most of the months, however, it should be realized that the length of available data records is not long and that there is always a chance of any meteorological extreme of record being exceeded.

TABLE 4.9 PROBABILITY THAT PRECIPITATION WILL NOT EXCEED A SPECIFIC AMOUNT IN ANY ONE DAY, VANDENBERG AFB, CALIFORNIA

Amount		Jan	Feb	March	Apr	May	June
(in.)	(mm)	%	%	%	%	%	%
0.00	0.00	69.4	70.4	61.7	70.4	71.8	70.0
Trace	Trace	79.1	75.9	72.2	80.4	94.0	94.8
0.01	0.25	81.1	76.9	74.6	82.5	96.8	97.7
0.05	1.27	83.5	81.4	83.9	87.9	98.0	100.0
0.10	2.54	88.3	84.4	85.9	90.8	98.8	100.0
0.25	6.35	91.5	90.4	91.5	95.4	99.6	100.0
0.50	12.70	95.1	94.4	96.3	97.5	100.0	100.0
1.00	25.40	98.3	96.9	98.7	99.2	100.0	100.0
2.50	63.50	99.9	99.9	99.5	100.0	100.0	100.0
5.00	127.00	100.0	100.0	99.9	100.0	100.0	100.0
Amount		July	Aug	Sept	Oct	Nov	Dec
(in.)	(mm)	%	%	%	%	%	%
0.00	0.00	62.4	63.4	77.9	79.4	73.3	73.8
Trace	Trace	98.2	94.9	95.4	95.1	82.6	80.6
0.01	0.25	98.9	98.1	95.8	95.5	83.3	83.1
0.05	1.27	100.0	98.8	97.5	95.9	85.9	87.4
0.10	2.54	100.0	99.5	97.9	96.7	87.4	89.2
0.25	6.35	100.0	99.9	98.7	97.5	90.0	93.5
0.50	12.70	100.0	100.0	99.9	98.7	94.4	97.1
1.00	25.40	100.0	100.0	100.0	99.5	98.8	99.6
2.50	63.50	100.0	100.0	100.0	99.9	99.9	100.0
5.00	127.00	100.0	100.0	100.0	100.0	100.0	100.0

The 100% values in the table indicate no chance of exceeding certain amounts of precipitation during most of the months, however, it should be realized that the length of available data records is not long and that there is always a change of any meteorological extreme of record being exceeded.

TABLE 4.10 PROBABILITY THAT PRECIPITATION WILL NOT EXCEED A SPECIFIC AMOUNT IN ANY ONE DAY, NEW ORLEANS, LOUISIANA

Amount		Jan	Feb	March	Apr	May	June
(in. )	(mm)	%	%	%	%	%	%
0.00	0.00	77.1	70.2	73.6	79.7	75.9	72.2
0.01	0.25	77.7	71.1	74.1	79.9	76.4	72.6
0.05	1.27	80.9	74.5	78.1	81.9	78.0	77.7
0.10	2.54	85.7	76.4	81.0	83.6	82.9	82.3
0.20	5.08	89.1	80.4	82.8	87.0	86.5	85.3
0.50	12.70	94.0	88.8	88.6	91.2	92.2	90.3
1.00	25.40	97.4	93.8	92.9	95.3	95.6	93.8
2.00	50.8	98.9	97.8	97.9	97.8	99.0	98.8
5.00	127.00	99.7	99.7	99.7	100.0	100.0	100.0
10.00	254.00	100.0	100.0	100.0	100.0	100.0	100.0
Amount		July	Aug	Sept	Oct	Nov	Dec
(in. )	(mm)	%	%	%	%	%	%
0.00	0.00	54.5	70.1	69.2	84.4	83.4	77.6
0.01	0.25	55.8	71.3	71.1	85.6	84.7	78.2
0.05	1.27	61.4	74.4	76.3	88.2	85.7	80.7
0.10	2.54	67.4	79.3	79.2	90.5	87.4	83.2
0.20	5.08	73.3	83.5	84.4	93.4	89.4	85.2
0.50	12.70	81.5	92.4	90.3	96.0	94.0	91.9
1.00	25.40	91.5	95.7	94.5	98.0	97.3	95.2
2.00	50.80	96.7	98.2	98.0	99.7	98.3	99.4
5.00	127.00	100.0	100.0	99.0	100.0	99.7	99.7
10.00	254.00	100.0	100.0	100.0	100.0	100.0	100.0

The 100% values in the table indicate no chance of exceeding certain amounts of precipitation during most of the months, however, it should be realized that the length of available data records is not long and that there is always a chance of any meteorological extreme of record being exceeded.

TABLE 4.11 HIGHEST RAINFALL RATE VERSUS DURATION FOR VARIOUS PROBABILITIES, GIVEN A DAY WITH RAIN FOR THE HIGHEST RAIN MONTH, KENNEDY SPACE CENTER, FLORIDA

Duration	PERCENTILE											
	50				95				99			
	(in.)	(mm)	in. hr <sup>-1</sup>	mm hr <sup>-1</sup>	(in.)	(mm)	in. hr <sup>-1</sup>	mm hr <sup>-1</sup>	(in.)	(mm)	in. hr <sup>-1</sup>	mm hr <sup>-1</sup>
5 min	0.22	5.6	2.6	66.0	0.72	18.0	8.7	221.0	1.00	25.0	12.0	305.0
15 min	0.23	5.8	0.93	24.0	0.88	22.0	3.5	89.0	1.30	33.0	5.2	132.0
1 hr	0.25	6.4	0.25	6.4	1.17	30.0	1.17	30.0	1.93	49.0	1.93	49.0
6 hr	0.28	7.1	0.05	1.3	1.55	39.0	0.26	6.6	3.18	81.0	0.53	13.0
24 hr	0.43	10.9	0.02	0.5	2.62	67.0	0.11	2.8	5.00	127.0	0.21	5.3

TABLE 4.12 DISTRIBUTION OF RAINFALL RATES WITH HEIGHT FOR ALL LOCATIONS (Ref. 4.5)

Height (Geometric) Above Surface (km)	% Surface Rate
SFC	100
1	90
2	75
3	57
4	34
5	15
6	7
7	2
8	1
9	0.1
10 and over	< 0.1

#### 4.3.6 Hydrometeor Characteristics with Altitude

Raindrops falling on the surface may originate at a higher altitude as some other form of hydrometeor, such as ice or snow. The liquid water content of these hydrometeors per unit volume would have a distribution similar to that given in Table 4.14 for rainfall. A summary of the hydrometeor characteristics from Reference 4.7 is given in Table 4.14

TABLE 4.13 ICE TYPES AS A FUNCTION OF TANK WALL TEMPERATURES

Temperature of Tank Wall		Type of Ice	Density Range		Remarks
° F	° C		lb ft <sup>-3</sup>	g cm <sup>-3</sup>	
23 to 32	-5 to 0	Clear ice	60	0.69	hard dense ice
15 to 23	-9 to -5	milky ice or clear ice with air bubbles	43-53	0.69-0.85	
below 15	below -9	Rime ice	18-25	0.29-0.40	crumbly

#### 4.4 Snow

The accumulation of snow on a surface produces stress. For a flat horizontal surface, the stress is proportional to the weight of the snow directly above the surface. For long narrow objects, such as pipes or wires lying horizontally above a flat surface (which can accumulate the snow), the stress can be figured as approximately equal to the weight of the wedge of snow with the sharp edge along the object and extending above the object in both directions at approximately 45 degrees to the vertical. (In such cases, the snow load would be computed for the weight of the snow wedge above the object and not the total snow depth on the ground). The weight of new-fallen snow on a surface varies between 0.5 kg m<sup>-2</sup> per cm of depth (0.25 lb ft<sup>-2</sup> in.<sup>-1</sup>) and 2.0 kg m<sup>-2</sup> per cm of depth (1.04 lb ft<sup>-2</sup> in.<sup>-1</sup>), depending on the atmospheric conditions at the time of the snowfall.

##### 4.4.1 Snow Loads at Surface

Maximum snow loads for the following areas are:

- a. Huntsville and Edwards Air Force Base. For horizontal surfaces a snow load of 25 kg m<sup>-2</sup> (5.1 lb ft<sup>-2</sup>) per 24-hour period (equivalent to a 10-in. snowfall) to a maximum of 50 kg m<sup>-2</sup> (10.2 lb ft<sup>-2</sup>) in a 72-hr period, provided none of the snow is removed from the surface during that time, should be considered for design purposes.
- b. Vandenberg Air Force Base and White Sands Missile Range. For horizontal surfaces, a maximum snow load of 10 kg m<sup>-2</sup> (2.0 lb ft<sup>-2</sup>) per one 24-hr period should be considered for design purposes.
- c. Kennedy Space Center and New Orleans area snow loads need not be considered.

TABLE 4.14 SUMMARY OF HYDROMETEOR CHARACTERISTICS [4.7]

Type of Hydrometeor	Altitude (km)	Drop Diameter ( $\mu\text{m}$ )		Concentration per Unit Volume ( $\text{cm}^3$ )		Liquid Water Content Per Unit Volume ( $\text{g m}^{-3}$ )		Ambient Temperature ( $^{\circ}\text{C}$ )
	Range	Range	Rep.	Range	Rep.	Range	Rep.	Range $\approx$
Layer Clouds	sfc-1.5	<1-40	11	<10-10 000	500	<0.1-1	0.2	+30 to -15
Layer Clouds	2.5-7.5	<1-50	12	<20-1000	100	<0.1-1	0.2	+20 to -25
Layer Clouds (ice crystals)	7.5-15.0	<10-10 000	100	<0.1-10	0.2	<0.01-0.1	0.02	-10 to -55
Convective Clouds								
Fair Weather								
Cumulus	0.5-8.0	<1-75	12	<10-10 000	300	<0.1-1	0.5	+20 to -30
Cumulus Congestus	0.5-13.0	<1-200	25	<10-10 000	150	<1-10	4.0	+20 to -55
Continuous Type Rain	sfc-6.0	<500-3000	1000	<50-3000*	500*	<0.05-0.7	0.1	+30 to -15
Shower Type Rain	sfc-13.0	<500-7000	2000	<10-3000*	500*	<0.1-30	1.0	+30 to -55
Coalescence (Warm) Rain	sfc-5.0	<100-1000	500	<500-50 000*	3000*	<0.05-0.1	0.1	+30 to 0
Hail	sfc-13.0	<0.01-13cm	0.8cm	<0.5-1000*	50*	<0.1-0.9**	0.8**	+30 to -55
Ice and Snow Crystals	sfc-13.0	<100-20 000	5000	<1-1000*	100*	<0.001-0.7***	0.07***	+5 to -55

1. Rep.: Representative value or value most frequently encountered

\* Per  $\text{m}^3$ \*\* Density of particles ( $\text{g cm}^{-3}$ )

\*\*\* Mass of crystals (mg)

#### 4.4.2 Snow Particle Size

Snow particles may penetrate openings (often openings of minute size) in equipment and cause a malfunction of mechanical or electrical components, either before or after melting. Particle size, associated wind speed, and air temperature to be considered are as follows:

- a. Huntsville and Edwards Air Force Base. Snow particles 0.1-mm (0.0039-in.) to 5-mm (0.20-in.) diameter; wind speed  $10 \text{ m sec}^{-1}$  (19 knots); air temperature  $-17.8^{\circ}\text{C}$  ( $0^{\circ}\text{F}$ ).
- b. Vandenberg Air Force Base and White Sands Missile Range. Snow particles 0.5-mm (0.020-in.) to 5-mm (0.20-in.) diameter; wind speed  $10 \text{ m sec}^{-1}$  (19 knots); air temperature  $-5.0^{\circ}\text{C}$  ( $24^{\circ}\text{F}$ ).

#### 4.5 Hail<sup>1</sup>

Hail is precipitation in the form of balls or irregular lumps of ice and is always produced by convective clouds. By definition, hail has a diameter of 5 mm (0.2 in.) or more. Hail falls are small-scale areal phenomena, with a relatively infrequent occurrence rate at any given geographical point. The resulting time and space variability of hail is its prime characteristic.

There are two areas of confusion regarding hail: (1) definition of it and (2) assessment of damage due to hail. First is the question of whether snow or ice pellets (often called "small hail") are hailstones. Sleet has also been confused with small hail, but convective cloud origin and size of stone are two factors which separate hail from any other form of frozen hydrometeors. The second area of confusion associated with hail concerns delineating crop loss due to hail. This type of loss often includes damage by wind, either that with the hail or that before or after the hail. The wind-induced damage can easily be mistaken as damage due to hail.

While North American hail data and information are generally sparse, there is much more information available than for any other location. In North America, very extensive hail data information are available for Alberta, Canada, and Illinois and Colorado in the United States. Hail phenomena studies have generally centered on hailstones, point hailfalls, hailstreaks, hailstorms, hailswaths, and hail days over areas of various sizes.

The principle hail area on the North American continent is located on the lee side of the Rocky Mountains where frequent and intense hail causes great damage over the Great Plains region. Another high-frequency hail area, related to spring storms, extends from Michigan to Texas. However, less crop damage is observed here because hail activity largely precedes the crop season.

The worldwide hail occurrence pattern is characterized by a greater hail frequency in continental interiors of mid-latitudes, with decreasing frequencies seaward, poleward, and equatorward. Most all hail is either orographically or frontally induced, although the Great Lakes affect the frequency close to that region. There are very few local-type hailstorms away from the mountains. The United States hail-days pattern is shown in Figure 4.3.

Four key hail characteristics (average frequency, primary cause of hail, peak hail season, and hail intensity) were analyzed in order to delineate hail regions within the United States. Figure 4.4 indicates that 14 hail regions exist across the United States, with a marine-effect influence on the West Coast and in the lee of the Great Lakes.

1. Paragraph 4.5 contains figures and information from Reference 4.8.



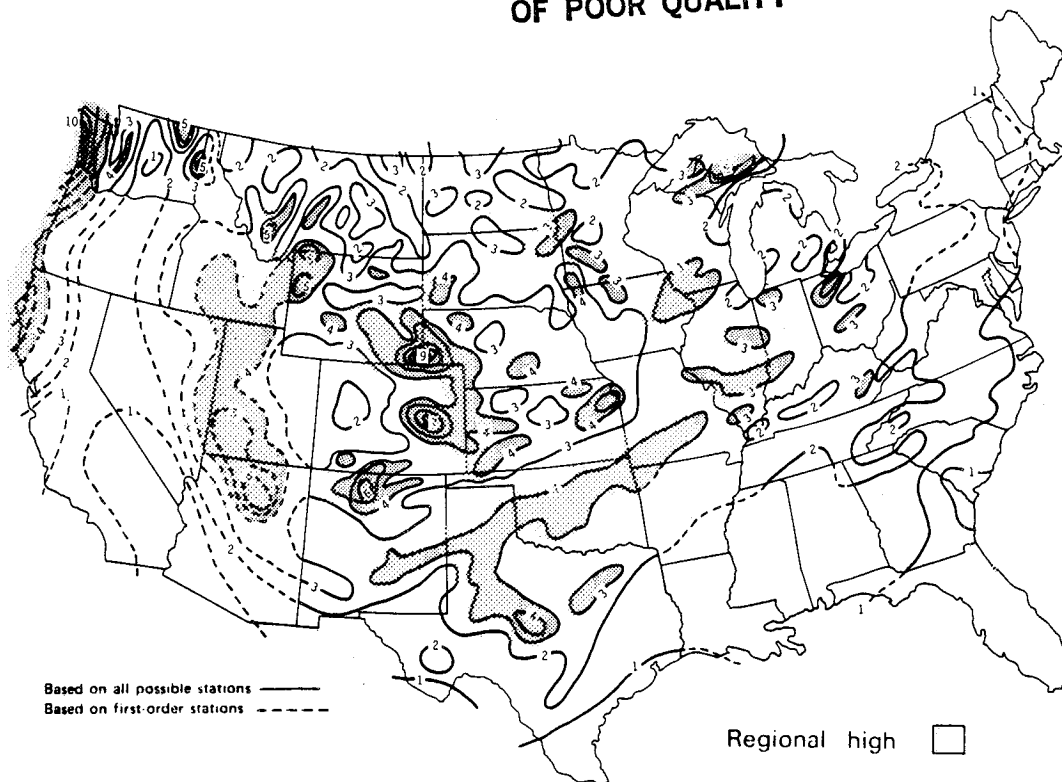


Figure 4.3 Average number of hail days based on point frequencies.

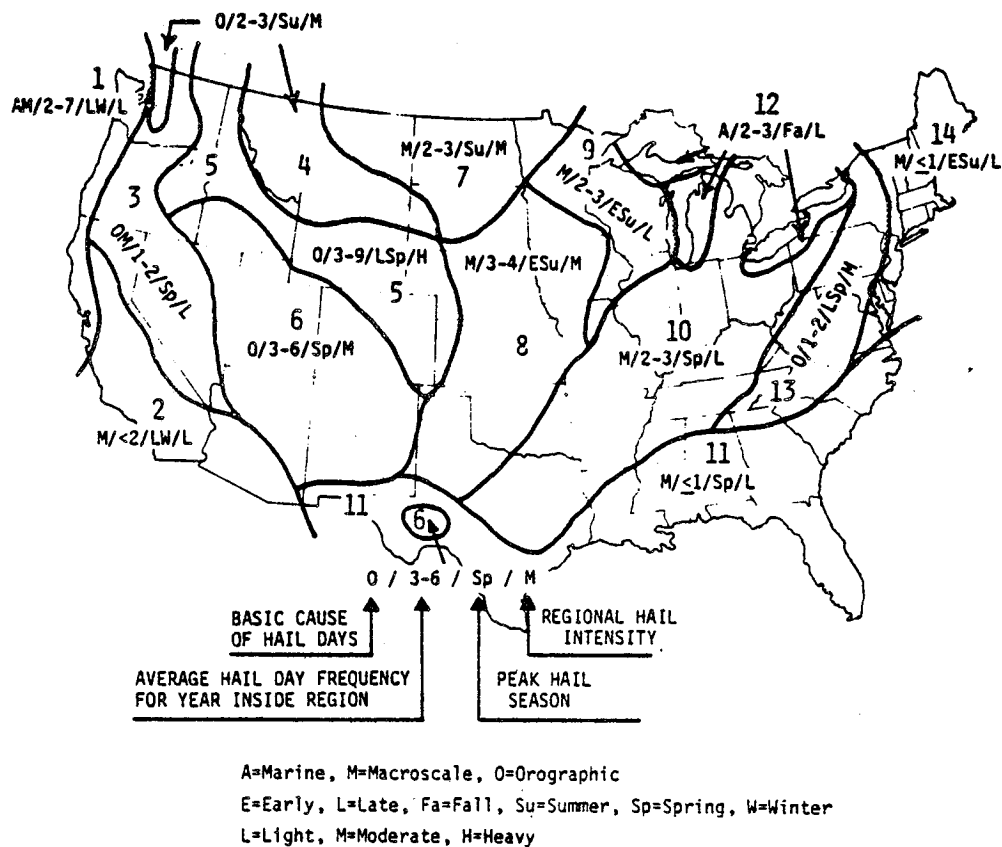


Figure 4.4 Hail regions of the United States.

Although most all hail is produced by thunderstorms, the special climatologies of these two phenomena differ in some respects. The main difference is that thunderstorms generally exhibit a latitudinal distribution across North America, whereas hail has an inner-continental maxima with frequency decreasing outward in all directions, as mentioned previously.

The "intensity" of hail produces the damage. Intensity is a direct function of the number of stones, their size, and the wind. A hail intensity pattern has been developed specifically for potential property loss. The development of this pattern incorporated insurance data, stone size data, and extreme wind frequency data. The hail intensity pattern is shown in Figure 4.5, which indicates a north-south oriented maximum located in the Great Plains region. This is the region of the continental United States in which large hailstones (the major factor in property loss) are most frequent and high winds occur most often.

Since hailstone sizes as well as the number of stones are important to intensity, size distributions help account for regional differences. Hailstone sizes have not been systematically measured throughout the United States, but small-area studies have provided some information. Figure 4.6 indicates that the greatest frequency of large stones is found in the lee of mountain localities like Colorado. Small hailstones dominate in Illinois, New England, and mountain-top areas of Arizona. An Illinois hailfall averages 24 stones per hailpad (1 ft<sup>2</sup> or 930 cm<sup>2</sup>), and only approximately 2 percent of these are more than 1.3 cm in diameter. In northeast Colorado, a hailfall averages 202 stones/ft<sup>2</sup>, and more than half (51 percent) of these are larger than 1.3 cm.

The season of high hail activity varies across the country. East of the Great Plains, maximum hail activity occurs in the spring months, starting in March in the far south and in May in the northern states. In the lee-of-the-mountain states, maximum hail activity occurs in the summer months. The Great Lakes area is the only place in North America where maximum hail occurs in fall months. Along the West Coast, certain areas have maximum hail in late winter or spring.

The duration of hailstorms is also variable. The average duration of hail near the mountains is 10 to 15 min, while in the Midwest it is 3 to 6 min. Hailstreaks, which have a median size of 20.7 km<sup>2</sup> (8 square miles), last an average of 10 min. A hailstreak is an area hit by a single volume of hail produced in a storm. A single storm may produce one or many hailstreaks.

In large areas, such as Iowa, Illinois, or Colorado, hail occurs on approximately 70 percent of all days with thunderstorms. In the Midwest, 50 percent of all thunderstorms connected with warm fronts and low pressure centers produce hail, but 75 percent of the thunderstorm days associated with cold fronts or stationary fronts are hail days.

Hail may also be accompanied by moderate to heavy rainfall, tornadoes, or wind. Crop-damaging hailstorms in Nebraska, Colorado, and Kansas are generally associated with moderate rains of 0.2 to 1.0 in., and 25 percent of the rain through the entire crop season falls with damaging hail. Hail days in Illinois typically have rainfall so heavy it averages nearly half (48 percent) of the monthly average. There have been cases where hailstones, falling at the same time or immediately before heavy rains, have blocked drains and downspouts, preventing much of the rain runoff from flat roofs and thereby causing roof collapse from the weight of the rainfall (Ref. 4.9).

A study of tornadoes in Illinois shows that major large tornadoes — those having tracks longer than 40 km (>25 miles) — always have hailfalls somewhere near their track. During 1951-1960, nearly 96 percent of the 103 tornado days in Illinois were also hail days, and 12 percent of all hail days in Illinois were tornado days as well.

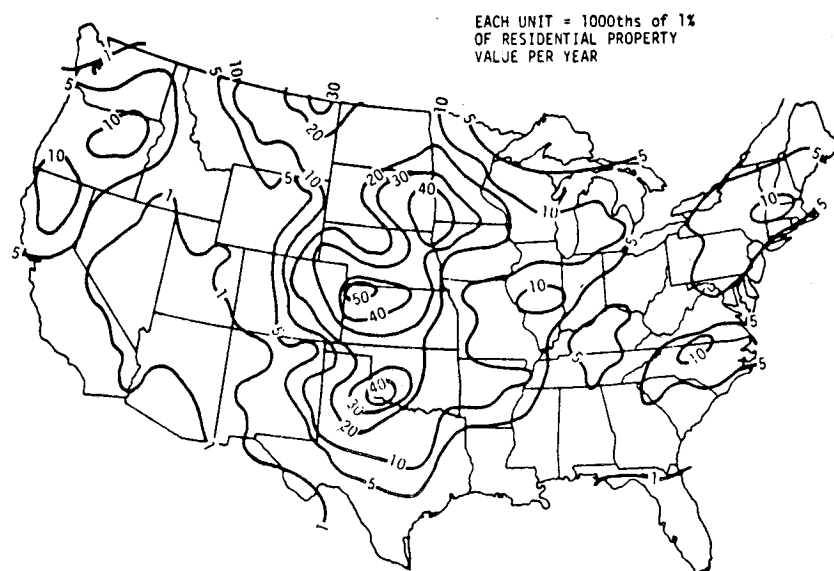


Figure 4.5 Index of potential hail damage to property.

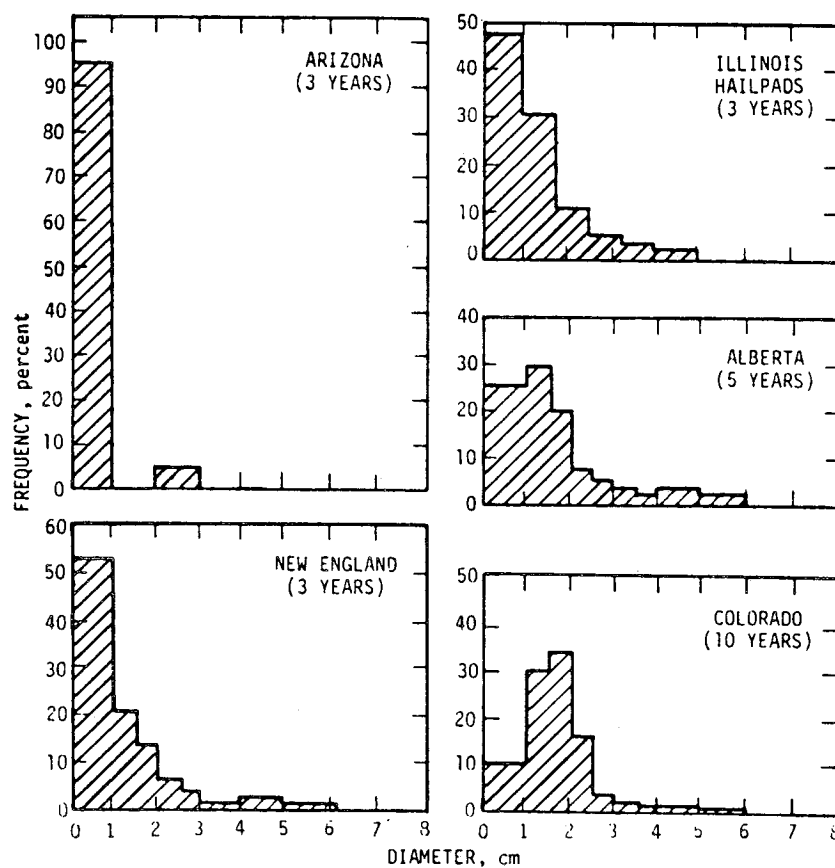


Figure 4.6 Frequency distributions of maximum hailstone sizes reported from many hailfalls at different locales.

Wind with hail is another critical factor in crop loss, and the Illinois studies show that windblown stones occurred in 60 percent of all hailfalls. Whenever this happens, an average of 66 percent of the stones at any one point are windblown.

#### 4.5.1 Hail at Surface

An estimate has been made of hail characteristics at selected space vehicle development and test locations. Figures 4.7, 4.8, 4.9, and Table 4.15 give estimated hail characteristics for KSC, VAFB, EAFB, White Sands, Northrup Strip, MSFC, and NSTL. Since no direct measurements, except for the number of hail days, exist for these locations, all other items were estimated from Illinois hailpad measurements reported by Changnon [4.8]. Hail characteristics estimated for use in evaluating hail protection needs and requirements are:

a. Hailstone Size. Figure 4.7 gives the risk in percent of a point hailfall producing stones larger than indicated sizes. For example, only 3 percent of the hailfalls at KSC will produce stones larger than 2.5 cm, while 50 percent will produce some stones larger than 0.9 cm.

b. Terminal Velocity. The best estimate of hailstone terminal velocity, as reported by several investigators, is given by the expression:

$$W = K \sqrt{D}$$

where

$W$  = terminal velocity in  $\text{ms}^{-1}$

$D$  = hailstone diameter in cm

$K = 11.5$

c. Number of Hailstones Per Hailfall. Values used for space vehicle locations were taken from Illinois measurements which showed that point hailfalls averaged 24 stones and that only 5 percent of the storms produced more than 300 stones per hailpad of  $930 \text{ cm}^2$  ( $1 \text{ ft}^2$ ). These numbers were used to prepare Figure 4.8.

d. Horizontal Velocity of Hailstones. These values (Fig. 4.9) were derived from peak wind speed distributions for each space vehicle location. These wind speeds may be different from other Shuttle design values because only hail season winds were used rather than the windiest period concept.

The reference height at KSC and VAFB is 61 m (200 ft). At all other locations it is 18.3 m (60 ft).

e. Density of Hailstones. A generally accepted value for the density of hail at all locations is  $0.89 \text{ g cm}^{-3}$  ( $56 \text{ lbs ft}^{-3}$ ).

f. Recommended Procedures for Evaluating Protection Requirements.

- (1) Use 50 percent values for stone size and number of stones.
- (2) Use 5 percent risk horizontal wind speeds.

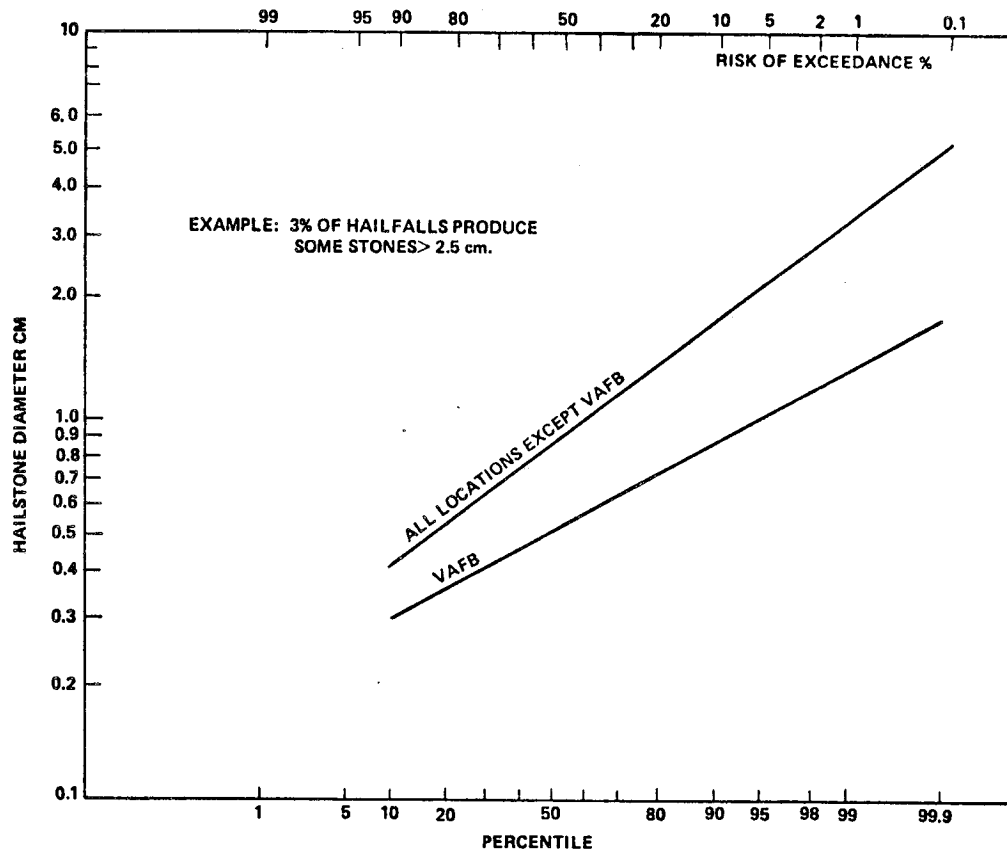


Figure 4.7 Maximum hailstone size per point hailfall.

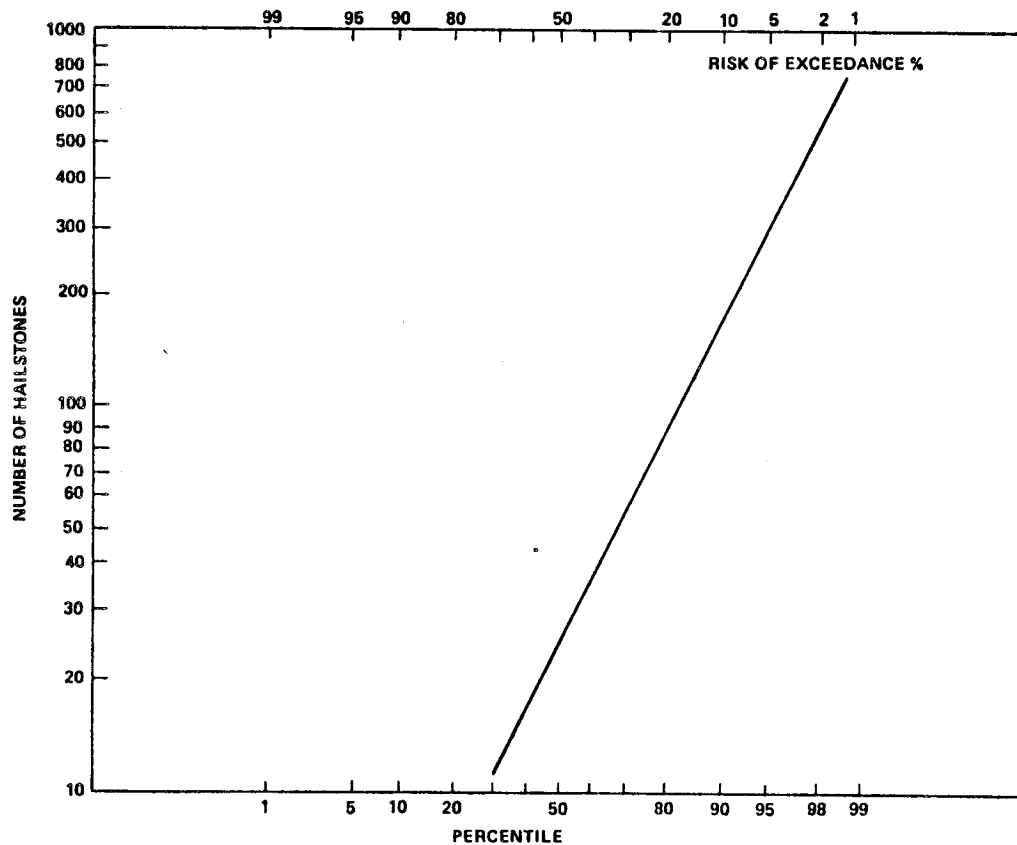


Figure 4.8 Probability (%) of number of stones per hailfall on hailpad of 930 cm² (1 ft²).

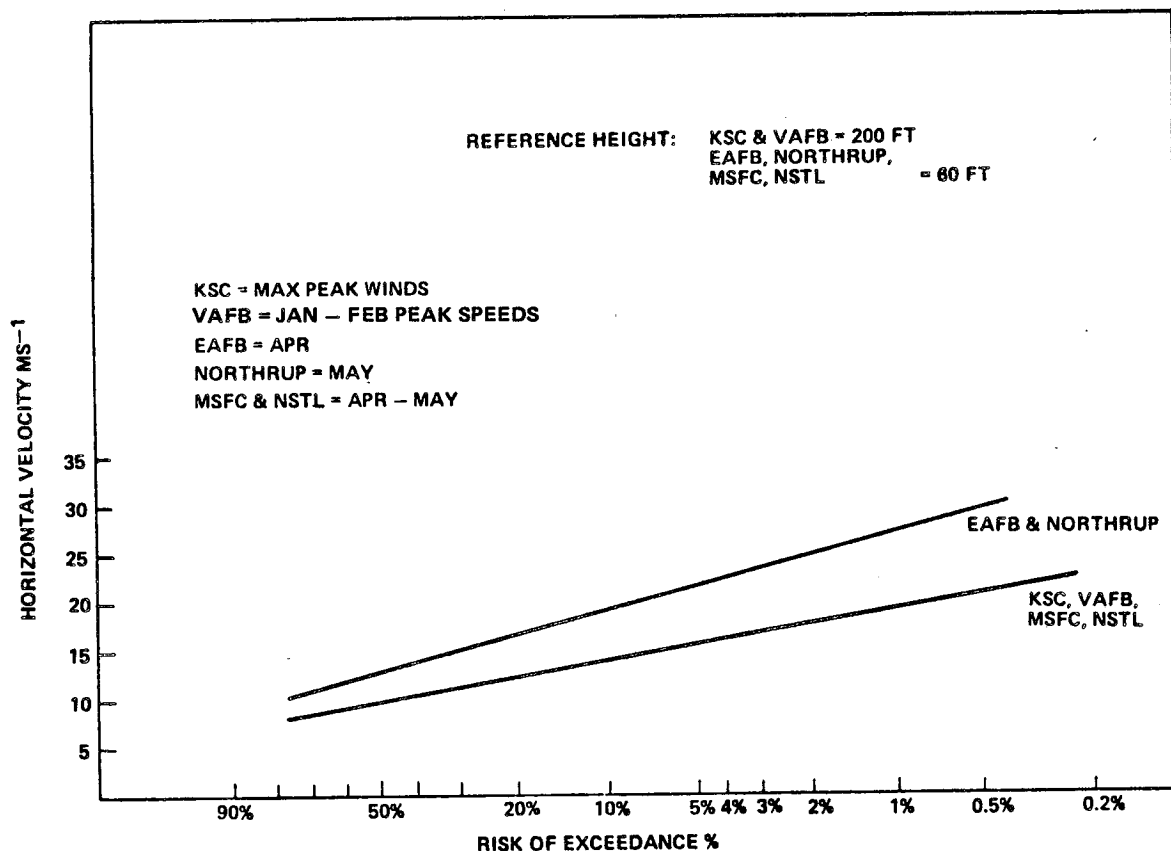


Figure 4.9 Horizontal hailstone velocity.

TABLE 4.15 ESTIMATED HAIL CHARACTERISTICS AT SELECTED SPACE VEHICLE LOCATIONS

ESTIMATED HAIL CHARACTERISTICS	KSC	VAFB	EAFB	NORTHROP	MSFC	NSTL
EXPOSURE TIME RISK (%) - WORST MONTH	1	8	5	12	17	3
- WORST 6 MONTHS	7	41	25	53	67	18
MEAN NO. OF HAILSTORM DAYS PER YEAR	0.1	1.1	0.6	1.5	2.2	0.4
AVERAGE POINT DURATION OF HAILFALL (MIN.)	5	5	5	5	5	5
AVERAGE NO. OF HAILSTONES PER 930 CM <sup>2</sup> (1 FT <sup>2</sup> )	24	24	24	24	24	24
DENSITY OF HAILSTONES (G/CM <sup>3</sup> )	0.9	0.9	0.9	0.9	0.9	0.9
SIZE-DIAMETER (CM) & TERMINAL VELOCITY (M/S)						
REPRESENTATIVE SIZE (50% RISK)	0.9	0.5	0.9	0.9	0.9	0.9
TERMINAL VELOCITY	11	8	11	11	11	11
LARGE SIZE (5% RISK)	2.2	1.0	2.2	2.2	2.2	2.2
TERMINAL VELOCITY	17	11.5	17	17	17	17
HORIZONTAL VELOCITY (M/S) - ALL DIRECTIONS <sup>1</sup>						
MEAN SPEED	9	9	13	13	9	9
5% RISK SPEED	15	15	22	22	15	15
MONTHS OF MAX FREQUENCY	MAY	JAN-FEB	FEB-APR	MAY-JUL	APRIL	APR-MAY
PERIOD OF RECORD - YEARS	22	20	28	30	9	28

<sup>1</sup>KSC and VAFB reference height = 61 m (200 ft). All others = 18 m (60 ft).

- (3) Calculate risk of experiencing a hailfall during a specified continuous exposure period from:

$$\text{Risk} = 1 - e^{-\lambda t}$$

where  $\lambda$  = mean number of independent hailstorm days per year

$t$  = exposure time in years

#### 4.5.2 Distribution of Hail with Altitude

Although it is not the current practice to design space vehicles for flight in thunderstorms, data on distribution with altitude are presented as an item of importance. The probability of hail increases with altitude from the surface to 5 km and then decreases rapidly with increasing height. Data on Florida thunderstorms, giving the number of times hail was encountered at various altitudes during aircraft flights (Ref. 4.10), are given in Table 4.16 for areas specified in Paragraph 4.5.1. It should be noted that the results presented in Table 4.16 are based on a very limited amount of available data.

TABLE 4.16 DISTRIBUTION OF HAIL WITH HEIGHT  
FOR ALL LOCATIONS [4.10]

Height (Geometric) Above Surface (km)	Occurrence of Hail % of Flights Through Thunderstorms
2	0
3	3.5
5	10
6	4
8	3

#### 4.6 Laboratory Test Simulation

In the laboratory, simulated rain droplets are usually produced by use of a single orifice, mounted above the equipment being tested. Such a test will not necessarily duplicate the natural occurrence of precipitation and may or may not reflect the true effect of natural precipitation on the equipment since a single orifice produces drops all nearly the same size.

Each test should be evaluated to determine if the following factors which occur in natural precipitation are important in the test.

##### 4.6.1 Rate of Fall of Raindroplets

Natural raindroplets will have usually fallen a sufficient distance to reach their terminal velocity (maximum rates of fall). Simulation of such rates of fall in the laboratory requires the droplets to fall a suitable distance. Large droplets (4-mm diameter and greater) will require approximately 12 m (39 ft) to reach terminal velocity.

Values of terminal velocities of water droplets were measured by Gunn and Kinzer (Ref. 4.11). Their results gave the values in Table 4.17. Reference 4.11 should be consulted for more detailed information.

Gunn and Kinzer (Ref. 4.11) found that water droplets greater than 5.8 mm would usually break up before the terminal velocity was reached.

TABLE 4.17 VALUES OF TERMINAL VELOCITIES  
OF WATER DROPLETS [4.11]

Drop Diameter (mm)	Terminal Velocity (m sec <sup>-1</sup> )
1	4.0
2	6.5
3	8.1
4	8.8
5	9.1
5.8	9.2

#### 4.6.2 Raindrop Size and Distribution

Normal rainfall has a variety of drop sizes with a distribution as shown in Figure 4.10, which illustrates the wider distribution of droplet sizes in the heavier rain which has the larger droplets. The maximum drop diameter distribution could be adequately simulated by a number of orifices, all at the same water pressure, to produce droplets of approximately 1-, 2-, 3-, and 4- and 5-mm diameter. For the median drop diameter, the use of a single orifice to produce 1-mm droplets would be suitable.

#### 4.6.3 Wind Speed

In most cases of natural rain there will be wind blowing near horizontal. This wind will modify the droplet paths from a vertical path to a path at some angle to the vertical, thus causing the rain droplets to strike at an angle. In addition, unless the equipment is streamlined in the direction of the wind, small vortices may develop at the surface of the equipment. These vortices may cause a considerable amount of the precipitation to flow in a variety of directions, including upward against the bottom of the equipment.

Studies of thunderstorms with rainfall rates from 12.7 to 76.2 mm hr<sup>-1</sup> (0.5 to 3.0 in. hr<sup>-1</sup>) with relationship to wind speeds occurring at the same time have shown an average mean wind speed of 5 m sec<sup>-1</sup> for all storms combined. Peak winds were as high as 16 m sec<sup>-1</sup>. All storms, except one with rates exceeding 25 mm hr<sup>-1</sup>, had peak winds at least 5 m sec<sup>-1</sup> greater than the mean wind for the same storm.

#### 4.6.4 Temperatures

The air temperature at the ground usually decreases several degrees at the start of rainfall. The amount of the temperature decrease is greatest in the summer, about 8°C (14°F), when the temperature is



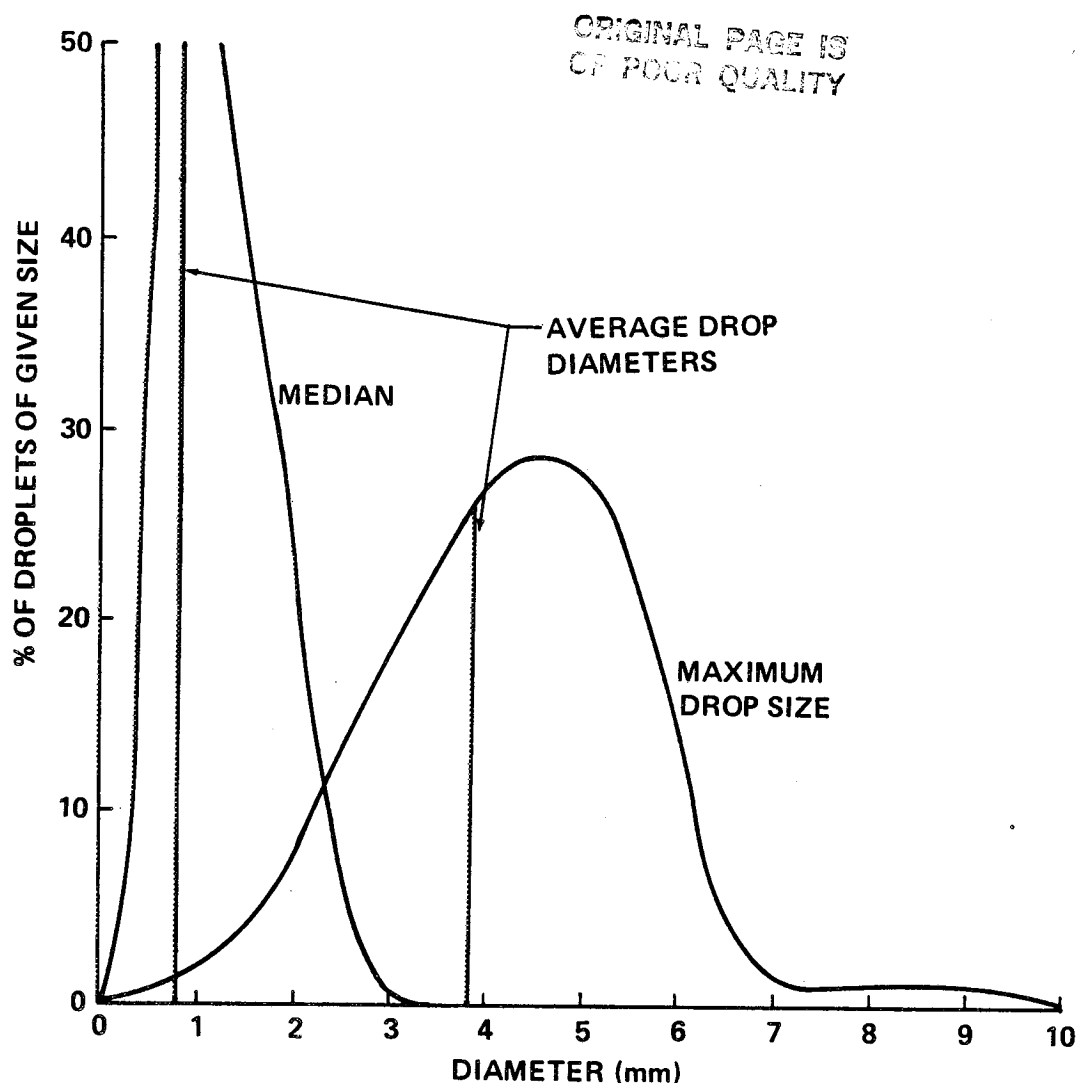


Figure 4.10 Distribution of drop sizes of rain.

high [greater than  $32^{\circ}\text{C}$  ( $90^{\circ}\text{F}$ )], with the final temperature approximately  $24^{\circ}\text{C}$  ( $75^{\circ}\text{F}$ ). In the winter the temperature decrease is usually about  $2.8^{\circ}\text{C}$  ( $5^{\circ}\text{F}$ ). At the end of the rainfall the summer temperature will increase again to nearly the same values as before the storm, but in the winter there is no general pattern of warming. This decrease in temperature is caused by the water droplets being colder than the surface air temperature.

#### 4.6.5 Recommended Items to Include in Laboratory Rainfall Tests

The following items need to be considered in rainfall tests in the laboratory:

- Raindrop size distribution.  
Rates less than  $25 \text{ mm hr}^{-1}$  — drop size of 1 mm.  
Rates greater than  $25 \text{ mm hr}^{-1}$  — drop size from 1 to 5 mm.
- Rate of fall of drops. Drops should fall at least 12 m to obtain terminal velocity.

c. Wind Speed. A mean wind of  $5 \text{ m sec}^{-1}$  with gusts of  $15 \text{ m sec}^{-1}$  of 30-sec duration at least once in each 15-min period.

d. Temperature. The temperature in the chamber should decrease from  $32^{\circ}\text{C}$  ( $90^{\circ}\text{F}$ ) to  $24^{\circ}\text{C}$  ( $75^{\circ}\text{F}$ ) at the start of rainfall for representative summer tests and should be maintained at  $10^{\circ}\text{C}$  ( $50^{\circ}\text{F}$ ) for winter tests. The decrease in air temperature may be obtained by using water at, or slightly below  $24^{\circ}\text{C}$  for the summer tests.

#### 4.6.5.1 Idealized Rain Cycle, Kennedy Space Center, Florida

For some studies and laboratory tests, it may be desirable to use an extreme rain cycle with associated drop sizes, wind speeds, and temperatures. The values from Table 4.12 can be used in any combination of rainfall rate and duration such that the total accumulation does not exceed the Table 4.12 value for the selected time period and percentile level. The percentile level should be compatible with the risk the operator is willing to accept. The 95 percentile values have a 5 percent risk of being exceeded – the 99 percentile values only a 1 percent risk.

If wind speed, temperature, and raindrop size are to be included in the test, the following values may be used with both 95 and 99 percentile rain rates:

Wind speed:  $5.1 \text{ m sec}^{-1}$ , gusts to  $15.4 \text{ m sec}^{-1}$   
 10 knots, gusts to 30 knots  
 gust lasting 2 min applied every 15 min.

	Summer		Winter	
	Before	During	Before	During
Temperature:	$32^{\circ}\text{C}$ ( $90^{\circ}\text{F}$ )	$24^{\circ}\text{C}$ ( $75^{\circ}\text{F}$ )	$13^{\circ}\text{C}$ ( $55^{\circ}\text{F}$ )	$10^{\circ}\text{C}$ ( $50^{\circ}\text{F}$ )
Drop Size:	Average = 2 mm Largest 1% = 5.9 mm			

The following are some rain cycle examples using 95 percentile values from Table 4.12:

<u>Period of Rainfall</u>	<u>Rate (in./hr)</u>	<u>Total Accumulation (in.)</u>
1 hr	1.17	1.17
3 hr	0.47	1.41
(1 hr) {	10 min {	1.17
	3 min {	
	5 min {	
	42 min {	
(3 hr) {	15 min {	1.41
	30 min {	
	5 min {	
	25 min {	
	105 min {	

## 4.7 Rain Erosion

### 4.7.1 Introduction

With the advent of high-speed aircraft a new phenomenon was encountered in the erosion of paint coatings, structural plastic components, and even metallic parts by the impingement of raindrops on surfaces. This was first observed soon after World War II on fighter aircraft capable of speeds over  $178 \text{ m sec}^{-1}$  (400 mph) (Ref. 4.12). This initiated rain erosion research at the Air Force Materials Laboratory, Wright-Patterson Air Force Base, and at the Royal Aircraft Establishment, Farnborough, England. Tests conducted by the British Ministry of Aviation at the Royal Aircraft Establishment (Ref. 4.13) have resulted in a table of rates of erosion for various materials and coatings. These materials and coatings were tested at speeds of  $220 \text{ m sec}^{-1}$  (428 knots). At the Air Force Materials Laboratory, a number of rotating (whirling) arm apparatuses have been used. The current rotating arm apparatus will permit testing of samples of materials at speeds up to  $403 \text{ m sec}^{-1}$  (900 mph) (Mach 1.2) with simulated rainfall variable through a wide variety of rates. Normally the tests are made at  $224 \text{ m sec}^{-1}$  (500 mph) and at  $25.4 \text{ mm hr}^{-1}$  (1 in.  $\text{hr}^{-1}$ ) or  $50.8 \text{ mm hr}^{-1}$  (2 in.  $\text{hr}^{-1}$ ) of rainfall (Ref. 4.14). A number of flight tests using F-80 aircraft in rain were made and compared with the rotating arm tests. The ranking of the test materials for rain erosion was similar for the variety of materials tested, but the time to erode materials varied because of differences in the intensities of the various environments. The natural erosion conditions included hail, ice crystal, and liquid water impingement (Ref. 4.15).

### 4.7.2 Rain Erosion Criteria

Rain erosion may be severe enough to affect the performance of a space vehicle. Sufficient data are not available to present specific extreme values of exposure for various materials used in design. Experience and results of the various tests indicate that materials should be carefully considered. Any materials in which failure in rain erosion would have an effect on the mission should be subjected to tests for rain erosion.

Tests by A. A. Fyall at the Royal Aircraft Establishment (Ref. 4.16) on single rain droplets have shown that the rain erosion rate may increase considerably with lower air pressure (higher altitude) because of the lower cushioning effect of the air on the droplets at impact.

## 4.8 Fogs

Fogs are classified as either warm or supercooled fog, depending upon whether the ambient temperature is above or below  $0^{\circ}\text{C}$ . In either case, fog consists of a considerable number of minute water drops suspended in the atmosphere near the Earth's surface and which reduce visibility to less than 1 km (American Meteorological Society's Glossary of Meteorology — Definitions).

The conditions most favorable for the formation of fog are high relative humidity, light surface winds, no overcast so that radiative cooling is most effective, and an abundance of condensation nuclei. Fog occurs more frequently in coastal areas than in inland areas since there is an abundance of water vapor.

Fogs are formed either by cooling the air until the water vapor condenses or by the evaporation of additional water vapor into the air. Common types are (1) radiation fogs, (2) advection fogs, (3) up-slope fogs, (4) frontal fogs, and (5) steam fogs. A brief description of each fog type follows.

Radiation Fog forms on clear nights when the Earth loses heat very rapidly to the atmosphere. When humidity is high and cooling takes place rapidly, condensation occurs. If there are no winds, the fog will be very shallow or will be reduced to a dew or frost deposit. If winds are present (about 5 knots), then the fog will thicken and deepen. These fogs do not occur at sea since the sea surface does not cool as the land does.

Advection Fog forms as warm, moist air moves over a colder surface. These fogs occur in coastal areas because the moist air moves inland by breezes over the colder land in the winter. In summer the warm, moist air is carried out to sea, where it forms a fog over the cool water and then the sea breezes advect the fog inland. These fogs are common along the coast of California in the summer.

Up-Slope Fog forms when stable, moist air moves up sloping terrain and is cooled by expansion. This cooling produces condensation, and fog forms. An up-slope wind is necessary for the formation and maintenance of this type of fog. Usually these fogs produce low stratus-type clouds.

Frontal Fog forms in the cold air mass of the frontal system. The precipitation from the warm air mass, overrunning the cold air mass, evaporates as it falls through and saturates the cold air, thus producing the frontal-type fog. These fogs form rapidly, cover large areas, occur frequently in winter, and are associated with slow-moving or stationary fronts.

Steam Fog forms by the movement of cold air over a warmer water surface. Steam fog rises from the surface of lakes, rivers, and oceans.

Although not classified as a common-type fog, there is a fog type called the ice (crystal) fog which is of interest. This fog occurs when the air temperature is approximately  $-34^{\circ}\text{C}$ , and as water vapor from the exhaust of aircraft engines, automobiles, etc., is produced, the vapor changes directly to ice crystals instead of condensing directly to liquid drops. The suspension of the ice crystals in the atmosphere produces the ice fog. These fogs can persist from a few minutes to several days and are quite a problem in arctic or polar regions.

Some typical microphysical characteristics of both radiation and advection types of fogs are as follows:

a. Radiation Fog (Inland)

- (1) Diameter of drops (av) —  $10\ \mu\text{m}$
- (2) Typical drop size —  $5 - 35\ \mu\text{m}$
- (3) Liquid water content —  $110\ \text{mg/m}^3$
- (4) Droplet concentration —  $200\ \text{cm}^{-3}$
- (5) Vertical depth
  - (a) Typical —  $100\ \text{m}$
  - (b) Severe —  $300\ \text{m}$
- (6) Horizontal visibility —  $100\ \text{m}$

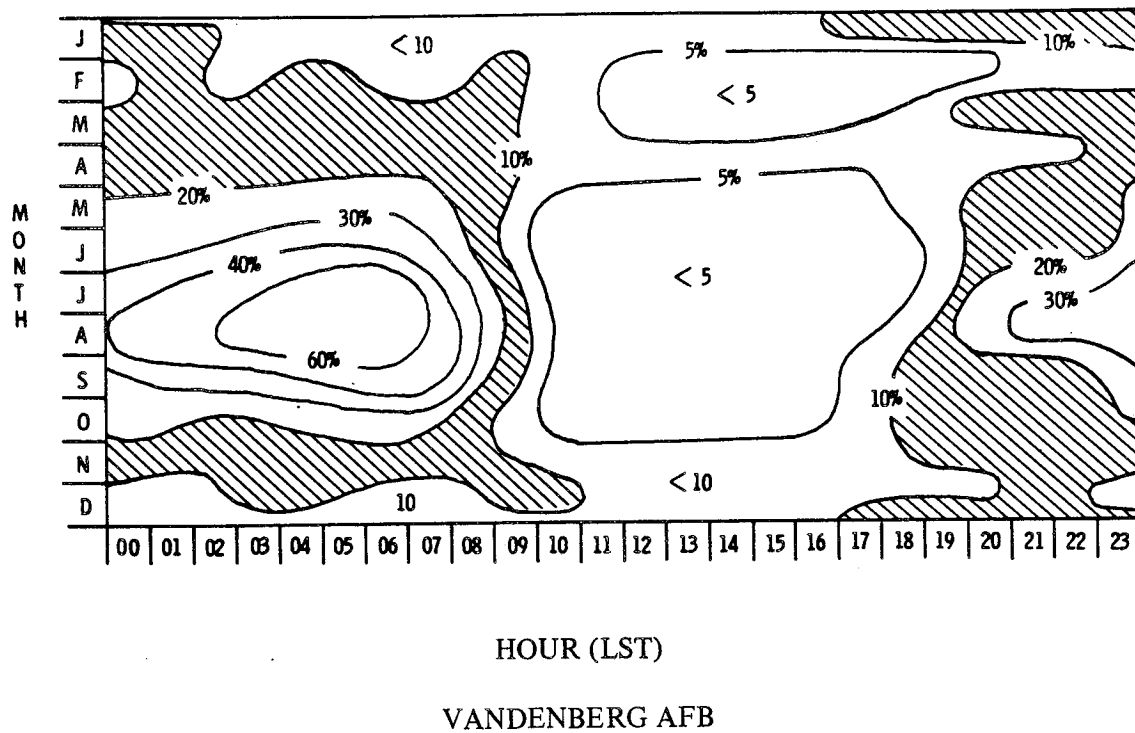
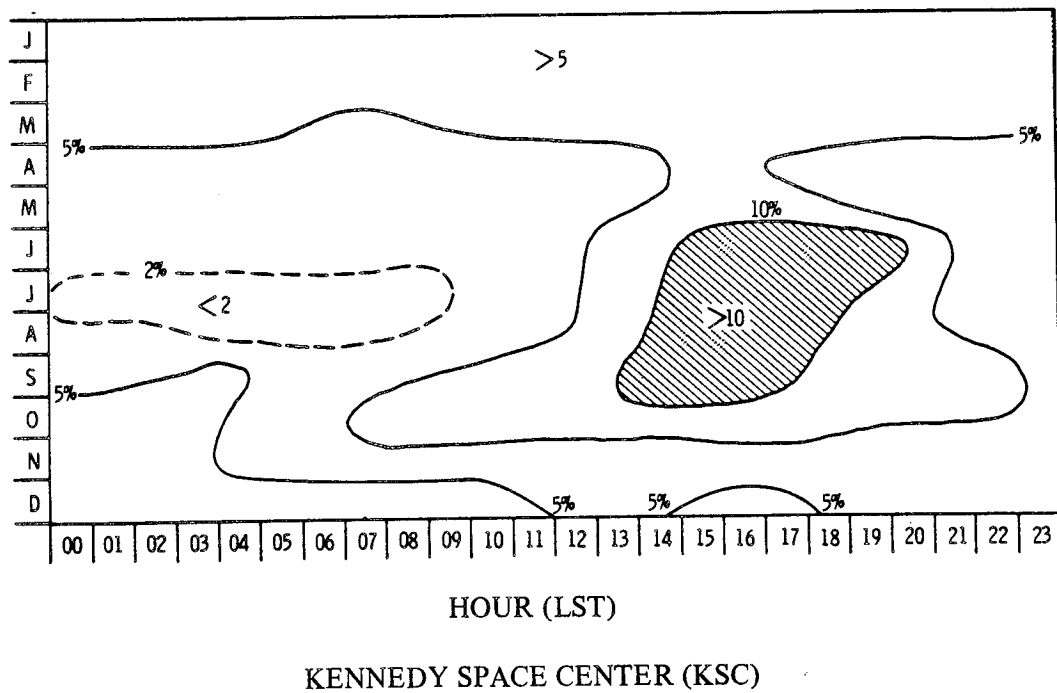
## b. Advection Fog (Coastal)

- (1) Diameter of drops (av) –  $20\ \mu\text{m}$
- (2) Typical drop size –  $7 - 65\ \mu\text{m}$
- (3) Liquid water content –  $170\ \text{mg/m}^3$
- (4) Droplet concentration –  $40\ \text{cm}^{-3}$
- (5) Vertical depth
  - (a) Typical – 200 m
  - (b) Severe – 600 m
- (6) Horizontal visibility – 300 m

4.9 Precipitation or Fog (VAFB and KSC)

Figures 4.11 and 4.12, showing the percentage frequency of precipitation or fog with visibility  $\leq 0.8\ \text{km}$  (0.5 mi.) at Vandenberg AFB and Kennedy Space Center, were developed from historical records of hourly observations. Certain Vandenberg and KSC climatic characteristics that may be of significance to aerospace mission planning and operations are immediately apparent. That is, potentially unfavorable climatic conditions occur mainly during summer night and early morning hours at VAFB but during summer afternoons at KSC. This, of course, is due to the high frequency of fog at VAFB and summer afternoon showers in central Florida.

For climatological studies useful in operational and design data for spacecraft and aircraft operations, the Department of Transportation-Federal Aviation Administration has produced a tabulation of ceilings, visibilities, wind, and weather data by various periods of the day and by various temperature and wind categories for 41 airports (Ref. 4.17).

Figure 4.11 Probability of precipitation or fog with visibility  $\leq 0.8$  km (0.5 mi.).Figure 4.12 Probability of precipitation or fog with visibility  $\leq 0.8$  km (0.5 mi.).

## REFERENCES

- 4.1 "Handbook of Aviation Meteorology, Second Edition." Her Majesty's Stationery Office, London, 1971.
- 4.2 "Rainfall Intensity-Duration-Frequency Curves for Selected Stations in the United States, Alaska, Hawaiian Islands, and Puerto Rico." Technical Paper No. 25, U. S. Department of Commerce, Washington, D.C., December 1955.
- 4.3 Gumble, E. J.: "Statistics of Extremes." Columbia University Press, 1958.
- 4.4 Billions, Novella S.: "A Study of Raindrop Size Distributions and Probability of Occurrence." Report No. RR-TR-65-1, U.S. Army Missile Command, Redstone Arsenal, Ala., 1965.
- 4.5 "Handbook of Geophysics," Revised Edition. The MacMillan Company, New York, 1960.
- 4.6 "Aviation Weather for Pilots and Flight Operations Personnel." Federal Aviation Agency, Department of Commerce, Weather Bureau, Washington, D. C., 1975.
- 4.7 Vaughan, William W.: "Distribution of Hydrometeors with Altitude for Missile Design and Performance Studies." ABMA DA-TM-138-59, Army Missile Command, Huntsville, Ala., 1959.
- 4.8 Changnon, Stanley A., Jr.: The Scales of Hail. Journal of Applied Meteorology, Vol. 16, No. 6, July 1977, pp. 626-648.
- 4.9 Changnon, Stanley A., Jr.: Heavy Falls of Hail and Rain Leading to Roof Collapse. Journal of the Structural Division, ASCE, Vol. 104, No. ST1, Technical Notes, January 1978, pp. 198-200.
- 4.10 Byers, Horace R. and Braham, Roscoe, R., Jr.: The Thunderstorm. United States Government Printing Office, Washington, D.C., 1949.
- 4.11 Gunn, Ross; and Kinzer, Gilbert D.: "The Terminal Velocity of Fall for Water Droplets in Stagnant Air," Journal of Meteorology, Vol. 6, August 1949.
- 4.12 Wahl, Norman E.: "Investigation of the Phenomena of Rain Erosion at Subsonic and Supersonic Speeds." Technical Report AFML-TR-65-330, Air Force Materials Laboratory, Research and Technical Division, Air Force Systems Command, Wright-Patterson Air Force Base, Ohio, October 1965.
- 4.13 Fyall, A. A.; King, R. B.; and Strain, R. N. C.: "Rain Erosion Aspects of Aircraft and Guided Missiles." Journal of the Royal Aeronautical Society, Vol. 66, July 1962.
- 4.14 Hurley, Charles J.; and Schmitt, George F., Jr.: "Development and Calibration of a Mach 1.2 Rain Erosion Test Apparatus." AFML-TR-70-240, Air Force Material Laboratory, Air Force Systems Command, Wright-Patterson Air Force Base, Ohio, October 1970.
- 4.15 Schmitt, George F., Jr.: "Flight Test-Whirling Army Correlation of Rain Erosion Resistance of Materials." AFML-TR-67-420, Air Force Materials Laboratory, Air Force Systems Command, Wright-Patterson Air Force Base, Ohio, September 1968.

## REFERENCES (Concluded)

- 4.16 Fyall, A. A.: "Single Impact Studies of Rain Erosion." Technical Air, Vol. 26, October 1970, pp. 4-11.
- 4.17 Climatological Summaries — Visibilities below 1/2 Mile and Ceilings Below 200 Feet. FAA-RD-69-22, FA-67-WAI-12, National Weather Record Center, Asheville, N. C., June 1969.



## SECTION V. SEA STATE\*

5.1 Introduction

Natural environment design specifications for all applicable Space Shuttle activities are given in the appropriate Level II (Ref. 5.1) or Level III (Ref. 5.2) Space Shuttle documents. Since those documents are controlled by the program or project manager, it is not appropriate to repeat the design values here. Instead, this section contains the empirical distributions of several natural environment parameters that may be useful in operational analyses and future design studies.

In deep water the characteristics (sea states) are determined not only by the mean wind speed but also by the fetch (the distance over which it blows) and duration of the wind over the open water. A sea state is generally described by significant wave height, which is the average height of the one-third highest waves. Of course, higher waves exist in any given sea state. For example, from the relationship between wind speed and wave height for a fully arisen sea, as shown in Figure 5.1, it can be seen that in a code 3 sea state with significant wave heights about 1.2 m, 10 percent of the waves will average about 1.5 m. In other words, a wind speed of  $8.2 \text{ m sec}^{-1}$  (fetch and duration unlimited) will produce a sea with the highest one-third waves averaging about 1.2 m and the highest one-tenth waves about 1.5 m.

Figure 5.1 shows the distribution of wave heights versus wind speed at any given instant — information applicable to vehicle water entry. For all other operations (afloat, secure, towback recovery) where some considerable time interval is involved, the exposure period concept must be considered; that is, the longer the exposure period, the greater the probability of encountering a larger wave. Wave heights at the 5 percent risk level for exposure periods from 1 to 100 hr in sea-state codes 3, 4, and 5 are shown in Figure 5.2. From Figure 5.2, for example, it can be seen that exposure for 1 hr in sea-state code 4 entails a 5 percent risk of encountering at least one wave greater than 5.3 m. If the exposure time is increased to 48 hr in the same sea-state code 4 condition, the wave height at the 5 percent risk level becomes 6.3 m.

The foregoing paragraphs dealt with general sea-state relationships valid in any deep-water area. This part will present empirical data applicable to the Kennedy Space Center SRB recovery area (27 deg to 31 deg N; 77 deg to 80 deg W) or the Vandenberg Air Force Base SRB recovery area (31 to 33 degrees N; 120 to 122 degrees W).

It is emphasized that the following tables were generated from observations of significant waves ( $H_{1/3}$  equals the average height of the one-third highest waves) without regard to fetch or duration (Ref. 5.3). In any given sea state there will always be waves higher than the significant heights. Also, exposure time increases the chances of higher waves occurring.

From Table 5.1, there is a 3 percent risk of exceeding sea-state code 5 and a 68 percent risk of exceeding sea-state code 3 in February. Also, in February there is a 95 percent chance that the significant wave height will be  $\leq 3.7$  m and, conversely, a 5 percent chance that it will exceed 3.7 m. On an annual basis the 95th percentile wave height is 2.9 m in the Kennedy Space Center recovery area versus 2.8 m in the Vandenberg AFB recovery area (Table 5.2). While the annual  $H_{1/3}$  values are very similar, some monthly distributions show considerable differences. In general, the Kennedy Space Center area shows greater seasonal variation and, consequently, a more severe environment.

---

\*Further information and/or interpretation of these sea state criteria should be directed to the Atmospheric Sciences Division, Space Sciences Laboratory, Marshall Space Flight Center, Alabama 35812.

5.2

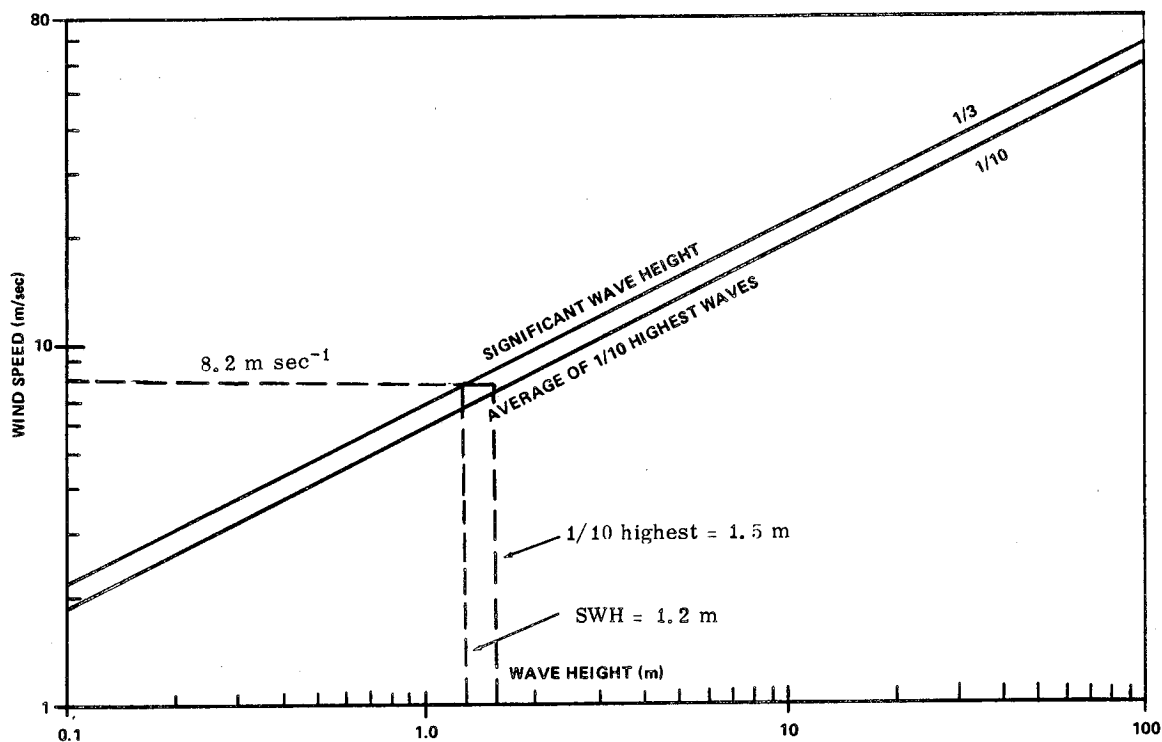


Figure 5.1 Relationship between wave height and wind speed in a fully arisen sea.

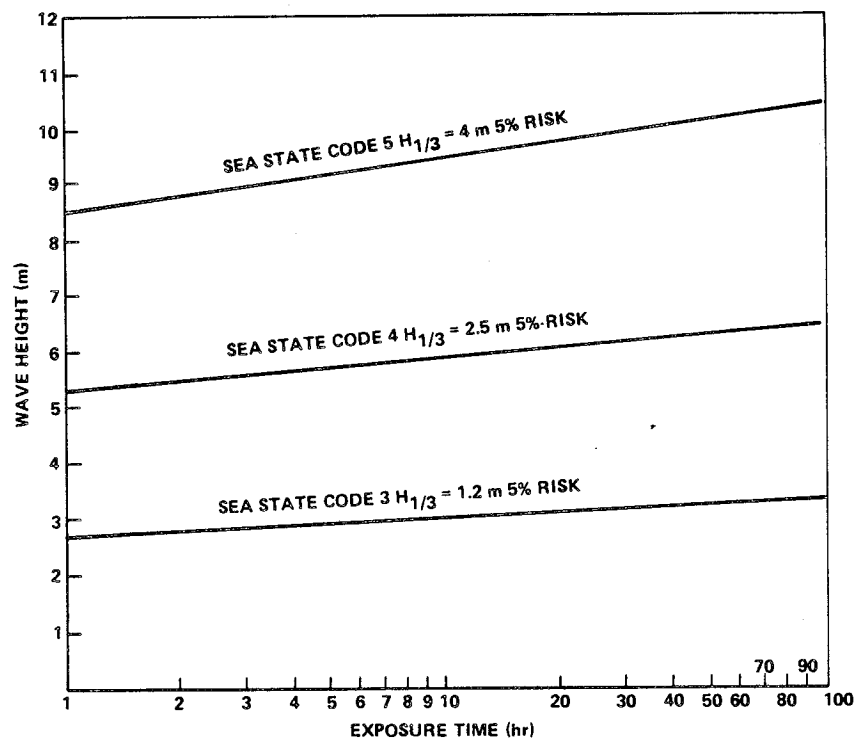


Figure 5.2 Five-percent risk wave height versus exposure time (assuming sea-state category remains unchanged for duration of exposure period).

TABLE 5.1 KENNEDY SPACE CENTER RECOVERY AREA SEA STATES  
(27 to 31 degrees north; 77 to 80 degrees west)

Significant Wave Heights, Avg. of 1/3 Highest		Sea State Codes	Percent Probability of Exceeding Indicated Heights												
			J	F	M	A	M	J	J	A	S	O	N	D	Avg.
m	ft														
0.6	2	2	86	90	84	87	68	70	68	58	82	82	84	84	80
1.2	4	3	60	68	54	50	27	35	30	22	55	58	56	56	50
2.4	8	4	14	20	10	8	5	6	3	2	15	12	13	10	9
4.0	13	5	2	3	1	0.5	0.8	0.8	0.2	0.2	2	1.8	1.2	0.8	1
6.1	20	6	0.2	0.3	0.2	<0.1	0.2	0.2	<0.1	<0.1	0.2	0.3	<0.1	<0.1	0.1
Percentiles															
50th (m)			1.4	1.6	1.4	1.2	0.8	0.9	0.8	0.7	1.3	1.4	1.4	1.4	1.2
95th (m)			3.3	3.7	2.8	2.7	2.4	2.6	2.2	2.1	3.3	3.2	3.0	2.8	2.9

TABLE 5.2 VANDENBERG AFB RECOVERY AREA SEA STATES  
(31 to 33 degrees north; 120 to 122 degrees west)

Significant Wave Heights, Avg. of 1/3 Highest		Sea State Codes	Percent Probability of Exceeding Indicated Heights												
			J	F	M	A	M	J	J	A	S	O	N	D	Avg.
m	ft														
0.6	2	2	74	67	76	78	82	82	81	83	77	58	69	74	76
1.2	4	3	42	38	45	49	50	51	47	45	44	37	34	49	44
2.4	8	4	9	9	10	11	10	9	5	6	6	5	4	13	8
4.0	13	5	1.4	1	1.8	1.8	1.2	0.4	0.2	0.1	0.4	0.4	0.5	3	1
6.1	20	6	<0.1	<0.1	<0.1	<0.1	<0.1	<0.1	<0.1	<0.1	<0.1	<0.1	<0.1	<0.5	<0.1
Percentiles															
50th (m)			1.0	0.9	1.1	1.2	1.2	1.2	1.1	1.1	1.1	0.7	0.9	1.2	1.1
95th (m)			2.9	3.2	3.2	3.0	3.2	2.8	2.4	2.5	2.6	2.4	2.4	3.5	2.8

Table 5.3 presents the international meteorological codes for the state of the sea (Ref. 5.4).

## 5.2 Wave Slopes

The wave slopes shown in Tables 5.4 and 5.5 were calculated along the wind direction after assuming a Gaussian distribution in a fully aroused sea. The entire distribution of significant wave heights was used for the calculations.

## 5.3 Surface Currents

a. Kennedy Space Center SRB Recovery Area. The dominant current, which is south to north, in the Kennedy Space Center SRB recovery area is the Gulf Stream. Although the mean speed and position of the maximum current shows little change from season to season, daily synoptic changes may be rapid and intense (Ref. 5.5).

TABLE 5.3 INTERNATIONAL METEOROLOGICAL CODES,  
CODE 3700, STATE OF SEA

Code Figure	Descriptive Terms	$H_{1/3}$ of Waves	
		m	ft
0	Calm (Glassy)	0	0
1	Calm (Rippled)	0-0.1	0-0.33
2	Smooth (Wavelets)	0.1-0.5	0.33-1.6
3	Slight	0.5-1.25	1.6-4.1
4	Moderate	1.25-2.5	4.1-8.2
5	Rough	2.5-4	8.2-13.1
6	Very Rough	4-6	13.1-19.7
7	High	6-9	19.7-29.5
8	Very High	9-14	29.5-45.9
9	Phenomenal	Over 14	Over 45.9

Note: Exact bounding height is assigned to lower code; e.g.,  
a height of 4 m is coded 5.

TABLE 5.4 KENNEDY SPACE CENTER RECOVERY AREA WAVE SLOPES  
(calculated from significant wave heights)

Risk of Exceeding	J	F	M	A	M	J	J	A	S	O	N	D	Avg.
5%	11°	12°	11°	10°	10°	10°	10°	9°	11°	11°	11°	11°	10°

TABLE 5.5 VANDENBERG AFB RECOVERY AREA WAVE SLOPES  
(calculated from significant wave heights)

Risk of Exceeding	J	F	M	A	M	J	J	A	S	O	N	D	A
5%	10°	10°	10°	10°	11°	11°	10°	10°	10°	10°	10°	11°	10°

The following means and standard deviations may be applied to all seasons (Fig. 5.3):

<u>Area</u>	<u>Mean</u>	<u>Standard Deviation</u>
22	0.4 m sec <sup>-1</sup> (0.8 knots)	0.6 m sec <sup>-1</sup> (1.27 knots)
26	1.3 m sec <sup>-1</sup> (2.5 knots)	0.6 m sec <sup>-1</sup> (1.25 knots)

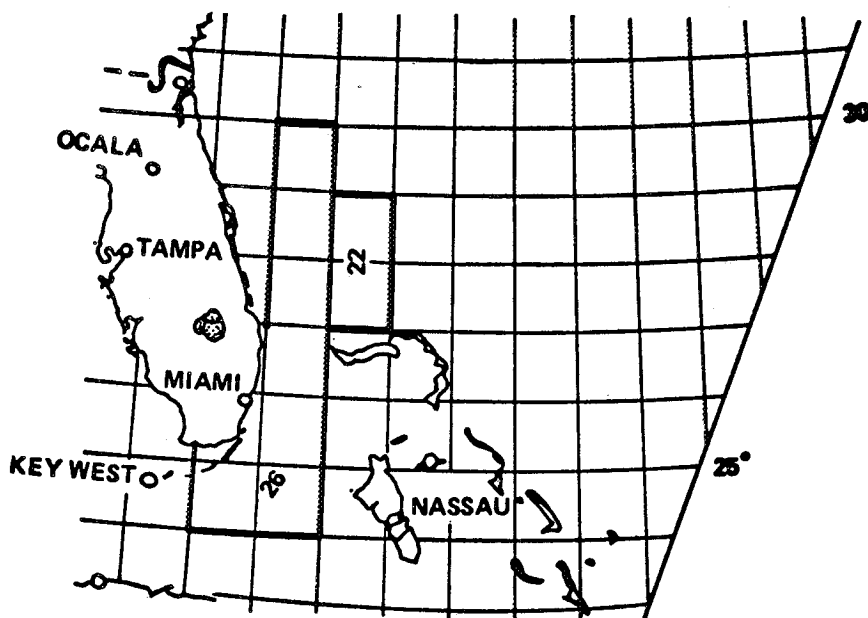


Figure 5.3 Surface current areas.

b. Vandenberg AFB SRB Recovery Area. While the predominant direction is from north to south in all seasons, the currents are generally weak in the Vandenberg AFB SRB recovery area – less than 1 knot.

The following mean and standard deviation may be used for the entire recovery area for all seasons:

<u>Mean</u>	<u>Standard Deviation</u>
0.3 m sec <sup>-1</sup> (0.54 knots)	0.3 m sec <sup>-1</sup> (0.56 knots)

#### 5.4 Sea-State Duration

The durations of rough seas (sea-state code 5 and greater) shown in Figure 5.4 are deduced values based upon the usual consequences of prevailing synoptic meteorological situations. There are no direct observations of sea-state duration in the SRB recovery areas.

Figure 5.4 provides information only on the duration – not on the frequency of occurrence – of sea states greater than or equal to code 5. For example, in the Kennedy Space Center recovery area there is a 5-percent risk that sea states greater than or equal to code 5 will last for 24 hours once they have developed. The risk of occurrence can be obtained from Table 5.1 (Ref. 5.3).

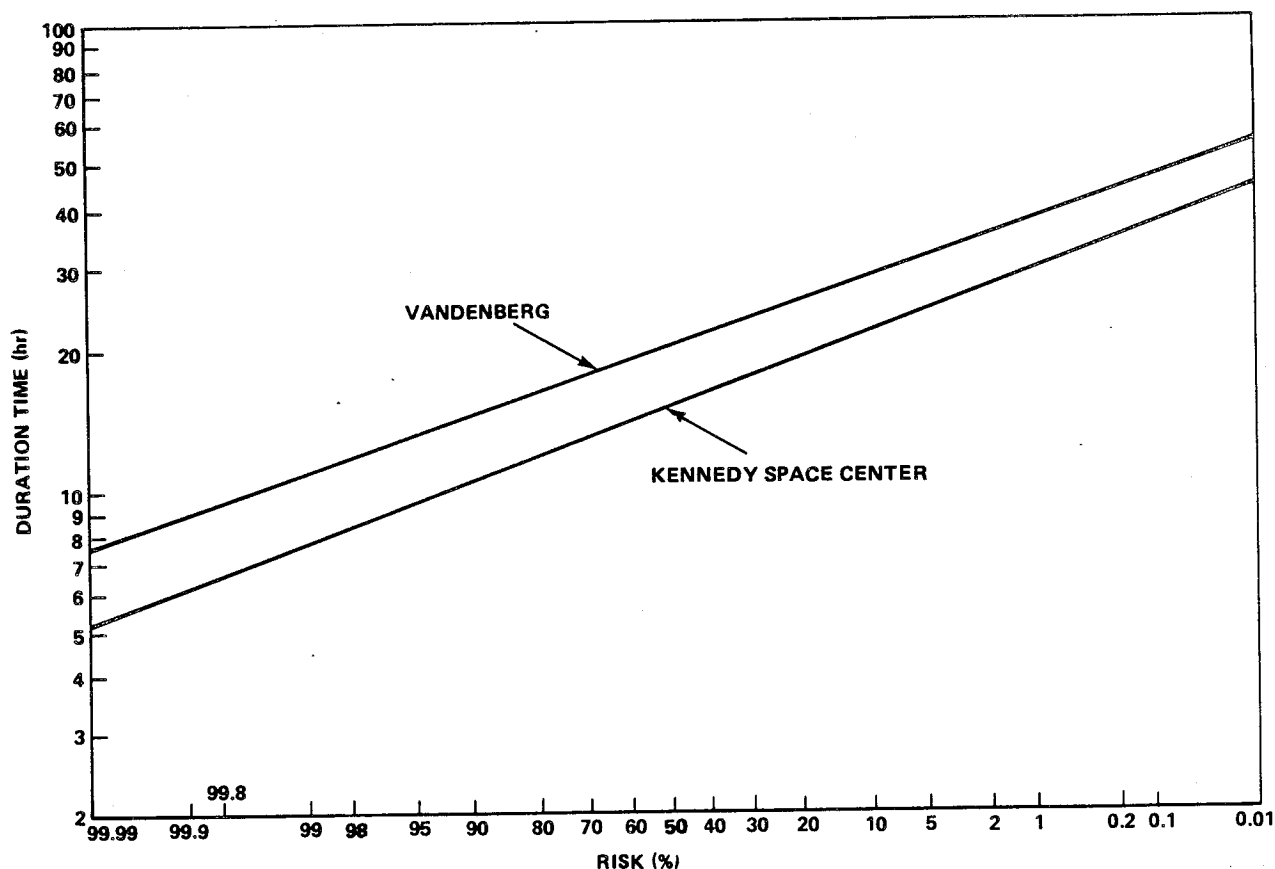


Figure 5.4 Distribution of duration times for sea states greater than or equal to code 5 in Kennedy Space Center and Vandenberg AFB SRB recovery areas.

### 5.5 Ocean Temperatures

Maximum, mean, and minimum water temperatures for 3-month periods from the surface to depths of 50 m for KSC and VAFB SRB recovery areas are given in Table 5.6 (Ref. 5.6).

### 5.6 Atmospheric Conditions

Climatological information applicable to SRB recovery and retrieval areas is given in Tables 5.7 and 5.8 (Refs. 5.3 and 5.7). These values, developed from observations made at 00, 06, 12, and 18Z by ships passing through the area, show the percent frequency of the indicated atmospheric condition. For example, in January the sky cover was 0, 1/8, or 2/8 ( $\leq 2/8$ ) on 20.3 percent of the observations. The sky was completely covered (8/8) on 20.8 percent of the observations.

TABLE 5.6 OCEAN TEMPERATURES IN THE SRB RECOVERY AREAS (°C)

Kennedy Space Center SRB Recovery Area

Months Depth (m)	Jan. — March			April — June			July — Sept.			Oct. — Dec.		
	Max.	Mean	Min.	Max.	Mean	Min.	Max.	Mean	Min.	Max.	Mean	Min.
0	26	23	16	29	26	21	31	29	27	29	26	19
10	26	23	16	29	26	20	30	29	26	29	26	19
20	26	23	17	29	26	19	30	28	23	29	26	20
30	26	23	16	28	26	17	29	28	21	29	26	21
50	26	23	17	28	25	17	29	27	19	28	26	22

VAFB SRB Recovery Area

Months Depth (m)	Jan. — March			April — June			July — Sept.			Oct. — Dec.		
	Max.	Mean	Min.	Max.	Mean	Min.	Max.	Mean	Min.	Max.	Mean	Min.
0	17	14	12	19	14	11	21	17	13	20	17	13
10	17	14	11	18	14	11	21	17	11	20	17	13
20	17	14	11	17	14	11	20	16	10	20	16	12
30	17	14	11	17	14	10	20	16	10	20	16	11
50	17	14	10	17	13	9	19	14	9	20	14	10

ORIGINAL PAGE IS  
OF POOR QUALITY

TABLE 5.7 KENNEDY SPACE CENTER SRB RECOVERY AREA ATMOSPHERIC CONDITIONS

Percent Frequency of Occurrence									
Month	Visibility (n.mi.)		Precip.	Sky Cover			Wind Speed (knots)		
	≤2	≥10		0-2/8	8/8	Mean	≤10	≥17	Mean
J	1.3	89.4	4.0	20.3	20.8	0.62	29.0	35.8	15.2
F	1.9	88.4	4.5	21.3	22.1	0.62	29.9	39.2	15.9
M	0.5	88.6	2.6	26.5	19.2	0.58	30.0	37.9	15.2
A	1.0	89.6	1.3	36.2	9.6	0.47	34.4	30.6	14.0
M	0.9	88.7	2.2	37.5	12.7	0.47	48.2	18.6	11.9
J	2.4	86.2	4.5	24.2	17.2	0.57	49.7	17.8	11.9
J	1.3	92.0	3.8	30.8	12.4	0.52	50.6	14.6	11.5
A	1.1	90.0	4.5	22.5	11.8	0.55	57.6	13.4	11.2
S	2.2	87.3	4.9	25.4	16.2	0.56	50.6	19.1	12.0
O	0.6	90.6	2.3	28.5	13.7	0.53	36.5	28.7	13.6
N	1.1	92.7	3.4	28.7	11.6	0.53	33.8	33.2	14.7
D	0.9	92.7	2.1	29.0	14.3	0.56	41.3	28.6	14.7

TABLE 5.8 VANDENBERG AFB SRB RECOVERY AREA ATMOSPHERIC CONDITIONS

Percent Frequency of Occurrence									
Month	Visibility (n.mi.)		Precip.	Sky Cover			Wind Speed (knots)		
	≤2	≥10		0-2/8	8/8	Mean	≤10	≥17	Mean
J	2.3	76.9	5.1	30.5	25.2	0.59	41.2	27.5	13.1
F	4.6	76.3	4.9	27.8	29.3	0.60	38.6	32.5	13.8
M	0.8	81.0	3.2	30.4	23.9	0.58	35.1	40.4	14.8
A	1.6	75.2	3.0	25.0	30.3	0.63	29.1	43.6	15.7
M	0.3	84.1	2.1	24.0	31.8	0.65	26.5	43.5	15.8
J	1.1	71.5	2.7	21.7	49.2	0.71	28.1	42.4	15.5
J	1.2	74.1	2.3	16.5	60.4	0.79	34.7	34.8	14.0
A	0.8	72.8	1.4	16.1	58.6	0.79	32.9	33.5	13.9
S	0.5	77.0	1.9	26.4	39.4	0.66	35.4	33.3	13.7
O	1.0	79.1	1.3	33.9	33.1	0.58	40.7	30.8	13.4
N	1.9	77.5	3.8	32.9	26.0	0.56	44.2	26.2	12.7
D	1.2	83.3	3.2	32.8	20.5	0.55	46.5	28.2	12.7



## REFERENCES

- 5.1 "Space Shuttle Flight and Ground System Specification." Vol. X, Appendix 10.10, Revision B, JSC 07700, NASA/Johnson Space Flight Center, April 27, 1978.
- 5.2 "Natural Environment for the Space Shuttle Solid Rocket Booster." MSFC SE-019-043-2H, Marshall Space Flight Center, Huntsville, Alabama, May 20, 1975.
- 5.3 "Summary of Synoptic Meteorological Observations." North American Coast Marine Areas, Vol. 4, Vol. 7 and Vol. 8, Nos. AD707701, AD709055, and AD710771, respectively, U.S. Naval Weather Service Command, Washington, D.C., May 1970.
- 5.4 "International Meteorological Codes, 1972." Hydrographic Office Publication No. 118, Naval Weather Service Environmental Detachment, Federal Building, Asheville, N.C., (reproduced and distributed to Naval Weather Service Command Units by direction of the Commander, Naval Weather Service Command), March 1972.
- 5.5 "Environmental Conditions Within Specified Geographical Regions." U.S. Department of Commerce, National Oceanic and Atmospheric Administration, Environmental Data Service, a United States Department of Commerce Publication, National Data Buoy Center, April 1973.
- 5.6 Churgin, J.; and Halminski, S. J.: "Temperature, Salinity, Oxygen, and Phosphate in the Waters Off United States." Key to Oceanographic Records, Documentation No. 2, Vol. 2, "Gulf of Mexico," National Oceanographic Data Center, March 1974.
- 5.7 "Marine Climatological Summaries." Vol. 1 through 9, U.S. Department of Commerce, NOAA, EDS, National Climatic Center, Asheville, N.C., June 1976.



## SECTION VI. HUMIDITY

6.1 Definitions (Ref. 6.1)

Absolute Humidity: In a system of moist air, the ratio of the mass of water vapor present to the volume occupied by the mixture; that is, the density of the water vapor component.

Condensation: The physical process by which a vapor becomes a liquid or solid; the opposite of evaporation.

Dew-Point Temperature: The temperature to which a given parcel of air must be cooled at constant pressure and constant water-vapor content in order for saturation to occur. When this temperature is below 0°C, it is sometimes called the frost point.

Dry-Bulb Temperature: The temperature of the air. The temperature registered by the dry-bulb thermometer of a psychrometer (sometimes referred to as ambient temperature).

Evaporation: The physical process by which a liquid or solid is transformed to the gaseous state; the opposite of condensation.

Frost Point: The highest temperature at which atmospheric moisture will sublime in the form of hoar frost on a cooled polished surface. It is analogous to the dew point, applying when the moisture in the atmosphere will not condense above 0°C.

Humidity: Generally, some measure of the water-vapor content in air. (See: absolute humidity, relative humidity, specific humidity, mixing ratio or dew point.)

Hydrology: That branch of physical geography which deals with the waters of the Earth exclusive of the oceans. The moisture (vapor, liquid, and solid) in the atmosphere is one phase of the "hydrologic cycle."

Hygrometer: An instrument which measures the water vapor content of the atmosphere.

Hygrometry: The study which treats the measurements of the humidity of the atmosphere and other gases.

Latent Heat of Condensation: The heat released per unit mass as water vapor condenses to form water droplets or ice crystals.

Latent Heat of Vaporization: The heat absorbed per unit mass as water or ice is vaporized into the gaseous state.

Mixing Ratio: In a system of moist air, the dimensionless ratio of the water vapor to the mass of dry air.

Moisture: A term usually referring to the water vapor content of the atmosphere, or to the total water substance (gaseous, liquid, and solid) present in a given volume of air.

Moisture Inversion: An increase with height of the moisture content of the air; specifically, the layer through which this increase occurs, or the altitude at which the increase begins.

Relative Humidity: The dimensionless ratio of the actual vapor pressure of the air to the saturation vapor pressure.

Saturation: The condition in which the partial pressure of any fluid constituent is equal to its maximum possible partial pressure under the existing environmental conditions, such that any increase in the amount of that constituent will initiate within it a change to a more condensed state.

Specific Humidity: In a system of moist air, the dimensionless ratio of the mass of water vapor to the total mass of the system.

Sublimation: The transition of a substance from the solid phase directly to the vapor phase, or vice versa, without passing through an intermediate liquid phase.

Supersaturation: The condition existing in a given portion of the atmosphere (or other space) when the relative humidity is greater than 100 percent; that is, when it contains more water vapor than is needed to produce saturation with respect to a plane surface of pure water or pure ice.

Vapor: Any substance existing in the gaseous state at a temperature lower than that of its critical point; that is, a gas cool enough to be liquefied if sufficient pressure were applied to it.

Vapor Concentration: [previously called absolute humidity (Ref. 6.2)] is the ratio of the mass of water vapor present to the volume occupied by the mixture, i.e., the density of the water content. This is expressed in grams of water vapor per cubic meter of air.

Vapor Pressure: The pressure exerted by the molecules of a given vapor. For a pure, confined vapor, it is that vapor's pressure on the walls of its containing vessel; and for a vapor mixed with other vapors or gases, it is that vapor's contribution to the total pressure (i.e., its partial pressure).

Water Vapor: Water substance in vapor form; one of the most important of all constituents of the atmosphere.

Wet-Bulb Temperature: The temperature an air parcel would have if cooled adiabatically to saturation at constant pressure by evaporation of water into it, all latent heat being supplied by the parcel.

## 6.2 Vapor Concentration

The physical state of water may exist in the gaseous, liquid, and solid phases in the atmosphere. The Earth's atmosphere contains a significant amount of moisture because of the ample supply of the substance. The equatorial region of the Earth is the main source from which moisture is supplied to the atmosphere. This is due to the vast oceanic area and moist land regions from which broad-scale evaporation of water takes place and is introduced into the air.

Water in vapor form is invisible. Since the partial pressure of water vapor is less than the partial pressure of the dry air it displaces, moist air is less dense than dry (drier) air. This contributes to the lower atmospheric pressure as is common to warm, moist air masses. Atmospheric pressure differentials are extremely significant between moist (warm) and dry (cold) air. This is the main driving factor which causes the dynamic variations of the global atmospheric circulation.

Humidity plays a significant role in the design, fabrication, operations, and flight of aerospace vehicles. In some cases moisture plays the main role, especially where long-term on-pad stay times must be encountered. Moisture is also of primary concern when satellites and any space probe, as well as delicate test equipment, must undergo exposure to the ambient air.

The following statements contain the reasons why detriments due to moist, humid air must be considered by researchers during the development of space vehicles and space probes in general.

a. Minute particulate material suspended in the air, especially at the lower altitudes, tends to settle on any surface. When combined with moisture, such debris can become very corrosive and react with many things on which it is deposited. Water, by itself, is a dissolving agent and associates with almost everything it comes into contact with. In general, water is the most important single agent affecting the surface of the Earth, and all materials exposed to the substance commonly undergo some chemical or physical change. Degradation of surfaces where dissimilar metals are in contact can take place at a rapid rate in the presence of moisture. The rate of corrosion of materials increases proportionally with humidity (Ref. 6.3). See Section XV of this report for additional details on atmospheric corrosion and abrasion.

b. Atmospheric humidity can impair or alter the performance of electronic equipment. Some of the primary problems are (1) dielectric constants of capacitors in tuned networks can change with variations of humidity, (2) electronic components may deteriorate as a result of metallic corrosion, and electrode chemical reactions with components can take place with the presence of moisture; examples of these are corrosive buildup on inductors, memory cores, etc., and parametric changes of components due to the formation of condensing vapor across contacts, and (3) the increase of humidity tends to decrease the breakdown voltage between potentials. These are a few problems that are identifiable when working with electronic components in a humid environment.

c. Organic growth, bacteria and fungi, multiply rampantly under conditions of high humidity and warm air temperature. Special emphasis must be placed on controlling the growth of these undesirable organisms where they may degrade the performance of aerospace systems and sensors. Stringent moisture controls must be placed within and around such systems.

d. A decrease in the temperature of the air to the dew point will result in the condensation of water vapor from the atmosphere into the liquid or frozen state. Considerable difficulty may result from ice forming on space vehicles when moist air is cooled by the low temperature of the fuel. Damage may result if pieces of this ice should drop onto vehicle or ground-support equipment before or during launch. Optical surfaces, such as lenses of optical equipment, may become coated with water droplets or ice crystals and become inoperative. Various other factors can result because of the condensation of water or ice at, or near, the vehicle launch site, causing many problems.

Controlled chamber tests are conducted where humidity is closely regulated. This is referred to as humidity cycling (Ref. 6.4). Relative humidity and temperature are gradually raised and lowered to simulate environmental conditions. The chamber shall be constructed and function, and accessories shall be arranged in the chamber, according to the specifications provided in Reference 6.4. This reference describes five different humidity test procedures that can be applied, depending upon the requirements needed.

A temperature of 71°C (160°F) and 95 percent relative humidity represents a dew-point temperature of 69°C (156°F) that is much higher than any natural extreme in the world. Dew points above 32°C (90°F) are extremely unlikely in nature (Ref. 6.5), since the dew-point temperature is limited by the source of the water vapor, i.e., the surface temperature of the water body from which the water evaporates (Ref. 6.6).

NASA's External Tank Verification Plan (Ref. 6.7) lists the following general statements under Test Controls and Test Methods: (1) the item is sealed or potted and subjected to a seal test, (2) the item is located in a controlled-humidity or air-conditioned environment during operation and is protected from humidity when nonoperating, (3) the item is subjected to propellant compatibility testing which is considered to be a more severe environment, and (4) the item is fabricated from materials which preclude corrosion by humidity. This, again, requires additional and different quality control standards than those discussed previously.

The Space Shuttle Program, Shuttle Master Verification Plan document, states that the humidity and other environmental parameter tests will use the procedures given in "Military Standard 810C" (Ref. 6.4).

Some information and test procedures have been provided on humidity-temperature chamber test criteria for various systems and their associated electrical-mechanical components. A wide variety of such tests are identified in the various system requirements documents. However, this document has been prepared to emphasize actual environmental criteria, including extreme values, in conducting any such tests of components to promote realism about the actual environment.

### 6.2.1 High Vapor Concentration at Surface

#### a. Huntsville, New Orleans, and Kennedy Space Center:

(1) The following extreme humidity cycle of 24 hr with a wind of less than  $5 \text{ m sec}^{-1}$  (9.7 knots) should be considered in design: Three hr of  $37.2^{\circ}\text{C}$  ( $99^{\circ}\text{F}$ ) air temperature at 50 percent relative humidity and a vapor concentration of  $22.2 \text{ g m}^{-3}$  ( $9.7 \text{ gr ft}^{-3}$ ); 6 hr of decreasing air temperature to  $24.4^{\circ}\text{C}$  ( $76^{\circ}\text{F}$ ) with relative humidity increasing to 100 percent (saturation); 8 hr of decreasing air temperature to  $21.1^{\circ}\text{C}$  ( $70^{\circ}\text{F}$ ), with a release of 3.8 grams of water as liquid per cubic meter of air (1.7 grains of water per cubic foot of air),<sup>1</sup> humidity remaining at 100 percent; and 7 hr of increasing air temperature to  $37.2^{\circ}\text{C}$  ( $99^{\circ}\text{F}$ ) and a decrease to 50 percent relative humidity (Fig. 6.1).

(2) An extreme relative humidity between 75 and 100 percent and air temperature between  $22.8^{\circ}\text{C}$  ( $73^{\circ}\text{F}$ ) and  $27.8^{\circ}\text{C}$  ( $82^{\circ}\text{F}$ ), which would result in corrosion and bacterial and fungal growths, can be expected for a period of 15 days. A humidity of 100 percent occurs one-fourth of the time at the lower temperature in cycles not exceeding 24 hr. Any loss of water vapor from the air by condensation is replaced from outside sources to maintain at least 75 percent relative humidity at the higher temperature.

#### b. The Vandenberg Air Force Base:

(1) The following extreme humidity cycle of 24 hr with a wind of less than  $5 \text{ m sec}^{-1}$  (9.7 knots) should be considered in design: Three hours of  $23.9^{\circ}\text{C}$  ( $75^{\circ}\text{F}$ ) air temperature at 75 percent relative humidity and a vapor concentration of  $16.2 \text{ g m}^{-3}$  ( $7.1 \text{ gr ft}^{-3}$ ); 6 hr of decreasing air temperature to  $18.9^{\circ}\text{C}$  ( $66^{\circ}\text{F}$ ) with relative humidity increasing to 100 percent; 8 hr of decreasing air temperature to  $12.8^{\circ}\text{C}$  ( $55^{\circ}\text{F}$ ) with a release of 5.0 grams of water as liquid per cubic meter of air (2.2 gr of water per cubic foot of air),<sup>2</sup> humidity at 100 percent; and 7 hr of increasing air temperature to  $23.9^{\circ}\text{C}$  ( $75^{\circ}\text{F}$ ) and the relative humidity decreasing to 75 percent (Fig. 6.2).

---

1. The release of water as a liquid on the test object may be delayed for several hours after the start of this part of the test because of thermal lag in a large test object. If the lag is too large, the test should be extended in time for each cycle to allow condensation.

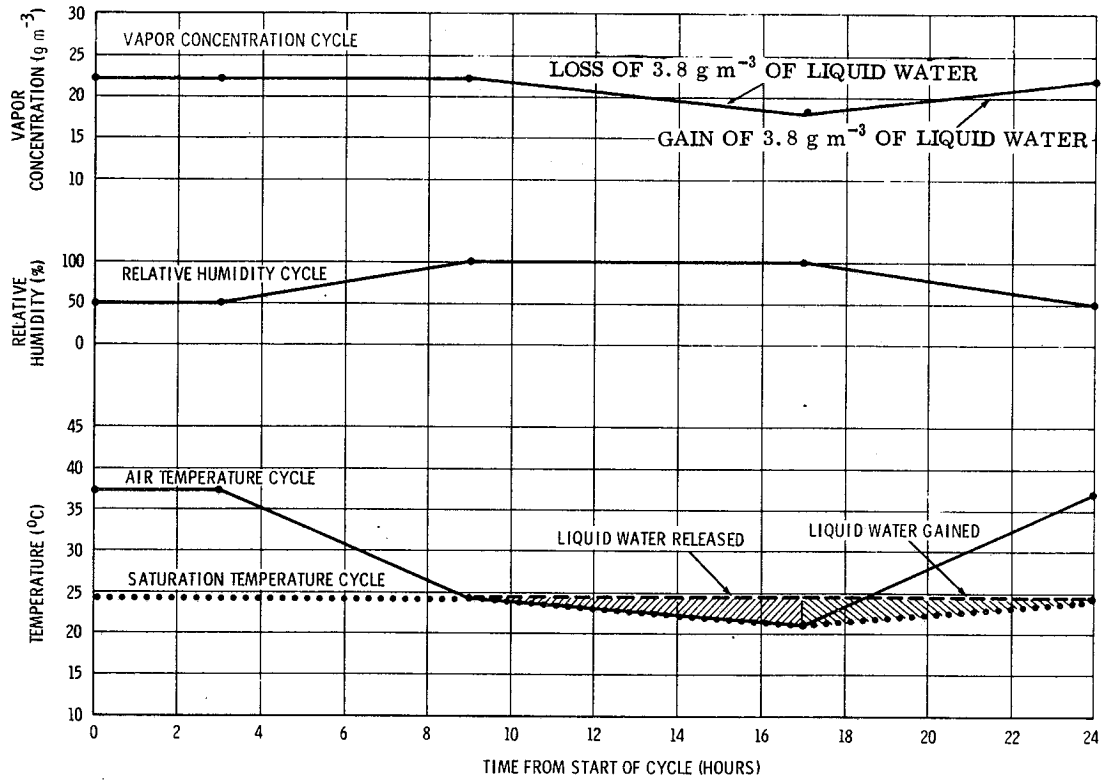


Figure 6.1 Extreme high vapor concentration cycle for Huntsville, New Orleans, and Kennedy Space Center.

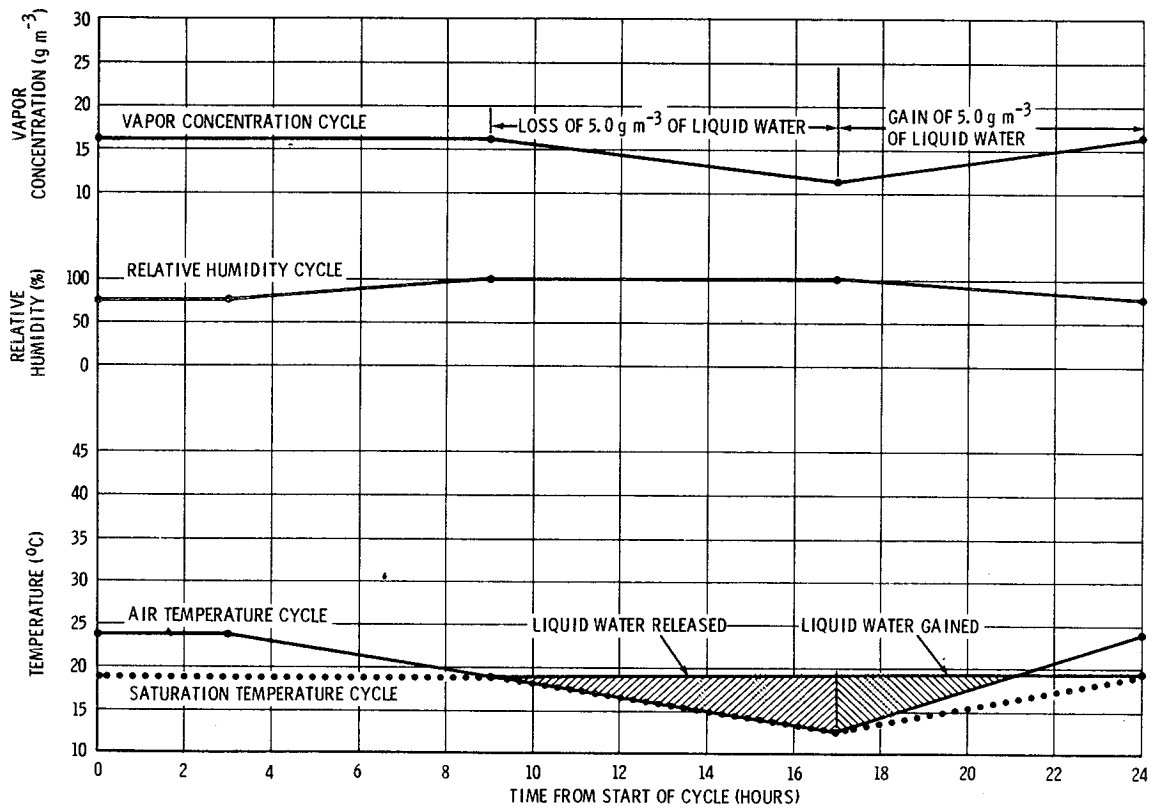


Figure 6.2 Extreme high vapor concentration cycle for the Vandenberg Air Force Base.

(2) Bacterial and fungal growth should present no problem because of the lower temperatures in this area. For corrosion, an extreme humidity of between 75 and 100 percent relative humidity and air temperature between 18.3°C (65°F) and 23.3°C (74°F) can be expected for a period of 15 days. The humidity should be 100 percent during one-fourth of the time at the lower temperature in cycles not exceeding 24 hr. Any loss of water vapor from the air condensation is replaced from outside sources to maintain at least 75 percent relative humidity at the higher temperature.

d. White Sands Missile Range: This area is located at 1216 m (4000 ft) above sea level and is on the eastern side of higher mountains. The mean annual rainfall of 250 cm (10 in.) is rapidly absorbed in the sandy soil. Fog rarely occurs. Therefore, at this location, a high vapor concentration over periods longer than a few hours need not be considered.

## 6.2.2 Low Vapor Concentration at Surface

### 6.2.2.1 Introduction

Low water-vapor concentration can occur at very low or at high temperatures when the air is very dry. In both cases, the dew points are very low. However, in the case of low dew points and high temperatures, the relative humidity is low. When any storage area or compartment of a vehicle is heated to temperatures well above the ambient air temperature (such as the high temperatures of the storage area in an aircraft standing on the ground in the sun), the relative humidity will be even lower than the relative humidity of the ambient air. These two types of low water-vapor concentrations have entirely different environment effects. In the case of low air temperatures, ice or condensation may form on equipment while in the high-temperature, low-humidity condition; organic materials may dry and split or otherwise deteriorate. When a storage area (or aircraft) is considerably warmer than the ambient air (even when the air is cold), the drying increases even more. Low relative humidities may also result in another problem — that of static electricity. Static electrical charges on equipment may ignite fuel or result in shocks to personnel when discharged. Because of this danger, two types of low water-vapor concentrations (dry extremes) are given for the surface.

### 6.2.2.2 Surface Extremes of Low Vapor Concentration.

#### a. Huntsville and White Sands Missile Range:

(1) A vapor concentration of  $2.1 \text{ g m}^{-3}$  ( $0.9 \text{ gr ft}^{-3}$ ), with an air temperature of  $-11.7^\circ\text{C}$  ( $+11^\circ\text{F}$ ) and a relative humidity between 98 and 100 percent for a duration of 24 hr, must be considered.

(2) A vapor concentration of  $4.5 \text{ g m}^{-3}$  ( $2.0 \text{ gr ft}^{-3}$ ), corresponding to a dew point of  $-1.1^\circ\text{C}$  ( $30^\circ\text{F}$ ) at an air temperature of  $28.9^\circ\text{C}$  ( $84^\circ\text{F}$ ) and a relative humidity of 15 percent occurring for 6 hr each 24 hr, and a maximum relative humidity of 34 percent at an air temperature of  $15.6^\circ\text{C}$  ( $60^\circ\text{F}$ ) for the remaining 18 hr of each 24 hr for a 10-day period, must be considered.

#### b. New Orleans and Kennedy Space Center:

(1) A vapor concentration of  $4.2 \text{ g m}^{-3}$  ( $1.8 \text{ gr ft}^{-3}$ ), with an air temperature of  $-2.2^\circ\text{C}$  ( $28^\circ\text{F}$ ) and a relative humidity of 98 to 100 percent for a duration of 24 hr, must be considered.

(2) A vapor concentration of  $5.6 \text{ g m}^{-3}$  ( $2.4 \text{ gr ft}^{-3}$ ) corresponding to a dew point of  $2.2^\circ\text{C}$  ( $36^\circ\text{F}$ ) at an air temperature of  $22.2^\circ\text{C}$  ( $72^\circ\text{F}$ ) and a relative humidity of 29 percent occurring for 8 hr, and a maximum relative humidity of 42 percent at an air temperature of  $15.6^\circ\text{C}$  ( $60^\circ\text{F}$ ) for the remaining 16 hr of each 24 hr for 10 days, must be considered.



c. Vandenberg Air Force Base:

(1) A vapor concentration of  $4.2 \text{ g m}^{-3}$  ( $1.8 \text{ gr ft}^{-3}$ ), with an air temperature of  $-2.2^{\circ}\text{C}$  ( $28^{\circ}\text{F}$ ) and a relative humidity of 98 to 100 percent for a duration of 24 hr, must be considered.

(2) A vapor concentration of  $4.8 \text{ g m}^{-3}$  ( $2.1 \text{ gr ft}^{-3}$ ), corresponding to a dew point of  $0.0^{\circ}\text{C}$  ( $32^{\circ}\text{F}$ ) at an air temperature of  $37.8^{\circ}\text{C}$  ( $100^{\circ}\text{F}$ ) and a relative humidity of 11 percent occurring for 4 hr each 24 hr, and a maximum relative humidity of 26 percent at an air temperature of  $21.1^{\circ}\text{C}$  ( $70^{\circ}\text{F}$ ) for the remaining 20 hr of each 24 hr for 10 days, must be considered.

### 6.2.3 Compartment Vapor Concentration at Surface

A low water-vapor concentration extreme of  $10.1 \text{ g m}^{-3}$  ( $4.4 \text{ gr ft}^{-3}$ ), corresponding to a dew point of  $11.1^{\circ}\text{C}$  ( $52^{\circ}\text{F}$ ) at a temperature of  $87.8^{\circ}\text{C}$  ( $190^{\circ}\text{F}$ ) and a relative humidity of 2 percent occurring for 1 hr, a linear change over a 4-hr period to an air temperature of  $37.8^{\circ}\text{C}$  ( $100^{\circ}\text{F}$ ) and a relative humidity of 22 percent occurring for 15 hr, then a linear change over a 4-hr period to the initial conditions, must be considered at all locations.

## 6.3 Vapor Concentration at Altitude

In general, the vapor concentration decreases with altitude in the troposphere because of the decrease of temperature with altitude. The data given in this section on vapor concentration are appropriate for design purposes.

### 6.3.1 High Vapor Concentration at Altitude

The following tables present the relationship between maximum vapor concentration and the associated temperature normally expected as a function of altitude (Ref. 6.8).

- a. Maximum Vapor Concentrations for Kennedy Space Center, Table 6.1.
- b. Maximum Vapor Concentrations for White Sands Missile Range, Table 6.2.
- c. Maximum Vapor Concentrations for Vandenberg AFB, Table 6.3.

### 6.3.2 Low Vapor Concentration at Altitude

The values presented as low extreme vapor concentrations in the following tables are based on data measured by standard radiosonde equipment.

- a. Minimum Vapor Concentrations for Kennedy Space Center, Table 6.4.
- b. Minimum Vapor Concentrations for White Sands Missile Range, Table 6.5.
- c. Minimum Vapor Concentrations for Vandenberg AFB, Table 6.6.

TABLE 6.1 MAXIMUM VAPOR CONCENTRATION FOR  
KENNEDY SPACE CENTER

Geometric Altitude		Vapor Concentration		Temperature Associated with Maximum Vapor Concentration	
(km)	(ft)	(g m <sup>-3</sup> )	(gr ft <sup>-3</sup> )	(°C)	(°F)
SFC (0.005 MSL)	(16)	27.0	11.8	30.5	87
1	3,300	19.0	8.3	24.5	76
2	6,600	13.3	5.8	18.0	64
3	9,800	9.3	4.1	12.0	54
4	13,100	6.3	2.8	5.5	42
5	16,400	4.5	2.0	-0.5	31
6	19,700	2.9	1.3	-6.8	20
7	23,000	2.0	0.9	-13.0	9
8	26,200	1.2	0.5	-20.0	-4
9	29,500	0.6	0.3	-27.0	-17
10	32,800	0.3	0.1	-34.5	-30
16.2	53,100	0.025	0.01	-57.8	-72
20	65,600	0.08	0.03	-47.8	-54

TABLE 6.2 MAXIMUM VAPOR CONCENTRATION FOR  
WHITE SANDS MISSILE RANGE

Geometric Altitude		Vapor Concentration		Temperature Associated with Maximum Vapor Concentration	
(km)	(ft)	(g m <sup>-3</sup> )	(gr ft <sup>-3</sup> )	(°C)	(°F)
SFC (1.2 MSL)	(3,989)	16.0	7.0	21.5	71
2	6,600	13.2	5.8	18.9	66
3	9,800	9.0	3.9	12.8	55
4	13,100	6.8	3.0	7.8	46
5	16,400	4.9	2.1	2.2	36
6	19,700	3.4	1.5	-2.2	28
7	23,000	2.2	1.0	-10.0	14
8	26,200	1.3	0.6	-16.1	3
9	29,500	0.6	0.3	-22.8	-9
10	32,800	0.2	0.1	-30.0	-22
16.5	54,100	0.08	0.03	-47.8	-54
20	65,600	0.05	0.02	-52.2	-62

TABLE 6.3 MAXIMUM VAPOR CONCENTRATION FOR  
VANDENBERG AFB

Geometric Altitude		Vapor Concentration		Temperature Associated with Maximum Vapor Concentration	
(km)	(ft)	(g m <sup>-3</sup> )	(gr ft <sup>-3</sup> )	(°C)	(°F)
SFC (0.113 MSL)	371	17.5	7.6	30.5	86.9
1	3,300	14.8	6.5	24.2	75.6
2	6,600	10.0	4.4	20.6	69.1
3	9,800	7.5	3.3	11.0	51.8
4	13,100	5.0	2.2	4.7	40.5
5	16,400	3.7	1.6	- 1.4	29.5
6	19,700	2.3	1.0	- 8.1	17.4
7	23,000	1.6	0.7	-12.5	9.5
8	26,200	0.8	0.3	-20.2	- 4.4
9	29,500	0.4	0.2	-28.2	-18.8
10	32,800	0.2	0.1	-34.3	-29.7

TABLE 6.4 MINIMUM VAPOR CONCENTRATION FOR  
KENNEDY SPACE CENTER

Geometric Altitude		Vapor Concentration		Temperature Associated with Minimum Vapor Concentration	
(km)	(ft)	(g m <sup>-3</sup> )	(gr ft <sup>-3</sup> )	(°C)	(°F)
SFC (0.005 MSL)	(16)	4.0	1.7	29	84.2
1	3,300	0.5	0.2	6	42.8
2	6,600	0.2	0.1	0	32.0
3	9,800	0.1	0.04	-11	12.2
4	13,100	0.1	0.04	-14	6.8

TABLE 6.5 MINIMUM VAPOR CONCENTRATION FOR  
WHITE SANDS MISSILE RANGE

Geometric Altitude		Vapor Concentration		Temperature Associated with Minimum Vapor Concentration	
(km)	(ft)	(g m <sup>-3</sup> )	(gr ft <sup>-3</sup> )	(°C)	(°F)
SFC (1.2 MSL)	(3, 989)	1.2	0.5	-1	30.2
2	6, 600	0.9	0.4	-5	23.0
3	9, 800	0.6	0.3	-12	10.4
4	13, 100	0.4	0.2	-20	-4.0
5	16, 400	0.2	0.1	-26	-14.8
6	19, 700	0.1	0.04	-36	-32.8
7	23, 000	0.09	0.03	-42	-43.6
8	26, 200	0.07	0.03	-49	-56.2
9	29, 500	0.03	0.01	-55	-67.0
10	32, 800	0.02	0.01	-60	-76.0

TABLE 6.6 MINIMUM VAPOR CONCENTRATION FOR  
VANDENBERG AFB

Geometric Altitude		Vapor Concentration		Temperature Associated with Maximum Vapor Concentration	
(km)	(ft)	(g m <sup>-3</sup> )	(gr ft <sup>-3</sup> )	(°C)	(°F)
SFC (0.113 MSL)	371	1.6	0.7	4.5	40.1
1	3, 300	0.7	0.3	- 1.4	29.5
2	6, 600	0.4	0.2	- 7.5	18.5
3	9, 800	0.3	0.1	-12.6	9.3
4	13, 100	0.1	0.04	-19.4	- 2.9
5	16, 400	0.07	0.03	-27.3	-17.1
6	19, 700	0.03	0.01	-35.1	-31.2
7	23, 000	0.02	0.009	-39.5	-39.1

## REFERENCES

- 6.1 "Glossary of Meteorology." American Meteorological Society, Boston, Mass., 1959.
- 6.2 Sheppard, P. A.: "The Physical Properties of Air With Reference to Meteorological Practice and the Air-Conditioning Engineer." ASME, Vol. 71, 1949, pp. 915-919.
- 6.3 "Climatic and Environmental Criteria for Aircraft Design." ANC-22 Munitions Board Aircraft Committee, 1952.
- 6.4 "Military Standard, Environmental Test Methods." MIL-STD-810C, March 10, 1975.
- 6.5 Sissenwine, Norman; and Court, Arnold: "Climatic Extremes for Military Equipment." Report No. 146, Environmental Protection Branch, Research and Development Division, Office of the Quartermaster General, Washington, D.C., 1951.
- 6.6 Sverdrup, H. V.: "Oceanography for Meteorologists." Prentice-Hall, Inc., New York, 1942.
- 6.7 "External Tank Verification Plan." MMC-ET-TM01-B, Contract No. NAS8-30300, WBS No. 1.6.2.2, DR. NO. TM01, Martin Marietta, Michoud Assembly Facility, New Orleans, La., Sept. 9, 1974.
- 6.8 Sissenwine, Norman; Grantham, D. D.; and Salmela, H. A.: "Mid-Latitude Humidity to 32 Km." Journal of the Atmosphere Sciences, Vol. 25, 1968, pp. 1129-1140.



## SECTION VII. ATMOSPHERIC PRESSURE AND DENSITY (SURFACE)

### 7.1 Atmospheric Pressure

#### 7.1.1 Definition

Atmospheric pressure (also called barometric pressure) is the force exerted, as a consequence of gravitational attraction, by the mass of the column of air of unit cross section lying directly above the area in question.

#### 7.1.2 Surface Pressure

The total variation of pressure from day to day is relatively small. Rapid but slightly greater variations occur as the result of the passage of frontal systems, while the passage of a hurricane can cause somewhat larger, but still not significant, changes for pressure environment design of space vehicles. Surface pressure extremes for various locations and their extreme ranges are given in Table 7.1. The data at these locations were mostly taken from their respective surface weather observation summaries (Ref. 7.1). See Section VIII for extreme pressures across the United States. The pressure drop in a tornado can exceed 20 percent of ambient during the few seconds of its passage.

#### 7.1.3 Pressure Change

- a. A gradual rise or fall in pressure of 3 mb ( $0.04 \text{ lb in.}^{-2}$ ) and then a return to original pressure can be expected over a 24-hr period.
- b. A maximum pressure change (frontal passage change) of 6 mb ( $0.09 \text{ lb in.}^{-2}$ ) (rise or fall) can be expected within a 1-hr period at all localities.

#### 7.1.4 Pressure Decrease with Altitude

- a. Pressure decrease is approximately logarithmic with height. Materials transported in mountainous terrain or in cargo compartments of aircraft must be packaged to stand the pressure differential without damage. Near sea level (i.e.,  $< 3 \text{ km}$ ) the pressure will vary about 1 mb for each 10-m change in altitude. Figure 7.1 shows the standard atmospheric pressure decrease with altitude (Ref. 7.2).

- b. More detailed data on pressure distribution with altitude are given in Section III.

### 7.2 Atmospheric Density

#### 7.2.1 Definition

Density is the ratio of the mass of a substance to its volume. (It also is defined as the reciprocal of specific volume.) Density is usually expressed in grams per cubic centimeter or kilograms per cubic meter.

TABLE 7.1 SURFACE PRESSURE EXTREMES (values apply to  
station altitude above MSL) [Ref. 7.1]

Location	Units	Pressure			Station Elevation	
		Maximum	Mean	Minimum**	ft	m
Huntsville	N m <sup>-2</sup> mb lb in. <sup>-2</sup>	102 080 1 020.8 14.8	99 540 995.4 14.4	97 210 972.1 14.1	644	196
Kennedy Space Center		103 600 1 036.0 15.0	101 670 1 016.7 } * 14.7	99 970 999.7 14.5	16 9***	5 2.7***
Vandenberg AFB		102 000 1 020.0 14.8	100 250 1 002.5 } * 14.5	99 010 990.1 14.4	371 368***	113 112.2***
Edwards AFB		95 560 955.6 13.9	93 410 934.1 } * 13.5	92 030 920.3 13.3	2316 2302***	706 701.7***
New Orleans		104 160 1 041.6 15.1	101 780 1 017.8 14.8	99 900 999.0 14.5	6	2
NSTL/Bay St. Louis		104 410 1 044.1 15.1	101 640 1 016.4 14.7	99 150 991.5 14.4	31	9
Johnson Space Center		103 960 1 039.6 15.1	101 530 1 015.3 14.7	99 530 995.3 14.4	50	15
White Sands Missile Range		89 010 890.1 12.9	87 130 871.3 } * 12.6	85 200 852.0 12.4	4239	1292

\* The mean values given here will differ from the median surface values as given in Tables 3.7, 3.8, 3.9, and Ref. 3.4 of Section III.

\*\* Hurricane-influenced low pressures are not given here.

\*\*\* Runway elevations above MSL.



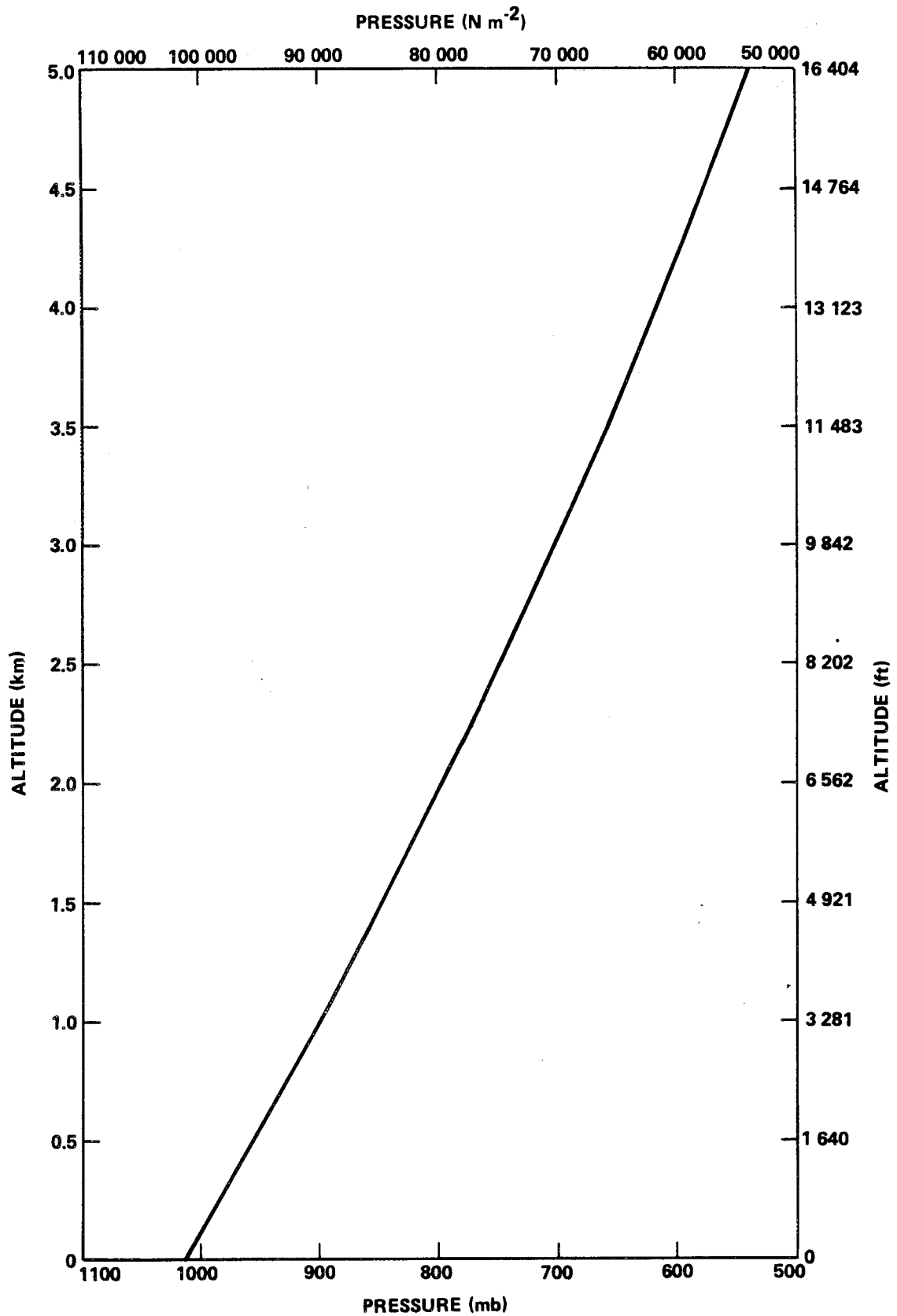


Figure 7.1 Pressure change with altitude for packaging materials (Ref. 7.2).

## 7.2.2 Surface Density

The variation of the density of the atmosphere at the surface from the average for any one station, and between the areas of interest, is small and should have no important effect on preflight operations. Table 7.2 gives the median density at the surface for the four test ranges.

TABLE 7.2 MEDIAN SURFACE DENSITIES

Area	Surface Altitude	Source of Data	Density	
	m*		kg m <sup>-3</sup>	lb ft <sup>-3</sup>
Kennedy Space Center	5	(Ref. 7.3)	1.1830	$7.385 \times 10^{-2}$
Vandenberg AFB	113	(Ref. 7.4)	1.2190	$7.610 \times 10^{-2}$
White Sands Missile Range	1292	(Ref. 7.5)	1.0418	$6.504 \times 10^{-2}$
Edwards AFB	706	(Ref. **)	1.1210	$6.998 \times 10^{-2}$

\* Station elevation above mean sea level.

\*\* Edwards surface density value from Section III, Table 3.9.

However, atmospheric density, especially low density, is important to aircraft takeoff and landing operations and should therefore be considered when planning Space Shuttle orbiter ferry flights. Table 7.3 gives low density values that are equaled or exceeded approximately 5 percent of the time during the hottest part of the day in summer. Typical associated temperatures needed for engine power calculations are also listed. Since low density is found at high elevation and high temperatures, only the highest enroute airfield and the ferry flight terminals were considered. Since Kennedy Space Center and Vandenberg AFB extremes are given in Section III, only Edwards AFB and Biggs AFB are listed here.

TABLE 7.3 LOW DENSITY (5 PERCENTILE WORST) AND ACCOMPANYING TEMPERATURES FOR ORBITER FERRY OPERATIONS

Location	Low Density		Temperature	
	kg m <sup>-3</sup>	% Departure <sup>a</sup> from US 76	°C	°F
Edwards AFB California	1.0246	-10.5	39.4	103
Biggs AFB Texas	0.97555	-10.5	38	100

a. Departure from U.S. Standard Atmosphere [7.2].

### 7.3 Surface Density Variability and Altitude Variations

Data on the variation of surface density and density aloft about its median annual values can be found in Section III. The Global Reference Atmosphere (Ref. 7.6) will also provide density values versus altitude together with variability, by month, for any point on the globe.

#### REFERENCES

- 7.1 "Revised Uniform Summary of Surface Weather Observations – Edwards AFB, California." Part F, USAF-ETAC, Data Processing Division, Air Weather Service (MAC), Federal Building, Asheville, North Carolina, March 20, 1974.
- 7.2 "U.S. Standard Atmosphere, 1976," United States Government Printing Office, Washington, D.C., October 1976.
- 7.3 Smith, O. E.; and Weidner, Don K.: "A Reference Atmosphere for Patrick AFB, Florida, Annual (1963 Revision)." NASA TM X-53139, 1964. NASA-Marshall Space Flight Center, Huntsville, Alabama.
- 7.4 Carter, E. A.; and Brown, S. C.: "A Reference Atmosphere for Vandenberg AFB, California, Annual (1971 Version)." NASA TM X-64590, NASA-Marshall Space Flight Center, Alabama, 1971.
- 7.5 "White Sands Missile Range Reference Atmosphere (Part I)," 1964. IRIG Document No. 104-63, Secretariat, Range Commander's Council, White Sands Missile Range, New Mexico.
- 7.6 Justus, C. G., et al.: "The NASA/MSFC Global Reference Atmospheric Model – MOD3 (with Spherical Harmonic Wind Model)." NASA CR-3256, March 1980, NASA-Marshall Space Flight Center, Huntsville, Alabama.



## SECTION VIII. UNITED STATES SURFACE EXTREMES

### 8.1 Introduction

Most NASA programs involving the launch and re-entry of space vehicles are conducted in the continental United States. This section provides the extremes of those meteorological variables not included elsewhere in this document that are critical to such programs. Statistical data discussed in this section include air temperature, snowfall, hail, and atmospheric pressure. Section IX, Worldwide Surface Extremes, provides a more general discussion of atmospheric extremes on a global scale.

### 8.2 Environments Included

- (a) Air temperature, extreme maximum and minimum;
- (b) Snowfall -- snow loads, 24-hr maximum and storm maximum;
- (c) Hail, maximum size;
- (d) Atmosphere pressure, extreme maximum and minimum.

Information is available for other extreme atmospheric parameters relative to the principal locations covered by this document, by consulting the appropriate section in this document.

### 8.3 Source of Data

The extremes presented have been prepared using data from National Weather Service stations and published articles, such as Reference 8.1. These extremes represent the highest or lowest extreme value measured at each station. The length of record varies from station to station, but most values represent more than 15 years of record. Where unusual geographical features in a local area affect an extreme value (such as the minimum temperature on a high mountain peak), it will not in general be shown on the maps presented unless a Weather Service station is located there.

The extremes noted reflect measurements during the available period of record for essentially all meteorological parameters. Because this period of record covers only a few decades for most locations, it is obvious that there is a finite risk that extreme values used will be exceeded in future years. However, the values shown are considered appropriate as criteria guidelines for use in critical engineering design studies relative to probable occurrence of meteorological extremes during expected operational lifetime.

## 8.4 Extreme Design Environments<sup>1</sup>

### 8.4.1 Air Temperature

The distribution, by state and location, of extreme maximum air temperatures in the United States is shown in Figure 8.1, while Figure 8.2 shows the extreme minimum temperature distribution. Given in Table 8.1 are the extreme U. S. temperatures (°F) together with their locations and dates of occurrence (Ref. 8.2). To convert to °C, use the formula: °C = 5/9(°F-32). The maps (Figs. 8.3 and 8.4) from Reference 8.3 show the mean temperature and standard deviations of the temperatures for January and July.

To estimate the temperature  $\hat{T}$  that is less than or equal to a probability  $p$  (corresponding to the normal distribution), from Figures 8.3 and 8.4, find from the appropriate figure, by interpolation as needed, the mean temperature  $\bar{T}$  and standard deviation  $S_T$  and substitute these in the equation

$$\hat{T} = \bar{T} + S_T \cdot y_s \text{ [°F]} .$$

Values of  $y_s$  for various normal probability levels are:

Cold Temperatures (Figure 8.3)		Hot Temperatures (Figure 8.4)	
$p$	$y_s$	$p$	$y_s$
0.20	-0.84	0.80	+0.84
0.10	-1.28	0.90	+1.28
0.05	-1.65	0.95	+1.65 (See footnote 2.)
0.025	-1.96	0.975	+1.96
0.01	-2.33	0.99	+2.33

### 8.4.2 Snowfall – Snow Load

The maps in Figures 8.5 and 8.6 show the maximum depth of snow and the corresponding snow loads. Figure 8.5 shows the maximum depth for a 24-hr period; Figure 8.6 shows the maximum depth and the corresponding snow loads for a storm period. The storm total map shows the same snow depth as in the 24-hr map in the southern low elevation areas of the United States since snow storms seldom exceed 24 hr in these areas. The greatest 24-hr snowfall was 1930 mm (76 in.) at Silver Lake, Colorado, on April 14-15, 1921. One storm gave 4800 mm (189 in.) at Mt. Shasta Ski Bowl, California, from February 13 to 19, 1959 (Ref. 8.4).

The terrain combined with the general movement of weather patterns has a great effect on the amount of fall, accumulation, and melting of the snow. Also, the length of a single storm varies for various areas. In some areas in mountain regions much greater amounts of snowfall have been recorded than shown

1. All values of extreme maxima and minima in this section are for design guidelines and may or may not exactly reflect extrapolations (theoretical or otherwise) of actual measured values over the available period of record.
2. The 95th percentile value is recommended for hot-day design ambient temperatures over runways for landing-takeoff performance calculation using Figure 8.4; the 5th percentile is for cold-day design.

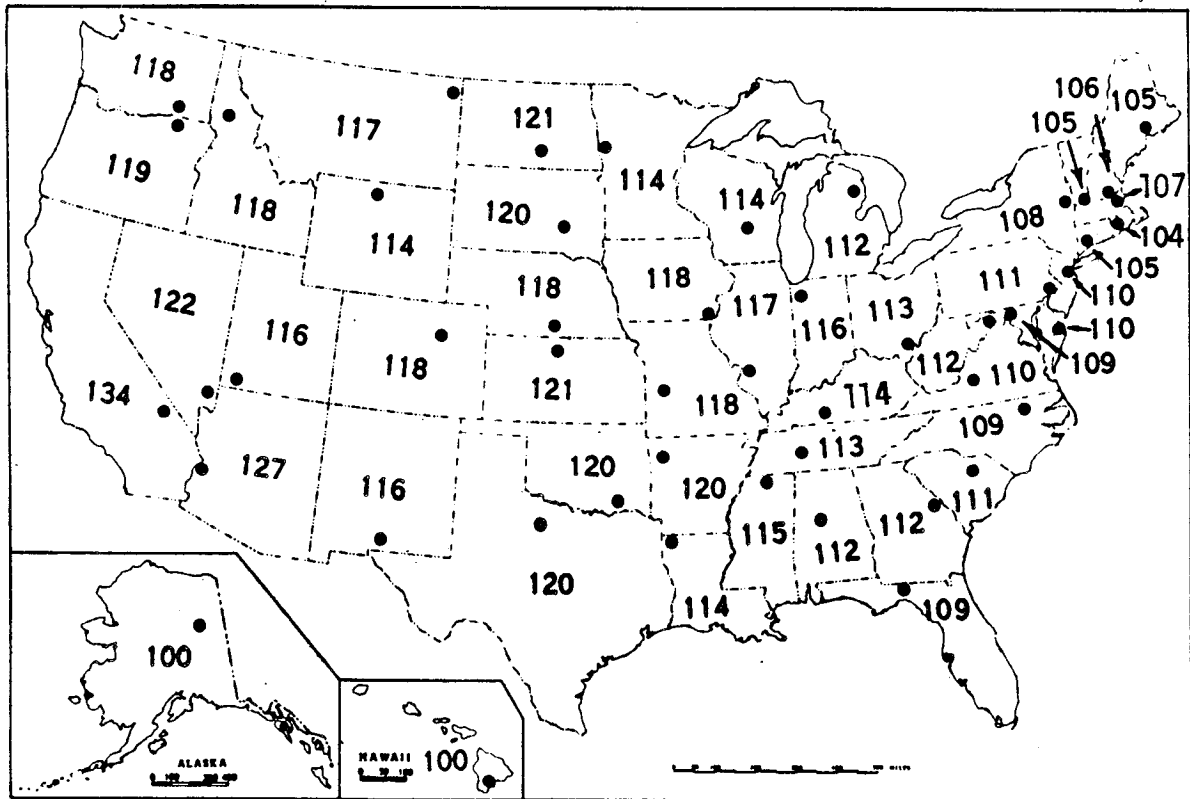


Figure 8.1 Highest temperatures (°F) of record and locations, by states.

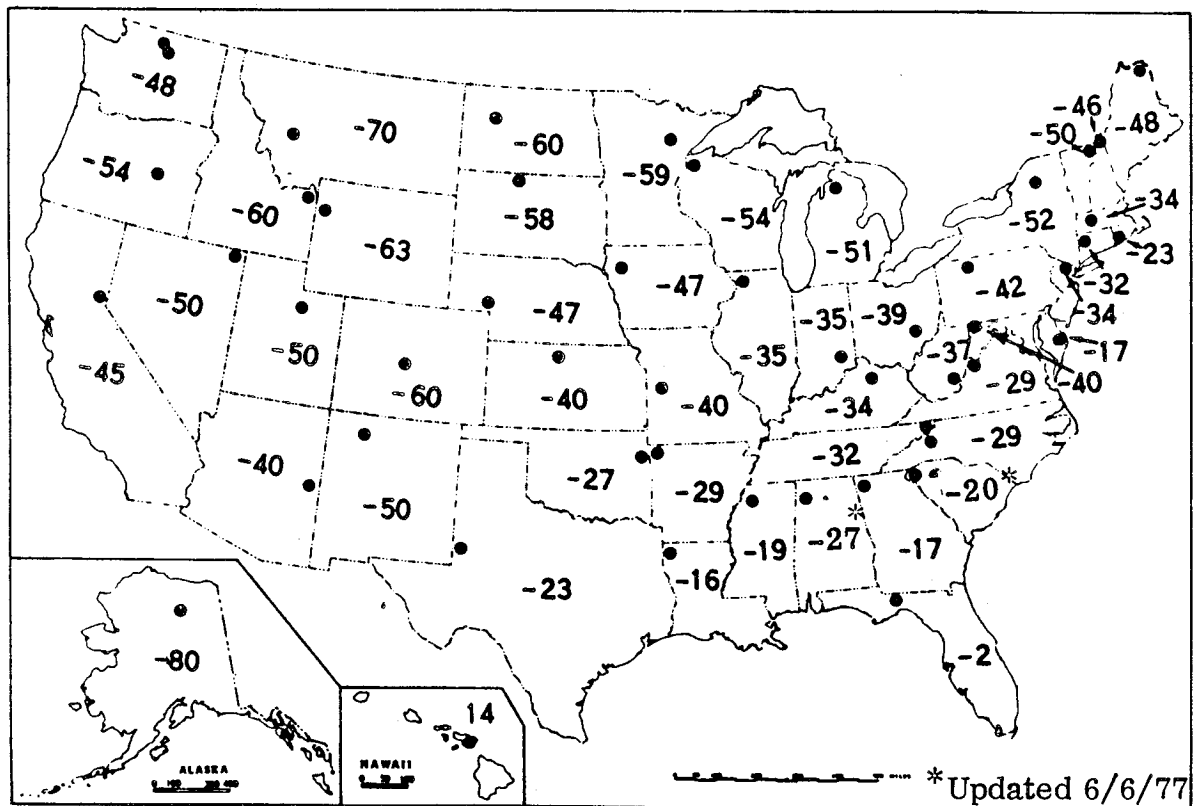


Figure 8.2 Lowest temperatures (°F) of record and locations, by states.

TABLE 8.1 EXTREMES OF TEMPERATURE AND SEA-LEVEL PRESSURE FOR THE UNITED STATES

Temperature [°C (°F)]		Location	Date	Sea-Level Pressure [N/m <sup>2</sup> (mb)(in.)]	Location	Date
High				High		
Contiguous United States	57 (134)	Greenland Ranch, Ca.	July 10, 1913	106 330 (1063.3) (31.40)	Helena, Mont.	Jan. 9, 1962
Hawaii	38 (100)	Pahala	April 27, 1931	102 670 (1026.7) (30.32)	Honolulu	Feb. 10, 1919
Alaska	38 (100)	Fort Yukon	June 27, 1915	106 430 (1064.3) (31.43)	Barrow	Jan. 3, 1970
Low				Low		
Contiguous United States	-57 (-70)	Rogers Pass, Mont.	Jan. 20, 1954	95 490 (954.9) (28.20)	Canton, N.Y. Block Island, R.I.	Jan. 3, 1913 Mar. 7, 1932
U.S. (Hurricane)				89 230 (892.3) (26.35)	Matecumbe Key, Fla.	Sept. 2, 1935
Hawaii	-11 (12)	Mauna Kea Observatory	May 17, 1979	99 050 (990.5) (29.25)	Lihue	Aug. 6, 1959
Alaska	-62 (-80)	Prospect Creek	Jan. 23, 1971	92 500 (925.0) (27.31)	Dutch Harbor	Oct. 25, 1977



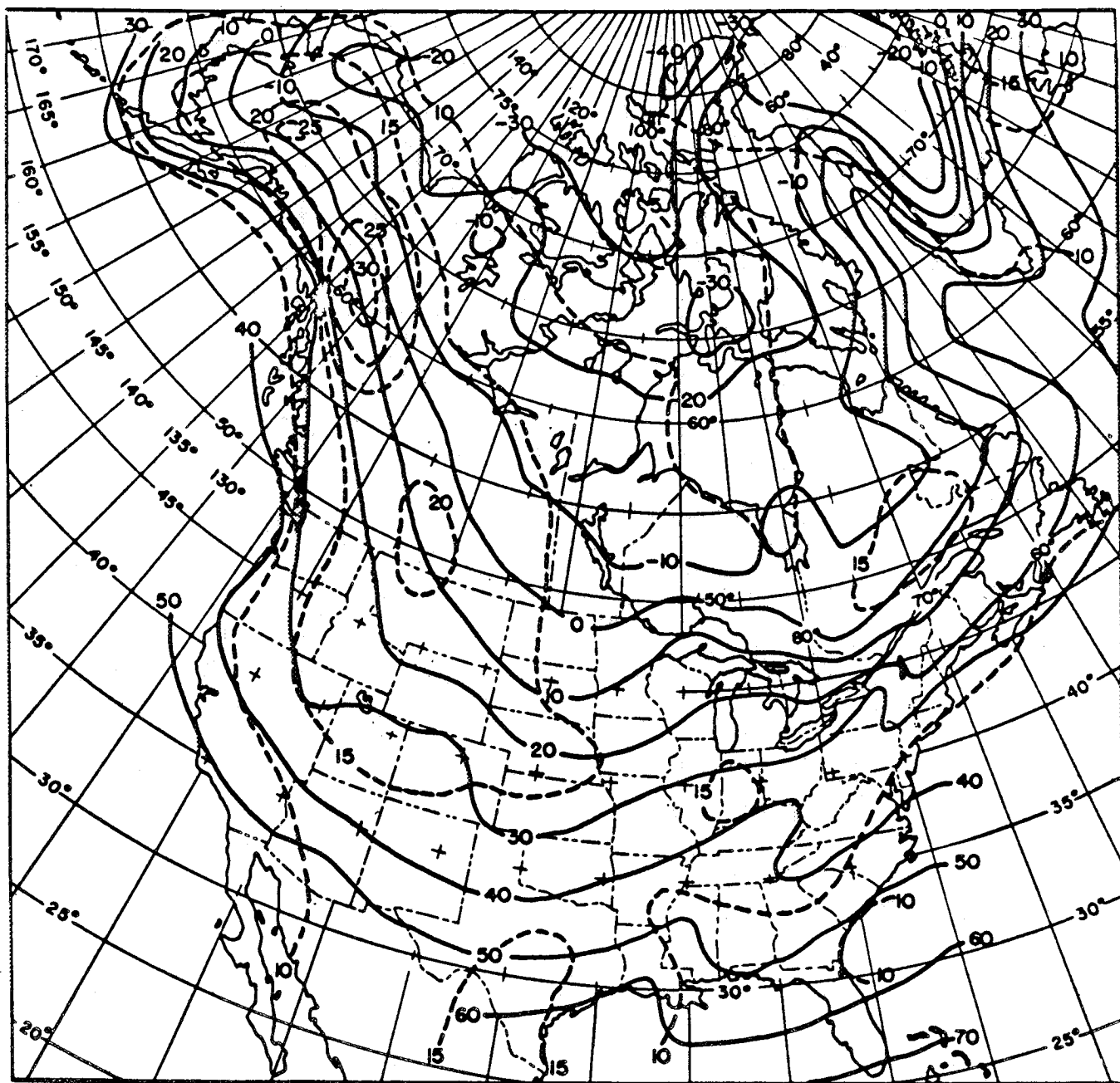


Figure 8.3 Isotherms of January hourly surface temperatures. (Approximate mean values ( $^{\circ}\text{F}$ ) are shown by solid lines, standard deviations ( $^{\circ}\text{F}$ ) by broken lines. The approximations were made to give best estimates of lower 1- to 20-percentile values of temperature by normal distribution [Ref. 8.3].)

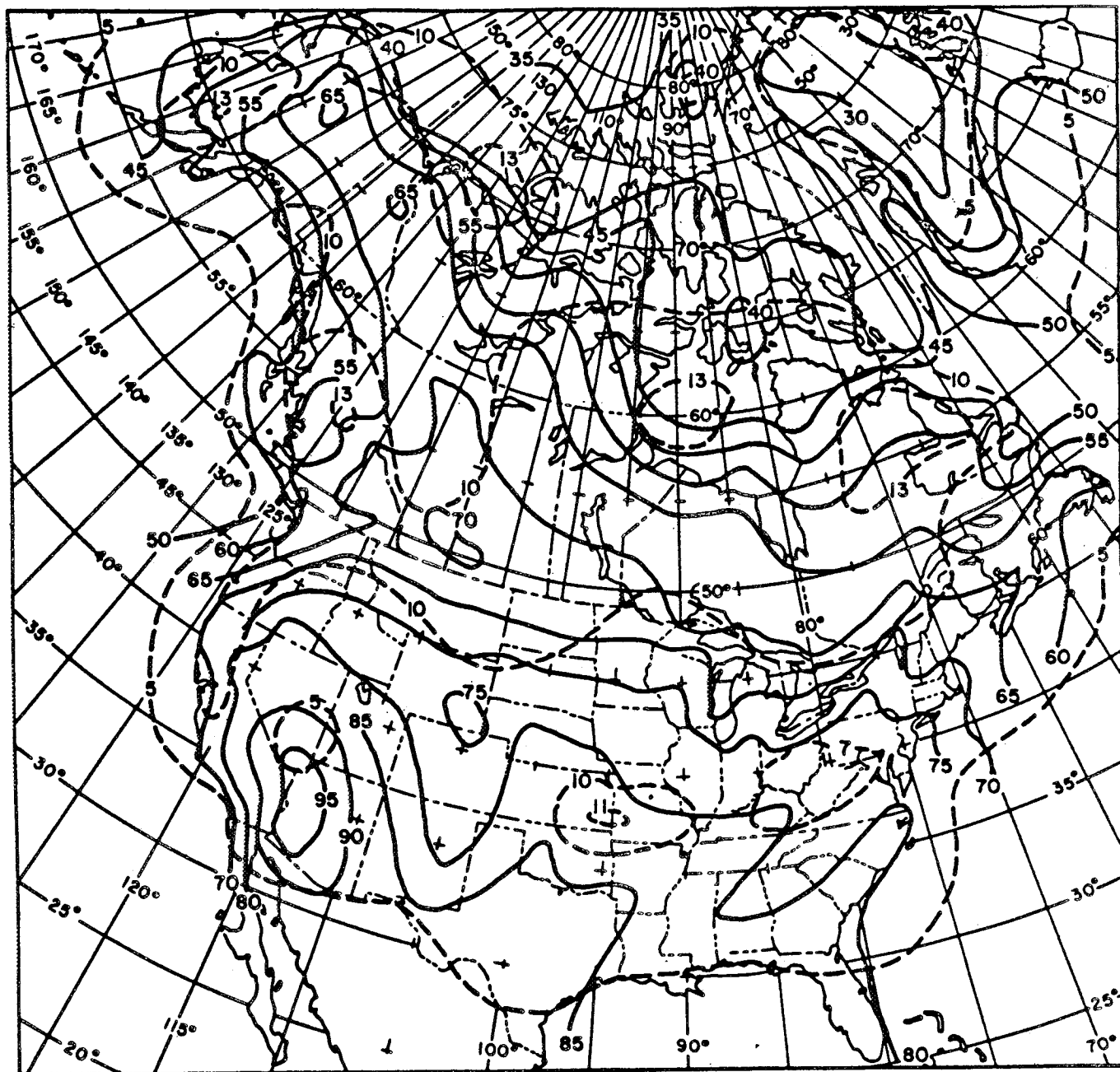
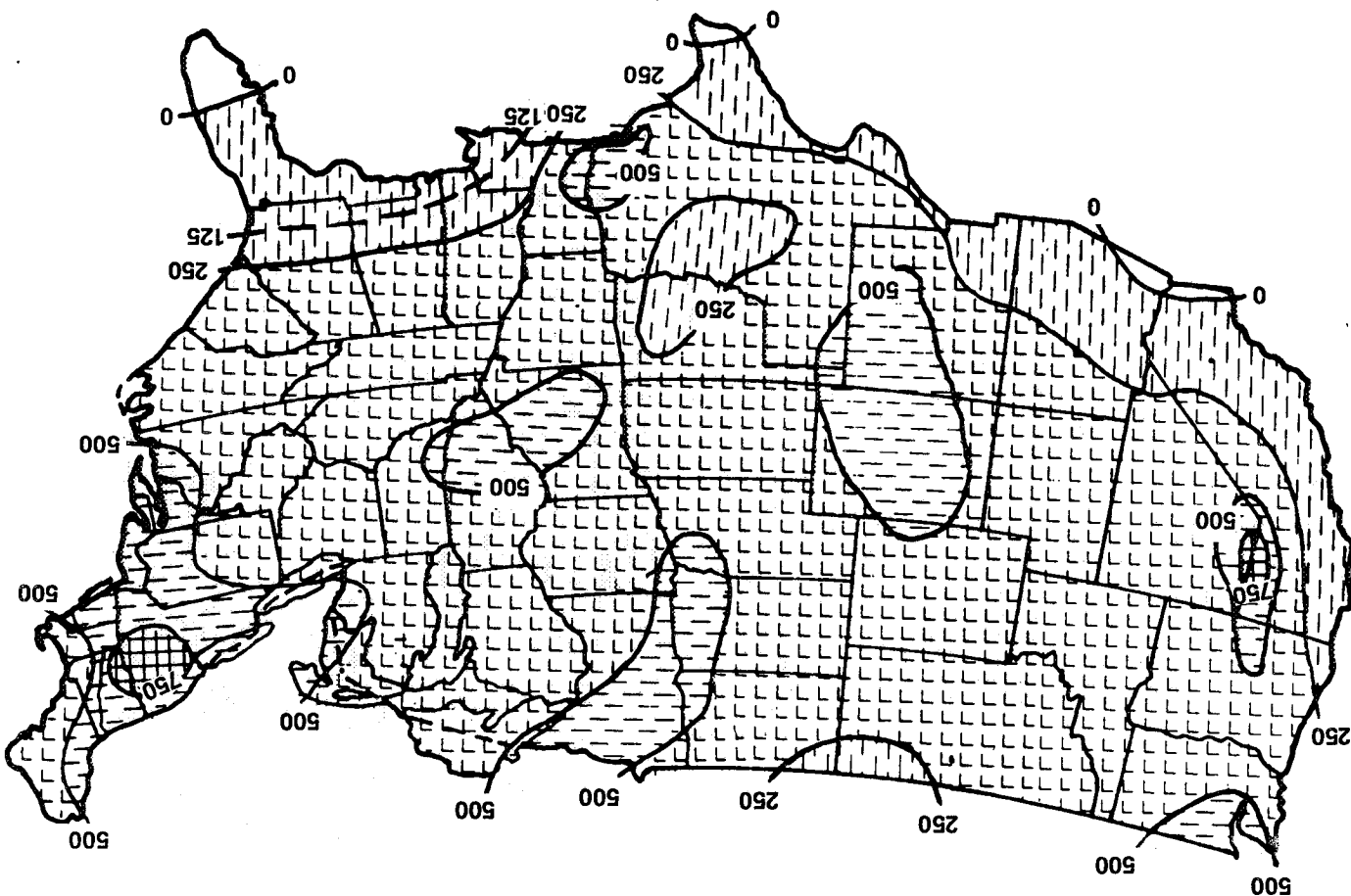


Figure 8.4 Isotherms of July hourly surface temperatures. (Approximate mean values ( $^{\circ}\text{F}$ ) are shown by solid lines, standard deviations ( $^{\circ}\text{F}$ ) by broken lines. The approximation were made to yield the best estimates of upper 80- to 99-percentile values by normal distribution [Ref. 8.3].)



### MAXIMUM SNOW LOAD

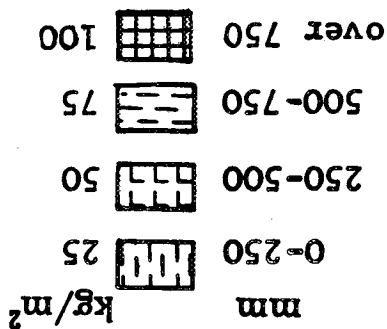
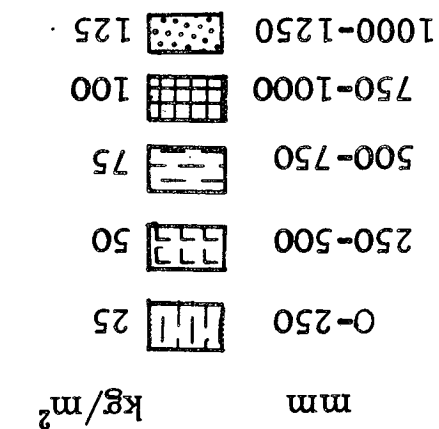
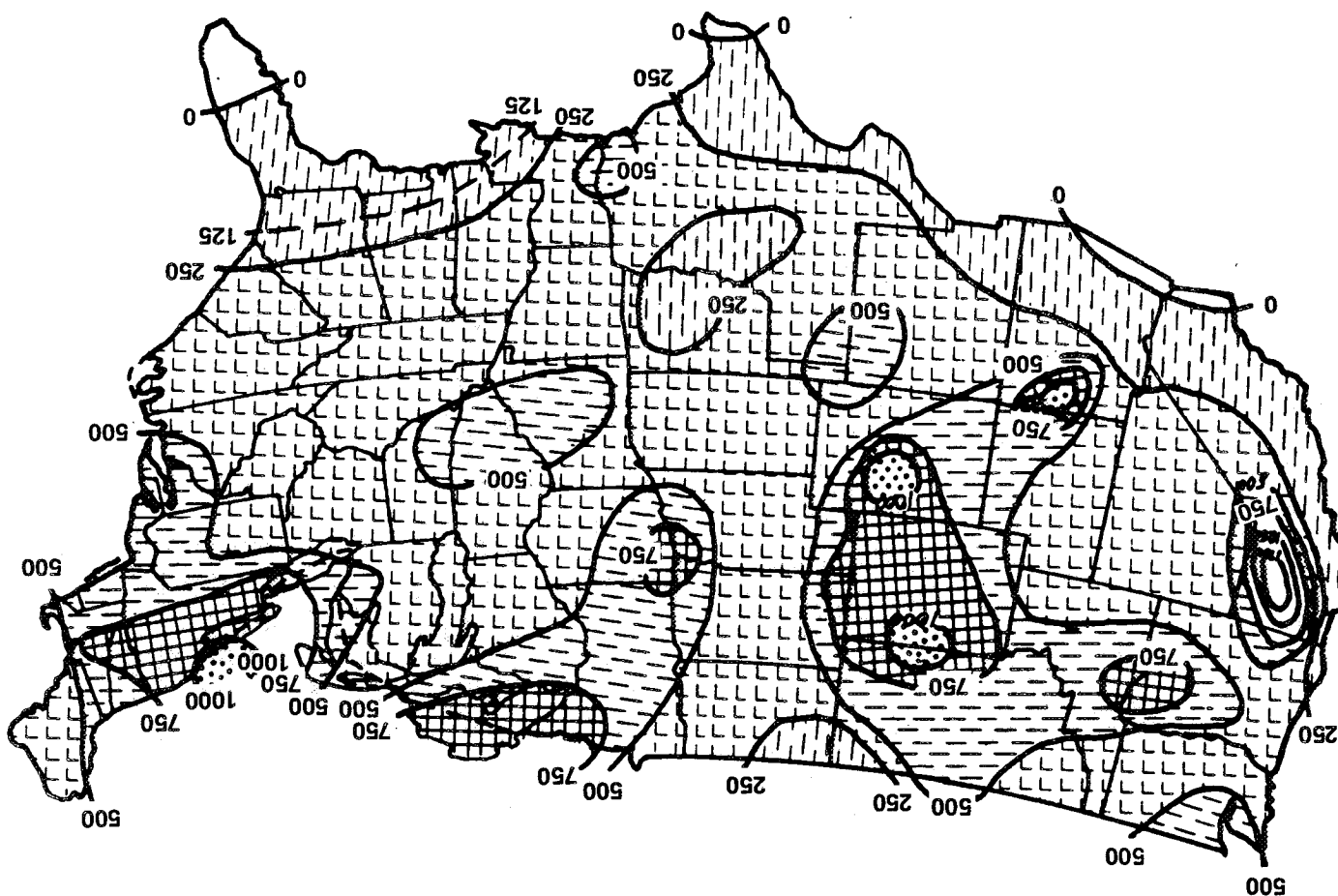


Figure 8.5 Extreme 24-hr maximum snowfall (mm).

Figure 8.6 Extreme storm maximum snowfall (mm).



# MAXIMUM SNOW LOAD



ORIGINAL PAGE IS  
OF POOR QUALITY

on the maps. Also, the snow in these areas may remain for the entire winter. For example, in a small valley near Soda Springs, California, a seasonal snow accumulation of 7.9 m (26 ft) with a density of about  $0.35 \text{ g/cm}^3$  was recorded. This gives a snow load of  $2772 \text{ kg/m}^2$  ( $567.7 \text{ lb/ft}^2$ ). Such a snow pack can do considerable damage to improperly protected equipment buried deep in the snow. This snow pack at Soda Springs is the greatest on record in the United States and was nearly double the previous records in the same area. A study of the maximum snow loads in the Wasatch Mountains of Utah (Ref. 8.5) showed that for a 100-year return period at 2740 m (9000 ft) altitude, a snow load of  $1220 \text{ kg/m}^2$  ( $250 \text{ lb/ft}^2$ ) could be expected.

#### 8.4.3 Hail

The distribution of maximum-sized hailstones in the United States is shown in Figure 8.7. The sizes are for single hailstones and not conglomerates of several hailstones frozen together. The largest officially recorded hailstone in the United States weighed 757 g (1.67 lb). It fell September 3, 1970, at Coffeyville, Kansas (Ref. 8.6).

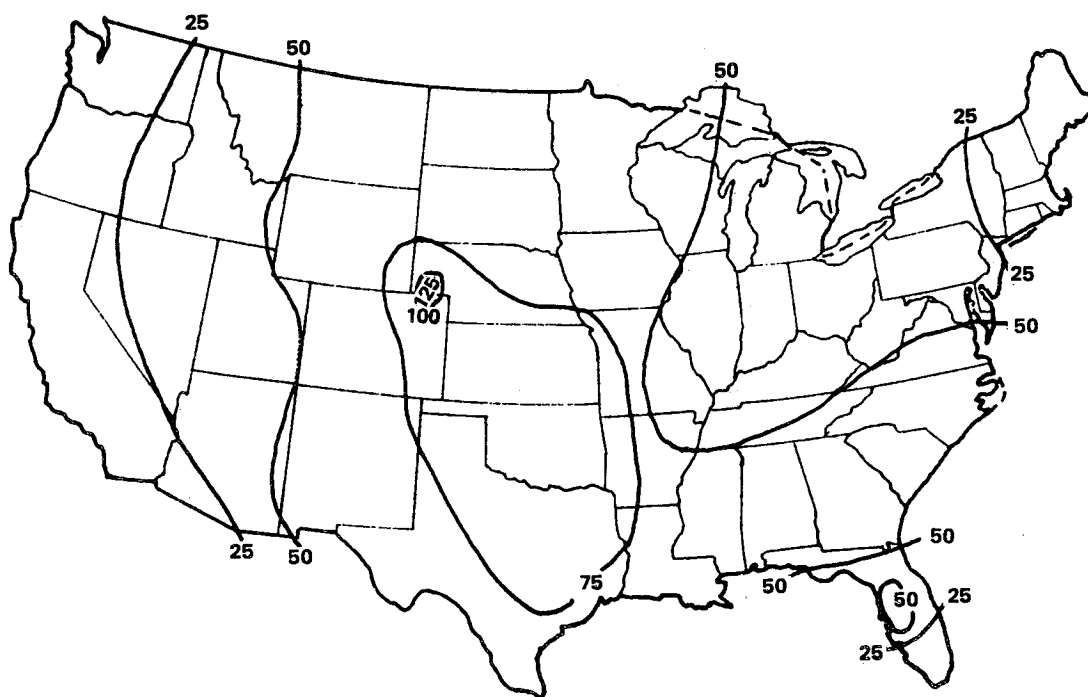


Figure 8.7 Extreme maximum hailstone diameters (mm).

#### 8.4.4 Atmospheric Pressure

Atmospheric pressure extremes normally given in the literature are given as the pressure which would have occurred if the station were at sea level. The surface weather map published by the United States National Weather Service uses sea-level pressures for the pressure values to assist in map analysis and forecasting. These sea-level pressure values are obtained from the station pressures by use of the hydrostatic equation:

$$-dP = \rho g dZ$$

where

$dP$  = pressure difference

$\rho$  = density

$g$  = gravity

$dZ$  = altitude difference.

These sea level data are valid only for design purposes at locations with elevation near sea level. As an example, when the highest officially reported sea level pressure observed in the United States of 106 330  $N/m^2$  (1063.3 mb) occurred at Helena, Montana (Ref. 8.7), the actual station pressure was approximately 92 100  $N/m^2$  (921 mb) because the station is 1187 m (3893 ft) above mean sea level.

Figures 8.8 and 8.9 show the general distribution of extreme maximum and minimum station pressures in the United States. Because of the direct relationship between pressure and station elevation, Figures 8.10 through 8.13 should be used with the station elevation to obtain the extreme maximum and minimum pressure values for any location in the United States. Similar maps and graphs in U. S. Customary Units are given in Reference 8.8.

Using References 8.2, 8.7, 8.9, and 8.10, extreme temperatures and sea-level pressures for the United States are given in Table 8.1. (See Section XIV for temperature extremes for selected sites and Section VII for station pressure extremes.) Reference 8.10 also contains surface atmosphere extreme criteria for vehicle launch and transportation areas.

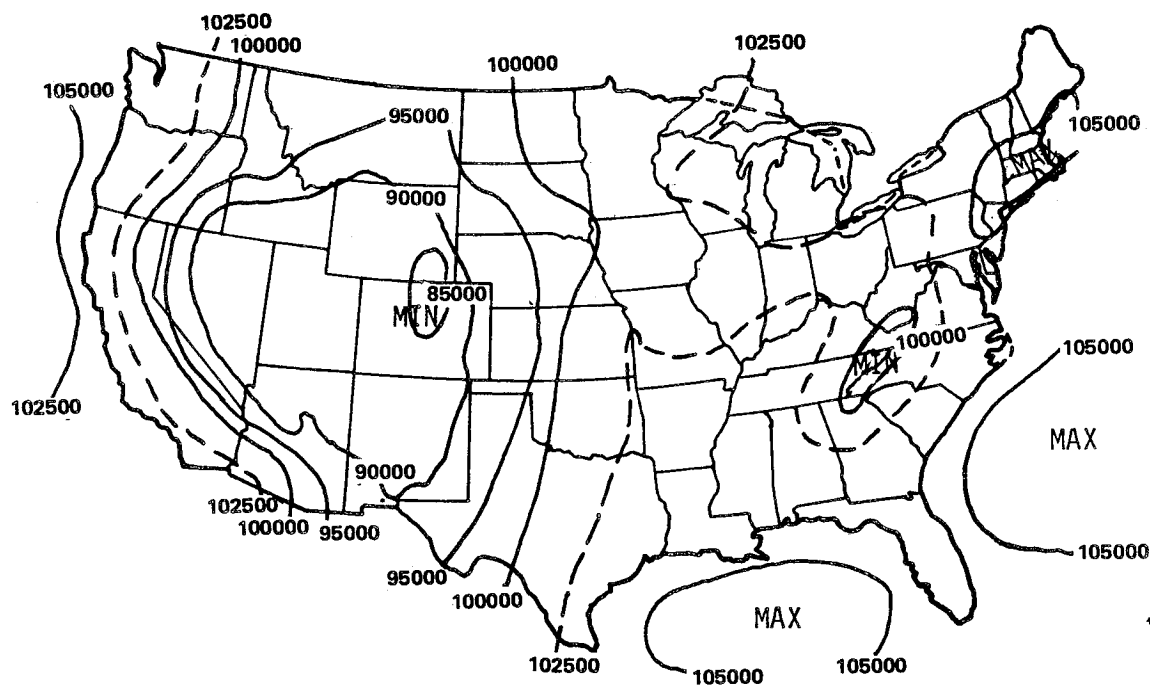


Figure 8.8 Maximum absolute station pressure ( $N/m^2$ ).

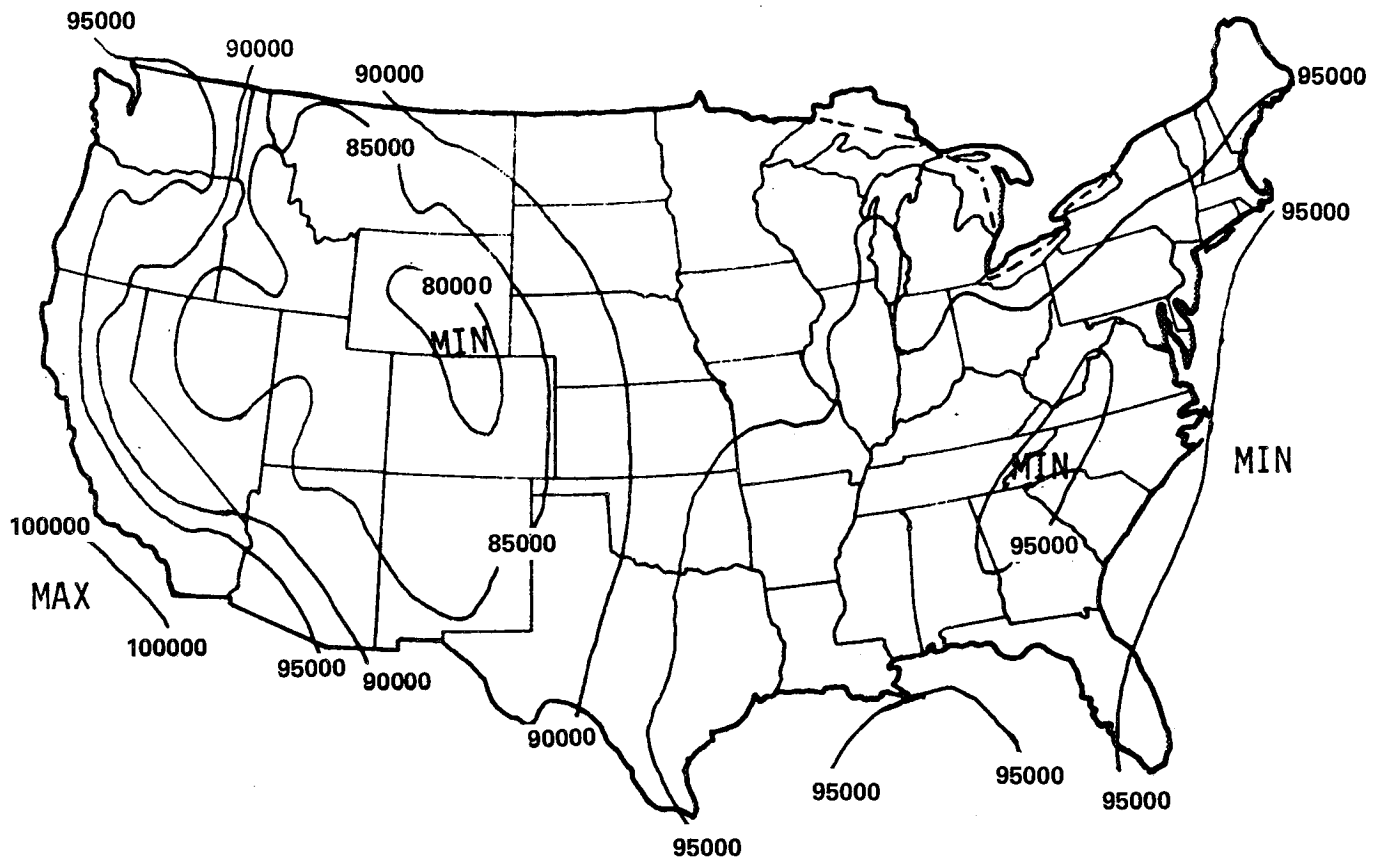


Figure 8.9 Minimum absolute station pressure ( $\text{N/m}^2$ ).

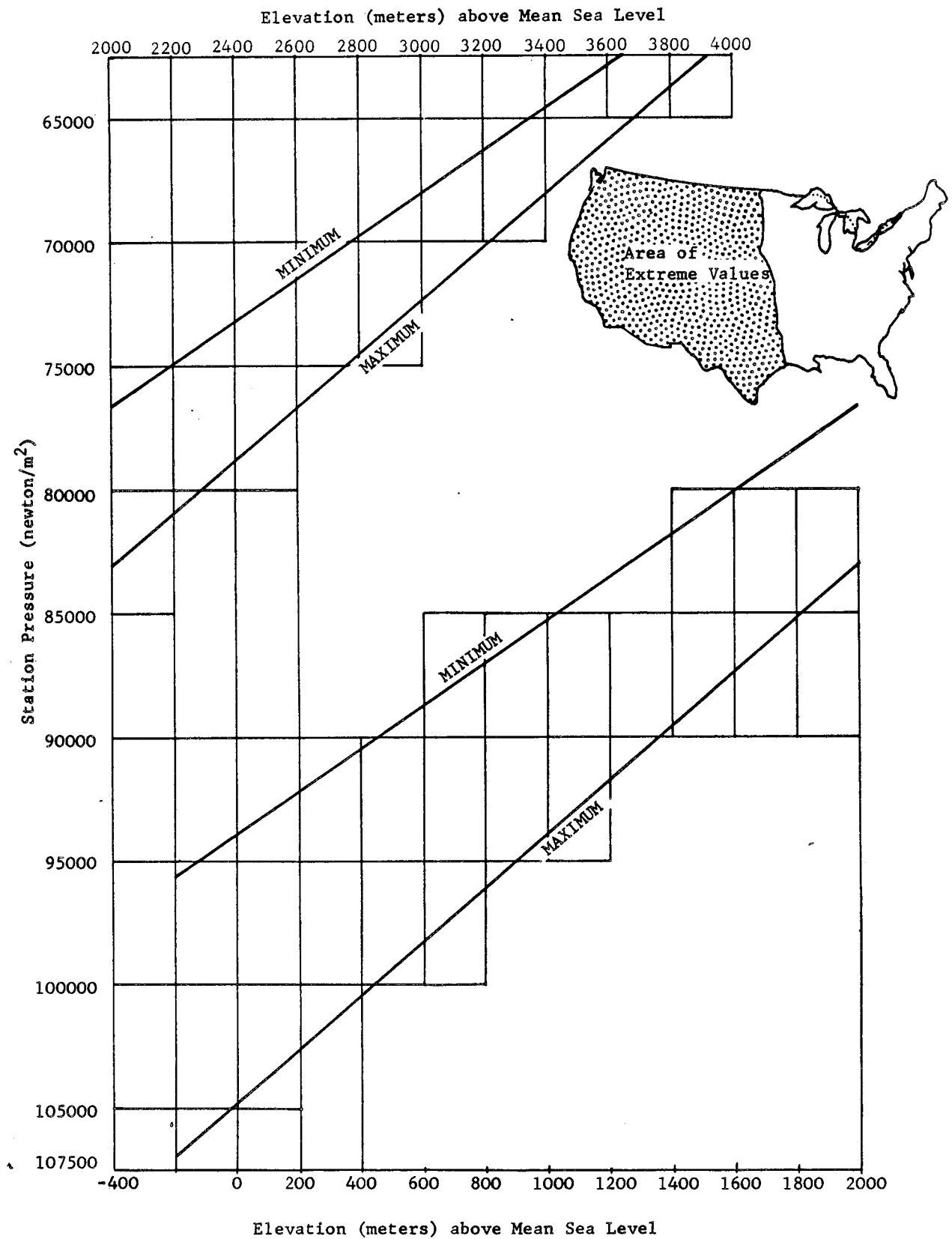


Figure 8.10 Extreme pressure values versus elevation for western United States.



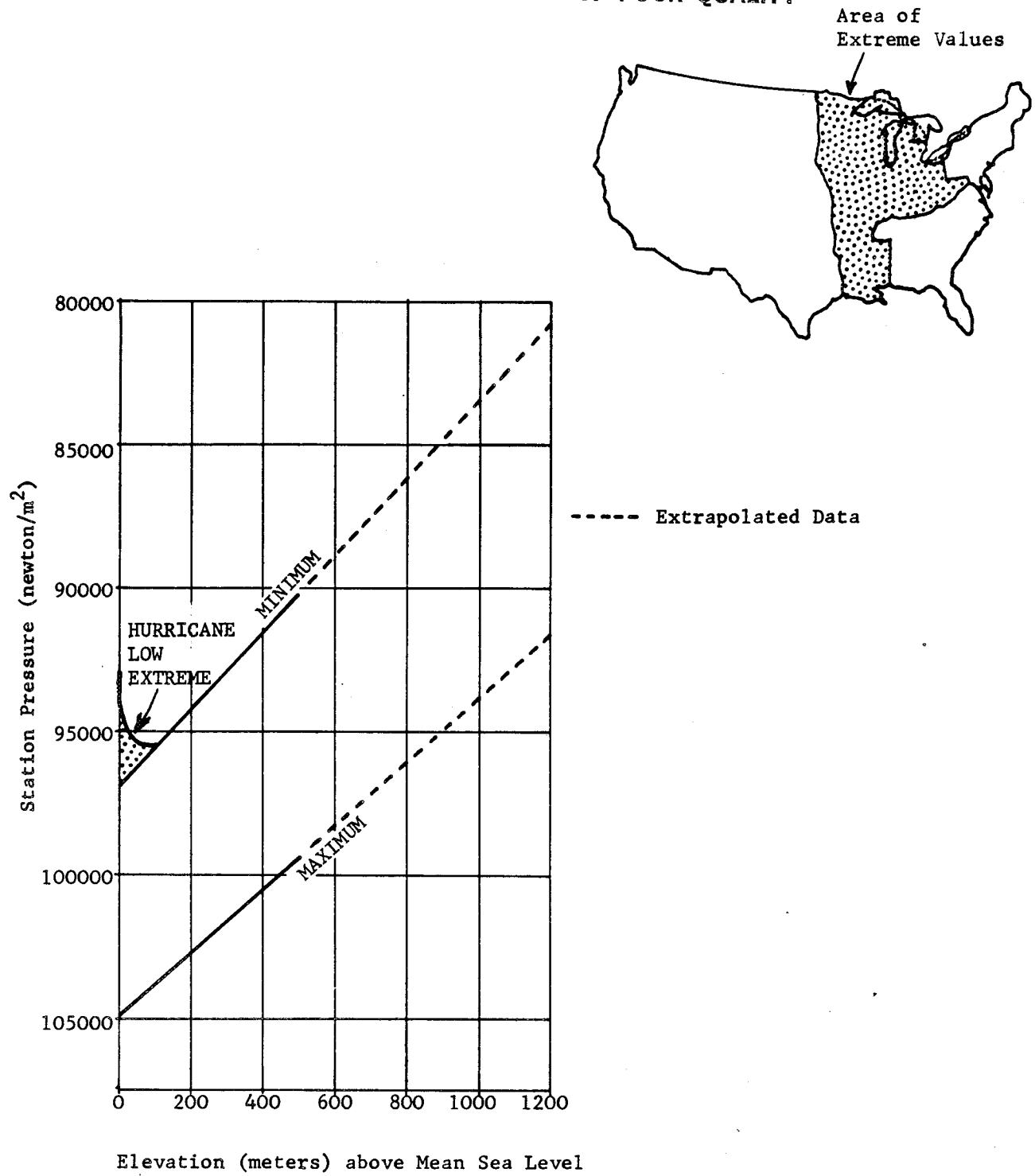


Figure 8.11 Extreme pressure values versus elevation for central United States.

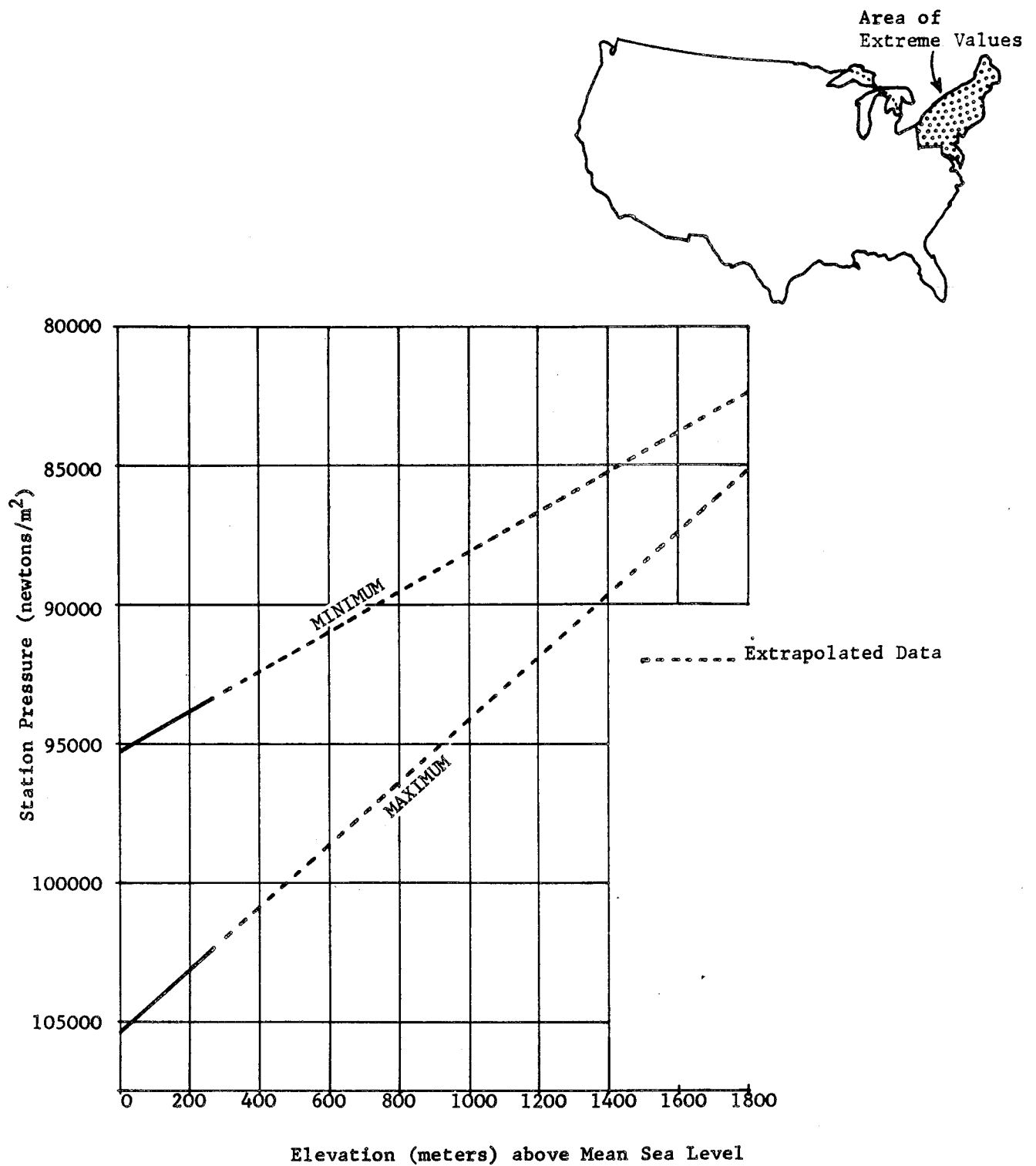


Figure 8.12 Extreme pressure values versus elevation for northeastern United States.

ORIGINAL PAGE IS  
OF POOR QUALITY

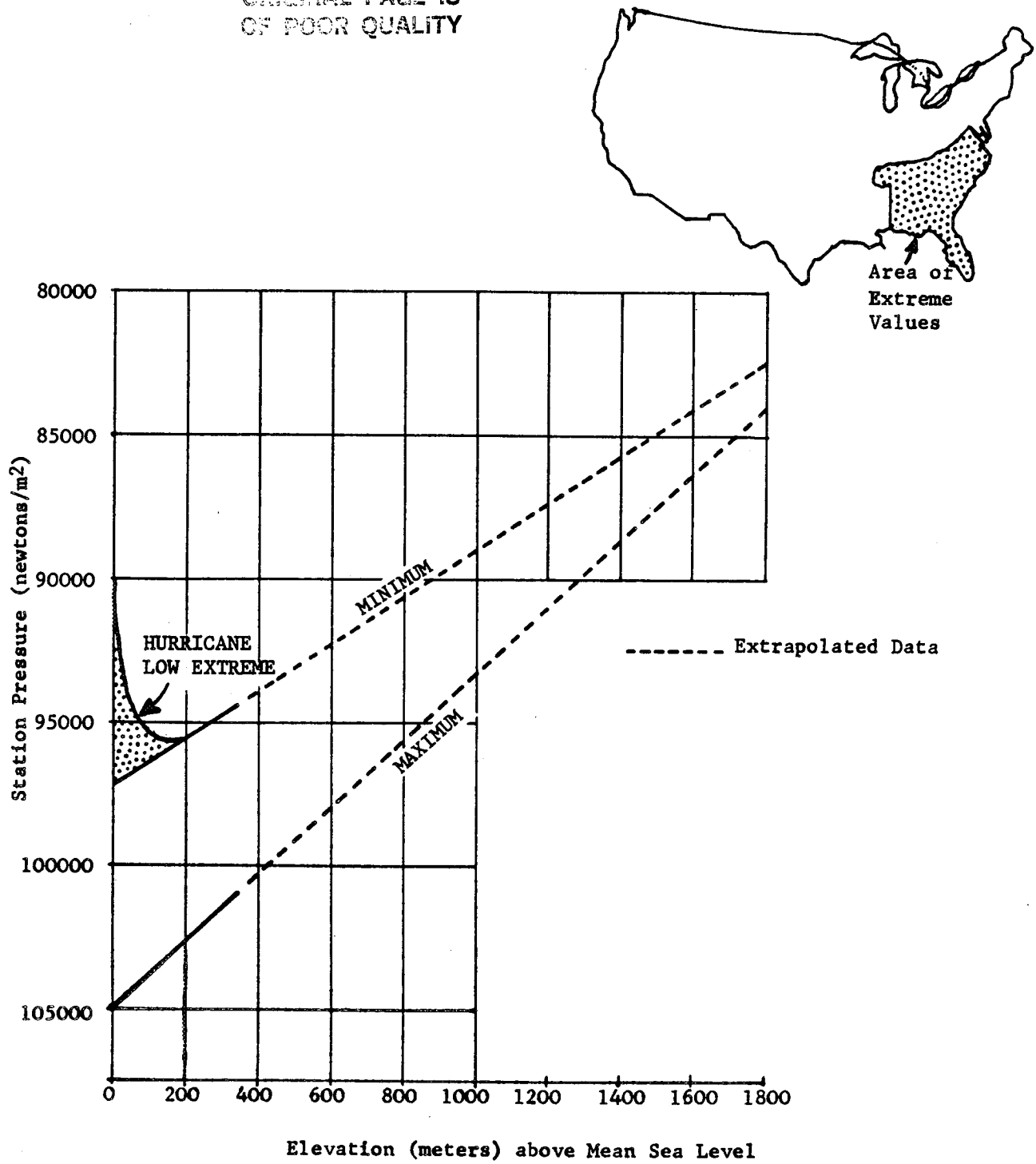


Figure 8.13 Extreme pressure values versus elevation for southeastern United States.

## REFERENCES

- 8.1 Schmidli, Robert J.: "Weather Extremes," NOAA Technical Memorandum NWS WR-28, Revised February 1981.
- 8.2 "Temperature Extremes in the United States." Environmental Information Summaries, C-5, NOAA Environmental Data Service, Asheville, N. C., May 1977.
- 8.3 Valley, Shea L.: "Handbook of Geophysics and Space Environments." McGraw-Hill Book Company, Inc., New York, 1965.
- 8.4 Riordan, Pauline: "Weather Extremes Around the World." Report ETL-TR-74-5, U. S. Army Engineer Topographic Laboratories, Ft. Belvoir, Virginia, April 1974.
- 8.5 Brown, Merly J.; and Williams, Philip Jr.: "Maximum Snow Loads Along the Western Slopes of the Wasatch Mountains of Utah." Journal of Applied Meteorology, Vol. 15, No. 3, 1962, pp. 123-126.
- 8.6 Ludlum, David M.: "The 'New Champ' Hailstone." Weatherwise, Vol. 24, No. 4, August 1971, p. 151.
- 8.7 Ludlum, David M.: "Extremes of Atmospheric Pressure in the United States." Weatherwise, Vol. 15, No. 3, 1962, pp. 106-115.
- 8.8 Daniels, Glenn E.: "Values of Extreme Surface Pressure for Design Criteria." Institute of Environmental Sciences, 1965 Proceedings, Institute of Environmental Sciences, Mt. Prospect, Ill., pp. 283-288.
- 8.9 Ludlum, David M.: "Extremes of Atmospheric Pressure." Weatherwise, Vol. 24, No. 3, 1971, pp. 130-131.
- 8.10 Surface Atmospheric Extremes (Launch and Transportation Areas) NASA Space Vehicle Design Criteria (Environment), NASA SP-8084, May 1972.

## SECTION IX. WORLDWIDE SURFACE EXTREMES

### 9.1 Introduction

This section provides worldwide extreme values for temperature, dew point, precipitation, pressure, wind speed, etc. Section VIII, United States Surface Extremes, provides more detailed statistics on atmospheric extremes for the United States.

### 9.2 Sources of Data

A great amount of meteorological data has been collected throughout the world. Various agencies have collected data in a form that may be used for statistical studies. Kendrew's "Climates of the Continents" (Ref. 9.1) is a summary of mean values of the meteorological parameters, temperature, pressure, and precipitation; and it is also the source of many interesting discussions of local meteorological conditions around the world. "World Weather Records" (Ref. 9.2), compiled by the Weather Bureau (now part of the National Oceanic and Atmospheric Administration), provides another summary of mean values of meteorological data. A publication entitled "Weather Extremes" (Ref. 9.3), by Robert J. Schmidli, is extremely valuable for its listing of extreme values of surface meteorological parameters. Climatological data have also been prepared for numerous worldwide airfield locations by the U.S. Air Force ETAC in support of the Naval Weather Service (Ref. 9.4). Eleven volumes have been published to date which contain monthly mean (some extreme) climatic information for all areas around the globe.

The Earth Sciences Laboratory, U. S. Army Topographic Laboratories, Fort Belvoir, Virginia, has collected worldwide data on meteorological extremes which are published in AR 70-38 (Ref. 9.5). For AR 70-38, the Earth Sciences Laboratory prepared world maps that show worldwide absolute maximum and absolute minimum temperatures.<sup>1</sup> These maps are reproduced in this section as Figures 9.1 and 9.2, and due credit is given to the Earth Sciences Laboratory, U. S. Army Engineer Topographic Laboratories, Fort Belvoir, Virginia. In addition, MIL-STD-210B, "Climatic Extremes for Military Equipment," (Ref. 9.6) issued on December 15, 1973, is a standard guidebook used by the U. S. military branches which contains worldwide extreme values. Reference 9.7, prepared by Air Force Cambridge Research Laboratories, gives more background information on the preparation of MIL-STD-210B.

The several climatic atlases for various areas of the world provide other sources of data; those of interest will be referred to in the following sections. For essentially all meteorological parameters, the extremes noted reflect measurements during the available period of record. Since this period of record covers only a few decades for most locations, it is obvious that there exists a finite risk that extreme values used will be exceeded in future years. However, the values shown are considered appropriate as criteria guidelines to establish critical engineering design problems requiring more in-depth assessment relative to probable meteorological extremes during expected operational lifetime.

---

1. Absolute is defined as the highest and lowest values of data of record.

### 9.3 Worldwide Extremes Over Continents

To present all the geographic extremes properly, many large maps similar to Figures 9.1 and 9.2 would be required; therefore, only worldwide extremes of each parameter will be discussed, and available references on each parameter will be given. Individual geographic extremes will be mentioned when pertinent.

#### 9.3.1 Temperature

Absolute maximum and absolute minimum world temperature extremes are shown in Figures 9.1 and 9.2. Some geographical extreme air temperatures of record are given in Table 9.1.

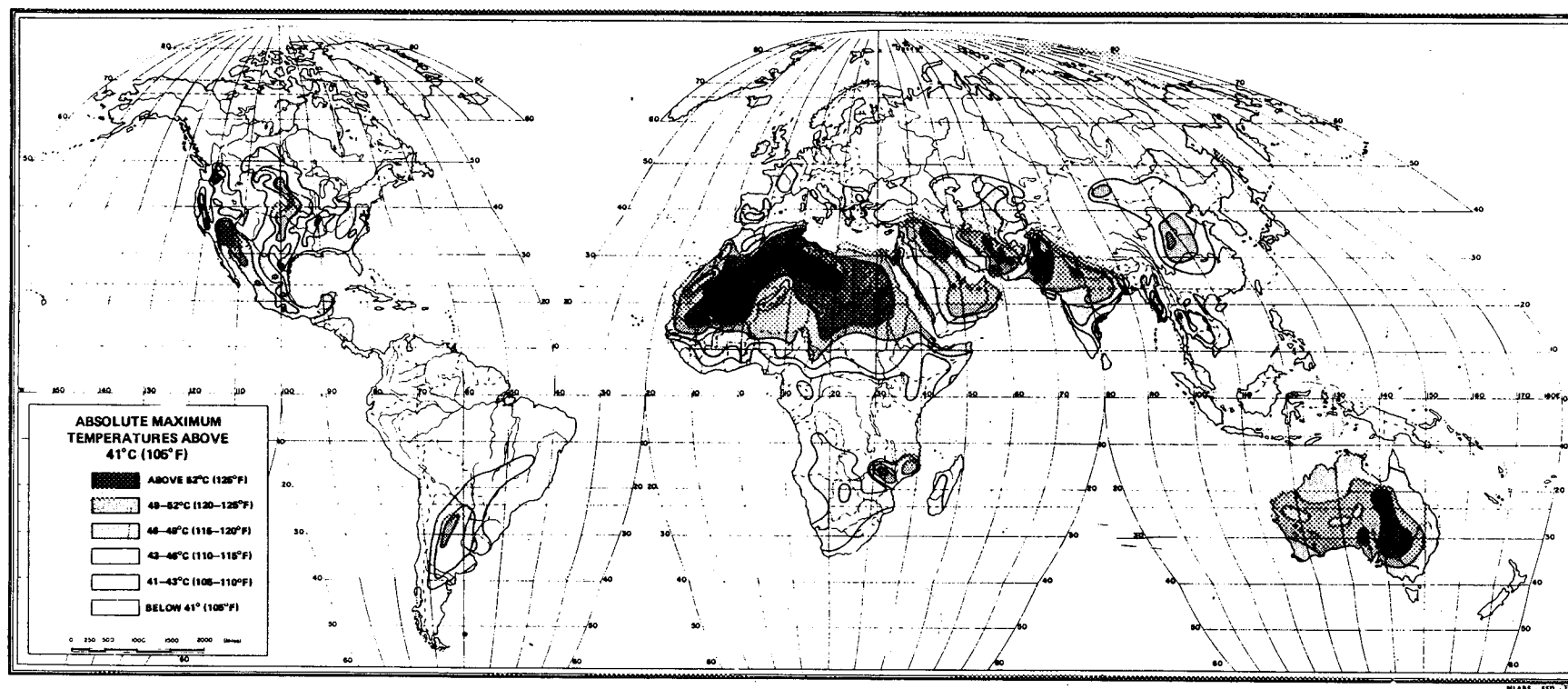
TABLE 9.1 EXTREME AIR TEMPERATURES OF RECORD

Location	Air Temperature of Record [ $^{\circ}\text{C}$ ( $^{\circ}\text{F}$ )]
Salah, Africa	48 (118), mean daily max. for 45 days 53 (127), absolute max.
El Azizia, Africa*	58 (136), absolute max.
Tirat Tsvi, Israel	54 (129), absolute max.
Death Valley, Calif.*	57 (134), absolute max. for U. S.
Cloncurry Queensland, Australia	53 (128), absolute max.
Vostok, Antarctica	-88.3 (-127), absolute min.
Oimekin, U.S.S.R.	-68 (-90), absolute min.
Northice, Greenland	-66 (-87), absolute min.
Prospect Creek Camp, Alaska	-62 (-80), absolute min.
Rogers Pass, Montana	-57 (-70), absolute min. for U. S.
Snag, Yukon Territory, Canada	-63 (-81), absolute min. for North America

\*The validity of these temperatures has been questioned; see Ref. 9.8.

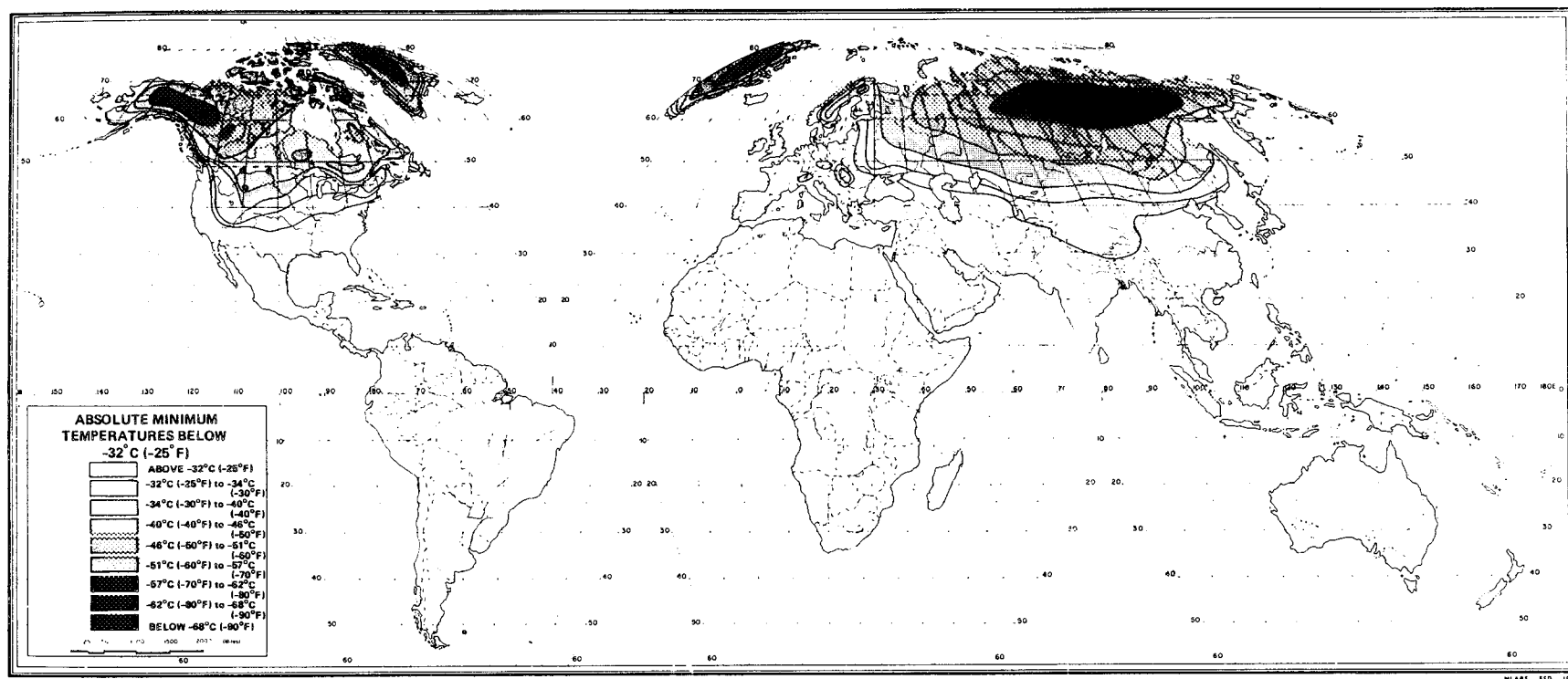
Temperatures of the ground are normally hotter than the air temperatures during the daytime. In Loango, Congo, Africa, temperatures of the ground as high as  $82^{\circ}\text{C}$  ( $180^{\circ}\text{F}$ ) have been measured. At Stuart, Australia, the sand has reached temperatures so hot that matches dropped into it burst into flame.

In the design of equipment for worldwide ground environment operations, MIL-STD-210B (Ref. 9.6) now uses extreme temperature values of  $58^{\circ}\text{C}$  ( $136^{\circ}\text{F}$ ) for a hot temperature and  $-68^{\circ}\text{C}$  ( $-90^{\circ}\text{F}$ ) for a cold temperature.



ORIGINAL PAGE IS  
OF POOR QUALITY

Figure 9.1 Worldwide geographic absolute maximum temperatures above 41°C (105°F). (Ref. 9.5)



ORIGINAL PAGE IS  
OF POOR QUALITY

Figure 9.2 Worldwide geographic absolute minimum temperatures below -32°C (-25°F). (Ref. 9.5)



The preceding data were used in an extreme value theory which resulted in the risk values given in Tables 9.2 and 9.3. The risk values for extreme high temperatures developed by the extreme value theory used 57 extreme annual temperatures at Death Valley, California (Ref. 9.7). Such temperatures persist for 1 or 2 hr during a day.

TABLE 9.2 EXTREME HIGH TEMPERATURES WITH RELATION TO RISK AND DESIRED LIFETIME

Risk (%)	Temperatures [ $^{\circ}\text{C}$ ( $^{\circ}\text{F}$ )] Planned Lifetime (years)				
	1	2	5	10	25
1	55 (131)	56 (133)	57 (134)	57 (135)	58 (136)
10	53 (127)	53 (128)	54 (130)	55 (131)	56 (133)
25	52 (125)	53 (127)	53 (128)	54 (129)	55 (131)
50	51 (124)	52 (125)	53 (127)	53 (128)	54 (130)

The recommendation for cold temperature was based upon the risk table, shown in Table 9.3, of extreme low temperatures, developed by extreme value theory using 18 annual low temperatures at two Siberian locations (Ref. 9.7). The extreme low temperatures will persist for longer periods since they occur during polar darkness. (Also see References 9.9 and 9.10 regarding probabilities of surface temperature extremes.)

TABLE 9.3 EXTREME LOW TEMPERATURES WITH RELATION TO RISK AND DESIRED LIFETIME\*

Risk (%)	Temperature [ $^{\circ}\text{C}$ ( $^{\circ}\text{F}$ )] Planned Lifetime (years)			
	2	5	10	25
10	-66 (-86)	-67 (-89)	-69 (-92)	-71 (-95)

\*Temperatures in Antarctica were not considered in the study.

### 9.3.2 Dew Point

High dew points associated with high temperatures near large bodies of water can be detrimental to equipment making living conditions very uncomfortable. Some examples of this atmospheric condition are

- The northern portion of the Arabian Sea in April and May, to  $29^{\circ}\text{C}$  ( $85^{\circ}\text{F}$ ) dew point.
- The Red Sea in July, to  $32^{\circ}\text{C}$  ( $89^{\circ}\text{F}$ ) dew point.
- The Caribbean Sea (includes the western end of Cuba and the Yucatan Peninsula, Mexico) in July, to  $27^{\circ}\text{C}$  ( $81^{\circ}\text{F}$ ) dew point.

d. The northern portion of the Gulf of California, to 30°C (86°F) dew point (data from Puerto Penasco, Mexico, Ref. 18.8).

The Air Force has published the "Atmospheric Humidity Atlas for the Northern Hemisphere" (Ref. 9.11), which shows maps for various percentile levels of dew point for midseason months (January, April, July, and October).

### 9.3.3 Precipitation

The worldwide distribution of precipitation is extremely variable; some areas do not receive rain for years, while others receive torrential rain many months of the year.<sup>2</sup> Precipitation is also seasonal; for example, Cherrapunji, India, with its world record total of 2647 cm (1042 in.) of precipitation in a year, has a mean monthly precipitation of less than 2.54 cm (1 in.) in December and January. The heaviest precipitation for long periods (greater than 12 hr) usually occurs in the monsoon type of weather. High rates of rainfall for short periods (less than 12 hr) usually occur in the thunderstorm type of rain and over much smaller areas than the monsoon rain. Some world records for various periods of rainfall are given in Table 9.4 (Refs. 9.1, 9.12, and 9.13).

TABLE 9.4 WORLD RAINFALL RECORDS

Station	Time Period	Amount (in.) (cm)
Unionville, Maryland	1 min.	1.23 (3.1)
Plum Point, Jamaica	15 min.	8.0 (20)
Holt, Mo.	42 min.	12.0 (31)
D'Hanis, Tex.	3 hours	20.0 (51)
Belouve, LaReunion Island	12 hours	53.0 (135)
Cilaos, LaReunion Island	1 day	73.62 (188)
Cherrapunji, India	30 days	366.14 (930)
Cherrapunji, India	1 year	1041.73 (2647)
<p>Highest average annual precipitation:</p> <p>World — 460 in. (1168 cm) — Mt. Waialeale, Kanai, Hawaii</p> <p>Contiguous U.S. — 144 in. (366 cm) — Wynoochee, Washington</p> <p>Lowest average annual precipitation:</p> <p>World — 0.03 in. (0.08 cm) — Arica, Chile</p> <p>U.S. — 1.63 in. (4.4 cm) — Death Valley, California</p>		

Even though the values given in Table 9.4 are considerably higher than the values given in Table 4.2 of Section IV, values in Table 4.2 are considered adequate for most space vehicle design problems within currently expected operational areas.

2. Arica, Chile, had no rain between October 1903 through December 1917. The longest dry period for a United States location was 767 days for Bagdad, California (October 3, 1912 to November 8, 1914).

### 9.3.4 Pressure

Surface atmospheric pressure extremes for use in design must be derived from the measured station pressures, not from the computer sea level pressures that are usually published.

Station pressures between stations have great variability because of the difference in altitude of the stations. The lowest station pressures occur at the highest altitudes. The highest station pressures occur at either the lowest elevation stations (below sea level), or in the arctic regions in cold air masses at or near sea level.

Court (Ref. 9.12) has published an interesting discussion on worldwide pressure extremes. Some typical extreme high and low pressure values are given in Table 9.5 (Refs. 9.1 and 9.12).

TABLE 9.5 EXTREME PRESSURE VALUES FOR SELECTED AREAS

Station	Elevation Above Sea Level [m (ft)]	Pressure (mb)	
		Lowest	Highest
Lahasa, Tibet	3685 (12 090)	645 <sup>a</sup>	652 <sup>a</sup>
Sedom, Israel	-389 (-1 275)	—	1081.8
Portland, Maine	-9 (61)	—	1056
Barrow, Alaska	4 (13)	—	1064.3
Qutdligssat, Greenland	3 (10)	—	1063.4
In Typhoon Tip, 16°44'N, 137°46'E October 12, 1979	~0	870 <sup>b</sup>	—

a. Monthly means.

b. Lowest sea level pressure of record.

### 9.3.5 Ground Wind

Worldwide extreme surface winds have occurred in several types of meteorological conditions: tornadoes, hurricanes or typhoons, mistral winds, and Santa Ana winds. In design, each type of wind needs special consideration. For example, the probability of tornado winds is very low compared with the probability of mistral winds, which may persist for days.

#### 9.3.5.1 Tornadoes

Tornadoes are rapidly revolving circulations normally associated with a cold front squall line or with warm, humid, unsettled weather; they usually occur in conjunction with a severe thunderstorm. Although a tornado is extremely destructive, the average tornado path is only about 400 m (1/4 mi.) wide and seldom more than 26 km (16 mi.) long, but there have been a few instances in which tornadoes have caused heavy destruction along paths more than 1.6 km (1 mi.) wide and 483 km (300 mi.) long. The probability of any one point being in a tornado path is very small; therefore, design of structures to withstand tornadoes is

usually not considered except for special situations where tornado shelters are built underground. Velocities have been estimated to exceed  $134 \text{ m s}^{-1}$  (260 knots) in tornadoes. See Section X for further information regarding tornadoes.

### 9.3.5.2 Hurricanes (Typhoons)

Hurricanes (also called typhoons, willy-willies, tropical cyclones, and many other local names) are large tropical cyclones of considerable intensity. They originate in tropical regions between the equator and 25 degrees latitude. A hurricane may be 1600 km (1000 mi.) in diameter with winds in excess of  $67 \text{ m s}^{-1}$  (130 knots). A hurricane is defined as a storm of tropical origin with winds equal to or greater than  $33 \text{ m s}^{-1}$  (64 knots). Hurricanes are always accompanied by heavy rain. Since the hurricanes of the West Indies are as intense as others throughout the world, design winds based upon these hurricanes would be representative for any geographical area. Section 2.3 gives hurricane design winds for the area of Kennedy Space Center, Florida. Although the highest winds recorded in a hurricane in the area of KSC, Florida, were lower than winds from thunderstorms in the same area, the probability still exists that much higher winds could result from hurricanes in the vicinity of Kennedy Space Center.

For extremes applicable to equipment, Table 9.6 from a study of 19 years of wind data for Naha, Okinawa (in the Pacific typhoon belt) (Ref. 9.7), is representative of all hurricane areas of the world. See Section X for further information regarding hurricanes.

TABLE 9.6 EXTREME WINDS IN HURRICANE (typhoon) AREAS WITH RELATION TO RISK AND DESIRED LIFETIME (3.1-m reference height)

Extreme Wind Speeds ( $\text{m s}^{-1}$ )*†				
Planned Lifetime (years)				
Risk (%)	2	5	10	25
10	* 69	79	86	97
	† 61	72	80	91

\*Based on 2-sec gusts (annual extreme)

†Based on 1-min steady wind associated with the 2-sec gust

### 9.3.5.3 Mistral Winds (Ref. 9.1)

The mistral wind is a strong polar current between a large anticyclone and a low pressure center. These winds frequently have temperatures below freezing. The mistral of the Gulf of Lions and the Rhone Valley, France, is the best known of these winds. Although winds of  $37 \text{ m s}^{-1}$  (83 mph) have been recorded in the area of Marseilles, France, much higher winds have occurred to the west of Marseilles in the more open terrain, where even railway trains have been blown over. Mistrals blow in the Rhone Valley for about 100 days a year.

#### 9.3.5.4 Santa Ana Winds

In contrast to the mistrals, the Santa Ana winds, which occur in Southern California west of the coast range of mountains, are hot and dry and have speeds up to  $21 \text{ m s}^{-1}$  (41 knots). Similar winds, called Fohn winds, occur in the Swiss Alps and in the Andes, but, because of the local topography, they have lower speeds. The destructiveness of these winds is not from their speeds, but from their high temperatures and dryness, which can do considerable damage to blooming trees, crops, exposed equipment and instruments that may be sensitive to prolonged heat and dryness.

## REFERENCES

- 9.1 Kendrew, W. G., "The Climates of the Continents," Oxford University Press, Amen House (London), 1961.
- 9.2 "World Weather Records," U. S. Department of Commerce, Weather Bureau, Superintendent of Documents, U. S. Government Printing Office, Washington, D. C., 1968.
- 9.3 Schmidli, Robert J., "Weather Extremes," NOAA Technical Memorandum NWS WR-28, Revised February 1981.
- 9.4 "Worldwide Airfield Climatic Data," Environmental Technical Applications Center, Air Weather Service, U. S. Air Force, Vol. XI, April 1973.
- 9.5 "Research, Development, Test, and Employment of Material for Extreme Climatic Conditions," AR-70-38, July 1, 1969.
- 9.6 Military Standard Climatic Extremes for Military Equipment, Department of Defense, MIL-STD-210B, December 15, 1973.
- 9.7 Sissenwine, Norman, and Cormier, René V., "Synopsis of Background Material for MIL-STD-210B, Climatic Extremes for Military Equipment," AFCRL-TR-74-0052, Air Force Cambridge Research Laboratories, January 24, 1974.
- 9.8 Billions, Novella S., "Frequencies and Durations of Surface Temperatures in Hot-Dry Climatic Category Areas. (Cat. 4, AR 70-38)," Technical Report RR-72-13, Dec. 1972, U. S. Army Missile Command, Redstone Arsenal, Alabama.
- 9.9 Tattleman, P., and Kantor, A. J., "Atlas of Probabilities of Surface Temperature Extremes: Part I -- Northern Hemisphere," AFGL-TR-76-0084, 1976.
- 9.10 Tattelman, P., and Kantor, A. J., "Atlas of Probabilities of Surface Temperature Extremes: Part II -- Southern Hemisphere," AFGL-TR-77-0001, December 27, 1976.
- 9.11 Dodd, Arthur V., "Aerial and Temporal Occurrence of High Dew Points and Associated Temperatures," Technical Report 70-4-ES, Department of the Army, U. S. Army Natick Laboratories, Earth Sciences Laboratory, Natick, Mass., August 1969.
- 9.12 Court, Arnold, "Improbable Pressure Extreme: 1070 mb," Bulletin of the American Meteorological Society, vol. 50, no. 4, Apr. 1969, pp. 248-250.
- 9.13 Riordan, Pauline, "Weather Extremes Around the World." Report ETL-TR-74-5, U. S. Army, Engineer Topographic Laboratories, Fort Belvoir, Virginia, April 1974.

## SECTION X. OCCURRENCES OF TORNADOES AND HURRICANES

10.1 Introduction

Severe weather may adversely affect the design, transportation, and operation of aerospace vehicles. This section contains a discussion of such atmospheric phenomena. (The reader is referred to Section XI for a discussion of thunderstorm activity and to Section IX for information regarding severe worldwide weather conditions.)

10.2 Tornadoes

Tornadoes are recognized as the most destructive wind force. Due to differential pressures created by tornadoes, buildings have been known to literally explode. Fortunately, the aerial extent of tornadoes is small compared with hurricanes. Tornadoes are observed at times in association with hurricanes in Florida and along the coastal states. Based on Thom's analysis of the number of tornado occurrences (Ref. 10.1), Table 10.1 has been prepared giving tornado statistics for stations of interest. The statistics included in Table 10.1 are based upon an area ( $A_2$ ) of a 1-degree square of latitude and longitude on the Earth's surface. The period of record is 1953-1979.

The probability of one or more tornadoes in  $N$  years in an area ( $A_1$ ) is given by<sup>1</sup>

$$P(A_1; N) = 1 - \exp\left(-\bar{x} \frac{A_1}{A_2} N\right) \quad (10.1)$$

where  $\bar{x}$  is the mean number of tornadoes per year in a 1-degree square. We choose the area size for  $A_1$  as  $7.3 \text{ km}^2$  ( $2.8 \text{ mi.}^2$ ) because Thom (Ref. 10.1) reports that  $7.2572 \text{ km}^2$  ( $2.8209 \text{ mi.}^2$ ) is the average ground area covered by tornadoes in Iowa, and the vital industrial complexes for most locations are of this general size. Thus, taking  $A_1 = 7.3 \text{ km}^2$  ( $2.8 \text{ mi.}^2$ ) and  $A_2 = 2.59 \text{ km}^2$  ( $1 \text{ mi.}^2$ ) and evaluating equation (10.1) for the values of  $\bar{x}$  and  $A_2$  for the stations given in Table 10.1 yields the data in Table 10.2. Table 10.2 gives the probability of one or more tornadoes in a  $7.3\text{-km}^2$  ( $2.8\text{-mi.}^2$ ) area and a  $2.59\text{-km}^2$  ( $1\text{-mi.}^2$ ) area in 1 year, 10 years, and 100 years for the indicated 8 locations. It is noted that for  $A_1 \ll A_2$  and  $N < 100$ , equation (10.1) can be approximated by

$$P(A_1; N) \doteq \bar{x} \frac{A_1}{A_2} N \quad (10.2)$$

An interpretation of the statistics in Table 10.2 is given using Kennedy Space Center as an example. There is a 12.5-percent chance that at least one tornado will "hit" within a  $7.3\text{-km}^2$  ( $2.8\text{-mi.}^2$ ) area at KSC in 100 years. For a  $2.59\text{-km}^2$  ( $1\text{-mi.}^2$ ) area at KSC, the chance of at least one tornado hit in 100 years is 4.7 percent. If several structures within a  $7.3\text{-km}^2$  ( $2.8\text{-mi.}^2$ ) area at KSC are vital to a space mission and these structures are not designed to withstand the wind and internal pressure forces of a tornado, then there is a 12.5 percent chance that one or more of these vital structures will be destroyed or damaged by a tornado in 100 years. If the desired lifetime of these structures [or  $7.3\text{-km}^2$  ( $2.8\text{-mi.}^2$ ) industrial complex] is 100 years and the risk of destruction by tornadoes is accepted in the design, then the design risk or calculated risk of failure of at least one structure due to tornado occurrences is 12.5 percent. This example serves to

1. Credit is due Dr. J. Goldman, International Center for the Solution of Environmental Problems, Houston, Texas, for this form of the probability expression.

TABLE 10.1 TORNADO STATISTICS FOR STATIONS SPECIFIED, 1953-1979

Station	Number of Tornadoes in 1 deg Square	Mean ( $\bar{x}$ ) No. of Tornadoes Per Year in 1 deg Square	Area ( $A_2$ ) of 1 deg Square		Mean (P) Probability of a Tornado Striking a Point in Any Year in a 1 deg Square	Mean (R) Recurrence Interval (yr) for a Tornado Striking a Point in a 1 deg Square
			(km <sup>2</sup> )	(mi <sup>2</sup> )		
Huntsville	68	2.52	10 179	3 930	0.001809	553
Kennedy Space Center	54	2.00	10 839	4 185	0.001348	742
Vandenberg AFB	2	0.07	10 179	3 930	0.000050	19 902
Edwards AFB	7	0.26	10 179	3 930	0.000187	5 358
New Orleans	50	1.85	10 645	4 110	0.001270	788
NSTL - Bay St. Louis	60	2.22	10 645	4 110	0.001524	656
Houston	109	4.04	10 736	4 145	0.002749	364
White Sands	6	0.22	10 412	4 020	0.000154	6 478

$$P = 2.8209 \bar{x} / A_2$$

$$R = 1/P$$

TABLE 10.2 PROBABILITY OF ONE OR MORE TORNADOES IN A 7.3-km<sup>2</sup> AREA AND  
A 2.59-km<sup>2</sup> AREA IN 1, 10, AND 100 YEARS

Station	Mean ( $\bar{x}$ ) No. of Tornadoes Per Year in 1 deg Square	P( $A_1;N$ ) for $A_1 = 7.3 \text{ km}^2 (2.8 \text{ mi.}^2)$			P( $A_1;N$ ) for $A_1 = 2.59 \text{ km}^2 (1.00 \text{ mi.}^2)$		
		N=1 Year	N=10 Years	N=100 Years	N=1 Year	N=10 Years	N=100 Years
Huntsville	2.52	0.001794	0.017794	0.164347	0.000641	0.006392	0.062110
Kennedy Space Center	2.00	0.001337	0.013292	0.125245	0.000478	0.004768	0.046666
Vandenberg AFB	0.07	0.000050	0.000499	0.004975	0.000018	0.000178	0.001780
Edwards AFB	0.26	0.000185	0.001851	0.018354	0.000066	0.000661	0.006594
New Orleans	1.85	0.001260	0.012524	0.118415	0.000450	0.004491	0.044014
NSTL-Bay St. Louis	2.22	0.001511	0.015010	0.140359	0.000540	0.005387	0.052582
Houston	4.04	0.002725	0.026922	0.238837	0.000974	0.009699	0.092868
White Sands	0.22	0.000153	0.001531	0.015207	0.000055	0.000547	0.005458

$$P(A_1;N) = 1 - e^{-\bar{x}(A_1/A_2)N}$$



point out that the probability of occurrence of an event which is rare in one year becomes rather large when taken over many years and that estimates for the desired lifetime versus design risk for structures discussed in subsection 2.3.10 of Section II should be made with prudence.

Figures 10.1 and 10.2 show tornado incidence statistics by state and area and also by month for the United States.

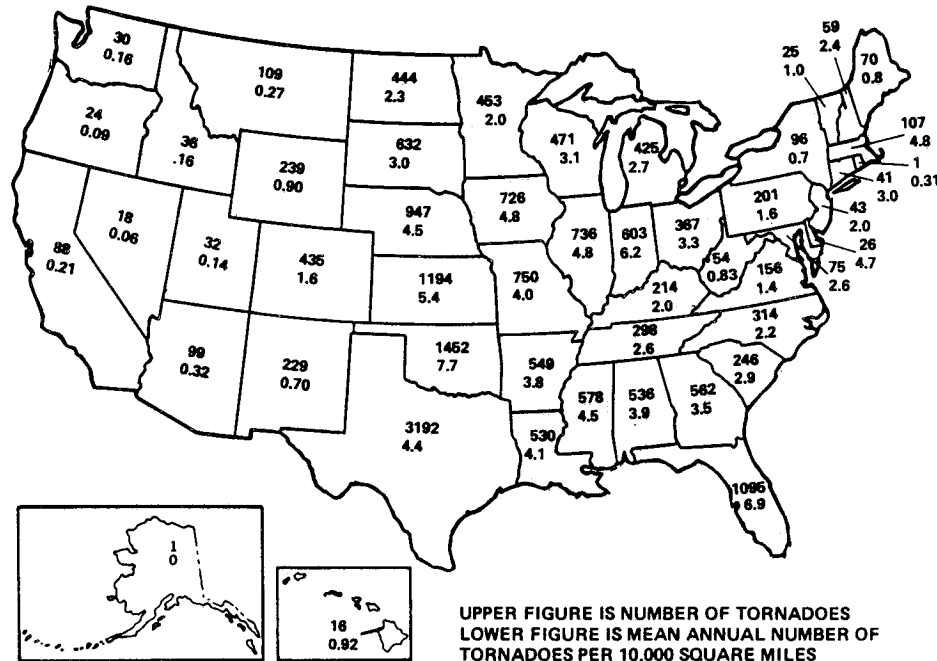


Figure 10.1 Tornado incidence by state and area, 1953-1979 (up-dated from NOAA<sup>2</sup>).

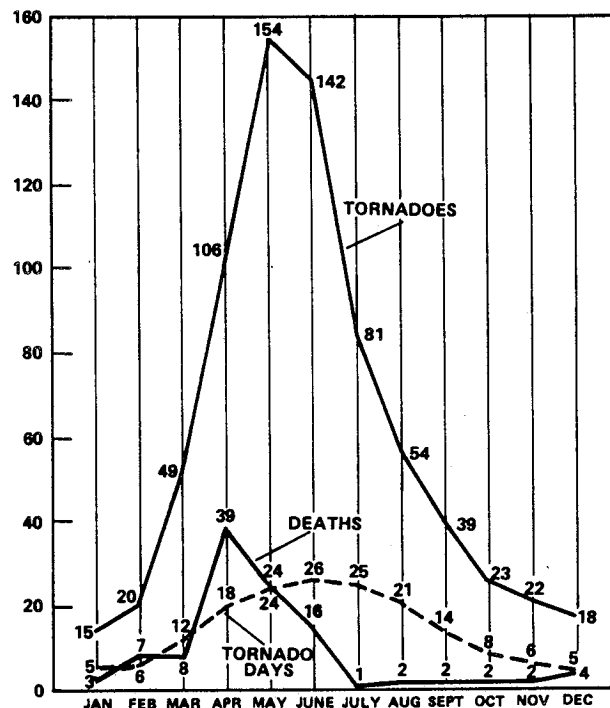


Figure 10.2 Tornado incidence by month for the U.S., 1953-1979 (up-dated from NOAA<sup>2</sup>).

2. "Severe Local Storm Warning Service and Tornado Statistics, 1953-1976," U.S. Department of Commerce, National Oceanic and Atmospheric Administration pamphlet, NOAA/PA 77018, 1981.

### 10.3 Hurricanes and Tropical Storms

The occurrence of hurricanes at Kennedy Space Center and other locations for the Eastern Test Range is of concern to the space program because of high winds and because range support for space operations is closed during passage or near approach of a hurricane. This discussion will be restricted to the frequency of tropical storms, hurricanes, and tropical storms and hurricanes combined (tropical cyclones) for annual reference periods and certain monthly groupings, as a function of radial distances from KSC only.

By definition, a hurricane is a storm of tropical origin with maximum sustained surface winds greater (1-min mean) than or equal to 33 m/sec (64 knots). A tropical storm is a cyclone whose origin is in the tropics with sustained winds less than 33 m/sec (64 knots) but greater than or equal to 17 m/sec (33 knots). There is no known upper limit for wind speeds in hurricanes, but speeds exceeding 90 m/sec (175 knots) have been measured. Also, tornadoes have been observed in association with hurricanes.

Tables 10.3 and 10.4 give a general indication of the frequency of tropical storms and hurricanes by months within 161- and 644-km (100- and 400-n.mi.) radii of Kennedy Space Center, Florida. From Table 10.3 it is noted that hurricanes within 161 and 644 km (100 and 400 n.mi.) of KSC have been observed as early as May and as late as December, with the highest frequency during September. In the 81-year period (1899 to 1979), there were 131 hurricanes whose path (eye) came within a 644-km (400-n.mi.) radius of KSC; there were 21 hurricanes that came within a 161-km (100-n.mi.) radius of KSC during this period. From available KSC wind records, and some observations along the coast from Melbourne, Florida, to Titusville, Florida, the highest wind gusts during the passage of 18 of the 21 hurricanes that came within a 161-km (100-n.mi.) radius of KSC were obtained. For the three hurricanes for the years 1899, 1906, and 1925, the peak gusts were not available. Of the 18 hurricanes that came within a 161-km (100-n.mi.) radius of KSC for which the maximum wind gust records are available, 7 produced wind gusts greater than 33.5 m/sec (65 knots),<sup>3</sup> 10 produced maximum wind gusts to 26 m/sec (50 knots), and 12 had extreme wind gusts less than 18.5 m/sec (36 knots). Thus, from these records, even if a defined hurricane path comes within a 161-km (100-n.mi.) radius of KSC, hurricane force winds [speeds  $> 33$  m/sec (64 knots)] are not always observed at KSC. Hurricanes at greater distances than 161 km (100 n.mi.) could possibly produce hurricane force winds at KSC. Hurricanes downgraded to tropical storms, and extreme nonhurricane-associated thunderstorms, have also produced strong peak winds in the KSC area; i.e., peak speeds of 38.8 m/sec at 150 m and 34.2 m/sec at 18 m were recorded from downgraded Hurricane Abby in June 1968. Nonhurricane-associated winds at KSC have reached 26.2 m/sec at 18-m, and 32.6 m/sec at 150-m levels (Ref. 10.2). It is recognized that hurricanes approaching KSC from the east (from the sea) will, in general, produce higher winds than those approaching KSC after crossing the peninsula from Florida (from land). Hurricane David, September 1979, was the first hurricane to strike the Cape Canaveral area directly since 1926. The eastern edge of the eye passed within an estimated 1.5 miles of the Space Shuttle runway. Hurricane David's peak speed of 34.5 m/sec (measured at 10.4 m) exceeded the design launch peak wind speed profile of the Space Shuttle natural environment requirements for a 5-percent risk of exceeding a 10-m level peak wind speed of 15.8 m/sec (30.8 knots) for the windiest 1-hr exposure period (Ref. 10.3).

#### 10.3.1 Distribution of Hurricane and Tropical Storm Frequencies

Knowing the mean number of tropical storms or hurricanes (events) per year that come within a given radius of KSC, without knowing other information, is of little use. If the distribution of the number of tropical storms or hurricanes is known to be a Poisson-type distribution, then the mean number of events per year (or any reference period) can be used to completely define the Poisson distribution function.

3. The highest recorded KSC hurricane-associated wind speed gust was 45.5 m/sec (88.4 knots) measured atop (96 m) the launch complex 34 service structure during Hurricane Dora, September 9, 1964. A simultaneous measurement of 42.4 m/sec (82.4 knots) from the 21-m level, Blockhouse location, was also recorded (Ref. 10.2).

TABLE 10.3 NUMBER OF HURRICANES  
IN AN 81-yr PERIOD (1899-1979) WITHIN  
A 161- AND 644-km (100- and 400-  
n.mi.) RADIUS OF KENNEDY  
SPACE CENTER

Month	Number of Hurricanes Within	
	161-km (100-n. mi. ) radius	644-km (400-n. mi. ) radius
Jan.	0	0
Feb.	0	0
Mar.	0	0
Apr.	0	0
May	1	1
Jun.	2	5
Jul.	2	12
Aug.	3	25
Sep.	6	48
Oct.	6	34
Nov.	0	5
Dec.	1	1
Total	21	131

TABLE 10.4 NUMBER OF TROPICAL STORMS  
IN A 109-yr PERIOD (1871-1979) WITHIN A  
161- AND 644-KM (100- and 400-  
n.mi.) RADIUS OF KENNEDY  
SPACE CENTER

Month	Number of Tropical Storms Within	
	161-km (100-n. mi. ) radius	644-km (400-n. mi. ) radius
Jan.	0	0
Feb.	1	1
Mar.	0	0
Apr.	0	0
May	2	4
Jun.	7	30
Jul.	6	29
Aug.	23	69
Sep.	23	111
Oct.	32	102
Nov.	1	17
Dec.	1	1
Total	96	364

From Figure 10.3, the probability of no event,  $P(E_0, r)$  where  $r$  = radius, for the following can be read: (1) tropical storms and hurricanes for annual reference periods; (2) tropical storms and hurricanes for July-August-September; and (3) tropical storms and hurricanes for July-August-September-October, versus radius, in kilometers, from KSC. To obtain the probability for one or more events,  $P(E_1, r)$ , from Figure 10.3, the reader is required to subtract the  $P(E_0, r)$ , read from the abscissa, from unity; that is,  $[1 - P(E_0, r)] = P(E_1, r)$ . For example, the probability that no hurricane path (eye) will come within 556 km (300 n.mi.) of KSC in a year is 0.33 [ $P(E_0, r = 300) = 0.33$ ], and the probability that there will be one or more hurricanes within 556 km (300 n.mi.) of KSC in a year is 0.67 ( $1 - 0.33 = 0.67$ ).

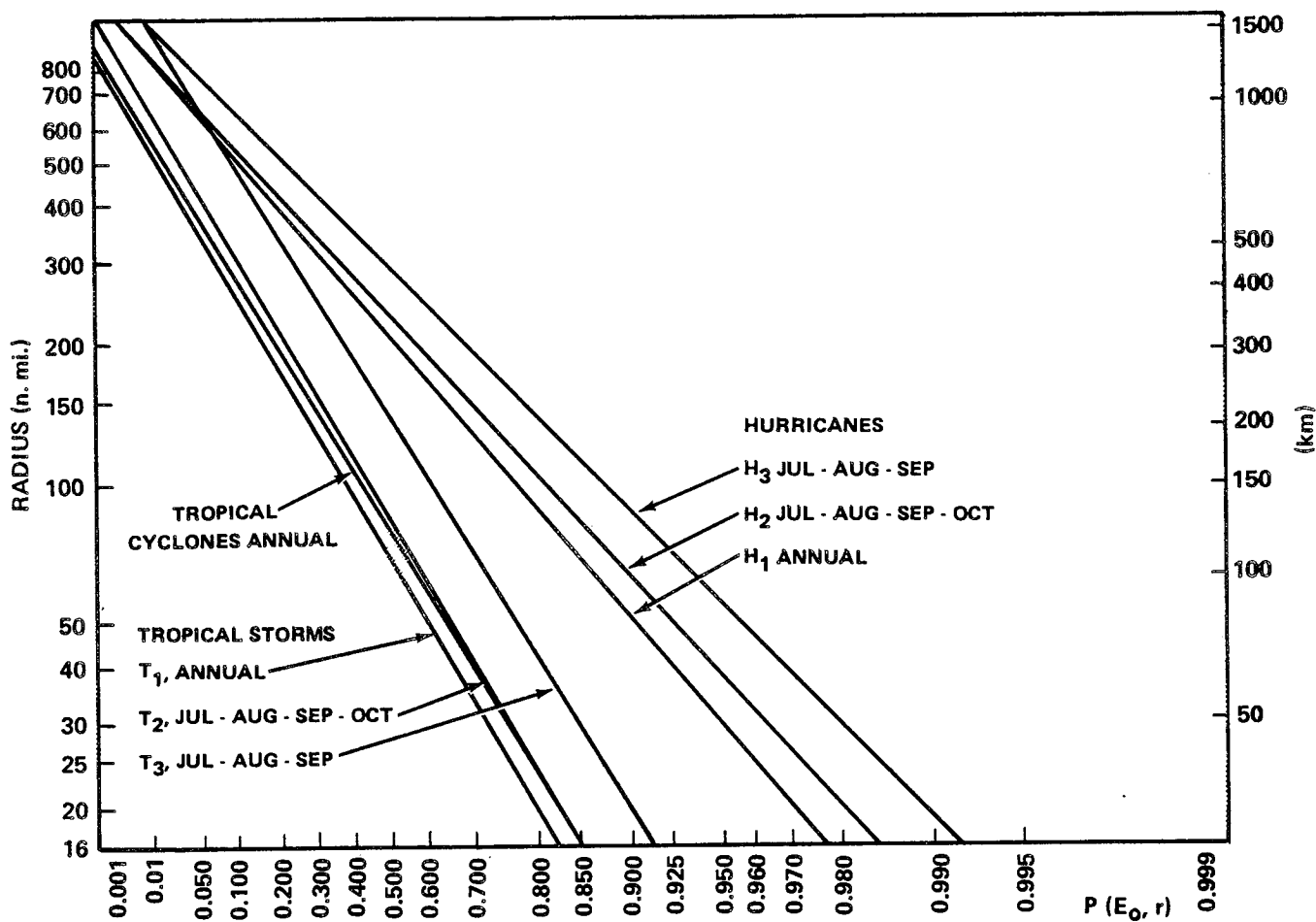


Figure 10.3 Probability of no tropical storms or hurricanes for various reference periods versus various radii from Kennedy Space Center.

## REFERENCES

- 10.1 Thom, H. C. S.: "Tornado Probabilities." Monthly Weather Review, Vol. 91, Nos. 10-12, Oct.-Dec. 1963, pp. 730-736.
- 10.2 Alexander, Margaret B.: "An Analysis of Maximum Horizontal Wind Speeds Recorded Since 1961 at Kennedy Space Center, Florida." NASA TM-78177, Marshall Space Flight Center, Alabama, May 1978.
- 10.3 Alexander, Margaret B.: "Hurricane David Wind Velocities." NASA-MSFC-ES82 Memorandum for Record, September 20, 1979.



## SECTION XI. ATMOSPHERIC ELECTRICITY

11.1 Introduction

At present there are no complete design handbooks, military specifications, or standards for atmospheric electricity hazards protection (Ref. 11.1). This is especially true where aerospace vehicles/systems ground launch and atmospheric flight operations are concerned. The Air Force Systems Command (AFSC) Design Handbook 1-4, "Electromagnetic Compatibility," is the most complete design handbook currently available (Ref. 11.2) which discusses lightning strike phenomena, design to prevent lightning, etc., but the information included on protection from lightning hazards is very limited. The Society of Automotive Engineers (SAE) Committee AE-4 on Electromagnetic Compatibility published a report defining lightning test waveforms and techniques for aerospace vehicles and hardware (Ref. 11.3). The committee is presently working on standards for transient test levels for aerospace electronics equipment.

Reference 11.4 contains Space Shuttle program lightning protection criteria. Also, some information regarding atmospheric electricity hazards associated with lightning and static electricity is documented in military standards entitled, "Electrical Bonding and Lightning Protection for Aircraft Systems" (Ref. 11.5), "General Specifications for Lightning Arresters" (Ref. 11.6), "Systems Electromagnetic Compatibility Requirements" (Ref. 11.7), and "Electromagnetic Interference Characteristics Requirements for Equipment" (Ref. 11.8). Portions of the material found in these documents are included in the technical statements of this section.

The Aerospace Safety Research and Data Institute of NASA's Lewis Research Center sponsored the documentation by the General Electric Company of a handbook, "Lightning Protection of Aircraft," (Ref. 11.9). Such information, together with the findings from lightning research tasks being conducted by Air Force, Navy, NASA, and private industry (General Electric, the Rand Corporation, Brunswick Company, McDonnell Aircraft Company, Stanford Research Institute, etc.), should provide excellent material for the preparation of a handbook on lightning and static electricity protection for aerospace vehicles and systems.

A document entitled, "Review of Lightning Protection Technology for Tall Structures," (Ref. 11.10) discusses the actions of corona-point arrays in strong electric fields. Some statistics are included relative to four tall structural facilities at Kennedy Space Center which have lightning dissipation arrays. These facilities are: (1) NASA's 150-Meter Ground Winds Tower, (2) Unified S-Band Station, (3) Mobile Service Structure, LC-39, and (4) Mobile Service Tower, LC-41 (Cape Canaveral Air Force Station).

Atmospheric electricity must be considered in the design, transportation, and operation of aerospace vehicles. The effect of the atmosphere as an insulator and conductor of high-voltage electricity, at various atmospheric pressures, must also be considered. Aerospace vehicles that are not adequately protected can be damaged by the following:

1. A direct lightning stroke to the vehicle or the launch support equipment while on the ground or after launch.
2. Current induced in the vehicle from changing electric fields produced by nearby lightning.
3. A large buildup of the atmospheric potential gradient near the ground as a result of charged clouds nearby.
4. High-voltage systems aboard the vehicle which are not properly designed can arc or break down at low atmospheric pressures.

## 11.2

The vehicle can be protected as follows:

1. By insuring that all metallic sections are connected by electrical bonding so that the current flow from a lightning stroke is conducted over the skin without any gaps where sparking would occur or current would be carried inside. Reference 11.5 gives the requirements for electrical bonding.
2. By protecting buildings and other structures on the ground with a system of lightning rods and solid grounding over the outside to carry the lightning stroke into the ground.
3. By providing a zone of protection (as shown in Ref. 11.11 for the lightning protection plan for Shuttle Launch Complex 39).
4. By providing protection devices in critical circuits (Ref. 11.12).
5. By using systems which have no single failure mode. [The Saturn V launch vehicle used triple redundant circuitry on the auto-abort system, which requires two out of the three signals to be correct before abort is initiated (Ref. 11.13)].
6. By appropriate shielding of units sensitive to electromagnetic radiation.
7. For horizontally flying vehicles, by avoiding potentially hazardous thunderstorm areas with proper flight planning and flight operations. Reference 11.14 has an excellent discussion on geographic areas where thunderstorms and thus potentially dangerous lightning discharges occur frequently.

If lightning should strike a vehicle or the test stand or launch umbilical tower (LUT), sufficient system checks should be made to insure that all electrical components and subsystems of the vehicle are functional.

### 11.2 Thunderstorm Electricity

On a cloudless day, the potential electrical gradient in the atmosphere near the surface of the Earth is relatively low ( $<300$  V/m); but when clouds develop, the potential gradient near the surface of the Earth increases. If the clouds become large enough to have water drops of sufficient size to produce rain, the atmospheric electrical energy often grows large enough to produce lightning discharges. In this situation, electric fields at the ground are generally thousands of volts per meter, while fields aloft are orders of magnitude stronger.

#### 11.2.1 Potential Gradient

The Earth-ionospheric system is sometimes described as a large capacitor, with the Earth's surface as one plate, the ionosphere the other plate, and the atmosphere the dielectric. The Earth is negatively charged with respect to the ionosphere.



### 11.2.2 Fair-Weather<sup>1</sup> Potential Gradients

The fair-weather electric field strength (the negative of the electrical gradient) measured near the ground is approximately 100 V/m and negative; i.e., the Earth is negatively charged with respect to the ionosphere. The fair-weather-value varies with time and location. These variations in the fair weather field are caused by local anomalies in the atmosphere conductivity as well as variations in the global circuit (Ref. 11.15). The fair-weather potential gradient decreases with altitude and has a value near 10 V/m at 10 km. Fair-weather potential gradient over a 100-m-high vehicle could effectively short the 10,000-V, or greater, potential difference between the air near the ground and the air around the vehicle top, causing an ungrounded vehicle to assume a high voltage with respect to the Earth.

### 11.2.3 Potential Gradients During Thunderstorms

When a cloud develops into the cumulonimbus state, lightning discharges result. For a discharge to occur, the potential gradient at a location reaches a value equal to the critical breakdown value of air at that location. Laboratory data indicate this value to be greater than  $10^6$  V/m at standard sea-level atmospheric pressure. Electrical fields measured at the surface of the Earth are much less than  $10^6$  V/m during lightning discharges for several reasons:

1. The total charge in a cloud tends to be much smaller than the net charge in a single charge region, again resulting in a rapid decrease of the field with distance. Each charge in the atmosphere and its image within the Earth resembles an electrical dipole, and the intensity of the electrical field decreases with the cube of the distance to the dipole.
2. The atmospheric electric field measured over land at the surface is limited by corona discharge from grounded points, such as grass, trees, and other structures, which produce local screening layers.

For these reasons, the measured electrical field at the surface is seldom more than about  $1 \times 10^4$  V/m. Potential gradient values at the surface are generally highest when the charged cloud is directly overhead. As the horizontal distance between the projection of the charged center of the cloud to the ground and the measuring equipment becomes greater, the readings become lower, reaching zero at some distance, and then change to the opposite sign at greater distances (References 11.5 and 11.15).

### 11.2.4 Corona Discharge

As the atmospheric potential gradient increases, the air surrounding exposed sharp points becomes ionized by corona discharge. The charge induced by a nearby lightning stroke may aid such a discharge. The corona discharge may be quite severe when lightning storms or large cumulus clouds are within approximately 16 km (10 mi.) of the launch pad.

## 11.3 Characteristics of Lightning Discharges

The following definitions define a lightning discharge and its parts:

- 
1. The term fair weather is used to mean without clouds. The term fine weather is sometimes used.

## 11.4

Lightning stroke, any one of the major electrical and luminous effects, the entire series of which combined make up the lightning flash. Many authors restrict the term "stroke" to the "return stroke" of the cloud-ground flash.

Continuing currents, the current which sometimes flows at the end of a large stroke for hundreds of milliseconds.

The characteristics of various types of lightning discharges are summarized in Table 11.1 and References 11.8 and 11.16.

### 11.3.1 Lightning Currents<sup>2</sup>

The current flows<sup>3</sup> in a lightning flash (cloud to ground) are conveniently separated into categories as follows:

a. Return stroke surges

Peak current from under 20,000 A to over 200,000 A, with durations of tens of microseconds.

b. Intermediate currents

Peak current from under 2,000 A to over 20,000 A, with duration of milliseconds.

c. Continuing currents

Peak current from under 200 A to over 2,000 A, with durations of hundreds of milliseconds.

Currents of category (a) mainly produce explosive effects and undesirable coupling transients, while categories (b) and (c) mainly cause hole-burning type damage.

The time structure of the lightning currents is usually less variable between individual flashes than the amplitudes. Furthermore, there is little connection within an individual discharge between the severity of the three categories; i.e., an initial severe return stroke has minimal influence on the severity of a following continuing current.

### 11.3.2 Lightning Characteristics for Design on the Launch Pad or During Ground Transportation

Three models of lightning flashes are presented in this section for use in design studies as follows:

Model 1. A very severe discharge model.

This model involves two high-current peak strokes (return strokes); the model is as follows:

a. The first return stroke surge with a current peak of 200,000 A and a maximum current rise at a rate of 100,000 A/ $\mu$ s (100 kA/ $\mu$ s) then falling off at a rate of about 2,000 A/ $\mu$ s for 98  $\mu$ s to 7,000 A.

2. The information in this section was prepared in cooperation with Dr. E. T. Pierce of Stanford Research Institute, Menlo Park, California. See Appendix A, Reference 11.4.

3. Note that a broad range of current values is given for each category.

TABLE 11.1 CHARACTERISTICS OF LIGHTNING DISCHARGES

Type of Lightning	Average Peak Current per Stroke (A)	Maximum Rate of Rise of Current (A/ $\mu$ sec)	Average Amount of Charge Transferred		Average Total Duration of Stroke (msec)	Average Number of Strokes (unitless)	Average Time Between Strokes (msec)	Remarks
			Per Stroke (C)	Total (C)				
Intercloud lightning	100-2000	100-500	1-5	1-5	300	1		
Discrete lightning strokes to ground								
Leader	100		1-5	5	20	1		
Return stroke	20 000	200 000	5	4-20	0.3	3 to 4	40	Peak current exceeding 100 000 A have been measured about 2 percent of the time.
Long continuing current lightning strokes to ground								
Leader	100		1-5	5	20	1		
Return stroke	20 000	10 000	12-40	12-40	200	1		Average current value of 185 A for long periods (175 msec).

b. An intermediate current, following the intermediate current, of an average of 700 A (1,000 to 400 A) for 50 ms.

c. A first continuing current, following the intermediate current, of an average of 700 A (1,000 to 400 A) for 50 ms.

d. A second continuing current, following the first intermediate of an average of 400 A, for 337 ms at constant current.

e. A second return stroke surge, during the first continuing current, with a peak current of 50,000 A and a maximum current rise at a rate of 25,000 A/ $\mu$ s and then falling off at a rate of about 500 A/ $\mu$ s for 98  $\mu$ s to 3,500 A.

f. An intermediate current, following the second return stroke surge, of an average of 2,000 A (3.5 kA to 400 A) for 5 ms.

The current time history for this model is shown in Figure 11.1 and Table 11.2. This model is the basis of the Space Shuttle Lightning Protection Design and was developed from measurements of Florida lightning by Dr. Uman (Ref. 11.17) and work by Dr. Pierce and Dr. Cianos (Ref. 11.18). Later measurements suggest significantly higher rates of change in the electric currents and electric and magnetic fields than these models indicate.

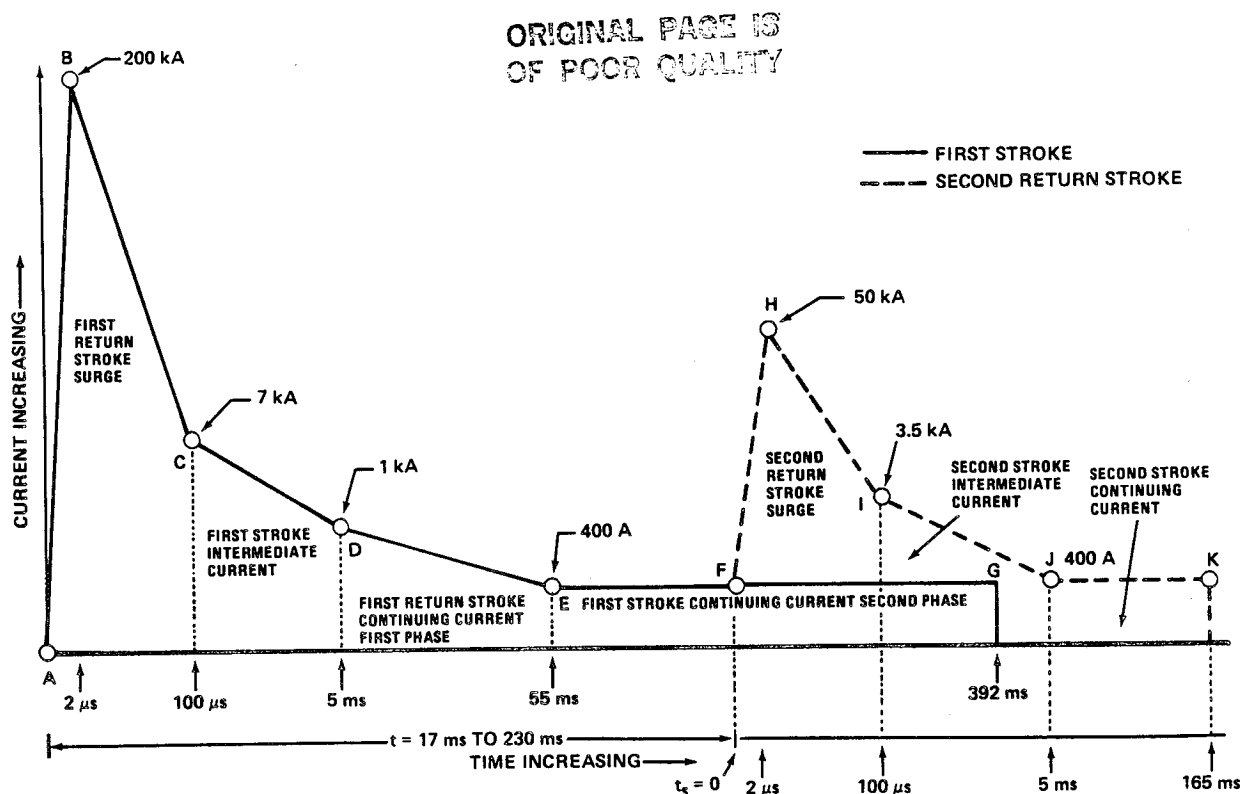


Figure 11.1 Diagrammatic representation of a very severe lightning model (Model 1)  
(note that the diagram is not to scale) January 1979 Revision.

TABLE 11.2 DETAILS OF A VERY SEVERE LIGHTNING MODEL (MODEL 1)

Stage	Key Points	Rate of Current Change	Charge Passing
1. First Return Stroke Surge	$t = 0$ $i = 0$ $t = 2 \mu s$ $i = 200 \text{ kA}$ $t = 100 \mu s$ $i = 7 \text{ kA}$	Linear Rise - $100 \text{ kA}/\mu s$ Linear Fall - $193 \text{ kA}$ in $98 \mu s$	$0.2 \text{ C}^*$ $\sim 10.2 \text{ C}$
2. First Stroke Intermediate Current	$t = 100 \mu s$ $i = 7 \text{ kA}$ $t = 5 \text{ ms}$ $i = 1 \text{ kA}$	Linear Fall - $6 \text{ kA}$ in $4.9 \text{ ms}$	$19.6 \text{ C}$
3. Continuing Current--First Phase	$t = 5 \text{ ms}$ $i = 1 \text{ kA}$ $t = 55 \text{ ms}$ $i = 400 \text{ A}$	Linear Fall - $600 \text{ A}$ in $50 \text{ ms}$	$35.0 \text{ C}$
4. Continuing Current--Second Phase	$t = 55 \text{ ms}$ $i = 400 \text{ A}$ $t = 392 \text{ ms}$ $i = 400 \text{ A}$	Steady Current	$135.0 \text{ C}$
5. Second Return Stroke Surge	$t = 17 \text{ ms} \rightarrow 230 \text{ ms}$ to $t_s = 0$ $t_s = 2 \mu s$ $i = 50 \text{ kA}$ $t_s = 100 \mu s$ $i = 3.5 \text{ kA}$	Linear Rise $\sim 25 \text{ kA}/\mu s$ Linear Fall - $46.5 \text{ kA}$ in $98 \mu s$	$\sim 0.05 \text{ C}$ $\sim 2.28 \text{ C}$
6. Second Stroke Intermediate Current	$t_s = 5 \text{ ms}$ $i = 3.5 \text{ kA}$ $t_s = 165 \text{ ms}$ $i = 400 \text{ A}$	Linear Fall - $3.1 \text{ kA}$ in $5 \text{ ms}$	$9.75 \text{ C}$

\* Coulomb (C) is the quantity of electricity transported in one second by a current of one ampere.

Note:  $t$  = Time associated with first return stroke.

$t_s$  = Time associated with second return stroke.

### Model 2. A 98 percentile peak current model.<sup>4</sup>

This model involves one high-current peak stroke (return stroke). The model is as follows:

- a. The first return stroke surge with a current peak of 100,000 A and a maximum current rise at a rate of 20,000 A/ $\mu$ s (20 kA/ $\mu$ s), then falling off at a rate of about 1,000 A/ $\mu$ s for 95  $\mu$ s to 3,500 A.
- b. An intermediate current, following the first return stroke surge, of an average of 2,000 A (3,500 to 500 A) for 5 ms (5,000  $\mu$ s).
- c. A first continuing current, following the intermediate current, of an average of 350 A (500 to 200A) for 50 ms.
- d. A second continuing current, following the first intermediate current, of an average of 200 A, for 300 ms at constant current.

This model current time history is shown in Figure 11.2 and Table 11.3.

### Model 3. An average peak current model

This model involves one high-current peak stroke (return stroke). The model is as follows:

- a. The first return stroke surge with a current peak of 20,000 A and a maximum current rise at a rate of 4,000 A/ $\mu$ s (4 kA/ $\mu$ s), then falling off at a rate of about 190 A/ $\mu$ s for 95  $\mu$ s to 2,000 A.
- b. An intermediate current, following the first return stroke surge, of an average of 1150 A (1700 to 850 A) for 5 ms (500  $\mu$ s).
- c. A first continuing current, following the intermediate current, of an average of 100 A, for 300 ms at constant current.
- d. A second continuing current, following the first intermediate current, of an average of 100 A, for 300 ms at constant current.

The current-time history for this model is shown in Figure 11.3 and Table 11.4.

#### 11.3.3 Lightning Characteristics for Design During Flight (Triggered Lightning)

The space vehicle while in flight should be capable of withstanding an electrical discharge from triggered lightning equal to Model 3, given in Section 11.3.2, for an average cloud-to-ground discharge. Designs of most solid and liquid rocket engines are such that more extreme lightning currents may result in serious damage when the engines are burning. Therefore, launch mission rules are needed to prevent a launch when any severe lightning discharges are possible (Ref. 11.19).

---

4. The intermediate and continuing currents are not necessarily the 98 percentile values, but are added to represent a more severe burning phase.

ORIGINAL PAGE IS  
OF POOR QUALITY

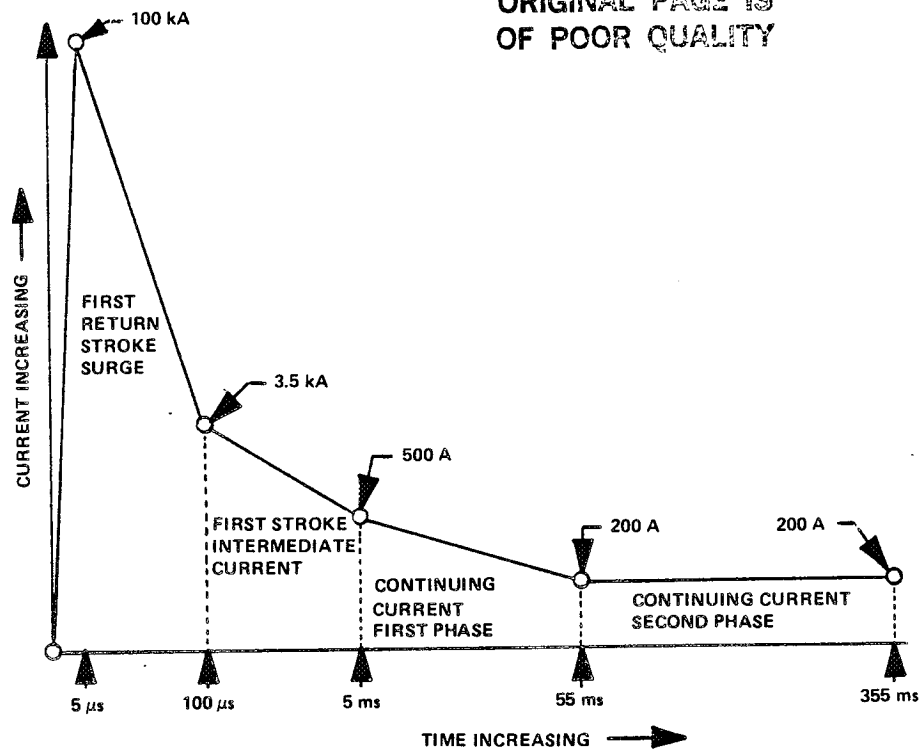


Figure 11.2 Diagrammatic representation of a 98 percentile peak current lightning model (Model 2). (Note that the diagram is not to scale).

TABLE 11.3 DETAILS OF A 98 PERCENTILE PEAK CURRENT LIGHTNING MODEL (MODEL 2)

Stage	Key Points	Rate of Current Change	Charge Passing
1. First Return Stroke Surge	$t = 0$ $i = 0$ $t = 5 \mu s$ $i = 100 \text{ kA}$ $t = 100 \mu s$ $i = 3.5 \text{ kA}$	Linear Rise - $20 \text{ kA}/\mu s$ Linear Fall - $96.5 \text{ kA}$ in $95 \mu s$	$0.3 \text{ C}$ $\sim 4.9 \text{ C}$
2. First Stroke Intermediate Current	$t = 100 \mu s$ $i = 3.5 \text{ kA}$ $t = 5 \text{ ms}$ $i = 500 \text{ A}$	Linear Fall - $3 \text{ kA}$ in $4.9 \text{ ms}$	$9.8 \text{ C}$
3. Continuing Current-- First Phase	$t = 5 \text{ ms}$ $i = 500 \text{ A}$ $t = 55 \text{ ms}$ $i = 200 \text{ A}$	Linear Fall - $300 \text{ A}$ in $50 \text{ ms}$	$17.5 \text{ C}$
4. Continuing Current-- Second Phase	$t = 55 \text{ ms}$ $i = 200 \text{ A}$ $t = 355 \text{ ms}$ $i = 200 \text{ A}$	Steady Current	$60 \text{ C}$

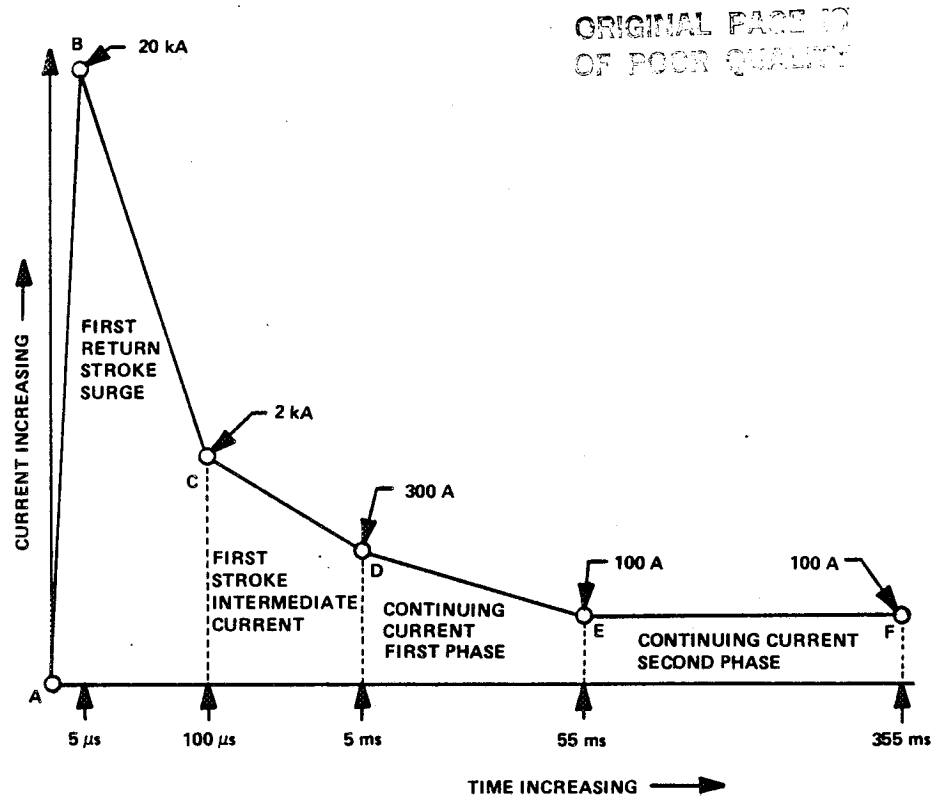


Figure 11.3 Diagrammatic representation of an average lightning model (Model 3).  
(Note that the diagram is not to scale.)

TABLE 11.4 DETAILS OF AN AVERAGE LIGHTNING MODEL (MODEL 3)

Stage	Key Points	Rate of Current Change	Charge Passing
1. First Return Stroke Surge	$t = 0$ $i = 0$ $t = 5 \mu s$ $i = 20 \text{ kA}$ $t = 100 \mu s$ $i = 2 \text{ kA}$	Linear Rise - $4 \text{ kA}/\mu s$ Linear Fall - $18 \text{ kA}$ in $95 \mu s$	$0.1 \text{ C}$ $\sim 1.0 \text{ C}$
2. First Stroke Intermediate Current	$t = 100 \mu s$ $i = 2 \text{ kA}$ $t = 5 \text{ ms}$ $i = 300 \text{ A}$	Linear Fall - $1.7 \text{ kA}$ in $4.9 \text{ ms}$	$5.6 \text{ C}$
3. Continuing Current -- First Phase	$t = 5 \text{ ms}$ $i = 300 \text{ A}$ $t = 55 \text{ ms}$ $i = 100 \text{ A}$	Linear Fall - $200 \text{ A}$ in $50 \text{ ms}$	$10.0 \text{ C}$
4. Continuing Current -- Second Phase	$t = 55 \text{ ms}$ $i = 100 \text{ A}$ $t = 355 \text{ ms}$ $i = 100 \text{ A}$	Steady Current	$30.0 \text{ C}$

#### 11.3.4 Current Flow Distribution from a Lightning Discharge

When lightning strikes an object, the current tends to follow the lowest conductivity path to the true Earth ground. However, because of the high-frequency components of lightning, the current does not always follow what appears to be the preferred, lowest resistance, path; but, rather, it often "jumps," following a path of lowest net impedance. The voltage drop along this path may be great enough over short distances to be dangerous to personnel and equipment. Cattle and humans have been electrocuted from the current flow through the ground and the voltage potential between their feet while standing under a tree struck by lightning.

Because lightning tends to strike the highest exposed point, the only way to be certain that damaging currents will not flow through a space vehicle on the launch pad is to either: (1) prevent the lightning discharge to the launch complex, (2) conduct the lightning discharge around the launch complex using low-impedance high-current capacity conductors well insulated (high-resistance supports) from the launch complex equipment, or (3) design the space vehicle to carry the currents without damage.

#### 11.3.5 Radio Interference

When an electrical charge produces a spark between two points, electromagnetic radiation is emitted. This discharge is not limited to a narrow band of frequencies but covers most of the electromagnetic radiation spectrum with varying intensities. Most static heard in radio reception is related to electrical discharges, with lightning strokes contributing much of the interference. This interference from lightning strokes is propagated through the atmosphere in accordance with laws valid for ordinary radio transmission and may travel great distances. With the transmission of interference from lightning strokes over great distances, certain frequencies remain prominent, with those near 30 kHz being the major frequencies. Interference with telemetering and guidance needs to be considered only when thunderstorms are occurring within 100 km (60 mi.) of the space vehicle launch site (Refs. 11.8 and 11.20).

#### 11.4 Frequency of Occurrence of Thunderstorms

According to standard United States weather observing and recording practice, a thunderstorm is reported whenever thunder is heard at the station. It is recorded together with other atmospheric phenomena on the standard weather observer's form, indicating when the thunder is heard. The report ends 15 min after thunder is last heard. This type of reporting of thunderstorms may contain a report as one, or one or more thunderstorms during a period. For this reason, these types of observations will be referred to as thunderstorm events, i.e., a period during which one or more thunderstorms are reported. Because of the method of reporting thunderstorms, most analyses of thunderstorm data are based on the number of days per year in which thunder is heard one or more times on a day; i.e., thunderstorm days. Reference 11.21 is a detailed study of frequencies of thunderstorms occurring in the KSC area.

##### 11.4.1 Thunderstorm Days per Year (Isoceraunic<sup>5</sup> Level)

The frequency of occurrence of thunderstorm days is an approximate guide to the probability of lightning strokes to Earth in a given area. The number of thunderstorm days per year is called the isoceraunic level. A direct lightning stroke is possible at all locations of interest, but the frequency of such an occurrence varies with location (Table 11.5).

---

5. This word is also spelled isokeraunic.



TABLE 11.5 FREQUENCY-OF-OCCURRENCE OF "THUNDERSTORM DAYS"  
(ISOCERAUNIC LEVEL)

Location	Mean Number of Days Per Year of Thunderstorms	Monthly Distribution ( $\frac{\% \text{ of Annual}}{\text{No. Days}}$ )											
		Jan.	Feb.	Mar.	Apr.	May	Jun.	Jul.	Aug.	Sep.	Oct.	Nov.	Dec.
Huntsville	70	1 0.70	3 2.10	6 4.20	8 5.60	11 7.70	19 13.30	22 15.40	18 12.60	9 6.30	1 0.70	1 0.70	1 0.70
River Transportation and New Orleans	75	3 2.25	3 2.25	5 3.75	5 3.75	8 6.0	16 12.0	21 15.75	20 15.0	10 7.5	3 2.25	3 2.25	3 2.25
Gulf Transportation	90	1 0.90	1 0.90	4 3.60	2 1.80	9 8.10	18 16.20	24 21.60	23 20.70	12 10.80	4 3.60	1 0.90	1 0.90
Eastern Test Range	70.09	0.77 0.54	1.94 1.36	4.28 3.00	4.02 2.82	9.73 6.82	18.55 13.00	21.27 14.91	20.23 14.18	13.22 9.27	3.89 2.73	1.18 0.82	0.92 0.64
Panama Canal Transportation	100	1 1.0	1 1.0	4 4.0	2 2.0	9 9.0	18 18.0	24 24.0	23 23.0	12 12.0	4 4.0	1 1.0	1 1.0
West Coast Transportation	6	9 0.54	11 0.66	19 1.14	13 0.78	7 0.42	4 0.24	3 0.18	7 0.42	8 0.48	8 0.48	3 0.24	8 0.48
Vandenberg AFB, California	2	5 0.1	15 0.3	15 0.3	5 0.1	2 0.04	1.5 0.03	10 0.2	10 0.2	25 0.5	1.5 0.03	5 0.1	5 0.1
Sacramento	4	6 0.24	16 0.64	12 0.48	15 0.60	9 0.54	6 0.24	3 0.12	3 0.12	10 0.40	12 0.48	5 0.20	3 0.12
Wallops Test Range <sup>a</sup>	40.6	0.5 0.2	1.2 0.5	5.2 2.1	8.4 3.4	12.6 5.1	17.2 7.0	21.7 8.8	20.4 8.3	7.9 3.2	3.2 1.3	1.0 0.4	0.7 0.3
White Sands Missile Range <sup>b</sup>	38.1	0.8 0.3	0.1 0.05	1.8 0.7	4.7 1.8	7.6 2.9	15.2 5.8	30.5 11.6	23.9 9.1	8.7 3.3	5.2 2.0	0.5 0.2	1.0 0.4
Edwards AFB, California	4.3	2.3 0.1	2.3 0.1	2.3 0.1	7.0 0.3	4.7 0.2	2.3 0.1	23.3 1.0	25.6 1.1	20.9 0.9	7.0 0.3	2.3 0.1	9 0
a. Data from Norfolk, Virginia													
b. Data from Holloman AFB, New Mexico													

## 11.4.2 Thunderstorm Occurrence per Day

In a study using weather observation data, which reports a thunderstorm when thunder is heard, the frequencies were computed on the number of days which had 0, 1, 2, ..., thunderstorms reported; i.e., none or more thunderstorm events. Tables 11.6 and 11.7 and Reference 11.21 give this information.

## 11.4.3 Thunderstorm Hits

There were sufficient data for the summer months (June-August) at Kennedy Space Center to make an analysis of the frequency of occurrence of thunderstorm hits as:

1. A thunderstorm actually reported overhead.
2. A thunderstorm first reported in a sector and last reported in the opposite sector, if it is assumed that thunderstorms move in straight lines over small areas. This information is listed in Tables 11.8 and 11.9 and Reference 11.21.

11.12

TABLE 11.6 FREQUENCIES OF THE OBSERVED NUMBER OF DAYS THAT EXPERIENCED  
x THUNDERSTORM EVENTS AT KSC FOR THE 11-YEAR PERIOD  
OF RECORD JANUARY 1957 THROUGH DECEMBER 1967

x	Jan	Feb	Mar	Apr	May	Jun	Jul	Aug	Sep	Oct	Nov	Dec	Spring	Summer	Fall
0	335	295	308	299	266	187	177	185	228	311	321	334	873	549	860
1	4	9	20	18	43	77	80	89	54	17	6	3	81	246	77
2	2	4	9	10	25	40	47	30	33	9	3	2	44	117	45
3		2	3	3	3	17	26	24	12	4		2	9	67	16
4			1		3	6	9	10	3				4	25	3
5					0	2	2	3					0	7	
6					1	1							1	1	
n	341	310	341	330	341	330	341	341	330	341	330	341	1012	1012	1001

TABLE 11.7 RELATIVE FREQUENCY OF DAYS THAT EXPERIENCED  
AT LEAST ONE THUNDERSTORM EVENT AT KSC

Jan	Feb	Mar	Apr	May	Jun	Jul	Aug	Sep	Oct	Nov	Dec	Spring	Summer	Fall
0.018	0.048	0.097	0.094	0.220	0.433	0.481	0.457	0.309	0.088	0.027	0.021	0.137	0.458	0.141

TABLE 11.8 FREQUENCIES OF THE OBSERVED NUMBER OF DAYS THAT EXPERIENCED  
x THUNDERSTORM HITS AT KSC FOR THE 11-YEAR PERIOD OF RECORD,  
JANUARY 1957 THROUGH DECEMBER 1967

x	Jun	Jul	Aug	Summer
0	293	305	300	898
1	27	24	30	81
2	5	6	7	18
3	3	3	2	8
4 or more	2	3	2	7
Total	330	341	341	1012

TABLE 11.9 RELATIVE FREQUENCY OF DAYS THAT EXPERIENCED  
AT LEAST ONE THUNDERSTORM HIT AT KSC

Jun	Jul	Aug	Summer
0.112	0.106	0.121	0.113

#### 11.4.4 Hourly Distribution of Thunderstorms

Figure 11.4 presents the empirical probability that a thunderstorm will occur in the Kennedy Space Center area at each hour of the day during each month. The highest frequency of thunderstorms (24 percent) is around 1600 EST in July. A thunderstorm is reported by standard observational practice if thunder is heard, which is possible over a radius of approximately 25 km. Thus, the statistics presented in Figure 11.4 are not necessarily the probability that a thunderstorm will "hit," for example, a vehicle on the launch pad, or occur at a given location at Kennedy Space Center.

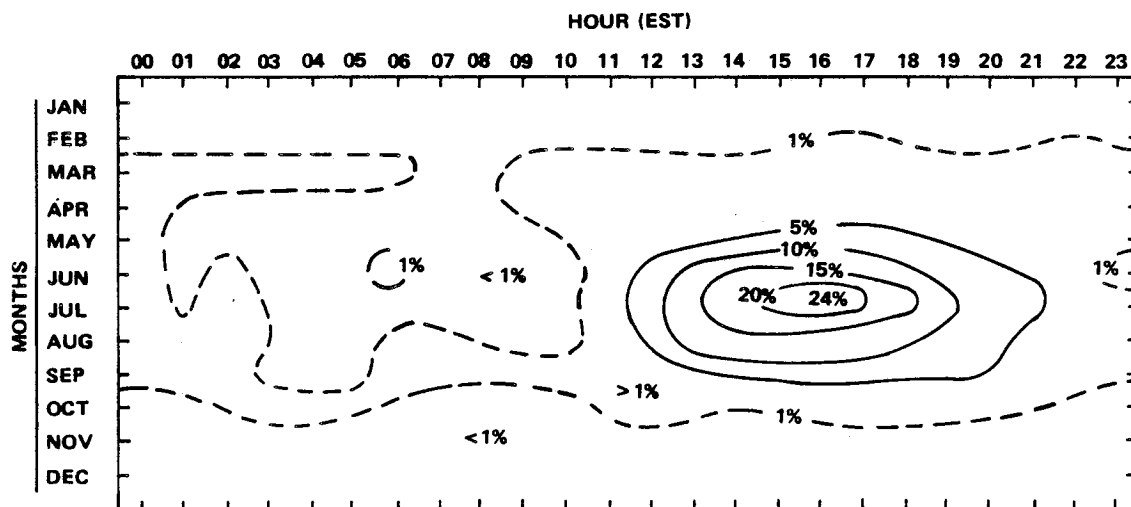


Figure 11.4 Probability (%) of occurrence of thunderstorms by months versus time of day in the KSC area.

#### 11.5 Frequency of Lightning Strokes to Earth

Only limited data have been obtained on the number of lightning strokes to ground. These data have been difficult to obtain because only recently could measuring equipment differentiate between cloud-to-ground and cloud-to-cloud strokes. This sophisticated equipment has only been installed in limited areas. Therefore, much data of cloud-to-ground lightning strokes have been obtained visually. Such observations are limited in both number and length of time of observations.

Comparison of data published on cloud-to-ground lightning strokes from measuring equipment, visual observations, actual strikes to objects from insurance claims and magnetic links, and electrical outages confirms that the average number of lightning strokes per year to objects of different heights given in Table 11.10 is realistic of the KSC area.

Table 11.10 should not be interpreted to mean that 4.4 lightning strokes will be observed on a 152-m (500-ft) object at KSC each year (Ref. 11.10). There may be no strokes or very few during a year, then in another year, a considerable number of strokes. Also, one can assume that all strokes that occur will not be observed or known to have occurred within the launch area. Although numerous aerospace vehicles have been launched from KSC during the last 15 years, only a few lightning strokes are known to have struck the launch complex until Apollo 15, when 11 separate strokes were known to have struck the launch complex during 5 different days between June 14 and July 21, 1971 (a period of 37 days) (Ref. 11.22).

11.14

TABLE 11.10 ESTIMATE OF THE AVERAGE NUMBER OF LIGHTNING STROKES  
PER YEAR FOR VARIOUS HEIGHTS FOR KSC

Height		Average Number of Lightning Strokes per Year
(m)	(ft)	
30.5	100	0.4
61.0	200	1.1
91.4	300	2.3
121.9	400	3.5
152.4	500	4.4
182.9	600	5.3
213.4	700	5.8

### 11.6 Static Electricity

Static electrical charge may accumulate on an object from its motion through an atmosphere containing raindrops, ice particles, or dust. A stationary object, if not grounded, can also accumulate a charge from windborne particles (often as nuclei too small to be visible) or rain or snow particles striking the object. This charge can build up until the local electric field at the point of sharpest curvature exceeds the breakdown field. The quantity of maximum charge will depend on the size and shape of the object (especially if sharp points are on the object). Methods of calculating this charge are given in Reference 11.16.

If a charge builds up on a vehicle on a launch pad which is not grounded, any discharges which occur could ignite explosive gases or fuels, interfere with radio communications or telemetry data, or cause severe shocks to personnel. Static electrical charges occur more frequently during periods of low humidity and can be expected at all geographical areas.

### 11.7 Electrical Breakdown of the Atmosphere

The atmosphere of the Earth at normal sea-level pressure ( $101\,325\text{ N/m}^2$ ) is an excellent insulator, having a resistance greater than  $10^{16}$  ohms for a column  $1\text{ cm}^2$  in cross section and  $1\text{ m}$  long. When ionization takes place in the atmosphere, the conductivity of the air generally increases. However large net charge can accumulate from either cloud buildups or in electrical equipment. When the charge density is increased sufficiently, breakdown fields are reached and discharges can occur.

The breakdown voltage (voltage required for a spark to jump a gap) for direct current is a function of atmospheric pressure. The breakdown voltage decreases with altitude until a minimum is reached of  $327\text{ V/mm}$  at an atmospheric pressure of  $760\text{ N/m}^2$  ( $7.6\text{ mb}$ ), representing an altitude of  $33.3\text{ km}$ . Above and below this altitude, the breakdown voltage increases rapidly (Ref. 11.23), being several thousands volts per millimeter at normal atmospheric pressure (Fig. 11.5).

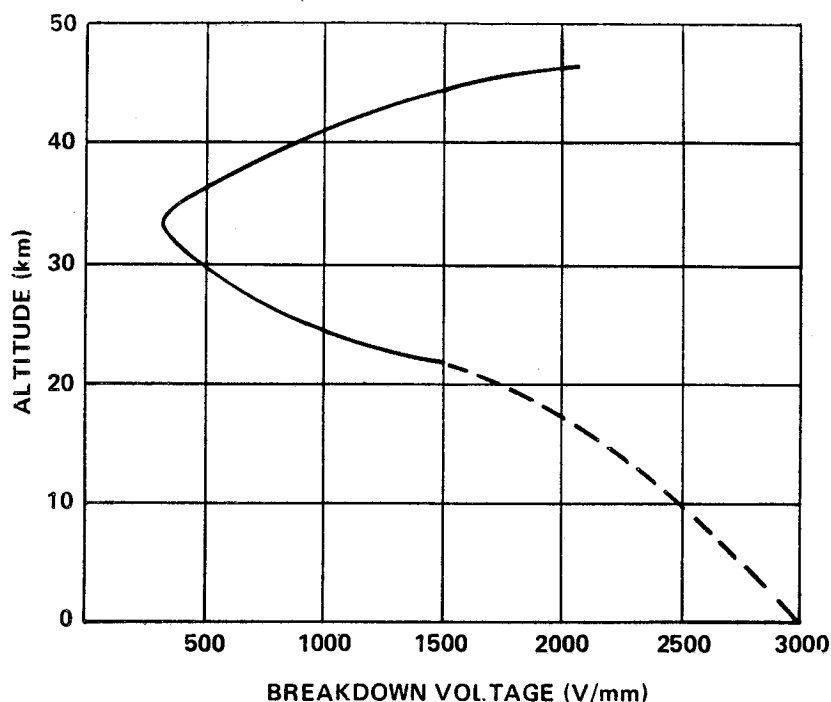


Figure 11.5 Breakdown voltage versus altitude.

The breakdown voltage is also a function of frequency of an alternating current. With an increase of frequency the breakdown voltage decreases. A more complete discussion can be found in Reference 11.24.

The following safety measures can be taken to prevent arcing of high voltage in equipment:

1. Have equipment voltages off at the time the space vehicle is going through the critical atmospheric pressures. Any high-voltage capacitors should have bleeding resistors to prevent high-voltage charges remaining in the capacitors.
2. Eliminate all sharp points and allow sufficient space between high-voltage circuits.
3. Seal high-voltage circuits in containers at normal sea-level pressures.
4. Have materials available to protect, with proper use, against high-voltage arcing by potting circuits.

## REFERENCES

- 11.1 Corbin, John C., Jr.: Protection of Systems Avionics Against Atmospheric Electricity Hazards – Lightning and Static Electricity. IEEE 1977 National Aerospace and Electronics Conference Proceedings, May 1977.
- 11.2 Electromagnetic Compatibility. Air Force Systems Command Design Handbook, AFSC DH1-4, Third Edition, January 5, 1975.
- 11.3 Lightning Test Waveforms and Techniques for Aerospace Vehicles and Hardware. Report of SAE Committee AE-4, Special Task F, May 5, 1976.
- 11.4 Space Shuttle Program Lightning Protection Criteria Document. Document No. JSC-07636, Johnson Space Center, National Aeronautics and Space Administration, November 4, 1975.
- 11.5 Military Specification, Bonding, Electrical (for Aircraft). MIL-B-5087B(ASG), 1964, and Amendment 1, February 6, 1968.
- 11.6 Military Specification, Arrester, Lightning, General Specification For. MIL-A-9094D (ASG), March 17, 1969.
- 11.7 Military Specification, Electromagnetic Compatibility Requirements, Systems. MIL-E-6051D, September 7, 1967.
- 11.8 Military Standard, Electromagnetic Interference Characteristics, Requirements for Equipment. MIL-STD-461A, August 1, 1968.
- 11.9 Fisher, Franklin A., and Plumer, J. Anderson: Lightning Protection of Aircraft. NASA RP-1008, National Aeronautics and Space Administration, Washington, D.C., 1977.
- 11.10 Review of Lightning Protection Technology for Tall Structures. Sponsored by Office of Naval Research, National Aeronautics and Space Administration, Federal Aviation Administration, and U.S. Air Force. Johnson Space Flight Center, November 6, 1975.
- 11.11 Statement on Space Shuttle Lightning Protection Shield (80-Foot Fiberglass Cylinder on Top of LC39 Launch Pad Structure) as Employed During ASTP-Apollo Mission on Launch Complex 39 at KSC. Official contacts: William B. Durrett and Clyde Whittaker, DD-EDD, Kennedy Space Center, Florida.
- 11.12 Lightning Protection Guidelines for STADAN Ground Equipment. NASA CR-94682, N68-24516, High Voltage Laboratory, General Electric Company, Pittsfield, Massachusetts, Goddard Space Flight Center, Greenbelt, Maryland, November 1967.
- 11.13 Analysis of Apollo 12 Lightning Incident. Document No. MSC-01540, prepared jointly by Marshall Space Flight Center, Kennedy Space Center, and Manned Spacecraft Center, National Aeronautics and Space Administration, February 1970.
- 11.14 Appleman, Herbert S.: Lightning Hazard to Aircraft. Technical Report 179 (Rev.), Headquarters Air Weather Service (MAC), United States Air Force, Scott AFB, Illinois, April 1971.

## REFERENCES (Concluded)

- 11.15 Chalmers, J. Alan: Atmospheric Electricity. Pergamon Press, New York, 1957.
- 11.16 Brook, M.; Holmes, C. R.; and Moore, C. B.: Lightning and Rockets – Some Implications of the Apollo 12 Lightning Event. Naval Research Reviews, Vol. 23, No. 4, April 1970, pp. 1-17.
- 11.17 Uman, Martin A.: Lightning, McGraw-Hill, 1969.
- 11.18 Cianos, N., and Pierce, E. T.: A Ground-Lightning Environment for Engineering Usage. Stanford Research Institute, 1972.
- 11.19 Prentice, S. A., and Mackerras, D.: Recording Range of Lightning-Flash Counter. Proceedings IEEE, Vol. 116, No. 2, February 1969, pp. 294-302.
- 11.20 Electromagnetic Interference Characteristics, Measurement of. MIL-STD-462, July 31, 1967.
- 11.21 Falls, Lee W.; Williford, W. O.; and Carter, M. C.: Probability Distributions for Thunderstorm Activity at Cape Kennedy, Florida. NASA TM X-53867, NASA/Marshall Space Flight Center, Alabama, 1970.
- 11.22 Apollo 15 Mission Report. MSC 05161, NASA, Manned Spacecraft Center (Johnson Space Center), Houston, Texas, December 9, 1971.
- 11.23 Spink, Bradley R.: A Practical Solution to the Arcing Problem at High Altitudes. Planetary and Space Science, Vol. 7, July 1961, pp. 11-18.
- 11.24 Paul, Fred W., and Burrowbridge, Donald: The Prevention of Electrical Breakdown in Spacecraft. NASA SP-208, National Aeronautics and Space Administration, Washington, D.C., 1969.





## SECTION XII. CLOUD PHENOMENA

### 12.1 Introduction

This section contains information on cloud processes, cloud types and classification, and cloud content and structure. It is designed to provide a general introduction to cloud phenomena which defines the major processes involved in cloud life cycles and a generalized description of cloud properties. The intent is also to provide a starting point when more specific information is required.

The term "cloud" refers to any visible collection of particles of water and/or ice suspended in the atmosphere at some elevation above the surface; fogs may properly be considered as clouds, but they are treated separately in Section IV of this document. It is important to point out that the properties of such "collections" are, for the most part, exceedingly difficult to measure with high precision, and they vary extensively both spatially and temporally. Significant variations in cloud properties occur on a time scale of minutes — indeed the entire life cycle of a thunderstorm cell is usually less than 50 min. Spatially, significant changes occur in mean cloud properties on all scales from a few meters — as between the updraft and downdraft regions within a convective cloud — to hundreds of kilometers. Thus, even when the best detailed information is obtained for clouds in a specific location and meteorological situation, extensive deviations from the expected cloud properties should be anticipated.

### 12.2 Cloud Processes

#### Cloud Formation

Air can retain only a limited amount of water in the vapor phase; the maximum amount is a strong function of temperature, as illustrated by Table 12.1. When an air parcel is cooled by any of various mechanisms (adiabatic expansion associated with updrafts caused by buoyancy or orographic features, radiative cooling, or mixing with another air parcel of lower temperature), the water remains largely in the vapor state until saturation is reached. Further cooling beyond that point causes the rapid growth of cloud droplets because the excess vapor readily condenses out on the submicron-sized atmospheric aerosol which is always present in abundance in the natural atmosphere. The process is somewhat self-limiting since sufficient numbers of cloud drops always nucleate and grow, removing the available water vapor as fast as it is released by the thermodynamic processes. Thus, supersaturations rarely exceed 2 percent in the atmosphere. In addition, the radial growth rate of a drop by condensation is inversely proportional to the drop radius. The result is a cloud of water drops of mean radius around 5 to 20  $\mu\text{m}$ , 10 to 3000/cm<sup>3</sup>, which rapidly forms and stabilizes. Further growth to precipitation-size particles must occur by other mechanisms. Condensational growth does continue but it is believed to be too slow, relative to other processes, to enter into the physics in an important way.

The cloud drop size distribution is an important determinant of the microphysical processes within the cloud. The initial distribution is primarily determined by the driving mechanism for the cloud formation (i.e., cooling rate or updraft velocity) and the initial aerosol concentration. Aerosol concentrations are classified broadly into two or three groups based on the origin of the air mass: maritime (50 to 100 particles/cm<sup>3</sup> capable of acting as cloud condensation nuclei (CCN) at 1 percent supersaturation), continental (300 to 700 particles/cm<sup>3</sup> active as CCN at 1 percent), and polluted continental (more than 1000 CCN/cm<sup>3</sup> at 1 percent). It is not the total aerosol concentration that is relevant, only the particles large enough and hygroscopic enough to serve as condensation nuclei. In general (particularly in cumulus clouds), the average droplet diameter, the width of the size distribution, and the tendency of the size distribution to be bimodal

TABLE 12.1 SATURATION VAPOR DENSITY AND SATURATION VAPOR PRESSURE OVER WATER AND ICE

Temperature (°C)	Over Water		Over Ice	
	Density (g/m <sup>3</sup> )	Pressure (mb)	Density (g/m <sup>3</sup> )	Pressure (mb)
20	17.30	23.37	—	—
15	12.83	17.04	—	—
10	9.399	12.27	—	—
0	4.847	6.108	4.847	6.107
- 10	2.358	2.863	2.139	2.597
- 20	1.074	1.2540	0.8835	1.032
- 30	0.4534	0.5088	0.3385	0.3798

all increase with height for several thousand feet above cloud base, while the total droplet concentration decreases with height. These variations with height are related to both the occurrence of droplet coalescence and entrainment, a mixing process between the cloud and the drier environment.

A typical value for the liquid water content averaged throughout a normal cumulus cloud is approximately 0.5 g/m<sup>3</sup>, although the peak value within the cloud may be two to six times this quantity. The liquid water content also increases with height for several thousand feet above cloud base before decreasing near the cloud top where entrainment of drier air is more pronounced.

Clouds having large concentrations of droplets generally consist of small droplets, while those with small concentrations generally contain comparatively more large droplets. Convective maritime clouds have larger droplets than continental clouds. The microphysical cloud parameters are also a function of the development stage of a cloud. Since the drop size spectra are a function of so many parameters, any "representative" drop spectra which might be presented must be overly simplified. Figure 12.1 shows the range of representative drop spectra for several different types of clouds. Cloud drop size spectra in maritime air are quite broad; they narrow in the continental air.

### Precipitation Formation

The development of precipitation in a cloud of micron-sized water drops requires the aggregation of roughly one million such drops into a single particle. A multitude of mechanisms contribute to this transition, and the physical picture is not yet complete; however, two basic processes can be identified. These are the "collision-coalescence" or "warm rain" process which is dominant in precipitation formation in maritime clouds in tropical climates and the "Wegener-Bergeron" process which dominates in continental clouds in temperate climates.

The "collision-coalescence" process consists, as the name implies, of the mutual collision of cloud drops and their subsequent coalescence into a single drop. Collision occurs because differences in the drop size produce different terminal fall velocities. The collision efficiency (or cross section) between small drops of nearly equal size is very small because the air tends to carry a drop around another in its path. Therefore, the initial breadth of the size distribution of clouds in maritime air masses is crucial. This mechanism enters into the development of precipitation in clouds in continental-type air masses only after other processes have

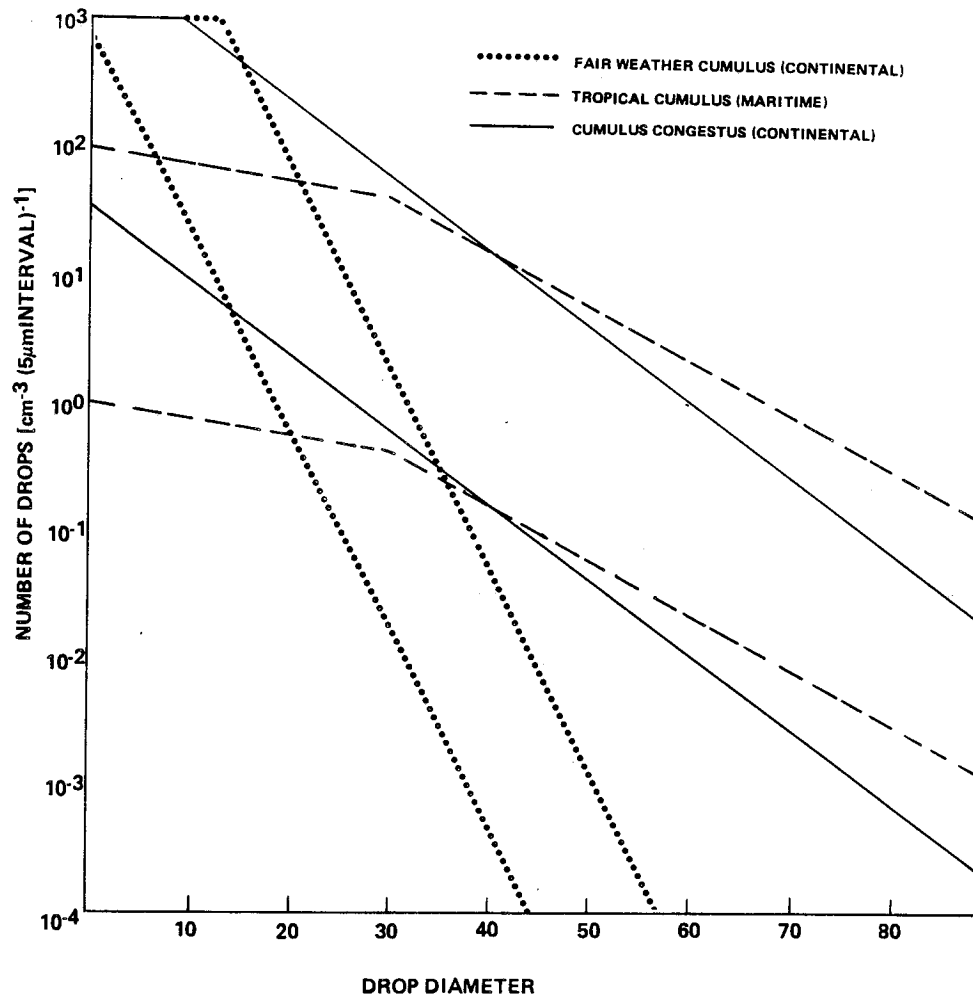


Figure 12.1 Upper and lower bounds on the typical number of cloud drops per cubic centimeter per 5 micron size interval for three principal cloud types: continental fair weather cumulus, continental cumulus congestus, and maritime tropical cumulus.

broadened the size distribution. As a drop grows by collecting others, its size and fall velocity increase with respect to the mean; thus the efficiency of the process also increases.

The Wegener-Bergeron process involves the ice phase in precipitation formation; thus it is only found where substantial portions of the cloud are below the freezing level. Small drops of very pure water will supercool to  $-40^{\circ}\text{C}$  in the laboratory. In the atmosphere, cloud drops are almost always sufficiently pure that they will supercool to  $-10^{\circ}\text{C}$ ; in clean air masses, supercooled water clouds at  $-20^{\circ}\text{C}$  are not uncommon. Such clouds form a severe hazard to aircraft and aerospace vehicles because of icing. Below  $-20^{\circ}\text{C}$  the number of substances which will initiate the freezing process, the "ice nuclei," increases dramatically; therefore, clouds at lower temperatures are nearly always heavily glaciated. Once ice is introduced into a cloud — either by nucleation in the colder regions at the cloud top or by mixing with the remnants of other clouds — the ice will spread throughout the cloud and the number of crystals may be multiplied by various mechanisms. Thus, mature clouds are frequently glaciated down to the freezing level.

The Wegener-Bergeron process derives from the simple fact illustrated by Table 12.1; the saturation vapor pressure over ice is lower than over water at the same temperature. Thus, an ice crystal in a

supercooled water cloud sees substantial supersaturation and it grows rapidly at the expense of the surrounding drops. This growth releases latent heat which feeds energy into the dynamic development of the cloud. As the size and fall velocity of the ice crystal increase, the condensational growth may be supplemented by collision-coalescence growth (riming) which further enhances the precipitation formation. In certain cases the collision-coalescence process becomes dominant and graupel or hail production results.

### 12.3 Basic Cloud Types

Most of the clouds which are important to aerospace activities (excepting fogs) are formed by the cooling of rising air parcels. The dynamic structure of these clouds can be characterized by three-dimensional turbulent motions superimposed upon the basic vertical motion. However, the physical mechanisms which drive both the basic motion and the superimposed turbulence differ from cloud to cloud in intensity and spatial/temporal scale, as well as in nature. Moreover, the turbulent fluctuations of various cloud microphysical properties can bring about interactions, usually nonlinear, with the basic flow state, also over a wide range of intensities and spatial/temporal scales. As a result of this wide variety of interactions each cloud is morphologically and microstructurally unique. The remainder of this section examines certain commonalities which exist in terrestrial clouds and which are useful for understanding cloud behavior.

Clouds which form at high altitudes in the lower troposphere (16,500 to 45,000 ft) are usually classed as cirriform clouds, from the Latin word cirrus (a filament of hair). At such altitudes, clouds are usually composed entirely of ice crystals. Mid-level clouds (6,500 to 23,000 ft), labeled with the prefix alto (middle), as well as lower clouds are usually composed of water droplets alone or a mixture of droplets and ice crystals. Water droplets evaporate more readily than ice particles in the subsaturated air outside clouds; hence, ice clouds tend to be marked by diffuse, streaky boundaries, whereas clouds of liquid water usually have more distinct boundaries. In general, the higher the altitude at which a cloud forms, the lower will be its hydrometeor (liquid and solid water) and gaseous water content. An extreme example is provided by the very tenuous Nacreous and Noctilucent clouds which form at elevations of 20 to 30 km and 80 to 100 km, respectively. Very little is known about the properties of these clouds.

Clouds can also be classified by the nature of the spatial/temporal scale of the driving mechanisms for the vertical motion. The driving mechanism most common in the atmosphere is the differential buoyancy between adjacent air parcels. If the characteristic scale of the horizontal density gradient is small (a few kilometers or so), the uplift begins as buoyant thermals, variously modeled as plumes or bubbles, which develop into cumulus (heaped) clouds. The highly turbulent nature of these clouds, combined with their large surface-to-volume ratio, drives rapid vertical and lateral entrainment (mixing) of the cloudy air with the surrounding air. Hence, the microstructure, the vigor, the size, and the lifetime of such clouds, as well as their potential for producing precipitation, depend critically on the temperature and water vapor profile of the surrounding air. For example, an overlying temperature inversion, such as at the tropopause or at the top of the boundary layer, will suppress the vertical development of all but the most vigorous clouds. Similarly, entrainment of dry ambient air will quickly destroy the buoyancy of developing clouds. Thus, cumulus humilis clouds, with vertical velocities of a few m/s, liquid water content (LWC) of approximately  $1 \text{ g m}^{-3}$ , generally ragged boundaries, depth of 1 to 2 km, and lifetimes of 20 to 30 min, are usually a sign of fair weather. Under more unstable conditions, with more available water vapor, some of the early convective clouds can develop into larger cumulus congestus, with vertical velocities of approximately 10 m/s, LWC of several  $\text{g m}^{-3}$ , uniform dark bases, sharp "cauliflower" boundaries, depth of several kilometers, and lifetimes of 30 to 60 min. Cumulonimbus (from nimbo, meaning rain) clouds are marked by the glaciation (rapid conversion of liquid water to ice) of the topmost section of the cloud, followed by the formation of the characteristic cirriform anvil, and the rapid development of precipitation. These clouds can have vertical velocities of tens of m/s, hydrometeor (water and ice) loadings of 5 to  $10 \text{ g m}^{-3}$ , cloud tops

reaching above the tropopause, and lifetimes of a few hours. Cumulonimbus clouds often contain large hailstones, develop very large internal wind shears, and maintain intense turbulence and electrical activity throughout the cloud. These characteristics, as well as the potential for some cumulonimbus clouds to spawn violent tornadoes, make these clouds a serious hazard to aerospace activity.

At the other extreme, if the air density varies significantly only on the synoptic scale, the uplift develops nearly uniformly over wide areas (100 to 1000 km<sup>2</sup> or more) with vertical velocities of a few cm/s. This type of uplift produces generally uniform stratus (layer) clouds. Depending on their stage of development, these clouds can attain vertical depths anywhere from several hundred meters up to 10 km or more. Thus, stratus clouds generally have a comparatively small surface-to-volume ratio, are less susceptible to decay by entrainment, and have lifetimes from several hours up to a day or more. The weak updrafts characteristic of stratus clouds drive only a very slow hydrometeor growth process because the rate at which water vapor is made available by adiabatic cooling is correspondingly slow. In addition, the weak updrafts allow hydrometeors to fall out of the cloud after they have attained a diameter of only several tens of microns. Hence, the hydrometeor water content (several tenths of a g m<sup>-3</sup> or less) and the accumulated precipitation from such clouds are likely to be quite low except in deeper supercooled or mixed stratus or in convective cores or bands embedded in the stratus deck.

Combinations of the various cloud formation mechanisms can produce cloud types which combine characteristic features of their respective parent cloud types. For example, thin layers of stratus, altostratus, or cirrostratus clouds, when warmed from below by the Earth's radiation and cooled from above by radiative loss to space, will develop a network of closely spaced convective cores, each surrounded by clear subsiding air. These layers of convective clouds are appropriately called stratocumulus, altocumulus, and cirrocumulus. The same names are given to convective clouds which are aligned in cloud streets or rolls by a vertical shear in the horizontal wind or to wave-like billow clouds induced by shear instability.

Clouds formed by forced uplift over prominent orographic features have some unique characteristics which can have important effects on aerospace activity. The vertical velocities in these clouds are determined by the ambient wind speed, the terrain slope parallel to the wind, the terrain geometry perpendicular to the wind, and stability of the ambient air mass. Cloud depths are determined by the stratification of water vapor; often multiple layers of orographic clouds can be seen. A particularly important type of orographic cloud is produced in a stable moist air mass overlaid by drier air which passes over mountain peaks or ridges. Under these conditions saucer or lens-shaped clouds appear directly above the mountain (cap cloud) or in the lee wave downwind of the ridge (wave or lenticular cloud). The upper boundary of these clouds is usually quite smooth and sharp, indicating nearly laminar flow with little or no turbulent entrainment across the cloud boundary. These clouds last for many hours as long as the local synoptic pattern is stable. The conditions which favor the development of cap and lee wave clouds can also lead to a highly turbulent vortex or rotor cloud below the lee wave downwind of the mountain. Wave clouds provide a visualization of the severe disturbance of the ambient air flow by the terrain. Under appropriate conditions of terrain geometry and overlying air mass stability, these disturbances can also propagate vertically through clear air well into the stratosphere. This mechanism is believed to be an important contribution to the phenomenon of clear air turbulence, or CAT.

A second important orographic cloud type is produced by the lifting of a deep layer of moist air on the upwind side of a mountain range. This condition can lead to the development of heavy precipitation on the upwind slopes of the mountain range. Stratiform precipitation tends to be favored in stable or weakly unstable air masses, while showery precipitation, possibly accompanied by thunderstorm development, is favored in the more unstable air masses.

The various types of clouds discussed previously can often be associated with a particular synoptic condition or storm system. For example, synoptic-scale, mid-latitude cyclonic storms are characterized by stratiform clouds overlying the warm front; patchy cirrus thickening to cirrostratus, lowering to a deep layer of altostratus and culminating near the surface front with dark nimbostratus and underlying "scud," or fragmentary clouds. The warm sector can be either clear, partially or completely obscured by small cumulus, stratus, or altostratus, or spotted by deep convection, especially in the summertime. Cold fronts are frequently accompanied by high winds, large wind shears, and deep convection with heavy precipitation. Several other types of smaller scale storm systems are characterized by deep cumulonimbus towers organized in nearly steady-state self-propagating structures. Severe storms, squall lines, and tropical storms or hurricanes fall into this category. These storm systems frequently are characterized by high winds, heavy precipitation, severe flooding, and intense electrical activity, each of which creates obvious hazards to aerospace vehicles.

The final general category which is useful for classifying clouds or cloud systems is the origin of the air mass in which the cloud or cloud system of interest is embedded. For example, the freezing level is likely to be closer to cloud bases in mid-latitude clouds than in tropical clouds. Cloud bases are more likely to be closer to the surface of the Earth in maritime clouds than in continental clouds. Summertime clouds are more likely to be isolated cumuliform clouds than are wintertime clouds. Finally, total cloud water content is likely to be higher in summer than in winter, in maritime air masses than in continental, and in the tropics than in the mid-latitudes. These general features together with the aerosol content of the embedding air mass have important consequences on the nature of the cloud particle size distribution, the cloud life cycle, and the consequent development of precipitation in these clouds.

## BIBLIOGRAPHY

- List, Robert J.: "Smithsonian Meteorological Tables," 6th ed. Smithsonian Institution, Washington, D.C., 1958, 527 pp.
- Mason, B. J.: "The Physics of Clouds," 2nd ed., Clarendon Press, Oxford, 1971, 671 pp.
- Pruppacher, Hans R. and Klett, James D.: "Microphysics of Clouds and Precipitation," D. Reidel Pub., Dordrecht, Holland, Boston, U.S.A.; London, U.K., 1978, 714 pp.
- Hobbs, Peter V. and Wallace, John M.: "Atmospheric Science, An Introductory Survey," Academic Press, New York, San Francisco, London, 1977, 467 pp.
- Mount, Wayne D. and Fow, Richard B.: "Models of Weather Environments Adverse to Electro-Optical Systems," U.S. Army Electronics Research and Development Command, Atmospheric Sciences Laboratory, White Sands Missile Range, NM, CR-81-0047-1, 1981, 107 pp.





## SECTION XIII. CLOUD COVER AND FOUR-D ATMOSPHERIC MODELS

13.1 Introduction

A most useful tool in planning experiments and applying space technology to Earth observation is a model of atmospheric parameters. For example, cloud cover data might be used to predict mission feasibility or the probability of observing a given target area in a given number of satellite passes.

To meet the need for atmospheric models, NASA-MSFC has sponsored the development of the four-dimensional atmospheric models (subsection 13.4) and the worldwide cloud model (subsection 13.3). The goal of this work was to produce atmospheric attenuation models to predict degradation effects for all classes of sensors for application to Earth-sensing experiments from spaceborne platforms. To insure maximum utility and application of these products NASA-MSFC also sponsored the development of an "Interaction Model of Microwave Energy and Atmospheric Variables," a complete description of the effects of atmospheric moisture upon microwaves.

13.2 Interaction Model of Microwave Energy and Atmospheric Variables

While the visible and infrared wavelengths find clouds opaque, the microwave part of the electromagnetic spectrum is unique in that cloud and rain particles vary from very weak absorbers and scatterers to very significant contributors to the electromagnetic environment. This is illustrated in Figures 13.1, 13.2, and 13.3, which are extracted from the final report on the interaction model (Ref. 13.1).

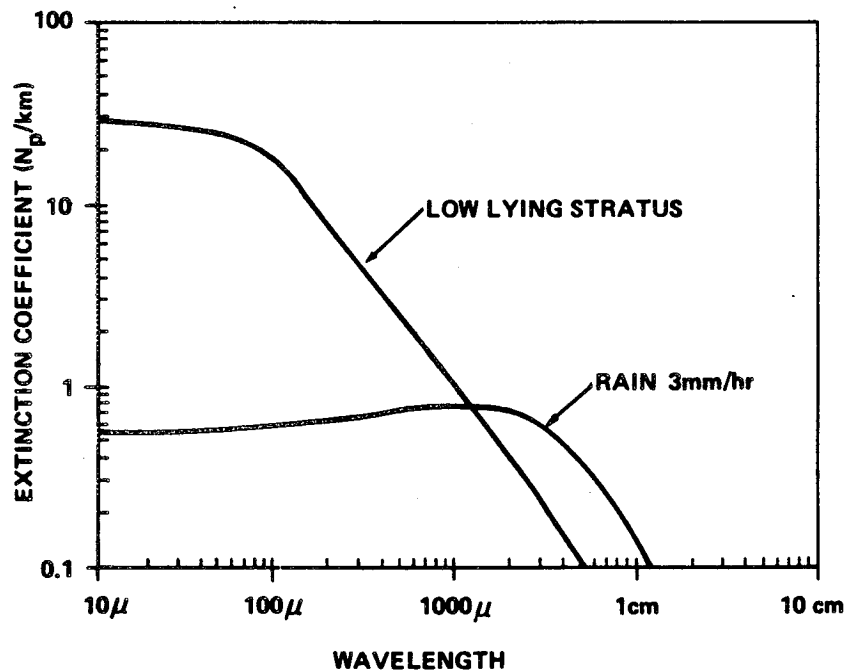


Figure 13.1 Extinction coefficient as a function of wavelength.

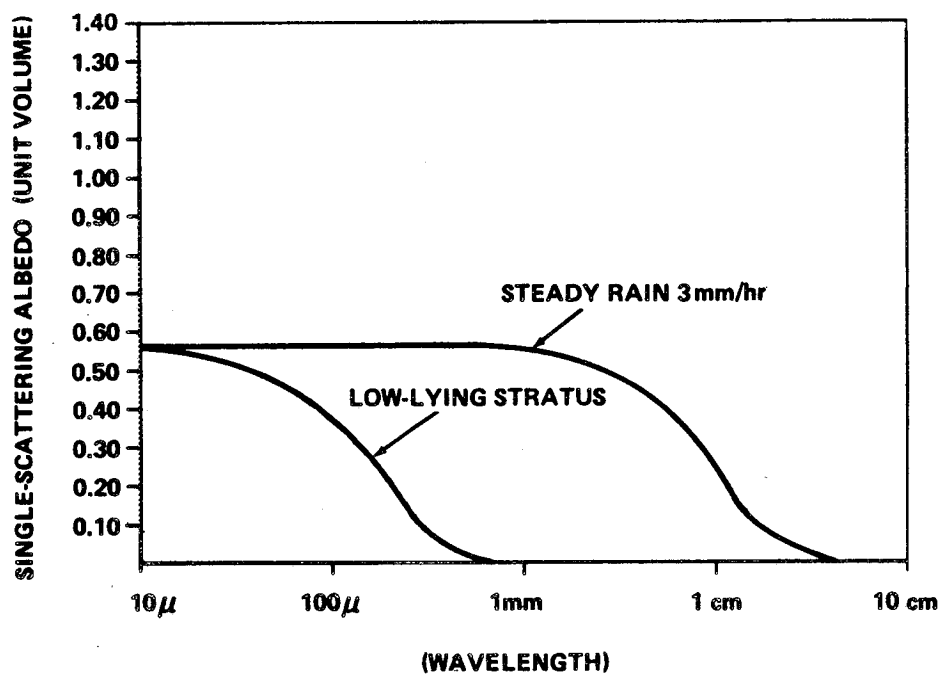


Figure 13.2 Single scattering albedo for two cloud models.

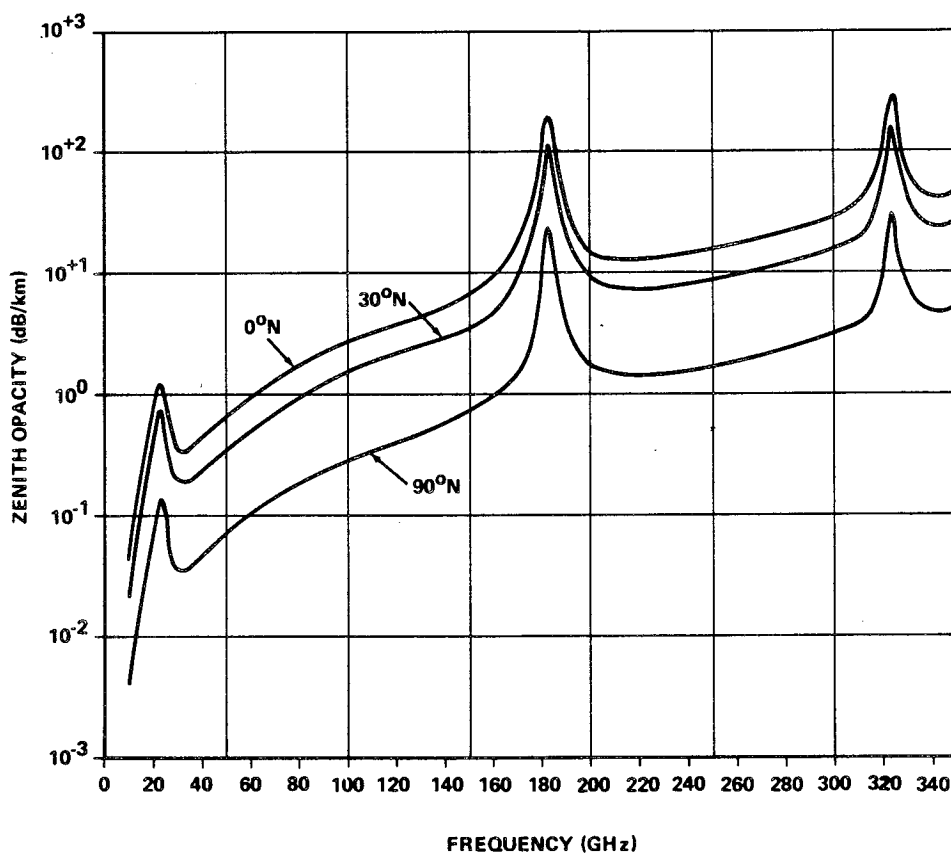


Figure 13.3 Zenith opacity.

### 13.2.1 Scattering and Extinction Properties of Water Clouds Over the Range 10 cm to 10 $\mu\text{m}$

Figures 13.1 and 13.2 show the unit-volume scattering and extinction properties of two modeled cloud drop distributions computed using the Mie theory. Figure 13.1 gives the extinction coefficient as a function of wavelength, while Figure 13.2 presents the single scattering albedo for two cloud models representing low clouds and rainy conditions. The curves show the wavelength regimes appropriate to the two cloud types in which scattering effects are relatively unimportant, and in which the extinction coefficient follows the simple Rayleigh ( $1/\lambda^2$ ) dependence.

### 13.2.2 Zenith Opacity due to Atmospheric Water Vapor as a Function of Latitude

In the preparation of Figure 13.3 five years of climatological data from the MIT Planetary Circulations Project were used to obtain mean water vapor distributions applicable to the latitudes  $0^\circ\text{N}$ ,  $30^\circ\text{N}$ , and  $90^\circ\text{N}$ , corresponding to tropical, mid-latitude, and arctic conditions. The total water vapor content for the three cases is 4.5, 2.5, and 0.5  $\text{g}/\text{cm}^2$ , respectively. The curves demonstrate the effect of climatological extremes in simulating and predicting the influence of atmospheric water vapor upon surface observations from a space observer, over the range from 10 to 350 gigahertz. A detailed report on the interaction model (Ref. 13.1) is available upon request to the Atmospheric Sciences Division, Space Sciences Laboratory, MSFC/NASA.

## 13.3 Global Cloud Model

### 13.3.1 Introduction

Cloud cover is a key factor to be considered in the planning of remote sensing missions of the Earth's surface. Depending upon the extent and thickness of a cloud and upon the wavelengths used by the space-borne sensor, a cloud has effects on the measured radiation ranging from slight attenuation to total absorption. The complexity of modern remote sensing systems, with wavelengths in the visible, infrared, and microwave, necessitates detailed information on expected cloud cover to permit intelligent planning and studies. Cloud cover is also a key element in the research strategy of the U. S. Climate Program. Information is needed to develop an understanding of the role played by clouds in the radiation balance and to aid in the parameterization of clouds in climate models. In recognition of this need, the Atmospheric Sciences Division at the Marshall Space Flight Center sponsored the development of a global data bank of cloud statistics (Ref. 13.2) and computer techniques to utilize the statistics in various simulation studies (Ref. 13.3).

Concurrent with these studies, MSFC also sponsored the development of another data bank (Refs. 13.4, 13.5). This data bank, known as the 4-D Atmospheric Model, contains means and variances of atmospheric pressure, temperature, water vapor, and density from the surface to 25 km above the Earth. Related computer programs were also written to permit the use of this data bank in specifying atmospheric profiles for any latitude, longitude, and month of the year.

By using the worldwide cloud cover statistics and the existing simulation procedure, it is possible to provide an evaluation of the consequence of cloud cover on Earth-viewing space missions or the receipt of solar radiation for individual target areas or swaths over small areas. While the present cloud model and simulation procedure provide a valuable first step toward global Earth radiation budget evaluation, both contain serious limitations which can be overcome by:

## 13.4

- Utilizing a more accurate cloud cover data base
- Developing a simulation procedure which includes a description of the satellite orbit in ground-referenced coordinates and observation characteristics such as field of view ground swath size and target lighting.

The revised global cloud cover data base will contribute to the climate program by:

- Providing up-to-date information readily available to users
- Providing a data set for use in climate models or by the climate research community
- Providing data to examine the inter-annual variability of cloud cover at any location
- Providing seasonal cycle information to validate seasonal cycle simulations for a hierarchy of climate models.

These data will contribute to a better understanding of the annual cycle of cloud cover as a first step in the continuing comprehensive climate program.

The revised simulation procedure will utilize observed cloud cover data. No statistical cloud summaries or distributions will be used; the assumption of homogeneity of cloud statistics within specific geographical areas will not be applicable; theoretical models for adjusting cloud statistics to account for temporal and spatial variability will not be required.

### 13.3.2 Background

#### Development of the Global Cloud Model

The first NASA-sponsored study by Sherr et al. (Ref. 13.2) defined the basic guidelines for a global data bank of cloud statistics. The primary purpose for the development of this data bank was to provide information for the proper planning and analysis of Earth-oriented space missions; hence, it was believed that climatological data of universal application were required and that at least the following should be provided:

1. Global coverage
2. Cloud cover distributions in a readily usable, standard form
3. Distributions by season, time of day, and some readily defined climatological region or grid
4. Expression of the spatial and temporal coherence of cloud cover
5. Expression of cloud cover distributions on a variety of scales of observation,

Based upon climatological considerations, 29 homogeneous cloud regions, with boundaries upon even latitudes and longitudes, were defined to represent the global cloud distribution. This facilitated the meeting of the preceding specifications without generating a data set too large or unwieldy to be of use. It would, of course, have been possible to define many more regions, indicating the great diversity of local climates,

but the resulting increase in information would be small compared to the increase in difficulty in using the model. A representative station was selected for each region, and all data given for that station was assumed applicable to locations within that region.

To derive the actual cloud statistics, cloud cover summaries of 5 to 30 years of data were obtained from the Weather Bureau for each representative station. Cloud cover reports were grouped into five categories (Table 13.1), and frequencies for each of the five categories were derived for every region, for 12 months of the year, and for 3-hour intervals throughout the 24-hour day beginning at 01 LST (Table 13.2). Spatial and temporal conditional statistics of cloud cover were also derived and were based primarily upon satellite photographs (Table 13.3).

TABLE 13.1 CLOUD CATEGORY DESIGNATION

Categories	Tenths	Eighths (Octas)
1	0	0
2	1,2,3	1,2
3	4,5	3,4
4	6,7,8,9	5,6,7
5	10	8

TABLE 13.2 BASIC CLOUD STATISTICS

Cloud Region: 19                      Month: January								
Cloud Category	Time (LST)							
	01	04	07	10	13	16	19	22
1	0.31	0.30	0.18	0.16	0.15	0.16	0.24	0.30
2	0.08	0.05	0.09	0.08	0.12	0.10	0.10	0.08
3	0.04	0.04	0.04	0.04	0.04	0.06	0.05	0.05
4	0.11	0.10	0.15	0.16	0.17	0.21	0.16	0.14
5	0.46	0.50	0.54	0.56	0.52	0.47	0.45	0.43

TABLE 13.3 CONDITIONAL CLOUD STATISTICS

Cloud Region: 19						Month: January					
Given Cloud Category	Space Conditionals					Given Cloud Category	Time Conditionals				
	Cloud Category						Cloud Category				
	1	2	3	4	5		1	2	3	4	5
1	0.76	0.05	0.05	0.05	0.09	1	0.52	0.07	0.06	0.18	0.17
2	0.17	0.17	0.08	0.08	0.50	2	0.33	0.18	0.08	0.19	0.22
3	0.13	0.12	0.15	0.30	0.30	3	0.21	0.18	0.11	0.32	0.18
4	0.14	0.09	0.14	0.45	0.18	4	0.23	0.10	0.05	0.35	0.27
5	0.13	0.06	0.12	0.16	0.53	5	0.23	0.04	0.07	0.20	0.46

As a final task in the study, a Monte Carlo technique was developed whereby the unconditional and conditional statistics, in the form of cumulative probabilities, were used to simulate the cloud cover conditions for various orbital missions. With some modifications, this simulation technique has remained the basic approach toward the application of the statistical data.

The second study, by Greaves et al. (Ref. 13.3), continued the development of statistics and statistical procedures for cloud simulation in a number of areas. The most important of these was the development of a Markov scaling technique to scale the 24-hour and 200-mile conditional cloud cover statistics to any other time or distance scale. Also developed was a relationship between ground and satellite-derived cloud frequency distributions. This relationship was used to introduce internal consistency between the ground-observed unconditional statistics and the conditional statistics derived from satellite observations.

### 13.3.3 The Simulation Procedure

The consequence of cloud cover is evaluated by a Monte Carlo computer simulation procedure using the basic and conditional cloud statistics described previously. Random numbers are used to select, from the appropriate probability distribution, a cloud cover category for each satellite pass.

Results of the simulations, which can be made for target areas of various size, are generally given in two forms. First, the satellite pass number and probability of success are considered as variables with the required percent photographic coverage of the target area fixed. For example, if 95 percent photographic coverage of the target area is required for success, the results would be given as the probability of success versus the pass number. A plot of these results, as illustrated in Figure 13.4, might show that there is a 60 percent chance of photographing 95 percent of the target area in six satellite passes. Second, the pass number is fixed, while the percentage of area photographed and the chance of success are treated as variables. Results in this case are given as the percent chance of achieving some percent photographic coverage of the target area by some limiting pass number. The results are illustrated in Figure 13.5, which indicates that, after eight satellite passes, there is a 60 percent chance of photographing 90 percent of the target area.

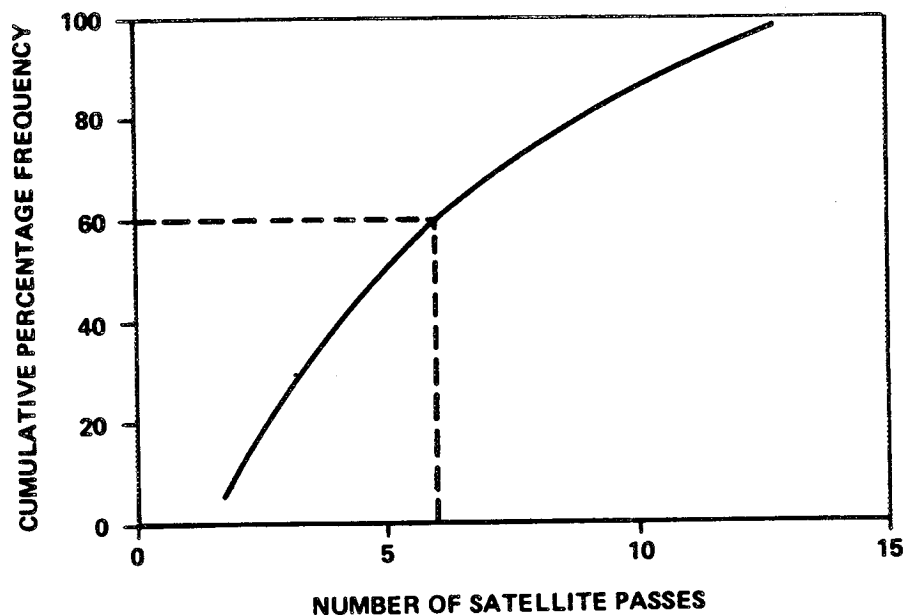


Figure 13.4 Analysis of 95 percent photographic coverage of target area.

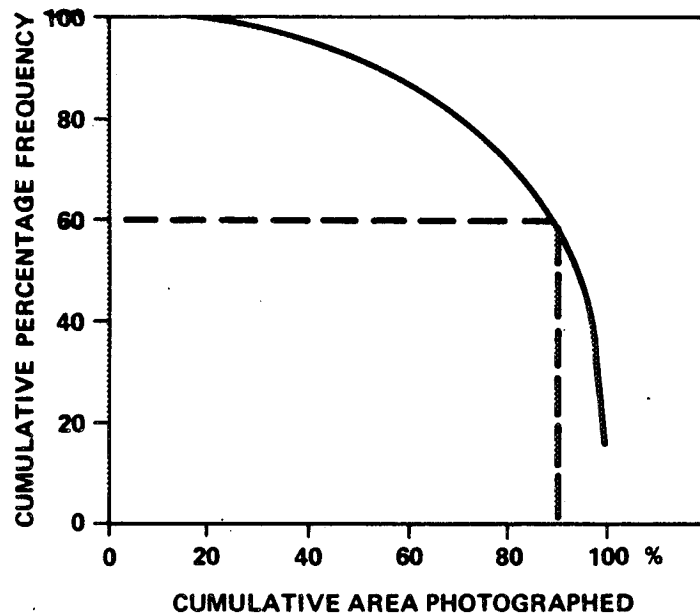


Figure 13.5 Photographic coverage of target area after eight satellite passes.

#### 13.3.4 Limitations of the Present Model

The number of cloud climatic regions was limited by data volume handling capability and by the amount of suitable data available. The entire United States, for example, is effectively covered in only four or five regions. Also, each region is assumed to be completely homogeneous. That is, the base station cloud distribution applies everywhere within that region. The cloud climatologies for nine of the Southern Hemisphere regions were taken as being seasonal reversals of similar Northern Hemisphere regions. For some oceanic regions, where representative data could not be obtained, statistics were modified from those of other regions based upon climatological considerations. The satellite-derived data base for the conditional statistics is generally weak. It was necessary to compute conditional probabilities on a seasonal basis to produce an adequate sample size for statistical manipulations. The consistency between ground-observed basic or unconditional statistics and satellite-observed conditional distributions has introduced uncertainties in the combined utilization of the two data bases.

The techniques for changing the cloud distributions to make them applicable to larger area sizes, temporal separations other than 24 hours, and spatial distances other than 200 n.mi. are all theoretical and have not been adequately verified.

The simulation procedure requires that either region number or latitude-longitude plus month and time of day be given as input values. Only three cloud regions can be evaluated in any one simulation, and cloud region boundaries are considered impervious — the statistics change abruptly at the region boundary. The scheme works well for individual selected targets, but at present it cannot evaluate large areas. Orbital parameters that affect target field of view and target lighting are not considered. To overcome these limitations, a new cloud model and more versatile simulation techniques are being developed.

### 13.3.5 The Revised Cloud Model

Development of the cloud model is divided into three phases, as follows:

- Prepare a worldwide cloud cover data base from Air Force Global Weather Central 3D Neph Analysis data files
- Verify the adequacy of the quantity and quality of the data base
- Analyze the seasonal and annual changes of cloud cover.

#### Preparation, Verification, and Analysis of Cloud Data Base

Data preparation involves the following tasks:

- Develop software for extraction of total cloud cover data at each grid point of the  $\frac{1}{4}$ -mesh global array ( $\sim 50$  n.mi. spacing at mid-latitudes)
- Develop and maintain an accessible data base of global cloud cover observations
- Create year-month-hour and month-hour files
- Extract detailed cloud information (high, middle, and low cloud amounts and types plus total sky cover) at selected grid points for detailed analyses.

Verification involves the following tasks:

- Establish the adequacy of the available period of record by studying the inter-annual variability of cloud cover for various climatic regimes
- Verify the data base by comparison of statistical summaries of selected grid point data to standard National Weather Service station data.

Analysis involves the following tasks:

- Develop information to assess the seasonal cycle cloud cover simulations for use in climate models
- Conduct comprehensive annual cycle cloud cover analyses for various geographic locations.

### 13.3.6 The Revised Simulation Procedure

The objective is to develop computer software to utilize cloud data in conjunction with a satellite orbit program to simulate the effect of cloud cover on Earth-oriented space missions. The simulation procedure will be designed to provide answers to such questions as: How confident can one be of success if the objective is to photograph all or part of the Earth's land masses? Considering cloud cover, is the mission feasible? A measure of success can be defined as a minimum acceptable percent of the target area photographed during the satellite lifetime or until expendables are depleted. The procedure will utilize the orbital parameters and lighting constraints to specify the appropriate ground track and cloud cover observations.



The mission simulation will use the observed cloud cover data (described in the previous paragraphs); no statistical cloud summaries or distributions will be required. Instead, the mission simulation will be repeated enough times to produce statistically stable values of the probability of success. Success can be defined as obtaining the required photographic coverage on a single pass over the target or as acquiring incremental coverage on each pass to form a mosaic of the target area. In either case the results can be given as the required number of trials to be X percent confident of acquiring Y percent of the target. The procedure will be valid for any target size, including areas from 50 n.mi. in diameter to the size of continents.

The simulation procedure will include software development to satisfy the following requirements:

- Adaptation of existing numerical or analytical integration satellite orbit software at NASA/MSFC to create an ephemeris (satellite location and ground track) data file
- Conversion of satellite ground track to nonoverlapping field-of-view areas and derivation of representative cloud cover data within each area
- Display of model simulation results.

### 13.3.7 Cloud Data for the Revised Model

An extensive investigation revealed no suitable summarized or statistical cloud distributions and only one source of cloud observations that provides global coverage and diurnal variation in a manageable volume. This is the 3D Neph Analysis prepared by the Air Force Global Weather Central (Ref. 13.6).

#### 3D Neph Analysis

The 3D Neph Analysis, a global cloud analysis, is prepared eight times (00Z, 03Z, 06Z, . . .) daily by the Air Force Global Weather Central, Offutt Air Force Base, Nebraska. The analysis, made from all available cloud data, includes satellite, aircraft, and ground/ship observations. These observations are fitted into a coherent global cloud structure which largely eliminates the risk of incorporating erroneous data or interpreting snow or sand as clouds. The analysis encompasses 15 altitude layers and includes 22 parameters on a fine mesh grid (approximately 25 n.mi. spacing at 45 degrees latitude).

The 3D Neph Analysis has all the attributes required for adequate mission simulations except that it is too voluminous to handle. The revised cloud model is based upon a smoothed version of the basic 3D Neph Analysis that doubles the spacing between grid points and greatly reduces the volume of data.

### 13.4 Four-Dimensional Atmospheric Models

In this part of the attenuation model project, the emphasis is placed on water vapor rather than clouds. Also, since attenuation calculations are usually made from reference atmosphere inputs, the other atmospheric parameters found in reference atmospheres were included in the MSFC 4-D model. The basic data comprise monthly statistics (mean and standard deviations) of pressure, temperature, density, and moisture content from 0 to 25 kilometers altitude on a global grid network. These data provide information on latitudinal, longitudinal, altitudinal, and temporal variations of the parameters; hence the name "four-dimensional atmospheric models." Of course, a profile of temperature, pressure, density, and moisture content for any global location may be retrieved from these data. Still, to reduce the data to a more manageable amount it was decided to outline homogeneous moisture content regions for which a single set of

profile statistics would apply. This procedure would permit the use of one set of profiles for all locations within a homogeneous region. For each region, analytical functions have been fitted to the statistical data. For moisture, exponential functions were most appropriate, while for temperature, a series expansion technique was used. Fitting analytic functions to the statistical climatological profile data produces a library of coefficients for the temperature and moisture profiles. These coefficients are then used to develop computer subroutines to regenerate the model profiles of temperature and moisture which are a function of the homogeneous region and month of the year.

In the compilation of the global statistics, pressure and density were determined from the hypsometric equation and the equation of state, rather than linear or logarithmic interpolation. The purpose of this was to insure hydrostatic consistency; thus, the pressure and density profiles can be generated from the temperature profile and the hydrostatic assumption.

The final result of this 4-D model analysis is a computer program that provides mean and variance profiles of moisture, temperature, pressure, and density from the surface to 25 kilometers altitude for any location on the globe and month of the year. The computer programs contain the equations, data, and library of coefficients necessary to produce the desired results.

The MSFC 4-D atmospheric model is described in References 13.4 and 13.5 and is available upon request to the Atmospheric Sciences Division, Space Sciences Laboratory, Marshall Space Flight Center, Alabama 35812.

## REFERENCES

- 13.1 Gaut, N. E., and Reifenstein, E. C. III, "Interaction Model of Microwave Energy and Atmospheric Variables," Environmental Research and Technology, Inc., Final Report of Contract NAS8-26275, Feb. 1971.
- 13.2 Sherr, P. E., et al., "World Wide Cloud Cover Distribution for Use in Computer Simulations," Allied Research Associates, NASA CR-61226, June 14, 1968.
- 13.3 Greaves, J. R., et al., "Development of a Global Cloud Model for Simulating Earth-Viewing Space Missions," Allied Research Associates, Final Report Contract NAS8-25812, Jan. 1971.
- 13.4 Spiegler, D. B. and Greaves, J. R., "Development of Four-Dimensional Atmospheric Models (World-wide), Allied Research Associates, Inc., NASA CR-61362, August 1971.
- 13.5 Spiegler, D. B. and Fowler, M. G., "Four Dimensional Worldwide Atmospheric Models (Surface to 25 km Altitudes), Allied Research Associates, Inc., NASA CR-2082, July 1972.
- 13.6 Fye, F. K., "The AFGWC Automated Cloud Analysis Model." AFGWC Technical Memorandum 78-002, HQ Air Force Global Weather Central, Offutt Air Force Base, Nebraska, 1978.



## SECTION XIV. THERMAL AND RADIATION

14.1 Introduction

The natural thermal environments, i.e., solar and sky radiation (thermal radiation) and temperature, can produce undesirable effects on space vehicles and ground support systems by:

- a) Unequal heating resulting in stresses of various types.
- b) Temperature extremes (high or low) occurring inside or on the vehicle surface which may cause equipment malfunctions or uncomfortable/undesirable conditions for manned missions.
- c) Difficulties in alignment of the vehicle parts at interfaces and calibration of R and D instruments on the vehicle because of variations of size and/or shape with temperature.

Because of these and other effects, information on the thermal environment at the Earth's surface and in space is required in space vehicle design.

14.2 Definitions

The following terms are used in this section:

Absorption bands are those portions of the solar (or other continuous) spectrum which have lesser intensity because of absorption by gaseous elements or molecules. In general, elements give sharp lines, but molecules such as water vapor or carbon dioxide in the infrared give broad diffuse bands.

Air mass is the amount of atmosphere that the solar radiation passes through, considering the vertical path at sea level as unity (i.e., when the Sun is at the zenith, directly overhead).

Air temperature (surface) is the free or ambient air temperature measured under standard conditions of height, ventilation, and radiation shielding. The air temperature is normally measured with liquid-in-glass thermometers in a louvered wooden shelter, painted white inside and outside, with the base of the shelter normally 1.22 m (4 ft) above a close-cropped grass surface (Ref. 14.1). Unless an exception is stated, surface air temperatures given in this report are temperatures measured under these standard conditions.

Atmospheric transmittance is the ratio between the intensity of the extraterrestrial solar radiation and intensity of the solar radiation after passing through the atmosphere.

Black body is an ideal emitter which radiates energy at the maximum possible rate per unit area at each wavelength for any given temperature and which absorbs all incident radiation at all wavelengths.

Diffuse sky radiation is the solar radiation reaching the Earth's surface after having been scattered from the direct solar beam by molecules and particles in the atmosphere. It is measured on the surface after the direct solar radiation is subtracted from the total horizontal radiation.

Direct solar radiation is the solar radiation received on a surface directly from the Sun and does not include diffuse sky radiation.

C-4

Emittance is the ratio of the energy emitted by a body to the energy which would be emitted by a black body at the same temperature. All real bodies will emit energy in different amounts from a black body at various wavelengths; i.e., colored bodies are colored because of higher emittance at specific wavelengths. In this document, the assumption is made that the absorptivity of an object is numerically equal to the emittance of the object at the same wavelengths. Therefore, the value of the emittance can be used to determine the portion of the energy received by the object which heats (or energy lost which cools) the object.

Extraterrestrial solar radiation is that solar radiation received outside the Earth's atmosphere at one astronomical unit from the Sun. The term "solar spectral irradiance" is used when the extraterrestrial solar radiation at small wavelength intervals is considered.

Fraunhofer lines are the dark absorption bands in the solar spectrum caused by gases in the outer portion of the Sun and Earth's atmosphere.

Horizontal solar radiation is the solar radiation measured on a horizontal surface. This is frequently referred to as "global radiation" or "total horizontal radiation" when solar and diffuse sky radiation are included.

Irradiation is often used to mean solar radiation received by a surface.

Normal incident solar radiation is the radiation received on a surface, normal to the direction of the Sun, direct from the Sun, and does not include diffuse sky radiation.

Radiation temperature is the absolute temperature of a radiating black body determined by Wien's displacement law, expressed as

$$T_R = \frac{w}{\lambda_{\max}} \quad , \quad (14.1)$$

where  $T_R$  is the absolute temperature of the radiating body ( $^{\circ}\text{K}$ ),  $w$  is the Wien's displacement constant ( $0.2880 \text{ cm}^{\circ}\text{K}$ ), and  $\lambda_{\max}$  is the wavelength of the maximum radiation intensity for the black body.

Sky radiation temperature is the average radiation temperature of the sky when it is assumed to be a black body. Sky radiation is the radiation to and through the atmosphere from outer space. While this radiation is normally termed nocturnal radiation, it takes place under clear skies even during daylight hours.

Solar constant is the rate at which solar radiation is received outside the Earth's atmosphere on a surface normal to the incident radiation and at the Earth's mean distance from the Sun. The solar constant equals  $1.940 \text{ cal cm}^{-2} \text{ min}^{-1}$  ( $0.1353 \text{ W cm}^{-2}$ ) (Ref. 14.2).

### 14.3 Spectral Distribution of Radiation

#### 14.3.1 Introduction

All objects radiate energy in the electromagnetic spectrum. The amount and frequency of the radiation distribution is a function of temperature. The higher the temperature, the greater the amount of total energy emitted and the higher the frequency (shorter the wavelength) of the peak energy emission.

### 14.3.2 Solar Radiation

The Sun emits energy in the electromagnetic spectrum from  $10^{-7}$  to greater than  $10^5$   $\mu\text{m}$ . This radiation ranges from cosmic rays through the very long wave radio waves. The total amount of radiation from the Sun is nearly constant in intensity with time.

Of the total electromagnetic spectrum of the Sun, only the radiant energy from that portion of the spectrum between 0.22 and 20.0  $\mu\text{m}$  will be considered in this document since it contains 99.8 percent of the total electromagnetic energy. The spectral distribution of this region closely resembles the emission of a gray body radiating at 6000°K. This is the spectral region which causes nearly all of the heating or cooling of an object.

Solar radiation outside the Earth's atmosphere is distributed in a continuous spectrum with many narrow absorption bands caused by the elements and molecules in the colder solar atmosphere. These absorption bands are the Fraunhofer lines, whose widths are usually very small ( $< 10^{-4}$   $\mu\text{m}$  in most cases).

The Earth's atmosphere also absorbs a part of the solar radiation such that the major portion of the solar radiation reaching the Earth's surface is between about 0.35 and 4.00  $\mu\text{m}$ . The distribution of the solar energy outside the Earth's atmosphere<sup>1</sup> (extraterrestrial) is as follows:

Region ( $\mu\text{m}$ )	Distribution (%)	Solar Intensity <sup>1</sup> g-cal $\text{cm}^{-2}$ ( $\text{min}^{-1}$ )
Ultraviolet below 0.38	7.003	0.136
0.38 to 0.75	44.688	0.867
Infrared above 0.75	48.309	0.937

The first detailed information published for use by engineers on the distribution of solar radiation energy (solar irradiation) wavelength was that by Parry Moon in 1940 (Ref. 14.3). These data were generally based on theoretical curves but are still used as the basic solar radiation in design by many engineers.<sup>2</sup>

### 14.3.3 Intensity Distribution

Table 14.1 presents data on the distribution with wavelength of solar radiation outside the Earth's atmosphere and at the Earth's surface after 1.0 atmosphere absorption. The solar radiation distribution data outside the Earth's atmosphere (solar spectral irradiance) are based on extraterrestrial data obtained by high-flying aircraft and published by Thekaekara (Ref. 14.4). The values of solar radiation for 1.0 atmosphere

1. At one astronomical unit on a surface normal to the Sun.

2. Additional information is provided by: Beckman, W. A.; Klein, S. S.; and Duffie, J. A.: "Solar Heating Design," John Wiley and Sons, New York, 1967; Daniels, G. E.; Smith, O. E.; and Greene, W. M.: "Application of Solar Radiation and Temperature in Design of Aerospace Vehicles," Internal Note ES-42, NASA Marshall Space Flight Center, April 15, 1976.

TABLE 14.1 SOLAR SPECTRAL IRRADIANCE (outside atmosphere)  
AND SOLAR RADIATION AFTER ABSORPTION  
BY CLEAR ATMOSPHERE

Wavelength (microns) $\lambda$	Solar Spectral Irradiance (watts cm <sup>-2</sup> $\mu^{-1}$ )	Area Under Solar Spectral Irradiance Curve (watts cm <sup>-2</sup> )	Solar Radiation After One Atmosphere Absorption (watts cm <sup>-2</sup> $\mu^{-1}$ )	Area Under One Atmosphere Solar Radiation Curve (watts cm <sup>-2</sup> )	Percentage of Solar Radiation After One Atmosphere Absorp- tion for Wavelengths Shorter than $\lambda$ (%)
0.120	0.000010	0.00000060	0.000000	0.000000	0.00
0.140	0.000003	0.00000073	0.000000	0.000000	0.00
0.150	0.000007	0.00000078	0.000000	0.000000	0.00
0.160	0.000023	0.00000093	0.000000	0.000000	0.00
0.170	0.000063	0.00000136	0.000000	0.000000	0.00
0.180	0.000125	0.00000230	0.000000	0.000000	0.00
0.190	0.000271	0.00000428	0.000000	0.000000	0.00
0.200	0.00107	0.000010	0.000001	0.000000	0.00
0.210	0.00229	0.000027	0.000003	0.000000	0.00
0.220	0.00575	0.000067	0.000007	0.000000	0.00
0.225	0.00649	0.000098	0.000007	0.000000	0.00
0.230	0.00667	0.000131	0.000008	0.000000	0.00
0.235	0.00593	0.000162	0.000007	0.000000	0.00
0.240	0.00630	0.000193	0.000007	0.000000	0.00
0.245	0.00723	0.000227	0.000008	0.000000	0.00
0.250	0.00704	0.000263	0.000008	0.000000	0.00
0.255	0.0104	0.000306	0.000012	0.000000	0.00
0.260	0.0130	0.000365	0.000015	0.000000	0.00
0.265	0.0185	0.000443	0.000021	0.000000	0.00
0.270	0.0232	0.000548	0.000026	0.000000	0.00
0.275	0.0204	0.000657	0.000023	0.000000	0.00
0.280	0.0222	0.000763	0.000025	0.000000	0.00
0.285	0.0315	0.000897	0.000036	0.000001	0.00
0.290	0.0482	0.001097	0.000055	0.000001	0.00
0.295	0.0584	0.001363	0.000066	0.000001	0.00
0.300	0.0514	0.001638	0.000077	0.000035	0.03
0.305	0.0603	0.001917	0.019830	0.000134	0.12
0.310	0.0689	0.002240	0.029084	0.000279	0.25
0.315	0.0764	0.002603	0.038941	0.000474	0.42
0.320	0.0830	0.003002	0.047684	0.000712	0.64
0.325	0.0975	0.003453	0.062018	0.001022	0.92
0.330	0.1059	0.003961	0.073829	0.001392	1.25
0.335	0.1081	0.004496	0.080896	0.001796	1.61
0.340	0.1074	0.005035	0.084636	0.002219	1.99
0.345	0.1069	0.005571	0.087080	0.002655	2.39
0.350	0.1093	0.006111	0.091327	0.003111	2.80
0.355	0.1083	0.006655	0.092186	0.003572	3.40
0.360	0.1068	0.007193	0.092857	0.004036	3.63
0.365	0.1132	0.007743	0.099873	0.004536	4.08
0.370	0.1181	0.008321	0.105507	0.005063	4.55
0.375	0.1157	0.008906	0.104596	0.005586	5.03
0.380	0.1120	0.009475	0.102971	0.006101	5.49
0.385	0.1098	0.010030	0.102273	0.006613	5.95
0.390	0.1098	0.010579	0.103977	0.007132	6.42
0.395	0.1189	0.011150	0.114309	0.007704	6.93
0.400	0.1429	0.011805	0.137403	0.008391	7.55
0.405	0.1644	0.012573	0.158076	0.009181	8.26
0.410	0.1751	0.013422	0.168365	0.010023	9.02
0.415	0.1774	0.014303	0.170576	0.010876	9.79
0.420	0.1747	0.015183	0.167980	0.011716	10.54
0.425	0.1693	0.016043	0.162788	0.012530	11.28
0.430	0.1639	0.016876	0.157596	0.013318	11.99
0.435	0.1663	0.017702	0.159903	0.014117	12.71
0.440	0.1810	0.018570	0.174038	0.014988	13.40
0.445	0.1922	0.019503	0.184807	0.015912	14.30
0.450	0.2006	0.020485	0.192884	0.016876	15.19
0.455	0.2057	0.021501	0.195904	0.017656	16.07
0.460	0.2066	0.022532	0.196761	0.018839	16.96
0.465	0.2048	0.023560	0.196923	0.019824	17.84
0.470	0.2033	0.024580	0.195480	0.020801	18.72



TABLE 14.1 (Continued)

Wavelength (microns) $\lambda$	Solar Spectral Irradiance (watts cm <sup>-2</sup> $\mu$ <sup>-1</sup> )	Area Under Solar Spectral Irradiance Curve (watts cm <sup>-2</sup> )	Solar Radiation After One Atmosphere Absorption (watts cm <sup>-2</sup> $\mu$ <sup>-1</sup> )	Area Under One Atmosphere Solar Radiation Curve (watts cm <sup>-2</sup> )	Percentage of Solar Radiation After One Atmosphere Absorp- tion for Wavelengths Shorter than $\lambda$ (%)
0.475	0.2044	0.025600	0.196538	0.021784	19.61
0.480	0.2074	0.026629	0.197523	0.022772	20.50
0.485	0.1976	0.027642	0.186415	0.023704	21.34
0.490	0.1950	0.028623	0.183962	0.024624	22.17
0.495	0.1960	0.029601	0.183177	0.025539	22.99
0.500	0.1942	0.030576	0.179814	0.026439	23.80
0.505	0.1920	0.031542	0.176146	0.027319	24.60
0.510	0.1882	0.032492	0.172660	0.028183	25.37
0.515	0.1833	0.033421	0.168165	0.029023	26.13
0.520	0.1833	0.034337	0.168165	0.029864	26.88
0.525	0.1852	0.035259	0.169908	0.030714	27.65
0.530	0.1842	0.036182	0.168990	0.031559	28.41
0.535	0.1818	0.037097	0.166788	0.032393	29.16
0.540	0.1783	0.037997	0.163977	0.033211	29.90
0.545	0.1754	0.038882	0.160917	0.034015	30.62
0.550	0.1725	0.039751	0.158256	0.034806	31.33
0.555	0.1720	0.040613	0.157798	0.035595	32.05
0.560	0.1695	0.041466	0.155504	0.036373	32.75
0.565	0.1705	0.042316	0.156422	0.037155	33.45
0.570	0.1712	0.043171	0.157064	0.037940	34.16
0.575	0.1719	0.044028	0.157726	0.038729	34.87
0.580	0.1715	0.044887	0.157339	0.039516	35.57
0.585	0.1712	0.045744	0.157064	0.040301	36.28
0.590	0.1700	0.046597	0.155963	0.041081	36.98
0.595	0.1682	0.047442	0.154311	0.041852	37.68
0.600	0.1666	0.048279	0.152844	0.042616	38.37
0.605	0.1647	0.049107	0.151100	0.043372	39.05
0.610	0.1635	0.049928	0.150000	0.044122	39.72
0.620	0.1602	0.051546	0.146972	0.045592	41.05
0.630	0.1570	0.053132	0.145370	0.047045	42.30
0.640	0.1544	0.054689	0.144299	0.048488	43.66
0.650	0.1511	0.056217	0.142547	0.049914	44.94
0.660	0.1486	0.057715	0.141523	0.051329	46.22
0.670	0.1456	0.059186	0.140000	0.052729	47.48
0.680	0.1427	0.060628	0.137211	0.054101	48.71
0.690	0.1402	0.062042	0.134807	0.055449	49.93
0.700	0.1369	0.063428	0.131634	0.056766	51.11
0.710	0.1344	0.064784	0.129230	0.058058	52.27
0.720	0.1314	0.066113	0.126346	0.059321	53.41
0.730	0.1290	0.067415	0.124038	0.060562	54.53
0.740	0.1260	0.068690	0.121153	0.061773	55.62
0.750	0.1235	0.069938	0.118750	0.062961	56.69
0.800	0.1107	0.075793	0.106442	0.068283	61.48
0.850	0.0988	0.081030	0.095000	0.073033	65.76
0.900	0.0889	0.085723	0.080090	0.077037	69.36
0.950	0.0835	0.090033	0.077314	0.080903	72.84
1.000	0.0746	0.093985	0.071730	0.084490	76.07
1.100	0.0592	0.100675	0.056923	0.090182	81.20
1.200	0.0484	0.106055	0.046538	0.094836	85.39
1.300	0.0396	0.110455	0.036000	0.098436	88.63
1.400	0.0336	0.114115	0.002240	0.098660	88.83
1.500	0.0287	0.117230	0.027333	0.101393	91.29
1.600	0.0244	0.119885	0.023461	0.103739	93.40
1.700	0.0202	0.122115	0.019423	0.105681	95.15
1.800	0.0159	0.123920	0.013826	0.107064	96.40
1.900	0.0126	0.125345	0.000126	0.107077	96.41
2.000	0.0103	0.126490	0.009809	0.108057	97.29
2.100	0.0090	0.127455	0.008653	0.108923	98.07
2.200	0.0079	0.128300	0.007596	0.109682	98.76
2.300	0.0068	0.129035	0.006538	0.110336	99.34

TABLE 14.1 (Concluded)

Wavelength (microns) $\lambda$	Solar Spectral Irradiance (watts cm <sup>-2</sup> $\mu^{-1}$ )	Area Under Solar Spectral Irradiance Curve (watts cm <sup>-2</sup> )	Solar Radiation After One Atmosphere Absorption (watts cm <sup>-2</sup> $\mu^{-1}$ )	Area Under One Atmosphere Solar Radiation Curve (watts cm <sup>-2</sup> )	Percentage of Solar Radiation After One Atmosphere Absorption for Wavelengths Shorter than $\lambda$ (%)
2.4	0.0064	0.129695	0.006153	0.110951	99.90
2.5	0.0054	0.130285	0.001080	0.111059	100.00
2.6	0.0048	0.130795	0.000005	0.111060	100.00
2.7	0.0043	0.131250	0.000004	0.111060	100.00
2.8	0.00390	0.131660	0.000004	0.111061	100.00
2.9	0.00350	0.132030	0.000004	0.111061	100.00
3.0	0.00310	0.132360	0.000003	0.111061	100.00
3.1	0.00260	0.132645	0.000002	0.111062	100.00
3.2	0.00226	0.132888	0.000002	0.111062	100.00
3.3	0.00192	0.133097	0.000002	0.111062	100.00
3.4	0.00166	0.133276	0.000001	0.111062	100.00
3.5	0.00146	0.133432	0.000001	0.111062	100.00
3.6	0.00135	0.133573	0.000001	0.111062	100.00
3.7	0.00123	0.133702	0.000001	0.111062	100.00
3.8	0.00111	0.133819	0.000001	0.111063	100.00
3.9	0.00103	0.133926	0.000001	0.111063	100.00
4.0	0.00095	0.134025	0.000001	0.111063	100.00
4.1	0.00087	0.134116	0.000001	0.111063	100.00
4.2	0.00078	0.134198	0.000000	0.111063	100.00
4.3	0.00071	0.134273	0.000000	0.111063	100.00
4.4	0.00065	0.134341	0.000000	0.111063	100.00
4.5	0.00059	0.134403	0.000000	0.111063	100.00
4.6	0.00053	0.134459	0.000000	0.111063	100.00
4.7	0.00048	0.134509	0.000000	0.111063	100.00
4.8	0.00045	0.134556	0.000000	0.111063	100.00
4.9	0.00041	0.134599	0.000000	0.111063	100.00
5.0	0.0003830	0.13463906	0.000000	0.111063	100.00
6.0	0.0001750	0.13491806	0.000000	0.111063	100.00
7.0	0.0000990	0.13505506	0.000000	0.111063	100.00
8.0	0.0000600	0.13513456	0.000000	0.111063	100.00
9.0	0.0000380	0.13518356	0.000000	0.111063	100.00
10.0	0.0000250	0.13521506	0.000000	0.111063	100.00
11.0	0.0000170	0.13523606	0.000000	0.111063	100.00
12.0	0.0000120	0.13525056	0.000000	0.111063	100.00
13.0	0.0000087	0.13526091	0.000000	0.111063	100.00
14.0	0.0000055	0.13526801	0.000000	0.111063	100.00
15.0	0.0000049	0.13527321	0.000000	0.111063	100.00
16.0	0.0000038	0.13527756	0.000000	0.111063	100.00
17.0	0.0000031	0.13528101	0.000000	0.111063	100.00
18.0	0.0000024	0.13528376	0.000000	0.111063	100.00
19.0	0.0000020	0.13528596	0.000000	0.111063	100.00
20.0	0.0000016	0.13528776	0.000000	0.111063	100.00
25.0	0.000000610	0.13529328	0.000000	0.111063	100.00
30.0	0.000000300	0.13529556	0.000000	0.111063	100.00
35.0	0.000000160	0.13529671	0.000000	0.111063	100.00
40.0	0.000000094	0.13529734	0.000000	0.111063	100.00
50.0	0.000000038	0.13529800	0.000000	0.111063	100.00
60.0	0.000000019	0.13529829	0.000000	0.111063	100.00
80.0	0.000000007	0.13529855	0.000000	0.111063	100.00
100.0	0.000000003	0.13529865	0.000000	0.111063	100.00
1000.0	0.000000000	0.13530000	0.000000	0.111063	100.00



absorption are representative of a very clear atmosphere which provides a minimum of atmospheric absorption. This gives a total normal solar radiation value (area under the spectral curve) equal to the highest values measured at the Earth's surface in mid-latitudes. These data are for use in solar radiation design studies when extreme solar radiation effects are desired at the Earth's surface. The same data are shown in graphical form in Figure 14.1.

#### 14.3.4 Atmospheric Transmittance of Solar Radiation

The atmosphere of the Earth is composed of a mixture of gases, aerosols, and dust which absorb radiation in different amounts at various wavelengths. If the ratio is taken of the solar spectral irradiance  $I_0$  to that of the solar radiation after absorption through one air mass  $I_{1.00}$ , an atmospheric transmittance factor  $M$  can be found [equation (14.2)]:

$$M = \frac{I_0}{I_{1.00}} \quad (14.2)$$

The atmospheric transmittance constant can be used in the following equation for computations of intensities for any other number of air masses:

$$I_N = I_0 (M^N) \quad (14.3)$$

where

$I_N$  = intensity of solar radiation for  $N$  air mass thickness

$N$  = number of air masses.

Equation (14.3) can also be used to obtain solar radiation intensities versus wavelengths for other total normal incident solar radiation intensities (area under curve) by computation of new values of atmospheric transmittance as follows:

$$M_N = M \frac{I_{TN}}{0.1111} \quad (14.4)$$

where

$I_{TN}$  = new value of total normal incident solar radiation intensity in  $W \text{ cm}^{-2}$

$M$  = value for atmospheric transmittance given in Table 14.1

$M_N$  = new value of atmospheric transmittance.

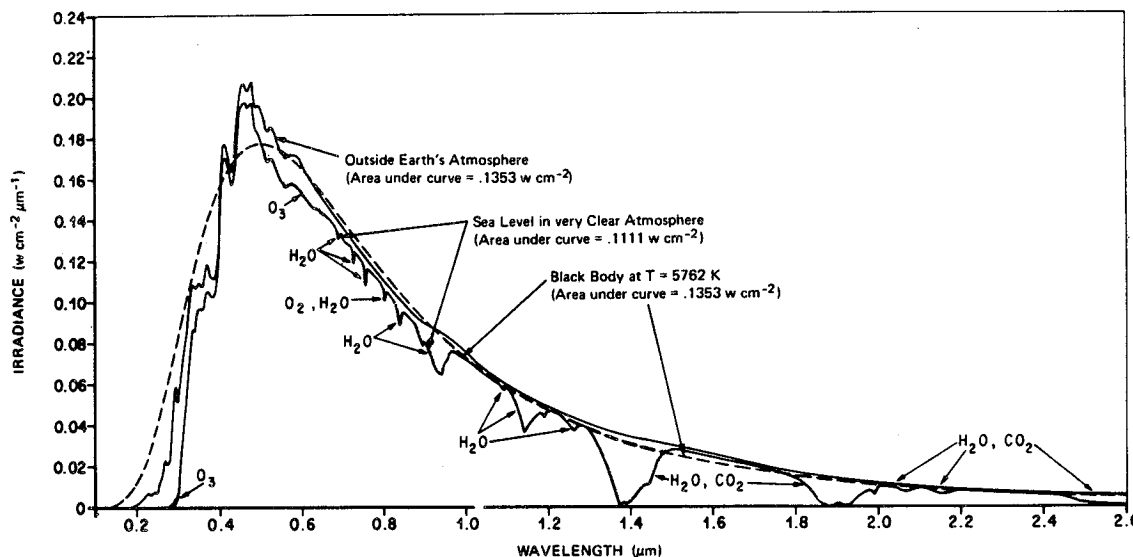


Figure 14.1 Normal incident solar radiation at sea level on very clear days, solar spectral irradiance outside the Earth's atmosphere at 1 AU (Ref. 14.4), and black body spectral irradiance curve at  $T = 5762^{\circ}\text{K}$  (normalized to 1AU).

Equations (14.3) and (14.4) are valid only for locations relatively near the Earth's surface (below 5 km altitude). For higher altitudes, corrections would be needed for the change of the amount of ozone and water vapor in the atmosphere. Also, equation (14.4) should be used only for values of  $I_{TN}$  greater than  $0.0767 \text{ W cm}^{-2}$  ( $1.10 \text{ g-cal cm}^{-2} \text{ min}^{-1}$ ) since values lower than this would indicate a considerably higher ratio of water vapor to ozone in the atmosphere and require that the curve be adjusted to give more absorption in the infrared water vapor bands at long wavelengths (infrared) and a smaller increase for the ozone at shorter wavelengths.

#### 14.3.5 Sky (Diffuse) Radiation

When solar radiation, which is a nearly parallel beam of light, enters the atmosphere of the Earth, molecules of air, dust particles, and aerosols such as water vapor droplets either diffuse or absorb a part of the radiation. The diffuse radiation then reaches the Earth as nonparallel light from all directions.

##### 14.3.5.1 Scattered Radiation

The scattered radiation gives the sky its brightness and color. The color is a result of selective scattering at certain wavelengths as a function of the size of the molecules and particles.

On a clear day the amount of scattering is very low because there are few particles and water droplets. The clear sky can be as little as  $10^{-6}$  as bright as the surface of the Sun. This sky radiation is called "diffuse radiation" in this document. On a clear day the total energy contribution from the diffuse radiation from the entire sky hemisphere to a horizontal surface is between  $0.0007$  and  $0.014 \text{ W cm}^{-2}$  ( $0.01$  and  $0.02 \text{ g-cal cm}^{-2} \text{ min}^{-1}$ ).

As a black body radiator, the clear sky is considered equivalent to a cold surface (Table 14.2). The temperature of the clear sky is the same during the daytime as at nighttime. Values of sky radiation for several localities are given in Table 14.3. It is the clear sky at night acting as a cold sink, without the solar radiation heating the surface of the Earth, that causes air temperatures to be lower than the daytime values.

TABLE 14.2 SURFACE AIR AND SKY RADIATION TEMPERATURE EXTREMES

Area	Surface Air Temperature Extremes <sup>a</sup>					Sky Radiation	
	Maximum		Minimum		Extreme Minimum Equivalent Temperature	Equivalent Radiation (g-cal cm <sup>-2</sup> min <sup>-1</sup> )	
	Extreme	95% <sup>b</sup>	Extreme	95% <sup>b</sup>			
Huntsville, Ala.	°C 40.0	36.7	-23.9	-12.8	-30.0	0.28	
	°F 104	98	-11	9	-22		
Kennedy Space Center, Fla.	°C 37.2	33.3	-3.9	1.7	-15.0	0.36	
	°F 99	92	25	35	5		
Space and Missile Test Center Vandenberg AFB, Calif.	°C 37.8	29.4	-3.3	1.1	-15.0	0.36	
	°F 100	85	26	34	5		
Edwards AFB, Calif.	°C 45.0	41.7	-15.6	-7.8	-30.0	0.28	
	°F 113	107	4	18	-22		
Honolulu, Oahu — Hickam Field	°C 33.9	32.8	11.1	15.6	-15.0	0.36	
	°F 93	91	52	60	5		
Guam — Andersen AFB	°C 34.4	31.1	18.9	22.2	-15.0	0.36	
	°F 94	88	66	72	5		
Santa Susana, Calif.	°C 42.2	36.1	-2.2	1.7	-15.0	0.36	
	°F 108	97	28	35	5		
Thiokol Wasatch Division, Utah	°C 38.3	35.6	-27.8	-16.1	-30.0	0.28	
	°F 101	96	-18	3	-22		
New Orleans, La.	°C 37.8	35.0	-10.0	-3.3	-17.8	0.35	
	°F 100	95	14	26	0		
National Space Tech. Lab., Miss.	°C 37.8	35.6	-13.9	-2.2	-17.8	0.35	
	°F 100	96	7	28	0		
Continent Transportation (rail, truck, river barge)	°C 47.2	—	-34.4	—	-30.0	0.28	
	°F 117	—	-30	—	-22		
Ship Transportation (West Coast, Panama Canal, Gulf of Mexico)	°C 37.8	—	-12.2	—	-15.0	0.36	
	°F 100	—	10	—	5		
Johnson Space Center, Tex.	°C 40.0	36.7	-9.4	-2.2	-17.8	0.35	
	°F 104	98	15	28	0		
Wallops Flight Center, Va.	°C 37.2	33.3	-20.0	-5.6	-17.8	0.35	
	°F 99	92	-4	22	0		
White Sands Missile Range, N.M.	°C 41.7	38.9	-23.9	-10.0	-30.0	0.28	
	°F 107	102	-11	14	-22		

a. The extreme maximum and minimum temperatures will be encountered during periods of wind speeds less than about 1 meter per second.

b. Based on daily extreme (maximum or minimum) observations for worst month.

TABLE 14.3 SOLAR RADIATION MAXIMUM VALUES ASSOCIATED  
WITH EXTREME WIND VALUES

Maximum Solar Radiation (Normal Incident)						
Steady-State Ground Wind Speed at 18 m Height	Huntsville, New Orleans, NSTL, JSC Gulf Transportation, Eastern Test Range, Western Test Range, West Coast Transportation and Wallops Test Range				White Sands Missile Range	
	(kJm <sup>-2</sup> sec <sup>-1</sup> )	(g-cal cm <sup>-2</sup> min <sup>-1</sup> )	(BTU ft <sup>-2</sup> hr <sup>-1</sup> )	(kJm <sup>-2</sup> sec <sup>-1</sup> )	(g-cal cm <sup>-2</sup> min <sup>-1</sup> )	(BTU ft <sup>-2</sup> hr <sup>-1</sup> )
10	0.84	1.20	265	1.05	1.50	322
15	0.56	0.80	177	0.70	1.00	221
≥ 20	0.35	0.50	111	0.56	0.80	177

With clouds the amount of diffuse radiation is greater. The total hemisphere during an overcast day may contribute as much as  $0.069 \text{ W cm}^{-2}$  ( $1.0 \text{ g-cal cm}^{-2} \text{ min}^{-1}$ ) of radiation to a horizontal surface.

The greater scattering by clouds makes the effective temperature of the clouds warmer than the clear air. At night the clouds act as a barrier to the outgoing radiation. Since they are warmer than the clear sky, the air near the ground will not cool to as low a temperature.

#### 14.3.5.2 Absorbed Radiation

The various gases in the atmosphere selectively absorb some of the incoming radiation. Absorption changes some of the radiation into heat or radiation at wavelengths different from that received. Absorption by gases is observed in the solar spectrum as bands of various widths. The major gases in the Earth's atmosphere, which show as absorption bands in the solar spectrum, are water vapor, carbon dioxide, ozone, and molecular oxygen.

#### 14.4 Average Emittance of Colored Objects

In thermal engineering studies, the color of a painted surface is not important when one considers low-temperature radiation, i.e., from  $10^\circ$  to  $68^\circ\text{C}$ , since most painted surfaces have the same absorptivity at these low temperatures. Colored surfaces may differ in absorptivity. A list of values of emissivity and absorptivity for various surfaces and different colors of paint exposed to solar radiation is presented in Reference 14.5. Similar data are given in other publications that give either a range of values or mean values for the type of surface. The change of temperature (above or below the air temperature), which is the amount of heating or cooling, is proportional to the emissivity or absorptivity; therefore, the accuracy of determining the temperature of a surface is related to the accuracy of the emissivity and absorptivity. Spectral distribution curves of emittance are available for many surfaces. The average emittance of any surface can be computed by the following method:

- a. Divide the spectral emittance curve (i.e., Figure 14.1) into small intervals that have little or no change of emittance within the interval.
- b. Using the same intervals from the spectral distribution of radiation (i.e., from Table 14.1), multiply each value of emittance over the selected interval by the percentage of radiation over the interval.
- c. Sum the resultant products to give the average emittance.

Table 14.4 and Figure 14.2 give an example of such computations with data from Figure 14.1 and Table 14.1 being used. Similar computations can be accomplished for other sources of radiation such as the night sky or from cloudy skies.

#### 14.5 Computation of Surface Temperature for Several Simultaneous Radiation Sources

The extreme value of temperature which a surface may reach when exposed to daytime (solar) or nighttime (night sky) radiation with no wind (calm), assuming it has no mass or heat transfer within the object, is

TABLE 14.4 COMPUTATION OF EMITTANCE OF WHITE PAINT EXPOSED TO DIRECT SOLAR RADIATION AT THE EARTH'S SURFACE

Wavelength ( $\mu$ )	Emittance	Average Emittance	Solar Radiation, 1 Atmo- sphere (%)	Solar Radiation over Interval (%)	Product of Aver- age Emittance and Percent Solar Radiation over Interval Divided by 100
0.300	0.73	0.590	0.03	1.22	0.0072
0.330	0.45	0.410	1.25	1.55	0.0063
0.350	0.37	0.365	2.80	21.00	0.0766
0.500	0.36	0.325	23.80	11.77	0.0382
0.580	0.29	0.260	35.57	15.54	0.0404
0.700	0.23	0.225	51.11	10.37	0.0233
0.800	0.22	0.260	61.48	7.88	0.0205
0.900	0.30	0.370	69.36	6.71	0.0248
1.000	0.44	0.520	76.07	9.32	0.0485
1.200	0.60	0.650	85.39	3.44	0.0224
1.400	0.70	0.745	88.83	4.57	0.0340
1.600	0.79	0.810	93.40	3.01	0.0244
1.900	0.83	0.830	96.41	3.59	0.0298
50.000	0.83		100.00		
Sum = average emittance = 0.396					

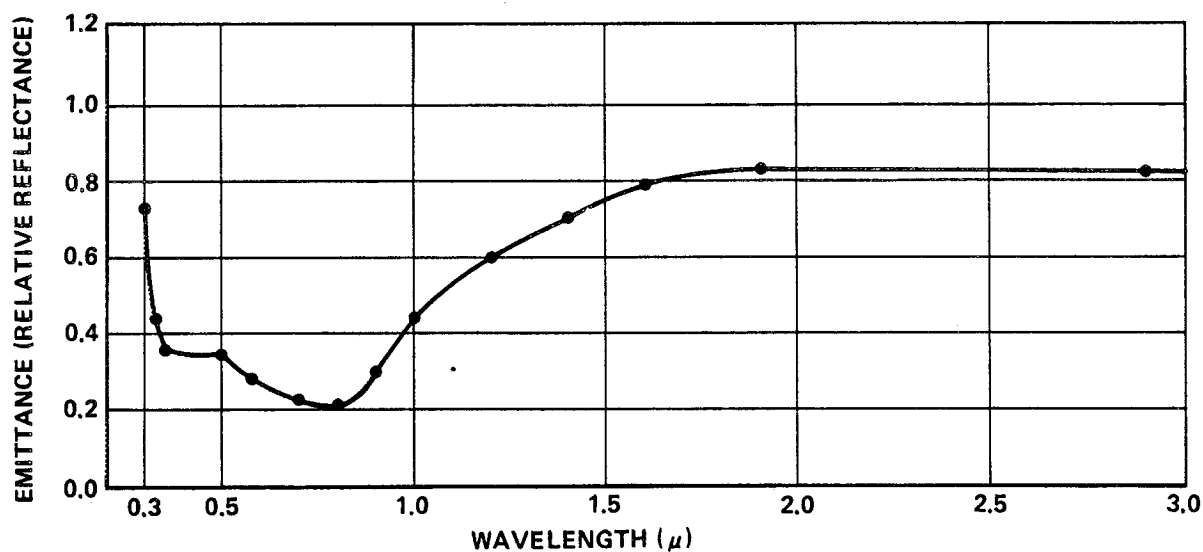


Figure 14.2 Emittance of barium sulphate and magnesium oxide versus wavelength.

$$T_S = T_A + E (\Delta T_{BS}) \quad , \quad (14.5)$$

where

$T_S$  = surface temperature ( $^{\circ}\text{K}$ )

$T_A$  = air temperature ( $^{\circ}\text{K}$ )

$E$  = emittance of surface

$\Delta T_{BS}$  = increase in black body temperature ( $^{\circ}\text{K}$ ) from daytime solar radiation (plus) or decrease in black body temperature ( $^{\circ}\text{K}$ ) from nighttime sky radiation (minus), calculated from

$$\Delta T_{BS} = \left( \frac{I_{TS}}{\sigma} \right)^{1/4} - T_A \quad . \quad (14.6)$$

Extreme values of  $\Delta T_{BS}$  can be obtained from Figure 14.3A or Table 14.5, where

$I_{TS}$  = total radiation (solar by day) (sky for night) received at surface. These values can be extremes from Tables 14.6, 14.7, or 14.2 from this report.

$\sigma$  = Stefan-Boltzman constant

$$= 8.1296 \times 10^{-11} \text{ g-cal cm}^{-2} \text{ K}^{-4}$$

$$= 5.6692 \times 10^{-12} \text{ W cm}^{-2} \text{ K}^{-4} \quad .$$

The term  $(I_{TS}/\sigma)^{1/4}$  is equal to the extreme black body surface temperature.

If a correction for wind speed is desired, equation (14.5) can be used as follows:

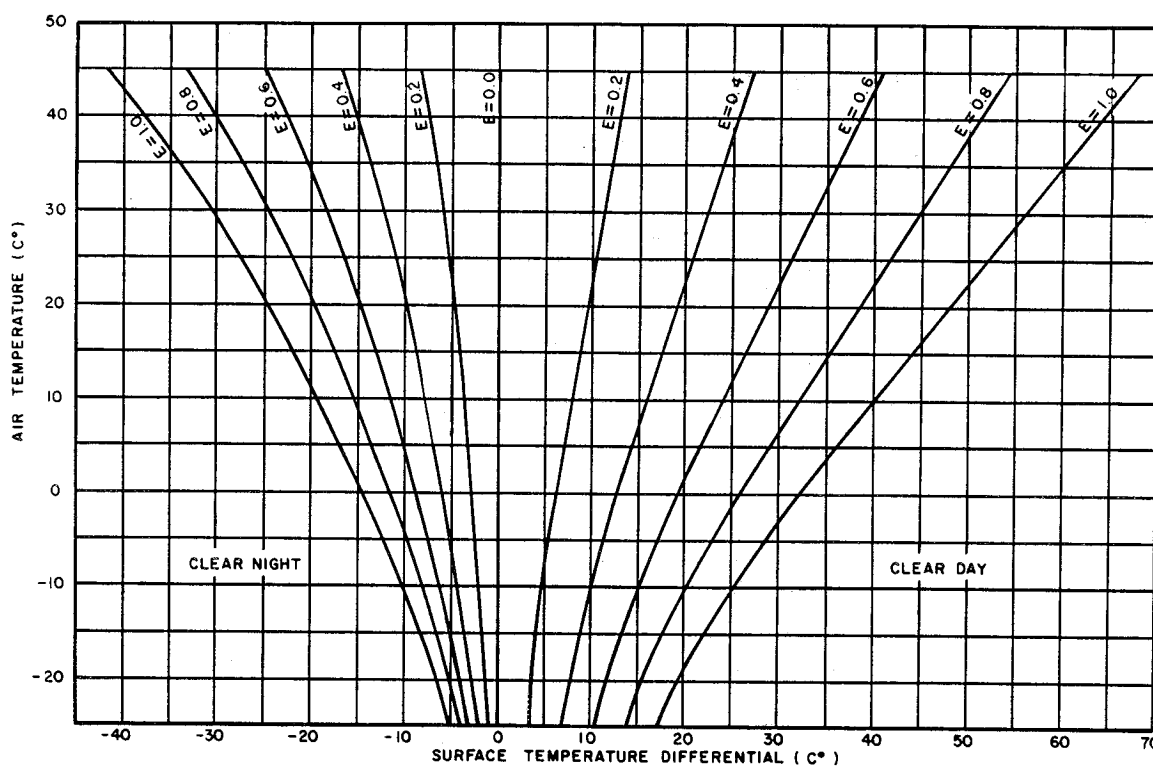
$$T_S = T_A + E(\Delta T_{BS}) \frac{Wc}{100} \quad , \quad (14.7)$$

where  $Wc$  is the correction for wind speed in percent from Figure 14.3B. Equations (14.5), (14.6), and (14.7) are only for computing the effect of one source of radiation on a surface. When more than one radiation source is received by an object, then a more complex method must be used, as given in the following discussion.

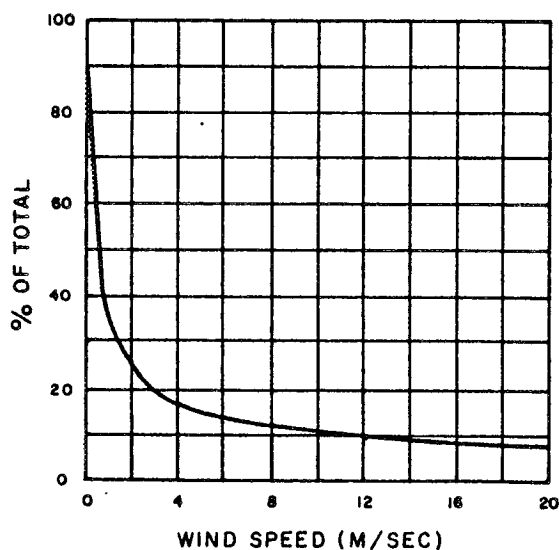
If we have a black body with several radiation sources and no convection, then

$$\sigma T^4 = \sum_{i=1}^n I_i \quad i = 1, 2, 3, \dots, n \quad . \quad (14.8)$$





- A. Surface temperature differentials with respect to air temperature for surface of emittance from 0.0 to 1.0 for calm wind conditions. Temperature difference after correction for wind is to be added or subtracted to the air temperature to give surface (skin) temperature.



- B. Correction for wind speed obtained from Graph A. Valid only for a pressure of one atmosphere.

Figure 14.3 Extreme surface (skin) temperature of an object near the Earth's surface (0 to 300 m) for clear sky.

TABLE 14.5 EXTREME SURFACE (skin) TEMPERATURE ABOVE OR BELOW  
AIR TEMPERATURE OF AN OBJECT NEAR THE EARTH'S SURFACE

Air Temperature  (°C)	Surface Temperature Differential (°C)									
	Clear Night					Clear Day				
	Wind Speed (m sec <sup>-1</sup> )					Wind Speed (m sec <sup>-1</sup> )				
	0	2	4	10	20	0	2	4	10	20
	Correction Factor					Correction Factor				
1.00	0.25	0.17	0.11	0.08	1.00	0.25	0.17	0.11	0.08	
-25	-5.0	-1.2	-0.8	-0.6	-0.4	16.9	4.2	2.9	1.9	1.4
-20	-6.5	-1.6	-1.1	-0.7	-0.5	19.2	4.8	3.3	2.1	1.5
-15	-8.2	-2.0	-1.4	-0.9	-0.6	22.0	5.5	3.7	2.4	1.8
-10	-10.2	-2.6	-1.7	-1.1	-0.8	25.1	6.3	4.3	2.8	2.0
- 5	-12.2	-3.0	-2.1	-1.3	-1.0	28.5	7.1	4.8	3.1	2.3
0	-14.5	-3.6	-2.5	-1.6	-1.2	32.0	8.0	5.4	3.5	2.6
5	-16.9	-4.2	-2.9	-1.9	-1.4	36.0	9.0	6.1	4.0	2.9
10	-19.4	-4.8	-3.3	-2.1	-1.6	40.0	10.0	6.8	4.4	3.2
15	-21.9	-5.5	-3.7	-2.4	-1.8	44.0	11.0	7.5	4.8	3.5
20	-24.6	-6.2	-4.2	-2.7	-2.0	48.0	12.0	8.2	5.3	3.8
25	-27.4	-6.8	-4.6	-3.0	-2.2	52.0	13.0	8.8	5.7	4.2
30	-30.5	-7.6	-5.2	-3.4	-2.4	56.0	14.0	9.5	6.2	4.5
35	-34.0	-8.5	-5.8	-3.7	-2.7	60.0	15.0	10.2	6.6	4.8
40	-37.7	-9.4	-6.4	-4.1	-3.0	64.0	16.0	10.9	7.0	5.1
45	-41.7	-10.4	-7.1	-4.6	-3.3	68.0	17.0	11.6	7.5	5.4

NOTE: Values are given for an emittance value of 1.0. Temperature differences for other emittance can be determined by multiplying tabular value by the appropriate emittance.

TABLE 14.6 EXTREME VALUES OF SOLAR RADIATION FOR THE SPACE AND MISSILE TEST  
CENTER, WEST COAST TRANSPORTATION, SANTA SUSANA, WHITE SANDS MISSILE  
RANGE, BRIGHAM CITY, AND EDWARDS AFB

TIME OF DAY (Local Stand- ard Time)	Total Horizontal Solar Radiation		Diffuse Radiation Associated with Total Horizontal Solar Radiation Extremes		Total Normal Incident Solar Radiation		Total 45° Surface Solar Radiation	
	g-cal cm <sup>-2</sup> min <sup>-1</sup>		g-cal cm <sup>-2</sup> min <sup>-1</sup>		g-cal cm <sup>-2</sup> min <sup>-1</sup>		g-cal cm <sup>-2</sup> min <sup>-1</sup>	
JUNE								
	EXTREME	95 Percentile	EXTREME	95 Percentile	EXTREME	95 Percentile	EXTREME	95 Percentile
0500	0	0	0	0	0	0	0	0
0600	0.16	0.11	.02	.04	1.14	0.78	0.04	0
0700	0.46	0.40	.05	.08	1.34	1.08	0.19	0.16
0800	0.82	0.76	.06	.09	1.54	1.38	0.34	0.31
0900	1.16	1.11	.04	.08	1.74	1.62	0.84	0.77
1000	1.45	1.42	0	.03	1.79	1.71	1.19	1.12
1100	1.64	1.56	0	.10	1.79	1.69	1.39	1.31
1200	1.69	1.63	0	.08	1.74	1.68	1.49	1.38
1300	1.69	1.64	0	.07	1.74	1.68	1.49	1.40
1400	1.59	1.54	.06	.12	1.74	1.68	1.34	1.29
1500	1.45	1.39	0	.06	1.79	1.70	1.14	1.09
1600	1.21	1.19	0	.02	1.79	1.71	0.89	0.78
1700	0.87	0.83	.03	.05	1.69	1.60	0.34	0.18
1800	0.46	0.42	.05	.08	1.39	1.23	0.19	0.13
1900	0.14	0.12	.02	.04	1.19	0.93	0.04	0
2000	0	0	0	0	0	0	0	0
DECEMBER								
	EXTREME	95 Percentile	EXTREME	95 Percentile	EXTREME	95 Percentile	EXTREME	95 Percentile
0800	0	0	0	0	0	0	0	0
0900	0.35	0.32	0.04	0.05	1.59	1.39	0.99	0.85
1000	0.65	0.60	0.03	0.05	1.64	1.53	1.29	1.21
1100	0.86	0.80	0	0.04	1.84	1.64	1.64	1.49
1200	0.96	0.89	0.02	0.06	1.79	1.69	1.74	1.63
1300	0.99	0.89	0	0.06	1.84	1.70	1.79	1.64
1400	0.85	0.80	0.01	0.04	1.79	1.64	1.59	1.49
1500	0.66	0.60	0.02	0.05	1.69	1.54	1.34	1.21
1600	0.38	0.31	0.02	0.05	1.64	1.38	1.04	0.87
1700	0	0	0	0	0	0	0	0

TABLE 14.7 EXTREME VALUES OF SOLAR RADIATION FOR EASTERN TEST RANGE, NSTL, JSC, NEW ORLEANS, GULF TRANSPORTATION, AND HUNTSVILLE

TIME OF DAY (Local Standard Time)	Total Horizontal Solar Radiation		Diffuse Radiation Associated with Total Horizontal Solar Radiation Extremes		Total Normal Incident Solar Radiation		Total 45° Surface Solar Radiation	
	g-cal cm <sup>-2</sup> min <sup>-1</sup>		g-cal cm <sup>-2</sup> min <sup>-1</sup>		g-cal cm <sup>-2</sup> min <sup>-1</sup>		g-cal cm <sup>-2</sup> min <sup>-1</sup>	
	JUNE							
	EXTREME	95 Percentile	EXTREME	95 Percentile	EXTREME	95 Percentile	EXTREME	95 Percentile
0500	0	0	0	0	0	0	0	0
0600	0.12	0.07	0	0	1.09	1.00	0	0
0700	0.42	0.36	0.05	0.07	1.29	1.04	0.19	0.16
0800	0.82	0.71	0.04	0.10	1.59	1.30	0.34	0.27
0900	1.23	1.02	0	0.10	1.59	1.48	0.49	0.41
1000	1.35	1.30	0.02	0.06	1.59	1.54	0.99	0.95
1100	1.52	1.45	0.03	0.09	1.59	1.54	1.19	1.14
1200	1.58	1.53	0.10	0.16	1.64	1.55	1.29	1.24
1300	1.58	1.50	0.10	0.20	1.64	1.53	1.29	1.24
1400	1.50	1.44	0.05	0.12	1.59	1.52	1.19	1.09
1500	1.35	1.30	0.02	0.06	1.59	1.52	1.04	0.95
1600	1.10	1.01	0.05	0.12	1.54	1.44	0.54	0.44
1700	0.77	0.72	0.05	0.09	1.49	1.33	0.34	0.30
1800	0.48	0.40	0.03	0.06	1.44	1.14	0.19	0.18
1900	0.11	0.08	0	0	1.14	1.00	0.14	0.03
2000	0	0	0	0	0	0	0	0

	DECEMBER							
	95 Percentile		95 Percentile		95 Percentile		95 Percentile	
	EXTREME	95 Percentile	EXTREME	95 Percentile	EXTREME	95 Percentile	EXTREME	95 Percentile
0700	0	0	0	0	0	0	0	0
0800	0.16	0.10	0	0	1.34	1.12	0.64	0.50
0900	0.46	0.42	0.04	0.06	1.44	1.36	0.94	0.89
1000	0.79	0.71	0.01	0.07	1.69	1.60	1.39	1.29
1100	0.95	0.92	0.02	0.04	1.79	1.68	1.64	1.56
1200	1.09	1.02	0	0.03	1.79	1.70	1.74	1.66
1300	1.05	1.02	0	0.03	1.79	1.78	1.74	1.66
1400	0.94	0.89	0.02	0.05	1.74	1.67	1.59	1.63
1500	0.79	0.70	0	0.03	1.74	1.57	1.39	1.27
1600	0.46	0.41	0.04	0.06	1.54	1.40	0.99	0.94
1700	0.16	0.10	0	0	1.34	1.12	0.64	0.50
1800	0	0	0	0	0	0	0	0

Then

$$T - T_A = \Delta T = \left( \frac{\sum_{i=1}^n I_i}{\sigma} \right)^{1/4} - T_A, \quad (14.9)$$

where  $T_A$  is the air temperature.

For any object exposed to radiation in the Earth's atmosphere

$$\Delta T = f_w \left( \frac{\sum_{i=1}^n E_i I_i}{\sigma} \right)^{1/4} - T_A, \quad (14.10)$$

where

$E_i$  = emittance of object for corresponding radiation source  $I_i$

$$\Delta T = T - T_A \quad (14.11)$$

$f_w$  = wind effect (convection)

$$f_w = \frac{0.325}{\sqrt{w}}$$

(14.12)

$w$  = wind speed (m/sec) .

## 14.6 Total Solar Radiation

### 14.6.1 Introduction

The standard solar radiation sensors measure the intensity of direct solar radiation from the Sun falling on a horizontal surface plus the diffuse (sky) radiation from the total sky hemisphere. Diffuse radiation is lowest with dry clear air; it increases with increasing dust and moisture in the air. With extremely dense clouds or fog, the measured horizontal solar radiation will be nearly all diffuse radiation. The higher ( $\geq 95$  percentile) values of measured horizontal solar radiation occur under clear skies or under conditions of scattered fair weather cumulus clouds which reflect additional solar radiation onto the measuring sensor.

In this document all solar radiation values given are intensities. Solar radiation intensities are measured in gram calories per square centimeter (same as langleys per square centimeter) by stations of the National Oceanic and Atmospheric Administration, National Weather Service; therefore, these units are used in this section.

### 14.6.2 Use of Solar Radiation in Design

When radiation data are used in design studies, the direct solar radiation should be applied from one direction as parallel rays, and, at the same time, the diffuse radiation should be applied as rays from all directions of a hemisphere (Fig. 14.4).

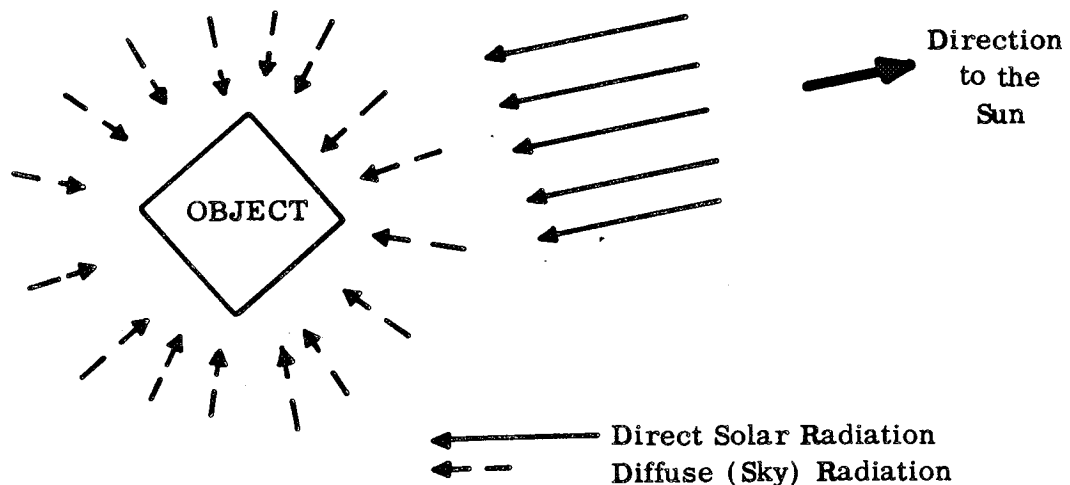


Figure 14.4 Method of applying radiation for design.

Because the Sun provides heat (from radiation) from a specific direction, differential heating of an object occurs; i.e., one part is heated more than another, resulting in stress and deformation. As an example, the Sun heats the side of the Space Shuttle vehicle facing the Sun, while the sky cools the opposite side.

This differential heating causes the vehicle to bend away from the Sun sufficiently at the top to require consideration in design of platforms surrounding the vehicle. These platforms are used to ready the vehicle on the launch pad and must be designed so as to prevent damage to the vehicle skin as the vehicle bends away from the Sun.

### 14.6.3 Total Solar Radiation Extremes

Ten years of total horizontal solar and sky radiation data at two stations were selected for analysis to determine the frequency distribution of solar radiation for use in design. The data analysis was made by The National Oceanic and Atmospheric Administration, National Climatic Center, under contract to NASA-Marshall Space Flight Center.

#### 14.6.3.1 Basic Data Computations

The basic data used were hourly totals of horizontal solar and sky radiation ( $I_{TH}$ ) for each hour of the day for 10-year periods at each of two stations: Apalachicola, Florida, and Santa Maria, California. The hourly totals were divided by 60 to obtain the average solar radiation values per minute for each hour. The average values per minute are numerically equal to intensity, and these values were used in the computations of frequency distributions. The diffuse sky radiation intensities  $I_{dH}$  were empirically estimated for each value based on the amount of total horizontal solar and sky radiation and solar altitude, similar to the method used in Reference 14.6. After the diffuse sky radiation is subtracted from the total horizontal solar and sky radiation, the resultant horizontal solar radiation  $I$  can be used to compute the direct normal incident solar radiation  $I_{DN}$  by using the following equation (Refs. 14.7 and 14.8):

$$I_{DN} = \frac{I}{\sin b} \quad , \quad (14.13)$$

where

$I_{DN}$  = direct normal incident solar radiation

$I$  = horizontal solar radiation =  $I_{TH} - I_{dH}$

$b$  = Sun's altitude (Refs. 14.9 and 14.14).

The total normal incident solar radiation  $I_{TN}$  values were found by adding the direct normal incident solar radiation  $I_{DN}$  and the diffuse sky radiation  $I_{dH}$  previously estimated. This method of finding the total normal incident solar radiation may result in a slight overestimate of the value for low solar altitudes because the sky hemisphere is intercepted by the ground surface. This error is insignificant, however, when extreme values are used and would be small for values equal to or greater than the mean plus one standard deviation.

Total solar radiation intensities on a south-facing surface, with the normal to the surface at 45 degrees to the horizontal, are calculated as follows:

$$I_{D45} = I(\sin 45 \text{ deg} + \cot b \cos a \cos 45 \text{ deg}) \quad , \quad (14.14)$$

where

$I_{D45}$  = intensity of direct solar radiation on a south-facing surface, with normal 45 degrees to the horizontal

$I$  = horizontal solar radiation =  $I_{TH} - I_{dH}$

$a$  = Sun's azimuth measured from the south direction

$b$  = Sun's altitude.

#### 14.6.3.2 Solar Radiation Extreme and 95 Percentile

To present the solar radiation data in a simplified form, the month of June was selected to represent the summer and the longest period of daylight and December for the winter and shortest period of daylight. The June data for normal incident solar radiation from Santa Maria, California, were increased for the period from 1100 to 1900 hours to reflect the higher values which occur early in July (first week) during the afternoon. Tables 14.6 and 14.7 give the frequency distributions for the extreme<sup>3</sup> values and the 95 percentile values of solar radiation for hours of the day. The values given for diffuse radiation are the values which occurred associated with the other extreme and 95 percentile values of the other solar radiations given. Since the diffuse radiation decreases with increasing horizontal radiation, the values given in Tables 14.6 and 14.7 are considerably lower than the highest values of diffuse radiation occurring during the period of record. Solar radiation data recommended for use in design are given in Table 14.8 and Figure 14.5.

#### 14.6.3.3 Variation with Altitude

Solar radiation intensity on a surface will increase with altitude above the Earth's surface, with clear skies, according to the following equation:

$$I_H = I_{DN} + (1.94 - I_{DN}) \left( 1 - \frac{\rho_H}{\rho_S} \right) \quad , \quad (14.15)$$

where

$I_H$  = intensity of solar radiation normal to surface at required height

$I_{DN}$  = intensity of solar radiation normal to surface at the Earth's surface assuming clear skies  
( $I_{DN} = I_{TN} - I_{dH}$ )

$\rho_H$  = atmospheric density at required height (from U. S. Standard, U. S. Supplemental Atmospheres, or this document) ( $\text{kg m}^{-3}$ )

---

3. Extreme as used in this section is the highest measured value of record.

TABLE 14.8 RECOMMENDED DESIGN OF SOLAR RADIATION DATA

Time of Day	Design High Solar Radiation		Design Low Solar Radiation	
Hour	BTU/ft <sup>2</sup> /hr	gm-cal/cm <sup>2</sup> /min	BTU/ft <sup>2</sup> /hr	gm-cal/cm <sup>2</sup> /min
0500	0	0.00	0	0.00
1100	363	1.64	70	0.32
1300			80	0.36
1400	363	1.64		
2000	0	0.00	0	0.00

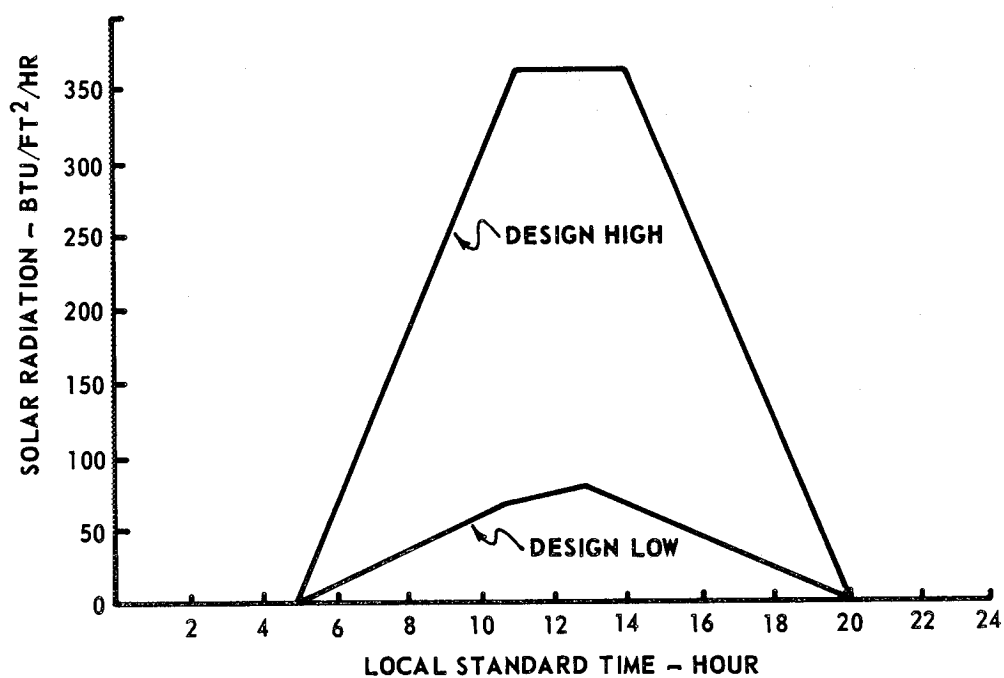


Figure 14.5 Recommended design solar radiation data.

$\rho_S$  = atmospheric density at sea level (from U. S. Standard, U. S. Supplemental Atmospheres, or this document) ( $\text{kg m}^{-3}$ )

1.94 = solar constant ( $\text{g-cal cm}^{-2}$ ).

The diffuse radiation  $I_{dH}$  decreases with altitude above the Earth's surface, with clear skies. A good estimate of the value can be obtained from the following equation<sup>5</sup> :

$$I_{dH} = 0.7500 - 0.4076 I_H , \quad (14.16)$$

where

$I_{dH}$  = intensity of diffuse radiation

$I_H$  = intensity of solar radiation normal to surface.

Equation (14.16) is valid for values of  $I_H$  from equation (14.15) up to  $1.84 \text{ g-cal cm}^{-2}$ . For values of  $I_H$  greater than  $1.84 \text{ g-cal cm}^{-2}$ ,  $I_{dH} = 0$ .

#### 14.6.3.4 Solar Radiation During Extreme Conditions

When ground winds occur exceeding the 95, 99, or 99.9 percentile design winds given in this document in Section II, the associated weather normally is such that clouds, rain, or dust is generally present; therefore, the intensity of the incoming solar radiation will be less than the maximum values given in Tables 14.6 and 14.7. Maximum values of solar radiation intensity to use with corresponding wind speeds are given in Table 14.3.

### 14.7 Temperature

Several types of temperatures at the Earth's boundary layer must be considered in design. These are as follows:

- a. Air temperature [normally measured at 1.22 m (4 ft) above a grass surface].
- b. Changes of air temperature (usually the rapid changes which occur in less than 24 hours are considered.)
- c. Measurement of surface or skin temperature of a surface exposed to radiation.
- d. Temperatures within a cloud compartment.

All of the above will be discussed in the following subsections.

#### 14.7.1 Air Temperature Near the Surface

Surface air temperature extremes (maximum, minimum, and the 95 percentile values) and the extreme minimum sky radiation (equal to the out-going radiation) are given in Table 14.2 for various geographical areas. Maximum and minimum temperature values should be expected to last only a few hours

---

5. Equation (14.16) is based on a cloudless and dust-free atmosphere.



during a daily period.<sup>6</sup> Generally, the maximum temperature is reached after 12 noon and before 5 p.m., while the minimum temperature is reached just before sunrise. Table 14.9A shows the maximum and minimum air temperatures which have occurred on each hour at Kennedy Space Center, but not necessarily on the same day, although these curves represent a cold and hot extreme day. The method of sampling the day (frequency of occurrence of observations) will result in the same extreme values if the same period of time for the data is used, but the 95 percentile values will be different for hourly, daily, and monthly data reference periods. Selection of the reference period depends on engineering application. Table 14.9B gives monthly mean temperatures, standard deviations, and 2.5 and 97.5 percentiles of values of temperature for Kennedy Space Center, Florida, and Vandenberg AFB, California. United States temperature extremes are given in Section XVIII. Worldwide extremes are given in Section IX.

TABLE 14.9A MAXIMUM AND MINIMUM SURFACE AIR TEMPERATURES  
AT EACH HOUR FOR EASTERN TEST RANGE<sup>a</sup>

Time	Annual Maximum		Annual Minimum	
	°C	°F	°C	°F
1 a.m.	28.9	84	1.1	34
2	28.9	84	0.6	33
3	29.4	85	-1.1	30
4	28.3	83	-0.6	29
5	28.3	83	-1.1	28
6	29.4	85	-1.1	27
7	30.6	87	-1.7	26
8	30.6	87	-2.2	25
9	31.7	89	-0.6	28
10	33.9	93	1.1	30
11	35.0	95	2.2	35
12 noon	35.6	96	5.0	41
1 p.m.	37.2	99	5.6	42
2	35.6	97	5.0	41
3	35.6	97	5.6	42
4	35.6	97	5.6	42
5	35.6	97	5.6	42
6	35.0	95	3.9	39
7	33.3	92	2.2	36
8	31.7	89	2.2	36
9	30.0	86	1.7	35
10	30.0	86	1.7	35
11	30.0	86	1.1	34
12 mid	30.0	86	1.1	34

a. Based on 10 years of record for Patrick Air Force Base and Kennedy Space Center.

6. The equivalent radiation values given here were computed from the equivalent temperature minimum extremes by using the Stefan-Boltzmann Law ( $\sigma T^4$ ).

TABLE 14.9B MONTHLY MEAN, STANDARD DEVIATIONS (STD), AND 2.5 AND 97.5 PERCENTILE  
VALUES OF TEMPERATURE FOR KENNEDY SPACE CENTER AND  
VANDENBERG AFB, CALIFORNIA

Kennedy Space Center					Vandenberg AFB			
Month	Monthly Mean or 50 Percentile (°F)	Standard Deviation 30-day avg.	Percentiles		Monthly Mean or 50 Percentile (°F)	Standard Deviation 30-day avg.	Percentiles	
			30-Day 2.5% <sup>a</sup> (°F)	Average 97.5% <sup>a</sup> (°F)			30-Day 2.5% <sup>a</sup> (°F)	Average 97.5% <sup>a</sup> (°F)
Jan.	60.3	2.9	54.6	66.0	52.2	2.0	48.3	56.1
Feb.	61.7	4.0	53.9	69.4	52.6	1.9	48.9	56.3
Mar.	65.3	3.3	58.8	71.8	52.3	1.8	48.8	55.8
Apr.	70.0	2.6	64.9	75.1	54.2	1.7	50.9	57.5
May	74.8	2.2	70.5	79.1	53.9	1.5	51.0	56.8
June	79.2	1.6	76.1	82.3	56.8	1.5	53.9	59.7
July	80.7	0.5	79.7	81.7	58.4	1.4	55.7	61.1
Aug.	80.9	0.8	79.3	82.5	59.8	1.5	56.9	62.7
Sept.	80.0	1.2	77.7	82.4	60.2	1.8	56.7	63.7
Oct.	75.2	2.3	70.7	79.7	60.1	1.9	56.4	63.8
Nov.	68.0	3.5	61.1	74.9	55.8	2.0	51.9	59.7
Dec.	61.7	4.0	53.9	69.5	53.1	2.5	48.2	58.0

a. Recommended for use in Solid Rocket Motor Propellant bulk temperature predictions for design analyses.

NOTE: See Office memorandum S & E-AERO-YT-15-73, subject "Ambient Temperature for Space Shuttle SRB Propellant Temperature Predictions", Atmospheric Sciences Division, Marshall Space Flight Center, Alabama 35812, for additional information.

### 14.7.2 Extreme Air Temperature Change

- a. For all areas the design values of extreme air temperature changes (thermal shock) are:

(1) An increase of air temperature of  $10^{\circ}\text{C}$  ( $18^{\circ}\text{F}$ ) with a simultaneous increase of solar radiation (measured on a normal surface) from  $0.50 \text{ g-cal cm}^{-2} \text{ min}^{-1}$  ( $110 \text{ Btu ft}^{-2} \text{ hr}^{-1}$ ) to  $1.85 \text{ g-cal cm}^{-2} \text{ min}^{-1}$  ( $410 \text{ Btu ft}^{-2} \text{ hr}^{-1}$ ) may occur in a 1-hour period. Likewise, the reverse change of the same magnitude may occur for decreasing air temperature and solar radiation,

(2) A 24-hour change may occur with an increase of  $27.7^{\circ}\text{C}$  ( $50^{\circ}\text{F}$ ) in air temperature in a 5-hour period, followed by 4 hours of constant air temperature, then a decrease of  $27.7^{\circ}\text{C}$  ( $50^{\circ}\text{F}$ ) in a 5-hour period, followed by 10 hours of constant air temperature.

- b. For Eastern Test Range (Kennedy Space Center), the 99.9 percentile air temperature changes are as follows:

(1) An increase of air temperature of  $5.6^{\circ}\text{C}$  ( $11^{\circ}\text{F}$ ) with a simultaneous increase of solar radiation (measured on a normal surface) from  $0.50 \text{ g-cal cm}^{-2} \text{ min}^{-1}$  ( $110 \text{ Btu ft}^{-2} \text{ hr}^{-1}$ ) to  $1.60 \text{ g-cal cm}^{-2} \text{ min}^{-1}$  ( $354 \text{ Btu ft}^{-2} \text{ hr}^{-1}$ ), or a decrease of air temperature of  $9.4^{\circ}\text{C}$  ( $17^{\circ}\text{F}$ ) with a simultaneous decrease of solar radiation from  $1.60 \text{ g-cal cm}^{-2} \text{ min}^{-1}$  ( $354 \text{ Btu ft}^{-2} \text{ hr}^{-1}$ ) to  $0.50 \text{ g-cal cm}^{-2} \text{ min}^{-1}$  ( $110 \text{ Btu ft}^{-2} \text{ hr}^{-1}$ ) may occur in a 1-hour period.

(2) A 24-hour temperature change may occur as follows: An increase of  $16.1^{\circ}\text{C}$  ( $29^{\circ}\text{F}$ ) in air temperature (wind speed under 5 m/sec) in an 8-hour period, followed by 2 hours of constant air temperature (wind speed under 5 m/sec), then a decrease of  $21.7^{\circ}\text{C}$  ( $39^{\circ}\text{F}$ ) in air temperature (wind speed between 7 and 10 m/sec) in a 14-hour period.

### 14.7.3 Surface (Skin) Temperature

The temperature of the surface of an object exposed to solar, day sky, or night sky radiation is usually different from the air temperature (Refs. 14.10 and 14.11). The amount of the extreme difference in temperature between the object and the surrounding air temperature is given in Table 14.5 and Figure 14.3, Part A, for exposure to a clear night (or day)<sup>7</sup> sky or to the Sun on a clear day. Since the flow of air across an object changes the balance between the heat transfers from radiation and convection-conduction between the air and the object, the difference in the temperature between the air and the object will decrease with increasing wind speed (Ref. 14.9). Part B of Figure 14.3 provides information for making the corrections for wind speed. Values are tabulated in Table 14.5 for various wind speeds.

### 14.7.4 Compartment Temperature

#### 14.7.4.1 Introduction

A cover of this material enclosing an air space will conduct heat to (or remove heat from) the inside air when the cover is heated by solar radiation (or cooled by the night sky). This results in the compartment air space being frequently considerably hotter or cooler than the surrounding air. The temperature reached in a compartment is dependent on the location of the air space with respect to the heated surface, the type

---

7. Without the sun's rays striking, the daytime sky is about as cold as the nighttime sky.

14.24

and thickness of the surface material, the type of construction, and the insulation; i.e., an addition of a layer of insulation on the inside surface of the compartment will greatly reduce the heating or cooling of the air in the compartment space (Refs. 14.12 and 14.13).

#### 14.7.4.2 Compartment Extreme High Temperature

A compartment probable extreme average high temperature of 87.8°C (190°F) for a period of 1 hour and an average high temperature of 65.6°C (150°F) for a period of 6 hours must be considered at all geographic locations while aircraft or other transportation equipment is stationary on the ground without air conditioning in the compartment. These extremes will be found at the top and center of the compartment.

#### 14.8 Data on Air Temperature Distribution with Altitude

Data on air temperature distribution with altitude are given in Section III.

## REFERENCES

- 14.1 Middleton, W. E. K.; and Spilhaus, A. F.: "Meteorological Instruments." University of Toronto Press, 3rd Edition, revised 1960.
- 14.2 "Solar Electromagnetic Radiation," NASA SP-8005, Rev. April 1971. National Aeronautics and Space Administration, Washington, D.C.
- 14.3 Moon, Parry: "Proposed Standard Solar Radiation Curves for Engineering Use." Journal of the Franklin Institute, vol. 230, Nov. 1940, pp. 583-617.
- 14.4 Thekaekara, Mathew P., Editor, "The Solar Constant and the Solar Spectrum Measured from a Research Aircraft." NASA TR R-351, National Aeronautics and Space Administration, Washington, D. C., Oct. 1970.
- 14.5 ASHRAE Handbook of Fundamentals. American Society of Heating, Refrigerating and Air Conditioning Engineers, New York, 1967.
- 14.6 Parmalee, G. V.: "Irradiation of Vertical and Horizontal Surfaces by Diffuse Solar Radiation from Cloudless Skies." Heating, Piping and Air Conditioning, vol. 26, Aug. 1954, pp. 129-136.
- 14.7 Becker, C. F.; and Boyd, J. S.: "Solar Radiation Availability on Surfaces in the United States as Affected by Season, Orientation, Latitude, Altitude, and Cloudiness." Journal of Solar Engineering, Science and Engineering, vol. 1, Jan. 1957, pp. 13-21.
- 14.8 Ornstein, M. P.: "Solar Radiation." Journal of Environmental Sciences, vol. 5, Apr. 1962, pp. 24-27.
- 14.9 "Tables of Computed Altitude and Azimuth," Publication H. O. No. 214, United States Hydrographic Office, United States Government Printing Office, 1940.
- 14.10 Fishenden, Margaret; and Saunders, Owen A.: "The Calculation of Heat Transmission." His Majesty's Stationary Office, London, 1932.
- 14.11 Daniels, Glenn E.: "Measurement of Gas Temperature and the Radiation Compensating Thermocouple." Journal of Applied Meteorology, vol. 7, 1968, pp. 1026-1035.
- 14.12 Porter, William L.: "Occurrence of High Temperatures in Standing Boxcars." Technical Report EP-27, Headquarters Quartermaster Research and Development Center, United States Army, Natick, Massachusetts, Feb. 1956.
- 14.13 Cavell, W. W.; and Box, R. H.: "Temperature Data on Standard and Experimental Cartridges in Pilot Ejection Devices in a B47E Aircraft Stationed at Yuma, Arizona." Memo Report No. M60-16-1, Frankford Arsenal, Pitman-Dunn Laboratories Group, Philadelphia, Pennsylvania, 1960.
- 14.14 Duffie, John A. and Beckman, William A.: "Solar Energy Thermal Processes," John Wiley & Sons, N. Y., 1974.



## SECTION XV. ATMOSPHERIC CHEMISTRY (Gaseous and Particulate)

### 15.1 Introduction

The chemistry of the atmosphere, both of its gases and its particles, must be taken into account in the development of aerospace vehicles for several reasons. Perhaps the most important is the deterioration of such vehicles and associated systems as the result of atmospheric constituents in flight or on the ground.

Although there is a very large variety of chemical elements and compounds in the Earth's atmosphere, the two most abundant gases (nitrogen and oxygen), carbon dioxide, water vapor, and ozone are the gases of primary concern because of their more direct influences on natural processes and their contribution to the needs of life in general. Various gases and constituents of the atmosphere selectively absorb solar radiation. The possible aspects of numerous types of airborne particles must also be considered. Such particles can cause abrasion and erosion and clog or otherwise interfere with essential parts of a space vehicle. Airborne particles affect visibility and the Earth's radiation balance and serve as condensation and freezing nuclei.

Much more knowledge is needed about the effects of variations in the composition of the atmosphere. The Space Shuttle design criteria commit the Space Shuttle program, as all NASA programs, to maintain the quality of the atmosphere.

### 15.2 Gaseous Composition

Nitrogen, oxygen, argon, and carbon dioxide make up more than 99.9 percent by volume of the atmosphere. The concentrations expressed as percentage by volume or by weight of the first three of these gases and of certain others (the "inert" gases) remain essentially constant except in the vicinity of local sources (power plants, active volcanoes, etc.) at least from ground level to 90 km altitude. The concentrations of these (Ref. 15.1) are shown in Table 15.1. Typical concentrations of other, variable, tropospheric trace constituents near the Earth's surface are shown in Table 15.2, based in part on Reference 15.1.

#### 15.2.1 Ozone ( $O_3$ )

Much of the ozone in unpolluted air in the troposphere is found in the stratosphere and brought to the Earth's surface by vertical transport processes. Additional ozone is produced in unpolluted air, and even more in polluted air, by photochemical processes. The concentrations of ozone in polluted air, especially in urban smog, are often an order of magnitude greater than in the "natural" atmosphere. The concentration range in the relatively unpolluted air of rural areas is about 0 to 80 parts per billion by volume (ppbv), zero concentration really meaning undetectable by presently existing methods. The ozone concentration in smog is occasionally as high as 1000 ppbv.

Ozone concentrations (mixing ratios) in the stratosphere increase with increasing altitude from the tropopause to about 30 km and then decrease. The maximum concentration is about 7 to 10 parts per million by volume (ppmv) (Ref. 15.1).

TABLE 15.1 NORMAL ATMOSPHERIC COMPOSITION FOR CLEAN, DRY AIR AT ALL LOCATIONS (VALID TO 90 km GEOMETRIC ALTITUDE)

Gas	Percent by Volume	Percent by Weight*
Nitrogen (N <sub>2</sub> )	78.084	75.520
Oxygen (O <sub>2</sub> )	20.9476	23.142
Argon (Ar)	0.934	1.288
Carbon dioxide (CO <sub>2</sub> )	0.0314	0.048
Neon (Ne)	$1.818 \times 10^{-3}$	$1.27 \times 10^{-3}$
Helium (He)	$5.24 \times 10^{-4}$	$7.24 \times 10^{-5}$
Krypton (Kr)	$1.14 \times 10^{-4}$	$3.30 \times 10^{-4}$
Xenon (Xe)	$8.7 \times 10^{-6}$	$3.9 \times 10^{-5}$

\*On basis of Carbon 12 isotope scale for which C<sup>12</sup> = 12,000, as adopted by the International Union of Pure and Applied Chemistry, Montreal, 1961.

TABLE 15.2 CONCENTRATIONS OF VARIOUS TROPOSPHERIC TRACE CONSTITUENTS ON THE EARTH'S SURFACE

Constituent	Typical Concentration, parts per billion by volume (ppbv)
N <sub>2</sub> O	270
NO	0.5
NO <sub>2</sub>	0.5
H <sub>2</sub> S	0.05
NH <sub>3</sub>	4
H <sub>2</sub>	500
CH <sub>4</sub>	1500
SO <sub>2</sub>	1.2
CO	190
CO <sub>2</sub>	$330 \times 10^5$
O <sub>3</sub>	40
HNO <sub>3</sub> (vapor)	0.1
COS	1
CS <sub>2</sub>	0.2



### 15.2.2 Nitrous Oxide ( $\text{N}_2\text{O}$ )

The concentrations of nitrous oxide in the troposphere are nearly constant at about 310 ppbv (Refs. 15.2, 15.3). Unpublished results by Cadle and Heidt obtained in 1980 varied from 312 to 318 ppbv. At altitudes of 13 to 18 km the concentration decreases from 250 to about 100 ppbv.

### 15.2.3 Nitric Oxide (NO) and Nitrogen Dioxide ( $\text{NO}_2$ )

A large amount of data exist concerning nitric oxide and nitrogen dioxide in smog, but very little data exist for the concentrations of these compounds in the unpolluted troposphere. The reported concentrations of nitric oxide vary from 0 to about 6 ppbv and of nitrogen dioxide from about 0 to 4 ppbv. Lodge et al. (Ref. 15.4) have reported concentrations ranging from 0.1 to 0.7 ppbv for NO and from 0.2 to 0.7 ppbv for  $\text{NO}_2$  in the American tropics. A background concentration of 0.5 ppbv for both NO and  $\text{NO}_2$  is suggested. In the stratosphere, measured concentrations of NO have ranged from about 0.1 to 5 ppbv and of  $\text{NO}_2$  from 1 to 10 ppbv. Concentrations of NO and  $\text{NO}_2$  as high as 200 ppbv are often found in smog (Ref. 15.5).

### 15.2.4 Nitric Acid Vapor ( $\text{HNO}_3$ )

Almost no information is available concerning the concentrations of nitric acid vapor in the troposphere. The only available data suggest a value of about 0.1 ppbv (Ref. 15.1). However, this value is for extremely clean air (the upper tropical troposphere), and concentrations over much of the United States may be much higher. Concentrations as high as 5 ppbv have been measured in the stratosphere.

### 15.2.5 Hydrogen Sulfide ( $\text{H}_2\text{S}$ )

Natusch et al. (Ref. 15.6) obtained values for hydrogen sulfide concentrations in the lower troposphere of about 0.05 ppbv. Hitchcock (Ref. 15.7) has suggested that  $\text{H}_2\text{S}$  concentrations in excess of 0.5 ppbv frequently occur near tidal flats, marshes, fresh water swamps, irrigated farmland, lakes, and rivers. This concentration is the approximate odor detection threshold.

### 15.2.6 Carbonyl Sulfide (COS) and Carbon Disulfide ( $\text{CS}_2$ )

Little is known about the concentrations of these two substances in the atmosphere. Probably the best value for tropospheric carbonyl sulfide is that of Torres et al. (Ref. 15.8), namely, a mean concentration of 0.988 ppbv and a standard deviation of 0.031 ppbv. The only published measurements of carbon disulfide concentrations in the "clean" troposphere are by Sandalls and Penkett (Ref. 15.9), who obtained a mean value at Harwell, England, of 0.190 ppbv.

### 15.2.7 Ammonia ( $\text{NH}_3$ )

A few measurements have been made of ammonia in the troposphere and indicate a mean value of about 4 ppbv (Ref. 15.1). Lodge et al. (Ref. 15.4) found higher values in the American humid tropics, varying from about 5 to 30 ppbv.

## 15.4

### 15.2.8 Hydrogen ( $H_2$ )

The concentrations of hydrogen in the atmosphere are better known than those of most trace constituents. Furthermore, the concentrations vary only slightly in the clean troposphere and apparently average about 500 ppbv. Hydrogen concentrations increase slowly with increasing altitude above the tropopause (Ref. 15.1).

### 15.2.9 Methane ( $CH_4$ )

Methane concentrations have often been measured in the troposphere and occasionally in the stratosphere. For example, measurements by Ehhalt (Ref. 15.10) at Scottsbluff, Nebraska, yielded a minimum concentration of 600 ppbv and a maximum concentration of 1600 ppbv. These appear to be about the extremes of the concentrations in the troposphere. The concentrations in the stratosphere slowly decrease with increasing altitude.

### 15.2.10 Sulfur Dioxide ( $SO_2$ )

The concentrations of sulfur dioxide in the troposphere have probably been measured more often than those of any other constituent. Measurements up to 1963 have been reviewed by Junge (Ref. 15.11), and more recent ones are given in Reference 15.1. Near the Earth's surface the concentration in clean air is probably about 1.2 ppbv. However, a major source of  $SO_2$  is the combustion of fossil fuels, and the air over most or all of the United States and other populated regions of the world is contaminated with  $SO_2$ . The actual concentrations depend on the proximity to sources and on the meteorological conditions. In the troposphere, concentrations of 1000 ppbv or more are not uncommon. The United States Environmental Protection Agency's standards for  $SO_2$  are a 20 ppbv annual arithmetic mean and a 100 ppbv maximum 24-hr concentration, not to be exceeded more than once per year (Ref. 15.12). Too few measurements have been made in the stratosphere to establish typical values there.

### 15.2.11 Carbon Monoxide ( $CO$ )

Carbon monoxide has both anthropogenic and natural sources. Mid-ocean concentrations are about 190 ppbv. Automobiles are a major source of  $CO$ . The United States primary ambient standards are a maximum 1-hr concentration of 35,000 ppbv and 8-hr concentrations of 9000 ppbv, not to be exceeded more than once a year (Ref. 15.13). A rapid decrease in carbon monoxide concentration with increasing altitude occurs in the stratosphere.

### 15.2.12 Carbon Dioxide ( $CO_2$ )

Carbon dioxide is produced by fossil fuel combustion, and its concentration in the ambient atmosphere is slowly increasing. Superimposed on this gradual, steady increase is an annual cycle of several ppmv. The mean concentration in 1970 was about 322 ppmv (Ref. 15.14). During the period 1959-1963 the general increase was linear and about 0.7 ppmv per year. Extrapolating to 1981 yields about 330 ppmv. On an annual mean basis carbon dioxide appears to be well mixed in the troposphere. The mixing ratio in the stratosphere has been estimated to be 0.6 ppmv less than the troposphere (Ref. 15.14).

15.2.13 Water (H<sub>2</sub>O)

Water vapor is discussed in detail in Section VI of this document.

15.3 Physical and Chemical Properties of Atmospheric Gases

Physical properties of some of the gases listed in Tables 15.1 and 15.2 are shown in Table 15.3. The values shown in Table 15.3 are from Ref. 15.1 and 15.15. Physical constants of the other gases are readily available in Ref. 15.16.

TABLE 15.3 PHYSICAL PROPERTIES OF SOME ATMOSPHERIC GASES

Constituent	Symbol	Molecular or Atomic Weight	Molecular or Atomic Mass (g)	Melting Point (°C)	Boiling Point (°C)	Density (g/l, 0°C) (760 Torr)	C <sub>p</sub> (15.0°C) (cal/g)
Nitrogen	N <sub>2</sub>	28.016	46.50880 × 10 <sup>-24</sup>	-209.8	-195.8	1.2506	0.2477
Oxygen	O <sub>2</sub>	32.000	53.12256 × 10 <sup>-24</sup>	-218.4	-182.96	1.429	0.2178
Nitrogen (atomic)	N	14.008	23.25440 × 10 <sup>-24</sup>	---	---	---	---
Oxygen (atomic)	O	16.000	26.56128 × 10 <sup>-24</sup>	---	---	---	---
Argon	A	39.944	66.31024 × 10 <sup>-24</sup>	-189.2	-185.7	1.784	0.1253
Carbon Dioxide	CO <sub>2</sub>	44.011	73.06168 × 10 <sup>-24</sup>	- 56.6 5.2 atm***	- 7.85 subl****	1.977	0.1989
Neon	Ne	20.183	33.50539 × 10 <sup>-24</sup>	-248.67	-245.9	0.9002	0.247
Krypton	Kr	83.800	139.11470 × 10 <sup>-24</sup>	-156.6	-152.9	3.708	0.0603*
Xenon	Xe	131.3	217.9685 × 10 <sup>-24</sup>	-112	-107.1	5.851	0.0384*
Helium	He	4.003	6.64530 × 10 <sup>-24</sup>	-272.2 26 atm***	-268.9	0.1785	1.24**
Hydrogen (atomic)	H	1.008	1.673361 × 10 <sup>-24</sup>	-259.14	-252.8	0.0899	3.389
Nitrous Oxide	N <sub>2</sub> O	44.016	73.07008 × 10 <sup>-24</sup>	-102.4	- 89.49	1.977	0.2004
Ozone	O <sub>3</sub>	48.000	79.68384 × 10 <sup>-24</sup>	-192.5	-111.9	2.144	0.1959

\*At 19°C

\*\*At -180°C

\*\*\*Must be pressurized to solidify.

\*\*\*\*Goes from solid to gaseous phase by sublimation process.

15.3.1 Nitrogen (N<sub>2</sub>)

Nitrogen is chemically inert and will have little chemical effect on space vehicles. It is converted to nitrous oxide (N<sub>2</sub>O) by bacterial action in soil (see nitrous oxide, Section 15.3.4).

## 15.6

### 15.3.2 Oxygen ( $O_2$ )

Oxygen is the most abundant oxidant (oxidizing agent) in the Earth's atmosphere. An oxidant can be defined as any substance which chemically donates one or more atoms of oxygen to another element or compound. A general definition of oxidation is that it is a chemical reaction in which either cations or anions lose electrons. Thus, an oxidizing agent is a substance that contains ions or atoms capable of taking up additional electrons. Similarly, a reducing agent can be defined as a substance capable of chemically removing oxygen from another substance or, more generally, capable of donating electrons to another substance. Almost by definition, the main chemical behavior of oxygen is as an oxidant. Of course, it supports combustion, but otherwise the oxidation by oxygen is quite slow, although it may be increased greatly by catalysts such as certain metals.

### 15.3.3 Argon (A), Neon (Ne), Krypton (Kr), Xenon (Xe), and Helium (He)

These so-called inert gases, which under very special conditions can combine with other elements to form compounds, are completely chemically inert in the atmosphere.

### 15.3.4 Nitrous Oxide ( $N_2O$ )

Nitrous oxide (laughing gas) readily decomposes into free oxygen and **nitrogen** and is, thus, a strong oxidizing agent. In relatively pure form it can support combustion. It reacts with **the first** electronically excited state of atomic oxygen ( $O^1D$ ) to form nitric oxide, an important reaction in **the stratosphere**.

### 15.3.5 Nitric Oxide (NO)

Nitric oxide does not decompose as readily as nitrous oxide, but in air it reacts very slowly with  $O_2$  and very rapidly with ozone, in each case to form nitrogen dioxide. It is an important ingredient of automobile exhaust gases and is a precursor of photochemical smog.

### 15.3.6 Nitrogen Dioxide ( $NO_2$ )

Nitrogen dioxide is a reddish-brown gas which contributes to the color of photochemical smog. It readily gives up half of its oxygen, being converted into nitric oxide, and is thus a strong oxidizing agent. It dissolves in water to form nitric acid ( $HNO_3$ ) and nitrous acid ( $HNO_2$ ) and thus contributes to the formation of the corrosive "acid rain."

### 15.3.7 Nitric Acid Vapor ( $HNO_3$ )

Nitric acid behaves chemically both as an acid and as a strong oxidizing agent. It is a major constituent of the acids in acid rain and acts upon most metals with the exception of gold, platinum, and a few of the rare metals. When nitric acid acts as an oxidizing agent, it usually decomposes, liberating nitric oxide and water.

### 15.3.8 Ammonia ( $\text{NH}_3$ )

Ammonia is very soluble in water, forming ammonium hydroxide ( $\text{NH}_4\text{OH}$ ). Ammonia and ammonium hydroxide are bases and react with acids such as nitric and sulfuric acid in the atmosphere, to form the corresponding salts. A number of metals, especially magnesium and lithium, react with ammonia at high temperatures, forming nitrides and liberating hydrogen. Ammonia also combines directly with a number of salts to form complex compounds.

### 15.3.9 Ozone ( $\text{O}_3$ )

Ozone is similar to molecular oxygen ( $\text{O}_2$ ) in its chemical behavior but is much more reactive. At a concentration of 1 ppmv, much lower than that in much of the stratosphere, humans begin to experience unpleasant symptoms when the air is pressurized to about 760 Torr (Ref. 15.17).

### 15.3.10 Hydrogen ( $\text{H}_2$ )

At ordinary temperatures hydrogen is inert, but at high temperatures it combines with metals to form hydrides, with nitrogen to form ammonia, with chlorine to form hydrogen chloride ( $\text{HCl}$ ), and with sulfur to form hydrogen sulfide ( $\text{H}_2\text{S}$ ). At relatively high concentrations hydrogen burns to form water. Hydrogen is a reducing agent, and at high temperatures will reduce metal oxides to the metal. However, in the atmosphere with its large excess of  $\text{O}_2$ , oxidation rather than reduction will predominate.

### 15.3.11 Hydrogen Sulfide ( $\text{H}_2\text{S}$ )

Hydrogen sulfide is an extremely poisonous gas, but not at the concentrations usually occurring in the atmosphere. Dissolved in water, it is slightly acidic. When heated to a moderately high temperature, it is decomposed into sulfur and hydrogen. It is a strong reducing agent. It reacts with a number of metals, especially at high temperatures, to form sulfides.

### 15.3.12 Carbon Disulfide ( $\text{CS}_2$ ) and Carbonyl Sulfide ( $\text{COS}$ )

The chemistry of these two gases has been reviewed by Peyton et al. (Ref. 15.18). Pure carbon disulfide at room temperature is a colorless volatile liquid of moderate solubility in water. It is a mild reducing agent and reacts with ozone to form  $\text{O}_2$ ,  $\text{SO}_2$ ,  $\text{COS}$ ,  $\text{CO}$ , and  $\text{CO}_2$ . Reactions of  $\text{CS}_2$  with atomic oxygen and with the free hydroxyl radical ( $\text{OH}$ ) are probably the main mechanisms of removal of both  $\text{CS}_2$  and  $\text{COS}$  in the troposphere and lower stratosphere. Carbonyl sulfide, like carbon disulfide, is photochemically decomposed in the stratosphere, the end product of a series of reactions being droplets of sulfuric acid. Carbonyl sulfide may be the principal source of sulfuric acid in the stratosphere after several years during which there has been little highly explosive volcanic activity. Both  $\text{CS}_2$  and  $\text{COS}$  are mild reducing agents.

### 15.3.13 Sulfur Dioxide ( $\text{SO}_2$ )

Sulfur dioxide is the well-known gas produced by the burning of sulfur, and it is the principal sulfur compound produced by the burning of fossil fuels. Depending upon conditions, sulfur dioxide can act as an oxidizing or a reducing agent, but in the atmosphere it is usually a reducing agent. In the air it reacts very

slowly, if at all, with ozone and  $O_2$  but reacts with atomic oxygen and with hydroxyl radicals to form sulfur trioxide ( $SO_3$ ), also in the gas phase. Sulfur trioxide is often mentioned as being an important atmospheric gas. Actually, it reacts with water vapor in the atmosphere so rapidly that its concentration is extremely small. The initial product of the reaction may be an addition product ( $SO_3 \cdot H_2O$ ), but the final product is sulfuric acid ( $H_2SO_4$ ) in droplet form.

Sulfur dioxide is very soluble in water, and in solution part of it combines with water to form sulfurous acid ( $H_2SO_3$ ). Thus, atmospheric  $SO_2$  dissolves in clouds, fog, and rain drops and is oxidized by dissolved  $O_2$  to form sulfuric acid, an important and probably the greatest contributor to the acidity of "acid rain." The extent of this oxidation is greatly increased by ammonium hydroxide present in the water (see Section 15.3.8). Furthermore, dissolved ozone rapidly oxidizes dissolved  $SO_2$  to  $H_2SO_4$ .

#### 15.3.14 Carbon Monoxide ( $CO$ )

Carbon monoxide is a colorless, odorless gas which is almost insoluble in water. Until recently it was believed to be almost inert in the troposphere, but it is now believed to be slowly oxidized in carbon dioxide ( $CO_2$ ) by a catalytic series of reactions involving hydroxyl radicals and nitric oxide. At high temperatures it is a strong reducing agent but, except for the preceding gas-phase reaction, as in the case of hydrogen, its reducing action in air is far outweighed by the oxidizing action of  $O_3$ .

#### 15.3.15 Carbon Dioxide ( $CO_2$ )

Carbon dioxide is a very stable substance, but like  $SO_2$  it is an acid anhydride and in aqueous solution reacts with water to form the weak acid carbonic acid ( $H_2CO_3$ ). Furthermore, it is a very weak oxidizing agent; and, if passed over carbon at temperatures above  $1000^\circ C$ , it is partially reduced to carbon monoxide.

#### 15.3.16 Methane ( $CH_4$ )

Methane is a colorless, odorless gas that is only slightly soluble in water. The chemistry of methane in the troposphere has been reviewed by Ehhalt (Ref. 15.19). It reacts slowly with atomic oxygen and with hydroxyl radicals to form carbon monoxide, hydrogen, and carbon dioxide. Otherwise it is very stable.

### 15.4 The Corrosive Effects of Gases

Several natural atmospheric gases play an important role in corroding materials. Oxidizing gases such as  $O_2$  and  $O_3$ , and various acids, described in Section 15.3, are the greatest offenders. However, with the ever-increasing amounts of pollutants on a regional and even global scale, the problem is becoming very harsh. Under certain atmospheric conditions, such as high humidity, intense radiation, high temperature, and intermittent condensation, the life expectancy of materials such as paint and plastics has been drastically reduced.

The corroding agent may be a single gas, but several agents may act simultaneously. Also, many types of corrosion can be the ultimate result of two or more successive corrosive processes; for example, rusting following the removal of a protective surface.

References 15.20 through 15.23 are useful detailed discussions of corrosion in general. Methods of corrosion testing are described and discussed in References 15.24 through 15.27.

#### 15.4.1 Rusting

Perhaps the best known type of corrosion resulting from oxidation is rusting, which notably attacks iron. The oxidizing agent is  $O_2$ , but rusting only occurs when the surface is moist, and apparently also involves atmospheric carbon dioxide. Iron rust is believed to consist of a mixture of iron oxide, hydroxide, and carbonate.

#### 15.4.2 Oxidation of Rubber and Synthetic Plastics

Rubber and many synthetic plastics become brittle, crack, or both when exposed to oxidizing agents such as  $O_3$ ,  $O_2$ , or  $NO_2$ . Rubber under tension may be especially rapidly attacked by  $O_3$ , forming characteristic cracks. In fact, a large number of organic compounds are subject to such oxidation. The rate of deterioration of plastics by oxidation depends on a number of factors, including the composition of the polymer, and the extent of the exposure to the oxidizing agent, heat, and light. Such degradation may be greatly retarded in most plastics by incorporating antioxidants. Often mixtures of antioxidants are used because they show a synergistic effect. An excellent discussion of the process of polymer oxidation, the polymers most susceptible to oxidation and antioxidants is given in Reference 15.28. Reference 15.29 describes the results of extensive research on atmospheric oxidants and antioxidants.

Antioxidants are also used in foods, especially in fats, since fats become rancid as a result of oxidation by atmospheric  $O_2$ , rather than bacterial action.

"Room temperature" oxidation of organic compounds is accelerated by sunlight and by the presence of certain metals, such as copper or its salts.

#### 15.4.3 "Weathering" of Paints

Paints and similar coatings are complex mixtures, and the mechanisms of their deterioration are also complex. The oxidation of organic components is responsible for much of the weathering. The affected properties of greatest concern are hardness, elongation, and adhesion. Critical deterioration factors include the intensity of solar radiation, the nature of temperature changes, and the quantity and periodicity of snow, rain, or dew. For a survey of paints and paint deterioration see Reference 15.30. It is ironic that the continuation of the oxidation by atmospheric  $O_2$  which is required to "dry" drying oils in paints can eventually destroy them.

#### 15.4.4 Corrosion by Sulfur Dioxide and Hydrogen Sulfide

Other than  $O_2$  and possibly  $O_3$ , probably no other gaseous compound in the atmosphere produces more corrosion than sulfur dioxide. Of course, as mentioned previously, water vapor promotes corrosion but is not itself corrosive. Sulfur dioxide corrodes many metals, especially at high relative humidities, and sulfates are formed. Possibly sulfuric acid is first formed and then attacks the metal. The corrosion products appear to be involved in the process. Copper exposed to polluted air forms a green coating called a patina which is, namely,  $CuSO_4 \cdot 3Cu(OH)_2$ . It is produced by sulfuric acid droplets and probably also by sulfur dioxide.

## 15.10

Hydrogen sulfide tarnishes silver and copper. Also, when present in the atmosphere at relatively high concentrations, it can cause "hydrogen cracking" in some stressed metals.

### 15.4.5 Nitric Acid Vapor and Hydrogen Chloride

Both of these gases are acids and react with various metals. In relatively clean air their concentrations are too low to do appreciable damage. But when dissolved in precipitation, they contribute to "acid rain" and then may be corrosive.

## 15.5 Particles

Airborne particles (liquids and solids) can cause problems for space vehicles in a number of ways. Direct impact of such particles on surfaces may abrade the surfaces. When dissolved in water, they may cause corrosion and may clog various mechanisms or produce electrical shorts.

When the particles are sufficiently small that they settle from the air very slowly, the particles together with the air in which they are suspended are termed aerosols. Sometimes the fine suspended particles themselves are called aerosols, but this use of the term should be avoided because it leads to confusion. Very fine particles can travel long distances. For example, approximately ten million tons of red dust from northwest Africa was deposited on England in 1903.

### 15.5.1 Sources of Particles

The mechanisms of formation of airborne particles can be divided into five groups (Ref. 15.31). The first is the condensation of vapor, including the formation of smoke. The second, chemical reactions involving trace gases in the atmosphere, might be considered to be an example of the first. The third is the mechanical breakup and dispersal of matter at the Earth's surface, including the production of sea-salt over the oceans and of various dusts, largely mineral, over land. The fourth is the coagulation of fine particles to form larger ones, and the fifth is the influx of extraterrestrial particles. Various combinations of these mechanisms occur. For example, the chemical reactions of the second category may occur between trace gases and particles formed by other means; similarly, complex particles are often formed by condensation (category 1) on particles produced by mechanism 3.

From the standpoint of corrosion, one of the most important types of particles in the atmosphere is sea-salt, largely sodium chloride. These particles are carried great distances and are widespread over the oceans and the continents. Over the oceans the concentrations may be as large as  $100/\text{cm}^3$  but  $1/\text{cm}^3$  is more common. Most airborne sea-salt started as droplets which evaporated when the relative humidity fell below about 75 percent. Conversely, since the particles are deliquescent, at relative humidities much above 75 percent the sea-salt particles once more become droplets.

Most droplets of sea-salt are formed by the breaking of myriads of air bubbles at the surface of the sea. The bubbles are produced by the breaking of small waves and, to a lesser extent, by rain or snow falling on the water. Sea-salt droplets are also formed by breaking waves such as surf. Such droplets are too large to remain airborne for long, but they can be an important source of corrosion near ocean shores. The accumulation of salt on exposed surfaces near the ocean is greatest during on-shore winds when many waves are breaking and forming white caps. Expected extremes have been discussed by Brierly (Ref. 15.32).



Sodium chloride associated with continental aerosol particles is not necessarily of marine origin, and much of the chloride associated with such particles is produced by various industrial processes.

Air pollution is another important source of corrosive particles. Sulfuric acid, either as droplets or absorbed in other particles, is probably the most corrosive compound, but various salts and absorbed acidic gases, organic and inorganic, can also corrode. The sulfuric acid is in part liberated directly into the atmosphere, but a large percentage of it is formed by the oxidation and hydration of sulfur dioxide in air. The sulfur dioxide is mainly from the combustion of fossil fuels.

Air pollution can no longer be considered to be largely a local problem. It is certainly a regional one and with regard to some contaminants a global one. For example, the highly corrosive acid rain, which has already been mentioned in Sections 15.3.7 and 15.3.13, occurs throughout the United States and Europe. Its high acidity (low pH), from which its name is derived, is directly or indirectly the result of air pollution. As mentioned previously, the main acidic constituents are sulfuric and nitric acids.

The chemistry of air pollution, including the formation of particles in photochemical smog, is highly complex (Refs. 15.31, 15.33, 15.34, 15.35). Photochemical smog is that form of air pollution formed by the action of sunlight on gasoline fumes, and oxides of nitrogen in air. The particles formed constitute a large percentage of those in urban atmospheres and in the air for large distances downwind of cities.

The production of airborne sand and dust depends on a number of factors such as wind speed, the nature of the soil, and the amount and nature of the vegetation. The subject has been studied in great detail by Gillette and his co-workers (Refs. 15.36 through 15.40).

Threshold air velocities for the input of soil particles into the air increased with different types of soil surfaces in the following order: disturbed soils (except disturbed heavy clay soils), sand dunes, alluvial and aeolian sand deposits, disturbed playa (dry lake) soils, skirts of playa centers, and desert pavements (alluvial deposits) (Ref. 15.38). Gillette et al. also concluded that the fine airborne particles (2 to 20  $\mu\text{m}$  equivalent diameter) from sandy soils are mainly clay minerals which are derived from the exposed soils by sandblasting during wind erosion (Ref. 15.37).

Particles in the stratosphere may at times pose a threat to space vehicles (Refs. 15.41, 15.42). This is especially true during the weeks and months following major volcanic eruptions such as that of Gunung Agung in Bali in 1963, of Vulcán Fuego in 1974, and of Mt. St. Helens in the State of Washington in 1980. Fine volcanic ash, much of which is shattered glass (Ref. 15.43), and sulfuric acid droplets are the main particulate constituents. For days to a week or two following such eruptions, meteorological analysis of air trajectories can indicate regions of the stratosphere where the volcanic particles are apt to be encountered. Later, the ash and sulfuric acid will tend to form a layer a few kilometers thick located a few kilometers above the tropopause and spreading in a matter of months over much or all of the globe. Volcanic ash in the troposphere is also highly damaging to any rapidly moving vehicle moving through it, but it usually remains in the air only a few days unless it is re-entrained.

Grass, brush, and forest fires put tremendous quantities of particles into the atmosphere. However, they are probably not especially corrosive or abrasive. This source of particles is reviewed in Reference 15.31.

## 15.5.2 Physical Properties

The physical properties of particles, such as hardness and shape (especially if they have jagged edges as does much volcanic ash), and also particle size, which is discussed in Section 15.5.3, have a great influence

on the extent of abrasion they may produce. Degrees of hardness are often compared using the Mohs' scale; the hardness of a number of minerals is compared using this scale in Table 15.4. The minerals other than halite and kaolinite were used to establish this scale.

TABLE 15.4 MOHS' SCALE-OF-HARDNESS FOR MINERALS

Mohs' Relative Hardness	Mineral
1	Talc
2	Gypsum
2-2.5	Kaolinite
2.5	Halite
3	Calcite
4	Fluorite
5	Apatite
6	Orthoclase
7	Quartz
8	Topaz
9	Carborundum
10	Diamond

Halite is naturally occurring solid sodium chloride and is included in Table 15.4 to indicate the approximate hardness of sea-salt particles. They may be cubes, but are usually more irregular. Kaolinite is a common clay mineral and is included in Table 15.4 to give an approximate value for clay particles, which make up much of the fine particle fraction of the airborne particles blown up by winds from sandy soils (see Section 15.5.1). These clay particles may be platelets. Much larger and harder are the sand particles, which may be largely quartz and are usually rounded. Gypsum, also listed in Table 15.4, is at times raised by winds over arid areas. Volcanic ash consists of glass and various minerals such as orthoclase; its hardness is about 6-7. The particles are often jagged. Most smog particles are droplets or soft organic particles or salts, although some harder particles such as fly ash from power plants may be present. Tables of hardness of many substances are given in Reference 15.16.

### 15.5.3 Particle Size Distributions

The size distributions of particles in the troposphere smaller than 1 or 2  $\mu\text{m}$  radius when the air is relatively clean have been studied extensively (Ref. 15.1, 15.11, 15.31, 15.44). The number concentrations increase rapidly with decreasing particle size, often down to sizes of 0.1  $\mu\text{m}$  radius or smaller. The more recent work cited (Refs. 15.1, 15.44) shows that the concentrations and size distributions are highly variable. Furthermore, the size distributions vary with altitude, as demonstrated in the preceding two references. Little information is available concerning larger particles except where airborne particle concentrations are very high, as in dust and sand storms and smog. The particle size distributions in urban smog are bimodal or trimodal when  $\Delta V/\Delta(\log D)$  per  $\text{cm}^3$  of air is plotted against  $\log D$ , where  $V$  is the particle volume and  $D$  is the diameter. The greatest volume concentrations are more than 10  $\mu\text{m}$  diameter. The number concentrations increase with decreasing size when  $\Delta N$ , the increment of number concentration, is substituted for  $\Delta V$ .

When the particles are mainly derived from soil, the  $\Delta V/\Delta(\log D)$  per  $\text{cm}^3$  versus  $\log D$  plots are bimodal, and both modes shift toward larger particle sizes with increasing aerosol loading (Ref. 15.39). A typical upper size mode for heavy loading is at about  $100 \mu\text{m}$  diameter. Information on atmospheric dust over selected geographical areas is also provided in Reference 15.45.

The particle size distribution of volcanic ash will vary greatly with distance from the source and the time elapsed since the eruption, largely due to the fallout of large particles.

#### 15.5.4 Variation With Altitude

The variations in the nature of atmospheric aerosols with changing altitude have already been mentioned briefly, but a few additional comments are appropriate. Atmospheric temperature inversion over the oceans, such as the tropical inversion, tend to keep sea-salt particles below a few kilometers in altitude. Above such inversions the particles are largely of continental origin.

The larger, more abrasive particles in dust and sand storms are mostly in the lower kilometer or two of the atmosphere, although the fine dust can reach great heights and travel great distances.

Atmospheric pollutants are often more or less trapped beneath atmospheric temperature inversions. Incidents of severe smog usually are associated with such inversions.

#### 15.5.5 Corrosion and Abrasion by Particles

Salt (sodium chloride) particles, whether from the ocean or areas where salt is used to melt ice, are harmful to space vehicles and associated systems mainly because of their corrosive rather than their abrasive properties. Salt especially attacks metals, and the corrosion is especially rapid at such high relative humidities that the salt is in solution. The action is probably largely electrochemical. Salt solutions can also provide a conductive path, altering or shorting out electric circuits.

Sulfuric acid can act in much the same way as salt particles but, in addition, can attack metals due to its acidity. In fact, any particles in the atmosphere containing electrolytes (acids and salts) can corrode many metals.

When an aerosol flows around an object, the aerosol particles will tend to flow around the object with the air. However, if the momentum of the particles is sufficiently great, they will deviate from the flow path of the air sufficiently to impact on the surface. Whether or not impacting occurs on the surface of an object depends on the particle shape, size, and density; the relative speed of the aerosol and object; and the size and shape of the object. Impaction theory is reviewed in Reference 15.46. The greater the size and density of the particles and the greater the relative aerosol velocity, the greater is the likelihood of impaction. Some particles will also collide with the surface merely by interception. Particles impacting on objects will abrade their surface, the extent of the abrasion depending on the hardness of the particles; their size, shape and density; the collision speed; and the nature of the object surface.

Airborne particles can cause a variety of damage in addition to that already mentioned, such as clogging of filters and orifices, fouling of moving parts, and making relays inoperative.

15.14

## 15.6 Snow, Hail, and Rain

Snow, hail, and even rain can cause abrasion. Also, they can cause corrosion if they contain appreciable amounts of salts (such as sea-salt) or acids, and acid precipitation is becoming ubiquitous. Snow and hail particles have a Mohs' scale hardness of about 2 at 0°C, increasing to 6 at -80°C (Ref. 15.47 and Table 15.5).

Although the flight time of a vehicle through a cloud layer may be extremely short, if the cloud layer contains a large concentration of moderate-sized hailstones (25 mm or larger) at temperatures below -20°C, considerable damage may be expected (especially to antennas and other protrusions) because of the kinetic energy of the hailstones at impact. Tests have shown a definite relationship between the damage to aluminum aircraft wing sections and the velocity of various-sized hailstones. Equal dents (sufficient to require repair) of 1 mm in 75 S-T aluminum resulted from the following impacts (Ref. 15.48):

- a. A 19-mm ice sphere at 190 m sec<sup>-1</sup> (369 knots).
- b. A 32-mm ice sphere at 130 m sec<sup>-1</sup> (253 knots).
- c. A 48-mm ice sphere at 90 m sec<sup>-1</sup> (175 knots).

Tests conducted by the British Ministry of Aviation (Ref. 15.49) have shown that paint coatings, structural plastic components, and even metallic parts of high-speed aircraft can be eroded by the impingement of raindrops. A table of rates of erosion of various materials and coatings was developed for speeds of 220 m sec<sup>-1</sup> (428 knots).

TABLE 15.5 HARDNESS OF HAIL AND SNOW

Temperature		Relative Hardness (Mohs' Scale)
(°C)	(°F)	
0	32.2	2
-20	- 4.0	3
-40	- 40.0	4
-60	- 76.0	5
-80	-112.0	6

## REFERENCES

- 15.1 "U.S. Standard Atmosphere, 1976." United States Government Printing Office No. 003-017-00323-0, Washington, D.C., October 1976.
- 15.2 Hahn, J.: "Improved Gas Chromatographic Method for Field Measurement of Nitrous Oxide in Air and Water Using a 5Å Molecular Sieve Trap." *Analytical Chemistry*, Vol. 44, 1972, pp. 1880-1892.
- 15.3 Schutz, K., Junge, C., Beck, R., and Albrecht, B.: "Studies of Atmospheric N<sub>2</sub>O." *Journal of Geophysical Research*, Vol. 75, 1970, pp. 2230-2246.
- 15.4 Lodge, J.P., Jr., Machado, P., Pate, J.B., Skeesly, D.C., and Wartburg, A.F.: "Atmospheric Trace Chemistry in the American Humid Tropics." *Tellus*, Vol. 26, 1974, pp. 250-253.
- 15.5 Butcher, S.S., and Charlson, R.J.: *An Introduction to Air Chemistry*. Academic Press, New York, 1972.
- 15.6 Natusch, D.F.S., Klonis, H.B., Axelrod, H.B., Tech, R.J., and Lodge, J.P., Jr.: "Sensitive Method for Measurement of Atmospheric Sulfur Dioxide." *Analytical Chemistry*, Vol. 44, 1972, pp. 2857-2910.
- 15.7 Hitchcock, D.: "Atmospheric Sulfates from Biological Sources," *Air Pollution Control Association Journal*, Vol. 26, 1976, pp. 210-215.
- 15.8 Torres, A.L., Maroulis, P.J., Goldberg, A.B., and Bandy, A.R.: "Measurements of Tropospheric OCS on the 1978 Gametag Flights." *EOS, Transactions of the American Geophysical Union*, Vol. 59, 1978, p. 1082.
- 15.9 Sandalls, F.J., and Penkett, S.A.: "Measurements of Carbonyl Sulfide and Carbon Disulfide in the Atmosphere." *Atmospheric Environment*, Vol. 11, 1977, pp. 197-199.
- 15.10 Ehhalt, D.H.: "Methane in the Atmosphere." *Journal of the Air Pollution Control Association*, Vol. 17, 1967, pp. 518-519.
- 15.11 Junge, C.E.: *Air Chemistry and Radioactivity*. Academic Press, New York, 1963.
- 15.12 United States Environmental Protection Agency: *Federal Register*, Vol. 36, No. 158, 1971, p. 15492.
- 15.13 United States Environmental Protection Agency: *Federal Register*, Vol. 36, No. 84, 1971, pp. 8186-8201.
- 15.14 Bolin, B., and Bischof, W.: "Variations in the Carbon Dioxide Content of the Atmosphere in the Northern Hemisphere." *Tellus*, Vol. 22, 1970, pp. 431-442.
- 15.15 *Handbook of Geophysics and Space Environments*. United States Air Force, Air Force Cambridge Research Laboratories, 1965.
- 15.16 *Handbook of Chemistry and Physics*. 4th Edition, The Chemical Rubber Co., Cleveland, Ohio, 1966. Also, later editions.

15.16

- 15.17 Liptak, B.A., Editor: Environmental Engineers' Handbook. Vol. 2, Air Pollution, Chilton Book Co., Radnor, Pennsylvania, 1974, p. 1069.
- 15.18 Peyton, T.O., Steck, R.V., and Mabey, W.R., : Carbon Disulfide, Carbonyl Sulfide. Literature Reviews and Environmental Assessment. National Technical Information Service, Springfield, Virginia, 1976.
- 15.19 Ehhalt, D.H.: "Methane in the Atmosphere." Carbon and the Biosphere, Woodwell, G.M. and Pecan, E.V., Ed. National Technical Information Services, No. CONF 720510, Springfield, Virginia, 1973, pp. 144-158.
- 15.20 Fontano, M.G.: Corrosion, A Compilation. Press of Hollenback, Columbus, Ohio, 1957, 200 pp.
- 15.21 Evans, U.S.: The Corrosion and Oxidation of Metals: Scientific Principles and Practical Applications. E. Arnold, London, 1967, 1094 pp.
- 15.22 Uhlig, H.H.: Corrosion and Corrosion Control. 2nd Ed., Wiley, New York, N.Y., 1971, 410 pp.
- 15.23 Corrosion in Natural Environments. American Society for Testing and Materials, Philadelphia, 1974, 347 pp.
- 15.24 Military Standards, Environmental Test Methods, MIL-STD-810C, March 10, 1975.
- 15.25 May, J.P., and Taylor, V.G.: "Corrosion Testing in Marine Atmospheres." Journal of the Atmospheric Sciences, Vol. 7, 1964, pp. 23-27.
- 15.26 Doyle, D.P., and Goddard, H.P.: "A Rapid Method for Determining the Corrosivity of the Atmosphere at Any Location." Nature, Vol. 200, 1963, pp. 1167-1168.
- 15.27 Airbor, W.H., Ed.: Handbook on Corrosion Testing and Evaluation, Wiley, New York, N.Y., 1971.
- 15.28 Simonds, H.R., and Church, J.M., Eds: The Encyclopedia of Basic Materials for Plastics. Reinhold, New York, N.Y., 1967, pp. 71-77.
- 15.29 Scott, G.: Atmospheric Oxidation and Antioxidation. Elsevier, New York, N.Y., 1965.
- 15.30 Clark, G.L., and Gessner, G.H. Eds.: The Encyclopedia of Chemistry, 2nd Ed. Reinhold, New York, N.Y. 1966, pp. 765-768.
- 15.31 Cadle, R.D.: Particles in the Atmosphere and Space. Reinhold, New York, N.Y., 1966, p. 226.
- 15.32 Brierly, W.B.: "Atmosphere Sea-Salts Design Criteria Areas." Journal of Environmental Science, Vol. 8, 1965, pp. 15-23.
- 15.33 Rasool, S.J.: Chemistry of the Lower Atmosphere. Plenum Press, New York, N.Y., 1973, p. 335.
- 15.34 Heicklen, J.: Atmospheric Chemistry. Academic Press, New York, N.Y., 1976.
- 15.35 Hidy, G.M., Mueller, P.K., Grosjean, D., Appel, B.R., and Wesolowski, J.J.: The Character and Origin of Smog Aerosols. Wiley-Interscience, New York, N.Y., 1980, p. 776.

- 15.36 Gillette, D. A., Clayton, R. N., Mayeda, T. K., Jackson, M. L., and Sridhag, K.: "Tropospheric Aerosols from Some Major Dust Storms of the Southwestern United States." *Journal of Applied Meteorology*, Vol. 17, 1978, pp. 832-845.
- 15.37 Gillette, D. A., and Walker, T. R.: "Characteristics of Airborne Particles Produced by Wind Erosion of Sandy Soil, High Plains of West Texas." *Soil Science*, Vol. 123, 1977, pp. 97-110.
- 15.38 Gillette, D. A., Adams, J., Endo, A., and Smith, D.: "Threshold Velocities for Input of Soil Particles Into the Air of Desert Soils." *Journal of Geophysical Research*, Vol. 85, 1980, pp. 5621-5630.
- 15.39 Patterson, E. M. and Gillette, D. A.: "Commonalities in Measured Size Distributions for Aerosols Having a Soil-Derived Component." *Journal of Geophysical Research*, Vol. 82, 1977, pp. 2074-2082.
- 15.40 Gillette, D. A.: "Fine Particulate Emissions Due to Wind Erosion." *Transactions of the American Society of Agricultural Engineers*, Vol. 20, 1977, pp. 890-897.
- 15.41 Cadle, R. D. and Grams, G. W.: "Stratospheric Particles and Their Optical Properties." *Reviews of Geophysics and Space Physics*, Vol. 13, 1975, pp. 475-501.
- 15.42 Cadle, R. D., Kiang, C. S., and Louis, J. F.: "The Global Scale Dispersion of the Eruption Clouds from Major Volcanic Eruptions." *Journal of Geophysical Research*, Vol. 81, 1976, pp. 3125-3132.
- 15.43 Heiken, G.: "Morphology and Petrography of Volcanic Ashes." *Geological Society of America Bulletin*, Vol. 83, 1972, pp. 1961-1988.
- 15.44 Blifford, I. H., and Ringer, L. D.: "The Size and Number Distribution of Aerosols in the Continental Atmosphere." *Journal of Atmospheric Sciences*, Vol. 26, 1969, pp. 716-726.
- 15.45 Hinds, D. B., and Hoidale, G. B.: *Boundary Layer Occurrence IV - Atmospheric Dust Over Selected Geographical Areas*. ECOM-DR-77-3 (OSD 1366), Atmospheric Sciences Laboratory, U. S. Army Electronics Command, White Sands Missile Range, New Mexico, 1977.
- 15.46 Cadle, R. D.: *The Measurement of Airborne Particles*. Wiley-Interscience, New York, N.Y., 1975, pp. 342.
- 15.47 Blackwelder, E.: "The Hardness of Ice." *American Journal of Science*, Vol. 238, 1940, pp. 61-63.
- 15.48 Sonter, R. K., and Emerson, J. B.: *Summary of Available Hail Literature and the Effect of Hail on Aircraft in Flight*. NASA TND-2734, Langley Aeronautical Laboratory, Langley Field, Virginia, 1952.
- 15.49 Zyll, A. A., King, R. B., and Strain, R. N.: "Rain Erosion Aspects of Aircraft and Guided Missiles." *Journal of the Royal Aeronautical Society*, Vol. 66, 1962, pp. 447-453.





## SECTION XVI. GEOLOGIC HAZARDS

### 16.1 Introduction

The American Geological Institute (AGI) Glossary of Geology defines a geologic hazard as "a naturally occurring or man-made geologic condition or phenomenon that presents a risk or is a potential danger to life and property." An understanding of geologic processes is essential if man is to anticipate and solve problems which arise from geologic hazards existing in areas which he intends to develop and occupy. In this chapter these hazards are discussed as they pertain to potential Shuttle sites at Vandenberg and Edwards Air Force Bases, California; and Cape Canaveral, Florida. A section on seismic environment, prepared for Space Shuttle GSE (Ground Support Equipment) design, has also been included. A bibliography is given at the end of the chapter, in addition to the references cited.

### 16.2 Specific Hazards

Geologic hazards include: earthquakes, tsunamis and seiches, slope processes, floods, volcanic activity, expanding ground, and ground subsidence.

#### 16.2.1 Earthquakes

Earthquakes are due to sudden releases of tectonic stresses which result in relative movement of rocks on opposite sides of a fault plane, as well as shaking of ground in areas near (and sometimes far from) the actual fault movement. Ground movement and shaking can trigger numerous other disasters, including landslides; liquefaction and sliding of unconsolidated sediments; destruction of buildings, dams, and roads; fires; tsunamis; seiches; changes in ground water level; and uplift of subsidence. They can also bring about far-reaching atmospheric pressure changes and sound waves and oscillations of the ionosphere (Ref. 16.1).

Relative movement of different sections (plates) of the Earth's crust causes stresses to build up near the boundaries between them. Movement along faults, releasing seismic waves, takes place when the stresses exceed either the strength of the solid rock or the frictional resistance between rocks on either side of a pre-existing break or fault. Since pre-existing fault surfaces usually have lower strength than the surrounding rock, movement takes place along them.

Earthquakes have proven to be one of the most disastrous and insurmountable of geologic hazards. Buildings constructed to withstand them have crumbled under their forces (Ref. 16.1). Prediction of earthquake likelihood, intensity, and timing for a given location has not yet proved reliable. Experience has shown that, to date, the best protection against earthquakes is identification of high-risk areas and avoidance of construction in them.

Definition of high-risk areas, a complicated process, includes mapping faults, dating movement on them to determine whether they are or might still be active, calculating theoretical maximum possible earthquake intensity for active faults, and predicting effects of possible earthquakes on sediments and rocks in the area. This information is then used to judge the safety of the area for construction.

#### 16.2.2 Tsunamis and Seiches

Tsunamis are seismic sea waves. They can be generated by submarine earthquakes that suddenly elevate or lower portions of the sea floor, by submarine landslides, or by submarine volcanic eruptions.

Tsunamis travel on the order of 500 km per hour and can cross an ocean in less than 1 day. Their wavelengths are long — 100 to 200 km. Their amplitudes in deep water are low, less than 1 m, but as they approach a shoreline, their large volume of water piles up into sizable “tidal waves.” Configuration of the shoreline and tidal and wind conditions can help to form waves over 10 m high. In 1948, the U. S. Coast and Geodetic Survey established a seismic sea wave warning system for the Pacific Ocean, so the arrival of tsunamis from distant sources can now be anticipated by a few hours.

A seiche is a long wavelength in an enclosed body of water. Its period is dependent on the dimensions of the basin, pond, lake, or enclosed bay. Commonly, seiches are low in amplitude and are not noticeable. When a large-scale disturbance takes place, however, larger amplitude waves result and can continue to be reflected back and forth across the body of water for hours or days. Large seiches can be caused when tsunamis arrive in bays, or when earthquakes and large slope movements initiate them in an enclosed body of water. Near enclosed bodies of water investigation of possible damaging seiche activity should be considered as a part of earthquake and slope movement studies.

### 16.2.3 Slope Processes

Slope processes refer to all types of movement of loose materials (soil and rock) on slopes. These processes range from imperceptible slow creep to rock-falls and mud-flows which can travel more than 100 m per second. Mass movements are often seasonal or periodic, but they may be catastrophic or spasmodic. The nature of slope instabilities and resultant downslope transferences depend upon:

- (1) Type and structure of materials, including composition, size of their particles, degree of consolidation, and structural discontinuities (cleavages, bedding, contacts, fractures, etc.).
- (2) Geomorphic setting, including climate, vegetation, shape and degree of slope, and slope orientation.
- (3) Triggering mechanisms, external factors which upset the delicate balance which maintains slope stability. These mechanisms include natural and man-caused activities such as earthquakes, addition of excessive fluids (especially water), and alteration of hillslope configuration (undercutting, etc.).

Tables 17.1a and 17.1b describe various types of mass movements, and Figure 16.1 depicts several forms of this class of hazards (Ref. 16.3).

Although some problem areas can be detected by examination of aerial photos, infrared photography, and topographic maps, potential-use areas should be examined on-site by competent engineering geologists and/or soil engineers.

Historically, several methods of prevention and control of slope processes have been used with varying degrees of success. They are:

1. Avoidance of problem areas;
2. Water control (drains, surface water diversions);
3. Excavations (slope reduction, unloading, terracing, total removal of slides); and
4. Restraining structures (walls, piles, bolts, grout, nets).
5. Planting, effective only in controlling shallow, small-scale slope processes.

TABLE 16.1a SLOPE PROCESSES

Movement		Composition of Mass and Process			Favoring Conditions
Kind	Rate	Material dry or with minor ice or water	Material and water	Material and ice	
Creep	Very slow	Soil creep	Rockcreep Talus creep	Solifluction	Unconsolidated sediment or structurally modified rock. Bedded or alternate resistant and weak beds. Rock broken by fractures, joints, etc. Slight to steep slopes. High daily and annual temperature ranges; high frequency of freeze and thaw; alternate abundant rainfall and dry periods. Balance of vegetation to inhibit runoff but not to anchor movable mass.
Flowage	Slow to rapid		Earthflow Mudflow Debris avalanche	Debris avalanche	Unconsolidated materials, weathering products; poorly consolidated rock. Alternate permeable and impermeable layers; fine-textured sediment on bedrock. Beds dipping from slight to steeper angles; beds fractured to induce water in cracks. Scarps and steep slopes well gullied. Alpine, humid temperature, semiarid climate. Absence of good-vegetative cover such as forest.
Sliding	Slow to very rapid	Slump Debris slide Debris fall	Rockslide Rockfall		Inherently weak, poorly cemented rocks; unconsolidated sediments. One or more massive beds overlying weak beds; presence of one or more permeable beds; alternate competent and incompetent layers. Steep or moderate dips of rock structures; badly fractured rock; internal deforming stress unrelieved; undrained lenses of porous material. Scarps or steep slopes. Lack of retaining vegetation.
Subsidence	Slow to very rapid		Subsidence		Soluble rocks; fluent clays or quicksand; unconsolidated sediments or poorly lithified rocks; materials rich in organic matter, water, or oil. Permeable unconsolidated beds over fluent layers. Rocks crushed, fractured, faulted, jointed inducing good water circulation. Level or gently sloping surface.

Compiled and modified from Sharpe (1938), by permission.

#### 16.2.4 Floods

Floods are defined as "any relatively high streamflow which overtops the natural or artificial banks in any reach of the stream." As a result, water and its sediment load are spread over the adjoining ground. Floods are natural, recurring events which become a problem only when they compete with man for the floodplain or flood channel. Rare catastrophic floods, in which water flows above and beyond the floodplains, may have disastrous consequences. Historically, catastrophic floods have resulted in loss of life and enormous property destruction. Initially, the greater than normal volumes of water, moving at abnormal velocities, are able to erode very quickly, picking up large volumes of sediment and debris. As water and its debris load continue downstream, large amounts of material (including man-made objects) are picked up or covered.

Floods normally occur as a result of cloudbursts, extended rain, and/or rapid snowmelt accompanied by rapid runoff. Natural dams such as those caused by landslide (as well as man-made dams) result in flooding of land upstream. Disastrous floods may occur as a result of sudden release of large amounts of water by dam failures.

TABLE 16.1b FACTORS CAUSING SLOPE PROCESSES

<p>Wedging and prying: by plant roots; swaying of trees and bushes in wind; expansion of freezing water and hydrostatic pressure of water in joints and cracks; diurnal, annual, irregular expansion due to heating; expansion due to wetting; animal activity. Filling and closing of cracks and voids caused by: burrowing of animals; decay of plant roots and other organic matter; gullyng or undercutting by streams; removal of soluble rocks and minerals; erosion of fine particles by sheet wash and rills; downslope mass movement; shrinkage due to drying or cooling. Increase in load: addition of material upslope; rainfall, snow, or ice; traffic of vehicles or animals; tectonic, meteorologic or animal disturbance.</p>
<p>Reduction in internal friction due to excessive amounts of water in mass. May start as slide; causes similar to landslides.</p>
<p>Removal of support: oversteepening of natural or artificial slopes by erosion; outflow, compaction, softening, burning out, solution, chemical alteration of subadjacent layer; disappearance of buttress against slope such as ice front. Overloading: by other mass-movement processes; by rain, snow, ice, and saturation, overburden in excavation. Reduction of internal friction and cohesion: by surface and ground water, oil seeps, chemical alteration by weathering. Wedging and prying: as in creep. Earth movement: produced by earthquakes; storms, traffic of vehicles and animals; drilling, blasting, gunfire; earth strains due to temperature and atmospheric pressure and tidal pull.</p>
<p>Removal of support of adjacent layers: by solution or chemical alteration; by outflow of fluent material; by natural or artificial excavation; by compaction caused by natural or artificial overloading, by reduction of internal friction, by dessication. Earth movement: by warping; by natural or artificially induced vibrations. Overloading: natural or artificial.</p>

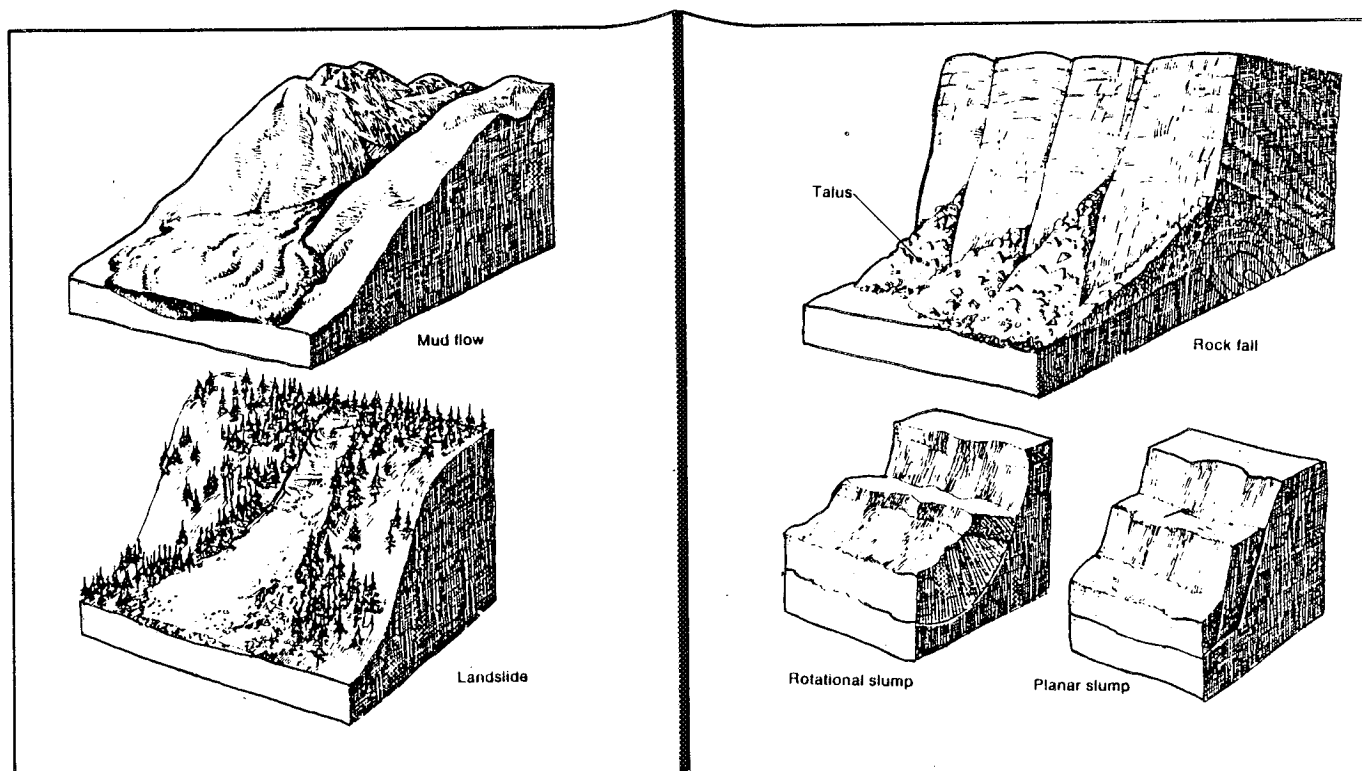


Figure 16.1 Slope processes.

Several approaches have been used to avoid the damaging effects of floods. All these approaches make use of flood predictability from stream flow records and historical flooding recurrences. Flood hazard maps are compiled as various areas are assigned risk factors. The type of approach used to reduce flood damage will depend upon the calculated or assumed risk:

1. Avoidance of high-risk areas for construction activities.
2. Detention or delay of runoff in smaller tributaries at higher reaches of the watershed.
3. Modification of the lower reaches of rivers, where floodplain inundation is expected, by channels and levees.

#### 16.2.5 Volcanic Hazards

Volcanic hazards fall into two categories: hazards near the volcanic activity and hazards distant from it.

##### 16.2.5.1 Hazards Near Volcanic Activity

Within a few tens of miles of a volcanic center, hazards include: lava flows, nuées ardentes (hot ash flows) and poisonous gases, ash falls and bombs, earthquakes and debris, and mud flows.

1. Some lava flows are much more dangerous to man than others. Lava flows vary a great deal in viscosity, depending on their chemistry and temperature. They can be up to 10 m thick, travelling a meter per hour, or they can form a sheet as thin as 1 m which travels up to 50 km per hour. The latter have been the most hazardous to man in the past. A trained geologist can predict, to some extent, the type of flow most likely to occur in a given volcanic area. If fast fluid flows are likely, guiding levees can be built to shunt them away from populous or otherwise valuable areas.
2. Nuées ardentes are heavier than air, gas-borne flows of incandescent volcanic ash released during explosive volcanic eruptions. Temperatures in the flows reach 800°C, and the gases that carry them may be poisonous. These flows, though gas-borne, are extremely dense. Their physical force is great enough to snap large trees and crumble strong buildings. It was a nuée ardente from Mt. Pelée that devastated St. Pierre, Martinique, in 1902, completely destroying the town and killing an estimated 40,000 people. Hot, dense, poisonous gases can also be emitted without ash.
3. Ash falls in the immediate vicinity of a volcano can be up to a few tens of meters deep and very hot. Near the eruption center they may contain sizable volcanic bombs of solid or solidifying rock, as well as pebble-sized fragments of pumice. They may give off gases for some time.
4. Earthquakes (see Section 16.2.1) usually accompany volcanic activity and often trigger debris flows and mud flows.
5. Debris and mud flows form from the unconsolidated material that makes up the flanks of active stratovolcanoes. The material becomes unstable because of doming of the volcano, rapid melting of snow by hot ash or lava, and/or percolation of hot volcanic gases through snow masses. Volcanic mud and debris flows have been known to travel 80 km at speeds of several tens of km per hour. Some flows from major volcanoes contain on the order of 2 to 4 cubic kilometers of material. Dams in the paths of mud flow may

break and contribute to the volume of flows that overtop them. In some places where mudslide hazard has been recognized, dams have been built and reservoirs kept empty to absorb them. In addition to downstream damage, volcano-caused landslides can cause instability at their point of origin: When a large volume of material is removed suddenly from the flank or summit of an active volcano, pressure is released and an eruption may be triggered (as in the May 18, 1980, eruption of Mt. St. Helens).

#### 16.2.5.2 Hazards Distant from Volcanic Activity

Far from volcanic centers, volcanic ash and tsunamis can still be serious hazards.

1. An ashfall's total volume depends on the size of the eruption that brought it about. Its distribution depends on the elevation reached by the volcanic cloud and on wind conditions at the time of the eruption. A sizable ashfall can damage areas several hundred kilometers from the eruption site. Ash is detrimental to human health and damaging to mechanical equipment. It reduces visibility if there is wind or traffic, and must be removed from buildings and pavement. Fine ash, if it reaches the stratosphere, may remain there for months or years, affecting climate by reducing insolation.

2. Tsunamis (see Section 16.2.2) may be caused by submarine volcanic explosions and debris slides, which can travel thousands of kilometers from the volcanism that caused them. They endanger life and all coastal construction within 40 m of sea level.

When considering volcanic hazards, it is important to realize that in any area volcanism is sporadic. A volcanic area which has been inactive throughout historic times may reawaken to violent activity in a few days or weeks, or it may remain inactive for centuries into the future. Earthquakes, almost always felt or recorded several days or weeks before activity commences, serve as a warning of impending danger. Once volcanism commences, danger is greatest within a few tens of kilometers of the eruption. The effects of volcanism can easily be catastrophic, especially since volcanoes are virtually uncontrollable by man. Important constructions should not be located in the immediate vicinity of active or dormant volcanoes, or in areas likely to be affected by distant volcanism.

#### 16.2.6 Expanding Ground

Expanding ground is caused by freezing of moisture in the ground or by rock components that expand when wet.

When water freezes, its volume increases by approximately 9 percent. When water in fine-grained, unconsolidated material freezes, additional water from the atmosphere and from unfrozen ground below slowly adds to the already frozen mass. Eventually, lenses of ice build up, lifting the soil above them. In areas where winters are cold and moist, or where day-night temperatures differ markedly, freezing and thawing may cause marked dislocation of surface and near-surface materials. Some clays contain minerals that increase in volume upon wetting and decrease in volume upon drying. The most common of these minerals are anhydrite and the montmorillonite clay group. Problems with expansive clays and the rocks and soil in which they occur are most frequently encountered in arid or semiarid areas with strong seasonal changes in soil moisture.

Expansive clays are particularly associated with volcanically derived materials. Shales containing clays of the montmorillonite group (including bentonite derived from volcanic ash) commonly swell 25 to 50 percent in volume (Ref. 16.4). Such swelling results from chemical attraction of water molecules and

their subsequent incorporation between submicroscopic, platy clay molecules. As more water becomes available, it infiltrates between the clay plates and, with freezing, pushes them farther apart.

Similarly, when the mineral anhydrite is subjected to hydration, it can alter to the mineral gypsum, a chemical change that causes up to 40 percent expansion.

These large increases in volume upon freezing or hydration, and associated decreases in volume with thawing or drying, can be very destructive. Volume increases of only 3 percent are considered to be potentially damaging and to require specially designed foundations. James and Holtz (Ref. 16.5) report that shrinking and swelling damage to foundations, roads, and pipelines in the United States amounts to more than twice the dollar value of damage incurred by floods, hurricanes, tornadoes, and earthquakes combined.

On-site inspection by a competent soil engineer or engineering geologist may pinpoint potential clay-expansion problems. Engineering soil tests are required to evaluate the extent and severity of the problem in construction sites.

Installation of well-designed drainage systems, or complete removal of expansive materials, may lessen the potential damage from expansive ground.

#### 16.2.7 Ground Subsidence

Ground subsidence is characterized by downward movement of surface material, caused by natural phenomena such as removal of underground fluid, consolidation, burning of coal seams, or dissolution of underground materials. It may also be caused by man's removal or compaction of earth materials.

Ground subsidence is ordinarily a relatively slow process; it has been known to continue for many decades. Usually the result is broad warping and flexing, with some cracking and offset at the ground surface. If the process causing subsidence persists, the surface may suddenly collapse. Foundation failures, ruptures of pipe and utility lines, dam collapses, salt water invasion, and disruption of roads and canals have all been directly attributable to ground subsidence.

Potential causes for ground subsidence include:

1. Removal of solids: Removal of the solid subsurface support base involves mining, natural or human solution of carbonate and other easily soluble minerals (including salt and sulfur), and underground burning of organic beds. Cavern collapse is the most catastrophic result. Alternatives to avoiding such areas for heavy loads include subsurface backfilling, cement-grouting, and installation of underground support pillars.
2. Withdrawal of fluids: Subsidence due to withdrawal of fluids (including gas, oil, and water) is the most common type of man-caused regional ground subsidence. As fluids are removed, and fluid pressure within the aquifer or reservoir rock is reduced, the aquifer skeleton must bear an increased grain-to-grain load. In permeable media, the increase in effective stress and subsequent compaction is immediate. Increasing percentages of clays in the aquifer cause the adjustment to take place more slowly. In extreme cases, subsidence of more than 7 m over a 60-year period has been directly attributed to withdrawal of water and/or petroleum. Injection of fluids back into the aquifer can often arrest and reverse the subsidence.
3. Oxidation of organic beds: Oxidation of organic beds, such as layers of peat, and resultant breakdown of support structures have been known to follow drainage of peat bogs. Raising the water table can inhibit this oxidation.

4. Application of surface loads: Compaction due to surface loading alone commonly results in only minor ground subsidence. However, application of surface loads may trigger more severe subsidence when added to already weakened substratum conditions.

5. Hydrocompaction: Wetting of some clays in moisture-deficient, low-density soils may lead to weakening of clay bonds which support soil voids, and ultimately to collapse of internal soil structure and compaction. Hydrocompaction commonly occurs in wind-deposited silts and fine-grained colluvial soils which have a high clay content. Some areas near the south and west borders of the San Joaquin Valley dropped 1.5 to 5 m in the early 20th century after application of water. Drainage installations and replacement of the offending clay-bearing materials are modifications used to circumvent potential hydrocompaction problems.

6. Tectonic movements: These movements include earthquakes and man-caused explosions which directly cause reordering and subsidence, and which commonly cause additional ground subsidence in already unstable areas. Some materials such as quick clays and quicksands lose all their cohesive strength and acquire the properties of a liquid upon being violently disturbed. Such materials can flow and envelope buildings constructed on them.

Ground subsidence is commonly caused by a combination of factors. Geologic conditions which are favorable for its occurrence include the presence of mines, soluble or flammable materials, oil, water or gas, windblown soils, fluent clays or quicksand, faults or fractured rocks, and good water circulation. It is imperative to recognize these potential problems before construction commences and to take corrective measures where they are called for.

#### 16.2.8 Other Hazards

Geologic hazards such as avalanches and other snow and ice processes do not influence the three areas concerned and are not discussed here.

#### 16.2.9 Conclusions

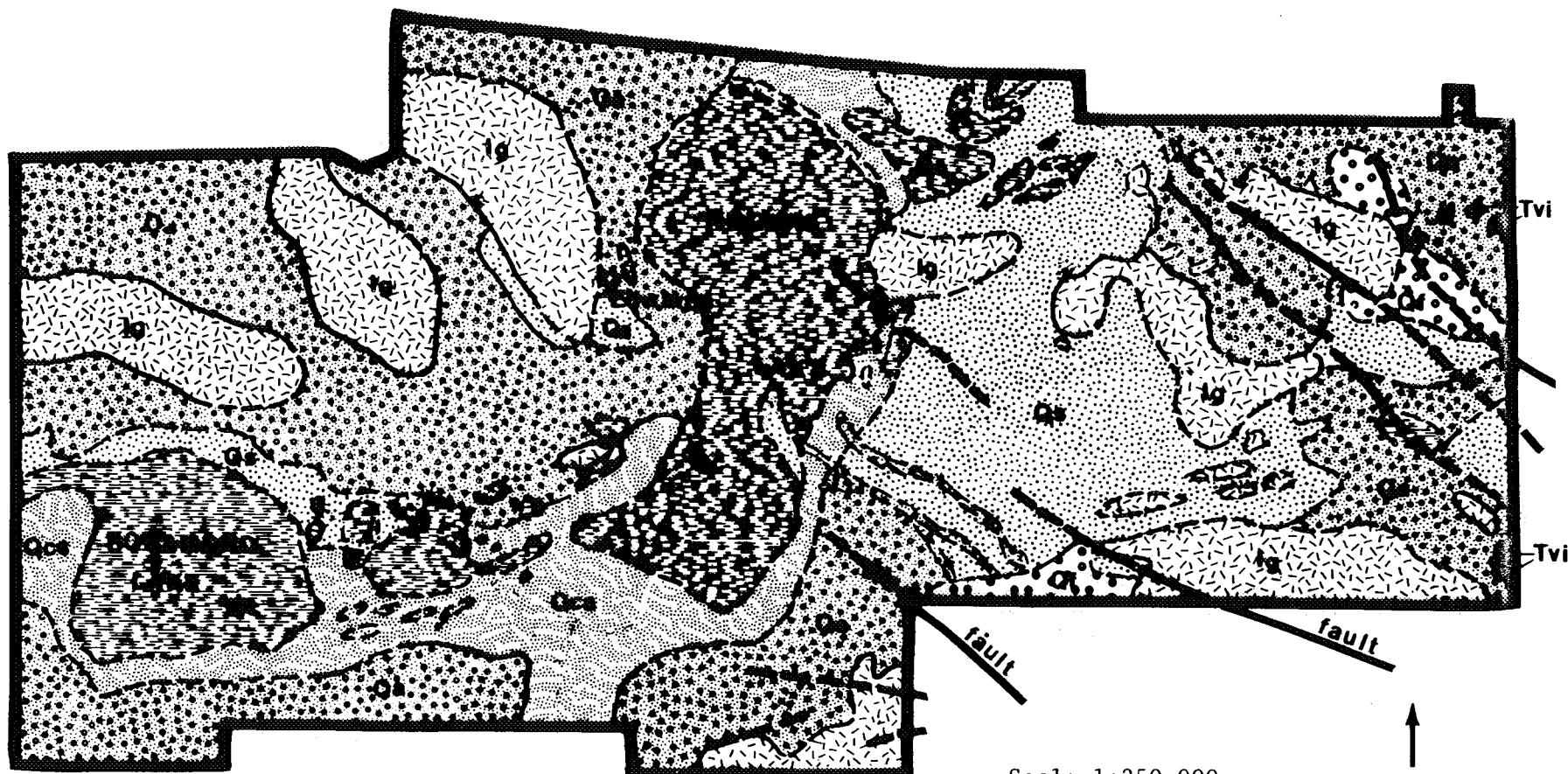
A word should be added to the preceding description of geologic hazards. Many of those described occur suddenly, while others take place over a long period of time. Almost all of these "hazardous" events are normal geologic processes and should be expected to occur from time to time. We have learned to predict and control some of these processes, but for others the best we can do is study the likelihood of their occurrence in different areas and avoid building where danger is great.

### 16.3 Geology and Geologic Hazards at Edwards Air Force Base, California

#### 16.3.1 Geology

Edwards Air Force Base is covered by rock materials of three distinct age groups (Ref. 16.6). The oldest rocks are pre-Tertiary (pre-65 million years ago) granite intrusive and metamorphic units (lg on Fig. 16.2). These rocks are similar in age and composition to the Sierra Nevada Batholith. They form most of the ridges and hills within the air base boundaries.





Alluvial sand, gravel, and beach sand



Playa clay



Windblown sand and playa clay



Windblown sand (less than 50' deep)



Fanglomerate, partially cemented



Tertiary volcanic rocks with sedimentary interbeds



Intrusive igneous rocks

Scale 1:250,000

0 5mi/8km



(Boundaries dashed where inferred or shifting)

Figure 16.2 Geology of Edwards Air Force Base, California (after Dibblee, Ref. 16.6).

ORIGINAL PAGE IS  
OF POOR QUALITY

Minor amounts of Tertiary age rocks (3 to 65 million years old) are exposed at Edwards Air Force Base (Tvi on Fig. 16.2). Most of these are dikes and sills of fine-grained rock. A few volcanic flows and pyroclastics, with interbedded sediments, crop out along the eastern boundary of the base. Some bentonite layers occur within the sedimentary units. Although the dikes and sills form stable slopes, some of the slopes covered by the pyroclastic and sedimentary interbeds are unstable.

Most of the terrain within the boundaries of Edwards Air Force Base is covered with thick units of Quaternary and Recent (3 million years old) unconsolidated and weakly consolidated materials which include alluvial sand and gravel (Qa on Fig. 16.2), beach dunes and bars (also Qa), playa clays (Qc), wind-blown sands (Qcs), and older, partly consolidated gravels (Qf). These deposits generally occupy areas of low relief.

Alluvial sand and gravel, deposited by action of flowing water, form channel and fan deposits. Wave-deposited bars and wind-deposited dunes occur along the northern "shore" of Rogers Lake. Minor clay balls occur in the wave-deposited bars. Windblown sand forms small dunes elsewhere within the base, and also covers parts of the desert floor with a thick veneer of sand.

The playa clays are mudflat facies of the alluvium. They are hard when dry but become soft and sticky when wet. Studies by Droste (Ref. 16.7) found that playa clays from Rogers Lake consist of 40 to 50 percent montmorillonite and 40 to 50 percent illite. Clays from Rosamond Lake consist of 20 to 30 percent montmorillonite, 50 percent illite, and 20 to 30 percent chlorite. Although in the desert climate thorough wetting of the playas is rare, these high-montmorillonite clays are subject to severe swelling and shrinking, which should be considered when planning construction activities near the dry lake beds.

Several high-angle, northwest-trending faults have been mapped in the southern and eastern parts of the air base. They have small displacements and seem to edge granitic domal features. The faults are at present inactive.

### 16.3.2 Geologic Hazards

The following subsections describe general locations of possible or potential geologic hazards which exist at Edwards Air Force Base (Fig. 16.3). On-site investigations and engineering properties tests are recommended on a location-by-location basis before initiation of any construction activities.

#### 16.3.2.1 Earthquakes

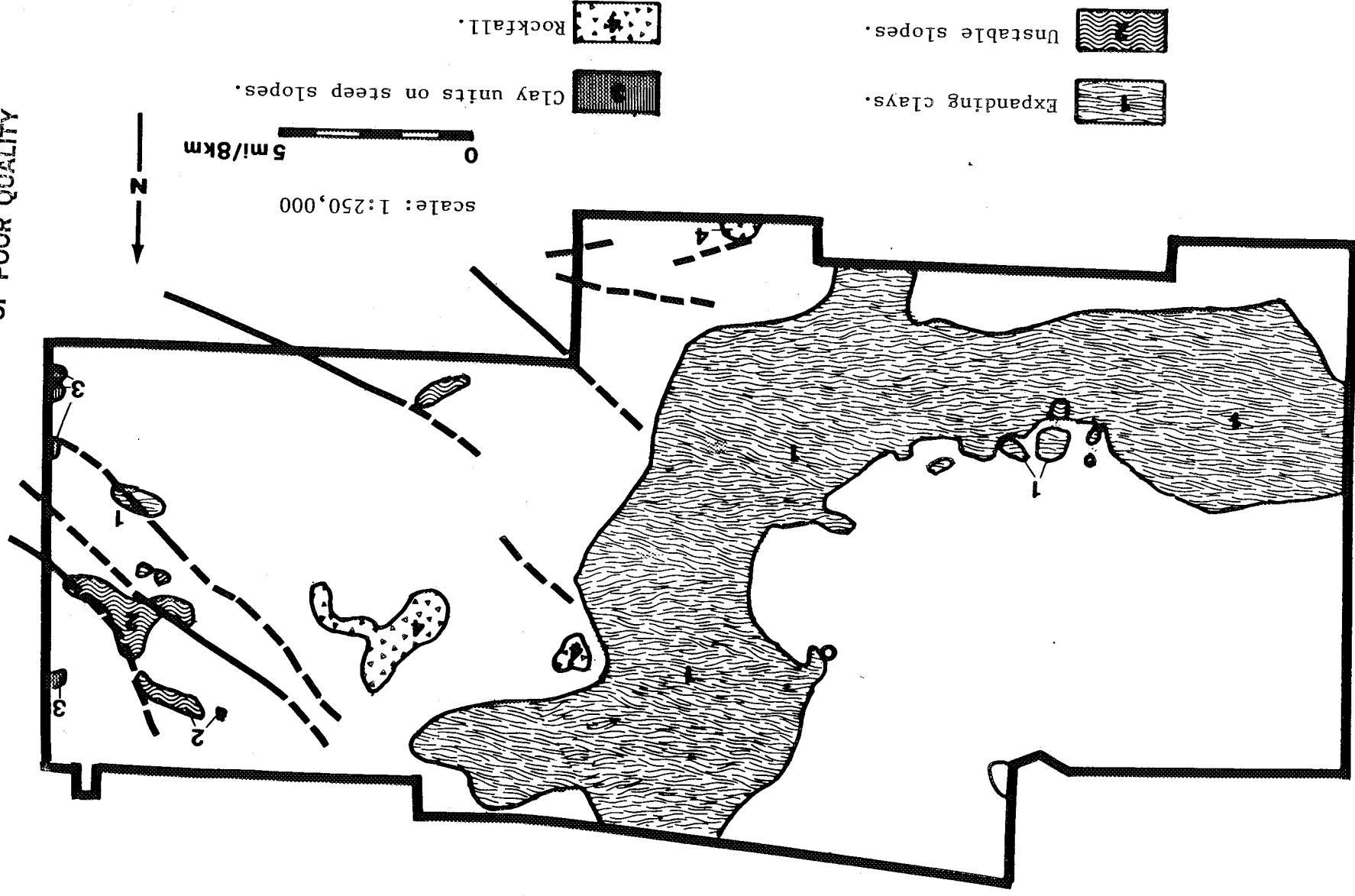
There were no recorded earthquakes with epicenter magnitude of 4 or greater at Edwards Air Force Base between 1910 and the present (Refs. 16.8, 16.9). The base is located on a relatively stable wedge between the San Andreas and Garlock faults, both of which are less than 40 miles from the base. The proximity of these major active faults indicates, of course, regional tectonic instability. However, the known faults mapped in the eastern and southern parts of the base seem to be inactive, and earthquake hazards are judged to be negligible.

#### 16.3.2.2 Slope Processes

All of the air base lies within an area designated as 1 by Radbruch and Crowther (Ref. 16.10). This designation identifies areas in California which have the lowest number and volume of landslides per given area. Hilly parts within a unit 1 area may experience landslides, but because of the overall low-to-moderate

Figure 16.3 Geological hazards of Edwards Air Force Base, California.

(Faults dashed where inferred.)



## 16.12

relief, few problems from slope processes are expected. Some hazards may exist on steep gravel-covered slopes. The fanglomerate units that form steep slopes in the Kramer Hills, near Jackrabbit Hill, and elsewhere on the base should be considered susceptible to mass movement. Slopes covered by Tertiary pyroclastics and interbedded sedimentary layers along the eastern boundary are potentially hazardous. Rockfall problems may exist at the bases of granite cliffs.

### 16.3.2.3 Flooding

Except for very local flash flooding, no flood hazards are likely. Flash flooding may turn playas into shallow temporary lakes.

### 16.3.2.4 Expanding Ground

Careful examination of the engineering properties of the playa clays should precede construction activities. The high montmorillonite content of these clays leads to swelling and shrinking when they are alternately wet and dry. Similar caution should be exercised when dealing with the Tertiary pyroclastics and their sedimentary interbeds.

### 16.3.2.5 Subsidence

Localized subsidence may occur near old mine diggings. There is also the possibility of hydrocompaction in playa clays.

### 16.3.2.6 Conclusions

Edwards Air Force Base, though mostly underlain by granite, is 65 percent covered by Pleistocene and recent unconsolidated sand, clay, and gravel. Despite proximity of major active faults, seismic risk is low. Slopes are generally less than 10 percent, so geologic hazards resulting from slope processes are localized and probably restricted to steep slopes consisting of weakly consolidated fanglomerate.

Approximately 30 percent of the air base is covered by unconsolidated clay-rich material. The clays include a high proportion of montmorillonite and are susceptible to expansion and shrinking. However, low precipitation of the Mojave Desert region greatly reduces the potential for such problems.

In summary, Edwards Air Force Base is located in a geologically low-risk area.

## 16.4 Geology and Geologic Hazards of Vandenberg Air Force Base, California

### 16.4.1 Introduction

Land use planning for Vandenberg Air Force Base should take into account possible danger from earthquakes, seismic waves, slope instability, floods, and burning ground. Volcanism, expanding clays and rocks, and subsidence are not expected to interfere with activities on the base.

### 16.4.2 Geology

Figure 16.4 is a geologic map of the Vandenberg Air Force Base area. The oldest rocks on the base, found in its northwest end, are Franciscan mafic and ultramafic igneous rocks and the sedimentary Knoxville Formation of Jurassic age. The remaining rocks, which cover the greater part of the base, are much younger, ranging in age from Oligocene to Recent. Oligocene poorly consolidated nonmarine sediments crop out near the older rocks. Miocene diatomaceous earth underlies the rest of the base and is overlain extensively by younger sediments. At most of its outcroppings, the diatomaceous earth is soft, lightweight, and porous, but resistant to weathering. It contains abundant water-soluble salts, which form an efflorescence on outcrops. This rock is a source and a reservoir for gas, oil, and tar, which have been removed in oilfields north and east of the base. Pliocene to Recent sediments are generally unconsolidated, fine-to-coarse sand and conglomerate. These sediments form terraces, fill valley bottoms, and are piled into extensive sand dunes near the coast. Sediments of Pliocene age contain hydrocarbons of Miocene derivation. Pliocene and older rocks have been extensively folded and locally faulted, probably as they were compressed during western drift of the continent.

### 16.4.3 Geologic Hazards

#### 16.4.3.1 Earthquakes

Although no recent fault scarps are known on the air base, earthquakes pose an everpresent threat to it. The base is in one of the most earthquake-prone parts of the country. Between 1910 and 1971, five earthquakes with magnitude between 4.0 and 4.9 had foci within 3 miles of the base (Fig. 16.5b). Ground shaking has been felt on the base during many other earthquakes. Although usually of short duration, such shaking can trigger building collapse, water waves and flooding, slope movements and/or release of flammable gases. Earthquakes are a definite hazard at this base.

#### 16.4.3.2 Tsunamis and Seiches

Seismic water waves (tsunamis) must be considered as a threat all along the shore of the Pacific Ocean. Land within 12 m of sea level is in the tsunami danger zone. (Actually, few documented tsunamis have reached that height.) Fresh-water dams should be examined to determine their strength should seiching take place. Areas on the base which could be affected by tsunamis or by seiching are shown in Figure 16.5b.

#### 16.4.3.3 Slope Processes

The potential for slow or fast slope changes exists in several parts of Vandenberg Air Force Base. These areas are described later and are illustrated on Figure 16.5b.

a. Gullying is cutting away diatomaceous earth around the edges of Burton Mesa and San Antonio Terrace. This slow, almost continuous process has formed very steep slopes which would be unstable in a strong earthquake.

b. Several large landslides have occurred in the Casmalia Hills, in and near the north end of the base. Surface material there is obviously unstable and should be examined carefully on site before any construction.

16.14

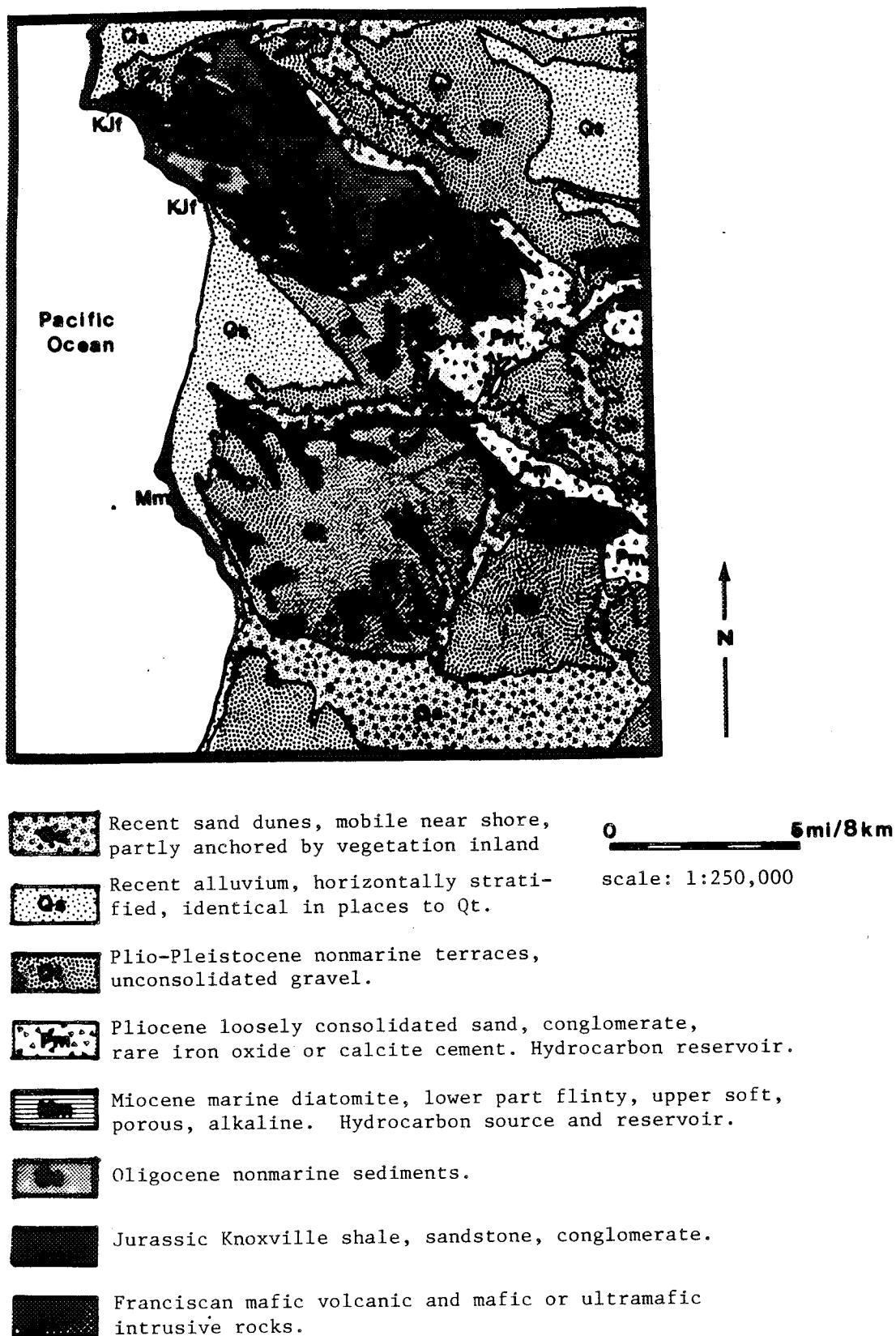


Figure 16.4 Geology of the Vandenberg Air Force Base area (after Jennings, Ref. 16.11).

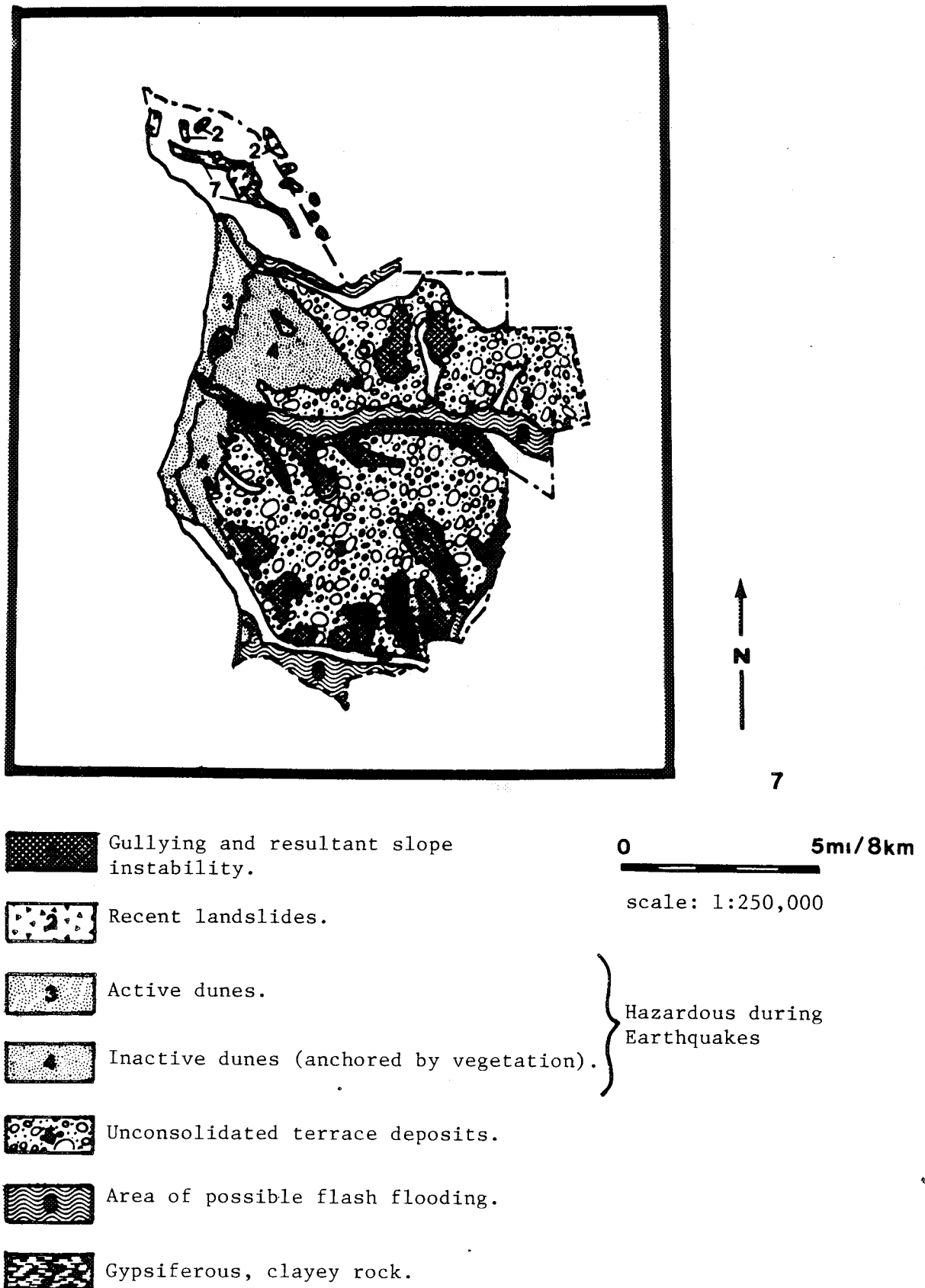


Figure 16.5a Geologic hazards of Vandenberg Air Force Base, California.

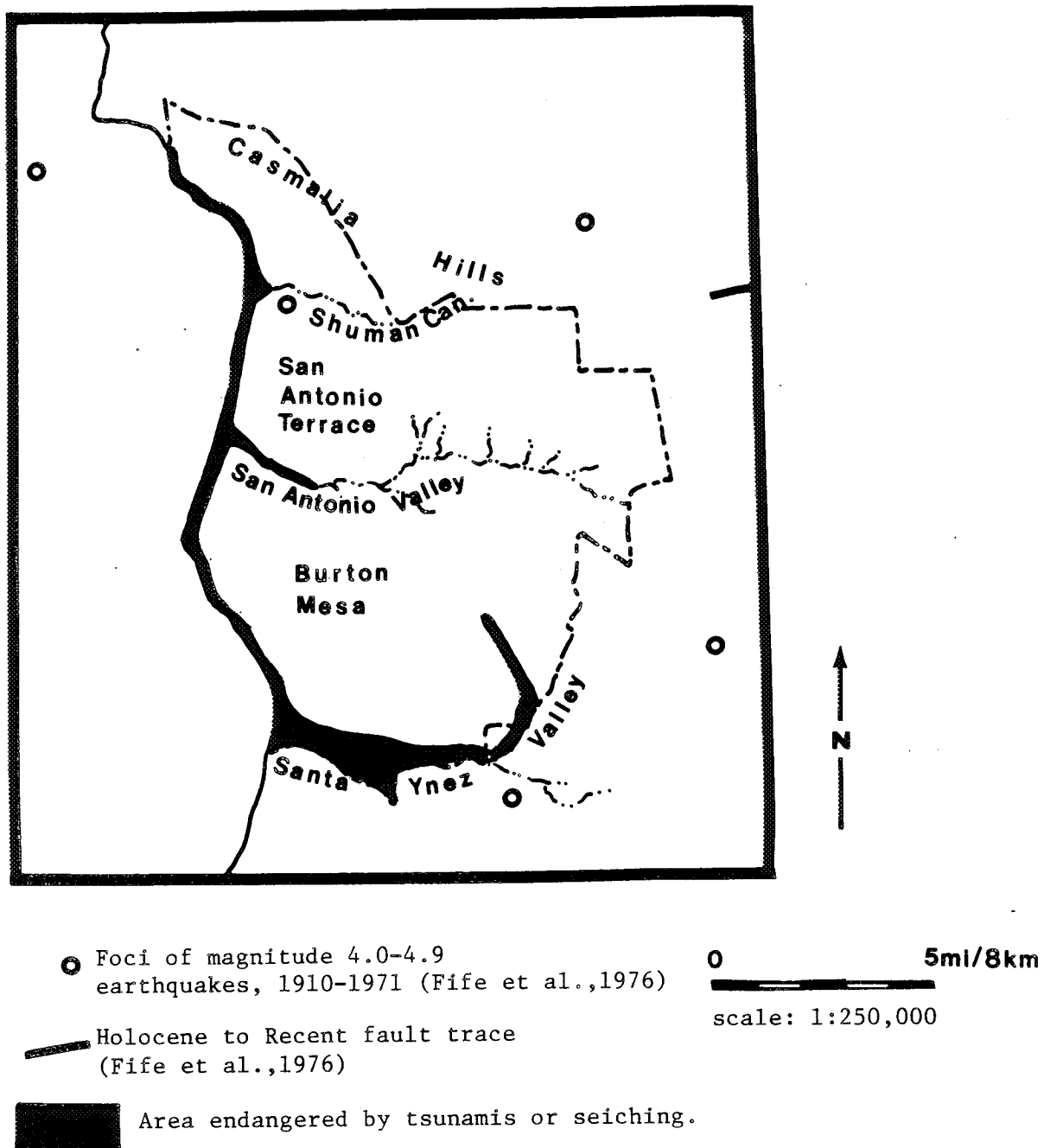


Figure 16.5b Geologic hazards (tsunamis or seiching) and place names, Vandenberg Air Force Base, California.



c. Roughly one quarter of the base is covered by recent sand dunes. Though much of the dune area is anchored by vegetation, including windbreaks at the landward edge of the dunefield, sand blasting should be expected on San Antonio Terrace and Burton Mesa during times of high winds (see Chapter II on Winds).

d. Although their surfaces are flat and nearly level, San Antonio Terrace and Burton Mesa are likely to be strongly affected by earthquake-induced surface movements because of the thick layer of unconsolidated sand and gravel terrace deposits which cover them. Shaking is highly amplified by thick, loose material, and buildings or other constructions on such material are at risk, especially if they are several stories high.

#### 16.4.3.4 Floods

Three flood plain systems exist on the base. From north to south they are Shuman Canyon, San Antonio Valley, and Santa Ynez Valley. All three should be considered possible sites for flash flooding, especially since, during times when their rivers are dry, dune and bar sand partially block their outlets to the ocean. In addition, small dams in the Santa Ynez drainage basin could break and cause flooding during an earthquake.

#### 16.4.3.5 Volcanic Hazards

No volcanic hazards are expected to affect this area, although tsunamis caused by distant volcanism are an always-present danger (see Subsection 16.4.3.2).

#### 16.4.3.6 Expanding Clays and Rocks

Expanding clays and rocks are not a major hazard on most of the base. Several hundred feet of gypsiferous, clayey, alkaline shale is present in the Casmalia Hills and should be avoided when locating construction sites.

#### 16.4.3.7 Subsidence

Burning of hydrocarbon-rich layers of diatomaceous earth is well documented in historic time in the Casmalia Hills area. Burnt ground has been encountered to depths as great as 300 m in nearby oil wells (Ref. 16.12). Red, hard, vesicular, scoriaceous rock ("clinker") results from this burning. However, no change in the volume of the burnt rock has been documented. Burning itself poses a threat, as it is next to impossible to stop it once it has been started (by lightning or man).

### 16.4.4 Conclusions

Numerous potential geologic hazards exist within Vandenberg Air Force Base. Earthquakes occur from time to time, and could set off other dangerous events. Tsunamis caused by remote earthquakes or volcanism could affect the area of the base within 12 m of sea level. Seicheing may pose a danger to small dams on the base. Widespread slope and surface instability is likely in the event of a strong earthquake. Blowing sand at times reduces the usefulness of some areas. Flash floods are possible in the valleys during rainy seasons. In some areas, hydrocarbon-soaked rocks have been known to catch fire. Use of different

areas of the air base should take these hazards into account. True, the surface of the base is stable until rare hazard-causing events occur. But if they do, extensive destruction is possible.

## 16.5 Geology and Geologic Hazards at Cape Canaveral and Kennedy Space Center, Florida

### 16.5.1 Introduction

Cape Canaveral, on the eastern coast of the Florida peninsula, covers an expanse of barrier bars, swamps, and lagoons between the Atlantic Ocean and the mainland. The entire Kennedy Space Center lies within 8 m of sea level. Surficial deposits on the center are roughly 30 m of Miocene to Recent shelly sand and clay and medium to fine-grained sand and silt (Ref. 16.13) (Fig. 16.6). These sediments overlie Eocene limestone and dolomite.

### 16.5.2 Geologic Hazards of Cape Canaveral and Kennedy Space Center

#### 16.5.2.1 Earthquakes

Earthquakes are extremely unlikely in this corner of the United States and should not be considered a hazard.

#### 16.5.2.2 Tsunamis and Seiches

Sea waves (tsunamis) induced by earthquakes and/or volcanism elsewhere could be a hazard to the entire space center because of its low elevation. However, tsunamis are not common in the Atlantic Ocean and, although not impossible, are considered unlikely. Nor are the lagoons and rivers likely to develop seiches.

#### 16.5.2.3 Slope Stability

The lack of topographic relief on Cape Canaveral and Kennedy Space Center means slope stability is not a problem there.

#### 16.5.2.4 Floods

Flooding could be a hazard to the center if high water is brought about by hurricane winds (see chapters on weather).

#### 16.5.2.5 Volcanic Hazards

Volcanism near the center is unknown in recent time. The only volcanic hazards to the center are tsunamis caused by distant volcanism.

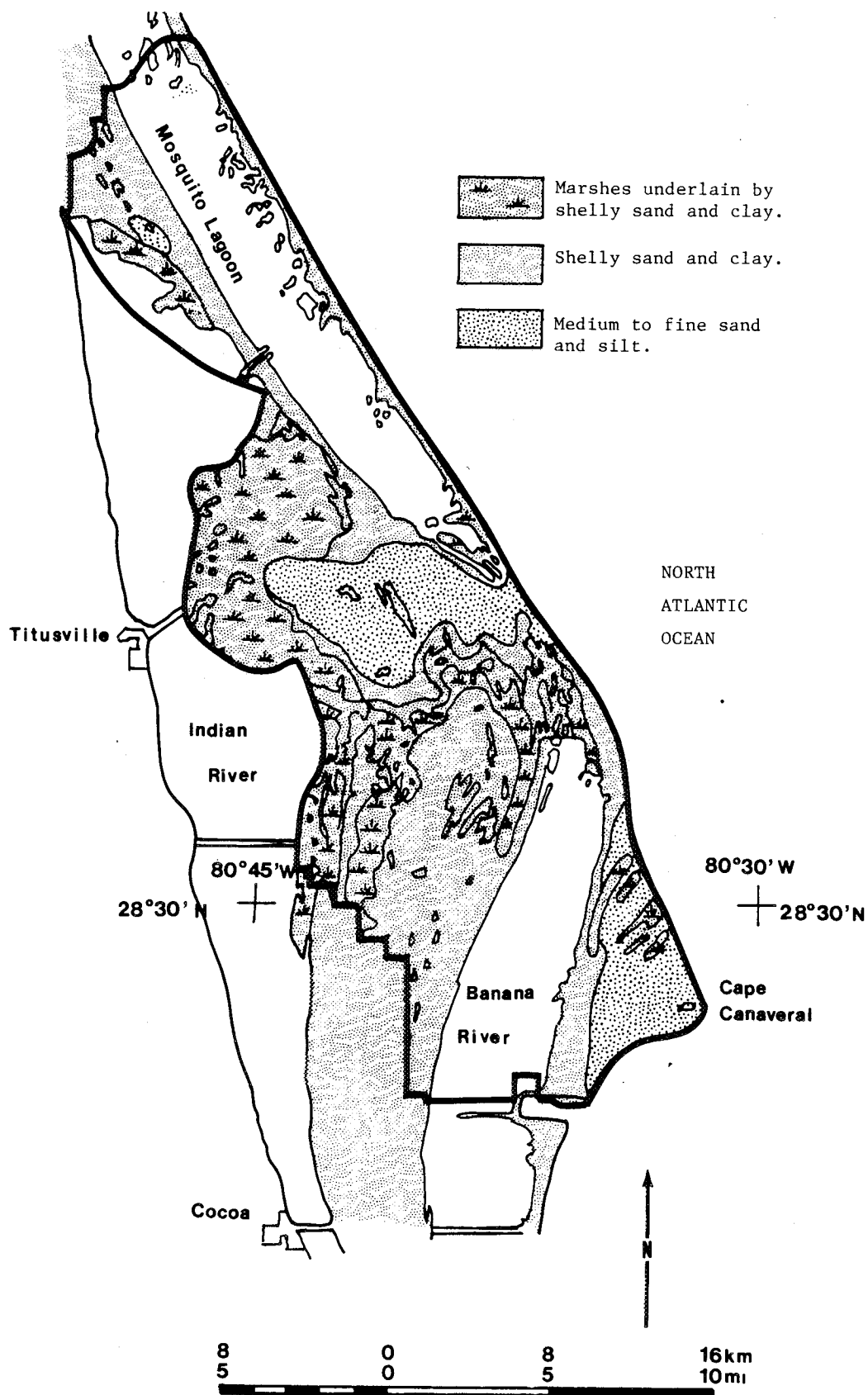


Figure 16.6 Geology of Cape Canaveral, Florida.

## 16.20

### 16.5.2.6 Expanding Soils and Rocks

Expanding soils and rocks are not a hazard to the center because of the high sand content of sediments and the consistently high humidity.

### 16.5.2.7 Subsidence and Uplift

Drilling results indicate the presence of caverns in the limestone and dolomite units which underlie the space center (Ref. 16.13). There is, therefore, potential for eventual caving. There is no apparent evidence of karst topography in the space center area, nor is collapse expected in the foreseeable future. Test drilling should in all cases precede building location and construction, however.

### 16.5.2.8 Conclusions

Cape Canaveral, Kennedy Space Center, is a low risk area for geologic hazards. Only flooding, due to hurricanes or seismically induced waves, is considered to be of possible importance. Crucial structures which would not survive high water should be protected by dikes.

## 16.6 Seismic Environment

GSE, which may be subjected to a high risk potential, seismic environment, shall be designed considering the hazards defined in this section, Geologic Hazards, and shall conform to the following requirements.

### 16.6.1 GSE Categories and Requirements

For seismic purposes, two categories of GSE have been established:

I. Equipment that can inflict structural damage on SSV elements by virtue of its operation, or by its failure to operate, during and after a seismic event.

II. Equipment located in close proximity to the SSV elements that can cause major structural damage due to support failure, or physical contact with the integrated SSV or SSV elements.

All GSE elements shall remain integrally constrained in their packages. Equipment shall not separate from the unit and become missiles. Equipment separated from SSV elements by strong physical barriers, such as walls or enclosures sufficient to prevent equipment contact with SSV elements, are exempt from this requirement.

### 16.6.2 Types of Design Analyses

A static or dynamic analysis shall be performed in accordance with paragraphs 16.6.3 and 16.6.4, which follow.

### 16.6.3 Dynamic Analysis

A rigorous dynamic analysis shall demonstrate that the equipment and its supporting mechanism/structure will withstand, without collapse or excessive deflection, the design loads induced in the system by a major seismic event. The effect of such an event on the system shall be determined using the GSE design response spectra for major seismic events at VAFB shown in Figure 16.7. The design loads shall equal the Root-Sum-Square (RSS) of the modal responses, where natural frequencies are determined by modal analysis and whose damping values are estimated by damping analysis, or by similarity to structures whose damping has been measured under actual or simulated earthquake motion.

### 16.6.4 Static Analysis

GSE shall be designed for seismic resistance according to the following:

1. GSE weighing less than 100 pounds shall have restraints designed to react a horizontal force of  $1.5 \times$  equipment weight from any direction applied at its center of gravity.

2. GSE weighing between 100 pounds and 1000 pounds shall be designed in accordance with the following equation:

$$F = ZKCW$$

$F$  = equivalent static lateral force in pounds applied at the center of gravity

$Z$  = seismic probability coefficient (no units), where  $Z = 1.5$  for high-loss potential equipment (damages SSV element),  $Z = 1.0$  for low-loss potential equipment (damages GSE only)

$C$  = seismic force coefficient (no units)

$K$  = coefficient based on building type (no units)

$W$  = weight in pounds of item under consideration.

$C$  may be calculated using the following equation:

$$C = (C_s) (A_h) (MF)$$

$$C_s = \text{soil constant (no units)} = 2.25 - 0.125 f_b \geq 1$$

$f_b$  = allowable soil bearing value in kips per square foot (see Geophysical Investigation Supplement for VAFB Station Set V23 (VCR-77-067 of 20 January 1977) (1 kip = 1000 pounds)

$$A_h = \text{design acceleration} = 0.10 + 0.15 (h/h_t)$$

$h$  = height of equipment in building above the building base

$h_t$  = height of building

$$MF = \text{magnification factor (no units)} = \frac{1}{\sqrt{[1 - (T_a/T)^2]^2 + [0.04 T_a/T]^2}}$$

$T_a$  = period of item under consideration in seconds

$T$  = period of building in seconds.

(For graphical solution to equation see Figs. 16.8 and 16.9).

The building characteristic constants for the Mobile Service Tower (MST), the Payload Changeout Room (PCR), and the Access Tower (AT) are shown in Table 16.2. For equipment in contact with or buried in the soil, or supported by footings, pedestals, or slabs supported by soil, use the following coefficients:  $K = 1.00$  and  $C = 0.15$ .

3. Items weighing more than 1000 pounds shall be subjected to a dynamic analysis. Items weighing more than 1000 pounds and with a ratio of 4 to 1 or greater between structural strength of tie down and limit load, as defined in paragraph 2, are exempt from dynamic analysis.

Equipment that is to be in use for not longer than eight hours in close proximity to, or supporting SSV elements, are exempt from these requirements.

Equipment that is mounted on casters or wheels shall have lockable casters/wheels, and shall further, be rigidly tied to primary or substantial secondary structure.

TABLE 16.2 BUILDING CHARACTERISTIC  
CONSTANTS

	K	h (ft)	T (sec)
MST	0.8	275	1.23
PCR	0.8	160	0.93
AT	0.8	192	0.61

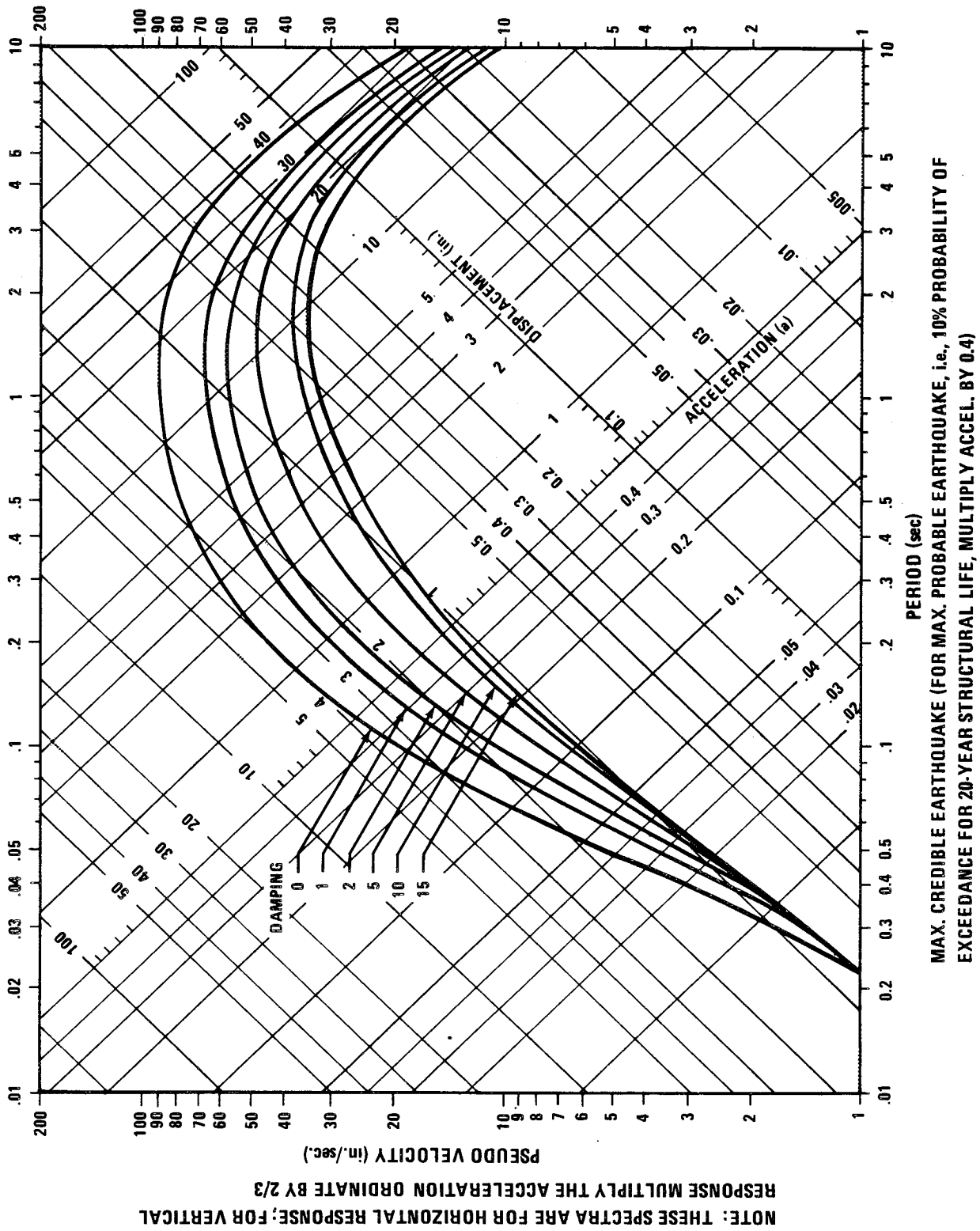


Figure 16.7 0.70E elastic design spectra for strongest potential vibratory ground motion.

ORIGINAL PAGE IS  
OF POOR QUALITY

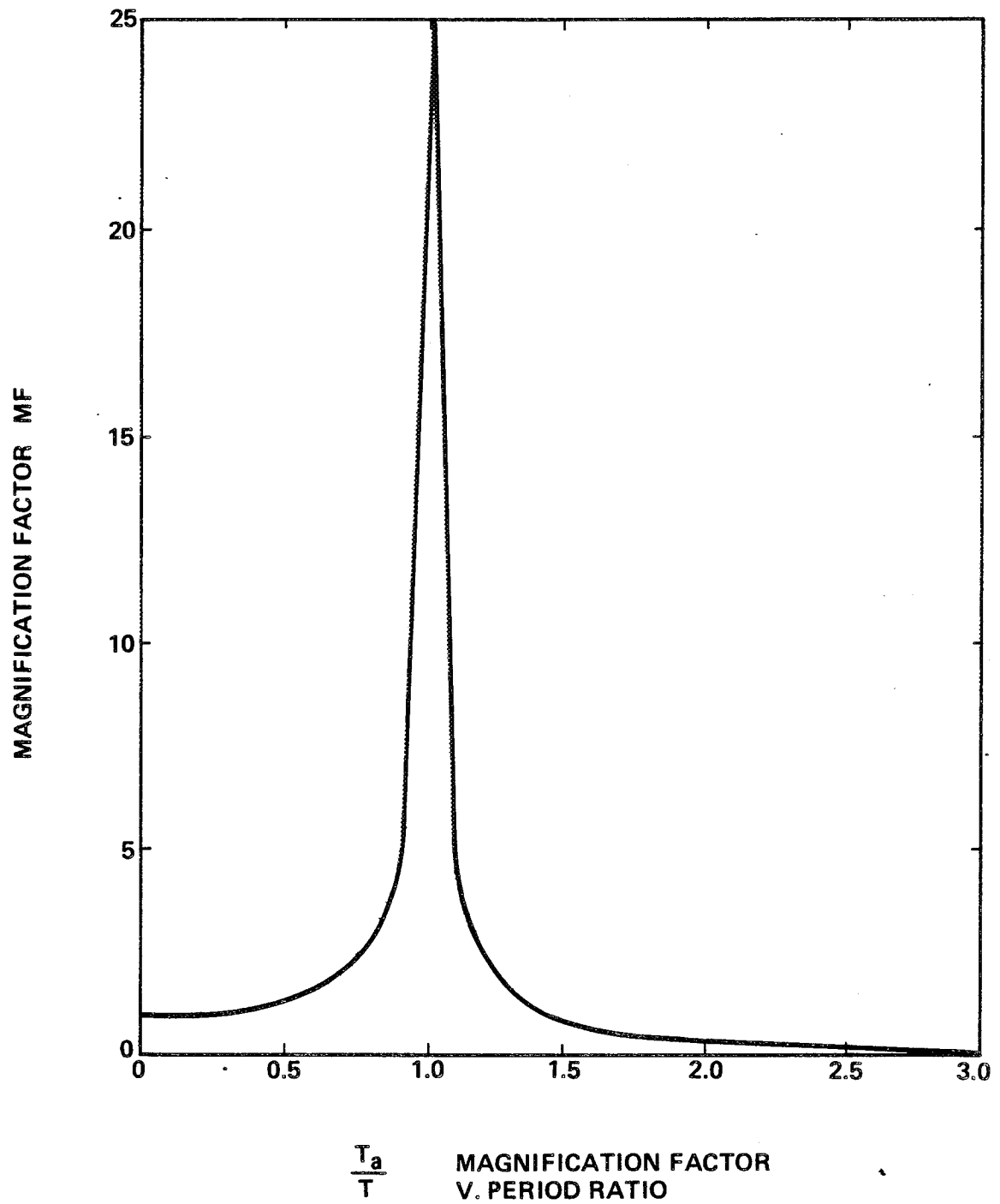


Figure 16.8 Magnification factor versus period ratio.



ORIGINAL PAGE IS  
OF POOR QUALITY

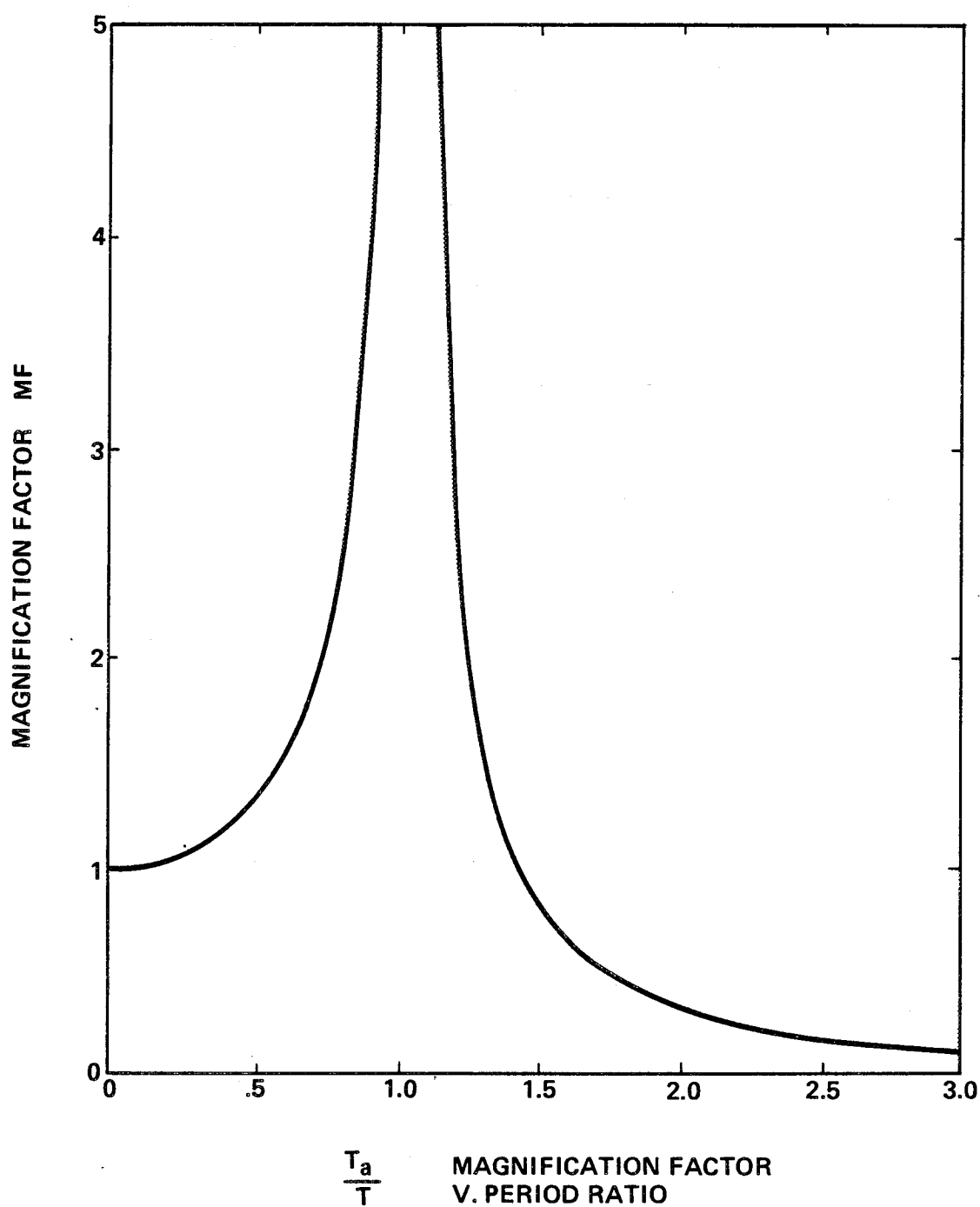


Figure 16.9 Magnification factor versus period ratio.

## REFERENCES

- 16.1 Van Dorn, W. G.: "Source Mechanism of the Tsunami of March 27, 1964." Alaska: Coastal Eng. Conf., 9th, Lisbon, 1964 Proc., pp. 166-190, 1964.
- 16.2 Tank, R. W., ed.: "Earthquake Activity." Focus on Environmental Geology (R. W. Tank, ed.), Oxford University Press, New York, pp. 36-118, 1973.
- 16.3 Ruhe, R. V.: Geomorphology. Houghton Mifflin Co., Boston, Mass., pp. 99-123, 1975.
- 16.4 Rogers, W. P., et al.: "Guidelines and Criteria for Identification and Land Use Controls of Geologic Hazard and Mineral Resource Areas." Colo. Geol. Survey Special Pub. No. 6, pp. 68-76, 1974.
- 16.5 James, D. E., Jr., and Holtz, W. G.: "Expansive Soils — The Hidden Disaster." Civil Eng., 43, No. 8, 1973.
- 16.6 Dibblee, T. W., Jr.: "Geology of the Rogers Lake and Kramer Quadrangle." U. S. Geol. Survey Bull. 1089-B, pp. 73-139, 1960.
- 16.7 Droste, J. B.: "Clay Minerals in the Playa Sediments of the Mojave Desert, California." California Div. Mines Special Report 69, 1961.
- 16.8 Mortan, D. M.: "Geologic Hazards in Southwestern San Bernardino County, California." California Div. Mines and Geol. Special Report 113, 1976.
- 16.9 Real, C. R., et al.: "Earthquake Epicenter Map of California, 1900-1974." California Div. Mines and Geol. MS 39, 1978.
- 16.10 Radbruch, D. H., and Crowther, K. C.: Maps showing areas of estimated relative amounts of landslides in California. U. S. Geol. Survey Misc. Geol. Inv. Map 747, 1973.
- 16.11 Jennings, C. W.: Santa Maria Sheet, Geologic Map of California. California Div. of Mines, 1:125,000, 1959.
- 16.12 Arnold, R., and Anderson, R.: "Geology and Oil Resources of the Santa Maria Oil District, Santa Barbara County, California." U. S. Geol. Survey Bull. 322, map (1:125,000), 1907.
- 16.13 Scott, T. M.: Orlando Sheet, Environmental Geology Series. Florida Geol. Survey MS 85, 1978.

## BIBLIOGRAPHY

Earthquakes

1. Allen, C. R., 1975, Geologic criteria for evaluating seismicity: Geol. Soc. Amer. Bull. 86, 1041-1057.
2. Bonilla, M. G., 1967, Historic surface faulting in continental United States and adjacent parts of Mexico: U. S. Geol. Survey of Report, 36 p.
3. Eckel, E. B., 1970, The Alaska earthquake, March 27, 1964: Lessons and conclusions: U. S. Geol. Survey Prof. Paper 546, 57 p.
4. Slemmons, D. B., 1977, State-of-the-art for assessing earthquake hazards in the United States: Report 6 – Faults and earthquake magnitude: U. S. Army Corps of Engineers, Waterways Experiment Station, Misc. Paper S-73-1, 166 p.

Tsunamis and Seiches

1. Bascom, W., 1964, Waves and Beaches: Garden City, N. Y., Anchor Books, Doubleday and Co., Inc., 267 p. (Chapters 5 and 6).
2. McCulloch, D. S., 1966, Slide-induced waves, seiching and ground fracturing caused by the earthquake of March 27, 1964, at Kenai Lake, Alaska: U. S. Geol. Survey Prof. Paper 543-A.
3. U. S. Coast and Geodetic Survey, 1965, The Story of the Seismic Sea Wave Warning System: U. S. Dept. of Commerce, U. S. Government Printing Office, 46 p.

Slope Processes

1. Coates, D. R., 1977, Landslides: Geol. Soc. Amer. Rev. Eng. Geol. 3.
2. Eckel, E. B., ed., 1958, Landslides and engineering practices: National Research Council, Highway Res., Board Spec. Report 29, 232 p.
3. Jackson, C., ed., 1973, Geology Today: Del Mar, Calif., Communications Research Books, 527 p. (300-304).
4. Sharpe, C. F. S., 1938, Landslides and Related Phenomena: New York, Columbia Univ. Press.
5. Verhoogen, J., Turner, F. J., Weiss, L. E., and Wahrhaftig, C., 1970, The Earth: and Introduction to Physical Geology, New York, Holt, Rinehart and Winston, Inc., 748 p. (327-333).

Floods

1. Bue, C. D., 1967, Flood information for floodplain planning: U. S. Geol. Surv. Circ., 539, 10 p.
2. Leopold, L. B., Wolman, M. G., and Miller, J. P., 1964: Fluvial processes in geomorphology: W. H. Freeman, San Francisco, Calif., 522 p.

3. Ruhe, R. V., 1975, *Geomorphology*: Houghton Mifflin Co., Boston, 47-98.
4. Strahler, A. N. and A. T., 1973, *Environmental geoscience*: John Wiley & Sons, Inc. (Hamilton Publ. Co.) Santa Barbara, Calif., 327-336.

#### Volcanic Hazards

1. Bolt, B. A., et al., 1975, *Geologic Hazards*: New York, Springer-Verlag, 328 p (chapter on evaluation of volcanic hazards).
2. Mullineaux, D. R., 1976, Preliminary map of volcanic hazards in the conterminous United States: U. S. Geol. Survey Misc. Field Inv. MF-786, scale 1:7,500,000.
3. Tank, R. W., ed., 1973, *Volcanism*, in Tank, R. W., ed., *Focus on Environmental Geology*: New York, Oxford University Press, 474 p.

#### Ground Subsidence

1. Allen, A. S., 1969, Geologic settings of subsidence: *Geol. Soc., Amer. Rev. Eng. Geol.*, 2, 305-342.
2. Forrester, F., 1974, Land subsidence in Utgard, R. O., and McKenzie, G. D., eds., *Man's Finite Earth*: Minneapolis, Minn., Burgess Pub. Co., 368p (199-202).
3. Hoffmaster, B. N., 19, *Subsidence: its effects and remedies*: Long Beach Harbor Dept., Long Beach, Calif.
4. Lofgren, B. E., 1969, Land subsidence due to the application of water: *Geol. Soc. Amer. Rev. Eng. Geol.* 2, 271-303.
5. Mayuga, M. N., and Allen, D. R., 1966, Long Beach Subsidence in Lung, and Proctor, eds., *Engineering Geology in Southern California*, 281-285.
6. Poland, J. F., 1969, Land Subsidence in Western United States in Olson and Wallace, eds., *Geologic Hazards and Public Problems*, May 27-28 Conference Proceedings, U. S. Gov't Printing Office, 77-96.
7. Rogers, W. P., et al., 1974, Guidelines and criteria for identification and land use controls of geologic hazard and mineral resource areas: *Colo. Geol. Survey Spec. Pub. No. 6*, 145 p. (61-67).

#### General

1. Cooke, C. W., 1945, *Geology of Florida*: Florida Geol. Survey Bull. 29.
2. Fife, D. L., et al., 1976, Geologic hazards in southwestern San Bernardino County, CA: Calif. Div. Mines and Geol. Special Report 113, plate 7, Earthquake epicenters in southern California, 1910-1917.
3. Shampine, W. J., 1963, Quality of Water from the Floridan Aquifer in Brevard Co., Florida: Florida Geol. Survey MS 17.
4. Woodring, W. P. and Bramlette, M. N., 1950, *Geology and paleontology of the Santa Maria District, CA*: U. S. Geol. Survey Prof. Paper 222, 185 pp and maps.

## SECTION XVII. AEROSPACE VEHICLE EFFLUENT DIFFUSION MODELING FOR TROPOSPHERIC AIR QUALITY AND ENVIRONMENTAL ASSESSMENTS

### 17.1 Introduction

NASA, and particularly MSFC, has pursued the development of computerized dispersion models for predicting the behavior of rocket exhaust clouds in the troposphere since the mid 1960's. These models are routinely used to assess the environmental impact of exhaust products from rocket engines with respect to air quality standards, toxicity thresholds, and potential bio-ecological effects and to evaluate requirements, if any, for launch constraints. The concept of using generalized multilayer dispersion models for these applications was first outlined in 1969 in Reference 17.1, and the models have been continuously updated and improved since that time (Refs. 17.2-17.5). In 1973, a joint program for rocket exhaust prediction and launch monitoring was initiated by NASA for all Titan launches from KSC. In this program, MSFC had the responsibility of supplying dispersion predictions, LaRC had responsibility for making concentration measurements of rocket exhaust products at the surface and aloft through the use of aircraft sampling techniques, and KSC provided local support for these activities. This program revealed the need for the development of a real-time dispersion prediction capability (Refs. 17.4-17.6), and the results of the program provided measurements for use in verifying the accuracy of model predictions (Ref. 17.7-17.11) as well as a data base which could be used in making model improvements.

The details of the current version of the Rocket Exhaust Effluent Diffusion (REED) code, which has been used to assess the environmental impact of Space Shuttle operations and to support the first two launches of the Space Shuttle, are described in subsection 17.2. The toxicity criteria relevant to exhaust products of solid rocket motors are given in subsection 17.3.

### 17.2 The NASA/MSFC REED Code

The burning of rocket engines during the first few seconds prior to and immediately following vehicle launches results in the formation of a large cloud of hot, buoyant exhaust products near ground level which subsequently rises and entrains ambient air until the temperature and density of the cloud reach an approximate equilibrium with ambient conditions. By convention, this cloud is referred to as the ground-cloud. The rocket engines also leave an exhaust trail from normal launches which extends throughout the depth of the troposphere. The NASA/MSFC REED code is designed to calculate peak concentration, dosage, and deposition (resulting from both gravitational settling and precipitation scavenging) downwind from normal launches and launch aborts for use in:

1. Mission planning activities and environmental assessments
2. Prelaunch forecasts of the environmental effects of launch operations
3. Postlaunch environmental analysis.

#### 17.2.1 Overview of the REED Code

Figure 17.1 is a schematic diagram showing the major components of the REED computer program. Requisite meteorological inputs to the computer program are obtained from the vertical profiles of wind direction, wind speed, air temperature, atmospheric pressure, and dew point or relative humidity between

17.2

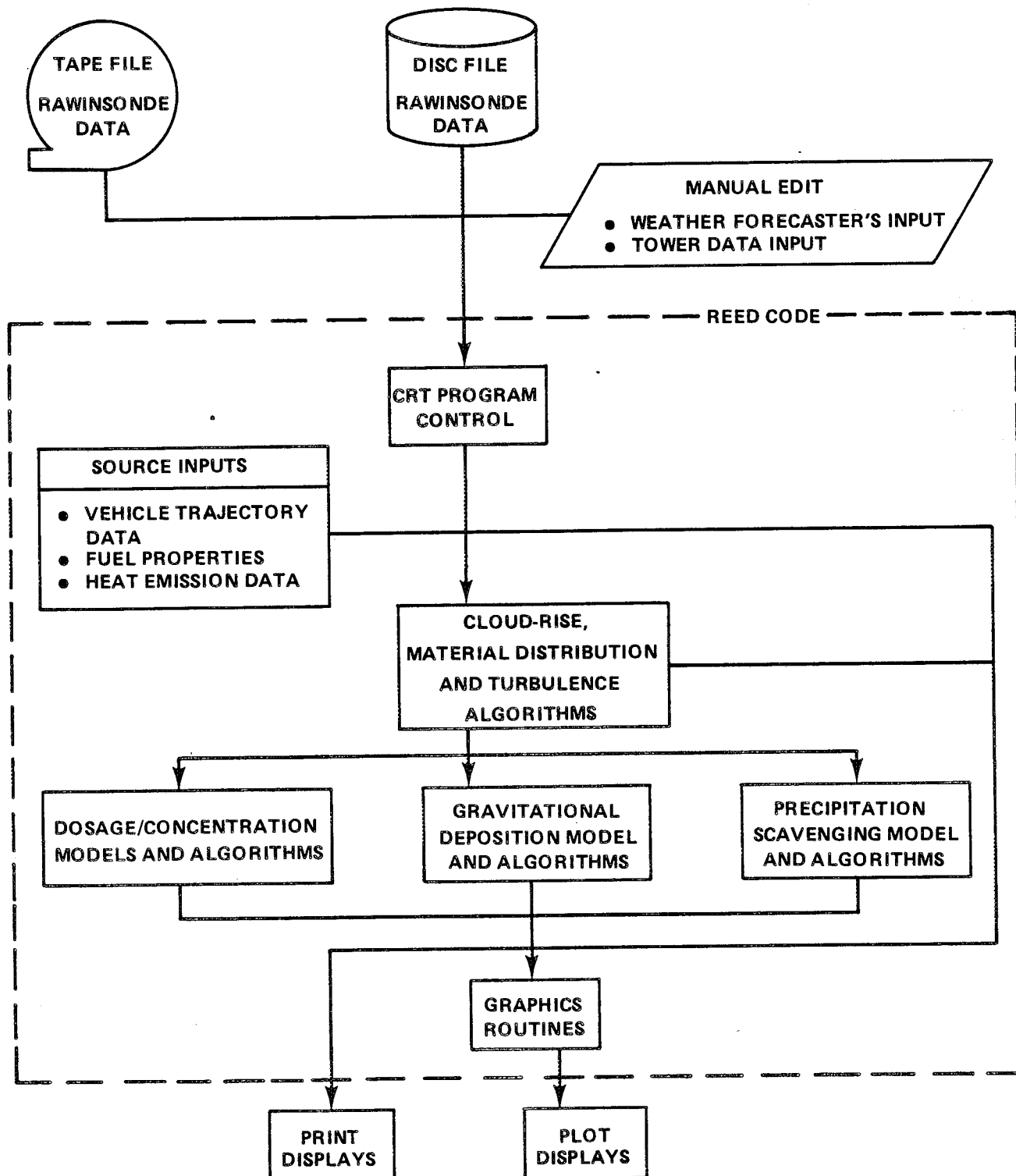


Figure 17.1 Schematic diagram illustrating major components of the REED computer program.

the Earth's surface and 3000 m. This information is obtained during launch support activities from rawinsonde measurements routinely made at scheduled times throughout the prelaunch countdown and after the launch has occurred. The REED program accepts the rawinsonde data from either a disc or data tape file. As shown in Figure 17.1, the rawinsonde data file can be manually edited to provide for any changes in the vertical profiles that weather forecasters assigned to the launch support team expect to occur between the time of the latest available rawinsonde measurements and the projected time of launch. Similarly, the meteorological inputs for the layers near the surface may also be manually adjusted to reflect changes in the low-level data available from the Wind System. The Wind System is a series of 30-m towers located throughout KSC and one 152-m meteorological tower instrumented to measure wind direction, wind speed, turbulence, and air temperature.

The REED program is controlled by operator input and internal management routines based on operator response to plain-language queries displayed on a CRT terminal. In Figure 17.1, this complex interactive function is simply designated by CRT Program Control. Once the operator has elected to perform calculations for the launch of a particular vehicle (for example, the Space Shuttle, Titan, or Delta Thor) and designated a normal launch or one of two launch-abort modes, the program automatically selects a proper set of source inputs for use in algorithms designed to calculate the following parameter values:

- Position in space of the rising ground cloud as a function of time after launch until the internal cloud temperature equals the ambient air temperature (cloud stabilization time)
- Dimensions of the ground cloud as a function of height
- Distribution of vehicle exhaust products within the cloud as a function of height.

At this point, the rawinsonde meteorological data, cloud-rise, cloud dimension, and exhaust-product distribution calculations are output to a printer and, if desired by the operator, also output to a plotted display of the vertical profiles of wind direction, wind speed, temperature, and virtual potential temperature as well as the dimensions of the stabilized cloud. The operator then has the option of modifying the default values selected and calculated by the program to represent the major meteorological layer structure parameters (the height of the base and top of the elevated inversion layer, for example) and the turbulence parameters that will be used in the dispersion calculations.

After the final selection of model input parameters has been made by the operator, the program performs the selected type of calculations (dosage/concentration, gravitational deposition, or deposition due to precipitation scavenging, etc.). When these calculations are completed, the results are printed and, at the operator's option, plotted. If the dosage/concentration option was selected, the print output includes peak concentration at 1-km intervals downwind from the launch pad, the cloud arrival and departure times at 1-im intervals downwind from the pad, and the total dosage and time-mean concentration for the period of interest at these distances. The operator has the option of requesting the REED program to plot these results versus distance from the pad and/or isopleths of these quantities on a map of KSC. The print output for the gravitational deposition model contains maximum ground-level deposition versus distance from the pad. If selected by the operator, plots are made of maximum gravitational deposition versus distance from the pad and of deposition isopleths on a map of KSC. Finally, if the operator chooses to calculate deposition due to precipitation scavenging, maximum deposition, or maximum surface water, pH is also printed and plotted.

Although not shown in Figure 17.1, there are three major run modes that an operator can choose for making calculations with the REED code (operational, research, and production). The operational mode is designed for use during launch support operations and automatically calculates various user inputs. For example, in the operational mode, the REED code uses an algorithm to calculate appropriate turbulence

parameters near the surface, although an option is provided permitting the operator to modify the values. Either the values calculated by the REED code or the operator input values are then used to automatically construct a vertical profile of turbulence for the first 3000 m above the surface which is used in the dispersion calculations. When the research mode of the REED code is selected, more information is usually input by the operator. For example, the operator can specify values of the turbulence parameters at each height where rawinsonde data are available. Finally, the production mode of the REED code is used to process multiple rawinsonde soundings which are read from the tape or disc file. While the production mode can be run interactively from the CRT terminal, the primary purpose of the production mode is to facilitate batch processing of multiple cases without operator attention. The graphics package is not used with the production mode.

### 17.2.2 Launch Types and Vehicle Parameters

The REED code is designed to provide dispersion estimates for normal launches and two types of launch failures. For a normal launch, the assumption is made that all engines and the pad deluge system operate normally. In the case of a launch failure (single engine burn on pad), one solid engine of the Space Shuttle, Titan III, and Delta vehicles is assumed to fail to ignite, causing the vehicle to remain on the pad in a hold-down configuration while the other solid engine ignites and burns with the pad deluge system operating normally. In the other failure mode (slow burn on pad), an on-pad explosion is assumed to rupture the casings of the solid engines, scattering solid propellant over the area in the vicinity of the launch pad. The scattered solid propellant continues to burn over an extended period at a constant rate. It is assumed that the heat liberated by the explosion of liquid propellant (Space Shuttle and Delta Thor vehicles) does not contribute to plume rise because this heat is liberated over a very short time period compared to the burn time of the scattered solid propellant.

The fuel expenditure, heat content, and burn time data currently used in the REED code are presented in Table 17.1 (Ref. 17.12). The fuel expenditure rates for normal launches were obtained by averaging the fuel expenditure rates for the engines over the approximate period from lift-off until the vehicle is approximately 3000 m above the surface. The fuel expenditure rates for the single engine burn are an average for the normal firing period of the engine. For the slow burn, the rates in the table are an average over the estimated total burn time of the scattered propellants. The effective fuel heat contents, which are used in calculating buoyant cloud rise for normal launches and plume rise for launch failures, include the effects of heat produced by afterburning as well as heat losses due to radiation.

Table 17.2 shows the exhaust cloud constituents expressed as a fraction of the total weight of the exhaust products. These fractions have been adjusted to yield the weight of HCl,  $\text{Al}_2\text{O}_3$ ,  $\text{CO}_2$ , and CO in the exhaust cloud when multiplied by the appropriate fuel expenditure rates in Table 17.1.

The cloud-rise and dispersion calculations for normal launches require specification of the time-height profile of the launch vehicle. The vehicle flight profile data for the first 3000 m above the surface were used to obtain a least-squares fit to the expression

$$T_k = az^b + c \quad , \quad (17.1)$$

where

$T_k$  = time for the vehicle to reach the altitude  $z$ .

The values thus obtained (Ref. 17.12) for the constants  $a$ ,  $b$ , and  $c$  in Equation (17.1) are given in Table 17.3.



TABLE 17.1 FUEL EXPENDITURE AND HEAT CONTENT DATA

Vehicle Type				
Property	Space Shuttle	Titan III	Delta 2914	Delta 3914
(a) Normal Launch				
Fuel Expenditure Rate $W$ ( $\text{g s}^{-1}$ )	$1.5219 \times 10^7$	$5.4375 \times 10^6$	$8.3607 \times 10^5$	$1.0576 \times 10^6$
Effective Fuel Heat Content $H$ ( $\text{cal g}^{-1}$ )	1479.1	2021.1	1766.0	1449.9
(b) Single Engine Burn				
Fuel Expenditure Rate $W$ ( $\text{g s}^{-1}$ )	$3.8451 \times 10^6$	$2.7188 \times 10^6$	NA <sup>1</sup>	NA
Effective Fuel Heat Content $H$ ( $\text{cal g}^{-1}$ )	1062.4	1010.6	NA	NA
Burn Time $t_B$ (s)	132.0	60.0		
(c) Slow Burn				
Fuel Expenditure Rate $W$ ( $\text{g s}^{-1}$ )	$9.8873 \times 10^5$	$1.3594 \times 10^6$	$2.7294 \times 10^5$	$3.7073 \times 10^5$
Effective Fuel Heat Content $H$ ( $\text{cal g}^{-1}$ )	1000.0	1000.0	690.0	411.2
Burn Time $t_B$ (s)	1027.0	240.0	69.0	126.0

1. NA – Not applicable.

TABLE 17.2 EXHAUST CLOUD CONSTITUENTS (FRACTION BY WEIGHT)

Constituent	Vehicle Type			
	Space Shuttle	Titan III	Delta 2914	Delta 3914
HCl	0.1146	0.1932	0.1218	0.1589
Al <sub>2</sub> O <sub>3</sub>	0.1828	0.2819	0.2214	0.1936
CO <sub>2</sub>	0.2503	0.2665	0.2055	0.2783
CO	0.00042	0.0222	0.0156	0.0331

TABLE 17.3 VALUES OF THE CONSTANTS IN THE EXPRESSION FOR VEHICLE ALTITUDE VERSUS TIME<sup>1</sup>

Vehicle	Constant		
	a	b	c
Space Shuttle	0.652213	0.468085	0.375
Titan III	0.429580	0.518422	5.0
Delta 2914	0.922156	0.432703	0.54
Delta 3914	1.245756	0.418095	0

1. See Equation (17.1).

### 17.2.3 Meteorological Layers

As noted previously, the primary meteorological input to the REED code is in the form of rawinsonde observations. Each level of information (standard, mandatory, and significant) in the rawinsonde data stream (kth observation level) is used in the REED calculations to obtain the wind and temperature profiles. The REED code is currently constructed to perform dispersion calculations in two major, meteorologically defined layers. The base of the lower layer ( $L=1$ ) is assumed to be at the Earth's surface and the top of the layer is assumed to be given by the base of an elevated inversion (top of the mixing layer). The boundaries of the upper layer ( $L=2$ ) are set by the operator. For example, if calculations are desired of dosage/concentration at the altitude of a sampling aircraft flying in an elevated inversion, the boundaries of the upper layer are defined by the base and top of the elevated inversion.

The selection of the boundaries of the two major layers is critical to the outcome of the dispersion calculations. Both gases (vapor) and particulates ( $Al_2O_3$ ) are assumed to be reflected toward the Earth's surface at the tops of major boundaries. Vapor and particulates can be totally or partially reflected at the base of the lower layer according to a user-specified input for the fraction of material reflected (1=complete reflection, 0=no reflection). Material is never reflected at the base of the upper layer when gravitational settling or precipitation scavenging calculations are made, but gases are always reflected at the base of the upper layer. Thus, gases are assumed to be trapped in the upper layer for dosage/concentration calculations. The boundaries of these two major layers are also used in the determination of vertical turbulence profiles, as explained below in subsection 17.2.6.

### 17.2.4 REED Code Cloud and Plume Rise Models

The determination of the stabilized height of the ground cloud for normal launches and of the plume generated by launch failures is an important factor in the dosage/concentration calculations because, in general, the maximum dosage/concentration calculated at the Earth's surface is inversely proportional to the cube of the stabilized height. In the case of normal launches of solid-fueled vehicles or vehicles with large solid boosters, vehicle hold-down times are minimal and the vehicle residence times in the first several hundred meters are relatively short. The ground cloud is therefore composed of buoyant gas emitted over a time period on the order of 10 sec. Experience to date shows that the buoyant rise of a ground cloud under these circumstances is best calculated using an instantaneous cloud-rise model. Limited experience in predicting the buoyant rise from the normal launch of Delta vehicles, with their large liquid-fueled first stage, indicates that an average of the rise predicted by a continuous plume-rise and instantaneous cloud-rise model is appropriate. No plume rise data are available for aborted launches of the vehicle types specified in the REED code. However, static tests of rocket engines indicate a continuous plume rise model is appropriate in these cases.

The buoyant rise models used in the REED program are based on the work of Briggs (Refs. 17.13 and 17.14).

#### 17.2.4.1 Instantaneous Cloud-Rise Model

The time for the ground-cloud produced by the normal launch of the Space Shuttle and Titan vehicles to reach a height  $z_k$  in a stable atmosphere is given by

$$t_I = s^{-0.5} \arccos \left[ 1 - \left( \frac{s \gamma_x \gamma_y \gamma_z z_k^4}{4 F_I} \right) \right] \quad (17.2)$$

where  $t_I$  is constrained to be less than the cloud stabilization time  $t^*$  and

$$t^* = \pi s^{-0.5} \quad (17.3)$$

$$s = \text{stability parameter} = \frac{g}{T} \frac{\Delta \Phi}{\Delta z}$$

$g$  = gravitational acceleration ( $9.8 \text{ m s}^{-2}$ )

$T$  = ambient air temperature ( $^{\circ}\text{K}$ )

$\frac{\Delta \Phi}{\Delta z}$  = vertical gradient of virtual potential temperature

$\gamma_x, \gamma_y, \gamma_z$  = alongwind, crosswind, and vertical entrainment coefficients

$F_I$  = initial buoyancy term

$$= \frac{3 g H W t_R}{4 \pi c_p T} \quad (17.4)$$

$H$  = effective fuel heat content ( $\text{cal g}^{-1}$ )

$W$  = fuel expenditure rate ( $\text{g s}^{-1}$ )

$t_R$  = time for the rocket to exceed the final cloud stabilization height  $z_I$

$$= a z_I^b + c \quad (17.5)$$

$\rho$  = air density ( $\text{g m}^{-3}$ )

$c_p$  = specific heat of air at constant pressure ( $0.24 \text{ cal g}^{-1} \text{ }^{\circ}\text{K}^{-1}$ )

$$z_I = \left[ \frac{8 F_I}{\gamma_X \gamma_Y \gamma_Z s} \right]^{1/4} \quad (17.6)$$

According to the preceding formulas, the quantities  $z_I$ ,  $t_R$ , and the height, over which  $\Delta\Phi/\Delta z$  is measured, are interrelated. The final cloud stabilization height  $z_I$  in Equation (17.6) must therefore be found by iteration. The iteration process begins by assuming that  $z_I$  lies in the first height interval ( $K=1$ ) above the surface bounded by the rawinsonde observation heights  $k=1$  and  $k=2$  and solving Equation (17.6) for  $z_I$  with

$$\frac{\Delta\Phi}{\Delta z} = \frac{\Phi_2 - \Phi_1}{z_2 - z_1}$$

If  $z_I$  exceeds  $z_2$ , the iteration continues, using the virtual potential temperature from the next highest  $k$ th observation level with the vertical gradient  $\Delta\Phi/\Delta z$  estimated from the least-squares approximation

$$\frac{\Delta\Phi}{\Delta z} = \frac{\sum_{i=1}^k \left\{ \left[ z_i - \left( \sum_{i=1}^k z_i/k \right) \right] \left[ \Phi_i - \left( \sum_{i=1}^k \Phi_i/k \right) \right] \right\}}{\sum_{i=1}^k \left[ z_i - \left( \sum_{i=1}^k z_i/k \right) \right]^2} \quad (17.7)$$

Providing that  $z_I < 3000$  m, the program finds a value of  $z_I$  within an interval ( $z_{i-1} \leq z_I \leq z_i$ ). At this point the program assumes that the gradient of virtual potential temperature in this height interval is linear and linearly interpolates to determine, within  $\pm 10$  m, the value of  $z_I$ .

The preceding cloud-rise model was theoretically derived for a thermally stable atmosphere ( $\Delta\Phi/\Delta z > 0$ ). A model based on similar considerations is easily derived for an adiabatic atmosphere. The cloud continues to rise over all time when this model is used, although the rate tends to approach zero asymptotically at long times. Experience shows that the height at which the rate of rise determined from the adiabatic model becomes negligible for practical purposes can be predicted using a small value of  $\Delta\Phi/\Delta z$  in the stable model. For this reason, the program sets  $\Delta\Phi/\Delta z$  equal to  $3.322 \times 10^{-4}$ . The program currently uses a default value of 0.64 for  $\gamma_X$ ,  $\gamma_Y$ , and  $\gamma_Z$ .

#### 17.2.4.2 Continuous Plume-Rise Model

The time for a continuous plume to reach the height  $z_R$  in a stable atmosphere is given by

$$t_c = s^{-0.5} \arccos 1 \left[ - \frac{s \bar{u}_c \gamma_x \gamma_y z_k^4}{3 F_c} \right] , \quad (17.8)$$

where  $t_c$  is constrained to be less than  $t^*$  given by Equation (17.3) and

$F_c$  = buoyancy flux

$$= \frac{g H W}{\pi \rho c_p T} \quad (17.9)$$

$\bar{u}_c$  = height-weighted mean wind speed between the surface and the stabilization height  $z_c$

$$z_c = \left( \frac{6 F_c}{\bar{u}_c \gamma_x \gamma_y s} \right)^{1/3} \quad (17.10)$$

As in the case of the instantaneous cloud-rise model, Equation (17.10) must be solved by iteration because  $\Delta\Phi/\Delta z$ ,  $z_c$ , and  $\bar{u}_c$  are interrelated. Also, the value of  $\Delta\Phi/\Delta z$  is set equal to  $3.322 \times 10^{-4}$  deg/m when the value calculated from Equation (17.7) is less than  $3.322 \times 10^{-4}$  (adiabatic atmosphere). For the continuous plume-rise model, the program default value for  $\gamma_x$  and  $\gamma_y$  is 0.5.

#### 17.2.5 Source Dimensions, Material Distribution, and Spatial Position of the Stabilized Ground-Cloud

The dispersion models are derived under the assumption that a vertical finite line source can be used to represent the source of material in each of the  $K$  layers defined by the rawinsonde measurement levels and that the alongwind ( $r_x$ ), crosswind ( $r_y$ ), and vertical ( $r_z$ ) radii of the cloud at the stabilization time  $t^*$  are consistent with the cloud-rise model, e.g.:

$$r_x = \gamma_x z_M$$

$$r_y = \gamma_y z_M \quad (17.11)$$

$$r_z = \gamma_z z_M ,$$

where

$$z_M = \begin{cases} z_I & ; \text{ instantaneous source} \\ z_C & ; \text{ continuous source} \end{cases} \quad (17.12)$$

Under these assumptions, the alongwind radius of the cloud in the Kth layer is

$$R_{xK} = \left[ r_x \left( 1 - \frac{z_o^2}{r_z^2} \right) \right]^{1/2}, \quad (17.13)$$

and the crosswind radius is

$$R_{yK} = \left[ r_y \left( 1 - \frac{z_o^2}{r_z^2} \right) \right]^{1/2}, \quad (17.14)$$

where

$$z_o = |\bar{z} - z_M| \quad (17.15)$$

$$\bar{z} = (z_{TK} + z_{BK})/2 \quad (17.16)$$

$z_{TK}$  = height of the top of the Kth layer

$z_{BK}$  = height of the base of the Kth layer

#### 17.2.5.1 Source Dimensions

For a normal launch, the source dimensions in the plane of the horizon are defined in terms of the standard deviations of the material distribution. For the source in the Kth layer, these dimensions are as follows:

Alongwind:

$$\sigma_{xO}\{K\} = \left\{ \begin{array}{ll} 0 & ; 0 < \bar{z} \leq (z_M - r_z) \\ R_{xK}/2.15 & ; (z_M - r_z) < \bar{z} \leq (z_M + r_z) \\ 93 \text{ m} & ; (z_M + r_z) < \bar{z} \end{array} \right\} , \quad (17.17)$$

Crosswind:

$$\sigma_{yO}\{K\} = \left\{ \begin{array}{ll} 0 & ; 0 < \bar{z} \leq (z_M - r_z) \\ R_{yK}/2.15 & ; (z_M - r_z) < \bar{z} \leq (z_M + r_z) \\ 93 \text{ m} & ; (z_M + r_z) < \bar{z} \end{array} \right\} , \quad (17.18)$$

under the assumption that the distribution of material in the plane of horizon is bivariate Gaussian and that the concentration of exhaust products at one radius from the centroid is 10 percent of the concentration at the centroid.

For launch failures, the corresponding dimensions in the horizontal plane are:

$$\sigma_{xO}\{K\} = \left\{ \begin{array}{ll} 50/2.15 & ; 0 < \bar{z} \leq (z_M - r_z) \\ R_{xK}/2.15 & ; (z_M - r_z) < \bar{z} \leq (z_M + r_z) \\ 0 & ; z_M + r_z \end{array} \right\} , \quad (17.19)$$

$$\sigma_{yO}\{K\} = \left\{ \begin{array}{ll} 50/2.15 & ; 0 < \bar{z} \leq (z_M - r_z) \\ R_{yK}/2.15 & ; (z_M - r_z) < \bar{z} \leq (z_M + r_z) \\ 0 & ; (z_M + r_z) < \bar{z} \end{array} \right\} . \quad (17.20)$$

#### 17.2.5.2 Material Distribution

For normal launches, the distribution of material within the ellipsoid with axes given by Equation (17.11) is assumed to be uniform in the vertical. Under this assumption, the amount of material  $F\{K\}$  in the  $K$ th layer is given by



$$F\{K=k-1\} = \left\{ \begin{array}{ll} W(\text{FM}) t_k/V_k & ; z_{\text{TK}} < z_M \\ W(\text{FM}) \left( \frac{t_R}{V_K} + \Delta t_K \right) & ; z_M < z_{\text{TK}} \leq z_M (1 + \gamma_z) \\ W(\text{FM}) \Delta t_k & ; z_M (1 + \gamma_z) < z_{\text{TK}} \end{array} \right\} , \quad (17.21)$$

where

FM = fraction of weight of the exhaust cloud constituent from Table 17.2

$$\Delta t_k = a \left( z_{\text{TK}}^b - z_{\text{BK}}^b \right) \quad (17.22)$$

$V_K$  = cloud volume in the Kth layer

$$= \pi r_x r_y \left\{ (z_{\text{TK}} - z_{\text{BK}}) - \left[ \frac{(z_{\text{TK}} - z_M)^3 - (z_{\text{BK}} - z_M)^3}{3 r_z^2} \right] \right\} . \quad (17.23)$$

For launch failures, the program assumes that the material has a Gaussian distribution in the vertical about the stabilization height  $z_M$ . Thus,

$$F\{K=k-1\} = W(\text{FM}) t_B \left[ P\{z_{\text{TK}}\} - P\{z_{\text{BK}}\} \right] , \quad (17.24)$$

where

$t_B$  = burn time from Table 17.1

$$P\{z\} = \frac{2.15}{\sqrt{2\pi} r_z} \int_{-\infty}^z \exp \left[ -\frac{1}{2} \left( \frac{2.15(z-z_M)}{r_z} \right)^2 \right] dz . \quad (17.25)$$

### 17.2.5.3 Spatial Position of the Stabilized Cloud

The spatial position in the plane of the horizon of the cloud in the Kth layer at the stabilization time  $t^*$ , with respect to the origin at the launch pad, is assumed to be given by the following polar coordinates:

$$R_{CK} = \left\{ \left[ x_K + \bar{u}_K(t^* - t_p) \sin \bar{\theta}_K \right]^2 + \left[ y_K + \bar{u}_K(t^* - t_p) \cos \bar{\theta}_K \right]^2 \right\}^{1/2}, \quad (17.26)$$

$$\theta_{CK} = \pi/2 - \tan^{-1} \left[ \frac{y_K + \bar{u}_K(t^* - t_p) \sin \bar{\theta}_K}{x_K + \bar{u}_K(t^* - t_p) \cos \bar{\theta}_K} \right], \quad (17.27)$$

where

$$x_K = x_{K-1} - \xi_K \sin(\Phi_{sK}) \quad (17.28)$$

$$y_K = y_{K-1} - \xi_K \cos(\Phi_{sK}) \quad (17.29)$$

$\bar{u}_K$  = mean wind speed in the Kth layer

$$t_p = \begin{cases} t_I\{z = z_{TK}\} & ; \text{ instantaneous cloud-rise model} \\ t_c\{z = z_{TK}\} & ; \text{ continuous cloud-rise model} \end{cases} \quad (17.30)$$

$\bar{\theta}_K$  = mean wind direction in the Kth layer.

For layers below the Kth layer containing  $z_M$ ,

$$\xi_K = t_p \bar{u}_K, \quad (17.31)$$

$$\Phi_{sK} = \bar{\theta}_K. \quad (17.32)$$

For an instantaneous source, the value of  $\xi_K$  in the Kth layer containing  $z_M$  is

$$\xi_K = \left[ \bar{u}_K \left( \frac{z_M - z_{BK}}{z_{TK} - z_{BK}} \right) + u_k \right] \left[ t_R - t_{I,k} \right]. \quad (17.33)$$

Similarly, for a continuous source,

$$\xi_K = \left\{ \frac{t_R - t_{c,k}}{z_m} \right\} \left\{ \left[ \bar{u}_K \left( \frac{z_M - z_{TK}}{z_{TK} - z_{BK}} \right) + u_k \right] [z_M - z_{BK}] + \sum_{i=1}^k [z_{i+1} - z_i] \left[ \frac{u_{i+1} + u_i}{2} \right] \right\} . \quad (17.34)$$

The value of  $\Phi_{sK}$  is

$$\Phi_{sK} = \frac{1}{2} \left[ \left( \frac{\theta_{k+1} - \theta_k}{z_{TK} + z_{BK}} \right) (z_M - z_{BK}) + 2 \theta_k \right] \quad (17.35)$$

for both the instantaneous and continuous sources.

For all K layers above  $z_M$  ( $z_{BK} < z_M$ ),

$$R_{CK} = t_R \bar{u}_K , \quad (17.36)$$

$$\theta_{CK} = \pi + \bar{\theta}_K . \quad (17.37)$$

#### 17.2.6 Turbulence Profile Algorithm

The REED dispersion model code uses profiles of the standard deviations of the azimuth wind angle  $\sigma_A'$  and elevation angle  $\sigma_E'$  as prime predictors of cloud growth. The program calculates default turbulence profiles, which can be adjusted by the program operator. The algorithm used to calculate the turbulence profiles begins by calculating a reference standard deviation of the wind azimuth angle  $\sigma_{AR}'\{\tau_o=600s\}$ , assumed representative of a measurement made over a 10-min period at the lowest height available from the rawinsonde data input (4.9 m at KSC).

##### 17.2.6.1 Calculation of the Default Value for $\sigma_{AR}'\{\tau_o=600s\}$

The calculation method (Ref. 17.12), based on the application of similarity relationships outlined in Ref. 17.15, assumes that

$$\sigma_{AR}'\{\tau_o=600s\} = \frac{\sigma_V\{600s\}}{\bar{u}} \simeq \frac{k_A f\{B\}}{\ln\left(\frac{\bar{z}}{z_o}\right) - \psi\{R_i\}} ; \quad R_i \neq 0 , \quad (17.38)$$

where

$\sigma_V$  = standard deviation of the crosswind component of the wind

$\bar{u}$  = mean wind speed at the measurement height of  $\sigma_V$

$\tau_0$  = reference time for the measurement of  $\sigma_{AR}'$  and  $\sigma_V$

$f\{B\}$  = function of the bulk Richardson number  $B$

$\bar{z}$  = geometric mean height of the layer of interest

$z_0$  = roughness length (0.20 m used for KSC)

$\psi\{Ri\}$  = function of the Richardson number  $Ri$ .

In the program, values of  $f\{B\}$  and  $\psi\{Ri\}$  are obtained from the expressions

$$f\{B\} = \left\{ \begin{array}{ll} 2.7 & ; B < -0.008 \\ 2.7 + 112 (0.008 + B) & ; -0.008 \leq B < -0.00175 \\ 3.4 - 725.5 (0.00175 + B) & ; -0.00175 \leq B < 0.0008 \\ 1.55 + 38.04 (B + 0.0008) & ; 0.0008 \leq B < 0.029 \\ 2.35 + 5.43 (B - 0.029) & ; 0.029 \leq B \end{array} \right\} \quad (17.39)$$

and

$$\psi\{Ri\} = \left\{ \begin{array}{ll} 2 \ln [(1+\xi)/2] + \ln [(1+\xi)^2/2] + 2 \tan^{-1} \xi + \pi/2 & ; Ri < 0 \\ 7Ri/(17Ri)^{1/4} & ; Ri > 0 \end{array} \right\}, \quad (17.40)$$

where

$$\xi = (1 - 16Ri)^{1/4}, \quad (17.41)$$

$$B = \frac{g \bar{z}^2}{T \bar{u}^2} \frac{\Delta\Phi}{\Delta\bar{z}}, \quad (17.42)$$

$\frac{\Delta\Phi}{\Delta\bar{z}}$  = vertical gradient of potential temperature over the height  $\bar{z}$

$$Ri = \left[ -\frac{1}{14 k_A \sqrt{B}} + \frac{1}{2} \sqrt{\frac{1}{49 k_A^2 B} + \frac{4(k_A+1)}{7 k_A}} \right]^2 ; Ri > 0, \quad (17.43)$$

For  $Ri < 0$ , the following equation is solved by Newton's method to obtain  $Ri$

$$0 = \frac{1 - \xi^4}{16^2 [\ln(z/z_0) + 0.050864 - 2[\ln(1+\xi)] - \ln(1+\xi^2) + 2\tan^{-1} \xi]} - B \quad (17.44)$$

Finally, for  $Ri=0$ ,  $\sigma_{AR}\{\tau_0=600s\}$  is calculated from the relationship

$$\sigma_{AR}\{\tau_0=600s\} = \frac{48.816}{\ln\left(\frac{z}{z_0}\right)} \quad ; \quad Ri = 0 \quad (17.45)$$

In no case does the program permit  $\sigma_{AR}\{\tau_0=600s\}$  to be greater than 0.524 radians (30 degrees).

#### 17.2.6.2 Vertical Profiles of $\sigma'_A$ and $\sigma'_E$

The dispersion models in the REED code use mean values of  $\sigma'_A$  and  $\sigma'_E$  in the two major layers ( $L=1,2$ ). In the case where the operator enters values of  $\sigma'_A$  and  $\sigma'_E$  at each rawinsonde level, the program computes the height-weighted mean values from the expression

$$\bar{\sigma}'_L = \frac{\sum_{k=z_{BL}}^{z_{BK}} (z_{k+1} - z_k) [(\sigma'_{k+1} + \sigma'_k)/2]}{z_{TL} - z_{BL}} \quad , \quad (17.46)$$

where

$\sigma'_L$  = mean value of standard deviation ( $\sigma'_A$  or  $\sigma'_E$ ) in the Lth layer

$z_{TL}$  = top of the Lth layer

$z_{BL}$  = base of the Lth layer .

When values of  $\sigma'_A$  and  $\sigma'_E$  are not entered at each k level, the program calculates the mean value of  $\sigma'_A$  under the assumption that, in general,  $\sigma'_A$  decreases with height in the surface mixing layer and that the decrease follows a power-law relationship (Refs. 17.16-17.18) given by

$$\sigma'_A\{z\} \approx \sigma'_A\{z=5m\} \left(\frac{z}{5}\right)^m \quad (17.47)$$

where  $m$  takes on negative values. The mean value of  $\bar{\sigma}_A'$  is defined as

$$\frac{\sigma_A'\{z=5\}}{(z_{TL} - 5) 5^m} \int_5^{z_{TL}} z^m dz = \frac{\sigma_A'\{z=5\} [z_{TL}^{1+m} - 5^{1+m}]}{(z_{TL} - 5) 5^m (1+m)} \quad (17.48)$$

It can be shown that, for reasonable values of  $m$ , Equation (17.48) is closely approximated by the simple expression

$$\bar{\sigma}_A'\{L=1; \tau_o=600s\} = \frac{\sigma_{AR}'\{\tau_o=600s\}}{2} \quad (17.49)$$

and the value at  $z=z_{TL}$  by

$$\sigma_A'\{z_{TL}=1; \tau_o=600s\} = \frac{\sigma_{AR}'\{\tau_o=600s\}}{2.7} \quad (17.50)$$

The assumption (Refs. 17.19 and 17.20) is also made that the value of  $\sigma_A'$  can be adjusted for the time required to form the source, in this case considered to be the cloud stabilization time  $t^*$ , by means of the expressions

$$\sigma_A'\{L=1; \tau=t^*\} = \sigma_A'\{L=1; \tau_o=600s\} \left(\frac{t^*}{600}\right)^{0.2} \quad (17.51)$$

and

$$\sigma_A'\{z_{TL}=1; \tau=t^*\} = \sigma_A'\{z_{TL}=1; \tau_o=600s\} \left(\frac{t^*}{600}\right)^{0.2} \quad (17.52)$$

Also, because the surface layer is capped by an elevated inversion where turbulence levels are expected to be minimal, the program reduces the value at the top of the second layer to 1 degree, as indicated by

$$\sigma_A'\{z_{TL}=2; \tau=t^*\} = 0.01745 \left(\frac{t^*}{600}\right)^{0.2} \quad (17.53)$$

If the program user has assigned the base of the second layer coincident with the top of the lower layer, the mean effective value of  $\sigma_A'$  in the upper layer is defined by the program as

$$\sigma_A'\{L=2;\tau=t^*\} = \frac{\sigma_A'\{z_{TL}=2;\tau=t^*\} + \sigma_A'\{z_{TL}=1;\tau=t^*\}}{2} \quad (17.54)$$

When the user chooses to assign the base of the upper layer at some kth height above the top of the lower layer, the program assumes that  $\sigma_A'$  has decreased to 1 degree in the Kth level just above the top of the lower layer. Thus, the effective value of  $\sigma_A'$  in the upper layer (L=2) is

$$\sigma_A'\{L=2;\tau=t^*\} = 0.01745 \left( \frac{t^*}{600} \right)^{0.2} \quad (17.55)$$

For the gravitational settling model described later in subsection 17.2.7.2, where material is assumed to fall through all layers, the program uses height-weighted values of  $\sigma_A'$  between the surface and the source in the Kth layer as given by

$$\sigma_{AK}' = \frac{\sum_{i=1}^K \sigma_{Ai}' (z_{i+1} - z_i)}{\sum_{i=1}^K (z_{i+1} - z_i)} \quad (17.56)$$

where  $\sigma_{Ai}'$  in the surface mixing layer ( $z_i < z_{TL}$ ) is given by Equation (17.51). In the next upper layer,  $\sigma_A'$  is obtained by linear interpolation, using the values from Equations (17.52) and (17.53), over the layer depth and by using Equation (17.53) at all greater heights.

Finally, the program assumes that turbulence over the layer depths of interest is approximately isotropic and thus that the mean effective value of  $\sigma_E'$  is equal to the mean effective value of  $\sigma_A'$ .

### 17.2.7 REED Code Dispersion Models

The dispersion models used in the REED code are based on Gaussian model concepts which experience has shown to be best suited for most practical applications. A detailed discussion of Gaussian modeling concepts and alternative approaches is found in References 17.21 and 17.22. As pointed out in this discussion (Ref. 17.22), the Gaussian approach, when properly used, "is peerless as a practical diffusion modeling tool. It is mathematically simple and flexible, it is in accord with much though not all of working diffusion theory, and it provides a reliable framework for the correlation of field diffusion trials as well as the results of both mathematical and physical diffusion modeling studies." In the REED dispersion code, the exhaust material

17.20

is assumed to be uniformly distributed in the vertical and to have a bivariate Gaussian distribution in the plane of the horizon at the point of cloud stabilization. It follows from these assumptions that the models are of the general form identified with Gaussian models for vertical line sources of finite extent.

#### 17.2.7.1 Dosage and Concentration Models

For convenience, the dosage and concentration formulas are written in a rectangular coordinate system with the origin at the ground beneath the cloud stabilization point in the Kth layer. The x axis is directed along the axis of the mean wind direction in the Lth layer, and the y axis is directed crosswind or perpendicular to the mean wind direction. In the programs, the origin of the coordinate system is placed at the launch pad.

The dosage or time-integrated concentration at any point (x,y,z) in the Lth layer due to the source in the Kth layer is given by the expression

$$\begin{aligned}
 D_{L,K} = & \frac{F\{K\}}{2\sqrt{2\pi} \sigma_{yL}(z_{TK} - z_{BK})} \left\{ \exp \left[ -\frac{1}{2} \left( \frac{y}{\sigma_{yL}} \right)^2 \right] \right\} \\
 & \left\{ \sum_{j=1}^N f_j \left[ \sum_{i=0}^{\infty} \left[ \gamma_j^i \left[ \operatorname{erf} \left( \frac{2i(z_{TL} - z_{BL}) - z_{BK} + z + V_j x / \bar{u}_L}{\sqrt{2} \sigma_{zL}} \right) \right. \right. \right. \right. \\
 & \left. \left. \left. + \operatorname{erf} \left( \frac{-2i(z_{TL} - z_{BL}) + z_{TK} - z - V_j x / \bar{u}_L}{\sqrt{2} \sigma_{zL}} \right) \right] \right. \right. \\
 & \left. \left. + \gamma_j^{i+1} \left[ \operatorname{erf} \left( \frac{2i(z_{TL} - z_{BL}) - 2z_{BL} + z_{TK} + z - V_j x / \bar{u}_L}{\sqrt{2} \sigma_{zL}} \right) \right. \right. \right. \\
 & \left. \left. \left. + \operatorname{erf} \left( \frac{-2i(z_{TL} - z_{BL}) + 2z_{BL} - z_{BK} - z + V_j x / \bar{u}_L}{\sqrt{2} \sigma_{zL}} \right) \right] \right] \right. \\
 & \left. + \sum_{i=1}^{\infty} \left[ \gamma_j^i \left[ \operatorname{erf} \left( \frac{2i(z_{TL} - z_{BL}) + z_{TK} - z - V_j x / \bar{u}_L}{\sqrt{2} \sigma_{zL}} \right) \right. \right. \right. \right.
 \end{aligned} \tag{17.57}$$



$$\begin{aligned}
 & + \operatorname{erf} \left( \frac{-2i(z_{TL} - z_{BL}) - z_{BK} + z + V_j x / \bar{u}_L}{\sqrt{2} \sigma_{zL}} \right) \Bigg] \\
 & + \gamma_j^{i+1} \left[ \operatorname{erf} \left( \frac{2i(z_{TL} - z_{BL}) + 2z_{BL} - z_{BK} - z + V_j x / \bar{u}_L}{\sqrt{2} \sigma_{zL}} \right) \right. \\
 & \left. + \operatorname{erf} \left( \frac{-2i(z_{TL} - z_{BL}) - 2z_{BL} + z_{TK} + z - V_j x / \bar{u}_L}{\sqrt{2} \sigma_{zL}} \right) \right] \Bigg] \Bigg] \Bigg\}
 \end{aligned}
 \tag{17.57}$$

Concluded

where, for convenience, 0 degree is set equal to unity and

$f_j$  = fraction of material with velocity  $V_j$

$\gamma_j$  = partial reflection coefficient (1 for complete reflection and 0 for no reflection) for the  $j$ th size category

$V_j$  = gravitational settling velocity for the  $j$ th size category

$N$  = total number of size categories describing the size distribution of interest ( $N \leq 10$  in the REED code)

$\sigma_{zL}$  = standard deviation of the vertical distribution of material in the  $L$ th layer due to the source in the  $K$ th layer

$$= \sigma_{EL}' \times \tag{17.58}$$

$\sigma_{EL}'$  = effective value of  $\sigma_E'$  in the  $L$ th layer (subsection 17.2.6)

$\sigma_{yL}$  = standard deviation of the crosswind distribution of material in the  $L$ th layer due to the source in the  $K$ th layer

$$= \left\{ \sigma_{AL}' \left[ x_{ry} \left( \frac{x + x_v - x_{ry}(1-\alpha)}{\alpha x_{ry}} \right)^\alpha \right]^2 + \left[ \frac{\Delta \theta_L' x}{4.3} \right]^2 \right\}^{1/2} \tag{17.59}$$

$x_{ry}$  = distance downwind from a virtual point source over which the crosswind cloud expansion is linear (default equals 100 m in the REED code)

$x_v$  = virtual distance

$$= x_{ry} \left( \frac{\sigma_{yo} K}{\sigma_{AL}' x_{ry}} \right)^{1/\alpha} + x_{ry} (1-\alpha) \quad (17.60)$$

$\alpha$  = coefficient of crosswind cloud expansion (default equals 1 for normal launches and 0.9 for abnormal launches in the REED code)

$\sigma_{AL}'$  = effective value of  $\sigma_A'$  in the Lth layer (see subsection 17.2.6)

$$\Delta\theta_L' = \begin{cases} (\theta_{TL} - \theta_{BL}) (\pi/180) & ; \quad V_j = 0 \\ \Phi_{j,k}' & ; \quad V_j \neq 0 \end{cases} \quad (17.61)$$

$\Phi_{j,k}'$  = effective wind-shear angle in radians for particles (drops) in the jth size category [see Equation (17.75)]

$$\bar{u}_L = \begin{cases} \left( \frac{1}{z_{TL} - z_{BL}} \right) \sum_{k=z_{BL}}^{z_{TL}} (z_{k+1} - z_k) \bar{u}_k & ; \quad v_j = 0 \\ \bar{u}_{j,k} & ; \quad v_j \neq 0 \end{cases} \quad (17.62)$$

$\bar{u}_{j,k}$  = effective mean wind-speed for particles (drops) in the jth size category [see Equation (17.69)].

The total contribution to a receptor position is calculated by summing the contributions from all sources,

$$\text{e.g., } D_L = \sum_k D_{L,K}.$$

The peak concentration, or highest concentration which occurs as the exhaust cloud passes the point (x,y,z), is given by the expression

$$x_{P,K} = D_L \left( \frac{\bar{u}_L}{\sqrt{2\pi} \sigma_{xL}} \right) \quad (17.63)$$

where

$\sigma_{xL}$  = standard deviation of the alongwind distribution of material in the Lth layer due to the source in the Kth layer

$$= \left[ \left( \frac{L\{x\}}{4.3} \right)^2 + \sigma_{x0}^2 \{K\} \right]^{1/2} \quad (17.64)$$

$L\{x\}$  = alongwind cloud length at the distance  $x$

$$L\{x\} = \left\{ \begin{array}{ll} \frac{0.28 \Delta \bar{u}_L x}{\bar{u}_L} & ; \quad \Delta \bar{u}_L \geq 0 \\ \frac{0.28 |\Delta \bar{u}_L| x}{\bar{u}_L} & ; \quad \frac{\Delta \Phi}{\Delta z} < 0, \Delta \bar{u}_L < 0 \\ 0 & ; \quad \frac{\Delta \Phi}{\Delta z} \geq 0, \Delta \bar{u}_L < 0 \end{array} \right\} \quad (17.65)$$

$$\Delta \bar{u}_L = \frac{\sum_{k=1}^{z_{TL}} (z_{k+1} - z_k) (\bar{u}_{k+1} - \bar{u}_k)}{z_{TL} - z_{BL}} \quad (17.66)$$

The peak time-mean concentration, or highest time-mean concentration to occur as the exhaust cloud passes the point  $(x,y,z)$ , is

$$x_{P,K} \{T_A\} = \frac{D_L}{T_A} \left\{ \operatorname{erf} \left( \frac{\bar{u}_L T_A}{2\sqrt{2} \sigma_{xL}} \right) \right\} \quad (17.67)$$

where

$T_A$  = time in seconds over which the concentration is averaged.

#### 17.2.7.2 Gravitational Deposition Model

The weight of material per unit area deposited on the ground as a result of the gravitational settling of particles (drops) with velocity  $V_j$  from the source in the  $K$ th layer is given by the expression

$$DEP_K = \frac{F\{K\}}{\sqrt{2\pi} \sigma_{yL} (z_{TK} - z_{BK})} \left\{ \exp \left[ -\frac{1}{2} \left( \frac{y}{\sigma_{yL}} \right)^2 \right] \right\} \quad (17.68)$$

Concluded  
(17.68)

$$\bar{v}_{j,k} = \frac{(X_{j,k}^2 + Y_{j,k}^2)^{1/2}}{z_{TK}} V_j \quad (17.69)$$

$$Y_{j,k} = \frac{\bar{u}_k}{V_j b_k} \left\{ \cos [b_k \Delta z_k / 2 + z_{BK}] - \cos (b_K z_{BK}) \right\} + \left\{ \sum_{i=1}^{k-1} \frac{\bar{u}_i}{V_j b_j} [\cos (b_i z_{Ti}) - \cos (b_i z_{Bi})] \right\} \quad (17.71)$$

$$b_k = \Delta\theta'_k / \Delta z_k \quad (17.72)$$

$$\Delta\theta'_k = \begin{cases} (\pi/180) (\theta_{TK} - \theta_{BK}) & ; \quad \Delta\theta'_k \neq 0 \\ 2 \times 10^{-3} & ; \quad \Delta\theta'_k = 0 \end{cases} \quad (17.73)$$

$$\Delta z_k = z_{TK} - z_{BK} \quad (17.74)$$

The effective wind-shear angle (change in direction of particle trajectory) for a particle in the jth size category falling to the surface from the Kth layer is

$$\Phi'_{j,k} = \tan^{-1} \left( \frac{Y_{j,k}}{X_{j,k}} \right) \quad (17.75)$$

In Equation (17.68), x is directed along an axis parallel with the direction  $(\pi + \theta'_k) + (\Phi'_{j,k})$  and y is crosswind to this direction. It should be noted that the deposition model given by Equation (17.68) assumes complete reflection of all material at the top of the L layers and partial reflection  $\gamma_j$  at the ground.

### 17.2.7.3 Precipitation Scavenging Model

The weight of material from the Kth layer deposited on the ground as a result of washout by rain is given by

$$WD_K = \frac{\Lambda F\{K\}}{\sqrt{2\pi} \sigma_{yL} \bar{u}_L} \left\{ \exp \left[ -\frac{1}{2} \left( \frac{y}{\sigma_{yL}} \right)^2 \right] \right\} \left\{ \exp \left[ -\Lambda \left( \frac{x}{\bar{u}_L} - t_i \right) \right] \right\} \quad (17.76)$$

where

$\Lambda$  = fraction of material removed per unit time

$t_i$  = time precipitation begins .

The principal assumptions made in deriving Equation (17.76) are:

1) The rate of precipitation is steady over an area that is large compared to the horizontal dimension of the cloud of material

2) The precipitation originates at a level above the top of the cloud so that hydrometeors pass vertically through the entire cloud

3) The time duration of the precipitation is sufficiently long so that the entire alongwind length of the cloud passes over the point (x,y).

The program uses the following expression (Ref. 17.23) to obtain a value of  $\Lambda$  for HCl scavenging

$$\Lambda = 5.2 \times 10^{-4} R^{0.567} \text{ sec}^{-1} \quad (17.77)$$

where

$R$  = rainfall rate (in./hr) .

The REED code also provides estimates of the maximum pH of ground-water collections of HCl at (x,y) under the assumptions that the rain begins just as the cloud reaches the receptor location, the rain ends just as the cloud passes the receptor, and the collection surface is impervious. Thus,

$$\text{pH}\{\text{HCl}\} = -\log_{10}[\text{WD}_K / (25.4 R M D)] \quad (17.78)$$

where

$D$  = rain duration (hr)

$M$  = molecular weight of HCl (36.465 g mole<sup>-1</sup>) .

### 17.3 Toxicity Criteria

An evaluation of the potential hazard arising from high near-field concentrations of toxic effluents from solid-rocket exhausts requires a knowledge of the applicable toxicity limits or thresholds. The Federal Air Quality Criteria do not presently include any of the solid-rocket exhaust effluents; however, the National Academy of Sciences provides guidelines for exposure to the toxic effluents associated with these exhausts. The Environmental Protection Agency (EPA) suggests that a safety factor of 10 be applied to the occupational exposure limits. These guidelines are based on the current limited knowledge of the effects of these effluents and are the basis of the toxicity criteria given in Table 17.4 (Ref. 17.24).

In Table 17.4, ceiling values are values that should not be exceeded for any period of time. The basis for the values in the table is reviewed in Reference 17.27.

The primary effluents from any solid-rocket exhaust are aluminum oxide ( $\text{Al}_2\text{O}_3$ ), hydrogen chloride (HCl), carbon monoxide (CO), carbon dioxide ( $\text{CO}_2$ ), hydrogen ( $\text{H}_2$ ), nitrogen ( $\text{N}_2$ ), and water vapor ( $\text{H}_2\text{O}$ ). While only the first four compounds are toxic in significant concentrations, there is always a potential hazard of suffocation from any gas which results in the reduction of the partial pressure of oxygen to a level below 135 mm Hg (18 percent by volume at standard temperature and pressure). Oxygen level reduction does not

TABLE 17.4 AIR QUALITY TOXICITY STANDARDS

Toxic Solid Rocket Exhaust Product	Time Interval (min)	Concentration		
		Public <sup>b</sup>	Emergency	Occupational
Alumina (Al <sub>2</sub> O <sub>3</sub> ) <sup>a</sup> (Aluminum Oxide)	10	5.0 mg/m <sup>3</sup>	—	50 mg/m <sup>3</sup>
	30	2.5 mg/m <sup>3</sup>	—	25 mg/m <sup>3</sup>
	60	1.5 mg/m <sup>3</sup>	—	15 mg/m <sup>3</sup>
	480	1.0 mg/m <sup>3</sup>	—	10 mg/m <sup>3</sup>
	Ceiling	8 ppm	14 ppm	30 ppm
Hydrogen Chloride (HCl) (Ref. 17.25)	10	4 ppm <sup>c</sup>	7 ppm	30 ppm Threshold
	30	2 ppm	3 ppm	20 ppm
	60	2 ppm	3 ppm	10 ppm
Carbon Monoxide <sup>a</sup> (CO)	10	90 ppm	275 ppm	1000 (1500) <sup>d</sup> ppm
	30	35 ppm	100 ppm	500 (800) <sup>d</sup> ppm
	60	25 ppm	66 ppm	200 (400) <sup>d</sup> ppm
	Dosage	200 ppm/ Time Interval		
Carbon Dioxide (CO <sub>2</sub> )	480	—	—	Average — 5000 ppm Peak — 6250 ppm
		—	—	
Nitrogen Dioxide (NO <sub>2</sub> ) (Ref. 17.26)	10	1 ppm	5 ppm	
	30	1 ppm	3 ppm	
	60	1 ppm	2 ppm	

- a. These values were reviewed by letter and telephone communication by Ralph C. Wands, Director, Advisory Center on Toxicology, National Academy of Sciences, Washington, D. C., April 1975.
- b. EPA suggests a safety factor of 10 be applied to occupational exposure limits.
- c. Parts of vapor or gas per million parts of contaminated air by volume at 25°C and 760 mm Hg.
- d. At these concentrations, headaches will occur along with a loss in work efficiency.

appear to be a hazard from solid-rocket exhaust due to the large volume of air which is entrained into these exhaust clouds; therefore, this potential hazard can be neglected in this discussion and attention directed only to the initial four toxic compounds.

The exposure levels for toxic effluents are divided into three categories (1) public exposure level, (2) emergency public exposure level, and (3) occupational exposure level. The public exposure levels are designed to prevent any detrimental health effects to all classes of human beings (children, men, women, the elderly, those of poor health, etc.) and to all forms of biological life. The emergency level is designed as a limit in which some detrimental effects may occur. The occupational level given is the maximum allowable concentration which a man in good health can tolerate — this level could be harmful to some aspects of the ecology. Public health levels for aluminum oxide are not given because the experience with these particulates is so limited that the industrial limits are, at best, very crude estimates.

Hydrogen chloride is an irritant; therefore, the concentration criterion for an interval should not be exceeded (Ref. 17.28). Since hydrogen chloride is detrimental to plant and animal life, and because most launch sites are encompassed by wildlife refuges, the emergency and industrial criteria for hydrogen chloride are not appropriate to the ecological constraints. Because of the large volume of air entrained in the exhaust cloud, the potential hazard from carbon monoxide and carbon dioxide can be neglected.

Any discussion of the detrimental health effects due to combined toxicological action of these ingredients has been omitted because of a lack of knowledge. However, investigations are currently underway to study this problem and to learn more about the biological effects of hydrogen chloride.



## REFERENCES

- 17.1 Dumbauld, R. K.; Bjorklund, J. R.; Cramer, H. E.; and Record, F. A.: "Handbook for Estimating Toxic Fuel Hazards." NASA-CR-61326, 1970, H. E. Cramer Co., NASA Contract NAS8-21453, 1969.
- 17.2 Dumbauld, R. K.; Bjorklund, J. R.; and Bowers, J. F.: "NASA/MSFC Multilayer Diffusion Models and Computer Program For Operational Prediction of Toxic Fuel Hazards." NASA CR-129006, 1973, H. E. Cramer Co., NASA Contract NAS8-29033.
- 17.3 Dumbauld, R. K.; and Bjorklund, J. R.: "NASA/MSFC Multilayer Diffusion Models and Computer Programs -- Version 5." NASA-CR-2631, 1975, H. E. Cramer Co., NASA Contract NAS8-29033.
- 17.4 Stephens, J. Briscoe; and Stewart, Roger B.: "Rocket Exhaust Effluent Modeling for Tropospheric Air Quality and Environmental Assessments." NASA TR R-473, 1977.
- 17.5 Bjorklund, J. R.; and Dumbauld, R. K.: "User's Instructions for the NASA/MSFC Cloud-Rise Preprocessor Program -- Version 6, and the NASA/MSFC Multilayer Diffusion Program -- Version 6 (Research Version for UNIVAC 1108 System)." NASA CR-2945, 1978, H. E. Cramer Co., Contract No. NAS8-31841.
- 17.6 Stephens, J. B.: "Diffusion Algorithms and Data Reduction Routine for Onsite Real-Time Launch Predictions for the Transport of Delta-Thor Exhaust Effluents." NASA TN-D-8194, 1976.
- 17.7 Gregory, Gerald L.; Hulten, William C.; and Wornom, Dewey E.: "Apollo Saturn 511 Effluent Measurements from the Apollo 16 Launch Operations -- An Experiment." NASA TM X-2910, March 1974.
- 17.8 Hulten, William C., et al.: "Effluent Sampling of Scout 'D' and Delta Launch Vehicle Exhausts." NASA TM X-2987, July 1974.
- 17.9 Gregory, Gerald L.; Hudgins, Charles H.; and Emerson, Burt R., Jr.: "Evaluation of Chemiluminescent Hydrogen Chloride and a NDIR Carbon Monoxide Detector for Environmental Monitoring." 1974 JANNAF Propulsion Meeting, San Diego, Calif., October 22-24, 1974.
- 17.10 Stephens, J. B., ed.: "Atmospheric Diffusion Predictions for the Exhaust Effluents from the Launch of a Titan IIIC, December 13, 1973." NASA TM X-64925, September 27, 1974.
- 17.11 Stephens, J. B.; Susko, M.; Kaufman, J. W.; and Hill, K. C.: "An Analytical Analysis of the Dispersion Predictions for Effluents from the Saturn V and Scout-Algol III Rocket Exhausts." NASA TM-X-2935, 1973.
- 17.12 Goldford, A. I.; Adelfang, S. I.; Hickey, J. S.; Smith, S. R.; Welty, R. P.; and White, G. L.: "Environmental Effects from SRB Exhaust Effluents -- Technique Development and Preliminary Assessment." NASA CR 2923, 1977, Science Applications, Inc., NASA Contract NAS8-31806.
- 17.13 Briggs, G. A.: "Plume Rise." TID-25075, 1969, Clearinghouse for Federal Scientific and Technical Information, Springfield, VA.

C-5

17.30

- 17.14 Briggs, G. A.: "Some recent analysis of plume rise observations." Paper ME-8E presented at the Second International Clean Air Congress, Washington, D.C., December 6-11, 1970.
- 17.15 Golder, D.: "Relations Among Stability Parameters in the Surface Layer." *Boundary-Layer Meteorology*, 3, 47-58, September 1972.
- 17.16 Swanson, R. N.; and Cramer, H. E.: "A Study of Lateral and Longitudinal Turbulence." *J. Appl. Meteor.*, 4, 409-417, 1965.
- 17.17 Cramer, H. E.; Record, F. A.; and Tillman, J. E.: "Round Hill Turbulence Measurements. Vols. II, III, IV and V." Techn. Rpt. ECOM-65-G10, Atmospheric Sciences Laboratory, Ft. Huachuca, Arizona, 1966.
- 17.18 Lumley, J. L., and Panofsky, H. A.: "The Structure of Atmospheric Turbulence." Interscience Publishers, 1964.
- 17.19 Cramer, H. E., et al.: "Meteorological Prediction Techniques and Data System." Tech. Rpt. 64-3-G, GCA Corporation, U. S. Army Dugway Proving Ground Contract DA-42-007-CML-552, 1964.
- 17.20 Osipov, Y. S.: "Diffusion From a Point Source of Finite Time of Action." AICE Survey of USSR Air Pollution Literature, National Technical Information Service, Springfield, VA, 1972.
- 17.21 Pasquill, F.: "The Dispersion of Materials in the Atmospheric Boundary Layer — The Basis for Generalization." Lectures on Air Pollution and Environmental Impact Analysis, Amer. Meteor. Soc., Boston, MA, 29 September-3 October, 1975.
- 17.22 Gifford, F. A.: "Atmospheric Dispersion Models for Environmental Pollution Applications." Lectures on Air Pollution and Environmental Impact Analyses, Amer. Meteor. Soc., Boston, MA, 29 September-3 October 1975.
- 17.23 Knutson, E. O.; and Fenton, D. L.: "Atmospheric Scavenging of Hydrochloric Acid." NASA-CR-2598, 1975, IIT Research Institute, NASA Contract NAS8-31947.
- 17.24 "National Primary and Secondary Ambient Air Quality Standards." Environmental Protection Agency, Part II of Federal Register, Vol. 36, No. 84, April 1971 (updated November 1971).
- 17.25 "Guides for Short-Term Exposures of the Public to Air Pollutants — II Guide for Hydrogen Chloride." Committee on Toxicology, National Academy of Sciences — National Research Council Report PB 203 464, August 1971.
- 17.26 "Guides for Short-Term Exposures of the Public to Air Pollutants, I. Guide for Oxides of Nitrogen." Committee on Toxicology, National Academy of Sciences, National Research Council Report PB 199 903, April 1971.
- 17.27 "Basis for Establishing Guides for Short-Term Exposures of the Public to Air Pollutants." Committee on Toxicology, National Academy of Sciences, National Research Council Report PB 199 904, May 1971.
- 17.28 "Guides for Short-Term Exposure of the Public to Air Pollutants, Vol. II Guide for Hydrogen Chloride." Committee on Toxicology of the National Academy of Sciences — National Research Council, Washington, D. C., August 1971.

## SECTION XVIII. CONVERSION UNITS

18.1 Physical Constants and Conversion Factors

This document lists the preferred metric units, alternative units, and conversion factors for a number of commonly used quantities in the aerospace industry. The selection presented, while not intended to be restrictive, will prove helpful in presenting values of quantities in an identical manner in similar contexts within the industry.

The preferred metric units, alternative units, and conversion factors are presented and grouped according to the categories listed below. For convenience, Tables I through VI list the SI base units, supplementary units, derived units, acceptable non-SI units, standard prefixes, and definition for selected physical constants and non-SI units.

1. Space and Time
2. Mass
3. Force
4. Mechanics
5. Flow
6. Thermodynamics
7. Electricity and Magnetism
8. Light
9. Acoustics
10. SI Base and Supplementary Units
11. SI-Derived Units
12. Non-SI Units Accepted for use with SI
13. Prefixes for SI Units
14. SI Definitions for Selected Physical Constants and Non-SI Units

When the preferred unit appears without a prefix, multiples of that unit per Table V may be used as necessary at the user's discretion. When a prefix appears with the unit, it is the preferred prefix. When the prefix is left to the user's discretion, however, units shall be consistent within any given document.

The conversion factors given are exact, unless the last digit is underlined. The level of error is 0.1 percent or less.

TABLE I. PREFERRED METRIC UNITS

	QUANTITY	PREFERRED METRIC UNIT	ALTERNATIVE UNITS	CONVERSION FACTORS
<b>1. SPACE &amp; TIME</b>				
1.1	TIME	S (SECOND)	MIN (MINUTE) H (HOUR) D (DAY)	
1.2	PLANE ANGLE	RAD (RADIAN)	° (DEGREE) ' (MINUTE) " (SECOND)	
1.3	SOLID ANGLE	SR (STERADIAN)		
1.4	LENGTH	MM (MILLIMETER)		1 IN = 2,54CM = 25,4MM 1 FT = 0,3048M = 304,8MM 1 YD = 0,9144M = 914,4MM
1.4.1	DISTANCE	KM (KILOMETER)	NAUTICAL MILE	1 STATUTE MILE = 1,609 344 KM 1 NAUTICAL MILE (US) = 1,852KM
1.4.2	DISTANCE	M (METER)		1 IN = 2,54CM = 25,4MM 1 FT = 0,3048M = 304,8MM 1 YD = 0,9144M = 914,4MM
1.4.3	VISIBILITY	KM (KILOMETER)		1 STATUTE MILE = 1,609 344KM
1.4.4	ALTITUDE	M (METER)		1 FT = 0,3048M
1.4.5	VIBRATION AMPLITUDE	MM (MILLIMETER)		1 IN = 25,4MM
1.4.6	POROSITY; SURFACE TEXTURE; THICKNESS OF SURFACE COATING	μ M (MICROMETER)		1 MICROINCH = 0,0254 μM
1.5	AREA	M <sup>2</sup> (SQUARE METER)		1 IN <sup>2</sup> = 645,16 MM <sup>2</sup> = 6,4516 CM <sup>2</sup> 1 FT <sup>2</sup> = 0,092 903 04 M <sup>2</sup> 1 ACRE = 0,4047 HM <sup>2</sup> 1 SQ MILE = 3,590 KM <sup>2</sup>
<div style="text-align: right;"> NASA—MSFC ES81 </div> <div style="text-align: right;">SHEET 1</div>				

TABLE I. (Continued)

	QUANTITY	PREFERRED METRIC UNITS	ALTERNATIVE UNITS	CONVERSION FACTORS
<b>1. SPACE &amp; TIME (CONTINUED)</b>				
1.6	VOLUME	M <sup>3</sup> (CUBIC METER)		$1 \text{ IN}^3 = 16\,387.064 \text{ MM}^3$ $1 \text{ FT}^3 = 0.028\,316\,847 \text{ M}^3$ $1 \text{ YD}^3 = 0.764\,554\,86 \text{ M}^3$ $1 \text{ GAL (DRY)} = 0.004\,405 \text{ M}^3$
1.6.1	FLUID TANK; WATER HEATING TANK; HIGH PRESSURE OXYGEN	L (LITER)	M <sup>3</sup> (CUBIC METER)	$1 \text{ FT}^3 = 28,317 \text{ L}$ $1 \text{ GAL (LIQ)} = 3,785\,412 \text{ L}$ $1 \text{ FL OZ} = 29,573\,53 \text{ CM}^3$
<b>2. MASS</b>				
2.1	MASS	KG (KILOGRAM)		$1 \text{ OZ (AVOIR)} = 28,349\,52 \text{ G}$ $1 \text{ LB (AVOIR)} = 0,453\,592\,37 \text{ KG}$ $1 \text{ LONG TON (2240 LB)} = 1016,047 \text{ KG}$ $1 \text{ SHORT TON (2000 LB)} = 907,1847 \text{ KG}$ $1 \text{ LONG TON} = 1,016\,047 \text{ METRIC TON}$ $1 \text{ SHORT TON} = 0,907\,185 \text{ METRIC TON}$
2.1.1	GROSS MASS; PAYLOAD	KG (KILOGRAM)	T (TONNE)	
2.1.2	HOISTING PROVISION	KG (KILOGRAM)	T (TONNE)	
2.1.3	CARGO CAPACITY	KG (KILOGRAM)	T (TONNE)	
2.1.4	FUEL CAPACITY (GRAVIMETRIC)	KG (KILOGRAM)	T (TONNE)	
2.2	LINEAR DENSITY	KG/M (KILOGRAM) PER METER)		$1 \text{ LB/FT} = 1,488\,16 \text{ KG/M}$ $1 \text{ LB/YD} = 0,496\,055 \text{ KG/M}$
2.3	DENSITY; CONCENTRATION	KG/M <sup>3</sup> (KILOGRAM PER CUBIC METER)	G/L (GRAMS PER LITER)	$1 \text{ LB/IN}^3 = 27\,679,9 \text{ KG/M}^3$ $1 \text{ LB/FT}^3 = 16,018\,46 \text{ KG/M}^3$ $1 \text{ SHORT TON/YD}^3 = 1186,5526 \text{ KG/M}^3$ $1 \text{ LB/GAL} = 119,8264 \text{ KG/M}^3$ $1 \text{ OZ/GAL} = 8,489\,152 \text{ KG/M}^3$
				<div>NASA-MSFC ES81</div> <div>SHEET 2</div>

TABLE I. (Continued)

	QUANTITY	PREFERRED METRIC UNIT	ALTERNATIVE UNITS	CONVERSION FACTORS
<b>2. MASS (CONTINUED)</b>				
2.3.1	AIR DENSITY	KG/M <sup>3</sup> (KILOGRAM PER CUBIC METER)		1 SLUG/FT <sup>3</sup> = 515,379 KG/M <sup>3</sup>
2.3.2	CARGO DENSITY	KG/M <sup>3</sup> (KILOGRAM PER CUBIC METER)	T/M <sup>3</sup> (TONNE PER CUBIC METER)	
2.3.3	GAS DENSITY	KG/M <sup>3</sup> (KILOGRAM PER CUBIC METER)		
2.3.4	LIQUID DENSITY	KG/M <sup>3</sup> (KILOGRAM PER CUBIC METER)	G/L (GRAM PER LITER)	
2.4	AMBIENT HUMIDITY	MG/G (MILLIGRAM PER GRAM)		
2.5	BALANCE MOMENT	KG M (KILOGRAM METER)	G MM (GRAM MILLIMETER)	
2.6	MOMENT OF INERTIA	KG M <sup>2</sup> (KILOGRAM SQUARE METER)		1 LB IN <sup>2</sup> = 2,9264 X 10 <sup>-4</sup> KG M <sup>2</sup> 1 LB FT <sup>2</sup> = 0,031 140 KG M <sup>2</sup>
2.7	MOMENTUM	KG M/S (KILOGRAM METER PER SECOND)		1 LB FT/S = 0,138 255 KG M/S
2.8	MOMENT OF MOMENTUM	KG M <sup>2</sup> /S (KILOGRAM SQUARE METER PER SECOND)		1 LB FT <sup>2</sup> /S = 0,042 140 KG M <sup>2</sup> /S
2.9	FLOOR LOADING	KG/M <sup>2</sup> (KILOGRAM PER SQUARE METER)	T/M <sup>2</sup> (TONNE PER SQUARE METER)	
2.10	WING LOADING	KG/M <sup>2</sup> (KILOGRAM PER SQUARE METER)	T/M <sup>2</sup> (TONNE PER SQUARE METER)	
<b>3. FORCE</b>				
3.1	FORCE	N (NEWTON)		1 LB <sub>F</sub> = 4,448 222 N
3.1.1	HANDLE OPERATING LOAD	N (NEWTON)		
3.1.2	JET AND ROCKET ENGINE THRUST	KN (KILONEWTON)		
3.1.3	ROCKET ENGINE TOTAL IMPULSE	N S (NEWTON SECOND)		
3.1.4	ROCKET ENGINE SPECIFIC IMPULSE	N S/KG (NEWTON SECOND PER KILOGRAM)		
				NASA-MSFC ES81
				SHEET 3

ORIGINAL PAGE IS  
OF POOR QUALITY  
TABLE I. (Continued)

18.5

	QUANTITY	PREFERRED METRIC UNIT	ALTERNATIVE UNITS	CONVERSION FACTORS
<b>3. FORCE (CONTINUED)</b>				
3.2	VACUUM	PA (PASCAL)		
3.3	PRESSURE	KPA (KILOPASCAL)		1 PSI = 6,894 757 KPA 1 IN H <sub>2</sub> O (39.2°F) = 0,249 08 KPA 1 IN H <sub>2</sub> O (60°F) = 0,248 84 KPA 1 IN HG (32°F) = 3,386 39 KPA 1 IN HG (60°F) = 3,376 85 KPA
3.3.1	AIR PRESSURE (GENERAL)	KPA (KILOPASCAL)		1 ATMOS (STD) = 101,325 KPA
3.3.2	AIR PRESSURE (METEOROLOGICAL)	KPA (KILOPASCAL)		1 TORR = 133, 322 PA = 0,133 32 KPA
3.3.3	HYDRAULIC PRESSURE	KPA (KILOPASCAL)		1 PSI = 6,894 757 KPA
3.4	STRESS	MPA (MEGAPASCAL)		1 KSI = 6,894 757 MPA
3.4.1	ELASTIC LIMIT; PROPORTIONAL LIMIT; ENDURANCE LIMIT	MPA (MEGAPASCAL)		
3.4.2	MODULUS OF ELASTICITY: YOUNG'S MODULUS; MODULUS OF RIGIDITY	MPA (MEGAPASCAL)		10 <sup>6</sup> PSI = 6894, 747 MPA
3.5	FRACTURE TOUGHNESS	MPA · M <sup>1/2</sup> (MEGAPASCAL METER <sup>1/2</sup> )		1 KSI - IN <sup>1/2</sup> = 1,098 843 MPA · M <sup>1/2</sup>
3.6	STRAIN ENERGY PER UNIT VOLUME	J/M <sup>3</sup> (JOULE PER CUBIC METER)		
				NASA-MSFC ES81
SHEET 4				

TABLE I. (Continued)

	QUANTITY	PREFERRED METRIC UNITS	ALTERNATIVE UNITS	CONVERSION FACTORS
<b>3. FORCE (CONTINUED)</b>				
3.7	TORQUE; MOMENT OF FORCE	N · M (NEWTON-METER)		1 IN LB <sub>F</sub> = 0,112 984 <u>8</u> N · M
3.8	BENDING MOMENT	N · M (NEWTON-METER)		1 FT LB <sub>F</sub> = 1,355 818 <u>N</u> · M
3.9	BENDING MOMENT PER UNIT LENGTH; TORQUE PER UNIT LENGTH	N M/M (NEWTON-METER PER METER)		1 LB <sub>F</sub> FT/IN = 53,378 <u>66</u> N M/M 1 LB <sub>F</sub> IN/IN = 4,428 <u>222</u> N M/M
3.10	STIFFNESS	N/M (NEWTON PER METER)		1 LB <sub>F</sub> /IN = 175,127 <u>N</u> /M
3.11	SURFACE TENSION	MN/M (MILLINEWTON PER METER)		
<b>4. MECHANICS</b>				
4.1	SECTION MODULUS	CM <sup>3</sup> (CUBIC CENTERMETER)		1 IN <sup>3</sup> = 16,387 064 CM <sup>3</sup>
4.2	SECOND MOMENT OF AREA	CM <sup>4</sup>		1 IN <sup>4</sup> = 41,623 <u>1</u> CM <sup>4</sup>
4.3	FREQUENCY	HZ (HERTZ)		
4.4	ROTATIONAL FREQUENCY	R/S (REVOLU- TIONS PER SECOND)	R/MIN. (REVOLUTIONS PER MINUTE)	
4.4.1	ROTATIONAL SPEED	R/MIN (REVOLU- TIONS PER MINUTE)		
4.5	ANGULAR VELOCITY	RAD/S (RADIAN PER SECOND)		
				NASA-MSFC ES81
				SHEET 5



TABLE I. (Continued)

	QUANTITY	PREFERRED METRIC UNIT	ALTERNATIVE UNITS	CONVERSION FACTORS
MECHANICS (CONTINUED)				
4.5.1	RATE OF TRIM	$^{\circ}/S$ (DEGREE PER SECOND)		
4.6	ANGULAR ACCELERATION	$RAD/S^2$ (RADIAN PER SECOND <sup>2</sup> )		
4.7	VELOCITY	M/S (METER PER SECOND)	KM/H (KILOMETER PER HOUR)	1 FT/S = 0,304 8 M/S 1 MILE/HOUR = 1,609 344 KM/H
4.7.1	AIRSPEED	KM/H (KILOMETER PER HOUR)		1 KNOT (US) = 1,852 KM/H
4.7.2	LAND SPEED	KM/H (KILOMETER PER HOUR)		1 MILE/HOUR = 1,609 344 KM/H
4.7.3	WINDSPEED	KM/H (KILOMETER PER HOUR)	$MS^{-1}$ (METER PER SECOND)	1 MILE/HOUR = 1,609 344 KM/H
4.7.4	VERTICAL SPEED	M/S (METER PER SECOND)		1 FT/S = 0.3048 M/S 1 FT/MIN = 0,005 08 M/S
4.8	LINEAR ACCELERATION	$M/S^2$ (METER PER SECOND <sup>2</sup> )		
4.9	ENERGY; WORK	J (JOULE)		1 FT LB/F = 1,355 818 J 1 HP H = 2,6845 MJ 1 KW H = 3,6 MJ
4.9.1	KINETIC ENERGY ABSORBED BY BRAKES	MJ (MEGAJOULE)		
4.10	IMPACT	$J/M^2$ (JOULE PER SQUARE METER)		
4.11	POWER	W (WATT)		

NASA—MSFC  
ES81

SHEET 6





TABLE I. (Continued)

	QUANTITY	PREFERRED METRIC UNIT	ALTERNATIVE UNITS	CONVERSION FACTORS
<b>6. THERMODYNAMICS (CONTINUED)</b>				
6.4	HEAT FLOW PER UNIT AREA	J/M <sup>2</sup> (JOULE PER SQUARE METER)		
6.5	HEAT FLOW RATE	KW (KILOWATT)		1 BTU/H = 0,293 071 W
6.5.1	HEAT RATE	MJ/(KW H) (MEGAJOULE PER KILOWATT HOUR)		1 BTU/(SHP H) = 1,415 KJ/(KW H)
6.6	DENSITY OF HEAT FLOW RATE	W/M <sup>2</sup> (WATT PER SQUARE METER)		1 BTU/H(H FT <sup>2</sup> ) = 3,154 59 W/M <sup>2</sup>
6.7	THERMAL CONDUCTIVITY	W/(M K) (WATT PER METER KELVIN)		1 BTU-IN/FT <sup>2</sup> ·H·°F=0, 144 23 W/(M K)
6.8	THERMAL CONDUCTANCE	W/(M <sup>2</sup> K) (WATT PER SQ. METER KELVIN)		1 BTU/(FT <sup>2</sup> ·H·°F) =5,678 26 W/(M <sup>2</sup> K)
6.9	COEFFICIENT OF HEAT TRANSFER	W/(M <sup>2</sup> K) (WATT PER SQ. METER KELVIN)		
6.10	THERMAL DIFFUSIVITY	MM <sup>2</sup> /S (SQUARE MILLI-METER PER SEC)		
6.11	THERMAL RESISTIVITY	M K/W (METER KELVIN PER WATT)		
6.12	THERMAL RESISTANCE	M <sup>2</sup> K/W (SQUARE METER KELVIN PER WATT)		
6.13	HEAT CAPACITY	KJ/K (KILOGOULE PER KELVIN)		
6.14	SPECIFIC HEAT CAPACITY	KJ/(KG K) (KILOJOULE PER KILOGRAM KILVIN)		1 BTU/(LB °F) = 4,1868 KJ/(KG K)
6.14.1	SPECIFIC HEAT	KJ/(KG K) (KILOJOULE PER KILOGRAM KELVIN)		
6.15	ENTROPY	KJ/K (KILOJOULE PER KELVIN)		1 BTU/°R = 1,8991 KJ/K
<div style="text-align: right;">NASA-MSFC ES81 SHEET 9</div>				

TABLE I. (Continued)

	QUANTITY	PREFERRED METRIC UNIT	ALTERNATIVE UNITS	CONVERSION FACTORS
<b>6. THERMODYNAMICS (CONTINUED)</b>				
6.16	SPECIFIC ENTROPY	KJ/(KG K) (KILOJOULE PER KILOGRAM KELVIN)		1 BTU/(LB °R) = 4,1868 KJ/(KG K)
6.17	GAS CONSTANT	J/(KG K) (JOULE PER KILOGRAM KELVIN)		1 FT LB/(LB °F) = 5,382 J/KG K
6.17.1	MOLAR GAS CONSTANT	J/(MOL K) (JOULE PER MOLE KELVIN)		$R_0 = 8,3143 \text{ J/(MOL K)}$
6.18	SPECIFIC ENERGY	J/KG (JOULE PER KILOGRAM)		
6.18.1	HEATING VALUE; ENTHALPY	MJ/KG (MEGAJOULE PER KILOGRAM)		1 BTU/LB = 2326 J/KG
6.19	SPECIFIC LATENT HEAT	J/KG (JOULE PER KILOGRAM)		
<b>7. ELECTRICITY &amp; MAGNETISM</b>				
7.1	ELECTRIC CURRENT	A (AMPERE)		
7.2	CURRENT DENSITY	A/M <sup>2</sup> (AMPERE PER SQUAREMETER)		1 A/IN <sup>2</sup> = 1,550 KA/M <sup>2</sup>
7.3	DIELECTRIC STRENGTH	V/MM (VOLT PER MILLIMETER)		
7.4	ELECTRIC POTENTIAL	V (VOLT)		
7.5	ELECTRIC FIELD STRENGTH	V/M (VOLT PER METER)		
7.6	POWER	W (WATT)		1 HP (550 FT LB <sub>F</sub> /S) = 0,7457 KW 1 HP (METRIC) = 0,7355 KW 1 HP (ELECTRIC) = 0.746 KW
7.7	POWER (APPARENT)	V A (VOLT AMPERE)		

TABLE I. (Continued)

	QUANTITY	PREFERRED METRIC UNITS	ALTERNATIVE UNITS	CONVERSION FACTORS
<b>7. ELECTRICITY &amp; MAGNETISM (CONTINUED)</b>				
7.8	ELECTRIC RESISTANCE; IMPEDANCE; MODULUS OF IMPEDANCE; REACTANCE	$\Omega$ (OHM)		
7.9	RESISTIVITY	$\Omega$ M (OHM METER)		
7.10	CONDUCTANCE; ADMITTANCE; MODULUS OF ADMITTANCE; SUSCEPTANCE	S (SIEMENS)		
7.11	CONDUCTIVITY	S/M (SIEMENS PER METER)		
7.12	QUANTITY OF ELECTRICITY	C (COULOMB)		1 A H = 3,6 KC
7.13	ELECTRIC CAPACITANCE	F (FARAD)		
7.14	PERMITTIVITY	F/MM (FARAD PER MILLIMETER)		
7.15	SELF INDUCTANCE; MUTUAL INDUCTANCE	H (HENRY)		
7.16	PERMEANCE	H (HENRY)		
7.17	RELUCTANCE	H <sup>-1</sup> (HENRY <sup>-1</sup> )		
7.18	PERMEABILITY	H/M (HENRY PER METER)		
7.19	MAGNETIC FLUX	WB (WEBER)		1 MAXWELL = 0,01 $\mu$ WB
7.20	MAGNETIC FLUX DENSITY	T (TESLA)		1 GAUSS = 0,1 MT
<div>NASA-MSFC ES81 SHEET 11</div>				

TABLE I. (Continued)

	QUANTITY	PREFERRED METRIC UNITS	ALTERNATIVE UNITS	CONVERSION FACTORS
<b>7. ELECTRICITY &amp; MAGNETISM (CONTINUED)</b>				
7.21	MAGNETIC FIELD STRENGTH	A/M (AMPERE PER METER)		1 OERSTED = $1000/4\pi$ A/M
7.22	ELECTROMAGNETIC MOMENT; MAGNETIC MOMENT	A M <sup>2</sup> (AMPERE SQUARE METER)		
7.23	ELECTRIC DIPOLE MOMENT	(COULOMB METER)		
<b>8. LIGHT</b>				
8.1	LUMINOUS INTENSITY	CD (CANDELA)		
8.2	LUMINOUS FLUX	LM (LUMEN)		
8.3	LUMINOUS EXITANCE	LM/M <sup>2</sup> (LUMEN PER SQUARE METRE)		
8.4	ILLUMINANCE	LX (LUX)		
8.4.1	CABIN ILLUMINATION	LX (LUX)		1 FT CANDLE = 10,764 LX
8.5	LUMINANCE	CD/M <sup>2</sup> (CANDELA PER SQUARE METER)		1 FOOTLAMBERT = 3,426 $\frac{26}{100}$ CD/M <sup>2</sup> 1 LAMBERT = 3183, $\frac{1}{100}$ CD/M <sup>2</sup>
<b>9 ACOUSTICS</b>				
9.1	NOISE LEVEL; SOUND LEVEL	DB (DECIBEL)		
9.2	PERIOD; PERIODIC TIME	S (SECOND)		
9.3	FREQUENCY	HZ (HERTZ)		
9.4	WAVELENGTH	M (METER)		
9.5	MASS DENSITY	KG/M <sup>3</sup> (KILOGRAM PER CUBIC METER)		
				NASA-MSFC ES81
				SHEET 12

TABLE I. (Concluded)

	QUANTITY	PERFERRED METRIC UNITS	ALTERNATIVE UNITS	CONVERSION FACTORS
<b>9. ACOUSTICS (CONTINUED)</b>				
<b>9.6</b>	<b>STATIC PRESSURE; INSTANTEANEOUS SOUND PRESSURE</b>	<b>PA (PASCAL)</b>		
<b>9.7</b>	<b>INSTANTANEOUS SOUND PARTICLE VELOCITY</b>	<b>M/S (METER PER SECOND)</b>		
<b>9.8</b>	<b>INSTANTANEOUS VOLUME VELOCITY</b>	<b>M<sup>3</sup>/S (CUBIC METER PER SECOND)</b>		
<b>9.9</b>	<b>VELOCITY OF SOUND</b>	<b>M/S (METER PER SECOND)</b>		
<b>9.10</b>	<b>SOUND ENERGY FLUX; SOUND POWER</b>	<b>W (WATT)</b>		
<b>9.11</b>	<b>SOUND INTENSITY</b>	<b>W/M<sup>2</sup> (WATT PER SQUARE METER)</b>		
<b>9.12</b>	<b>SPECIFIC ACOUSTIC IMPEDANCE</b>	<b>PA S/M (PASCAL SECOND PER METER)</b>		
<b>9.13</b>	<b>ACOUSTIC IMPEDANCE</b>	<b>PA S/M<sup>3</sup> (PASCAL SECOND PER CUBIC METER)</b>		
<b>9.14</b>	<b>MECHANICAL IMPEDANCE</b>	<b>N S/M (NEWTON SECOND PER METER)</b>		
<div>NASA—MSFC ES81</div> <div>SHEET 13</div>				



TABLE II. SI BASE AND SUPPLEMENTARY UNITS

QUANTITY	NAME	SYMBOL
<b>BASE UNITS:</b>		
LENGTH	METER	M
MASS	KILOGRAM	KG
TIME	SECOND	S
ELECTRIC CURRENT	AMPERE	A
THERMODYNAMIC TEMPERATURE	KELVIN	K
AMOUNT OF SUBSTANCE	MOLE	MOL
LUMINOUS INTENSITY	CANDELA	CD
<b>SUPPLEMENTARY UNITS</b>		
PLANE ANGLE	RADIAN	RAD
SOLID ANGLE	STERADIAN	SR

TABLE III. SI DERIVED UNITS

QUANTITY	NAME	SYMBOL	DERIVATION
FREQUENCY	HERTZ	HZ	$1 \text{ Hz} = 1 \text{ s}^{-1}$
FORCE	NEWTON	N	$1 \text{ N} = 1 \text{ kg m/s}^2$
PRESSURE; STRESS	PASCAL	PA	$1 \text{ Pa} = 1 \text{ N/m}^2$
ENERGY; WORK; QUANTITY OF HEAT	JOULE	J	$1 \text{ J} = 1 \text{ N m}$
POWER	WATT	W	$1 \text{ W} = 1 \text{ J/s}$
ELECTRIC CHARGE; QUANTITY OF ELECTRICITY	COULOMB	C	$1 \text{ C} = 1 \text{ A s}$
ELECTRIC POTENTIAL; ELECTROMOTIVE FORCE	VOLT	V	$1 \text{ V} = 1 \text{ W/A}$
ELECTRIC CAPACITANCE	FARAD	F	$1 \text{ F} = 1 \text{ A s/V}$
ELECTRIC RESISTANCE	OHM	$\Omega$	$1 \Omega = 1 \text{ V/A}$
ELECTRIC CONDUCTANCE	SIEMENS	S	$1 \text{ S} = 1 \text{ A/V}$
MAGNETIC FLUX	WEBER	WB	$1 \text{ WB} = 1 \text{ V s}$
MAGNETIC FLUX DENSITY; MAGNETIC INDUCTION	TESLA	T	$1 \text{ T} = 1 \text{ V s/m}^2$
INDUCTANCE	HENRY	H	$1 \text{ H} = 1 \text{ V s/A}$
LUMINOUS FLUX	LUMEN	LM	$1 \text{ LM} = 1 \text{ CD sr}$
ILLUMINANCE	LUX	LX	$1 \text{ LX} = 1 \text{ LM/m}^2$

TABLE IV. NON-SI UNITS ACCEPTED FOR USE WITH SI

QUANTITY	NAME	SYMBOL	DEFINITION
TIME	MINUTE	MIN	1 MIN = 60 S
	HOUR	H	1 H = 60 MIN = 3600 S
	DAY	D	1 D = 24 H = 86 400 S
	WEEK	WK	1 WK = 7 D
	MONTH	MO	1 MO
	YEAR	YR	1 YR = 365.26 DAYS
PLANE ANGLE	DEGREE	°	1° = ( $\pi/180$ ) RAD
	MINUTE	'	1' = (1/60)°
	SECOND	"	1" = (1/60)'
VOLUME	LITER	L	1 L = 1 DM <sup>3</sup> = 10 <sup>-3</sup> M <sup>3</sup>
AREA	HECTARE	HA	1 HA = 1 HM <sup>2</sup> = 10 <sup>4</sup> M <sup>2</sup>
PRESSURE	BAR	BAR	1 BAR = 10 <sup>5</sup> PA
ENERGY	KILOWATT-HOUR	KWH	1 KWH = 3.6 MJ
TEMPERATURE	DEGREE CELSIUS	°C	
MASS	METRIC TON	T	1 T = 10 <sup>3</sup> KG

TABLE V. PREFIXES FOR SI UNITS

FACTOR BY WHICH THE UNIT IS MULTIPLIED	PREFIX		FACTOR BY WHICH THE UNIT IS MULTIPLIED	PREFIX	
	NAME	SYMBOL		NAME	SYMBOL
10 <sup>18</sup>	EXA	E	10 <sup>-1</sup>	DECI*	D
10 <sup>15</sup>	PETA	P	10 <sup>-2</sup>	CENTI	C
10 <sup>12</sup>	TERA	T	10 <sup>-3</sup>	MILLI	M
10 <sup>9</sup>	GIGA	G	10 <sup>-6</sup>	MICRO	U
10 <sup>6</sup>	MEGA	M	10 <sup>-9</sup>	NANO	N
10 <sup>3</sup>	KILO	K	10 <sup>-12</sup>	PICO	P
10 <sup>2</sup>	HECTO*	H	10 <sup>-15</sup>	FEMTO	F
10 <sup>1</sup>	DEKA*	DA	10 <sup>-18</sup>	ATTO	A
*TO BE AVOIDED WHERE POSSIBLE					

TABLE VI. SI DEFINITIONS FOR SELECTED PHYSICAL CONSTANTS AND NON-SI UNITS

UNIT	SI EQUIVALENT
ANGSTROM UNIT ( Å )	10 <sup>-10</sup> METER
MICRON ( μ )	10 <sup>-6</sup> METER
LIGHT YEAR	9,460 55 X 10 <sup>12</sup> KILOMETER
SPEED OF LIGHT	299 337,98 KILOMETER PER SECOND
SPEED OF SOUND (SEA LEVEL)	340,461 6 METER PER SECOND
GRAVITATIONAL CONSTANT ( G <sub>N</sub> )	NEWTON - METER 9,806 65 - KILOGRAM - SECOND <sup>2</sup>
CENTISTOKE	10 <sup>-6</sup> SQUARE METER/SECOND

## REFERENCES

- 18.1 Mechtly, E. A.: "The International System of Units: Physical Constants and Conversion Factors." NASA SP-7012, Second Revision, National Aeronautics and Space Administration, Washington, D. C., 1973.
- 18.2 "Units of Weight and Measure (United States Customary and Metric) Definitions and Tables of Equivalents." United States Department of Commerce, National Bureau of Standards, Miscellaneous Publication 233, 1960.
- 18.3 "NBS Guidelines for Use of the Metric System." U. S. Department of Commerce, National Bureau of Standards, LC 1056, November 1974.

